Molecular mechanisms of drug resistance and invasion in a human lung carcinoma cell line

A thesis submitted for the degree of Ph.D.

by

Helena Joyce B.Sc. Hons, M.Sc.

This research work described in thesis was performed
under the supervision of Prof. Martin Clynes,
National Institute for Cellular Biotechnology

Dublin City University

2014

I hereby certify that this material, which I now submit for assessment on the programme of study leading to the award of Ph D. is entirely my own work, that I have exercised reasonable care to ensure that the work is original, and does not to the best of my knowledge breach any law of copyright, and has not been taken from the work of others save and to the extent that such work has been cited and acknowledged within the text of my work.

Signed:_____ ID No.: 99130394

Date:_____

Acknowledgements

I would like to express my sincere gratitude to my supervisor Professor Martin Clynes for providing me with the opportunity to do a PhD and for his constant advice, help, kindness and encouragement throughout this research project. I am also very grateful to Dr. Annemarie Larkin for her endless advice, help and friendship over the years and for listening to me drone on about my research.

I would like to acknowledge the many people who have assisted me with the numerous technical assays in pursuit of my research. Dr. Niall Barron's help with the molecular work including my PCR and methylation studies was invaluable. Thanks also to Dr. Padraig Doolan for his help with the microarray and bioinformatics analysis. Thanks also to Dr. Paul Dowling and Michael Henry for their help with the proteomics analysis and to Dr. Sinead Aherne for her help with the miRNA analysis. Thanks to Dr. Annemarie Larkin for teaching me the fundamentals and art of Immunohistochemistry. In addition, I would also like to thank Dr. Colin Clarke and Dr. Jai Mehta for their help with the bioformatics analysis. Thanks also to Dr. Sinead Toomey, RCSI, for doing the Sequenom analysis. Thanks to Dr. Finbarr O'Sullivan for his help with confocal microscopy, Dr. Stephen Madden for his advice on bioinformatics and to Mr. Vincent Lynch for those weekly chats. Thank you to Dr. Joanne Keenan who was always there to give me advice on all matters. A very special thanks goes to Andrew McCann who kept me informed of his work to back up my results. Thanks also to Edel McAuley, Emma Hughes and Laura Dowling for help with immunoblots and IHC and to Dr. Erica Hennessy for her help with the stem cell marker analysis. Thank you to Joanne, Laura and Justine for those early morning chats.

Thanks to past and present colleagues at NICB who have helped me over the years. From Gillian's and Joe's tireless work in the Prep room and Carol, Mairead, Geraldine, Mick and Yvonne for all the things that make our life easier on a day-to-day basis and always trying to help.

Finally, I thank my parents John and Veronica Joyce for all their love and encouragement and my brothers and sisters Marie, Paraic, Linda, Fiona and Micheál for their faith and support. And most of all for my loving, supportive, encouraging, and patient husband Brendan whose faithful support during the final stages of this PhD is so appreciated, and to my sons, Darragh, Ciarán and Cillian for providing a challenging alternative to scientific life.

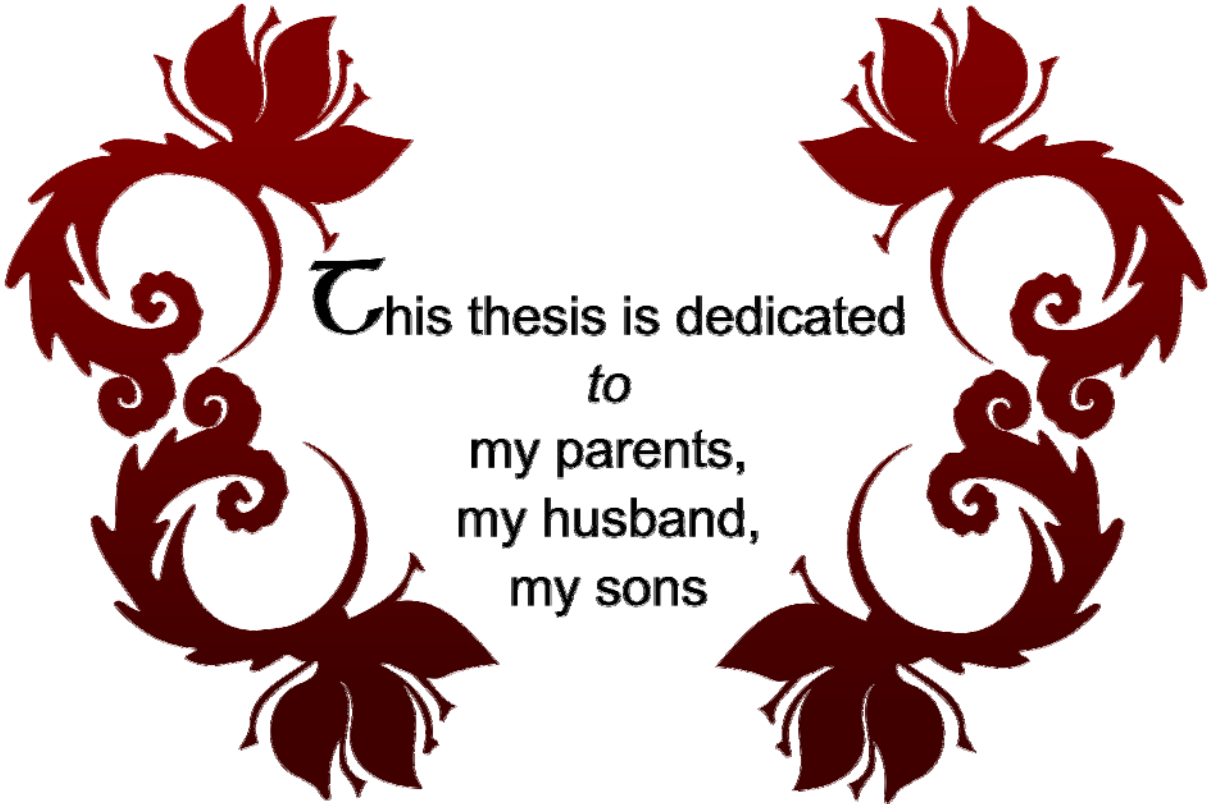
This thesis is dedicated
to
my parents,
my husband,
my sons

Contents

Abbreviations

%	Percentage
Ab	Antibody
ABC	ATP Binding Cassette
ABC/HRP	Streptavidin/biotin-Horseradish Peroxidase
ATCC	American Type Culture Collection
ATP	Adenosine Triphosphate
BSA	Bovine Serum Albumin
BCRP	Breast Cancer Resistance Protein
CAM	Cell Adhesion Molecules
cDNA	Complementary DNA
Ct	Cycle Threshold
DAB	3,3' Diaminobenzidine
dH20	Distilled water
DMEM	Dublecco's Minimum Essential Medium
DMSO	Dimethyl Sulfoxide
DNA	Deoxyribonucleic Acid
dNTP	Deoxynucleotide Triphosphate (N = A, C, T, G)
DTT	Dithiothreitol
ECACC	European Collection of Animal Cell Culture
ECM	Extracellular matrix
EDTA	Ethylene Diamine Tetraacetic Acid
EGF-	Epidermal Growth Factor
EGFR	Epidermal Growth Factor Receptor
EMT	Epithelial to Mesenchymal Transition
FCS	Foetal Calf Serum
GAPDH	Glyceraldehyde-6-Phosphate Dehydrogenase
IC50	Inhibitory Concentration 50%
IHC	Immunohistochemistry
HRP	Horseradish Peroxidase
IGFR	Insulin-like Growth Factor Receptor

kDa	Kilo Daltons
LRP	Lung resistance-related protein
MAPK	Mitogen Activated Protein Kinase
MDR	Multiple drug resistance
MET	MNNG (N-Methyl-N'-nitro-N-nitroso-guanidine) HOS Transforming gene
Min	Minutes
miRNA	microRNA
MMPs	Matrix Metalloproteases
mRNA	Messenger RNA
MRP	Multi-drug resistance-associated protein
NSCLC	Non-Small Cell Lung Cancer
PNP	Paranitrophenol phosphate
PBS	Phosphate Buffered Saline
P-gp	P-glycoprotein
PTKs	Protein Tyrosine Kinases
PTEN	Phosphatase and Tensin Homolog
RNA	Ribonucleic Acid
RNase	Ribonuclease
RNAi	Ribonucleic Acid interference
RPM	Revolutions Per Minute
RT	Room temperature
RT-PCR	Reverse Transcription Polymerase Chain Reaction
SCR	Scrambled
SD	Standard Deviation
SF	Serum-free
siRNA	Small interfering RNA
SDS-PAGE	Sodium Dodecyl Sulfate - Polyacrylamide Gel Electrophoresis
SNP	Single Nucleotide Polymorphism
TLDA	Taqman Low Density Array
TMA	Tissue Microarray
TBS	Tris Buffered Saline

UHP	Ultra High Pure Water
v/v	Volume/Volume

Abstract

Metastasis and drug resistance present as major problems to patients during cancer chemotherapy. The research outlined in this thesis aims to further our knowledge about the molecular mechanisms involved in these processes and the relationship between drug resistance and cancer invasion and/or metastasis.

One explanation for the link between resistance and metastasis is that resistance facilitates tumour progression and invasion into both surrounding and distal tissues. Investigations were conducted on a clonal sub-population of poorly differentiated human lung squamous carcinoma cells (DLKP). These were pulsed with mitoxantrone and the resulting cell populations extensively characterised. Two sub-lines emerged: SQ-Mitox-BCRP and SQ-Mitox-MDR cell lines. These two cell lines typically exhibited resistance to the selecting agent (ranging approx. 210 to 320-fold). This occurred as an early event during the pulsing process. The two sublines differed in their morphology and pattern of gene expression. In addition, BCRP was significantly increased in one population (SQ-Mitox-BCRP) while P-gp was significantly increased in the other population (SQ-Mitox-MDR).

A crucial step in human lung cancer progression appears to be the acquisition of invasiveness. The population of cells arising from the 4^{th} drug pulse remained noninvasive but had acquired a high level of drug resistance. However, after two additional drug pulses, all cell lines acquired invasiveness. The invasive, drug resistant BCRP and MDR cell line variants were characterised in depth and microarray analysis was used to find functionally significant changes in the transition from the preinvasive to the invasive phenotype. Functional and cellular signaling analyses were performed on the cell lines using pharmacological inhibitors, function-blocking antibodies, and gene silencing by RNA interference.

The DLKP cell line appears to contain at least three morphologically distinct sub-populations of cells with different levels of invasiveness. Microarray analysis generated gene lists that were specific to an invasive phenotype, identifying possible genetic markers for invasion. Proteins (including the cell adhesion molecules, N-cadherin and ALCAM and the axon guidance molecule SLIT2) were also identified as possible and alternative markers capable of distinguishing between the different cell line clones.

CHAPTER 1

A comprehensive literary review.

1.1 Lung cancer

1.1.1 Lung Cancer:the clinical problem

Unfortunately, lung cancer is the most common cause of cancer-related death in Ireland and indeed the world. Lung cancer was the single most common cause of cancer death in Ireland in 2011, with a total of 1,848 deaths, just over one-fifth of all cancer deaths[1]. In the United States in 2007, there were 203,536 people diagnosed with lung cancer and of this number, 158,683 people died from the disease[2]. Despite the advances in platinum-based chemotherapy[3], lung cancer remains the most frequent cause of cancer-related mortality worldwide[4] and has a 5-year overall survival (OS) rate of just 16% for all stages.

1.1.2 Pathogenesis and classification

Lung cancer is a disease characterised by un-controlled cell growth in the tissues of the lung. If left untreated, this growth can spread beyond the lung in a process called metastasis into nearby tissues or more distally to other parts of the body. Most cancers that arise in the lung, known as primary lung tumours, are carcinomas that derive from epithelial cells. Lung cancers can be histologically classified into two main groups, non small cell lung cancer (NSCLC) and small cell lung cancer (SCLC) – with 80% of cases falling into the first group and the remaining 20% into the second group[5].

The most common cause of lung cancer is long-term exposure to tobacco smoke, which causes 80 – 90% of all incidences[6]. Nonsmokers account for 10 – 15% of lung cancer cases, and these cases are often attributed to a combination of genetic factors, exposure to radon gas, asbestos fibres (in the rare case of mesothelioma), and air pollution, including second-hand smoke[7]. Since only approximately 20% of smokers develop lung cancer[6], it is believed that some people are more susceptible to the carcinogens in tobacco than others. Lung cancer, it may be argued, is one of the easiest cancers to prevent, but remains one of the most difficult to treat.

In small-cell lung carcinoma (SCLC), the cells contain dense neurosecretory granules (vesicles containing neuroendocrine hormones), which give this tumour an endocrine/paraneoplastic syndrome association[5]. These tumours are normally centrally located and are strongly associated with smoking. Relapse is very common, even after an initial, successful response to treatment[8]. They grow quickly and spread early in the course of disease. Sixty to seventy percent of patients typically have metastatic disease at clinical presentation.

There are three main subtypes of non small cell lung cancer (NSCLC) – (1.) adenocarcinoma, (2.) squamous-cell lung carcinoma, and (3.) large-cell lung carcinoma[9] (figure 1-1). Nearly 55% of lung cancers are adenocarcinoma, which usually originates in peripheral lung tissue[9]. Most cases of adenocarcinoma are associated with smoking; however, among people who have smoked fewer than 100 cigarettes in their lifetimes ("never-smokers"), adenocarcinoma is the most common form of lung cancer[10]. A subtype of adenocarcinoma, the bronchioloalveolar carcinoma (BAC), is more common in female never-smokers and eastern Asians, and may have a better long term survival[11] relative to other forms of non-small cell lung cancer, especially when it is caught early and only one tumour is present.

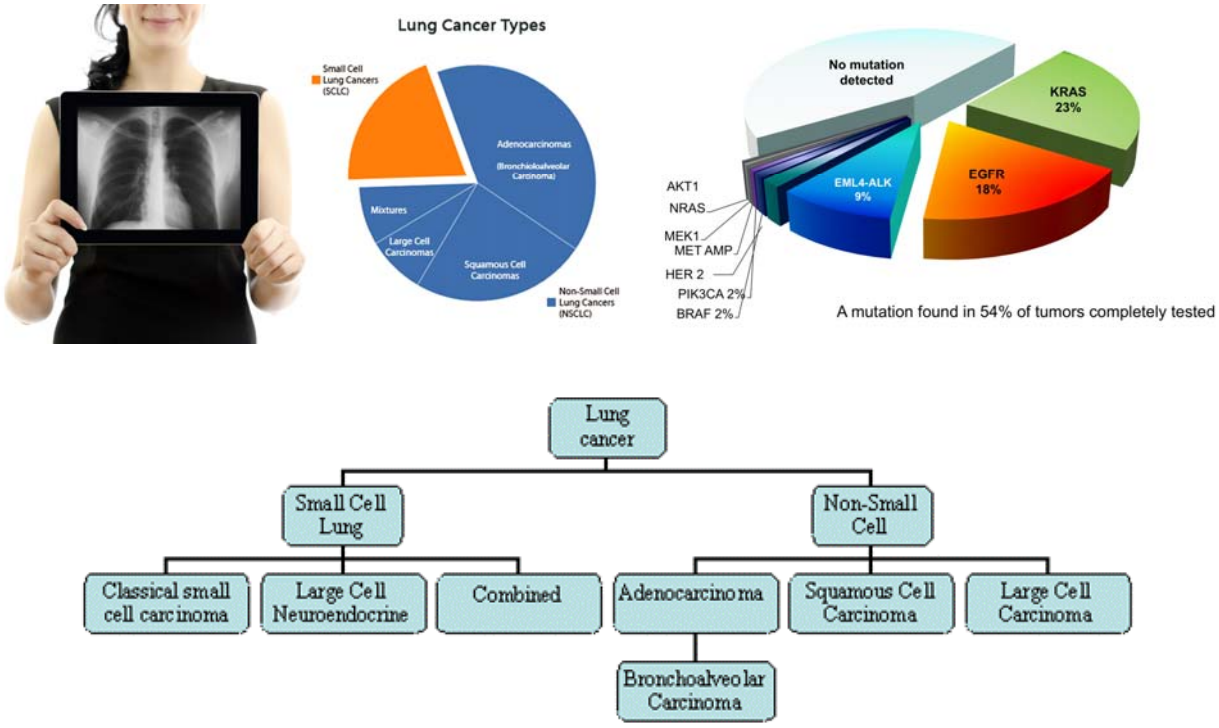

Figure 1-1: Small cell carcinoma is usually the most aggressive type of lung cancer with the poorest prognosis. Thus, often patients are told they have small cell carcinoma or non-small cell carcinoma, combining the three non-small cell types together, as they are relatively less aggressive. The only way to distinguish between these types of lung cancer is by a tissue biopsy.

Squamous cell carcinomas account for approximately 30% of all lung cancers and they are typically centrally located[12,13]. They are very common in Europe, and are often accompanied by the late development of distant metastasis[9]. Generally, NSCLC is associated with a poor

prognostic outcome and, despite surgery being the first line of treatment, approximately 70% of patients present with unresectable disease[14].

1.1.3 Treatment of lung cancer

The objective in cancer treatment is to control or eradicate the tumour and prevent its spread. Treatment for lung cancer can involve surgical removal, chemotherapy, or radiation therapy, as well as combinations of all these treatments. Despite huge developments in cancer treatment in the last few years, the outcome for many patients with advanced disease is still not promising.

Surgical removal of the tumour is generally performed for limited-stage (stage I or sometimes stage II) NSCLC and is the treatment of choice for cancer that has not spread beyond the lung[9]. About 10% to 35% of lung cancers can be removed surgically, but removal does not always result in a cure, since the tumours may already have spread and can recur later. Among people who have an isolated and slow-growing lung cancer removed, 25% to 40% are still alive 5 years after diagnosis.

1.1.3.1 Chemotherapy in the management of lung cancer

Many single anti-cancer agents have activity against NSCLC and these include cisplatin, carboplatin, paclitaxel, docetaxel, vinorelbine and gemcitabine; however, a modest increase in response rates is seen with combinations of these drugs with platinum derivatives to form the standard care[15]. Paclitaxel or docetaxel in combination with cisplatin have been recommended as an option in the first-line treatment of advanced NSCLC. However, response rates are often low due to the increasing development of resistance to the cytotoxicity of these drugs by the tumour cells being targeted.

Chemotherapy is the treatment of choice for most SCLC since these tumours are generally widespread in the body when they are first diagnosed. Only half of the people who present with SCLC survive for greater than four months without chemotherapy. With chemotherapy, their survival time is increased up to four- or five-fold. Several drugs are primarily used for the treatment of SCLC and include; cisplatin, carboplatin VP-16, cyclophosphamide, adriamycin, vincristine, lomustine and ifosfamide. Although combination therapy has shown good response rates, the median survival time of SCLC patients remains low. The most frequent combination therapy in the treatment of SCLC is etoposide and cisplatin[8,14,16].

Despite progress in the development of drugs that target unique cancer-specific pathways, traditional chemotherapeutics still yield significant survival advantages in many instances and so continue to be the tools that form the first line of defence used in the clinic.

1.1.3.2 Novel therapies in the management of lung cancer NSCLC

Modern treatment strategies focus on the pathological classification of NSCLC, which includes the assessment of protein expression by immunohistochemistry (IHC) to identify the presence of cell differentiation markers such as TTF1 and p63 (the splice variant p40). Also involved is the detection of molecular predictive markers, including validated driver mutations in genes associated with cell growth and survival[17] (figure 1-2). However, lung cancer is a heterogenous disease and it can display a great number of genetic aberrations within different tumours[18]. Lung cancers develop through a multistep process involving development of multiple genetic and epigenetic alterations, particularly activation of growth promoting pathways and inhibition of tumour suppressor pathways[19].

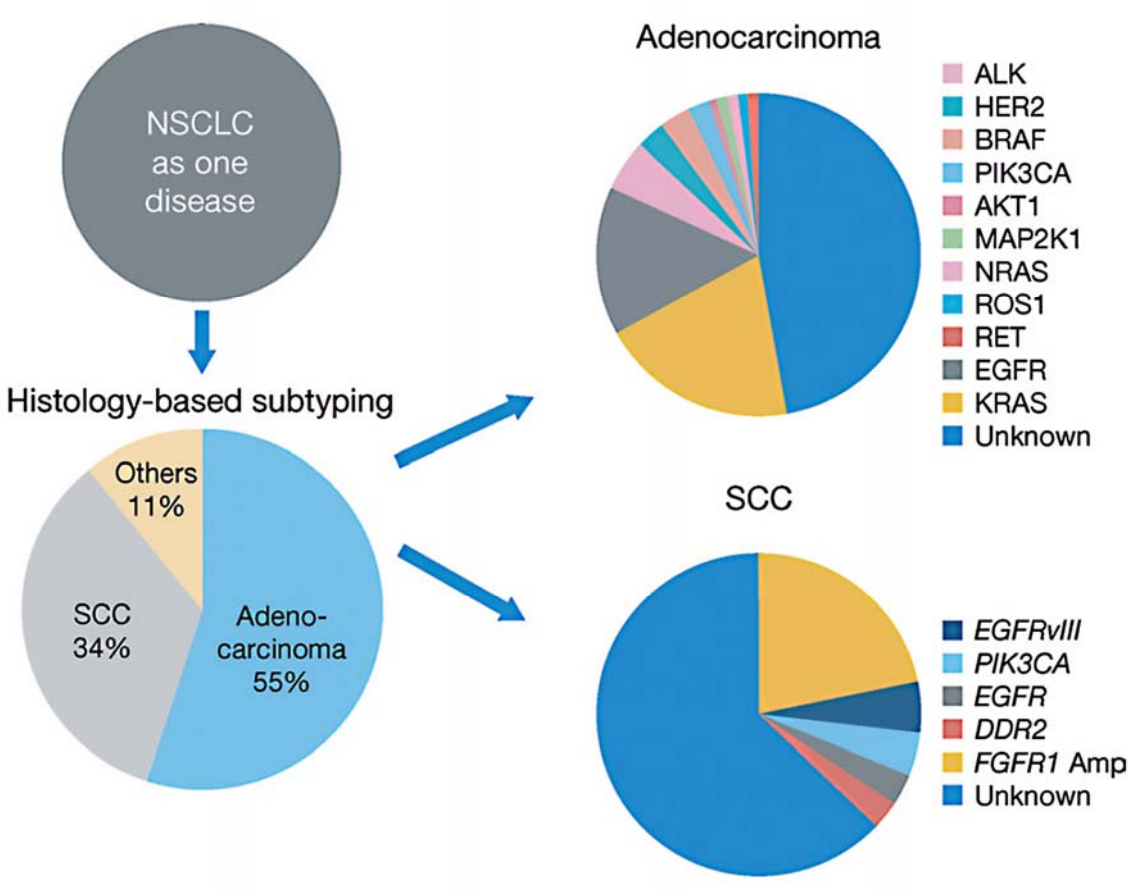

Figure 1-2: Evolving genomic classification of NSCLC. *Li et al.,* (2013)[20].

Characterisation of the molecular changes in lung cancer is becoming increasingly well-defined, helped by the continued advancement of both clinical and genomic tools. Figure 1-3 shows the major signalling pathways implicated in lung cancer[21]. These stimulatory signalling pathways are led by oncogenes, which drive cells towards a malignant phenotype, promoting proliferation and escape from apoptosis. Mutated oncogenic proteins cause an "addiction" of tumour cells to their abnormal functions, a concept referred to as "oncogene addiction"[22].

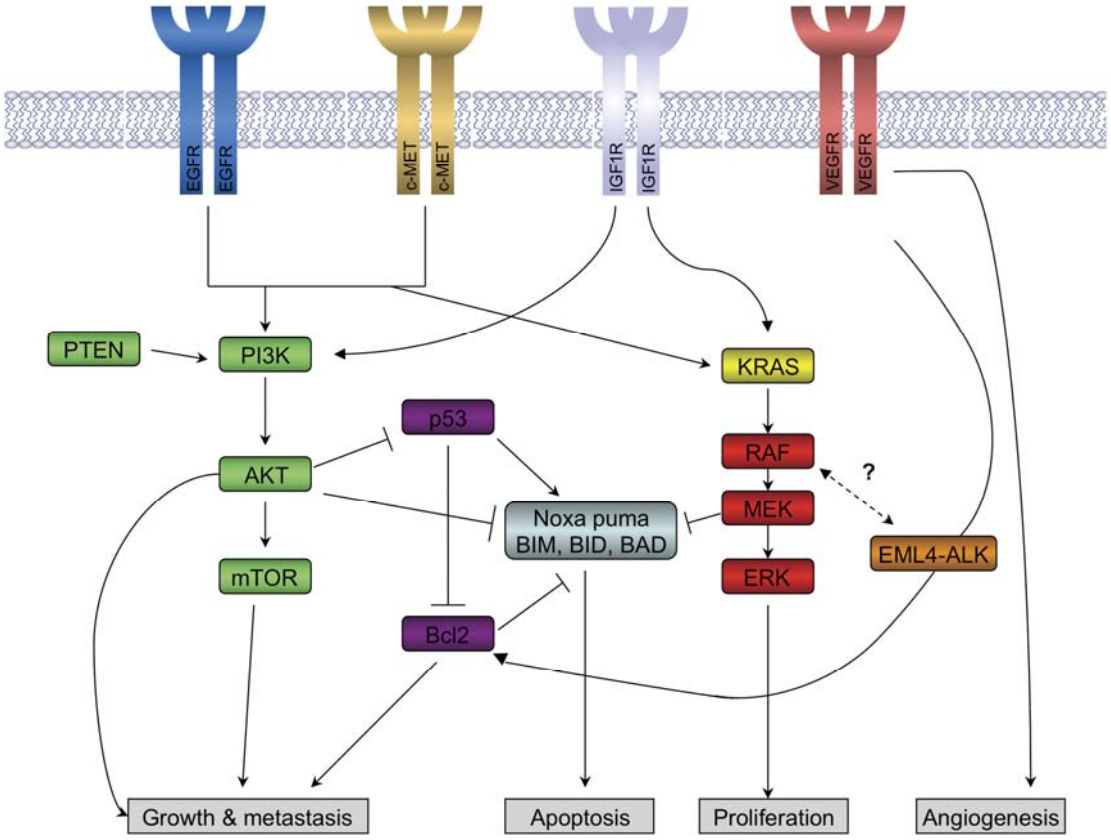

Figure 1-3: A major signalling pathway implicated in lung cancer is the EGFR pathway which signals to both the AKT/PI3K pathway (green) and the MAPK pathway (red) which regulate cell growth, proliferation and cell death. There is significant cross-talk between these pathways and their downstream effectors, which may be classified into six pathways for simplicity to account for differences in treatment modalities. The additional four pathways are: EGFR (blue), KRAS (yellow), EML4-ALK (orange), and P53/BCL (purple). It is thought that the RAS/RAF/MEK/MAPK pathway may be constitutively activated by the EML4-ALK fusion oncogene. The complex relationship between this pathway and EML4-ALK is indicated with a dashed line. (From West *et al.,* 2012[21])

It has been shown that EGFR overexpression is most frequent in squamous (84%), large cell (68%) and adenocarcinoma (65%) with very little expression in SCLC[23]. Mutations and amplification of EGFR are common in non-small-cell lung cancer and provide the basis for

treatment with EGFR-inhibitors. The Ras/mitogen-activated protein kinase and PI3K/Akt pathways are major signalling networks linking EGFR activation to cell proliferation and survival. Activation of the RAS/RAF/MEK/MAPK pathway occurs frequently in lung cancer, most commonly via activating mutations in KRAS which occur in ~20% of lung cancers, particularly adenocarcinomas [24, 25]. In lung cancer, 90% of mutations are located in KRAS (80% in codon 12, and the remainder in codons 13 and 61), with HRAS and NRAS mutations being only occasionally documented[18].

Mutation results in constitutive activation of downstream signalling pathways, such as PI3K and MAPK, rendering KRAS mutant tumours independent of EGFR signaling and therefore resistant to EGFR TKIs as well as chemotherapy. KRAS mutations are mutually exclusive with EGFR and ERBB2 mutations and are primarily observed in lung adenocarcinomas of smokers[18].

Lung cancer mutations have also been identified in BRAF and the parallel phosphatidylinositol 3-kinase (PI3K) pathway oncogenes and more recently in MEK and HER2 while structural rearrangements in ALK, ROS1 and possibly rearranged during transfection (RET) provide new therapeutic targets. The roles of tumour suppressor genes are increasingly recognised with aberrations reported in TP53, PTEN, RB1, LKB11 and p16/CDKN2A. Identification of biologically significant genetic alterations in lung cancer that lead to activation of oncogenes and inactivation of tumour suppressor genes has the potential to provide further therapeutic opportunities[19].

Genetic instability: Chromosomal aberration and loss of heterozygosity

Cells possess checkpoint pathways important for genome stability and preventing cancer. Like many solid tumours, genomic instability is a hallmark of lung cancer. Amplification is a mechanism for the activation of oncogenes such as MET in adenocarcinoma, fibroblast growth factor receptor 1 (FGFR1) and discoidin domain receptor 2 (DDR2) in squamous cell carcinoma (SCC). Intriguingly, many of these genetic alternations are associated with the smoking status of a population and also with particular racial and gender differences, which may provide further insights into the mechanisms of carcinogenesis and the role for various host factors in the development of lung cancer and its progression[26]. Chromosomal damage can lead to a loss of heterozygosity, i.e. a gross chromosomal event that results in the loss of the entire gene and the surrounding chromosomal region. This can cause inactivation of tumour suppressor genes. Damage to chromosomes 3p, 5q, 13q, and 17p are particularly common in small-cell lung carcinoma. Additionally, genetic alterations in several genes have been implicated in the

development of lung cancer and include the activation of MYC, RAS, EGFR, NKX2-1, ERBB2, SOX2, BCL2, FGFR2, and CRKL as well as inactivation of RB1, CDKN2A, STK11 and FHIT3[18].

P53

The many roles of the protein p53 as a tumour suppressor include the ability to induce cell cycle arrest, DNA repair, senescence, and apoptosis, to name only a few[27]. In humans, the *TP53* gene is reported to be mutated in approximately 50% of non-small-cell lung cancer cases and more than 70% of small-cell lung cancers[28]. The majority of these mutations are missense, resulting in the expression of a full-length p53 protein which is compromised in its ability to bind directly to DNA and activate anti-proliferative and pro-apoptotic target genes. Tobacco smoke is one of the best-known and studied mutagen mixtures involved in lung carcinogenesis, and TP53 mutational patterns differ between smokers and nonsmokers, with an excess of G to T transversions in smoking-associated cancer[29,30]. These particular transversions, which are uncommon in most cancers with the exception of hepatocellular carcinoma (HCC), is found to be associated with specific carcinogenic agents. The most prominent carcinogens in tobacco smoke, polycyclic aromatic hydrocarbons (PAHs) and especially benzo(a) pyrene, were found to be able to form DNA adducts in the coding region of the TP53 gene. In addition, there is a correlation between the mutational hotspots of TP53 in lung cancer (at codons 154, 157, 158, 245, 248, and 273) and the hotspots of adducts formation by PAHs in tobacco smoke.

Targeted lung cancer treatments in current use

More recently, targeted therapies have shown promise in the treatment of NSCLC (table 1-1). The drugs erlotinib (Tarceva) and gefitinib (Iressa) are so-called targeted drugs, which may be used in certain patients with NSCLC who are no longer responding to chemotherapy[31]. Targeted therapy drugs more specifically target cancer cells, resulting in less damage to normal cells than general chemotherapeutic agents. Erlotinib and gefitinib target the epidermal growth factor receptor. Cetuximab, a monoclonal antibody added to first-line chemotherapy has been shown to improve survival in patients with high epidermal growth factor receptor (EGFR) expression in their tumours[32].

Table 1-1. Current molecular targets in adenocarcinoma

Target	Prevalence (%)	Therapeutic agents
EGFR	Asians ~40; Caucasians ~10	Erlotinib, gefitinib, afatinib
ALK	< 5	Crizotinib
HER2	< 3	Afatinib, neratinib, dacomitinib
PIK3CA	< 5	GDC-0941, XL-147, BKM120
BRAF	< 5	Vemurafenib, GSK2118436
MEK	~1	AZD6244
ROS1	~2	Crizotinib
RET	~2	Sunitinib, sorafenib, vandetanib, cabozantinib
MET	1–11	Onartuzumab, rilotumumab, cabozantinib, tivantinib, crizotinib
FGFR1	~3	AZD4547, S49076, ponatinib, brivanib
PTEN	< 10	Vandetanib
PD-1/PD-L1	~30	Nivolumab, MPDL3280A
NaPi2b	~70	DNIB0600A (early development)

ALK, anaplastic lymphoma kinase; EGFR, epidermal growth factor receptor; FGFR1, fibroblast growth factor receptor 1; PD-L1, interaction of programmed death ligand 1; PIK3CA, phosphatidylinositol 3-kinase, catalytic subunit alpha. From Shames and Wistuba 2014[33]

Other attempts at targeted therapy include drugs known as anti-angiogenesis drugs, which block the development of new blood vessels within a tumour. Without adequate blood vessels to supply oxygen-carrying blood, the cancer cells will die. In this regard, the VEGF pathway has become an important therapeutic target in lung cancer. The antiangiogenic drug bevacizumab (Avastin) which targets VEGF has also been found to prolong survival in advanced lung cancer patients when it is added to the standard chemotherapy regimen[34]. This demonstrates the use of VEGF as a target for therapy.

Crizotinib also shows benefit in a subset of non-small cell lung cancer that is characterised by the EML4-ALK fusion oncogene, found in some relatively young, never or light smokers with adenocarcinoma[35].

1.1.4 Chemotherapy resistance

A major obstacle in the use of chemotherapy for cancer treatment is the development of resistance. Consequently, a better understanding of the mechanisms of drug resistance would help to overcome this obstacle. Intrinsic and acquired drug resistance are believed to result in treatment failure in over 90% of patients with metastatic cancer[36]. Resistance constitutes a lack of response to drug-induced tumour growth inhibition; it may be inherent in a subpopulation of

heterogeneous cancer cells or be acquired as a cellular response to drug exposure. Principal mechanisms include: (1) altered membrane transport involving the P-glycoprotein product of the multidrug resistance (MDR) gene as well as other associated proteins; (2) altered target enzyme (e.g. mutated topoisomerase II); (3) decreased drug activation; (4) increased nuclear receptor activation; (5) increased drug metabolism and elimination due to altered expression of cytochrome P_{450} enzymes; (6) drug inactivation due to conjugation with increased glutathione; (7) subcellular redistribution; (8) drug interaction; (9) enhanced DNA repair and (10) failure to apoptose as a result of mutated cell cycle proteins such as p53. Treatment with one agent can often lead to associated resistance to a number of unrelated agents. The development of resistance to a variety of unrelated chemotherapeutic drugs is called multiple drug resistance (MDR). MDR is caused by a variety of changes in the cancer cells and is almost always multifactorial.

1.1.4.1 P-gp and Multiple Drug Resistance.

The mechanism of multi-drug resistance was originally described in the 1970s when cells selected with just one agent, showed resistance to the cytotoxic effects of multiple unrelated agents. Cells treated with actinomycin D showed resistance to mithramycin, vinblastine, vincristine, puromycin, daunomycin, demecolcine and mitomycin C[37]. The protein responsible was identified as P-glycoprotein or P-gp, a 170kDa plasma membrane glycoprotein encoded by the MDR1 gene present on chromosome 7q21 [38]. In addition to the cross-resistance of agents, a decreased intracellular concentration of the target drugs was also noted[37]. This was attributed to the active efflux of the agent from the cells [39,40,41]. *Gottesman et al.,* [42] showed that P-gp is an ATP-dependent drug pump involved in the transport of a broad range of structurally unrelated compounds. *Bellamy et al.,* [43] identified that P-gp also confers taxane resistance and can cause intracellular redistribution of the drug. The list of compounds now known to interact with this transporter is well in excess of 300[44,45]. Many of the "new generation" anticancer compounds (e.g., kinase inhibitors) are also substrates for transport by P-gp[46,47] (table 1-2).

P-gp is a member of a family of ATP-dependent transporters found in all living organisms that are called ABC (for ATP-binding cassette) transporters. It is expressed in many distinct types of cancer as well as numerous normal tissues[48]. In the human, there are 48 such transporters, and many are involved in the transport of lipophilic substances, such as cholesterol and phospholipids, into cellular organelles and out of the cell[49].

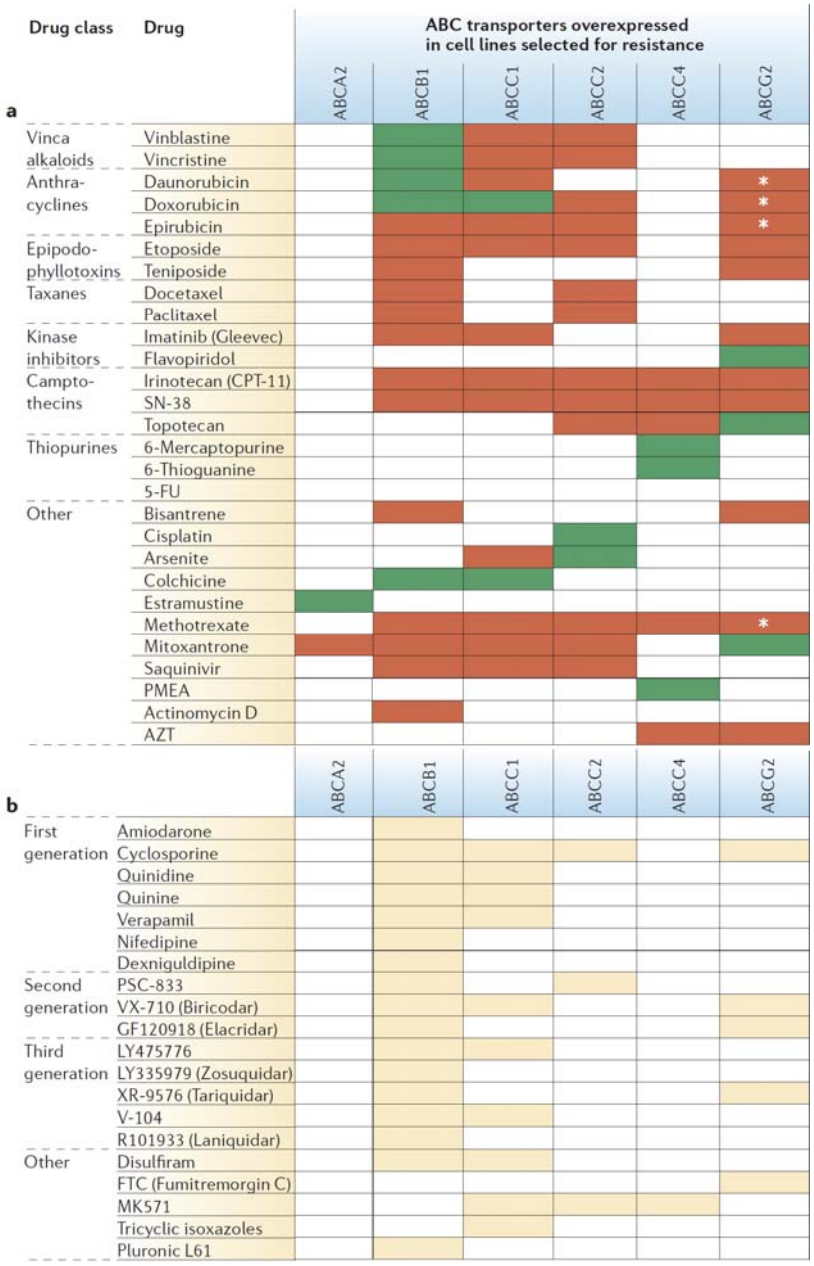

Table 1-2: Substrates and inhibitors of ATP-binding cassette transporters. **a**. Overlapping substrate specificities of the human ATP-binding cassette (ABC) transporters confering drug resistance to cancer cells. A single drug can be exported by several ABC transporters (rows), and each ABC transporter can confer characteristic resistance patterns to cells (columns). To determine which ABC transporters are involved in multidrug resistance (MDR), two different experimental procedures are common. Cells could be selected in increasing concentrations of a cytotoxic drug, which could result in the increased expression of a specific ABC transporter (see green boxes representing drug–gene pairs in which an ABC transporter was found to be overexpressed in cell lines selected for resistance to the respective drug). Resistant cells overexpressing a single ABC transporter often show characteristic cross-resistance to other, structurally unrelated, drugs (red boxes). **b**. The ability of ABC transporters to alter cell survival, drug transport and/or drug accumulation can be inhibited or altered by various modulators (yellow boxes). As in a, white boxes denote unexplored or absent drug–gene relationships. *The transport of these drugs by ABCG2 is dependent on an amino acid variation at position 482 (wild type is R; variants include R482G and R482T). Numbers in boxes refer to references. AZT, azidothymidine; 5-FU, fluorouracil; PMEA, 9-(2-phosphonylmethoxyethyl)adenine. (Adapted from *Szakacs et al.,* 2006[50]).

P-gp is synthesized as a 140-kDa polypeptide precursor that is later N-glycosylated to a final molecular weight of 170 kDa[51]. Glycosylation of P-gp was not found to be necessary for its drugtransport activity[52,53] but was shown to be important for the proper control of P-gp in the endoplasmic reticulum[54] and transport of P-gp to the plasma membrane[52]. It is made up of two homologous halves, which contain six transmembrane domains and an ATP-binding domain, separated by a linker protein (figure 1-4). P-gp is an energy dependent pump, capable of transporting hydrophobic compounds out of the cell[55].

The ABCB1 (mdr1) gene is also up-regulated in response to a range of chemotherapeutic drugs[56] as well as to diverse stress stimuli, such as the alteration of oxygen supply or deregulation of intracellular pH[57]. In addition, there are several nuclear receptors which are known to be modulators of *mdr1* gene transcription:

1. The Pregnane X Receptor (PXR), which is also known as the steroid and xenobiotic receptor. PXR is most often described as being involved in P-gp transcriptional control. This receptor is characterised by its interaction and activation by a large spectrum of ligands and represents an example of a promiscuous xenobiotic sensor. PXR is also known to regulate transcription of other very important players in cell resistance, i.e., cytochrome P450, particularly the CYP3A subfamily. The substrates and inhibitors of P-gp overlap considerably with those of CYP3A isoenzymes. For this reason P-gp expression may be enhanced upon application of a substance that is not a substrate of P-gp but is a ligand of PXR. For example, cisplatin, which cannot be transported by P-gp, frequently enhances the expression of P-gp as a side effect in both normal and cancer cells. Cisplatin is a known PXR ligand, and this transcription factor is involved in the mechanisms of cellular protection against this substance[56].
2. The Constitutive Androstane Receptor (CAR) is also recognised as a xenobiotic-sensor which can up-regulate the functional expression of drug transporters, such as P-glycoprotein (P-gp)[58]. .
3. Vitamin D receptor (VDR) identified as a positive regulator of P-gp expression in rat brain capillaries[59].
4. Thyroid hormone receptor (TR). *Nishio et al.,* suggest that thyroid hormone induces P-gp expression in a tissue-selective manner[60,61].
5. Peroxisome Proliferator Activated Receptors (PPARs). PPARs are ligand-activated transcription factors that regulate genes involved in fat and glucose metabolism, and inflammation. Activation of PPAR signaling is also reported to regulate ABC gene expression[62].

P-gp is frequently overexpressed in post-chemotherapy tumours where it hinders the cytotoxic response to drugs thus desensitising the cancerous cells. It is most likely to be associated with clinical multidrug resistance in cancer, including multiple myeloma, certain types of leukemia, breast cancer and ovarian cancer[49]. Overexpression of P-gp is associated with decreased cellular uptake of a drug, which allows cells to survive in the presence of higher drug concentrations originating from the vasculature. This drug transport can happen against a concentration gradient. Drug enters the cells via a non-energy dependent mechanism and leaves via this active ATP pump[63].

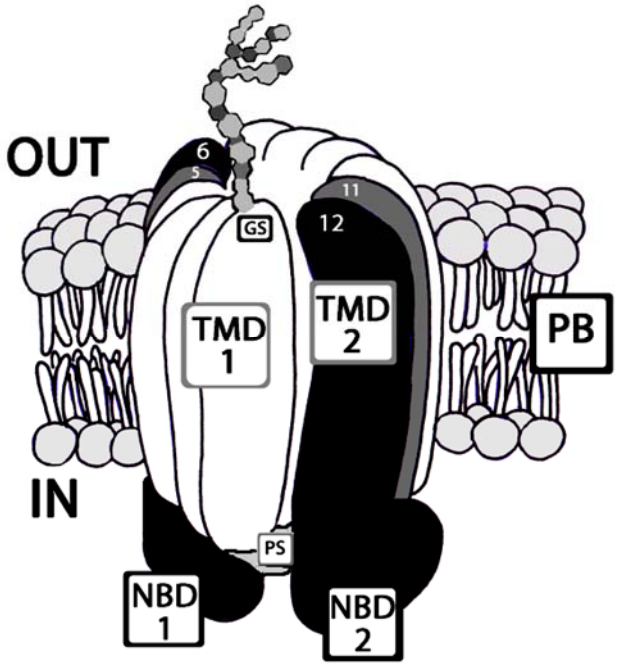

Figure 1-4: Assembly of P-gp in the plasma membrane. Both transmembrane domains (TMD1 and TMD2) of P-gp consist of six transmembrane α-helical spans (1-6 and 7-12) that form an active pore in the plasma membrane. Both nucleotide binding domains (NBD1 and NBD2) are oriented toward the cytoplasm. The glycosylation site (GS), which is located on the first external loop, is oriented toward the extracellular space and includes asparagines 91, 94 and 99. Phosphorylation sites (PS) for protein kinases A and C are oriented toward the cytoplasm and correspond to serines 669 and 681 of the linker region of murine P-gp, which is encoded by the mdr1b gene. Other symbols: PB, phospholipid bilayer; out, extracellular space; in, intracellular space. From Breier *et al.,* 2013[56]

1.1.4.2 BCRP

Breast Cancer Resistant Protein (BCRP), also called ABCG2, and MXR (mitoxantrone resistance protein) or ABCP (placental ABC protein), is also another member of the ATP-binding cassette (ANC) transporter superfamily. The ABCG2 gene was cloned independently from both drug-selected model cell lines and human cDNA libraries in 1998[64,65] and 1999[66]. BCRP mRNA encodes a 655-amino acid, 72kDa protein with a single nucleotide-binding domain (NBD) and six transmembrane domains (TMD). Because of its half size nature, ABCG2 has been thought to exist and work as a homo-dimer[67,68] (figure 1-5). However, emerging evidence suggests that ABCG2 may exist as a higher order of homo-oligomers on plasma membranes[69]. BCRP undergoes N-linked glycosylation at asparagine 596, and formation of an intramolecular disulfide bond between cysteines 592 and 608 which maintain its protein stability. Mature, oligomeric, fully glycosylated BCRP is degraded mainly via the lysosome, while underglycosylated, misfolded BCRP or BCRP without the intramolecular disulfide bond is targeted to the proteasome for degradation[70].

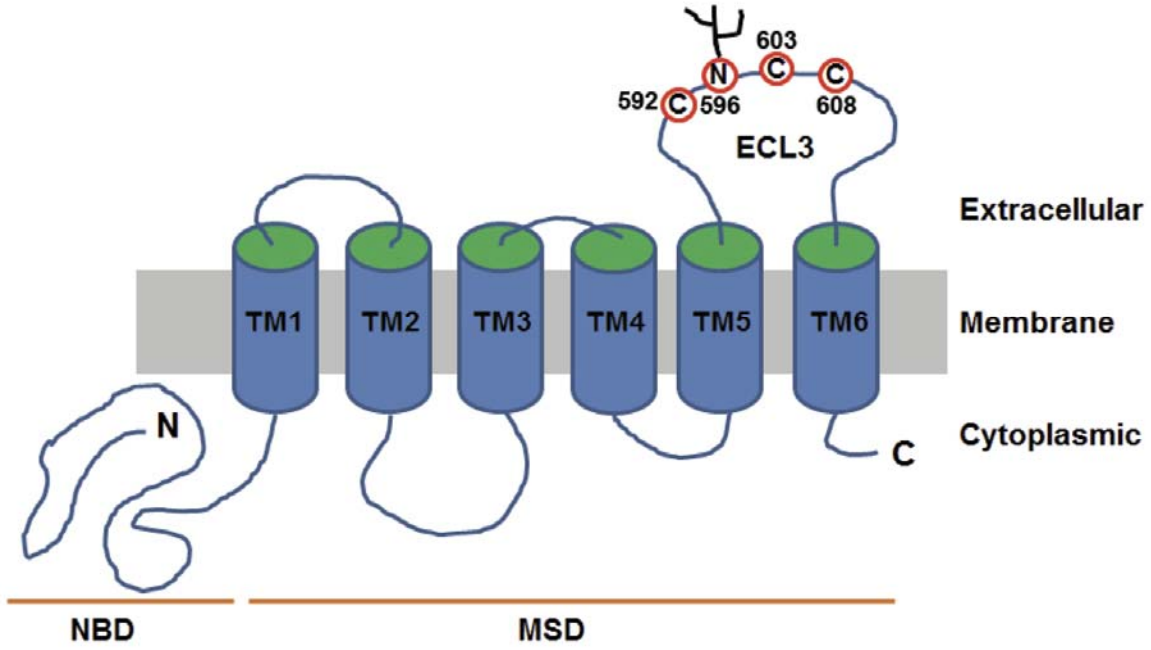

Figure 1-5: Membrane topology model of BCRP (ABCG2). The schematic topological model was constructed on the basis of sequence analysis and the available experimental data. Nucleotide-binding domain (NBD), membrane-spanning domain (MSD), transmembrane (TM) segments, and extracellular loop 3 (ECL3) are indicated. The cysteine residues and N-linked glycosylation sites in ECL3 are also shown. From *Mo & Zhang 2012*[71]

There may be multiple functions for the ABCG2 protein (BCRP), depending on the cellular context. For example, the expression of BCRP in several different tissues (including the placenta, colon, large and small intestine, sebaceous glands, islets and acinar cells of the pancreas) suggests a physiologically protective role. *Jonker et al.,* [72,73] have suggested that the protein may be responsible for either the transport of compounds in the foetal blood supply or the removal of toxic metabolites. In addition, ABCG2's different functional roles are potentially reflected in its transcriptional control (figure 1-6). ABCG2 expression has been shown to be up-regulated by the aryl hydrocarbon receptor[74], suppressed by DNA methylation[75] and, with specific respect to hepatobiliary cancer, up-regulated by Oct4[76].

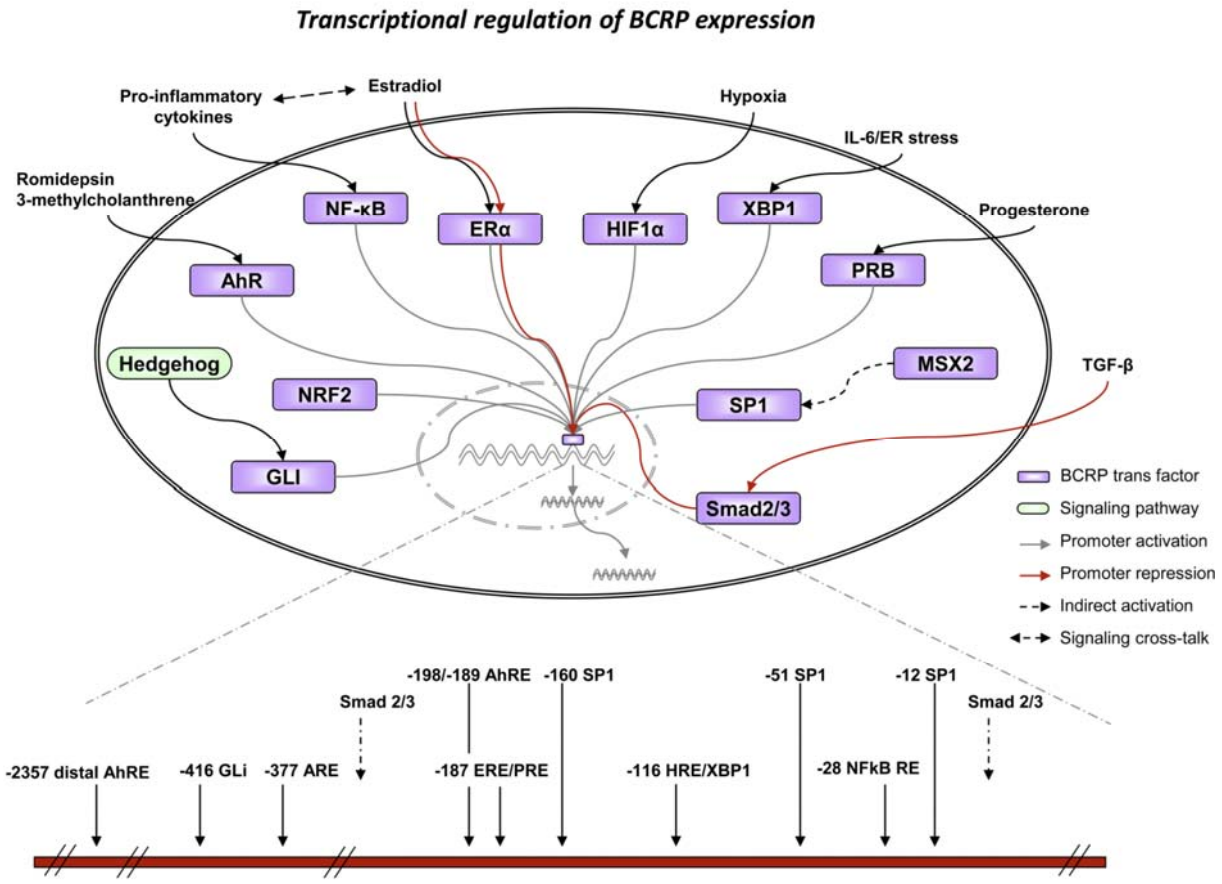

Figure 1-6: Schematic representation of transcriptional regulation of BCRP expression. Transcription factors that bind to *cis* elements upstream of the BCRP E1B/C promoter with subsequent activation or repression of the promoter are depicted diagrammatically. Signaling pathways and extracellular stimuli that stimulate binding of the transcription factors are also shown. The position of the various experimentally verified BCRP *cis* regulatory elements in relation to the transcription start site of the BCRP E1B/C first exon are also shown. (From *Natarajan et al.,* 2012[70]).

The upstream region contains functional oestrogen[77] and hypoxia[78] response elements, consistent with its expression in mammary glands and a role in haemopoietic stem cell protection. Various other potential transcriptional control points have been identified in the ABCG2 promoter, including putative Sp1, AP1 and AP2 binding sites[79].

BCRP has been detected in various *in vitro* cancer models, particularly following exposure to mitoxantrone. Mutant forms of BCRP in which amino acid arginine at codon 482 is substituted with threonine or glycine have been reported in various cancer cells when cells were selected with a BCRP substrate chemotherapeutic drug such as doxorubicin[80]. So far, expression of these mutants has not been reported in clinical specimens[81-83].

While the P-gp substrates vinblastine, paclitaxel and verapamil are not substrates of BCRP, BCRP does transport a variety of dyes (e.g. Hoechst 33462), chemotherapeutics such as flavopiridol topotecan, irinotecan and its active metabolite SN-38 as well as the tyrosine kinase inhibitors erlotinib, imatinib and gefitinib[69] (table 1-2). Both the R482G and R482T mutants and the wild-type ABCG2 are able to efflux mitoxantrone, topotecan, SN38 and Hoechst 33342 [84]. However, the R482G and R482T mutants have higher affinity with anthracyclines, including doxorubicin, daunorubicin, epirubicin. Only the wild type ABCG2 can effectively transport methotrexate (MTX)[85]. These data suggest that amino acid 482 may be a 'hot spot' for mutation and this mutation affects the substrate specificity of ABCG2[86].

1.1.4.3 MRP family

Multidrug resistance-associated proteins (MRPs) are ATP-binding cassette, transmembrane transporter proteins. MRP1 is the most characterised member of the group. The MRP1 gene encodes a 190kDa transmembrane protein whose structure is somewhat homologous to P-gp/MDRl. Although P-gp and MRP-1 share only 15% sequence homology, both function in an energy-dependent drug efflux system which reduces the intracellular accumulation of drug. It is located in the plasma membrane and endoplasmic reticulum of drug-resistant cells. While there is significant overlap with the substrate specificity of P-gp, MRP1 transports a broader range of xenobiotics used as antineoplastic or therapeutic agents, including folate-based antimetabolites, anthracyclines, vinca alkaloids, antiandrogens, and numerous glutathione (GSH) and glucuronide-conjugates of these compounds as well as organic anions and heavy metals. MRP1 also transports diverse physiological substrates such as folates, GSH and GSH disulfide (GSSG) as well as sulphate-, GSH- and glucuronide- conjugates of steroids, leukotrienes and

prostaglandins[87]. MRPs are often over-expressed in NSCLC[88]. MRP1 expression has also been shown to be predictive of poor response to chemotherapy in SCLC[89,90]. Other members of the ABC family of transporters include MRP2, MRP3, MRP4, MRP5 and BCRP. These family members are also involved in drug efflux, however, they are not as extensively studied as P-gp and MRP1.

1.1.4.4 Reversal of MDR

A large number of studies have focussed on blocking the function of multidrug resistance pumps, in an attempt to reverse MDR. Some non-toxic compounds can inhibit drug transport by acting as competitive or non-competitive inhibitors or by preventing ATP binding. Non-steroidal anti-inflammatory drugs (NSAIDS) such as sulindac and indomethacin have been shown to increase the cytotoxic effects of commonly used chemotherapy drugs in cells which have become resistant[91]. Early studies in this area observed that P-gp inhibitors such as verapamil and cyclosporin A were efficient *in vitro* but were poor inhibitors *in vivo*[92,93] (table 1-2b). This led to the development of second-generation P-gp inhibitors such as alspodar (PSC 833), dexverapamil, and dofequidar fumarate. However, these second generation inhibitors inhibit drug metabolism enzymes and ABC transporters, which results in impaired drug metabolism and elimination[94-96]. The third generation of P-gp inhibitors, which are currently undergoing clinical trials, include zosuquidar (LY335979), elacridar (GF120918)[97,98], CBT-1, and XR9576[99-102]. Several of these later-generation inhibitors act on multiple ABC transporters. Biricodar (VX-710) and GF-120918 for example, bind P-gp as well as MRP1 and ABCG2[103]. These generations of inhibitors have been examined in preclinical and clinical studies; however to date these trials have largely failed to demonstrate an improvement in therapeutic efficacy[104].

1.1.4.5 Mitoxantrone

Mitoxantrone, a Pgp substrate, is a synthetic anthracenedione which was developed based on the anthracycline structure, in an attempt to find anthracycline analogues with decreased cardiotoxicity while being able to maintain the same antitumour efficacy[105]. However, various reports showed that mitoxantrone causes chronic cardiotoxicity[106-108]. Unlike the anthracyclines, mitoxantrone is not active against a wide spectrum of tumours. Instead, it is used specifically for

the treatment of advanced breast cancer, non-Hodgkins lymphoma, non-lymphocytic leukemia and melanoma[109].

The structure of mitoxantrone is shown in figure 1-7. It has a planar heterocyclic ring, substituted with two positively charged nitrogen containing side chains. The anticancer mechanisms of mitoxantrone are believed to be related to its capacity to bind DNA and inhibit DNA topoisomerase II in the nuclear compartment of cells[110,111]. In addition, the action of its metabolites in the intracellular cytosolic compartment may also contribute to its antineoplastic activities[112].

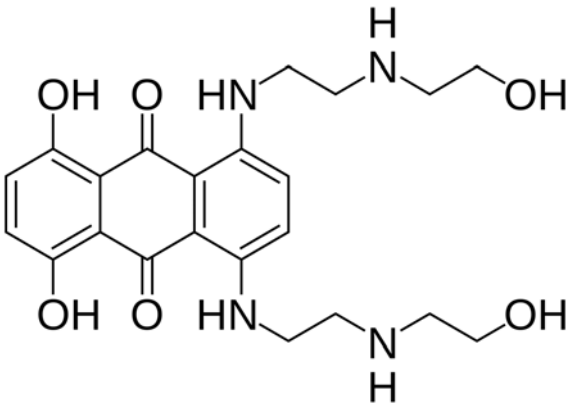

Figure 1-7: Chemical formula of mitoxantrone

1.1.4.6 Drug resistance in lung cancer

Most lung cancers already exhibit an intrinsic resistance to chemotherapy by the time of diagnosis. Most SCLCs are chemotherapy sensitive at diagnosis, but any recurrence of the disease usually displays acquired drug resistance. NSCLC, on the other hand, are predominantly intrinsically resistant to chemotherapy. It is likely that both acquired and intrinsic resistance share common factors, such as the expression of drug transporters, modulation of internal regulatory pathways, upregulation of defense pathways and the promotion of an antiapoptotic environment.

Drug transporters involved in the efflux of chemotherapeutic drugs

Studies have shown a large expression of P-gp in lung tumours, notably higher in NSCLCs than in SCLCs. Other studies have shown that lung tumour cell lines that were resistant to vincristine demonstrated cross-resistance to doxorubicin[113]. Molecular analysis revealed that these drug-

resistant cell lines had a higher expression of both P-gp and the MDR1 gene than did the parental cell lines. In addition, *in vitro* studies have also demonstrated higher expression of P-gp in NSCLC cell lines derived from smokers[114].

A further role for MDR1 in drug resistance was demonstrated by gene array studies where the expression of various genes were analysed in paclitaxel sensitive (NCI-H460) and resistant (NCI-H40/PTX250) human large-cell lung carcinoma cell lines. The results indicated a 1,092 fold increase in the expression of MDR1 observed in the paclitaxel resistant cell line [115].

Although P-gp has been shown to play a major role in drug resistance, other non-P-gp mediated mechanisms attributed to proteins such as MRP1 have also been implicated in NSCLC drug resistance. To date, seven isoforms of MRP have been identified (MRP1-MRP7). The major isoforms that have been shown to play a role in drug resistance are MRP1, MRP2, MRP3 and MRP5. Comparative studies performed with a panel of 30 lung cancer cell lines showed that NSCLC cell lines expressed higher levels of MRP3, MRP1 and MRP2 protein than in SCLC cell lines[88].

Other ABC transporters may also be involved in the pathogenesis of cancer, including ABCC10/MRP7[116]. A higher expression of ABCC10/MRP7 was demonstrated in 12 out of 17 lung cancer vinolrelbine resistant cell lines thereby demonstrating the involvement of other ABC transporter proteins other than MDR-1 in drug resistance[116]. *Zhao et al.,* recently suggested that ABCC3 expression may serve as a marker for MDR and multidrug resistance in NSCLC[117]. Another study reported the involvement of a non-ABC transporter protein, RLIP, in contributing to vinolrelbine resistance[118]. RLIP76 is a transporter involved in catalysing energy-dependent efflux of various chemotherapeutic drugs, such as doxorubicin[119]. Thus resistance to a chemotherapeutic drug may not only be due to one particular ABC transporter protein but may also be due to a defect in multiple transporter proteins.

Other pathways and mechanisms involved in drug resistance in lung cancer

Although drug efflux is a major mechanism associated with drug resistance, another mechanism by which cancer cells avoid drug cytotoxicity is by conjugation of the drug with sulphur-containing macromolecules such as metallothioneins (MTs) and glutathione (GSH). Furthermore, antioxidants such as, superoxide dismutase (SOD) have also been shown to be implicated in drug resistance[114]. The MTs are low molecular-weight intracellular proteins with a high cysteine content that can bind to several heavy metal ions. MTs can also bind to drugs such

as cisplatin, thereby leading to decreased sensitivity in lung cancer and other cancer types[120-122]. There was also a correlation found between MT expression and doxorubicin in NSCLC[123]. However, there are conflicting studies concerning MT expression and drug resistance in lung cancer[120,124]. MT expression was also found to be higher in tumours with high metastatic and proliferative potential[125].

The glutathione-S-transferases (GSTs) are another group of enzymes that are often up-regulated in drug-resistant cell lines. The GSTs are a family of phase II detoxification enzymes which ordinarily protect the normal cells from reactive endogenous and exogenous electrophiles, such as prostaglandins, aromatic hydrocarbons, and chemotherapy agents, by conjugating those compounds to the sulphur containing macromolecule glutathione-S-hydroxylase (GSH), thus detoxifying them[114]. The same may be described for cancer cells, so conferring on them resistance to chemical stress imposed by antineoplastic agents. The GSTs have two distinct roles in drug resistance – drug detoxification and MAPK pathway inhibition. Many chemotherapeutic drugs that form electrophilic moieties are detoxified through the GSH mechanism, thereby leading to resistance. Numerous drugs used in lung cancer treatment, such as cisplatin, kill tumour cells by inducing apoptosis arising from the activation of the JNK/MAPK pathway. Inhibition of this pathway by GSTs leads to decreased cisplatin-induced apoptosis, thereby also conferring resistance to the drug[114].

Another mechanism by which cancer cells develop resistance is by overexpression of antioxidants that protect cells from chemotherapy-induced oxidative stress and cell death. Numerous chemotherapeutic drugs such as epirubicin cause oxidative damage by generation of superoxide and hydrogen peroxide moieties, thereby leading to cancer cell death. However, overexpression of antioxidant systems such as SOD and GSH can neutralise the drug-induced oxidative stress, thereby leading to drug resistance[114].

Drug resistance and DNA repair

The primary target for most lung cancer chemotherapeutic agents is cancer cell DNA. For instance, cisplatin induces apoptosis primarily by forming DNA–platinum adducts and by introducing oxidising agents, thus causing oxidative damage to the DNA of cancer cells[126]. Dealing with resistance to DNA repair enzymes is a challenge as there are many different DNA repair pathways and enzymes and each tumour has its own unique genetic profile of overexpressed repair enzymes.

1. The nucleotide excision-repair (NER) pathway which is involved in platinum-based drug resistance[127]. The ERCC1 removes the DNA adducts so that DNA polymerase can repair and/or synthesise new DNA, and the tumour cell can divide normally again[114,128].

2. Mismatch-repair pathway (MMR) which repairs base–base and insertion–deletion mismatches generated during DNA replication or recombination of DNA. MMR is usually a cancer-preventing pathway that helps to maintain genomic stability, but it can also lead to resistance against certain chemotherapeutic agents such as 5-Fluorouracil[129]. The MMR pathway does not appear to play a major role in chemotherapy resistance in lung cancer[114].

3. Base excision–repair (BER) pathway which uses DNA glycosylase to recognise and catalyse the removal of damaged DNA bases and the gaps are then repaired which prevents the apoptotic affects of chemotherapy-induced DNA damage[130].

4. Non-homologous endjoining (NHEJ) pathway, is the major pathway used for repairing double-strand breaks (DSBs) in human DNA. It leads to resistance of cancer cells to multiple chemotherapy drugs and ionizing radiation by repairing DNA damage and stopping apoptosis. It involves the Ku protein which is a heterodimer composed of two polypeptides, Ku70 (XRCC6) and Ku80 (XRCC5). The Ku protein acts as a molecular scaffold which helps in binding of other proteins involved in DNA repair[114]. The drug doxorubicin also induces more apoptosis in cancer cells when those cells are deficient in DNA ligase IV or DNAPKcs; two of the integral proteins in the NHEJ pathway[131].

5. Homologous-recombination (HR) pathway which can repair the same kind of DNA-platinum adducts that occur in the NER pathway. This pathway begins with the recruitment of proteins to form the M/R/N complex (consisting of Mre11, Rad50, and NBS1) together with recruitment of replication protein A (RPA), which is a single-stranded DNA-binding factor. These bind the broken ends of the DNA strands together and begin the process of homologous DNA pairing for which the HR mechanism is named. This enables cancer cells to have two separate pathways for resisting the damage caused by alkylating agents[114].

Drug resistance and apoptosis

Failure to activate the process of programmed cell death or apoptosis represents an important mode of drug resistance and survival in cancer cells. Even though drugs such as cisplatin and carboplatin induce tumour cell death by damaging DNA, the final result is usually the activation of the apoptotic pathways. The loss of apoptotic control will eventually lead to tumour cell survival and progression of the cancer by enabling the cells to be more resistant to

chemotherapy[114]. Drugs such as cisplatin, taxol, etoposide and gemcitabine induce tumour cell death by activation of the intrinsic and extrinsic apoptotic pathways. A defect in either of these pathways can also lead to drug resistance. For example, drugs such as paclitaxel which can induce cell death by regulating cellular microtubule dynamics, kill cells in a Fas/Fas ligand (FasL)-dependent manner[132]. Furthermore, overexpression of Bcl-2 causes resistance to chemotherapeutic drugs in SCLC[128]. In addition, drugs such as cytarabine, doxorubicin, and methotrexate, which activate the apoptotic pathways, reportedly can confer resistance to cancer cells if their caspases are defective[114]. Thus, many factors appear to be involved in order to establish the drug resistance phenotype (figure 1-8).

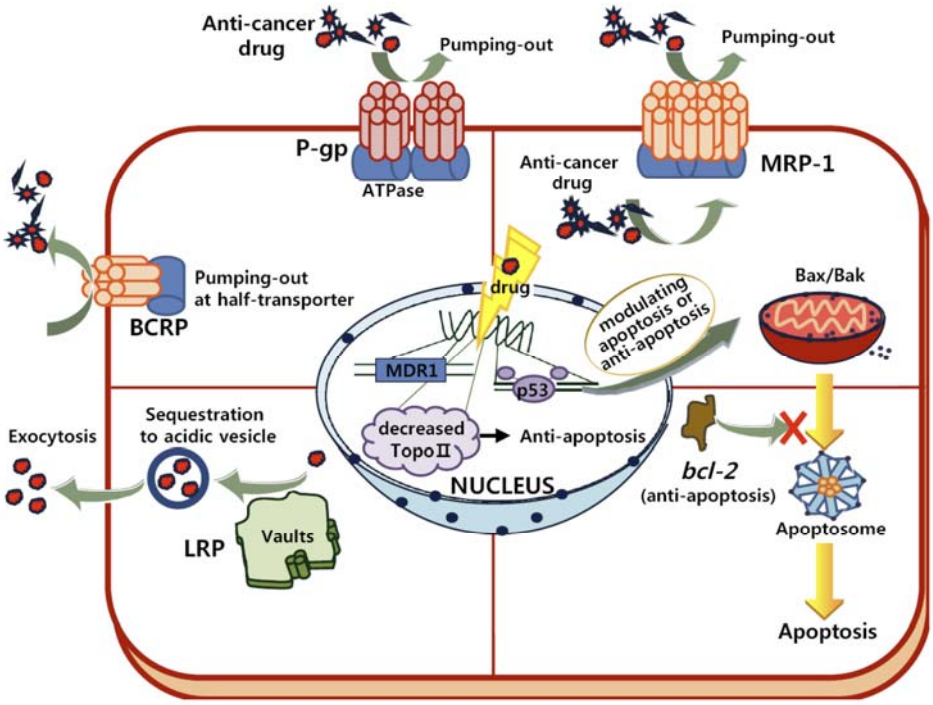

Figure 1-8: Drug-resistance mechanisms in tumour cells. Broad-based drug resistance, either intrinsic or acquired, exists in tumours and is believed to result from a multitude of factors. Various tissue culture studies have consistently shown that MDR in most cultured cancer cells involves ATP-binding cassette (ABC) transporters in the human such as P-glycoprotein (P-gp, ABCB1), multidrug resistance protein (MRP, MRP-1/ABCC1) breast cancer resistant protein (BCRP, ABCG2), lung resistant protein (LRP), bcl-2, p53, and Topoisomerase II (TopoII). Taken from *Oh et al.,* 2009[133].

Drug-resistance in the Microenvironment of tumours

Oh et al., (2009)[133] suggest drug resistance due to the microenvironment of tumours is one of the most important obstacles to tumour treatment (figure 1-9). In clinical tumours, a poorly

organised vasculature where cells are located far from blood vessels gives rise to a hypoxic region resistant to chemotherapy because drug penetration into this region is very limited. Since tumour cells in this hypoxic region are non-proliferating or slowly proliferating with increasing distance from tumour blood vessels, most anticancer drugs are less active. Such regions may encourage the elevation of anti-apoptosis proteins to prevent cell death and up-regulate growth factors for cell survival. Indeed, several growth factors such as epidermal growth factor (EGF), fibroblast growth factor (FGF), insulin-like growth factor (IGF), and hepatocyte factor (HGF), all have important functions in regards to MDR, cell proliferation, metastasis, and angiogenesis.

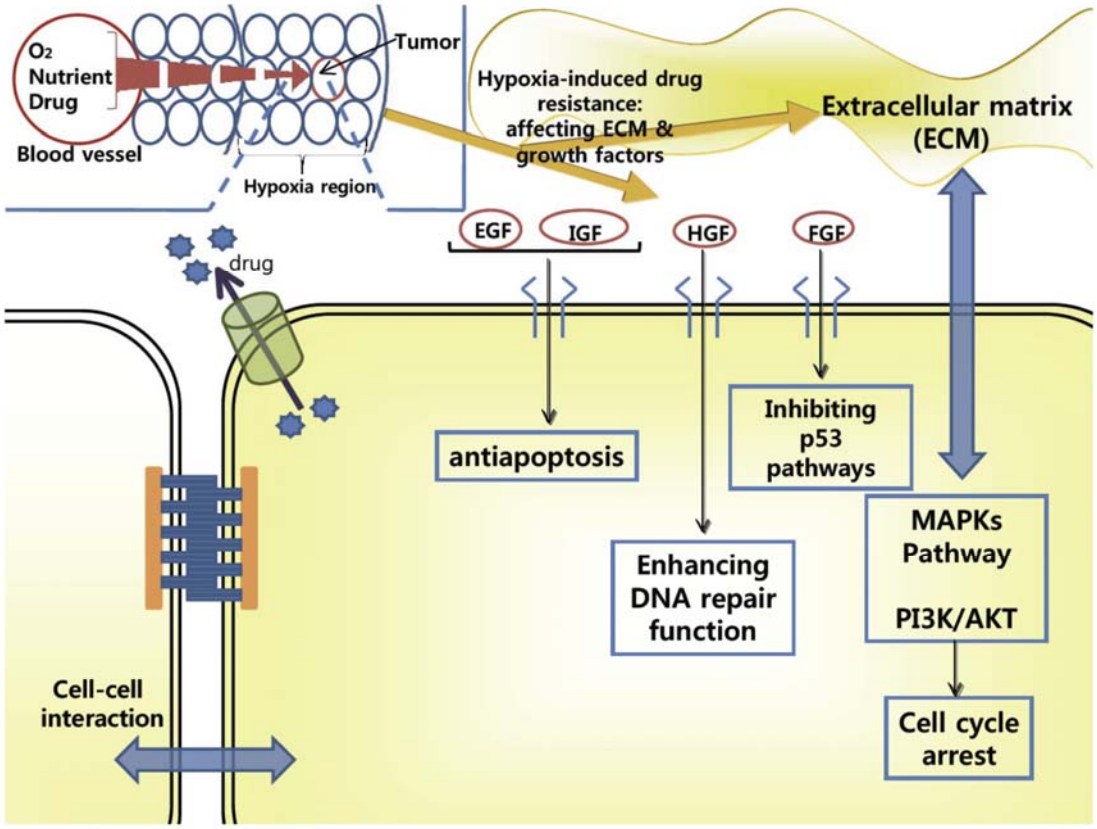

Figure 1-9: Drug-resistance mechanisms (such as soluble growth factors, ECM-based drug resistance, cell-cell interaction, and hypoxia-induced drug resistance) in the tumour microenvironment. Taken from *Oh et al.,* 2009[133].

As shown in figure 1-9, binding of EGF, FGF, and IGF to their receptors leads to up-regulation of anti-apoptotic proteins (bcl-2 family members such as bcl-2, bcl-XL, and LAPs), resulting in inhibition of apoptosis. In addition, binding of FGF to its receptor mediates obstruction of p53 pathways while HGF binding to its receptor enhances DNA repair functions. Altered expression

of extracellular matrix (ECM) components (such as fibronectin, collagen, tenacin, laminin, and hyalurona) contributes to protecting tumour cells from anticancer drugs, by activation of MAPKs and PI3K/AKT survival signaling, decreasing TopoII level, and arresting cell proliferation due to the increased cyclin-dependent kinase (CDK) inhibitor p27/Kip1 protein. In addition, cadherins, selectins, and cell adhesion molecules (CAMs) can make cell-cell contact and exhibit further drug-resistance.

1.1.5 Invasion and metastasis

1.1.5.1 Key molecular mechanisms in cancer invasion and metastases

Around 90% of all cancer deaths are the result of metastases, rather than through the effects of the primary tumour[134]. The majority of patients with lung cancer are diagnosed at late stages, when they are already beyond the possibility of treatment by surgery or radiotherapy – due to the extent of local invasion or distal metastases.

Nevertheless, the processes of invasion and metastasis are still insufficiently understood. In fact, there are currently no effective treatments available that target invading tumour cells. For example, the question is still unanswered, why some cancers, such as melanomas, tend to metastasize, whereas others, such as squamous carcinomas of the skin, scarcely form secondary tumours. *Bissell et al., [135]* suggest that the micro-environment surrounding the tumour may provide tumour-suppressive signals as long as the architecture or the tissue homeostasis is essentially controlled and maintained. However, once tissue homeostasis is lost, the altered microenvironment can itself become a potent tumour promoter.

A tumour which has not yet reached an invasive phenotype is often referred to as 'carcinoma *in situ*'. Invasiveness does not only mean the ability to thrust aside adjacent tissues, but also to actively invade and, therefore destroy these tissues at the contact borders. Metastasis refers to the capability to leave a primary tumour site, travel via the circulation to a distant tissue site, and there, form a secondary tumour[136].

Most deaths from cancer are due to metastasis that are resistant to conventional therapies. Current therapies fail to eradicate metastasis for three major reasons. Firstly, when initially diagnosed, most tumours are well advanced and metastasis has already occurred. Secondly, the specific organ environment can modify the response of a metastatic tumour cell to systemic therapy and alter the efficiency of anticancer agents. The third reason, and the greatest obstacle

to the success of therapy, is the heterogeneous composition of tumours, where highly metastatic cells can escape from the effect of therapeutic agents.

Micro-metastases can remain in the body of a cancer patient after successful chemotherapy or radiotherapy. It is possible that these remaining tumour cells start to proliferate uncontrollably years after the patient is thought to be cured of the primary disease, leading to the redevelopment of a new cancer.

Fortunately, metastasis is thought to be an inefficient process, a phenomenon which is often referred to as 'metastatic inefficiency'[137] and animal modeling suggests that less than 0.02% of tumour cells in circulation can survive to form metastases[138]. Up to one million cells per day can leave a primary mouse tumour of only 1g mass (~10^9 cells), and enter the invasion metastasis cascade. In direct contrast, the amount of micro-metastases which evolve into clinically relevant secondary tumours is negligible[136]. This is because tumour cells often encounter significant obstacles as they attempt to reactivate their growth machinery at metastatic sites. In 1889, *Paget*[139] concluded that metastasis occurred only when certain favoured tumour cells (the "seed") had a special affinity for certain specific organs (the "soil").

The formation of metastases requires the interaction of the right cells with the compatible organ environment. More recently, a number of genes whose expression facilitates the metastatic colonisation of breast cancer cells, specifically to either bone, lung, brain or liver, have been identified. These genes seem to dictate organ-specific metastatic tropism due to their ability to compensate for and overcome incompatibilities between the intrinsic growth programs of the disseminated carcinoma cells and the demands imposed by the particular foreign tissue micro-environment around them[140].

The cascade of events in lung cancer metastasis all require the participation of fundamental mechanisms such as cellular motility (which is an early event in metastasis) angiogenesis, degradation of matrix barriers, disruption of cell-cell and cell-matrix adhesion (figure 1-10) [141]. Genes that regulate functions like unlimited growth potential, survival, genomic instability, angiogenesis, epithelial to mesenchymal transition (EMT) and apoptosis evasion, are involved in giving lung cancer tumours invasive and metastatic competence[141].

1.1.5.2 The epithelial-mesenchymal transition

To begin, lung tumour cells undergo a transformation known as the epithelial-mesenchymal transition, or EMT[142]. EMT is regulated by growth factors and cytokines including transforming growth factor (TGF)-beta and can be deregulated in cancer cells during tumour progression resulting in invasiveness with metastatic characteristics.

Carcinomas can invade as cohesive multi-cellular units through a process termed "collective invasion" but individual tumour cells may also invade via two distinct programs: the protease-, stress-fiber-, and integrin-dependent "mesenchymal invasion" program or the protease-, stress-

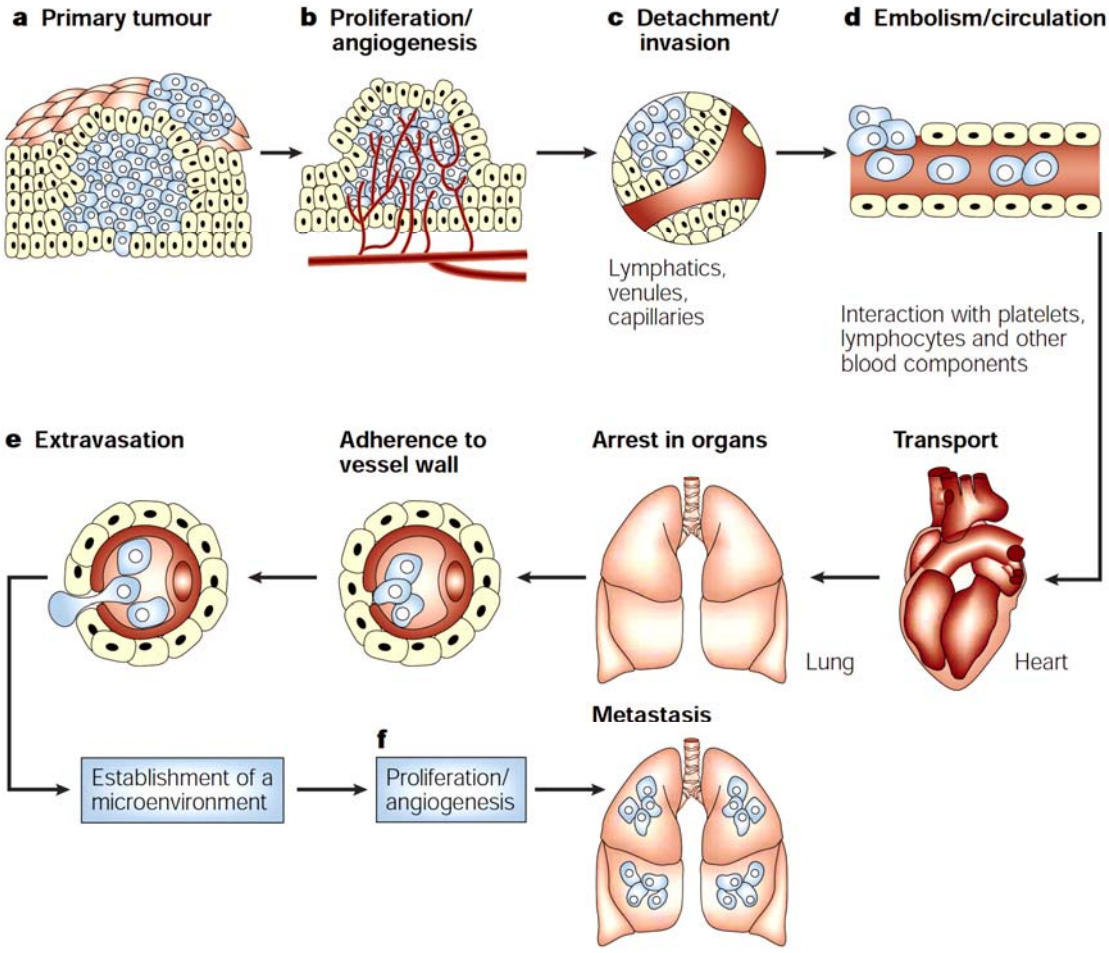

Figure 1-10: The cascade of events in lung cancer metastasis include: (1) Detachment of tumour cells from the extracellular matrix (ECM) and degradation of the ECM by several proteolytic enzymes. (2) Invasion of neighboring tissues and basement membrane. (3) Intravasation into the blood stream or lymphatic vessels, by attachment on the endothelial cells with adhesion molecules, infiltration of the vessels, survival and transport through the blood stream. (4) Arrest and extravasation at a distal site and formation of a metastatic lesion. (From Fidler, 2003[143])

fiber-, and integrin-independent, Rho/ROCK-dependent "amoeboid invasion" program[140]. It is believed that tumour cells interconvert between these various invasion strategies in response to changing microenvironmental conditions[140]. To achieve this, carcinoma cells may use a cell-biological program known as EMT, which is a differentiation program essential for morphogenesis during embryo development.

EMT features include loss of cell polarity, reorganisation of the cytoskeletal architecture, redistribution of the intracellular organelles, upregulation of fibroblast markers and increased motility[144]. Cells that undergo EMT assume a spindled shape, lose desmosomes and adherence junctions, and secrete increased amounts of enzymes to degrade the ECM[144,145].

EMT is driven by a network of transcription factors including Snail1, Snail2, and Snail3, ZEB1 and ZEB2 (zinc-finger E-box binding factor), Twist, and others. The general features of EMT include the downregulation of epithelial markers in adherence junctions, tight junctions and cytoketarin filament network (for example, E-cadherin, occludins, claudins, desmoplakin, type IV collagen, laminin 1, cytokeratins, catenins, ZO-1 and mucin1) and upregulation of mesenchymal markers, such as N-cadherin, vimentin, α5β1 and αVβ6 integrins, tenascin C, laminin β1 and 5, type I and VIα collagen, fibronectin, fibroblast specific protein 1 and α-smooth muscle actin[141].

Loss of expression of the cell cell adhesion molecule E-cadherin is a key characteristic trait of EMT and in the progression of epithelial tumours to become invasive, metastatic cancers. The loss of E-cadherin is generally seen to coincide with a gain of expression of the mesenchymal cadherin, N-cadherin in many cancer types; this 'cadherin switch' is thought to be necessary for tumour cells to gain invasive properties and is also a characteristic of EMT. N-cadherin has an affinity to stroma cells and upregulation of N-cadherin enhances migration towards the stroma[136]. Interestingly, the expression of N-cadherin promotes tumour cell metastasis irrespective of E-cadherin status of a given cell[146]. Interestingly *Marsen et al*., 2014[147] suggest that the acquisition of a mesenchymal morphology is the end-point of EMT but the routes towards that end-point might differ between conditions and cells. They identified a set of core invasiveness genes, the expression of which was associated with epithelial-mesenchymal transition in breast cancer cell lines and in human tissue samples but were unable to demonstrate a link between the core invasiveness gene signature and enhanced metastatic potential[147].

The transcription factors Slug, Snail, Goose-coid, Twist, and ZEB1, which are highly expressed by metastatic cells, have been suggested to have a role in inducing epithelial-mesenchymal

transitions[148]. However, the central EMT regulator is TGFβ. In non-small cell lung cancer, TGFβ inhibits tumour growth in early stages, whereas in late stages the same pathways promote tumour invasiveness and metastasis. TGFβ also activates Erk and p38 MAPKs, PI3K and Ras and Rho GTPases. All these signalling pathways end up promoting EMT by regulating genes that control cell proliferation, apoptosis, differentiation, motility and migration[149].

MicroRNAs (miRNAs) are also involved in regulating EMT and tumour metastasis. miRNAs are a class of small non-coding RNAs that negatively regulate gene expression at the post transcriptional level by blocking translation and inducing mRNA degradation[150]. The miR-200 family has been identified as potent negative regulator of EMT in lung adenocarcinoma, by controlling ZEB1 and ZEB2 and thus leading to increased E-cadherin expression[151]. MiR-126 has been shown in squamous cell lung cancer to downregulate Crk protein, reducing invasive potential[151]. Other regulatory circuits including the epigenetic machinery and post-translational control are also crucial in enabling cancer cells to maintain a defined cellular state or switch between the epithelial and mesenchymal states in response to stromal cues[152,153].

1.1.5.3 Invasion/Metastasis

The process of EMT is followed by invasion which initiates the metastatic process. Invasiveness involves entry of cancer cells that have resided within a well-confined primary tumour, across tissue boundaries and through host cellular and extracellular matrix barriers. The 'stroma' consists of fibroblasts, vasculature, immune cells and interstitial ECM. In order to invade the stroma, carcinoma cells must first breach the ECM, which plays a vital role in organising epithelial tissues, in part by separating their epithelial and stromal compartments. Components of this ECM contain proteinases, growth factors molecules and cytokines, which can be activated and released by the invading cells. Moreover, the ECM also plays crucial roles in signalling events within carcinoma cells via pathways initiated by integrin-mediated cell-matrix adhesions, leading to alterations in cell polarity, proliferation, invasiveness, and survival[135]. The controlled tissue architecture of normal epithelium serves as an intrinsic barrier to invasiveness that must be overcome by incipient metastatic carcinoma cells before they can develop into overt malignancies[140].

1.1.5.4 Cell adhesion molecules

Numerous adhesion molecules mediate the tumour cell-ECM adhesion process. The cell adhesion molecules (CAMs) can be divided into four major families: the immunoglobulin superfamily, the integrins, selectins and the cadherins[154]. Cadherins, whose main function is cell–cell adhesion, are well studied for their role in cell signaling during critical processes such as epithelial-to-mesenchymal transition (EMT), cell migration and gene regulation through catenins, especially the β-catenin/Wnt signling pathway[155].

Selectins and immunoglobulin superfamily (IgSF) members are mainly involved in the wound healing (recruiting platelets and leukocytes) process and the immune response (communication between immune cells and other constituents of the inflammatory process as well as among components of the immune system). Among other roles, they are 'traffic regulators' in the lymphatic system and attract immunocompetent cells to the site of inflammation[154].

Integrins are transmembrane receptors that mediate the attachment between a cell and its surroundings, such as other cells or the ECM itself. During signal transduction, integrins pass information about the chemical composition and mechanical status of the ECM into the cell. So, in addition to transmitting mechanical forces across otherwise physically vulnerable membranes, integrins are involved in cell signaling and the regulation of cell cycle, shape, and motility. Many studies suggest that various integrin subunits can contribute either positively or negatively to the transformed cell phenotype. Although cell-type-dependent changes in integrin signalling make it impossible to rigidly assign each of the integrins to the 'anti-neoplastic' or the 'pro-neoplastic' category, present evidence indicates that α2β1 and α3β1, at least in some cases, suppress tumour progression, whereas αvβ3, αvβ6 and α6β4 often promote it[156].

This family of proteins can form at least 25 distinct pairings of its 18 α and 8 β subunits, with each integrin consisting of a noncovalently linked α- and β-subunit, with each subunit having a large extracellular domain, a single membrane-spanning domain and a short, non-catalytic cytoplasmic tail[157]. Integrins also induce the expression of different ECM degrading proteases, especially members of the MMP family which can cleave ECM components to remodel the overall ECM structure, thereby promoting cell migration. The interplay between integrins and the matrix metalloproteinases may be one of the key phenomena in the invasion process.

1.1.5.5 MMPs

MMPs are a family of structural and functional related endopeptidases. They are, with the exception of MMP-11, secreted as inactive zymogens and activated outside the cell by other activated MMPs or serine proteases (e.g trypsin, plasmin, kallikrein). Proteolytic removal of the propeptide-domain is required for their activation. This enables access to the catalytic site of the MMPs. The cleavage of the ECM by activated MMPs facilitates the invasion of tumour cells as well as the release of ECM bound growth factors (e.g. insulin like growth factors and fibroblast growth factors). MMPs degrade fibronectin, collagen, laminin and proteoglycans. They also affect tumour neoangiogenesis and also break cell–cell and cell-ECM connections by cleaving adhesion molecules such as E-cadherin and CD44[158,159].

MMPs can thus change the structural and mechanical properties of the ECM[160]. MMP-1, MMP-2 and MMP-9 have all been correlated with increased risk of metastasis in human lung cancer[161,162]. However, MMP activity is held in check by the the TIMPs (tissue inhibitors of metalloproteinases) which prevent excessive ECM degradation and the resulting tissue instability that would ensue. Current thinking stresses the importance of the balance between TIMPs and MMPs, considering this to be of vital importance for invasion and metastasis[163]. At present, greater than 20 distinct MMPs are known: collagenases (MMP-1/8/13/18), gelatinases (MMP-2/9), stromalysines (MMP-3/10/11), matrilysines (MMP-7/26), membrane-bound MMPs (MMP-14/15/16/ 17/24/25) and other MMPs, which do not fit into the listed groups[164].

1.1.5.6 Evasion of apoptosis

In order for a cancer cell to migrate, it needs not only motility, but also the ability to evade apoptosis. Apoptosis is regarded as the central mediator of programmed cell death and is often defective or simply ineffective in cancer cells. Apoptosis is stimulated by a broad range of conditions and signals. The main mechanisms of cancer resistance to apoptosis are the loss of p53 activity and the overexpression of the Bcl2/BclxL[165,166] that play important roles in inhibiting mitochondria-dependent extrinsic and intrinsic cell death pathways. The anti-apoptotic proteins (Bcl-2, Bcl-xL) function to preserve mitochondrial integrity and prevent the loss of mitochondrial membrane potential and cell death by interfering with the action of Bax and Bak. Mitochondrial p53 can complex with Bcl-2 and Bcl-xL resulting in cytochrome c release and apoptosis. However, p53 mutants found in tumours are often defective in their binding to Bcl-xL implying that inhibition of p53-mediated apoptosis may contribute to the continued survival of

tumour cells. The pro-proliferative function of mortalin (mot-2, a member of the Hsp 70 – heat-shock protein 70 family, predominantly present in mitochondria) has been demonstrated by several studies including its overexpression resulting in lifespan extension of normal human fibroblasts and the malignant transformation of mouse and human immortal cells[167,168]. The pro-proliferative effects of mortalin in cancer cells have been assigned, at least in part, to its binding with the tumour suppressor protein, p53 that results in its retention in the cytoplasm and inhibition of its transcriptional activation and control of centrosome duplication function[169,170]. Overexpression of mortalin overrides the p53-dependent suppression of centrosome duplication and abnormal amplification of centrosomes, commonly found in human cancer, is the major cause of mitotic defects and chromosome instability in cancer cells.

Specific types of apoptosis in normal cells are also induced by integrin detachment resulting in the loss of cell adhesion to neighbouring cells or the ECM (anoikis) or loss of the internal cell cytoskeletal architecture (amorphosis). Anchorage independent growth is a critical step in the tumourigenic transformation of cells. Breaching the anoikis barrier disrupts the normal cell's defenses against transformation[141]. Evasion of anoikis is mainly regulated by integrins[171]. Integrins protect the cell from anoikis, and so also do several kinases activated by integrins, like SRC, FAK and ILK[172,173]. Altered integrin receptors or elevated levels of integrin-activated kinases are found in tumour cells, facilitating survival and metastasis[174]. Apoptosis evasion is also associated with EMT, since downregulation of E-cadherin[175] and activation of Snail and Twist lead to anoikis suppression[141].

1.1.5.7 Intravasation, circulation and extravasation

The circulation of the blood plays a significant role in determining where cancer cells travel. This is facilitated by the creation of new blood and lymph vessels that not only provide the primary tumour with all it needs in order to grow, but also reduce to a minimum the distance that metastasising cells need to move in order to enter the vasculature[176]. Therefore, angiogenesis is a fundamental step in the transition of tumours from a benign state to a malignant one. Normal angiogenesis is regulated by the balance of a vast range of activators and inhibitors[177]. The most important regulators include cytokines, acidic and basic fibroblast growth factor (aFGF and bFGF), vascular endothelial cell growth factor (VEGF), the CXC chemokines, the angiopoietin/ TIE ligand–receptor system, peptides including angiostatin, endostatin, tumstatin and thrombospondin 1, platelet-derived growth factor (PDGF), epidermal growth factor (EFG) and

hypoxia-inducible factors (HIF1A, HIF2A)[178]. In lung cancer, angiogenesis has mainly been associated with VEGF, bFGF and the CXC chemokines family[179].

Cancer cells usually become trapped in the first set of capillaries they encounter downstream from their point of entry. Frequently these sites are in the lungs, since deoxygenated blood leaving many organs is returned first to the lungs for re-oxygenation before being distributed throughout the rest of the body. Once in a new site, the cells must again penetrate the basement membrane of the blood vessel and establish themselves in the new tissue[141].

1.1.5.8 Drug resistance, metastasis and cancer stem cells

Cancer stem cells are cancer cells (CSC, found within tumours or haematological cancers) that possess characteristics associated with normal stem cells, specifically the ability to give rise to a multitude of different cell types. It is well established that CSCs can drive primary, metastatic and recurrent tumourigenesis in many malignancies. They are also believed to play a role in metastasis and the development of resistance to chemo- or radiotherapy[180]. Small populations of cells with properties similar to stem cells have been reported in small cell lung cancer[181] and non-small cell lung cancer[182]. Several studies have identified CD133, CD44, ALDH (aldehyde dehydrogenase) and ABCG2 (ATP-binding cassette sub-family G member 2) as lung cancer stem cell markers[183,184]. These markers also happen to be validated CSC markers in multiple other cancer types. Embryogenesis signaling pathways, such as the hedgehog, wnt and notch pathways have also been implicated as determinants of the lung CSC phenotype. With a central role for CSCs in tumour recurrence, metastasis and drug-resistance, targeting CSC markers and/or signaling pathways to eradicate lung cancer and enhance patient outcome is an attractive clinical approach[184].

1.1.6 MDR and invasion and metastasis

The major causes of treatment failure in cancer are the development of metastases and drug resistance. For more than two decades, these two important but not clearly understood aspects in the biology of cancer have been extensively studied. An important goal of cancer research is to determine whether a common factor exists that activates two sets of genes or pathways, one responsible for drug resistance, and the other responsible for increased tumour cell invasion and metastasis. Although direct evidence linking ABC transporters to metastasis is currently lacking,

roles are emerging for these proteins in cell migration and invasion. Research indicates that there is a change towards a more malignant phenotype indicating cancer progression [185,186,187,188,189,190].

Role of ABC transporters in cell migration

Several ABC transporters have roles in the migration of normal cells. Induced migration of peripheral dendritic cells to lymph nodes is greatly reduced in Abcc1–/– mice[191], and Abcc1-deficient dendritic cells also have markedly attenuated chemotactic responses *in vitro*. However, exogenous addition of the ABCC1 substrates leukotriene C4 (lTC4) and lTD4 overcame the absence of the transporter *in vivo* and *in vitro*[191], suggesting a role for ABCC1 in autocrine signalling in mouse dendritic cell migration. Other ABC transporters might also have a role, as ABCB1-specific neutralising antibodies and the inhibitor verapamil prevented the migration of dendritic cells from human skin explants [192]. However, comparison of these results across species is complicated by differences in the roles of various family members. In human dendritic cells, ABCC4 seems to have a more prominent role than ABCC1 in migration, with ABCC4 knockdown or pharmacological inhibition by sildenafil preventing their migration from human skin explants[193].

The apparent roles of ABC transporters in dendritic cell migration are also reflected in cancer cell lines. The original work by *Meyers and Biedler*[194] in highly resistant multidrug-resistant (MDR) cell lines suggested that P-glycoprotein overexpression leads to decreased tumourigenicity. Moreover, the expression levels of a panel of metastasis- and drug resistance-related genes were analysed in a study carried out on a human prostate carcinoma cell line (PC-3M) and its variants with different metastatic ability. Highly metastatic cells growing in culture expressed higher levels of mRNA for b-FGF, IL-8, MMP-2, MMP-9, and Pgp than poorly metastatic cells and parental cells. This suggests a possible correlation between metastasis and Pgp-mediated drug resistance[195]. Tumour cells selected for resistance to chemotherapeutic drugs often become more invasive relative to sensitive parental cells[196] and it has been observed that secondary metastatic tumours are in some cases more resistant to chemotherapy than primary tumours[197]. Studies on the human nasal carcinoma cell line, RPMI- 2650, indicate that pulse-selection with taxol, while leading to an increase in drug resistance, does not promote *in vitro* invasiveness in the human nasal carcinoma cell line. However, selection with the anticancer agent melphalan appears to increase *in vitro* invasiveness[198]. Furthermore, mitoxantrone, 5-FU, methotrexate, BCNU, cisplatin and chlorambucil all induce an invasive phenotype in the human lung cancer cell line DLKP[196].

A doxorubicin-selected, multidrug-resistant human melanoma line expressing high levels of ABCB1 showed a more invasive phenotype than the parental cell line[199]. Although it is possible that other genetic changes contributed to this phenotype, knock down of ABCB1 by siRNA substantially reduced the invasiveness of this cell line in vitro. Also, reduction of ABCB1 levels by siRNA reduced the migration of MCF-7 breast cancer cells in transwell migration and matrigel invasion assays. Expression of ABCB1 in the canine kidney cell line MDCK also stimulated increased migration, and inhibition of ABCB1 reduced migration of the rat brain endothelial cell line RBE4 [200].

Drugs that interfere with the function of P-glycoprotein also interfere with the cell's motility and invasion. *Nokihara et al.* [201] confirmed the importance of P-glycoprotein in metastatic changes when they showed that the rate at which metastatic sites were formed by MDR human small cell lung cancer cells (SBC-3/ADM, P-glycoprotein positive) was higher than that produced by the sensitive parental cells (SBC-3, P-glycoprotein negative) in SCID mice. *Bjornland et al.*[202] observed that MDR hepatoma cells displayed an elevated capacity to migrate when compared with that of P-glycoprotein (−) parental cells. Treatment of the MDR hepatoma cells with the P-glycoprotein inhibitor PSC833 decreased their migration rate**.**

Other studies make the connection between these two phenotypes more apparent. *Yang et al*[203], reported that the extracellular matrix metalloproteinase inducer (EMMPRIN), a cell membrane glycoprotein involved in invasion and metastases is overexpressed in MDR cells and not in drug-sensitive parental cell lines[204,205]. *Miletti-González et al.* [206,207] reported that the functional interaction between CD44 and P-glycoprotein (P-gp) was one step in a complex molecular organisation that results in the concomitant multidrug resistance (MDR) phenotype as well as increased cell migration, *in vitro* invasion, and metastasis. The knockdown of MDR1 by short hairpin RNA (shRNA) impairs the migration and invasion abilities of tumour cells. *Misra et al.,*[208] reported that MDR in cancer cells could be regulated by the ubiquitous extracellular matrix component, hyaluronan, a major ligand for the metastases-related CD44 receptor. *Zhang et al.,* [209] also showed that Anxa2 was up-regulated in multidrug-resistant MCF-7/ADR cells and might play essential roles in modulating MDR-induced tumour invasion/metastasis. More recently *Zhang et al.,* showed that P-gp interacts with Src, a tyrosine kinase upstream of Anxa2[210]. They suggest that P-gp may promote the invasion of MDR breast cancer cells by modulating the tyrosine phosphorylation of Anxa2.

ABC transporters and metastasis in vivo

Although it remains to be determined whether ABC transporters contribute to metastasis *in vivo*, several studies indicate such a link. For example, *Slotman et al.,* [211] found an increased incidence of haematogenous metastases with induction chemotherapy for patients with advanced head-and-neck squamous carcinomas, compared to patients receiving only surgery and radiotherapy. They also found an increase in metastases at sites other than the usual pulmonary site[211]. *Stefani* and coworkers reported that the use of hydroxyurea in combination with radiotherapy for the treatment of head and-neck cancer yielded no benefit in terms of response rate or survival, but rather increased the incidence of distant metastases from 8% to 23% [212]. The administration of a single drug dose may be sufficient to induce spontaneous metastasis[213]. In another study it was found that MDR1 gene expression can be rapidly activated in human tumours after transient *in vivo* exposure to doxorubicin[214]. In a breast cancer study, ABCC1 expression was higher in metastatic lymph nodes than in the corresponding primary tumour[215], and in melanoma, ABCC1 and ABCC4 were more highly expressed in cell lines derived from metastases than in those derived from primary tumours[216].

Role of EMT in drug resistance and metastasis

One of the early steps in the invasion-metastasis cascade includes the epithelial–mesenchymal transition. There are many studies on the role of EMT in cancer progression, in terms of drug resistance and metastasis[217]. For example overexpression of some of the transcription factors associated with EMT such as Snail, Twist and Slug has also been associated with chemoresistance, although their depletion has been shown to increase drug sensitivity[218-220]. *Saxena et al*.[221] investigated the role of EMT-inducing transcription factors in drug resistance mediated by ABC transporters in breast cancer cells. They showed that the transcription factors that lead to EMT and invasion also orchestrate the overexpression of drug transporters by directly modulating their promoter activity, thus providing a novel molecular mechanism for the long-standing association between invasiveness and drug resistance[221]. Irradiation has also been shown to predispose breast cancer cells to EMT, i.e., the transition into the more immature and malignant mesenchymal phenotype[128].

Therapy induced stress

Huang et al., 2013[222] suggest that progression toward a resistant tumour is not only due to the selection of cells that are genetic or epigenetic variants and "happen" to survive because they express a phenotype that is more drug-tolerant but may be also due to the therapy itself. A frequent clinical observation is that metastasis correlates with therapeutic resistance. It is hypothesised that metastatic competence and drug resistance are common traits of tumour stem cells[223]. As indicated previously, there is increasing evidence in many cancers that enhanced tumourigenicity resides in a tumour cell population that exhibits stem cell-like properties such as self-renewal, differentiation, cell mobility and toxicity resistance, designated as cancer stem cells (CSC) or tumour initiating cells (TIC) [224,225]. There is evidence to indicate that therapy induces stemness or drug resistance. For instance, irradiation induces stem cell-like behavior and drug tolerance in leukemic cells [226] and in hepatocarcinoma cells, including the expression of key pluripotency genes, such as Sox2 and Oct4[227]. It was also been shown that the chemotherapy agent cisplatin which may cause a genome-wide response; can also induce the same response. Therapy-induced trauma caused by surgery, irradiation or cytostatic treatment can also increase or decrease oxygen and nutrient levels and activate the production of chemokines and growth factors by stromal cells. Multiple pathways are then activated that may boost cancer cell invasion, metastasis, and resistance responses[228].

Joint pathways to resistance and invasion

Evidence is accumulating that cancer invasion and drug resistance are interconnected[228]. Molecular changes in different signalling pathways including apoptosis signalling or cell cycle regulation may be involved in cancer cell chemoresistance and increased malignancy[185,190,229]. Table 1-3 summarises the molecules important in resistance and invasion. Figure 1-11 summarises the overlap between migration-inducing and pro-survival pathways – particularly those concerning PI3K, Akt, Ras and Rho GTPases, integrins, cadherins and p53. Strategies to target these pathways have been explored in both preclinical and clinical studies[228]. For example, the tumour suppressor transcription factor TP53 is dysfunctional in many cancer types and controls many genes including the DNA checkpoint kinases and apoptosis regulators, so allowing unlimited growth. As a result it is a master regulator of cell susceptibility to cytotoxic stimuli, the constitutive deregulation of which supports resistance[228].

Unlimited growth is also mediated by mutations within RAS *(H-RAS, K-RAS, and N-RAS*) which activates the mitogen activated kinases (MAPKs;MEK.ERK, JNK, and p38), PI3K/Akt, and mammalian target of rapamycin (mTOR), thereby favouring cell cycle progression[228]. Active Ras proteins also contribute to invasion regulation as direct and indirect upstream activators of Rho GTPases and enhance motility and invasion through PI3K, mTOR, the Rac1-activating guanine-nucleotide exchange Tiam, and the MAPKs p38 and JNK. Ras pathways also activate the integrin-mediated focal adhesion and growth factor receptor signaling that interact with the MAPK and ERK pathways and results in regulation of the expression of the MMPs[228].

Preclinical animal models are necessary to detect tumour cell and stromal cell responses to therapy at a cellular level. In addition, investigation of gene transcription and protein expression profiles in the invasion and resistance pathways should be carried out on patient tumour cells, stroma and circulating tumour cells. There is a substantial redundancy involved in cancer cell survival in response to therapy and multipathway targeting is necessary for cancer treatment[228].

Table 1-3: Molecules important in resistance and invasion. Taken from *Alexander & Friedl, 2012*[228].

	Factor, molecule, or pathway	Alteration	Function in survival and resistance	Function in cytoskeletal control, invasion and metastasis
Classical tumour suppressors and oncogenes	p53 (transcription factor)	LOF mutation	Defective cell cycle arrest after DNA damage (abortive p21 expression / activation); impaired apoptosis response (via downregulated death receptors and Bax)	Enhanced mesenchymal and amoeboid migration in vitro (via Rho GTPases); increased ECM degradation (via MMP2 upregulation); EMT induction (via Slug, Twist)
		GOF mutation	Impaired DNA repair (via Mre11/ATM) and apoptosis response (via inhibition of p63/p73 and Notch signaling)	EMT induction (via Twist); increased invasion in vitro and metastasis *in vivo* (via TAp63 inhibition)
	Ras superfamily (N-ras, H-ras, K-ras)	GOF mutation	Increased cell proliferation (via Ras/MAPK, PI3K, mTOR); inhibition of apoptosis (via PI3K/Akt, mTOR)	Increased motility [via PI3K/Tiam (Rac), mTOR (RhoA/Rac)]; increased expression of c-Met, K-ras (via p38/JNK)
	Growth factors and their receptors	Amplification, overexpression, GOF mutation, constitutive activation	EGFR: increased cell proliferation (via Ras, PI3K/Akt, JAK/STAT); decreased apoptosis (via PI3K/Akt)	EGF/EGF-receptors: increased migration, chemotaxis (via PI3K, Src; STAT3; PKCδ)
			FGFR: increased cell proliferation (via Ras, PI3K); decreased apoptosis (via PI3K/Akt)	FGF/FGFR: increased migration/invasion, chemotaxis (via PI3K)
			c-Met: increased cell proliferation (via CD44/Ras, PI3K, JAK/STAT), decreased apoptosis (via PI3K/Akt)	HGF/c-Met: increased invasion, chemotaxis (via CD44/Ras, Src, PI3K)
			TGFβ/EMT: increased survival (via Ras, MAPK, PI3K/Akt, Src, STAT, Smad and Notch)	TGFβ/TGFR: increased invasion, chemotaxis (via PI3K/Cdc42/Rac, Smad/RhoA); TGFβ/EMT: expression regulation of N-cadherin, Rho GTPases, integrins, MMPs and GFRs
Cell adhesion receptors	Integrins	Constitutive expression and ligation to ECM	Enhanced survival (via Src/Grb2/Ras, FAK/PI3K); chemoresistance and radioresistance (via PINCH, STAT3, GSK3)	Adhesion to ECM, actin dynamics and mechanotransduction (via talin, vinculin, FAK); control of migration mode
	CD44 and variants	Upregulation (cancer stem cells); alternative splicing	Prosurvival signaling (via Ras as coreceptor for GFRs; via Src and ROCK activation of PI3K/Akt); multidrug resistance (via MDR1 upregulation)	Interaction with ECM; EMT induction (via c-Met interaction); putative role in mechanotransduction
	Cadherins	Altered expression pattern; downregulation	Prosurvival signaling (via β-cat/Wnt, p120-cat/Rac/Cyclin D1; coengagement of integrins	Control of cell–cell cohesion and detachment; supports collective invasion; EMT (E-cadh via integrins; N-cadh via p120-catenin)
Classical drivers of invasion	Rho superfamily members	Rac (Rac1) activation / overexpression	Increased proliferation (via MAPK, PI3K, JNK, NFκB, PAK, Cyclin D1); apoptosis inhibition (via Bad)	Promotes actin assembly and branching (via WAVE/Scar/Arp2/3); required for lamellipodia formation and invasion
		Rho (RhoA, RhoC) overexpression	Increased proliferation [via Cyclin D1, LIMK2 (RhoC)]	Controls actomyosin contraction required for migration/invasion (via ROCK and myosin II); supports roundish/amoeboid migration
		Cdc42 overexpression	Increased proliferation and decreased apoptosis (via PI3K, PAK, EGFR signaling, NFκB, STAT3), oncogene	Controls actin assembly (via WASP) and cell protrusion formation (filopodia, invadopodia)
	Chemokines/ cytokines and their receptors	CXCL12/CXCR4: enhanced release	Increased proliferation (via Ras); increased resistance (via PI3K/Akt)	Promotion of invasion and chemotaxis (via PI3K/Cdc42, FAK, Pax)
		IL-6/IL-6R: enhanced release	Increased cell proliferation (via Ras, J AK/STAT); increased resistance (via PI3K)	Promotion of invasion and chemotaxis (via MAPK, STAT)
	MMPs	Upregulation	Increased growth factor/chemo-/cytokine release and signaling (via ectodomain shedding, ECM degradation)	Tissue degradation underlying tissue invasion and remodeling; control of migration mode

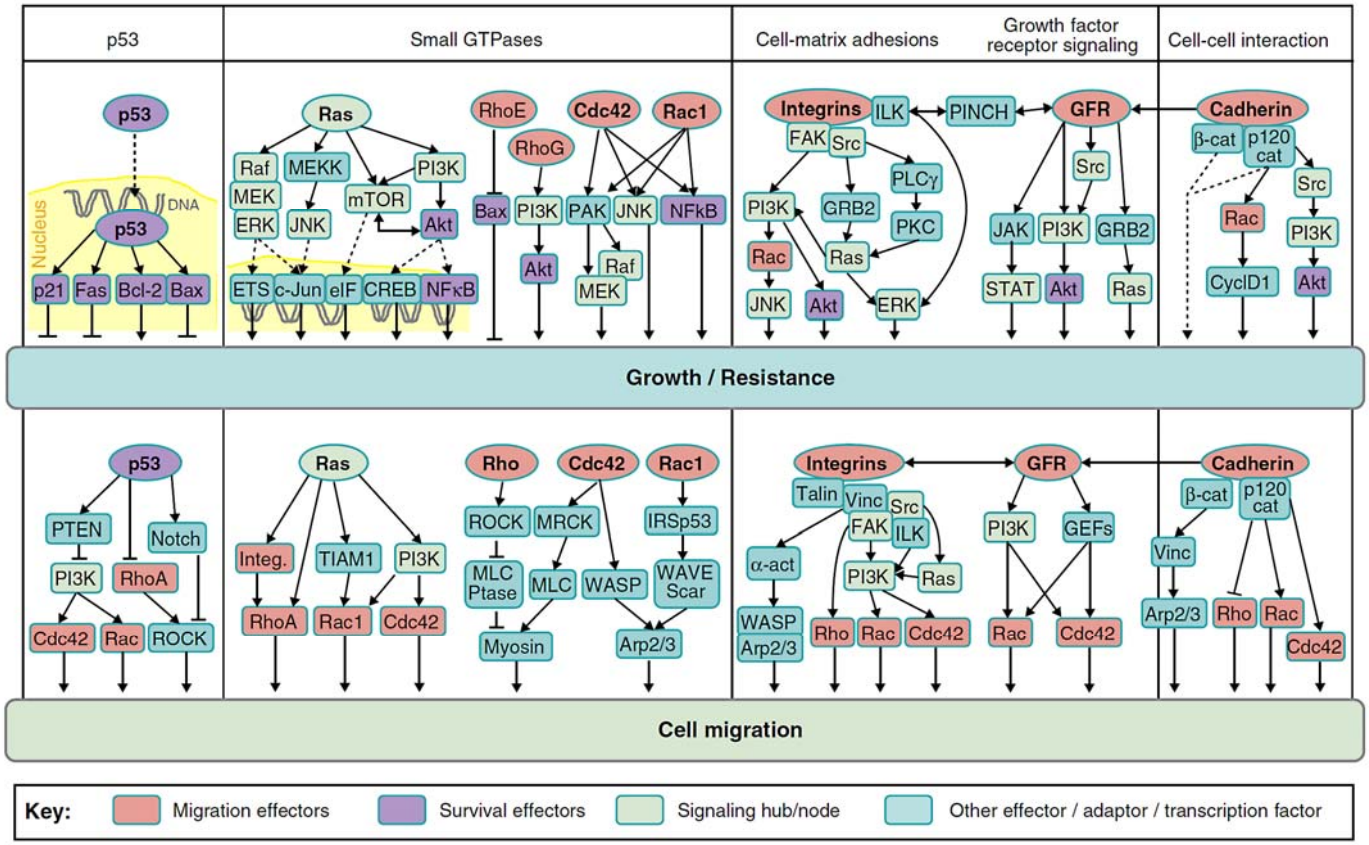

Figure 1-11: Signalling pathways controlling tumour cell growth, survival and invasion. The pathways of p53, Ras GTPase, small Rho GTPases, integrins, growth factor receptors and cadherins with a dual role in controlling cell growth and survival (upper row), as well as cell migration and invasion (lower row). Migration effectors are marked in red; survival effectors in purple; and signaling hubs in bright green. Arrows indicate signaling direction. Transcription factors are shown bound to DNA. Some abbreviations: a-act., aactinin; cat, catenin; Cdc42, cell division cycle 42; CREB, cAMP response element-binding; CyclD1, Cyclin D1; eIF, eukaryotic initiation factor; ERK, extracellular signal-related kinase; ETS, erythroblast transformation specific (transcription factor); FAK, focal adhesion kinase; GEF, guanine nucleotide exchange factor; GFR, growth factor receptor; GRB2, growth factor receptor-bound protein 2; ILK, integrin-linked kinase; Integ., integrin; JNK, Janus kinase; MEK, mitogen-activated protein kinase/extracellular signalregulated kinase kinase; MEKK, MEK kinase; mTOR, mammalian target of Rapamycin; MLC, myosin light chain, etc. Taken from *Alexander & Friedl, 2012*.

1.2 Background to techniques

1.2.1 Gene expression microarrays

Microarray-based gene expression profiling refers to the analysis of thousands of genes in a single experiment, where the labelled target (ie sample RNA, cRNA or cDNA) is interrogated with probes that are immobilized to a solid matter (eg fibrous mesh membrane, glass slide, beads). Through biostatistical and bioinformatics methods, the relative expression levels of each gene represented by a probe in the microarray can be obtained. After obtaining these values, numerous approaches and algorithms to interrogate microarray data can be applied[230].

The core principle behind microarrays is hybridization between two DNA strands, the property of complementary nucleic acid sequences to specifically pair with each other by forming hydrogen bonds between complementary nucleotide base pairs. A high number of complementary base pairs in a nucleotide sequence means tighter non-covalent bonding between the two strands. After washing off non-specific bonding sequences, only strongly paired strands will remain hybridized. Fluorescently labeled target sequences that bind to a probe sequence generate a signal that depends on the hybridization conditions (such as temperature), and washing after hybridization. Total strength of the signal, from a spot (feature), depends upon the amount of target sample binding to the probes present on that spot. Microarrays use relative quantization in which the intensity of a feature is compared to the intensity of the same feature under a different condition, and the identity of the feature is known by its position.

The microarray experiments carried out in our study employed the Affymetrix GeneChip system. Affymetrix probes are designed using publicly available information. The sequences, from which the probe sets were derived, were selected from GenBank, dbEST, and RefSeq. The sequence clusters were created from the UniGene database (Build 133, April 20, 2001) and then refined by analysis and comparison with a number of other publicly available databases, including the Washington University EST trace repository and the University of California, Santa Cruz Golden-Path human genome database (April 2001 release). Sequences from these databases were collected and clustered into groups of similar sequences.

The probes are manufactured on the chip using photolithography (a process of using light to control the manufacture of multiple layers of material), which is adapted from the computer chip industry. Each GeneChip contains approximately 1,000,000 features. Each probe is spotted as a pair, one being a perfect match (PM), and the other with a mismatch (MM) at the centre. These probe pairs allow the quantitation and subtraction of signals caused by non-specific cross-

hybridisation. The differences in hybridisation signals between the partners, as well as their intensity ratios, serve as indicators of specific target abundance. Each gene or transcript is represented on the GeneChip by 11 probe pairs. The probe sets are given different suffixes to describe their uniqueness and/ or their ability to bind different genes or splice variants.

"_at" describes probes set that are unique to one gene.

"_a_at" describes probe sets that recognise multiple transcripts from the same gene.

"_s_at" describes probe sets with common probes among multiple transcripts from separate genes.

The "_s_at" probe sets can represent shorter forms of alternatively polyadenylated transcripts, common regions in the 3‟ ends of multiple alternative splice forms, or highly similar transcripts. Approximately 90% of the _s_at probe sets represent splice variants. Some transcripts will also be represented by unique _at probe sets.

"_x_at" designates probe sets where it was not possible to select either a unique probe set or a probe set with identical probes among multiple transcripts. Rules for cross-hybridisation are dropped in order to design the _x_at probe sets. These probe sets share some probes identically with two or more sequences and therefore, these probe sets may cross-hybridise in an unpredictable manner.

A sample must be registered and an experiment defined in GCOS (GeneChip Operating Software) before processing a probe array in the fluidics station or scanning. Once the array is scanned, an image file is created called a ".dat" file. The software then computes cell intensity data (".cel" file) from the image file. It contains a single intensity value for each probe cell delineated by the grid (calculated by the Cell Analysis algorithm). The amount of light emitted at 570nm from stained chip is proportional to the amount of labelled RNA bound to each probe. Each spot correspond to individual probe (either perfect match or mismatch). The probes for each gene are distributed randomly across the chip to nullify any region specific bias. Following this, data analysis algorithms combine the probes to the respective intensity of individual transcripts.

1.2.2 2D-DIGE MALDI-TOF MS

Two-dimensional difference gel electrophoresis (2D-DIGE) is a high performance proteomic technology, allowing quantitative protein expression profiles across many clinical specimens in a reproducible, sensitive and high-throughout manner. Originally introduced in 1975, Farrell and Klose[231] demonstrated the ability to separate proteins based on their isoelectric points and molecular weights by 2-DE on polyacrylamide gels. Proteins in a 2D gel are separated by two separate unrelated elements. In the first dimension, proteins are separated according to their isoelectric point (pi) called isoelectric focusing. In the second dimension proteins are separated according to their molecular weights in SDS-PAGE.

2D-DIGE technology involves prelabelling the protein samples with different spectrally-resolvable fluorescent dyes so they can be mixed together, co-separated and visualised on a single 2-DE gel. The CyDye DIGE Fluor dyes (Cy2, Cy3 and Cy5) are matched for mass and charge, but possess distinct excitation and emission spectra. During labelling, the dyes undergo a nucleophilic substitution reaction with the s-amino group of lysine residues on protein resulting in the formation of an amide bond. The dye: protein ratio is optimised so that only 5% o f the protein sample is labelled (where the protein is abundant). This method ensures that only proteins with a single dye molecule are visualised and those containing multiple dye molecules are minimised. Consequently, the same protein labelled with any of the dyes will migrate to the same position on the 2D gel. By using different dyes to separately label proteins isolated from normal and diseased tissues, multiple samples (up to three) can be co-separated and quantitated by three different set of wavelengths (figure 1-12). The inclusion of a pooled internal standard (Cy2), containing every protein from all samples is used to match protein patterns across gels. This feature, counteracts inter-gel variation, allows normalisation of individual experiments and accurate quantification of differences between samples with significance[232 233].

The fully optimised system (including CyDye fluorescent dyes, imager, and DeCyder Differential Analysis Software) offers increased throughput, ease of use, reproducibility, and accurate quantitation of protein expression differences. Reduced system variability enables accurate study of protein expression differences against a baseline of biological variation. DeCyder biological variation analysis (BVA) processes multiple gel images, performs gel-gel spot matching and quantatively compares protein abundance across gels.

Mass spectrometry identifies the proteins corresponding to any spots observed by 2D-DIGE and utilises the gene and literature database to interpret the proteomic data.

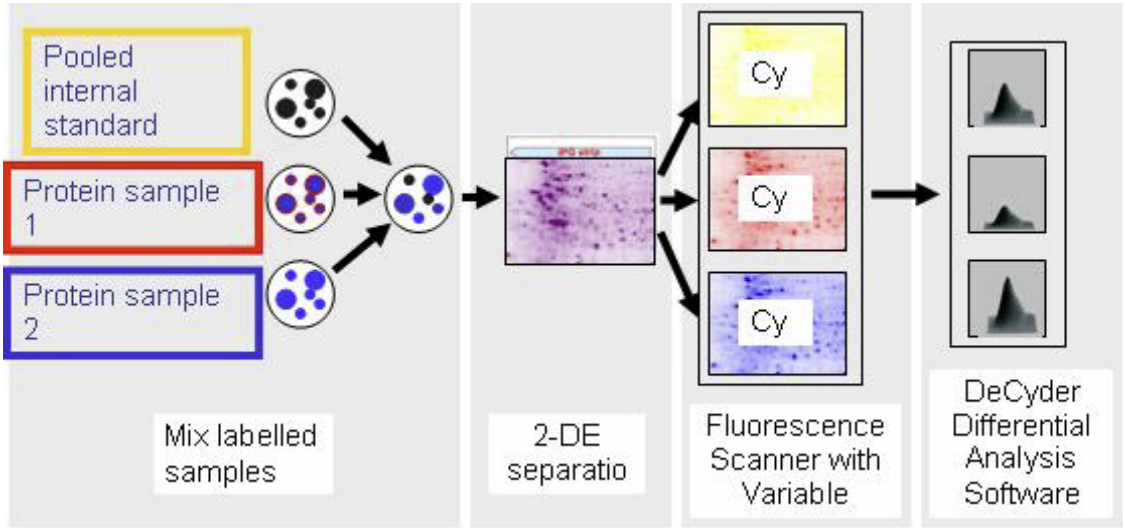

Figure 1-12 Outline of 2D-DIGE system where three CyDye DIE Fluor minimal dyes are separated in one gel

Matrixassisted Laser Desorption/Ionisation (MALDI) developed by Karas and Hillenkamp[234] involves the deposition of sample molecules with an excess of matrix material (α-cyano-4-hydroxycinnamic acid or dihydroxybenzoic acid) in a solvent. The water in the solvent evaporates and the sample proteins are surrounded by the matrix, which forms a crystal lattice. The precipitant is then bombarded with laser pulses that imparts energy. The matrix materials have absorbances at the wavelength of the laser, and are subject to desorption and ionisation, accompanied by fragmentation. The MS measures the mass-to-charge ratio (m/z) of the protein, peptide or peptide fragments (figure 1-13). The time-of-flight (TOF) analyser measures the time it takes for the ions to fly from one end of the analyzer to the other end and strike the detector. The smaller ions possess higher velocity relative to larger/heavier ions. Separated ion fractions arriving at the end of the drift tube are detected by an appropriate recorder that produces a signal upon impact of each ion group. The TOF mass spectrum is a recording of the detector signal as a function of time. This peptide mass fingerprint can then be used to search databases to identify the protein[235].

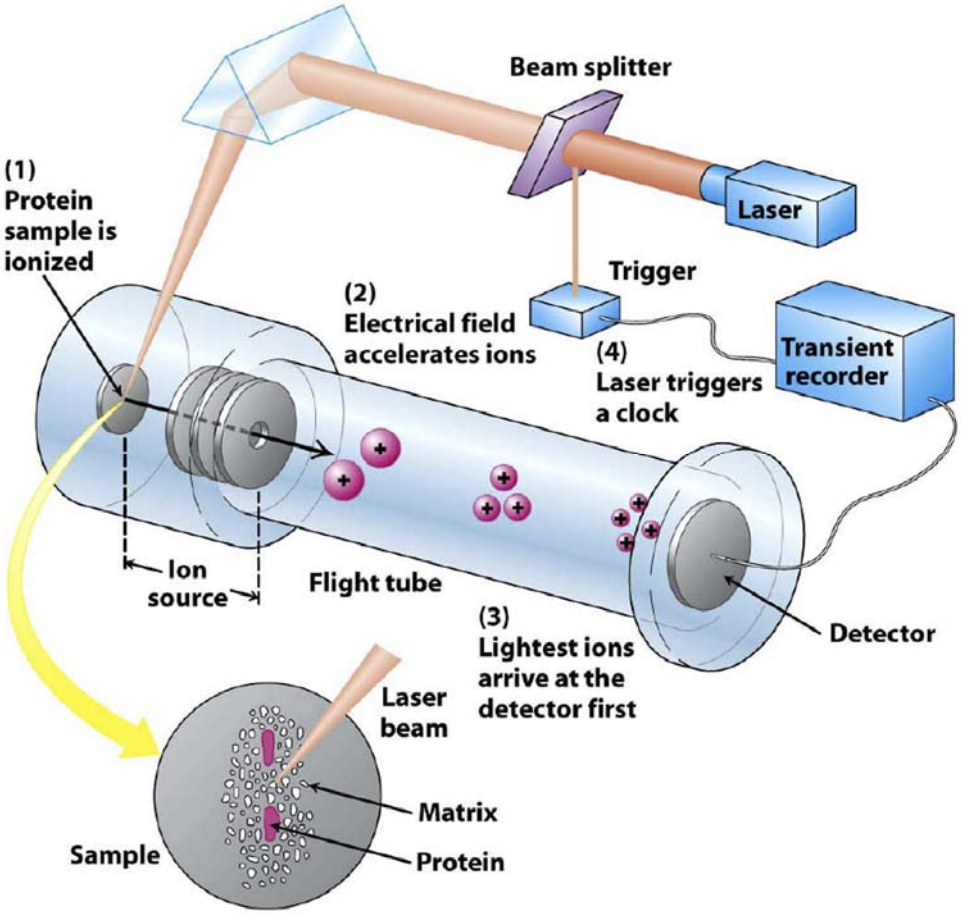

Figure 1-13 A schematic diagram of MALDI-TOF-MS.

1.2.3 siRNA and shRNA

The discovery of RNAi, a powerful tool to induce loss-of-function phenotypes through the posttranscriptional silencing of gene expression, has provided new possibilities for cancer therapy[236-238]. RNA interference (RNAi) is the mechanism for RNA-guided regulation of gene expression, in which the introduction of double-stranded RNA (dsRNA) into a diverse range of organisms and cell types causes degradation of the complementary mRNA. Small interfering RNA (siRNA) is also known as short interfering RNA or silencing RNA (figure 1-14). It is a class of 20-25 nucleotide-long double-stranded RNA molecules. In the late nineties RNA silencing was discovered in plants during the course of transgenic experiments that eventually led to the silencing of the introduced transgene and, in some cases, of homologous endogenous genes or resident transgenes[239] (Matzke *et al*., 1989; Linn *et al*., 1990; Napoli *et al*., 1990; Smith *et al*., 1990; van der Krol *et al*., 1990). However, this approach could not be used in mammalian cells

as the long double-stranded RNAs (dsRNAs) triggered a cytotoxic reaction leading to cell death (Hunter *et al*., 1975). Further studies in plants and invertebrates demonstrated that the actual molecules that led to RNAi were short dsRNA oligonucleotides, 21 nucleotides in length, processed internally by an enzyme called "Dicer". It was then demonstrated in 2001, that siRNA could directly trigger RNAi in mammalian cells without evoking nonspecific effects. RNAi technology takes advantage of the cell's natural machinery, facilitated by short interfering RNA molecules, to effectively knock down expression of a gene of interest. There are several ways to induce RNAi, synthetic molecules, RNAi vectors, and in vitro dicing.

1.2.3.1 Mechanism of action

Long double-stranded RNAs (typically >200 nt) can be used to silence the expression of target genes in a variety of organisms. Long double-stranded RNA (dsRNA) enters a cellular pathway that is commonly referred to as the RNA interference (RNAi) pathway. The dsRNA triggers a two-step reaction. During the initiation stage, dsRNA is processed by a ribonuclease (RNase) III enzyme, called Dicer, into small interfering RNAs (siRNAs)[240]; mediated by type III RNase Dicer enzyme. RNase III family members are among the few nucleases that show specificity for dsRNAs[241] and are evolutionarily conserved in worms, flies, fungi, plants, and mammals[242]. Complete digestion by RNase III enzymes results in dsRNA fragments of 20-25 base pairs[243]. During the effector stage, the siRNAs assemble into endoribonuclease-containing complexes known as RNA-induced silencing complexes (RISCs). siRNAs undergo unwinding before being incorporated into a high-molecular-weight protein complex called RISC[244]. Dicers are part of the RISC complex, which includes several different proteins such as the Argonaute gene family members and an ATP-dependant RNA helicase activity that unwinds the two strands of RNA. Functional RISCs contain only single stranded siRNA[245]. The siRNA strands subsequently guide the RISC to complementary RNA molecules, where base pairing takes place between the antisense strand of the siRNA and the sense strand of the target mRNA. This leads to endonuclease cleavage of the target RNA[246,247].

1.2.4 microRNA

MicroRNAs (miRNAs) are a class of naturally occurring small non-coding RNA molecules (21-25 bases in length) that regulate a variety of developmental and physiological processes[248]. They control gene expression by mRNA cleavage, mRNA destabilization, or inhibition of

translation[249]. The discovery of let-7 in *Caenorhabditis elegans* in 2000 as a regulator of developmental cellular fate[250] and discovery of let-7-related genes in multiple species indicated the importance of these miRNAs[251]. Since then, miRNA research has revealed multiple roles in negative regulation (transcript degradation and sequestering, translational suppression) and possible involvement in positive regulation (transcriptional and translational activation). By affecting gene regulation, miRNAs are likely to be involved in most biological processes[252].

Almost half of miRNAs reside in clusters and are transcribed as polycistronic precursor miRNAs[253]. Other miRNAs, located in intergenic regions, are transcribed by their own promoters, and those present in intronic regions are likely under the control of the host genes'promoters[254]. There are currently approximately 2,600 unique mature miRNAs in human (miRBase version 20)[255]. Almost 50% of these are located at fragile sites on chromosomes known for having common alterations (i.e. amplification, deletion, and rearrangements) in cancer[256]. Roles of miRNAs in cellular processes like cell cycle progression, proliferation, metabolism, apoptosis, and stress resistance cannot be overlooked as more than 60% of human protein coding genes are predicted to be under selective pressure to be regulated by miRNAs[257,258].

The uncapitalized "mir-" refers to the pre-miRNA, while a capitalized "miR-" refers to the mature form. miRNAs with nearly identical sequences except for one or two nucleotides are annotated with an additional lower case letter. For example, miR-123a would be closely related to miR-123b. Pre-miRNAs that lead to 100% identical mature miRNAs but that are located at different places in the genome are indicated with an additional dash-number suffix. For example, the pre-miRNAs hsa-mir-194-1 and hsa-mir-194-2 lead to an identical mature miRNA (hsa-miR-194) but are located in different regions of the genome. Both strands of a pre-microRNA may be processed into two mature microRNAs, with similar efficiencies which are discriminated by -5p and -3p, or with one dominantly processed and the recessive one star-labeled (*), which function differently against different target genes. For example, miR-123 and miR-123* would share a pre-miRNA hairpin, but more miR-123 would be found in the cell[259,260].

1.2.3.1 microRNA transcription and function

miRNA genes are usually transcribed by RNA polymerase II (Pol II). The first step in miRNA maturation is the nuclear cleavage preformed by the Drosha RNase III endonuclease to give an approximately 60–70 nt stem loop intermediate, having a 5' phosphate and an approximately 2 nt

3'overhang (figure 1-14). This pre-miRNA is actively transported from the nucleus to the cytoplasm by Ran-GTP and the export receptor Exportin-5. The nuclear cut by Drosha defines one end of the mature miRNA, and the other is processed in the cytoplasm by Dicer, which recognizes the double-stranded portion of the pre-miRNA and cuts about two helical turns away from the base of the stem loop. This eliminates the loop itself and leaves the 5' phosphate and approximately 2nt 3' overhang characteristic of the RNase III products. This process results in a mature miRNA, and siRNA-like imperfect duplex ready for RISC. Once loaded on RISC, there is no substantial difference between miRNA and siRNA toward the target messenger RNA. Both of them are capable of undertaking two possible post-transcriptional mechanisms: mRNA cleavage, translational repression. The choice is determined by the degree of complementarity with the target. A total identity between siRNA or miRNA and mRNA will specify cleavage, while partial complementarity of any of the two RNAs in the 30-untranslatable (30-UTR) region of the messenger will induce translational repression[261].

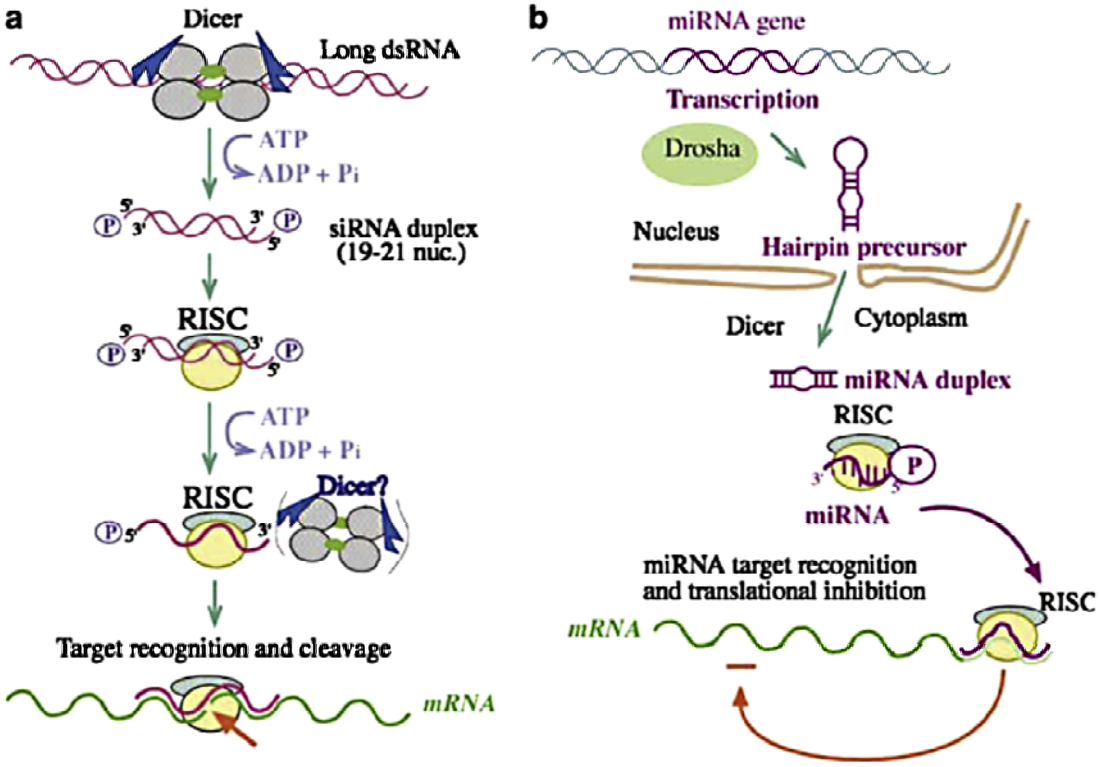

Figure 1-14: (a) siRNA and (b) miRNA (From Izquierdo et al., 2005[261]).

1.2.5 Methylation analysis

Methylation has been shown to play a vital role in numerous cellular processes, including embryonic development, genomic imprinting, X-chromosome inactivation, and preservation of chromosome stability[262]. DNA methylation occurs at the cytosine bases of eukaryotic DNA, which are converted to 5-methylcytosine by DNA methyltransferase (DNMT) enzymes. The altered cytosine residues are usually immediately adjacent to a guanine nucleotide, resulting in two methylated cytosine residues sitting diagonally to each other on opposing DNA strands. Different members of the DNMT family of enzymes act either as *de novo* DNMTs, putting the initial pattern of methyl groups in place on a DNA sequence, or as maintenance DNMTs, copying the methylation from an existing DNA strand to its new partner after replication[263].

In mammals, methylation is found sparsely but globally, distributed in definite CpG sequences throughout the entire genome, with the exception of CpG islands, or certain stretches (approximately 1 kilobase in length) where high CpG contents are found. The methylation of these sequences can lead to inappropriate gene silencing, such as the silencing of tumour suppressor genes in cancer cells (figure 1-15).

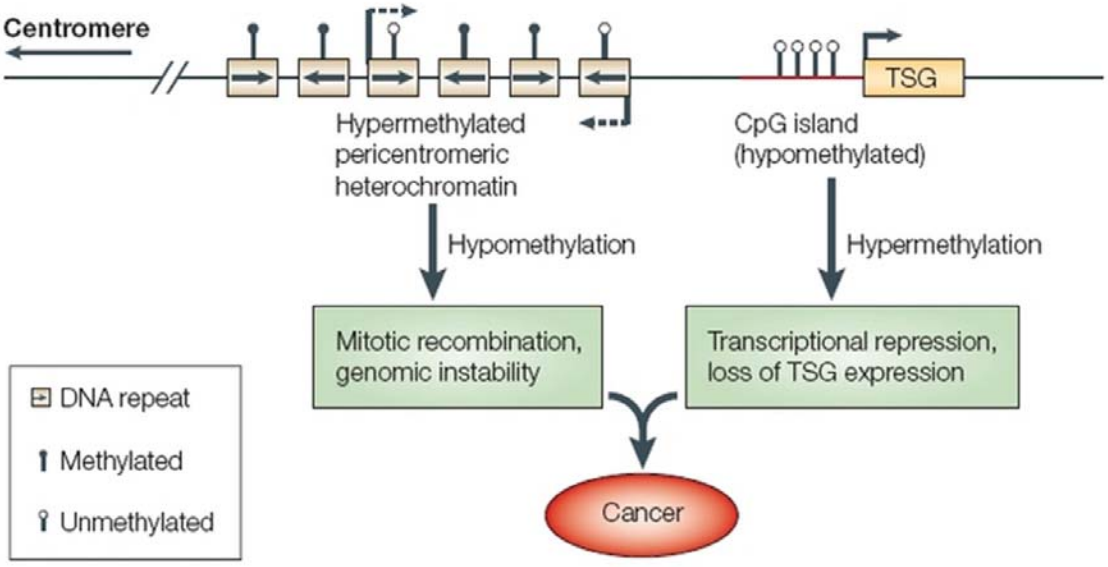

Figure 1-15: DNA methylation and cancer. The diagram shows a representative region of genomic DNA in a normal cell. The region shown contains repeat-rich, hypermethylated pericentromeric heterochromatin and an actively transcribed tumour suppressor gene (TSG) associated with a hypomethylated CpG island (indicated in red). In tumour cells, repeat-rich heterochromatin becomes hypomethylated and this contributes to genomic instability, a hallmark of tumour cells, through increased mitotic recombination events. De novo methylation of CpG islands also occurs in cancer cells, and can result in the transcriptional silencing of growth-regulatory genes. These changes in methylation are early events in tumourigenesis (From Robertson, K. DNA methylation and human disease. Nature Reviews Genetics 6, 598[262]).

Currently, the mechanism by which *de novo* DNMT enzymes are directed to the sites that they are meant to silence is not well understood. However, researchers have determined that some of these DNMTs are part of chromatin-remodeling complexes and serve to complete the remodeling process by performing on-the-spot DNA methylation to lock the closed shape of the chromatin in place. The global pattern of methylation in mammals makes it difficult to determine whether methylation is targeted to certain gene sequences or is a default state, but the CpG islands tend to be near transcription start sites, indicating that there is a recognition system in place[263].

1.2.5.1 Bisulfite modification

A major advance in DNA methylation analysis was the development of a method for sodium bisulfite modification of DNA to convert unmethylated cytosines to uracil, leaving methylated cytosines unchanged[264]. Bisulfite modification of genomic DNA was first employed for the detection of varying methylation patterns in individual strands of particular genomic sequences[264]. Incubation of target DNA with sodium bisulfite, results in conversion of unmethylated cytosine residues into uracil, leaving methylated cytosines unchanged. This allows one to distinguish methylated from unmethylated DNA via PCR amplification and analysis of the PCR products. During PCR amplification, unmethylated cytosines amplify as thymine and methylated cytosines amplify as cytosine (figure 1-16).

In this reaction, a bisulfite ion is added to the 5-6 double bond of the cytosine molecule, which is converted to a uracil-bisulfite derivative by hydrolytic deamination. The final alkali treatment of the DNA removes the sulphonate group to give uracil [265-267]. Under these conditions, 5-Methylcytosine (5-mC) remains unchanged. During PCR amplification, with primers designed to anneal with bisulfite-converted DNA only, all uracil and thymine nucleotides are amplified as thymine, whereas only 5-mC is amplified as cytosine (figure 1-16).

1.2.5.2 Methylation sensitive PCR (MSP)

Methylation sensitive PCR (MSP) is a rapid and very sensitive technique to screen for methylation. First reported in 1996 by *Herman et al.,*[268], MSP has become a widely used technique that is good for a "yes or no"indication concerning methylation of CpG sites. MSP primer-based methods include MethyLight[269], SYBER green-based quantitative MSP[270],

sensitive melting analysis after real-time MSP (SMART-MSP)[271], and methylation-specific fluorescent amplicon generation (MS-FLAG)[271].

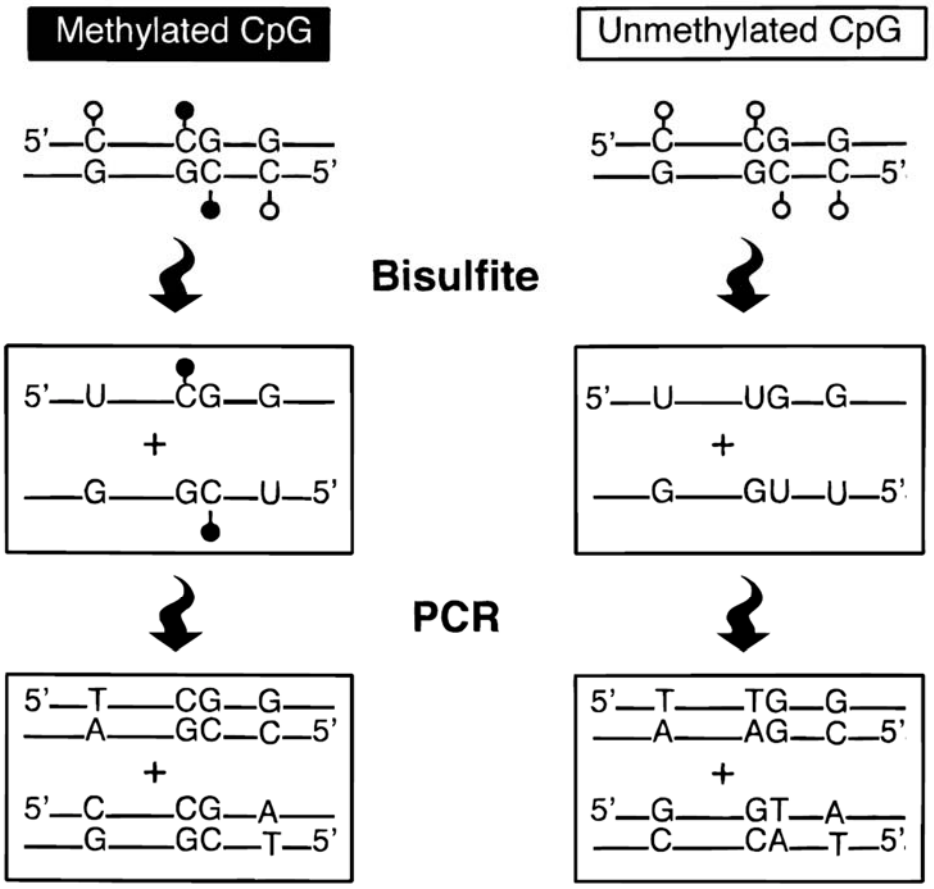

Figure 1-16: Sodium bisulfite conversion. Sodium bisulfite modifies the sequence of genomic DNA by converting unmethylated cytosines to uracils while leaving methylated cytosines unmodified. PCR amplification results in the replacement of uracil residues by thymines. Bisulfite conversion destroys the self-complementarity of the original genomic DNA, so that two different PCR products can be generated: one derived from the top strand, and one derived from the bottom strand.(From SpringerImages.com).

The design of primers is essential for reliable results; ideally, the 'methylated' and 'ummethylated' primer sets should be designed for the same CpG sites and include multiple CpG sites at the 3' ends[272]. Following bisulfite modification, PCR is performed using two sets of primers designed to amplify either methylated or unmethylated alleles. The methylated primer set assumes the CpG's are fully methylated and thus the primer will have all four bases in the sequence. The unmethylated primer set anneals to gDNA that is not methylated in the (same)

primer binding site, and therefore will have a T in place of C in the primer sequence. It is important to test the primer sets with a control gDNA of known methylation status. The properly designed methylated primer set will only amplify the control methylated gDNA, and not the unmethylated gDNA, and the unmethylated primer set will only amplify the unmethylated gDNA.

1.2.5.3 Quantitative methylation specific PCR

Eads and colleagues first introduced the high-throughput technology known as MethyLight or quantitative methylation specific PCR (QMSP) for the analysis of DNA methylation that utilises fluorescence-based real-time PCR (TaqMan®) technology[269] (figure 1-17). The use of three oligonucleotides (forward and reverse primers, and interpositioned probe) in MethyLight, any one or more of which can be used for methylation discrimination, allows for a high degree of specificity, sensitivity, and flexibility in methylation detection[273]. Figure 1-17 (application C) illustrates the primer design strategy for a quantitative version of MSP where the probe is designed to avoid covering CpG dinucleotides. A greater degree of methylation discriminatory capability can be achieved by designing the probe to include CpG dinucleotides in addition to the forward and reverse primers and this is the most commonly used application of MethyLight (figure 1-17, application D). The design of primers and probe that do not overlap CpG nucleotides (figure 1-17, application A) results in a reaction without any methylation discriminatory capability and serves as a control reaction for the amount of input DNA. The inclusion of methylation discrimination only in the probe (figure 1-17, application B) provides a quantitative method for determining the relative amounts of various permutations of methylation within the sequence covered by the probe.

A disadvantage of the MethyLight technique is that it cannot quantify methylation at the individual nucleotide level; rather, it can assess methylation levels at the primer sites and/or a probe site as a whole. These assays were designed to detect completely methylated or unmethylated alleles, but do not detect partial allelic methylation. In contrast, bisulfite-sequencing, such as bisulfite-pyrosequencing[274] can achieve resolution at the individual nucleotide level. More recently mass spectrometry has been widely used in methylation analyses[275].

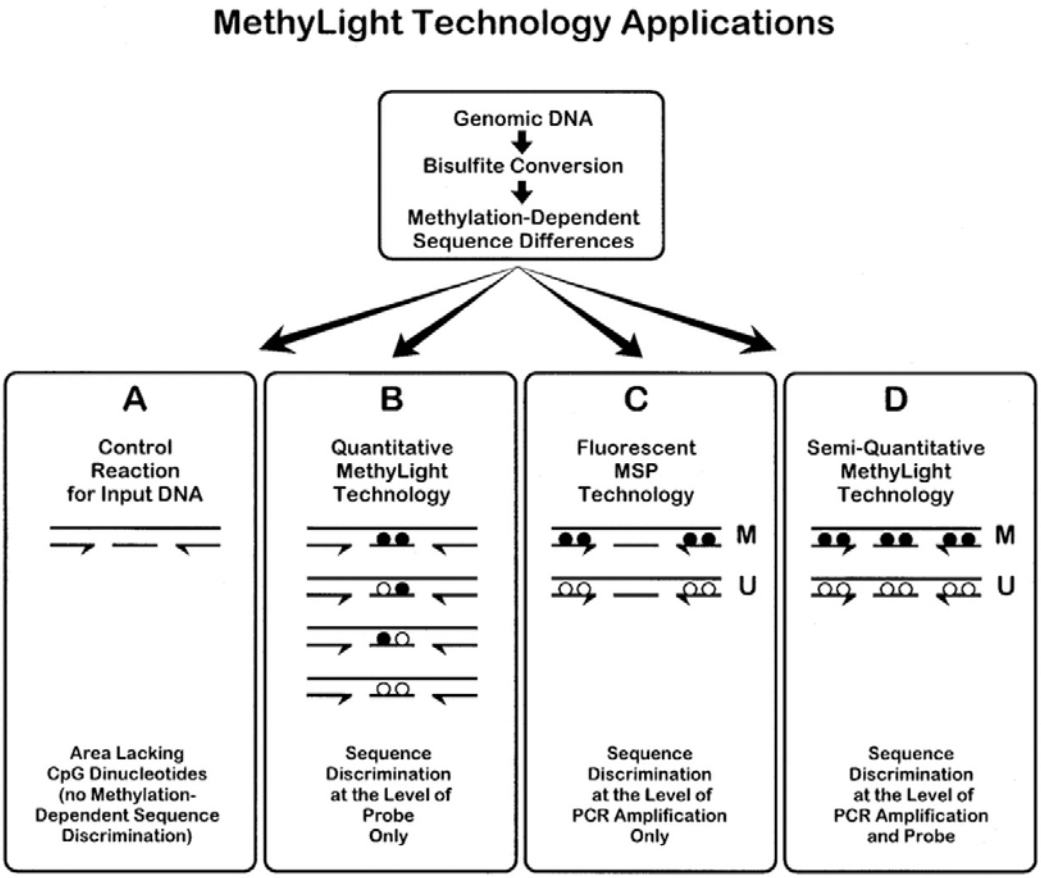

Figure 1-17: Schematic of the theoretical basis of MethyLight technology. Genomic DNA is first chemically modified by sodium bisulfite. This generates methylation-dependent sequence differences at CpG dinucleotides by converting unmethylated cytosine residues (locations indicated by white circles) to uracil, while methylated cytosine residues (locations indicated by black circles) are retained as cytosine. Fluorescence-based PCR is then performed with primers that either overlap CpG methylation sites or that do not overlap any CpG dinucleotides.

Sequence discrimination can occur either at the level of the PCR amplification process or at the level of the probe hybridisation process, or both. Sequence discrimination at the PCR amplification level requires the primers and probe (application D), or just the primers (application C), to overlap potential methylation sites (CpG dinucleotides). The MethyLight assay can also be designed such that sequence discrimination does not occur at the PCR amplification level. If neither the primers nor the probe overlap sites of CpG dinucleotides (application A), then no methylation-dependent sequence discrimination occurs at the PCR amplification or probe hybridisation level. This reaction represents amplification of the converted genomic DNA without bias to methylation status, which can serve as a control for the amount of input DNA. When just the probe overlaps methylation sites (application B), then sequence discrimination can occur through probe hybridisation. The design of separate probes for each sequence variant resulting from different methylation patterns (22 = 4 probes in the case of two CpGs, as illustrated) can potentially serve as a quantitative version of the MethyLight technology[269].

1.2.6 Sequenom Oncogenotype Mutational Analysis

The Sequenom MassARRAY® system is a DNA analysis platform that efficiently and precisely measures the amount of genetic target material and/or variations and is suitable for a variety of research applications including Somatic Mutation Profiling, Genotyping, Methylation Analysis, Molecular Typing and Quantitative Gene Expression (QGE). Detection by MALDI-TOF mass spectrometry (MS) offers high sensitivity and accuracy.

The assay is based on primer extension and offers two levels of specificity. First, a locus-specific PCR reaction takes place, followed by a locus-specific primer extension reaction (iPLEX assay) in which an oligonucleotide primer anneals immediately upstream of the polymorphic site being genotyped. The PCR primers are designed in a region of approximately 100 base pairs around the SNP of interest and an extension primer is designed immediately adjacent to the SNP. In the iPLEX assay, the primer and amplified target DNA are incubated with mass-modified dideoxynucleotide terminators (figure 1-18). The primer extension is made according to the sequence of the variant site, and is a single complementary mass-modified base. Through the use of MALDI-TOF mass spectrometry, the mass of the extended primer is determined. The primer's mass indicates the sequence and, therefore, the alleles present at the polymorphic site of interest. Sequenom supplies software (SpectroTYPER) that automatically translates the mass of the observed primers into a genotype for each reaction[276].

Figure 1-19 outlines the steps involved in the iPLEX assay. Firstly, the DNA needs to be amplified by PCR prior to performing an extension reaction of the SNP of interest. Sequenom's MassARRAY Designer software automatically designs PCR and extension primers (probes) for each SNP to be investigated. All oligos for PCR and iPLEX reactions are unmodified, with standard purification. The goal of an optimal multiplex PCR reaction is to evenly amplify many individual loci of DNA with minimal nonspecific byproducts. Purified amplicons are then used as templates for the primer extension reaction. Following the PCR, treatment with shrimp alkaline phosphatase (SAP) is performed in order to remove remaining, nonincorporated dNTPs from amplification products. SAP dephosphorylates unincorporated dNTPs by cleaving the phosphate groups from the 5′ termini.

After PCR amplification of the region of interest from genomic DNA, a genotyping primer is annealed adjacent to the polymorphic site in the presence of DNA polymerase and a mixture of dNTPs and ddNTPs. During the iPLEX reaction, the primer is extended by one mass-modified nucleotide depending on the allele and the design of the assay. Such a reaction mixture generates

allele specific products of different lengths, which allows easy interrogation by MALDI-TOF-MS.

The primer extension reaction is then desalted, as cations are known to interfere with MALDI. This cleanup step is important to optimize mass spectrometry analysis of the extended reaction products. A slurry of resin is added directly to primer extension reaction products to remove salts such as Na^{+}, K^{+}, andMg^{2+} ions. If not removed, these ions can result in high background noise in the mass spectra.

The DNA/RNA analyte mixture is transferred to a SpectroCHIP® Array. The SpectroCHIP® Array is coated with a matrix which allows crystallization of the PCR product on its surface. The chip is placed into the mass spectrometer and a laser is fired at the crystal which ionizes the molecules. These ions travel through a vacuum tube to an ion detector based on their mass. Smaller molecules travel faster than larger ones. Time of flight measures the difference in time different molecules hit the detector and the software calculates the mass of the fragments. MALDI-TOF can resolve mass differences of 16 Daltons.

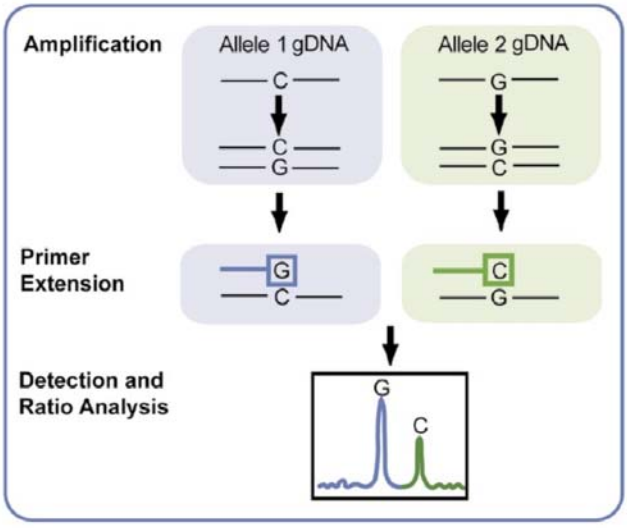

Figure 1-18: Single-base primer extension assay. In the iPLEX assay, the primer and amplified target DNA are incubated with mass-modified dideoxynucleotide terminators. The primer extension is made according to the sequence of the variant site, and is a single complementary mass-modified base. Through the use of MALDI-TOF mass spectrometry, the mass of the extended primer is determined.

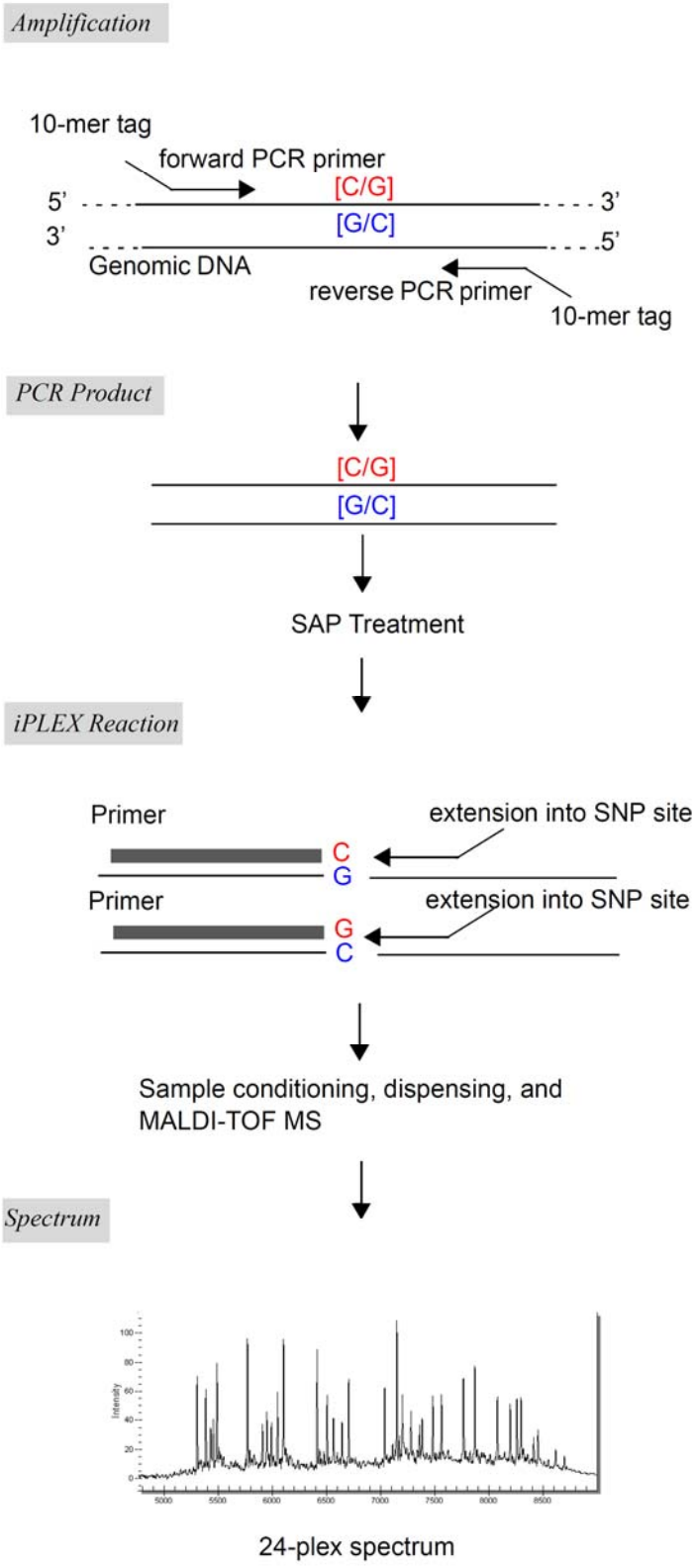

Figure 1.19 iPLEX Assay (The scheme depicts a single assay). The starting point of the iPLEX assay is PCR amplification, followed by the addition of Shrimp Alkaline Phosphatase (SAP) to inactivate remaining nucleotides in the reaction. Following a brief incubation, the primer mixture is added and conducted using a standardised cycling programme, placed on a SpectroChip and analysed by MALDI-TOF MS (diagram taken from *Oeth et al, 2006*, Sequenom Application Note Doc. No. 8876-006).

1.3 Introduction and Aims of thesis

The DLKP cell line has great potential for studying human lung cancer phenotypes for several reasons. First of all, although it is sensitive to most chemotherapeutic drugs, resistant variants can be readily generated[196,277]. Secondly, it is itself quite poorly invasive *in vitro*, but highly invasive variants can be readily generated[196,278,279]. Thirdly, it has been shown to contain at least three clonal subtypes which can interconvert through one of the clonal types only, and which have marked differences in invasiveness, adhesiveness, migration and anoikis resistance *in vitro*[280,281]. Finally, having been established from a tumour biopsy in our laboratory, it is available at early passage number, close to the patient tumour.

In the work described in this thesis, I have exploited the availability of clonal populations to investigate the time course and mechanism of development of resistance to a chemotherapeutic drug (mitoxantrone) and development of *in vitro* invasiveness and to investigate some aspects of the mRNA and protein expression changes associated with these changing phenotypes.

Aims

The aims of this thesis were as follows:

1. To examine the temporal relationship between emergence of drug resistance and invasiveness in a human lung carcinoma cell line model of mitoxantrone resistance development in order to better understand the link between multidrug resistance and cancer invasion.

2. To characterise the resistant phenotype of mitoxantrone resistant lung cancer cell lines – using toxicity assays, gene copy number assays, methylation assays, microarray expression analysis and proteomic analysis.

3. To use microarray analysis to search for changes which may be functionally significant in the transition from preinvasive to invasive phenotype in the newly developed lung cancer cell line models of mitoxantrone resistance.

4. To explore the association between the expression of ABC transporter proteins and cell signalling pathways.

5. To characterise, at the molecular level, three distinct clonal subpopulations of the lung cancer cell line DLKP which display different levels of *in vitro* invasiveness, and to identify reliable protein markers which could characterise these clones in a mixed cell population.

CHAPTER 2

Materials and methods

2.1 Cell lines and reagents

Table 2-1 outlines details and sources of the human lung tumour cell lines and their media components and serum concentrations used in this thesis. All cells were maintained under standard culture conditions, 5% CO_2 at 37°C. Cell culture procedures were strictly adhered to as outlined in NICB SOP. All cell lines were determined to be mycoplasma free; testing was carried out in-house. Table 2-2 outlines the chemotherapeutic drugs and inhibitors used in this project.

Table 2-1 Cell lines used in this thesis

Cell Line	Source	Media	Cell Type
DLKP parent	NICB	ATCC + 5% FCS	Human poorly differentiated lung carcinoma
DLKP-SQ McBride et al., 1998[280])	NICB	ATCC + 5% FCS	Intermediate Sub-Population Cloned from DLKP
DLKP-I (McBride et al., 1998[280])	NICB	ATCC + 5% FCS	Intermediate Sub-Population Cloned from DLKP
DLKP-M (McBride et al., 1998[280])	NICB	ATCC + 5% FCS	Intermediate Sub-Population Cloned from DLKP
SQ-Mitox-BCRP-4P	NICB	ATCC + 5% FCS	Mitoxantrone selected variant of DLKP-SQ
SQ-Mitox-BCRP-6P	NICB	ATCC + 5% FCS	Mitoxantrone selected variant of DLKP-SQ
SQ-Mitox-BCRP-6P (Isolate 1)	NICB	ATCC + 5% FCS	Mitoxantrone selected variant of DLKP-SQ
SQ-Mitox-MDR-4P	NICB	ATCC + 5% FCS	Mitoxantrone selected variant of DLKP-SQ
SQ-Mitox-MDR-6P	NICB	ATCC + 5% FCS	Mitoxantrone selected variant of DLKP-SQ
DLKP-A (Heenan *et al.,* 1997[277])	NICB	ATCC + 5% FCS	Adriamycin selected of DLKP
DLRP (Law *et al.,* 1992[282])	NICB	ATCC + 10% FCS	Human poorly differentiated lung carcinoma
Limbal stromal (O'Sullivan and Clynes[283])	NICB	DMEM + 10% FCS	Corneal epithelia

NICB: National Institute for Cellular Biotechnology, DCU, Dublin, Ireland. ATCC (Hams F12/DMEM 1:1)

Table 2-2 Chemotherapy drugs and inhibitors used in this project

Drug	Storage	Source
Mitoxantrone	Room temperature in dark	SVUH
Taxol	Room temperature in dark	SVUH
Epirubicin	4°C in dark	SVUH
Vinblastine	4°C in dark	SVUH
Irinotecan	-20°C	SVUH
Cisplatin	Room temperature in dark	SVUH
VP16	Room temperature in dark	SVUH
5FU	Room temperature in dark	SVUH
Elacridar (GF120918)	-20°C	Sequoia
PD98059	-20°C	Promega
U0126	-20°C	Promega
AZD6244	-20°C	Selleck

2.2 *In vitro proliferation assays*

Cells in the exponential phase of growth were harvested by trypsinisation. Cell suspensions containing 1×10^4 cells/ml were prepared in cell culture medium. To each well of a 96 well plate 100 µl of the cell suspension was added (Costar, 3599). Plates were agitated gently in order to ensure even dispersion of cells over the surface of the wells. Cells were incubated overnight. Cytotoxic drug dilutions were prepared at 2× their final concentration in cell culture medium. A volume of 100 µl of drug dilution was added to each well. Plates were mixed gently as above. Cells were further incubated for 6 – 7 days until the control wells had reached approximately 80-90% confluency. Assessment of cell survival in the presence of drug was determined by the acid phosphatase assay (section 2.2.2). The concentration of drug which caused 50% cell kill (IC_{50} of the drug) was determined by using Prism software from GraphPad Software (section 2.16). Results were graphed as percentage survival (relative to the control cells) versus cytotoxic drug concentration.

2.2.1 Combination toxicity assays

DLKP cells (2000 cells/well) were seeded into 96 well plates and incubated overnight as described in 2.2. Cytotoxic drug dilutions and MAPK kinase inhibitors (PD98059 and U0126)

were prepared at 2× their final concentration in cell culture medium. Elacridar (GF120918) was used as a control and prepared at 2× final concentration in cell culture medium. A volume of 100 µl of the final drug dilutions were added to each well and mixed gently. Cells were incubated for 48 hours. Assessment of cell survival in the presence of drug was determined by the acid phosphatase assay (section 2.2.2).

2.2.2 Assessment of cell number - Acid Phosphatase assay

Following the incubation period, media was removed from each plate/well. Each well on a plate was washed with 100 µl PBS. This was removed and 100 µl of freshly prepared phosphatase substrate (10 mM p-nitrophenol phosphate (Sigma 104-0) in 0.1 M sodium acetate (Sigma, S8625), 0.1% triton X-100 (BDH, 30632), pH 5.5) was added to each well. The plates were wrapped in tinfoil and incubated in the dark at 37°C for 2 hours. The enzymatic reaction was stopped by the addition of 50 µl of 1 M NaOH to each well. Plates were read in a dual beam plate reader at 405 nm with a reference wavelength of 620nm.

2.3 Extracellular matrix studies

2.3.1 *In vitro* invasion assays

Matrigel (BD Biosciences, 354234) was diluted to a working stock of 1 mg/ml in serum- free DMEM. Aliquoted stocks were stored at -20^{o}C. Invasion assays were performed using the method of Albini et al. (1987)[284]. A volume of 100 µl of matrigel was placed into each insert (BD Biosciences, 353097) (8.0µm pore size, 24 well format) and kept at 4 ^{o}C for 24 hours. The insert and the plate were then incubated for one hour at 37 ^{o}C to allow the proteins to polymerise. Cells were harvested and resuspended in culture media containing 5% FCS at 1×10^{6} cells/ml. Excess media/PBS was removed from the inserts, and they were rinsed with culture media. A volume of 100 µl of the cell suspension was added to each insert. A further 100 µl of culture media was added to each insert and 500 µl of culture media containing 5% FCS was added to the well underneath the insert. Cells were incubated for 24 hours.

To investigate the effect of MMP-2 (Millipore MAB13405) and MMP-10 (R&D Systems MAB9101) blocking antibodies on cell invasion, cells were seeded in culture media containing 5% FCS and 5µg/ml blocking antibody MMP-2 or 10µg/ml MMP-10.

To investigate the effect of the MAPK kinase inhibitor U0126 (Promega U0126 V112A) on cell invasion, cells were seeded in culture media containing 5% FCS and either 5μM or 10μM and 500 μl of culture media containing 5% FCS and either 5μM or 10μM was added to the well underneath the insert.

After the 24 hour incubation, the inside of the insert was wiped with a cotton swab dampened with PBS, while the outer side of the insert was stained with 0.25% crystal violet for 10 minutes and then rinsed in distilled water (dH2O) and allowed to dry. The inserts were viewed and photographed under the microscope. The invasion assays were quantified by counting cells in 10 random fields within a grid at 20× objective and graphed as the total number of cells invading at 200× magnification. A minimum of 2 inserts were used per sample tested.

2.3.2 Motility assay

Motility assays were carried out as described in section 2.3.1, without the addition of extracellular proteins.

2.3.3 Adhesion assay

The CytoMatrix SCREEN kit (Chemicon Millipore, ECM205) contains five individual 96-well plates, one each for fibronectin, vitronectin, laminin, collagen I and collagen IV. Each 96-well plate contains 12 × 8-well removable CytoMatrix Cell Adhesion Strips in a plate frame. The wells in rows A – G have been coated with a human ECM protein. Row H of each strip is coated with BSA which serves as a negative assay control. Cells are seeded onto the coated substrate. Subsequently, adherent cells are fixed and stained. Relative attachment was determined using absorbance readings. The CytoMatrix SCREEN kit was used according to the manufacturerer's instructions.

2.3.4 Preincubation of cells with matrigel coated flasks

Matrigel was coated onto flasks (1 ml/25 cm^2) at a concentration of 1 mg/ml. Flasks were shaken gently to ensure complete coverage of the bottom of the flask. The coated flasks were then placed at 4^oC overnight to allow the matrigel settle. Before seeding flasks with cells, the flasks were placed into an incubator at 37^oC for approximately 2 hours to allow the matrigel polymerise. The excess media in the flasks was then removed and fresh complete media

containing the cell suspension was added. Cells attached to the matrigel on the bottom of the flask and after 24 hrs were removed with 0.5 ml/25 cm^2 dispase (BD Biosciences, 354235). Dispase is a bacillus derived neutral metalo protease that recovers cells cultured on matrigel.

2.4 Zymography Assay

2.4.1 Collection of Conditioned Media

Cells were cultured until 50 – 60% confluent. Cells were washed 3× in serum-free (SF) media. Cells were incubated in SF media (12 ml/T75 cm^2 flask) for 60 min. After this time, cells were washed again 3× in SF media. A volume of 12mls of media was added to the cells and incubated for 72 hrs. After such time, conditioned media was collected, centrifuged for 5 min at 1000rpm, filter sterilised through a low-protein binding 0.22µm filter, concentrated (to 10× of the starting volume of the conditioned media) in a Vivaspin concentrator (Vivaspin-20, cat VS2012) with a 5 kDa cut-off and stored at –80°C.

2.4.2 Zymography of Matrix Metalloproteinases

Conditioned media supernatants were prepared in a 4× non-reducing loading buffer (Invitrogen, NP0007) before being separated on a 10% zymogram (gelatin) gel (Invitrogen, EC6175BOX) which allows for the visualisation of MMP-2 and MMP-9 or 12% zymogram (casein) gel (Invitrogen, EC6405BOX) which allows for the visualisation of MMP-10. The gels were run at a constant voltage of 125V, 45mA for 90 minutes, or until the bromophenol blue dye front reached the end of the gel, in a 1× Tris-Glycine SDS running buffer (Biorad, 161-0732). After electrophoresis, the gel was incubated with a 1× Zymogram Renaturing Buffer (Invitrogen Developing buffer (LC2671) containing 2.5% Triton-X100 (BDH, 30632), for 30 minutes at room temperature. The Renaturing Buffer is decanted, and 1× Zymogram Developing Buffer (Invitrogen LC2671) was added, followed by an additional 30 minute incubation at room temperature. Fresh Developing Buffer was added, and the gel incubated at 37°C overnight. The gel was stained with Brilliant blue G Colloidal Coomassie (Sigma, B2025).

2.5 Immunohistochemistry

2.5.1 Immunofluorescence studies on fixed cells

Aliquots of 30 µl of 1×10^6 cells/ml from actively growing cultures were plated directly onto 10 well, 7mm microscope slides (Erie Scientific Company, 465-68X). Cells were allowed to attach overnight. After such time, slides were washed 3× in PBS and allowed to air dry. Slides were then foil wrapped and stored at -80^{o}C until required. Cells were later thawed and fixed in ice-cold acetone for 5-10 minutes and allowed to air dry for 15 min prior to immunostaining. The primary antibody (table 2-3) was added and incubated for 1 hr at RT. Cells were washed 3× in PBS and secondary antibody, fluorescein isothicyanate-linked (FITC) anti-mouse IgG (Dako, F0261) which was diluted 1/40 was added for 30 min at RT. Secondary antibody was removed and cells washed as outlined. Slides were mounted with ProLong Gold mounting medium (P36930) and covered using a glass cover slip. Cells were viewed and photographed using a Nikon phase contrast microscope fitted with an FITC filter. Counterstaining was performed with propidium iodine nuclic acid stain (Invitrogen P3566).

2.5.2 Immunohistochemistry

All immunohistochemical (IHC) staining was performed using the DAKO Autostainer (DAKO, S3800) (table 2-4). Deparaffinisation and antigen retrieval was performed using Epitope Retrieval 3-in-1 Solution (pH 6) (DAKO, S1699) or the Epitope Retrieval 3-in-1 Solution (pH 9) (DAKO, S2375) and the PT Link system (DAKO, PT101). For epitope retrieval, slides were heated to 97°C for 20 minutes and then cooled to 65°C. The slides were then immersed in wash buffer (DAKO, S3006). On the Autostainer slides were blocked for 10 minutes with 200 µL HRP Block (DAKO, S2023). Cells were washed with 1× wash buffer and 200 µL of antibody added to the slides for 20 minutes. Slides were washed again with 1× wash buffer and then incubated with 200 µL Real EndVision (DAKO, K4065) for 30 minutes. A positive control slide was included in each staining run. Each slide was also run with Negative Control Reagent (1× TBS/0.05% Tween-20), to allow evaluation of non-specific staining and allow better interpretation of specific staining at the antigen site. All slides were counterstained with haematoxylin (DAKO) for 5 minutes, and rinsed with deionised water, followed by wash buffer. All slides were then dehydrated in graded alcohols (2 x 3 minutes each in 70% IMS, 90% IMS and 100% IMS), and cleared in xylene (2 x 5 minutes), and mounted with coverslips using DPX mountant (Sigma, 44581).

Table 2-3: Antibodies used in immunofluorescence analysis

Primary Antibody	Dilution	Company
N-cadherin	5 µg/ml	ab19348 Abcam
Piccolo, clone 4G3.3	1:300	Millipore
Robo-2	10 µg/ml	ab75014 Abcam
MMP-2	1:50	MAB13405 Millipore
MMP-10	1:50	MAB9101 R&D Systems
ALCAM	1:150	ab109215 Abcam

Table 2-4: Antibodies used in immunohistochemical analysis

Primary Antibody	Dilution	Company
BCHE	9 µg/ml	AV44208 Sigma
DSCAM	5 µg/ml	LS-B5787 LSBio

2.6 Western blot analysis

2.6.1 Preparation of Protein Lysates

2.6.1.1 Preparation of whole cell lysates

Cells were grown to 80-90% confluency in culture flasks (T75cm^2 flask), media was removed, cells were trypsinised, pelleted and washed twice in ice cold PBS. All procedures from this point forward were performed on ice. Cells were resuspended in 500µl (per T75cm^2 flask) RIPA lysis buffer (Sigma, R0278) containing 1× protease inhibitor (Complete MiniTM, 04693124001, Roche Diagnostics, GmbH) (Sigma, R0278) and incubated on ice for 20 minutes. Following centrifugation at 16,000 g for 5 minutes at 4°C the resulting lysate was stored at -80°C. Protein concentration was quantified using the Pierce BCA Protein Assay Kit (Cat no. 23227).

2.6.1.2 Preparation of membrane proteins

Membrane proteins were isolated from cells using the ProteoExtract Native Membrane Protein Extraction Kit (Calbiochem, 444810) and used according to the manufacturerer's instructions.

2.6.2 Gel Electrophoresis

Proteins for Western blotting were separated by SDS-PAGE gel electrophoresis (Laemmli *et al*., 1970[285]), using 4-12% gradient gels (Invitrogen NP0335, NP0321). Approximately 15µg of protein was applied to each well of the polyacrylamide gel. Pre-stained molecular weight markers (Invitrogen, LC5800) were also loaded onto the gel for the determination of the molecular weight of the protein samples. Gels were run at 200 volts and 250 milliamps for 1 - 1.5 hours with 1× MOPS, Tris/ Glycine/ SDS running buffer (Invitrogen, NP0001). When the dye front of the molecular weight markers had reached the end of the gel, electrophoresis was stopped.

2.6.3 Enhanced chemiluminescence (ECL) detection

Proteins were transferred to nitrocellulose membranes (Invitrogen, IB3010-01) using the iBlot transfer system (Invitrogen, IB1001). Protein transfer was visually confirmed using Ponceau S staining (Sigma, P7170). The membrane was blocked with 5% milk powder (170-6404, Biorad) in 0.1 % TBS-Tween (10× TBS, Sigma, T5912) at room temperature for 1 hour, then incubated overnight at 4°C in primary antibody (table 2-4) with 0.1 % TBS-Tween in 5 % milk powder. The membrane was washed three times with 0.5 % TBS-Tween and then incubated at room

temperature with secondary antibody (table 2-5) in 5 % milk powder with 0.5 % TBS-Tween for 1 hour. The membrane was washed three times with 0.5 % TBS-Tween followed by one wash with TBS alone. Immunoblots were developed using ECL reagents (Amersham, RPN 2105), which facilitated the detection of bound peroxidase-conjugated secondary antibody. Following the final washing membranes were incubated with ECL reagent and approximately 3 ml of a 50:50 mixture of ECL reagent was used to cover the membrane. The membrane was then exposed to Amersham HyperfilmTM, chemiluminescence film (GE Healthcare, 28906837) for various times (from 10 seconds to 30 minutes depending on the signal). The exposed autoradiographic film was developed for 3 minutes in developer (Kodak, LX-24). The film was then washed in water for 15 seconds and transferred to a fixative (Kodak, FX-40) for 5 minutes. The film was then washed with water for 5-10 minutes and left to dry at room temperature.

Table 2-5: List of primary, secondary antibodies and dilutions used in Western blot analysis

Primary Antibody	Dilution	Company
BCRP (BXP-21)	1:25	ALX-801-029 Enzo
P-gp (C219)	1:50	ALX-801-002 Enzo
Anti-EF1α, clone CBP-KK1	1:1000	05-235 Upstate-Millipore
Anti-human Integrin αV/CD51	1:1000	AF1219 R&D Systems
PA2G4/EBP1	1 µg/ml	LS-B6878 LSBio
DSCAM	1 µg/ml	LS-B5787 LSBio
ALCAM	1:1000	ab109215 Abcam
BCHE	1:800	AV44208 Sigma
SLIT2	1:1000	ab134166 Abcam
IGF1Rβ	1:200	IGF1Rβ (C-20):sc-713 Santa Cruz
pERK	1:1000	#9101 Cell Signaling
tERK	1:1000	#4695 Cell Signaling
GAPDH	0.05 µg/ml	R&R Systems
α-tubulin	1 µg/ml	Sigma
Swine Anti-Rabbit HRP	1/2000	P0399 Dako
Goat Anti-Mouse HRP	1/2000	P0477 DAKO
Goat Anti-Rabbit HRP	1/2000	P0448 DAKO

2.7 Human Phospho-MAPK array

The Human Phospho-MAPK array (catalog number ARY002B) was used to show the effect of the MAPK kinase inhibitor, U0126 on specific pathways. DLKP-I and DLKP-M cells were grown overnight on matrigel coated flasks (section 2.3.4). After 24 hrs, one flask of each was treated with 10 μM of the MEK inhibitor U0126 for 1 hour (DMSO used as control). Following the removal of the cells with dispase (section 2.3.4) the cells were rinced with PBS and solubilized at 1×10^7 cells/mL in Lysis Buffer 6. The lysates were pipetted up and down to resuspend and then gently rocked at 4°C for 30 minutes. They were then microcentrifuged at 14,000 × g for 5 minutes, and the supernatant transferred into a clean Eppendorf. Quantitation of sample protein concentrations was performed using the Pierce BCA Protein Assay Kit (Cat no. 23227) and the arrays were incubated with 250 μg of lysate.

2.8 RNA Analysis

2.8.1 RNA Extraction

RNA extraction was achieved using the Qiagen RNeasy mini kit (Qiagen, 74104), following the manufacturer's instructions. The RNA was then quantified spectrophotometrically at 260nm and 280nm using the NanoDrop® (ND-1000 spectrophotometer). The ND-1000 software automatically calculated the quantity of RNA in the sample based on an OD260 of 1 being equivalent to 40mg/mL RNA. The software simultaneously measured the OD_{280} of the samples allowing the purity of the sample to be estimated from the ratio of OD_{260}/OD_{280}. This was typically in the range of 1.8-2.0. A ratio of <1.6 indicated that the RNA may not be fully in solution. RNA samples were stored at -80 °C.

2.8.2 Reverse Transcriptase Reaction

To form cDNA, the following reagents (table 2-6) were mixed in a 0.5ml eppendorf (Eppendorf, 0030 121.023) heated to 72°C for 10 min and then cooled to 37°C. Added directly to this mixture was 4μl DEPC water and lμl Moloney murine leukaemia virus reverse transcriptase (MMLV-RT) (40,000U/μl) (Sigma, M-1302). The RT reaction was carried out by incubating the eppendorfs at 37°C for 1 hour. The MMLV-RT enzyme was inactivated by heating to 95°C for 5

min. The cDNA was stored at -20°C until required for PCR reactions as outlined in Section 2.8.3.

Table 2-6 Reaction components for reverse transcriptase reaction

Reaction Component	Reaction volume
25 mM $MgCl_2$ (Sigma, M-8787)	1.2µl
l0x PCR Buffer (Sigma, P-2317)	2µl
Oligo (dT) primers (0.5ng/µl) (MWG/Sigma)	2µl
dNTP's (10mM of each dNTP; Sigma, DNTP-100)	0.4µl
RNAsin (40U/µl) (Sigma, R-2520)	0.5µl
total RNA (500ng/ul)	2µl
DEPC water	6.9µl

2.8.3 Real-Time PCR

Taqman real time PCR was used for the mRNA quantification in this study. Real-time PCR is the technique of collecting data throughout the PCR process as it occurs, thus combining amplification and detection into a single step. Reactions are characterized by the point in time (or PCR cycle) where the target amplification is first detected. This detection occurs when the quencher dye that is found in the 3' end of the probe is separated from the fluorescent dye which is found in the 5' end of the probe due to cleaving of the probe with the target. This value is usually referred to as cycle threshold (Ct), the time at which fluorescence intensity is greater than background fluorescence. Consequently, the greater the quantity of target DNA in the starting material, the faster a significant increase in fluorescent signal will appear, yielding a lower Ct[286]. Ct is defined as the fractional cycle number at which the fluorescence passes the fixed threshold[287].

RNA was extracted (Section 2.8.1) and cDNA synthesised as per Section 2.8.2. The Taqman® Real Time PCR analysis was performed using the Applied Biosystems Assays on Demand PCR kits (TaqMan® gene expression assays) (table 2-7) on a 7900 fast real-time PCR instrument (Applied Biosystems). A volume of 22.5µl of qPCR master mix was added to was added to the relevant wells of a 96-well PCR plate (cat no. 4366932). A volume of 2.5µl of each cDNA sample was added to give a final reaction volume of 25µl. Each cDNA sample was analysed in

triplicate for the separate measurement of target gene expression and endogenous control (GAPDH). The components of the PCR were as follows are shown in table 2-8. The plate was then covered with an optical adhesive cover and placed in the ABI 7500 Real Time PCR instrument. The thermal cycling conditions were set using the default settings outlined in table 2-9. The sample volume was changed to 25µl and the run started.

Table 2-7 TaqMan assays used in this study

Gene	TaqMan assay catalog number
ABCB1	HS00184491_m1
ABCG2	HS00242273_m1
Actin	HS00184979_m1

Table 2-8 Components of Real Time PCR master mix

Reaction Component	Volume/well per 25µl reaction	Final Concentration
TaqMan universal PCR mastermix (2×) (Cat no. 4318157)	12.5µl	1×
20× assays on demand gene expression assay mix (primers)	12.5µl	1×
RNase –free water	8.75µl	-
cDNA	2.5µl	

Table 2-9 Thermal cycling conditions for TaqMan Gene Expression Assays

Stage	Temp (°C)	Time (mm:ss)
Hold	50	2:00
Hold	95	10:00
Cycle	95	0:15
(40 cycles)	60	1:00

Each real time PCR run was analysed on the 7500 system software under Relative Quantification ddCt study. A calibrator sample was selected and set to a value of one, allowing for the comparison of all other samples in relation to the calibrator. For the analysis of target gene or endogenous control amplification, the baseline was set to average, normalised fluorescent signal before detectable increase (usually 3-15 cycles) and the cycle threshold was set in the exponential part of the curve. The well information was then analysed. The Ct standard error was ideally less than +/-0.161. Ct errors with values greater than this were removed as outliers. The endogenous control was used automatically to normalise the data. When this was achieved for both the target and endogenous control, the relative quantity values for the run were generated and plotted relative to the calibrator sample.

2.9 Copy number assignment using real time qPCR

TaqMan Copy Number Assays are run simultaneously with a TaqMan Copy Number Reference assay in a duplex real-time polymerase chain reaction (PCR). The copy number assay detects the target gene of interest, and the Reference Assay detects a sequence that is known to exist in two copies in a diploid genome. In this study, the Reference Assay used is the RNase P H1 RNA gene. The number of copies of the target sequence in each test sample is determined by relative quantitation (RQ) using the comparative Ct (ΔΔCt) method. This method measures the Ct difference (ΔCt) between target and reference sequences, then compares the ΔCt values of test samples to a calibrator sample known to have two copies of the target sequence.

Quantitative PCR analysis of *ABCG2* and *ABCB1* gene content was performed in the SQ-Mitox cell line DNA samples using commercially available, predesigned TaqMan Copy Number Assays (Assay IDs: Hs00670096_cn and Hs02314130_cn for ABCB1 and ABCG2, respectively, each consisting of a pair of unlabeled primers and a FAM labeled, MGB probe) and the *RNase P* Copy Number Reference Assay, with a VIC-labeled TAMRA probe (Applied Biosystems, Foster City, CA). DNA was prepared using the Wizard SV Genomic DNA Purification System (Promega, A2360). The PCR consisted of 20 µl reactions containing 4 µl DNA (20 ng total gDNA), 10 µl Taqman Genotyping Master Mix (Applied Biosystems) and 1.0 µl each of one target gene and reference CNV assay mixes (20× working stock) and 4 µl nuclease-free water. Following the manufacturer's instructions, all qPCR reactions were run using four replicates on an ABI 7900HT instrument (Applied Biosystems) and thermal cycling conditions were 95°C, 10 min followed by 40 cycles of 95°C for 15 s and 60°C for 1 min.

2.10 Affymetrix GeneChips®

The microarray gene expression experiments carried out in this body of work were performed using Affymetrix GeneChips® Whole genome arrays (Affymetrix, 900470). Affymetrix GeneChip probe microarrays are manufactured using photolithography and combinatorial chemistry.

Table 2-10 Equipment required for microarray experiment

Item	Catalogue no.	Supplier
20× SSPE	US51214	Cambrex
Anti-Strep Biotinylated Ab (Goat)	BA-0500	LABKEM
Wheaton 1L sterile bottles	219980	Scientific
Herring sperm DNA	D1811	MSc
10% Tween 20	28320	MSc
BSA	15561-020	Biosciences
R-Phycoerythro Streptavidin	S-866	Biosciences
GeneChip Human Genome U133 Plus 2.0 Array	900470	Affymetrix
Test3 Array	900341	Affymetrix
One-Cycle Target Labelling Kit	900493	Affymetrix
Two-Cycle Target Labelling Kit	900494	Affymetrix
0.5M EDTA	E7889	Sigma
MES Free Acid Monohydrate	M5287	Sigma
MES Sodium Salt	M5057	Sigma
DMSO	D5879	Sigma
Goat IgG	15256	Sigma
Sodium Hypochlorite	42,504-4	Sigma
20× SSPE	85637	Sigma
5M NaCl, RNase-free, DNase-free	9760G	Ambion
1.5 ml eppys	12400	Ambion
0.5 ml eppys	12300	Ambion
Rnase Zap	9780	Ambion
RNA ladder	7152	Ambion
0.5M EDTA	9260G	Ambion
Rnase-free UHP	9932	Ambion
5× Megascript T7 kit	1334 (or B1334-5)	Ambion
Rneasy Mini Kit	74104	Qiagen
QIA Shredder	79656	Qiagen
RNA 6000 Nano Labchip Kit	5065-4476	Carl Stuart Ltd.

Tens to hundreds of thousands of different oligonucleotide probes are synthesised and located in a specific area on the microarray slide, called a probe cell. Each probe cell contains millions of copies of a given oligonucleotide and each feature size on the Affymetrix U133 plus 2.0 is 11 microns.

Microarray analysis was performed on RNA isolated from three biological repeat experiments (i.e. RNA was isolated from three independent stocks of the cells, each of which resulted in a set of data). Table 2-10 lists the items used in the analysis.

2.10.1 cDNA synthesis from total RNA

RNA was prepared using the RNeasy Mini Prep Kit® (QIAGEN, 74104) (section 2.8.1). The concentration of RNA was calculated using the Nanodrop (Nanodrop ND-1000, Labtech International, Ringmer, East Sussex, UK). The Agilent Bioanalyser was used to assess RNA qualitatively after isolation. cDNA was synthesised using the GeneChip® One-Cycle cDNA Synthesis Kit from l0 µg total RNA. Total RNA (10 µg), diluted poly-A RNA controls and T7-Oligo-dT) primer were mixed in a 0.2 mL PCR tube (table 2-2). RNase-free water was added to a final volume of 11 µL. The tube was gently flicked a few times to mix, and then centrifuged briefly to collect the reaction at the bottom of the tube. The reaction was then incubated for 10 minutes at 70°C. The sample was cooled at 4°C for at least 2 minutes. The tube was centrifuged briefly to collect the sample at the bottom of the tube. The First-Strand Master Mix was prepared by mixing 4 µl 5× First Strand Reaction Mix, 2 µl DTT (0.1M) and 1 µl dNTP (10mM) for a single reaction. A volume of 7 µl of First Strand Master Mix was added to each RNA/T7-Oligo (dT) Primer mix. The tube was mixed thoroughly be flicking the tube a few times and centrifuged briefly and then incubated for 2 minutes at 42°C. A volume of 2 µl of SuperScript II was then added to each RNA sample and the tube was mixed, centrifuged and immediately placed at 42°C for 1 hour and then cooled for at least 2 minutes at 4°C.

The Second-Strand Master Mix was prepared as shown on table 2-12 (for a single reaction). The tube was mixed and centrifuged. A volume of 130 µl of Second-Strand Master mix was added to each first-strand synthesis sample for a total volume of 150 µl. The tube was then mixed, centrifuged briefly and incubated for 2 hours at 16°C. A volume of 2 µl of T4 DNA polymerase was added to each sample and the tube was incubated for 5 minutes at 16°C. After incubation with T4 DNA Polymerase a volume of 10 µl EDTA (0.5M) was added. The double-stranded cDNA was then cleaned up using the GeneChip Sample Cleanup module (section 2.10.2).

2.10.2 Sample cleanup module cDNA cleanup

Sample cleanup was carried out using GeneChip Sample Cleanup module (Affymetrix, 900371), following the manufacturer's instructions. Biotin-labeled cRNA was then prepared using the GeneChip IVT Labeling Kit (section 2.10.3).

2.10.3 cRNA synthesis from cDNA IVT Amplification

The components listed in table 2-11 were added into a 1.5 mL eppendorf. The tubes were mixed centrifuged and then incubated at 16°C for 16 hours. The labelled cRNA was stored at -20°C, or at -70°C if not purifying immediately.

Table 2-11 cRNA synthesis from cDNA IVT amplification

Component	Volume (µl)
Template cDNA (total RNA 8.1 to 15 µg)	6
Water	14
10× IVT labelling buffer	4
IVT labelling NTP mix	12
IVT labelling enzyme mix	4
37°C overnight (16 hours)	

2.10.4 Biotin-Labeled cRNA Cleanup

Sample cleanup was carried out using GeneChip Sample Cleanup module (Affymetrix, 900371), following the manufacturer's instructions. The sample was run on the Agilent Bioanalyser (1:1 dilution) and concentration determined using the nanodrop (Read at A260, 1:50 dilution; in duplicate). The cRNA was stored at -20°C, or at -70°C if not quantitated immediately.

Table 2-12 cDNA reaction for total RNA (10µg)

Reaction	Volume (µl)
First strand cDNA synthesis:	
RNA + RNase free water	7
Diluted poly-A RNA controls	2
T7-Oligo(dT) Primer (50 µMol)	2
70°C for 10 min	
Cooled to 42°C.	
5× 1st strand buffer buffer	4
DTT (0.1 M)	2
dNTP's (10 mM)	1
42°C for 2 min	
Superscript II	2
42°C – 1 hr spin/ice	
Second strand cDNA synthesis:	
(< 90 min on ice)	
RNase free water	91
5× 2nd strand buffer	30
dNTP's (10mM)	3
E. coli DNA ligase	1
RNase H	1
E. coli DNA polymerase I	4
130 µl of second strand master mix was added to each of the first strand synthesis samples	
16°C for 2 hr (thermocycler)	
2 µl T4 DNA polymerase added	
16°C for 5 min.	
10µl 0.5M EDTA added to stop reaction.	
Spin/ice.	

2.10.5 Hybridisation of cRNA to chip

The components listed in table 2-13 (fragmentation reaction) were added into a 0.5 mL Eppendorf. The samples were incubated at 94°C for 35 minutes and then placed on ice. A aliquot was saved for analysis on the Bioanalyzer. Undiluted, fragmented cRNA samples were stored at -20°C or (-70°C for longer-term storage) until ready to perform the hybridisation.

The components listed in table 2-13 (hybridisation reaction for a single probe array) were added into a 1.5 mL Eppendorf. Volumes were scaled up for hybridisation to multiple probe arrays. The probe array was equilibrated to room temperature immediately before use. The hybridisation cocktail was heated to 99°C for 5 minutes in a heat block, transferred to a 45°C heat block for 5 minutes and then centrifuged at maximum speed for 5 minutes to remove any insoluble material from the hybridisation mixture. The array was pre-wet with 200 µl 1× Hybridisation Buffer and incubated at 45°C for 10 minutes with rotation. This buffer was then removed from the probe array cartridge and 200 µl of the clarified hybridisation cocktail was added. The probe arrays were then incubated at 45°C for 16 hours with rotation at 16 rpm.

Table 2-13 Hybridisation of cRNA to chip

Reaction	Volume (µl)
Fragmentation reaction: (15µg cRNA in 0.5ml Eppendorf)	
cRNA + water	15µg (1 to 24 µl)
5× fragmentation buffer	6
Incubate 35 min at 94°C	
Hybridisation reaction:	
Fragmented cRNA	15 µg
Control Oligonucleotide B2 (3 nM)	5
20× Eukaryotic Hybridisation Controls	15
Herring sperm DNA (10 mg/ml)	3
BSA (50 mg/ml)	3
2× Hybridisation buffer	150
DMSO	30
Water	to final vol. of 300 µl
Pre-wet chips	
Added 200µl 1× hybridisation buffer	
Rotated 15 min at 45°C, 60 rpm	
Removed buffer	
Hybridise chips	
Preheated hybridization solution – 5 min at 95°C	
45°C (for > 5min)	
Rotated overnight (16 hours) at 45°C, 60 rpm	

2.10.6 Fluidics on chip

The fluidics station was primed and the hybridisation solution was removed from the chips. The chips were then filled with 200 µl non-stringent buffer.

The SAPE and antibody solutions (tables 2-14 and 2-15) were added to the fluidics station and the fluidics protocol was run on the selected chips (EukGEvs450 for U133 Plus 2.0 chips). The Affymetrix Genechip Operating Software (GCOS) managed the fluidics protocol. All relevant data from the fluidics was stored in the Report file (*.RPT) for each chip.

Table 2-14 Preparation of SAPE solution

Reaction	Volume (µl)
SAPE solution (stains 1 & 3)	
2× stain buffer	600
50 mg/ml BSA	48
1 mg/ml SAPE	12
Distilled water	540
Total/chip	1200

Table 2-15 Preparation of antibody solution

Reaction	Volume (µl)
Ab solution (stain 2)	
2× stain buffer	300
50 mg/ml BSA	24
10 mg/ml goat IgG stock	6
0.5mg/ml biotinylated antibody	3.6
Distilled water	266.4

2.10.7 Chip Scanning

The chips were placed in the scanner and scanned. The GCOS software was used to manage the scanning protocol. The scan generated an initial image file (*.DAT) that contained the values for each gene probe. As there were 11 probes for each gene (one probeset), these values were averaged out into another file that was generated automatically by GCOS (*.CEL). The user then

gets GCOS to generate another file from the .CEL file which contains numerical values for each probeset (*.CHP). Finally, a quality control report file (*.RPT) is generated which is used to check the reliability/QC of each sample.

2.10.8 Microarray Data Normalisation

The purpose of data normalisation is to minimise the effects of experimental and technical variation between microarray experiments so that meaningful biological comparisons can be drawn from the data sets and that real biological changes can be identified in microarray experiments. Normalisation is the first step in the data analysis process. The challenge of normalisation is to remove as much of the technical variation as possible while leaving the biological variation untouched. Some of the common normalisation algorithms for Affymetrix arrays are MAS5[288], RMA[289] and dChip[290]. MAS5 developed by Affymetrix uses a reference (baseline) chip which is used to normalise all the experimental chips. The procedure is to adjust the intensity of each probe against the corresponding probes on the baseline chip; eliminate the highest 1% of probes (and for symmetry the lowest 1%), and fit a regression line to the middle 98% of probes. dChip uses an array with median overall intensity as the baseline array against which other arrays are normalised at probe level intensity. Subsequently a subset of PM ("perfect match") probes, with small within-subset rank difference in the two arrays (also known as invariant set), serves as the basis for fitting a normalisation curve. RMA employs normalisation at probe level using the quantile method. This normalisation method makes the chips have identical intensity distribution.

2.10.9 Microarray QC

The quality of the data generated with Affymetrix microarray chips was assessed based on different criteria including the scaling factor, background and noise levels, GAPDH 3′/ 5′ ratios and the %Present call.

Scaling factor

The scaling factor was the multiplication factor applied to each signal value on an array. A scaling factor of 1.0 indicates that the average array intensity was equal to the target intensity. Scaling factors vary across different samples and so there were no set guidelines for any particular sample type. However, Affymetrix advise that for replicates and comparisons

involving a relatively small number of changes, the scaling/normalisation factors (calculated by the global method) should be comparable among arrays. Larger discrepancies among scaling/normalisation factors (e.g., three-fold or greater) may indicate significant assay variability or sample degradation leading to noisier data.

Background and noise levels

Although there are no official guidelines regarding background, Affymetrix has found that typical average background values range from 20 to 100 for arrays scanned with the GeneChip® Scanner 3000. Arrays being compared should ideally have comparable background values. A high background implies that impurities, such as cell debris and salts, are binding to the probe array in a non-specific manner, and that these substances are fluorescing at 570nm (the detection wavelength). These non-specific binding causes a low signal-to-noise ratio (SNR), meaning that transcripts present at very low levels in the sample may be incorrectly called as "Absent". High background creates an overall loss of sensitivity in the experiment. The noise is a measure of the pixel-to-pixel variation of probes cells on a GeneChip array.

GAPDH 3′/ 5′ ratios

β-actin and GAPDH are used to assess RNA sample and assay quality for the majority of GeneChip® expression arrays. Specifically, the Signal values of the 3′ probe sets for -actin and GAPDH are compared to the Signal values of the corresponding 5′ probe sets. The ratio of the 3′ probe set to the 5′ probe set is generally no more than 3 for the 1-cycle assay. A high 3′ to 5′ ratio may indicate degraded RNA or inefficient transcription of ds cDNA or biotinylated cRNA. 3′ to 5′ ratios for internal controls are displayed in the Expression Report (.rpt) file.

% Present call

The number of probe sets called "Present" relative to the total number of probe sets on the array is displayed as a percentage in the Expression Report (.rpt) file. Percent present (%P) values depend on multiple factors including cell/tissue type, biological or environmental stimuli, probe array type, and overall quality of RNA.

Replicate samples should have similar %P values. Extremely low %P values are a possible indication of poor sample quality.

Quality inspection

The following Quality Controls were taken to estimate the quality of chip:

1. **Median Intensity:** Median intensity is the median intensity of the un-normalized probe values.
2. **P call %:** Calls indicate if the transcript is expressed or not. It can be 'P' for present, 'M' for marginally present and 'A' for absent. Total P calls in an array can vary widely based on the different nature of samples.
3. **% Signal outlier:** The signal value greater than 80th percentile multiplied by 3 is taken as signal outlier and is represented as % signal outlier.
4. **% Array outlier:** The array-outliers are the arrays whose probe pattern for selected probe set is different from the consensus probe pattern seen in most arrays.
5. **Warning**: If the array outlier increases over 5%, the chip is marked as outlier chip and is marked by '*', indicating potential image contamination or sample hybridisation problems of that array.

In addition to the above parameters, a manual inspection was also performed to estimate the quality of individual chips.

Hierarchical Clustering: Clustering is a way of finding and visualizing patterns in the data. It allows the grouping of objects based on similarity. In other words, it is the partitioning of a data set into subsets, so that the data in each subset share some common trait. Hierarchical clustering is a mathematical technique, the measure for a common trait is defined before the clustering is performed and is often a distance metric defining the relative similarity among two or more objects. The sample/genes with similar expression patterns are grouped together and are connected by a series of branches, which is called a dendrogram or clustering tree. Hierarchical

clustering was used to see how well the replicate samples cluster, identify any sub-groups in the samples and identify correlated genes.

2.10.10 Finding significant genes

In general, a combination of filtration criteria was used to pick up the differentially-regulated genes. These criteria are discussed below.

Fold change

Fold change is the ratio of mean of experimental group to that of baseline. It's a metric to define the gene's mRNA-expression level between two distinct experimental conditions. Fold change of 1.2, 1.5 and 2 was used for different types of analysis.

Difference

The difference of Affymetrix expression units was also taken for finding differentially-regulated genes. Difference of 100 was taken for most of the comparisons.

t-test

The t-test assesses whether the means of two groups are statistically different from each other. The output of the t-test is the p-value. The p-value of less than 0.05 was taken as significantly different.

Combination of parameters

A combination of a fold-change of 1.2, difference of 100 and p-value <0.05 was taken for up regulated genes. Similarly a combination of fold change of 1.2, difference of 100 and p-value < 0.05 was taken for down-regulated genes.

2.11 Proteomic analysis

Studies have shown that differential mRNA expression does not always correlate with protein expression[291,292]. Distinct changes may occur during the transformation of a healthy cell to a neoplastic cell that may not be apparent in gene changes. In addition, there may be less that 40% agreement between protein and mRNA levels in cultured cells, less for regulatory proteins like tyrosine kinases. The location, structure and function of proteins can also change dramatically within an organism due to malignant transformation, cell cycle and external/internal signalling.

2.11.1 Sample preparation

Cells were grown to 60-70% confluency in 175cm^2 flasks and trypsinised. Cell pellets were then washed twice in ice cold PBS and twice in sucrose buffer and the resulting pellet was stored at -80 ^{o}C.

2.11.2 Total protein extraction

All proteomic analysis detailed in this thesis was carried out by Dr. Paul Dowling. Cell pellets were reconstituted with 1ml of the following complete lysis buffer: (4% w/v CHAPS, 7 M urea, 2 M thiourea, 10 mM Tris-HCL, 5 mM magnesium acetate pH 8.5). Immediately before use, 10µl of 100x stocks of DNase and RNase were added to 1ml of lysis buffer. The lysate was then homogenised by passing through a 25-gauge needle 6 times. The cell lysate was placed on an orbital shaker and shaken for 1 hour at room temperature. The protein lysate was then transferred to an eppendorf and centrifuged at 14,000 rpm for 20 minutes at 10 ^{o}C to remove insoluble material. The resulting supernatant was transferred to a fresh microcentrifuge tube and its pH was checked to ensure it was between pH 8.0-9.0 by spotting 3 µl onto a pH indicator strip. The sample was then divided into smaller aliquots and stored at –80 ^{o}C. The protein concentration was quantified using the Biorad method. Biological replicates (n=3) of each cell line were prepared.

2.11.3 Protein sample labelling

2.11.3.1 Preparation of dye stock solution (1 nmol/µl)

The three CyDye DIGE Fluor Minimal dyes (Cy3, Cy5 and Cy2 (GE Healthcare, 25-8010-65) were thawed from –20^{o}C to room temperature for 5 minutes. To each microfuge tube dimethylformamide (DMF) (Aldrich, 22,705-6) was added to a concentration of 1 nmol/µl. Each microfuge tube was vortexed vigorously for 30 sec to dissolve the dye. The tubes were then centrifuged for 30 sec at 14,000 rpm in a microcentrifuge. The reconstituted dyes were stored at –20^{o}C for up to two months.

2.11.3.2 Preparation of 10 µl working dye solution (200 pmol/µl)

On thawing, the dye stock solutions were centrifuged in a microcentrifuge for 30 seconds. To make 10 µl of the three working dye solutions, 8 µl of DMF was added to 2 µl of 1 nmol/µl stock

of Cy2, Cy3 and Cy5 i.e. 200 pmol/µl working stock. The dyes were stored at -20 ^{o}C in tinfoil in the dark for 3 months.

2.11.3.3 Protein labelling

Protein samples equivalent to 50 µg were placed into eppendorf tubes and labelled with the Cy3 and Cy5 minimal dyes. Each tube was mixed by vortexing, centrifuged and then left on ice for 30 minutes in the dark. The reaction was quenched with a 50-fold molar excess of free lysine to dye for 10 minutes on ice in the dark. The labelled samples were stored at –80^{o}C. The Cy2 pool for each gel (50 µg) contained an equal concentration aliquot of each of the protein samples. To this 1 µl of each dye (200 pmol/µl) was added to 50 µg of protein sample. An equal volume of 2× sample buffer (2.5 ml rehydration buffer stock solution (7 M urea, 2 M thiourea, 4 % CHAPS), pharmalyte broad range pH 4-7 (2%) (GE Healthcare, 17-6000-86), DTT (2%) (Sigma, D9163)) was added to the labelled protein samples. The mixture was left on ice for at least 10 minutes then applied to Immobiline DryStrips for isoelectric focussing.

2.11.4 First dimension separation - isoelectric focussing

2.11.4.1 Strip rehydration

Immobiline 24 cm linear pH gradient (GE Healthcare, IPG) strips, pH 3-11 were rehydrated in rehydration buffer solution (7 M urea, 2 M thiourea, 4% CHAPS, 0.5% IPG buffer, 50 mM DTT). Each strip was overlaid with about 3 ml IPG Cover Fluid (GE Healthcare, 17-1335-01) and allowed to rehydrate overnight (or at least 12 hours) at RT.

2.11.4.2 Isoelectric focussing

IEF was performed using an IPGphor apparatus (GE Healthcare). The cover of the IPGphor unit was closed and the desired programme selected (40 kV/h at 20°C with resistance set at 50 mA). On completion of the IEF run, the strips were drained of the cover fluid and stored in glass tubes at –80^{o}C or used directly in the second dimension.

2.11.5 Second Dimension – SDS polyacrylamide gel electrophoresis

2.11.5.1 Equilibration of focussed Immobiline DryStrips

Strips were equilibrated for 20 min in 50 mM Tris-HCL, pH 8.8, 6 M urea, 30% v/v glycerol, 1% w/v SDS containing 65 mM DTT and then for 20 min in the same buffer containing 240 mM iodoacetamide. The 12.5 % acrylamide gel solution was prepared in a glass beaker (acrylamide/bis 40 %, 1.5 M Tris pH 8.8, 10 % SDS). Prior to pouring, 10 % ammonium persulfate and 100 µl neat TEMED were added. The gels were overlaid with 1 ml saturated butanol. The gels were left to set for at least three hours at RT. Equilibrated IPG strips were transferred onto 24 cm 12.5% uniform polyacrylamide gels poured between low fluorescence glass plates. Strips were overlaid with 0.5% w/v low melting point agarose in running buffer containing bromophenol blue. Gels were run at 2.5 W/gel for 30 min and then 100 W total at 10°C until the dye front had run off the bottom of the gels. All the images were collected on a Typhoon 9400 Variable Mode Imager (GE Healthcare).

2.11.5.2 Scanning DIGE labelled samples

The appropriate emission filters and lasers were then selected in the Typhoon Variable Mode Imager (GE Healthcare) for the separate dyes (Cy2 520 BP40 Blue (488), Cy3 580 BP30 Green (532) and Cy5 670 BP 30 Red (633)). Gels were scanned at 100 pixel resolution, resulting in the generation of three images, one each for Cy2, Cy3 and Cy5. Once the scanning was completed, the gel images were imported into the ImageQuant software. All gels were cropped identically to facilitate spot matching in the Decyder BVA module (version 6.5).

2.11.6 Analysis of gel images

2.11.6.1 Differential in-gel analysis (DIA)

The DIA module processes a triplet of images from a single gel. The internal standard is loaded as the primary image followed by the secondary and tertiary image, derived from, for example, a control and treated sample. Spot detection and calculation of spot properties were performed for each image from the same gel. The software determined the margins of the spots, quantified the spot intensities and calculated the relative spot intensity as the ratio between the total intensity of the gel and the intensity of each individual spot. The protein spots were then normalised using the in-gel linked internal standard. The data from the first gel was XML formatted and exported

into the Biological Variation Analysis (BVA) software for further analysis. This procedure was repeated for each gel in the experiment.

2.11.6.2 Biological variation analysis (BVA)

Once all gels from the experiment were loaded into the BVA module, the experimental design was set up and the images were assigned into three groups (standard, control and treated). The spots on the gels were then matched across all gels in the experiment.

This module detects the consistency of the differences between samples across all the gels. The software standardises the relative spot intensity of the Cy5 image to that of the Cy3 image in the same gel. The standardised spot intensity was then averaged across the triplicate gels. The BVA module calculates the degree of difference in the standardized protein abundance between 2 spots from different groups and expressed these differences as average ratio. The values by the software are displayed in the range of $-\infty$ to -1 for a decrease in expression and +1 to $+\infty$ for an increase in expression. For example, a two-fold increase and decrease is represented by +2 and-2, respectively (not by 2 and 0.5). The 'average ratio' has been termed as 'fold change' in this thesis. The software also calculates the consistency of the differences between samples across all the gels and applies statistics to associate a level of confidence (p-value) for each of the differences. The spots with statistically significant changes in protein expression ($\pm$1.2 fold with p-value $\leq$ 0.05) were considered as differentially expressed proteins. A $\pm$1.2 fold change was chosen with p-values less than 0.05 to look for even subtle changes in expression across the cell lines.

The protein spots with statistically significant protein expression changes were designated "proteins of interest" and placed in a pick list. Preparative gels for spot picking with 300 µg of protein/gel were focussed and run out on SDS-PAGE gels. The gels were then stained with colloidal coomassie and deep purple (section 2.14.3, 2.14.4). Spots that showed differential protein expression were picked with the ETTAN Spot Picker (section 2.14.3).

2.11.6.3 Staining- Brilliant blue G Colloidal coomassie staining of preparative gels for spot picking

After electrophoresis, the smaller lower plates with the gels attached were placed in the gel boxes containing fixing solution (7% glacial acetic acid in 40% (v/v) methanol (Aldrich, 200-659-6))

for at least 1 hour. During this step a 1× working solution of Brilliant Blue G colloidal coomassie (Sigma, B2025) was prepared by adding 800ml UHP to the stock bottle. When the fixing step had nearly elapsed a solution containing 4 parts of 1× working colloidal coomassie solution and 1 part methanol was made, mixed by vortexing for 30 seconds and then placed on top of the gels. The gels were left to stain for 2 hours. To destain, a solution containing 10% acetic acid in 25% methanol was poured over the shaking gels for 60 seconds. The gels were then rinsed with 25% methanol for 30 seconds and then destained with 25% methanol for 24 hours. Alternatively, after fixing solution, gels were washed 3 times in wash buffer (35 mM sodium hydrogen and 300 mM sodium carbonate in water) and further washed in water. Deep purple stain (GE Healthcare, RPN6305) was then added to the gels, diluted 1/200 in water, and incubated for 1 hr. Gels were destained in 7.5% (v/v) acetic acid in the dark for 15 min and repeated. The glass surface was dried and two reference markers (GE Healthcare) attached to the underside of the glass plate before scanning. The resulting image was imported into the ImageMaster software (GE Healthcare) and the spots were detected, normalised and the reference markers selected. All spots of interest were manually selected. The resulting image was saved and exported into the Ettan Spot Picker software.

2.11.6.4 Spot picking

The stained gel was placed in the tray of the Ettan Spot Picker (GE Healthcare, 18- 1145-28) with reference markers (GE Healthcare, 18-1143-34), aligned appropriately and covered with UHP. The imported pick list was opened, the syringe primed and the system was set up for picking the spots from the pick list. The spots were robotically picked and placed in 96-well plates (Greiner), which were stored at 4^{o} C until spot digestion.

2.11.6.5 Spot digestion

The 96-well plate was placed in the Ettan Digester (GE Healthcare, 18-1142-68) to digest the protein. The gel plugs were washed 3 times for 20 minutes each with 50µl 50mM ammonium bicarbonate (Sigma, A6141) in 50% methanol, followed by 3 × washes for 15 min with 50µl 70% acetonitrile (Sigma, 34967). The gel plugs were left to dry. After drying, the individual gel pieces were rehydrated in 10µl digestion buffer (12.5ng trypsin (Promega, V5111) per µl of 10% acetonitrile, 40mM ammonium bicarbonate). Exhaustive digestion was carried out overnight at 37^{o}C. A volume of 40µl of 0.1% trifluoroacetic acid (Sigma, 302031) in 50% acetonitrile was

added to the wells, mixed and left for 20 minutes. A volume of 60µl of this solution was transferred to a fresh 96 well plate. A volume of 30 µl of 0.1% trifluoroacetic acid in 50% acetonitrile was added to the wells, mixed and left for 20 minutes. A volume of 50µl of this solution was transferred to the fresh 96-well plate. The liquid in the plate was vacuum-dried in a Maxi dry plus (Speed Vac, MSC, Dublin). After drying, the 96-well plate was placed in the Ettan Spotter (GE Healthcare, 18-1142-67) for spotting onto the target plates. A volume of 3 µl of 0.5% trifluoroacetic acid in 50% acetonitrile was added to desiccated peptides and mixed 5 times. A volume of 0.3 µl of this mixture was spotted onto the target plate after which a volume of 0.3 µl matrix solution [7.5 mg/ml a-cyano-4-hydroxycinnamic acid (LaserBio labs, 28166-41-8) n 0.1% trifluoroacetic acid in 50% acetonitrile] was added.

2.11.6.6 Identification of proteins with MALDI-TOF

The target plate was placed in the MALDI-ToF (GE Healthcare, 11-0010-87) instrument. Spectra were acquired by selective accumulation of 250 individual laser shots and processed using Ettan MALDI evaluation software. The spectra were internally calibrated with trypsin enzyme autolysis peptide peaks at m/z 842.51 and m/z 2211.10, and externally calibrated with Pep4 mix with the five individual peaks covering the 500-3500 Da mass range and include bradykinin fragment 1-5 (573.315), angiotensin II human(1046.5424), neurotensin (1672.9176) and insulin Bchain oxidised (3494.6514). Known contaminant peaks were removed from the resulting mass spectra and remaining sample-related peaks were used for database searching. The identification sequencing method were set for the mass range 0-300kDa, pI 1-14, missed cleavage 1. The artificial modifications of peptides (carbamidomethylation of cysteines and partial oxidation of methionines) were also considered. Protein identification was achieved using Ettan MALDI-ToF Pro evaluation software (GE Healthcare) incorporating the ProFound database search engine for peptide mass fingerprints. The sequence database searched was the NCBI-nr database (2007/12/02) using subset species Homo sapiens and NR_NICB_Human070308. Protein identifications were accepted if they could be established at greater than 99% probability and had at least 3 identified peptides. The unidentified protein spot that had promising spectr um to get identification were desalted and concentrated using C-18 Zip-Tips (Millipore) and were reanalysed by MALDI-ToF MS to get identification. For this, the mixtures of tryptic peptides from individual samples were desalted using Millipore C-18 Zip-

Tips (Millipore) and eluted onto the sample plate with the matrix solution (5 mg/mL CHCA in 50% ACN/0.1% TFA V/V) and analysed with MALDI-ToF.

2.12 Methylation analysis

2.12.1 Bisulfite modification of genomic DNA

DNA (2 μg) obtained from cell lines was submitted to bisulfite modification using the EpiTect Bisulfite Kit (Qiagen, 59104) following the manufacturer's protocol. Bisulfite-treated DNA was resuspended in 20μl elution buffer and was used in the MethyLight assay. Since accurate quantification of DNA after bisulfite treatment was not possible due to its high degradation, the presence of amplifiable DNA was tested by real time PCR using a primer pair and a Taqman probe for the bisulfite converted sequence of a non-CpG-containing region of β-actin (section 2.12.5).

2.12.2 MethyLight assay

MethyLight assays were done using established protocols according to the protocol of QIAGEN EpiTect MethyLight PCR kit (59496, QIAGEN). Briefly, CpG island sequences were identified using the University of California Santa Cruz genome browser (http://genome.ucsc.edu/ webcite). MethyLight primers were designed usung MethPrimer (section 2.10.3) and Taqman probes were designed manually inhouse. Sequences of primers and probes are listed in table 2-16 (PrimeTime Mini qPCR Assay, Integrated DNA Technologies, IDT). DLKP-SQ and SQ-Mitox-BCRP-4th pulse DNA was converted using EpiTect Bisulfite Kit (Qiagen). For MethyLight, 1 μl of bisulfite-converted DNA solution was combined with 0.4 μM of each primer and 0.2 μM of probe in 1× EpiTect MethyLight master mix.

Amplification was carried out at 95°C for 5 min, followed by 40 cycles at 95°C for 15s, 60°C for 60s in an ABI 7500 Real-Time PCR cycler. The EpiTect Control DNA set were used as methylation controls (59695, QIAGEN).

Table 2-16 MethylLight primer and probe sequences

IDT primers/probes	Gene	Sequense	Type
Prime Time ABCG2-m	ABCG2-m.p	ACTTCCTAAACCGCGCTTCGAACTA	Probe
Prime Time ABCG2-m	ABCG2-m.s	ATTGCGTTTAGTTTTGGCG	Primer
Prime Time ABCG2-m	ABCG2-m.as	AACGAACTCAAACAACGCTA	Primer
Prime Time ABCG2-nm	ABCG2-nm.p	aAACTTCCTAAACCaCaCTTCaAACTATAAAC	Probe
Prime Time ABCG2-nm	ABCG2-nm.s	GGTTATTGTGTTTAGTTTTGGT	Primer
Prime Time ABCG2-nm	ABCG2-nm.as	AAACAAACTCAAACAACACTAAC	Primer
Prime Time ACTB-bis	ACTB.p	ACCACCACCCAACACACAATAACAAACACA	Probe
Prime Time ACTB-bis	ACT-bis.s	TGGTGATGGAGGAGGTTTAGTAAGT	Primer
Prime Time ACTB-bis	ACT-bis.as	AACCAATAAAACCTACTCCTCCCTTAA	Primer

m – methylated; nm – non methylated; bis – bisulfite; m.p – methylated probe; m.s – methylated sense; m.as – methylated antisense.

2.12.3 MethyLight primer and probe sequences

Three sets of inhouse PCR primers and probes, designed specifically for bisulfite converted DNA sequences were used: a set representing fully methylated and fully unmethylated DNA for the ABCG2 gene, and an internal reference set for the ACTB gene to control for input DNA. The methylated and unmethylated primers and the probe were designed to overlap the CpG dinucleotide site of ABCG2. The primer and probe sequences are listed above in table 2-16. In all cases, the first primer listed is the forward PCR primer, the second is the TaqMan® probe and the third is the reverse PCR primer.

The primer and probe sequences were designed using the web-based tool MethylPrimer Express (Applied Biosystems). MethylPrimer Express is a program for designing PCR primers for primers for bisulfite sequencing (BSP) and/or for methylation-specific PCR (MSP). The software searches DNA sequences for CpG islands, simulates bisulfite modification on the CpG-containing sequences, then recommends primer pairs for MSP or BSP. Primer design for either method can be adjusted to accommodate variation in experimental design.

2.12.4 Methylation Controls

The EpiTect PCR Control DNA Set (59695, Qiagen) consists of three different types of human DNA.:

- Amplified human genomic DNA (completely unmethylated)
- Completely unmethylated human genomic DNA – bisulfite converted
- Completely methylated human genomic DNA – bisulfite converted

The unmethylated and unconverted human control DNA of the EpiTect PCR Control DNA Set allows us to check that primers designed for the specific detection of unmethylated and converted DNA (U-converted DNA), and for methylated, converted DNA (M-converted DNA) do not bind to untreated genomic DNA. In case bisulfite conversion was not complete, leaving certain unmethylated C residues unconverted, false positives would result if the primer specific for M-converted DNA binds to untreated gDNA. This control DNA can also be used to check conversion efficiency during bisulfite treatment.

2.12.5 MethyLight Primer/Probe Preparation

The MethyLight assay utilises the TaqMan PCR principle which requires forward and reverse primers as well as an oligomeric probe which emits fluorescence only after it is degraded by the 5'-3' exonuclease activity of Taq polymerase. Each PCR reaction uses the same basic reaction set-up – the choice of primer/probe sets is the only variable in these reactions. All primer/probe sets used are diluted to the same stock concentrations to standardise the PCR reaction set-up as well as the running of the PCR program.

Designing primers and probes to target and amplify small regions of fully methylated bisulfite-modified DNA of the promoter CpG island of interest and analysing the ratio between this reaction and an endogenous control reaction (*ACTB*), which is impartial to methylation status, provides a measure for the frequency of methylated molecules at a given locus.

2.12.6 Checking the specificity of primers and PCR conditions

The presence of amplifiable DNA was tested by real time PCR using a primer pair and a Taqman probe for the bisulfite converted sequence of a non-CpG-containing region of β-actin. The Ct values obtained when using control DNA and ACTB primer pairs are shown in table 2-17.

Table 2-17 Primer for unmethylated actin gene

Sample	Ct (Ct std err)
Unmethylated control DNA	Undetermined
Unmethylated control DNA (bisulfite converted)	30.373 (0.366)
Methylated control (bisulfite converted)	28.997 (0.407)
No template control	Undetermined

2.12.7 5-Aza-2' deoxycytidine (5-aza-dC) treatment of DLKP-SQ cells

Cell viability was assessed using the acid phosphatase assay (section 2.2) and 5-Aza-dT concentrations up to 5μM were shown to have a minimal effect (approx. 10%) on cell viability. DLKP-SQ, Sq-Mitox-MDR and SQ-Mitox-BCRP cells were incubated in ATCC with 1μM of DNA methyltransferase inhibitor, 5-aza-2-deoxycytidine (5-aza-dC) (Sigma Chemical Company). After culture for 24 hours, cells were treated with 1μM 5-aza-dC for 72 hours. Whole cell lystates were prepared as outlined in section 2.6.1.1 and 10μg of protein from each sample were separated by Western blotting as outlined in section 2.6.2.

2.13 microRNA Expression Analysis

Megaplex™ Pools (Table 2-18) are designed to detect and quantitate up to 380 microRNAs (miRNAs) per pool in either human, mouse, or rat species using Applied Biosystems real-time instruments. The TaqMan® Array Human MicroRNA A card v2.0 contains 384 TaqMan microRNA Assays enabling quantitation of 377 human microRNAs. Three TaqMan MicroRNA Assay endogenous controls are included to aid in data normalization and one TaqMan® MicroRNA Assay not related to human is included as a negative control. The TaqMan® Array Human MicroRNA B Card v2.0 contains 290 TaqMan® MicroRNA Assays. Megaplex Pools consist of matching primer pools and TaqMan® Arrays:

- **Megaplex™ RT Primers** is a set of two predefined pools (Pool A and Pool B) of up to 380 stem-looped reverse transcription (RT) primers per pool that enable the simultaneous synthesis of cDNA for mature miRNAs.
- **Megaplex™ PreAmp Primers** (Optional) is a set of two pools (Pool A and Pool B) of gene-specific forward and reverse primers intended for use with very small

quantities of starting material. The primers enable the unbiased preamplification of the miRNA cDNA target by PCR prior to loading the TaqMan®MicroRNA Array. These primers were used for this study even though large quantities of starting material were available as it gives a better signal.

- **TaqMan® MicroRNA Arrays** is a set of two 384-well microfluidic cards (Array A and Array B) containing dried TaqMan primers and probes. The array enables quantitation of gene expression levels of up to 380 miRNAs and controls without the need to use multi-channel pipettors to fill the card. This is accomplished by loading the cDNA product (with or without preamplification) onto the array for PCR amplification and realtime analysis.

Table 2-18 Materials for microRNA Expression Analysis

Description	Part No.
TaqMan Human Micro RNA Array A	4398977
TaqMan Human Micro RNA Array B	4398978
MegaPlex RT & Preamp Human Pool Set	4401091
M-Plex RT Primers Human Pool A	4399966
M-Plex RT Primers Human Pool B	4399968
M-Plex Preamp Primers Human Pool A	4399233
M-Plex Preamp Primers Human Pool B	4399201
TaqMan MicroRNA RT kit	4366596
MirVana™ miRNA isolation kit	AM1560

2.13.1 Overall workflow

1. Isolate total RNA that contains small RNAs such as miRNA, siRNA, and snRNA.
2. Convert miRNA to cDNA prior to real-time PCR quantitation.
3. Dilute RT product.
4. TaqMan® Universal Master Mix II is added to each sample and pipetted into the sample loading ports of a TaqMan® Array Card.

5. The Taqman array card is run, performing real-time PCR. Resulting data analysed.

2.13.2 Run Megaplex Pools with Preamplification

2.13.2.1. Prepare the Megaplex RT Reaction

The MegaPlex RT reverse transcription kit components were thawed on ice. The dNTPs were vortexed after thawing. The directions and volumes listed below were for a single sample and were scaled appropriately using 2.2× volumes. A separate master mix was prepared for both M-Plex RT Primers Human Pool A and M-Plex RT Primers Human Pool B. The tube was inverted six times to mix, then the tubes were centrifuged briefly. A volume of 3µl (300ng) total RNA (or 3µL of water for the NoTemplate Control reactions) were placed into each tube containing the RT reaction mix. The tubes were inverted six times and spun briefly. The tubes were placed on ice for 5 mins. The run method was set up as shown in table 2-19 for a total reaction volume of 7.5 µL. The thermal cycling conditions are documented in table 2-20.

Table 2-19 Preparation of RT master mix

Component	Vol 1 × sample (µl)	Vol 10 × samples (µl)
Megaplex RT Primers (10×)	0.80	9.00
dNTPs with dTTP (100mM)	0.20	2.25
MultiScribe™ reverse transcriptase, (50 U/µl)	1.50	16.88
10X RT Buffer	0.80	9.00
$MgCl_2$	0.90	10.12
RNase inhibitor, 20U/µl	0.125	1.25
Nuclease-free water	0.20	2.25
Total	4.50	50.62

Table 2-20 Thermal–cycling conditions for Megaplex RT Reaction

Stage		Temp	Time
Cycle (40 Cycles, each of…)	(i)	16°C	2 min
	(ii)	42°C	1 min
	(iii)	50°C	1 sec
HOLD		85°C	5 min
HOLD		4°C	∞

2.13.2.2. Run the preamplification reaction.

The PreAmp reaction mix was prepared in a 1.5 mL microcentrifuge tube as shown in table 2-21. The microcentrifuge tubes were capped and mixed gently. The tubes were centrifuged to eliminate air bubbles from the mixture, and placed on ice. The thermal cycling conditions are documented in table 2-22. The tubes were then briefly centrifuged and a volume of 75 µl 0.1× TE pH 8.0 was added.

Table 2-21 Preparation of PreAmp reaction mix

PreAmp Reaction MixComponent	Vol 1 × sample (µl)	Vol 10 × samples (µl)
TaqMan® PreAmp Master Mix, 2×	12.5	140.62
Megaplex™ PreAmp Primers (10×)	2.5	28.13
Nuclease-free water	7.5	84.37
Total	22.5	253.12

Table 2-22 Thermal–cycling conditions for PreAmp reaction

Stage		Temp	Time
HOLD		95°C	10 min
HOLD		55°C	2 min
HOLD		72°C	2 min
Cycle (12 Cycles, each of…)	(i) (ii)	85°C 60°C	15 sec 4 min
HOLD		99.9 °C	10 min
HOLD		4°C	∞

2.13.2.3. Run the real-time PCR reaction

The PCR reaction mix was prepared in a 1.5 mL microcentrifuge tube as shown in table 2-23. The tubes were inverted to mix and then centrifuged briefly. The array was loaded and run as outlined in section 2.13.2.4.

Table 2-23 Preparation of Real-Time PCR reaction

Component	Volume for One Array (µl)
TaqMan Universal PCR Master Mix, No AmpErase UNG, 2×	450
Diluted PreAmp product	9
Nuclease-free water	441
Total	900

2.13.2.4. Loading and running the Taqman Array.

When the TaqMan array had equilibrated to room temperature, the card was carefully removed from the packaging, and placed foil side down on the lab bench. A volume of 100 µl of the RT reaction-specific PCR reaction mix was loaded into the corresponding ports. This was dispensed so that it went in and around the fill reservoir toward the vent port; the entire 100 µl was pipetted into the fill reservoir.

The TaqMan Arrays were centrifuged and sealed according to the user bulletin: Applied Biosystems TaqMan® Low Density Array (P/N 4371129). The set up and running of the plated document were carried out following the user bulletin: Applied Biosystems TaqMan® Low Density Array (P/N 4371129) and Applied Biosystems 7900HT Fast Relative Quantitation Using Comparative C_T Getting Started Guide (P/N 4364016). The analysis of the PCR reactions was carried out with reference to the SDS online help, 7900HT system user guide and troubleshooting using the Megaplex Pools Protocol (P/N 4399721).

2.14 Sequenom Oncogenotype Mutational Analysis

The Sequenom oncogenotype mutational analysis carried out in this study was outsourced to Professor Bryan Hennessy's laboratory, Department of Medical Oncology, Royal College of Surgeons in Ireland, Beaumont Hospital, Dublin 9. The Sequenoms Mass-ARRAY® system is a mass spectrometry based technique aimed at evaluating single nucleotide polymorphisms (SNPs), which can facilitate rapid, high-throughput and cost-effective detection of hot-spot gene mutations. Mutations were identified in the DNA isolated from the cell lines using the Sequenom Mass-ARRAY® system (See section 1.2.6).

DNA extraction was achieved using the Qiagen QIAamp genomic DNA kit (Qiagen, 513304) and approximately 500 ng of each cell line was submitted at a concentration of 10 ng/µl. The technique involves a PCR reaction which amplifies the region of the DNA to be sequenced, followed by a clean-up reaction where shrimp alkaline phosphatase (SAP) is added to remove excess nucleotides. An iPLEX assay was then carried out, where the primer and amplified target DNA were incubated with dideoxynucleotide terminators which have a modified mass. Using these terminators the DNA is extended by one base. Prior to sequencing, 6mg of clean resin was added to each sample, and samples were spotted directly from the PCR plate onto a Sequenom Spectrochip using the Sequenom nanodispenser RS1000. Transferred volumes were checked to ensure they were greater than 5nL and less than 20nL. If the volume was less than or greater than this, the speed of the machine was adjusted until the target volume was achieved. Spotted spectrochips were run on the MassArray Analyser Compact and through the use of MALDI-TOF mass-spectrometry the mass of the extended primer is determined. The mass of the primer indicates the sequence and, therefore the alleles present at the polymorphic site of interest. The mass of the observed primers can then be translated into a genotype for each reaction[20]. The aquisition parameters were: Shots (number of laser shots attempted during processing)-15, maximum acquisitions-9, minimum good spectra (Number of spectra collected before starting analysis) -5, maximum good spectra (Acquisition stops after this number) -5. The Sequenom panel used in this analysis offers parallel analysis of 284 mutations (Appendix 1).

2.15 RNA interference (RNAi)

RNAi using small interfering RNA's (siRNAs) was carried out to silence specific genes. The siRNAs used were chemically synthesised (Ambion Inc). These siRNAs were 21-23 bps in length and were introduced to the cells via reverse transfection with the transfection agent siPORT NeoFX^{TM} (Ambion Inc., 4511).

2.15.1 Transfection optimisation

In order to determine the optimal conditions for siRNA transfection, optimisation with kinesin siRNA (Ambion Inc., 16704) was carried out for each cell line. There were a number of different parameters that had to be determined to establish an optimised protocol for the siRNA transfection of the DLKP cells.

Cell suspensions were prepared at 1×10^5, 3×10^5 and 5×10^5 cells per ml. Solutions of negative control and kinesin siRNAs at a final concentration of 30nM were prepared in optiMEM (Gibco^{TM}, 31985047). NeoFX solutions at a range of concentrations were prepared in optiMEM in duplicate and incubated at room temperature for 10 minutes. After incubation, either negative control or kinesin siRNA solution was added to each NeoFX concentration. These solutions were mixed well and incubated for a further 10 minutes at room temperature. To each well of a 6-well plate 100µl of the siRNA/NeoFX solutions was added. A volume of 1 ml of the relevant cell concentrations were added to each well. The plates were mixed gently and incubated at 37°C for 24 hours. After 24 hours, the transfection mixture was removed from the cells and the plates were fed with fresh medium. The plates were assayed for changes in proliferation at 72 hours using the acid phosphatase assay (Section 2.2.1). Optimal conditions for siRNA transfection were determined as the combination of conditions, which gave the greatest reduction in cell number after kinesin siRNA transfection and also the least cell kill in the presence of transfection reagent. The optimised conditions for the DLKP cell lines were 2µl NeoFx to transfect 30nM siRNA in a cell density of $2\times l0^5$ per well of a 6-well plate.

2.15.2 Proliferation assays on siRNA transfected cells

Cells were seeded using 0.2µl NeoFX to transfect 30nM siRNA in a cell density of 2.5×10^3 per well of a 96-well plate. After 24 hrs, transfection medium was replaced with fresh media and cells were allowed to grow until they reached 80-90% confluency, a total of 5 days. Cell number

was assessed using the acid phosphatase assay (section 2.2.1). All experiments were carried out independently at least three times.

2.15.3 Invasion analysis of siRNA transfected cells

To assay for changes in invasive capacity, siRNA experiments in 6-well plates were set up using 2 µl NeoFx to transfect 30nM siRNA in a cell density of 2×10^5 per well of a 6-well plate. Transfection medium was removed after 24hr and replaced with fresh growth medium. The transfected cells were assayed for changes in invasion capacity at 72hr using the optimised *in vitro* invasion assay described in Section 2.3.1.

2.15.4 Chemosensitivity assay on siRNA-transfected cells

Assays were set up as described above (section 2.15.2). 24 hrs after addition of fresh media, appropriate concentrations (2×) of chemotherapeutic drugs were added to the wells in replicates of 4 and incubated for 3 days. The plates were assayed for changes in proliferation at 96 hrs using the acid phosphatase assay (Section 2.2.1).

Table 2-24 List of siRNAs used in this study

Silencer ® Select target name	Life technologies ID
ABCG2 # 1	S18056
ABCG2 # 2	S18057
ABCB1 # 1	S10420
ABCB1 # 2	S10418
ITGAV # 1	S3685
ITGAV # 2	S7568
BCHE # 1	S1906
BCHE # 2	S1907
Negative Control No. 1 siRNA	S4390843
Kinesin	AM4639

2.16 Statistical analysis

Software: Prism, Instat and Excel

IC_{50} values were calculated using GraphPad Prism (Version 5.01, GraphPad Software, Inc., USA). GraphPad Instat (Version 3) allowed simple descriptive statistics and 1-way ANOVA. Excel 2010 was used for t-tests and simple graphs.

Analysis of the difference of comparisons, as well as untreated versus siRNA treated mean invasion and percentage survival calculated, were performed using a student t-test (two-tailed with equal variance), on Microsoft Excel.

Error bars were plotted using plus and minus the standard deviation on duplicate inserts interexperimentally.

In the siRNA experiments, siRNA scrambled transfected cells were used as control compared to siRNA treated samples. This was to ensure no 'off-target' effects of the siRNA transfection procedure. Non-treated controls were used to ensure scrambled siRNA was having no effect and to normalise data.

Significance may be assumed as follows:

* A p value of ≤ 0.05 was deemed significant

** A p value ≤ 0.01 was deemed more significant

*** A p value ≤ 0.005 was deemed highly significant

2.17 Bioinformatics

Bioinformatics is the collection, organization and analysis of large amounts of biological data, using networks of computers and databases. Software packages are available to analyse microarray data e.g. Genespring and Spotfire. The data analysis software used for the analysis of the microarray experiments reported in this thesis was dChip[293].

2.17.1 dCHIP

DNA-Chip Analyzer (dChip) is a software package implementing model-based expression analysis of oligonucleotide arrays [290] and several highlevel analysis procedures. This model-based approach allowed probe-level analysis on multiple arrays. By pooling information across multiple arrays, it was possible to assess standard errors for the expression indexes. In this normalisation procedure an array with median overall intensity was chosen as the baseline array against which other arrays were normalised at probe level intensity. Subsequently a subset of PM probes, with small within-subset rank difference in the two arrays, served as the basis for fitting a normalisation curve. This approach also allowed automatic probe selection in the analysis stage to reduce errors due to cross-hybridizing probes and image contamination. High-level analysis in dChip included comparative analysis and hierarchical clustering. Gene filters employed for this analysis included a raw value difference of at least 100, and a fold change of at least 1.2. After these filters are in place and the relevant genes have been removed, a T-test is carried out to generate pvalues for each probe. Only p-values of less than 0.05 were accepted. This normalisation was downloaded from (http: //dchip. or g/) along with other data analysis modules.

2.17.2 R

The name "R" refers to the computational environment initially created by Robert Gentleman and Robert Ihaka, similar in nature to the "S" statistical environment developed at Bell Laboratories (http://www.r-project.org/about.html). It has since been developed and maintained by a strong team of core developers (R-core), who are renowned researchers in computational disciplines. R has gained wide acceptance as a reliable and powerful modern computational environment for statistical computing and visualisation, and is now used in many areas of scientific computation. R is free software, released under the GNU General Public License; this means anyone can see all its source code, and there are no restrictive, costly licensing arrangements. One of the main reasons that computational biologists use R is the Bioconductor project (http://www.bioconductor.org), which is a set of packages for R to analyse genomic data[294].

2.17.3 David

DAVID (the Database for Annotation, Visualization and Integrated Discovery) is a free online bioinformatics resource and was used for gene-term enrichment analysis. (http://david.niaid.nih.gov)[295,296].

2.17.4 Panther

Genelists were analysed using PANTHER Classification System (available from www.pantherdb.org). The PANTHER (Protein ANalysis THrough Evolutionary Relationships) Classification System is a unique resource that classifies genes by their functions, using published scientific experimental evidence and evolutionary relationships to predict function even in the absence of direct experimental evidence[297]. In this thesis, PANTHER was used to define a list of enriched pathways that are represented by lists of genes.

CHAPTER 3

Development of P-gp- and BCRP-mediated mitoxantrone resistant lung cancer cell lines using identical selection schedules.

3.1 Establishment of Mitoxantrone-resistant Cell Lines

3.1.1 Introduction

The resistance of tumours to cytotoxic drugs is a major cause of chemotherapy failure. In one type of multidrug resistance (MDR), that is caused by overexpression of multidrug efflux pumps belonging to the ABC family, cells display resistance to a variety of structurally and functionally unrelated chemotherapeutic drugs. The chemotherapeutic drugs to which the cells are resistant generally include the anthracyclines, vinca alkaloids, podophyllotoxins, peptide antibiotics and taxol, but usually exclude nucleotide analogues, metabolic inhibitors, alkylating agents and platinum analogues.

The MDR phenotype may be an inherent property of the cells or acquired following exposure to one or more cytotoxic agents. Studies with drug-selected model cell lines have repeatedly demonstrated that overexpression of some members of the ATP-binding cassette (ABC) transporter superfamily including P-glycoprotein (Pgp or ABCB1), breast cancer resistance protein (BCRP or ABCG2), and multidrug resistance associated protein 1 (MRP1 or ABCC1) as one of the major mechanisms responsible for MDR. Therefore, blocking BCRP- and P-gp-mediated active efflux may provide a therapeutic benefit for cancers. Delineating the precise molecular mechanisms for BCRP and P-gp gene expression may lead to identification of a novel molecular target to modulate BCRP- and P-gp mediated MDR.

It was previously demonstrated that exposure of the human lung carcinoma cell line, DLKP to mitoxantrone, an anthracenedione, can result in not only an MDR phenotype but also enhanced cell invasion *in vitro*[196]. One aim of the work described in this chapter was to use an *in vitro* model of development of mitoxantrone resistance to investigate whether resistance and invasion emerge together or sequentially. I also aimed to identify changes in gene expression associated with the selection of a mitoxantrone – resistant cell population. In the present study, I established two mitoxantrone resistant cell lines from DLKP-SQ by sequential pulsing. Although both cell lines showed resistance to mitoxantrone over 200 times more than the parent cells and cross-resistance to other anticancer drugs, the mechanism of resistance was different.

3.1.2 Choice of cell line and drug

Liang *et al* [196], have previously demonstrated that exposure of the human lung carcinoma cell line, DLKP to mitoxantrone, an anthracenedione, can result in not only an MDR phenotype but

also enhanced cell invasion *in vitro*. In addition, mitoxantrone is a substrate for both BCRP and P-gp. The aim of this study was to establish an *in vitro* model of mitoxantrone resistance to identify changes in gene expression associated with the selection of a mitoxantrone – resistant cell population and to establish if the resistant and invasion phenotypes emerged at the same or at different times. Selections can be performed on individual clones or on mass populations of cells. In this study, DLKP-SQ, a clone of DLKP was chosen for the establishment of a mitoxantrone resistant cell line. The strategy of deriving isogenic drug resistant cell lines from the DLKP-SQ clone eliminates variability due to intrinsic genetic differences between cell lines.

3.1.3 Cell culture and establishment of DLKP-SQ-Mitox

DLKP-SQ cells were cultured in ATCC containing 5% FBS, in a humidified incubator with atmosphere of 5% CO_2. DLKP-SQ-Mitox variants were selected by a high mitoxantrone concentration (the final concentration was 5 ng/ml, IC_{90}), for 4 hours and washed with drug-free medium. Triplicate flasks were set up. Medium was changed after 3 days to wash out dead cells. When the cells started growing exponentially they were pulsed with 5 ng/ml of mitoxantrone. The cells in one of the triplicate flasks died after one pulse.

This cyclic treatment was repeated four times over a period of four months, generating the replicate DLKP-SQ-Mitox resistant sublines.

3.1.4 Generation of mitoxantrone resistant cell lines

In the process of pulse treatment using high-dose Mitoxantrone, most of the cells enlarged in cell volume and the cells gradually died and floated. A few cells without drug treatment survived after a period of time (approximately 5%), and resumed to logarithmic growth. The DLKP-SQ-Mitox cell lines were established after four months and exhibited stable resistance to mitoxantrone. SQ-Mitox (flask A, figure 3.1-1) cells acquired levels of resistance to mitoxantrone that was 210 fold higher than the DLKP-SQ parent cells. DLKP-SQ-Mitox cells (Flask B) acquired levels of resistance to mitoxantrone that was 320 fold higher than the parent cells. IC_{50} values for SQ-Mitox sublines (flask A and B) ranged from 16 ng/ml to 25 ng/ml, whereas the IC_{50} for DLKP-SQ was 0.08 ng/ml.

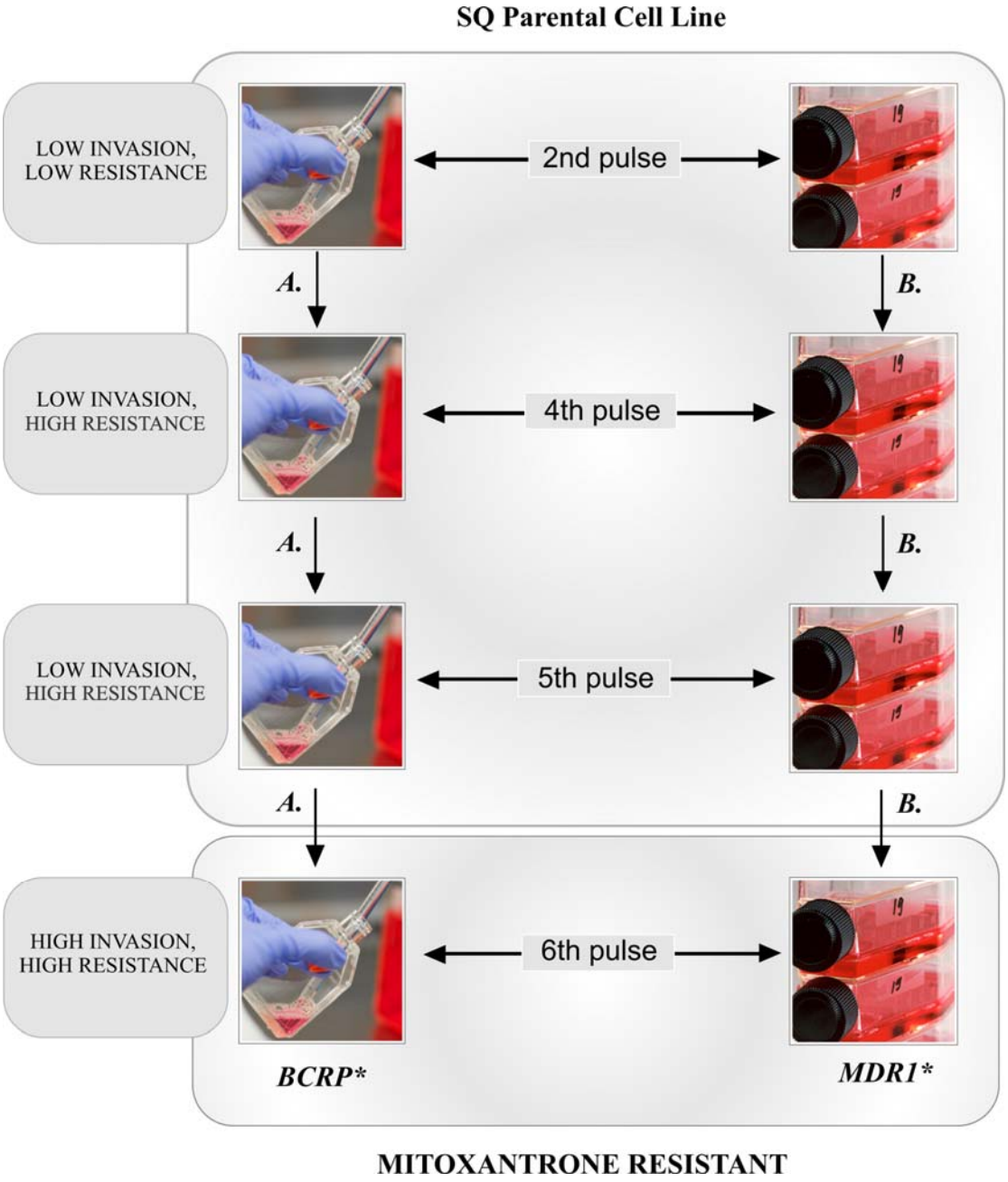

Figure 3.1-1: Flow diagram outlining the generation of the mitoxantrone resistant cell lines. *These eflux pumps were later identified through microarray analysis and revealed to be overexpression of BCRP and P-gp in flasks A and B respectively.

3.1.5 Morphology of mitoxantrone resistant cell lines

As described in the previous section, two independent mitoxantrone resistant cell lines were generated (Flask A and B, figure 3.1-1) and microarray analysis revealed that the two variants had completely different mechanisms of resistance. The two replicate flasks contained cells with two different morphologies. One replicate flask contained cells with a spindle like morphology (SQ-Mitox-BCRP) while the other flask contained cells with a more regular morphology and was closest to the parental cells (SQ-Mitox-MDR), figure 3.1-2.

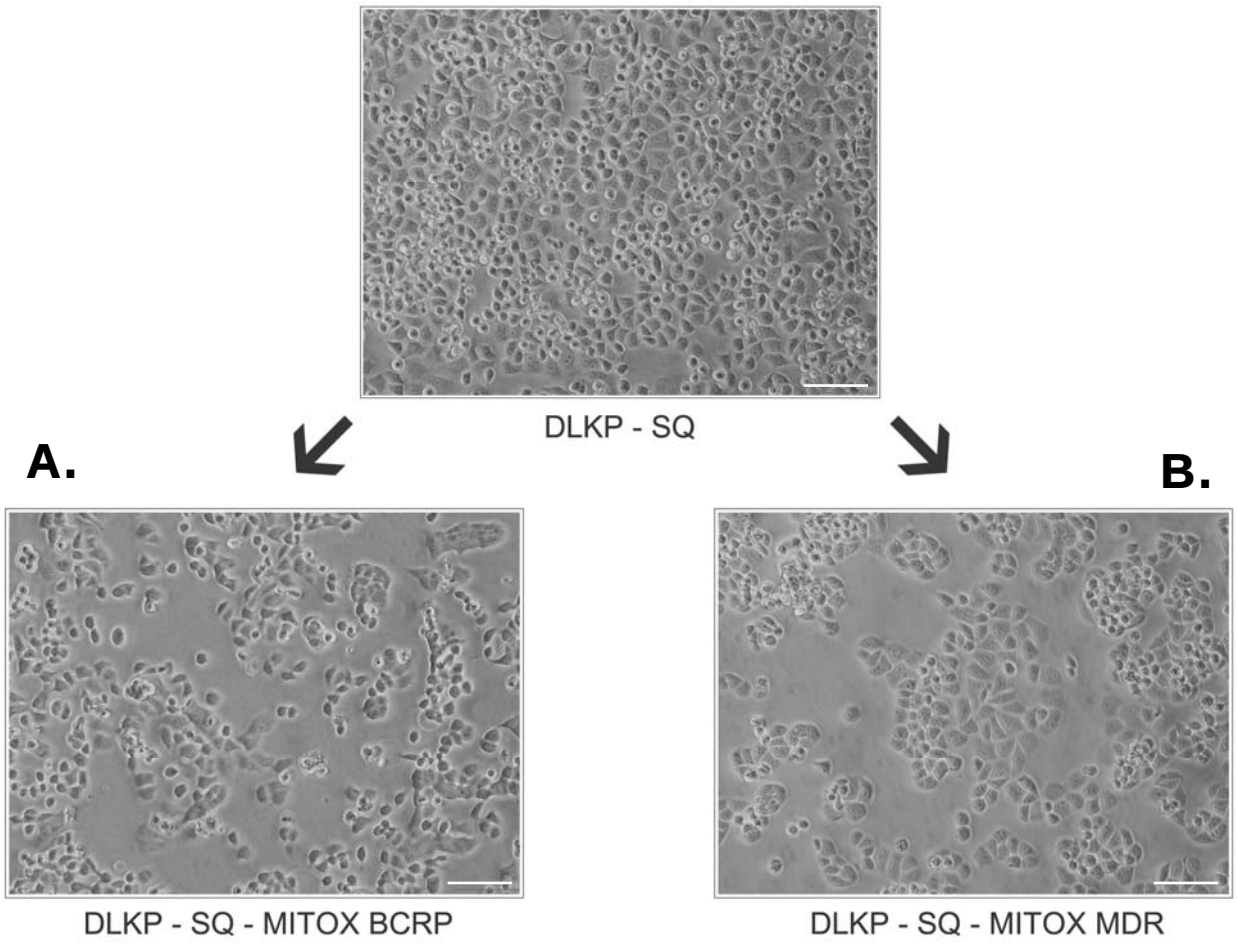

Figure 3.1-2: Cell morphology The DLKP-SQ cells are compact with distinct boundaries while the size of the Flask A cells were unequal and slightly larger (later shown to be BCRP overexpression). The morphology of the Flask B cells was irregular (later shown to be MDR1 overexpression) Magnification ×100, scale bar 200μm..

3.1.6 Invasion assays of mitoxantrone resistant cell lines

As the the aim of this study was to establish if the resistant and invasion phenotypes emerged at the same or at different times, the differences in invasion between the mitoxantrone resistant SQ cells and poorly invasive SQ parent were monitored during the development of resistance as described in section 2.3.1. Results show the trend that invasion was increased in the 6th pulse relative to the 4th pulse and the SQ parent in both the BCRP and P-gp over-expressing cells (figure 3.1-3). High standard deviations were observed in these assays and may have been due to the instability of the invasive phenotype in these new drug resistant cells. Interestingly, induction of invasion was independent of the type of transporter expressed. Further investigations (microarray analysis) of these cell lines will be described in chapter 4.

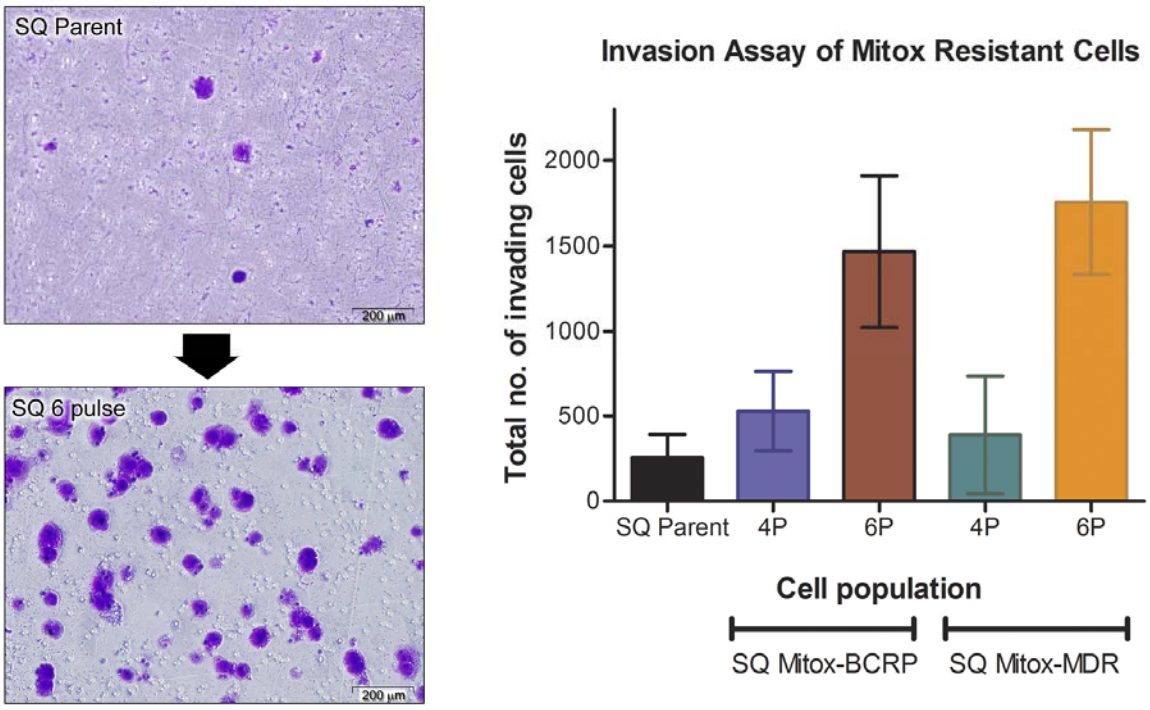

Figure 3.1-3: The invasive capacity of panel of DLKP-SQ-Mitox cells. The total number of invading cells was determined by counting the number of cells per field in 10 random fields, at 200× magnification. The average number of cells per field was then multiplied by a factor of 140 (growth area of membrane/field area viewed at 200× magnification (calibrated using a microscope graticule)). Error bars represent the standard deviation of triplicate invasion assay experiments (n=3).

3.1.7 Cross resistance drug profiles of mitoxantrone resistant cell lines

When cells are repeatedly treated with a chemotherapeutic drug, the drug resistant variant, which is eventually produced, typically not only displays resistance to this singular drug, but also to different groups of drugs. To determine if the SQ-Mitox-BCRP and SQ-Mitox- MDR cell lines similarly displayed cross-resistance to multiple pharmacological agents, a panel of drugs with differing structure and function were tested as described in section 2.2. As observed in table 3.1-1 below, the SQ-Mitox-MDR cells demonstrate a "typical" MDR phenotype which has been correlated with P-gp-mediated drug resistance and its associated cross-resistance to taxol, epirubicin, vinblastine, irinotecan and VP16.

In contrast, the SQ-Mitox-BCRP cell line exhibited resistance to mitoxantrone and irinotecan, but not to taxol, epirubicin, vinblastine, VP16 or 5-FU. Irinotecan and its active metabolite SN-38 are substrates of BCRP[298].

3.1.8 *ABCB1*/P-gp and *ABCG2*/BCRP RNA and protein expression

Significant differences confirmed between parent and resistant cell lines

Having developed MDR variants overexpressing BCRP and P-gp, the gene expression profiles of these cell lines were compared using microarray analysis (section 3.1.10). Significant differences in transcript levels from the microarray data were confirmed by qRT-PCR and Western blotting for BCRP and P-gp (figure 3.1-4). DLKP-A, an adriamycin-selected variant of a human lung epithelial carcinoma cell line, was used in these studies as a positive control. This cell line has previously been shown to overexpress P-glycoprotein[277]. There was perfect concordance between the microarray and qRT-PCR results for significant changes in expression of the P-gp and BCRP. Real Time PCR and Western blot analysis revealed that BCRP is highly upregulated in SQ-Mitox- BCRP and that P-gp is also highly upregulated in SQ-Mitox-MDR. Interestingly, Western blot analysis showed that BCRP and P-gp overexpression occurs early on in the pulsing process in the SQ-Mitox-BCRP and SQ-Mitox-MDR cell line respectively (as early as the 2nd pulse).

Table 3.1-1: IC_{50} and fold resistance of the DLKP-SQ Mitox resistant variants compared to the parental DLKP-SQ cell line (ng/ml).

Drug	DLKP-SQ	error	SQ-BCRP	error	SQ-Pgp	error
Mitox:						
IC_{50}	0.08	0.01	16.79	2.27	25.59	3.27
fold (n)	*1 (3)*		*209.87 (3)*		*319.87 (3)*	
Taxol:						
IC_{50}	1.65	0.647	1.11	0.379	501.2	40.58
fold (n)	*1 (2)*		*0.67 (3)*		*303 (2)*	
Epirubicin:						
IC_{50}	10.39	1.49	13.93	0.91	1861	208.59
fold (n)	*1 (3)*		*1.34 (3)*		*179.1(3)*	
Vinblastine:						
IC_{50}	0.63	0.36	0.68	0.4	81	1.41
fold (n)	*1 (2)*		*1.07 (2)*		*128 (2)*	
Irinotecan:						
IC_{50}	337	67	1359	207	1948	432.7
fold (n)	*1 (3)*		*4.03 (3)*		*5.8 (3)*	
Cisplatin:						
IC_{50}	731.8	136.33	467.85	11.80	582	75.51
fold (n)	*1 (2)*		*0.63 (2)*		*0.79 (2)*	
VP16:						
IC_{50}	1.20	0.076	1.51	0.40	2073.5	57.27
fold (n)	*1 (2)*		*1.25(2)*		*1727.5 (2)*	
5FU:						
IC_{50}	822.55	325.9	1850	544.47	1434	470.93
fold (n)	*1 (2)*		*2.25 (2)*		*1.74 (2)*	

error: standard deviation

n value indicates the number of times each toxicity assay done.

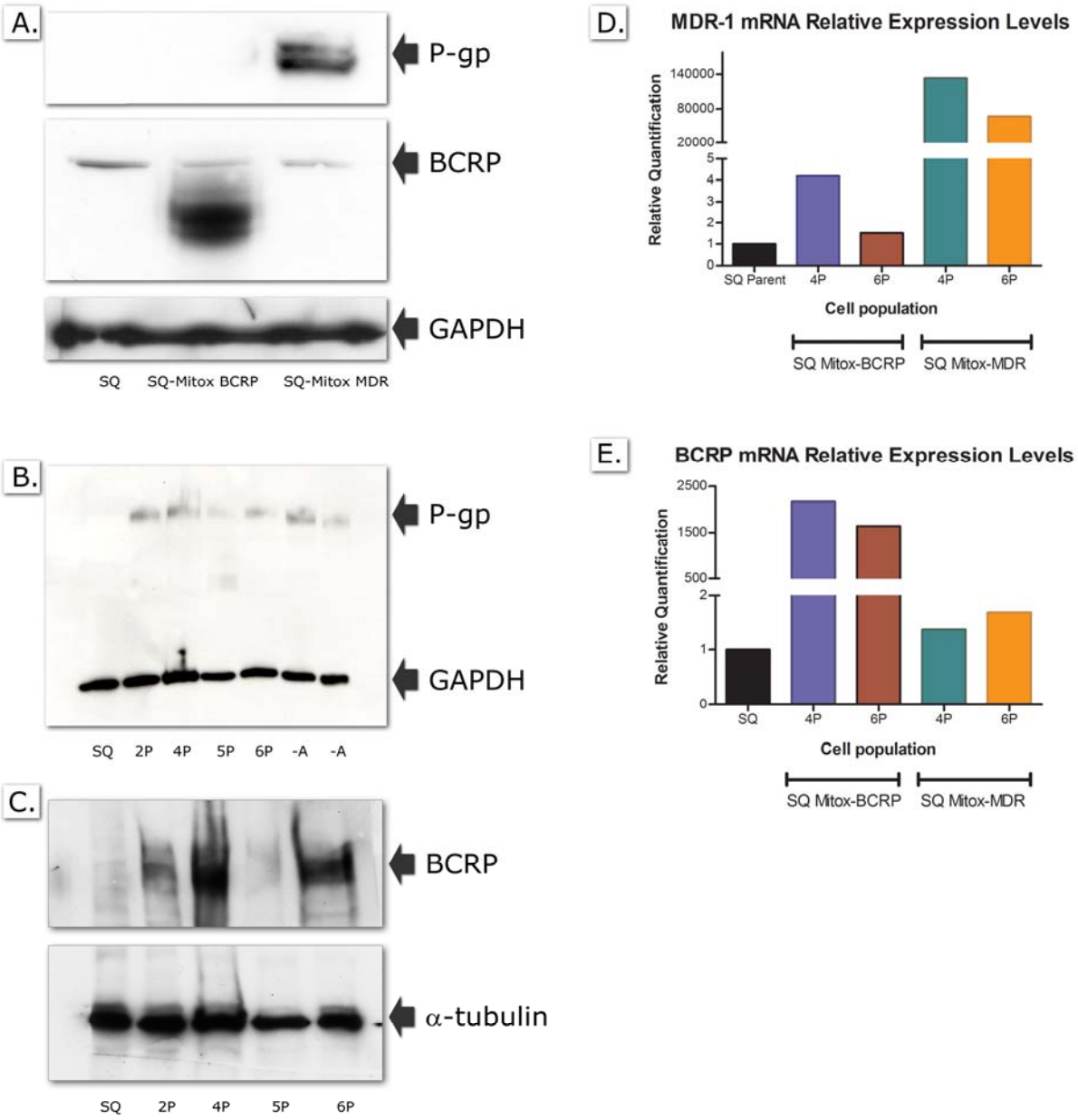

Figure 3.1-4: (**A**.) Western blotting for P-gp (170kD) and BCRP (70kD) in the SQ-Mitox cells. DLKP-A served as a positive control (**B. and C)**. Western blot shows that P-gp and BCRP overexpression occurs early on in the pulsing process (Pulse 2). (**D.)** Real time PCR shows MDR1 mRNA relative expression levels and **(E.)** BCRP mRNA relative expression levels.

3.1.9: MDR and BCRP confer drug resistance to Mitoxantrone-selected DLKP-SQ

Effect of ABCB1 siRNA on drug resistance

To further evaluate if *ABCG2* was conferring resistance to mitoxantrone in the BCRP and P-gp overexpressing cell line, we performed cytotoxicity assays in the presence and absence of elacridar, a specific inhibitor of *ABCG2* and *ABCB1* as described in section 2.15 and section 2.2). A concentration of 443nM Elacridar was chosen for the inhibitor experiment as previously used in this laboratory[299]. With the addition of 443nM Elacridar, the *ABCG2*-mediated and *ABCB1*-mediated resistance to mitoxantrone was reversed (figures 3.1-5 and 3.1-6). The addition of elacridar resulted in an approximately 30% enhancement of the toxicity of mitoxantrone on the SQ-Mitox-BCRP and SQ-Mitox-MDR cells. This indicates that the inhibition of BCRP (*ABCG2*) and P-gp (*MDR1* or *ABCB1*) results in greater toxicity to mitoxantrone exhibited by the SQ-Mitox-BCRP and SQ-Mitox-MDR cells respectively.

To confirm that BCRP was the ABC transporter conferring resistance to SQ-Mitox-BCRP, RNA interference (RNAi) studies were performed as described in section 2.15. Standard characterisation analysis determined the degree of silencing mediated by a synthetic siRNA corresponding to BCRP. Using 30nM siRNA, BCRP protein expression was found to be reduced (figure 3.1-7).

Following validation, cytotoxicity assays were performed on cells treated with BCRP (*ABCG2*) siRNA or scrambled siRNA (the negative control). The BCRP siRNAs induced a shift of the drug response curve down, below 50% cell survival, indicating less resistance to mitoxantrone (figure 3.1-5). Together with the results from the elacridar cytotoxicity studies, this suggests that BCRP is critical for the drug resistance observed in the SQ-Mitox-BCRP cell line.

To confirm that P-gp (*MDR1/ABCB1*) was the ABC transporter conferring resistance to SQ-Mitox-MDR, RNA interference (RNAi) studies were also performed. Standard characterisation analysis was conducted to determine the degree of silencing mediated by a synthetic siRNA corresponding to P-gp. Using 30nM siRNA, P-gp protein expression was found to be reduced (figure 3.1-7). Following validation, cytotoxicity assays were performed on cells treated with P-gp siRNA or scrambled siRNA. The P-gp siRNA induced a similar shift of the drug response curve below 50% in the case of P-gp siRNA1, indicating less resistance to mitoxantrone (Figure 3.1-6). Together with the results from the elacridar cytotoxicity studies, this suggests that P-gp is likewise critical for drug resistance in the SQ-Mitox-MDR cell line.

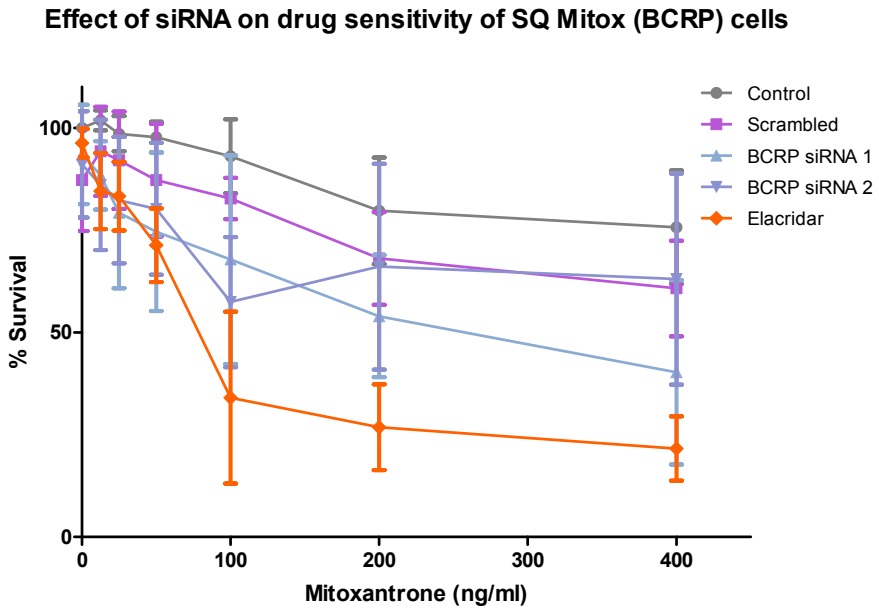

Figure 3.1-5 Evaluating the combination effect of small interfering RNA (siRNA) and mitoxantrone treatment in SQ-Mitox-BCRP cells. Cells were treated first with BCRP siRNA or scrambled siRNA for 24 hours followed by mitoxantrone treatment at different concentrations. 72 hours after the mitoxantrone treatment, cell viability was evaluated by acid phosphatase assay. The BCRP inhibitor Elacridar was used as a control. Data shown is mean ± standard deviation (n=3).

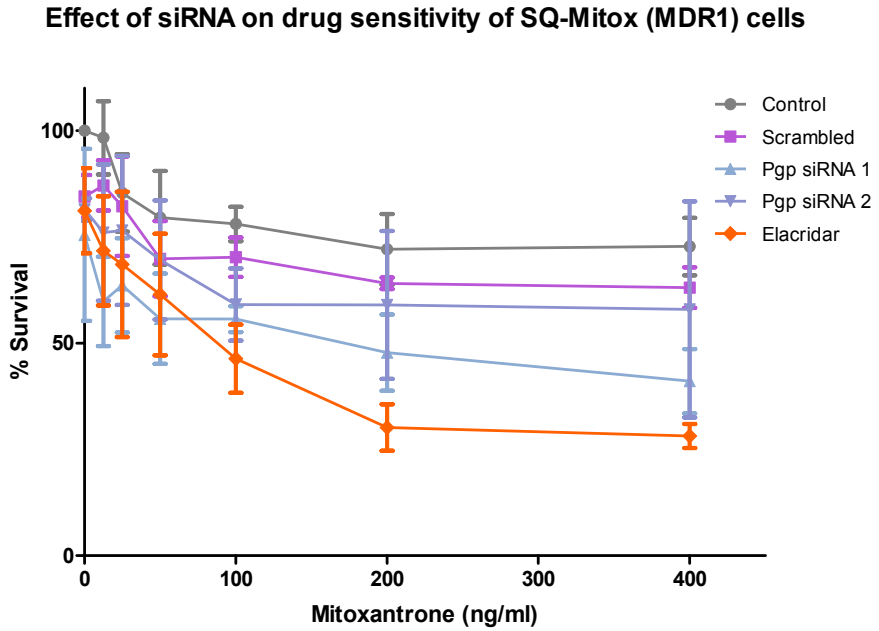

Figure 3.1-6 Evaluating the combination effect of small interfering RNA (siRNA) and mitoxantrone treatment in SQ-Mitox-MDR cells. Cells were treated first with P-gp siRNA or scrambled siRNA for 24 hours followed by mitoxantrone treatment at different concentrations. 72 hours after the mitoxantrone treatment, cell viability was evaluated by acid phosphatase assay. The P-gp inhibitor Elacridar was used as a control. Data shown is mean ± standard deviation (n=3).

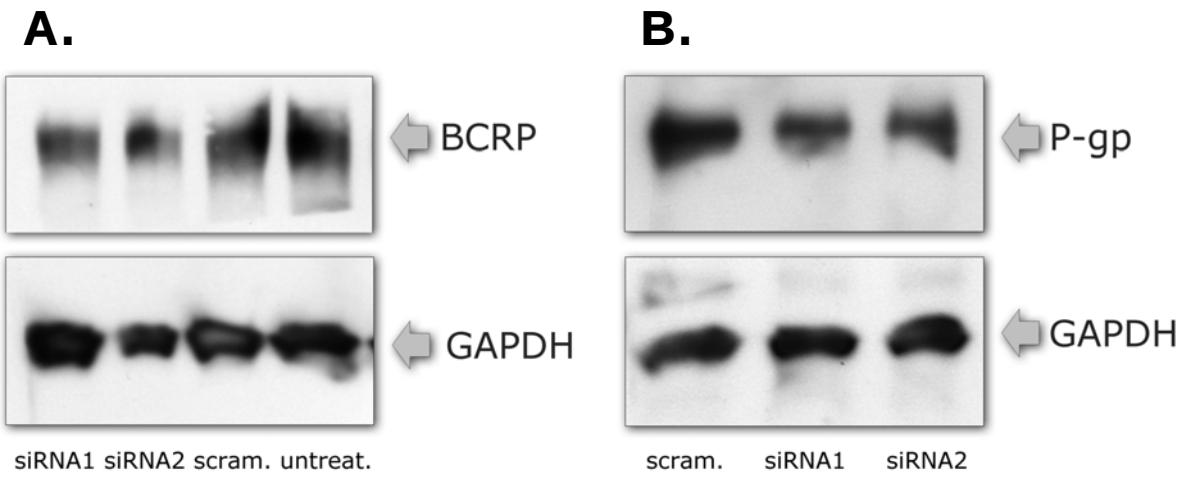

Figure 3.1-7: Effect of BCRP and P-gp siRNA on drug resistance – Western blot analysis of BCRP expression in SQ-Mitox-BCRP cells treated with BCRP siRNA and P-gp expression in SQ-Mitox-MDR cells treated with P-gp siRNA. **(A.)**: Western blot showing knockdown of BCRP at 48 hours post-transfection in SQ-Mitox-BCRP cells transfected with two independent siRNAs targeting BCRP relative to scrambled control siRNA transfected cells and untreated cells. (**B.**) Western blot showing knockdown of P-gp at 48 hours post-transfection in SQ-Mitox-MDR cells transfected with two independent siRNAs targeting P-gp relative to scrambled control siRNA transfected cells and untreated cells.

3.1.10 Gene Expression data analysis for DLKP-SQ and its mitoxantrone resistant variants

In order to further elucidate the mechanism of resistance in the mitoxantrone resistant variants, gene-lists were generated from the raw array data that may potentially serve as a genotypic signature for drug resistance in the SQ-Mitox variants. Changes in gene expression between DLKP-SQ parental cells and the derived drug resistant cell lines were generated using the statistical software environment R (www.r-project.org), section 2.17.2., and the aroma affymetrix package using the robust multichip average (RMA) algorithm[300,301], with a P-value adjustment of $p \leq 0.05$.

3.1.10.1 Changes in gene expression associated with resistance by microarray analysis

Two fold lists of probesets with significant changes in expression ($p \leq 0.05$) in each cell line compared to the drug sensitive parental cell line were generated. The 2 fold list showed that 1623 probesets (502 probesets over-expressed and 1121 probesets down-expressed) were significantly different in the SQ-Mitox- BCRP line, and 1313 probesets (296 probesets over-expressed and 1017 probesets down-expressed) were significant in the SQ-Mitox-MDR cell line.

The top 10 over- and down-expressed genes, with their primary functions, are summarised in table 3.1-2. *ABCG2* was the top over-expressed gene in the SQ-Mitox-BCRP cell line. *ABCB1* was similarly the top over-expressed gene in the SQ-Mitox-MDR cell line.

Since the BCRP (*ABCG2*) and MDR1 (*ABCB1*) genes were highly over-expressed compared to the fold changes for the other genes, it was decided to analysis the gene lists for over-represented categories of genes. The online tool DAVID enabled functional annotation analysis using the BP_FAT category of Gene Ontology (GO). Functional annotation analysis was conducted on probesets differentially expressed using gene ontology (GO) categories for biological processes. This allows for the discovery of overrepresented categories of genes. Functional annotation analysis of probesets significantly different in the BCRP overexpressing cell line (table 3.1-3) revealed that the most significant GO categories were associated with the regulation of neurogenesis, intracellular signalling cascades and mRNA metabolic processes. Functional annotation analysis of probesets significantly different in the MDR1 overexpressing cell line revealed that the most significant GO categories were associated with mRNA metabolic processes, mRNA processing and RNA splicing.

3.1.10.2 Generation of gene lists associated with BCRP- and P-gp – mediated mitoxantrone resistance

The mitroxantrone selection exclusively activated, and in parallel, a P-gp and a BCRP-related resistance mechanism. There may be alternate exclusive pathways, activated randomly by drug exposure.

The bioinformatics analysis had the following aims:

- To identify the genes that change with drug exposure.
- To identify the genes that change with drug resistance.
- To identify the genes which differ between the BCRP and MDR1 overexpressing variants.

Lists of probesets were generated using a 1.5-fold cutoff value for significant changes in expression levels ($p \leq 0.05$) relative to the drug sensitive parental cell line. These lists were overlapped using a Venn diagram to find genes that were significantly different in the two cell lines (figure 3.1-8). The 1.5-fold list showed 1872 probesets were significantly different in the

Table 3.1-2: Top ten gene transcripts significantly over- and down-expressed in SQ-Mitox-BCRP and SQ-Mitox-MDR relative to DLKP-SQ.

DLKP-SQ vs DLKP-SQ-Mitox-BCRP			*DLKP-SQ vs DLKP-SQ-Mitox-MDR*		
Gene symbol	**Log ratio**	**Main function**	**Gene symbol**	**Log ratio**	**Main function**
Up-regulated					
ABCG2	9.889	Nucleotide binding, transporter activity	*ABCB1*	10.106	Nucleotide binding, transporter activity
SPP1	8.501	Ossification, cytokine activity	*TMEM47*	6.498	Plasma membrane, cell junction
CDH10	6.318	Calcium ion binding	*SH3BP4*	5.624	Signal transducer activity
SAMD5	6.204	Unknown	*PCDH7*	5.572	Calcium ion binding, cell adhesion
PRSS12	5.514	Serine- type endopeptidase activity	*ARL4C*	5.131	Nucleotide binding, GTPase activity
AMPH	4.566	Synaptic transmission	*CAB39L*	4.996	Protein binding
DKK1	4.468	Signal transducer activity	*ZIC2*	4.415	Zinc ion binding, cell differentiation
LOC440934	4.318	Unknown	*CYP26A1*	4.252	Retinoic activity
HS6ST2	4.206	Sulfotransferase activity	*COL23A1*	3.911	Collagen catabolic process
AUTS2	4.07	Neurodevelopment	*SETDB2*	3.621	DNA binding
Down-regulated					
MALAT1	–7.244	Associated with metastasis	*MALAT1*	–7.11	Associated with metastasis
CD36	–6.391	Positive regulator of cell matrix adhesion	*CD36*	–6.309	Positive regulator of cell matrix adhesion
RBP7	-5.952	Retinol binding, transporter activity	*RBP7*	-5.954	Retinol binding, transporter activity
KIF1A	-5.408	Microtubule motor activity	*KIF1A*	-5.394	Microtubule motor activity
SERPINH1	-5.315	Serine type endopeptidase activity	*SERPINH1*	-5.315	Serine type endopeptidase activity
MDK	-9.467	Signal transduction	*MDK*	-4.923	Signal transduction
MYH10	-9.194	Microfilament motor activity	*SEM3C*	-5.691	Neural cell crest migration
THRAP3	-5.148	Mediator complex	*THRAP3*	-5.148	mRNA processing
TRIM59	-5.115	Ubiquitin-protein transferase activity	*LAYN*	-5.14	Carbohydrate binding
QSER1	-5.022	Unknown	*TFPI2*	-5.069	Serine type endopeptidase activity

Table 3.1-3: The gene ontology (GO) identified by functional analyses – differentially expressed genes in SQ-Mitox

Go ID	Go term	Foreground Freq.	Background Freq	P-value	Benjamini -Hochberg	FDR
SQ-Mitox-BCRP:						
GO:0050767	Regulation of neurogenesis	28/933	166/209875	2.5E-5	0.0742	0.0443
GO:0007242	Intracellular signalling cascade	121/933	1256/206424	1.10E-4	0.1577	0.1975
GO:00016071	mRNA metabolic process	46/933	370/226320	1.40E-4	0.1325	0.2452
GO:00046907	Intracellular transport	71/933	657/226320	1.60E-4	0.1170	0.2862
GO:0007049	Cell cycle	81/933	776/236620	1.60E-4	0.0971	0.2937
GO:0022402	Cell cycle process	63/933	565/225818	1.70E-4	0.0853	0.3077
GO:0006397	mRNA processing	41/933	321/226320	1.90E-4	0.0810	0.3398
GO:0044265	Cellular macromolecule catabolic process	76/933	725/226652	2.30E-4	0.0854	0.4107
SQ-Mitox-MDR:						
GO:00016071	mRNA metabolic process	44/761	370/226320	4.6E-6	0.0128	0.0082
GO:0006397	mRNA processing	39/761	321/226320	1.10E-5	0.0150	0.0192
GO:0008380	RNA splicing	35/761	284/226320	2.50E-5	0.0227	0.0439
GO:0050767	Regulation of neurogenesis	24/761	166/208850	5.40E-5	0.0373	0.0969
GO:0045664	Negative regulation of neuron differentiation	10/761	33/1569472	6.00E-5	0.0333	0.1080
GO:0007242	Intracellular signalling cascade	103/761	1256/206424	7.60E-5	0.0347	0.1348
GO:0000398	nuclear mRNA splicing, via spliceosome	22/761	153/226320	1.30E-4	0.0506	0.2312
GO:0000377	RNA splicing, via transesterification reactions	22/761	153/226320	1.30E-4	0.0506	0.2312

SQ-Mitox- BCRP line, and 1472 probesets were significant in the SQ-Mitox-MDR line.

Approximately half the total number of probesets were identified as changed as a consequence of selection for drug resistance (55.91% for SQ-Mitox-MDR and 43.96% for SQ-Mitox-BCRP) and 45-57% of changes in gene expression are unique in each cell line (figure 3.1-8).

Functional annotation analysis of probesets, exclusively and differentially expressed (totalling 1049) in the BCRP overexpressing cell line, revealed that the most significant GO categories were related to RNA processing, intracellular transport and cellular response to stress (table 3.1-4).

Functional annotation analysis of genes exclusively differentially expressed (totalling 649) in the P-gp overexpressing cell line revealed that the most significant GO categories were related to chromatin modification, embryonic morphogenesis and chromatin organization (table 3.1-4). Specific analysis of the common 823 probesets showed that the most enriched categories were mRNA processing and RNA splicing.

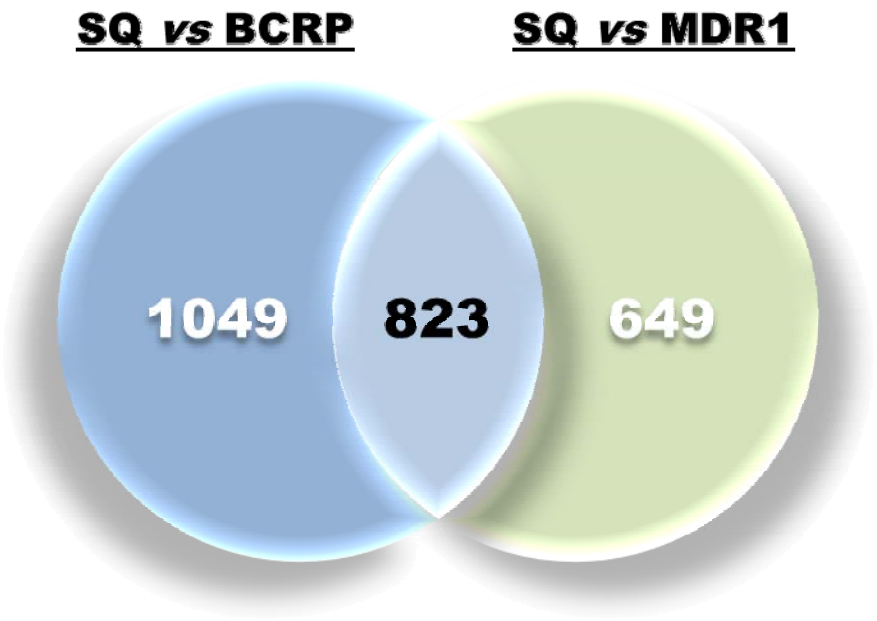

Figure 3.1-8: The generation of gene-lists may potentially serve as a gene signature for P-gp and BCRP expression. A pairwise comparison was employed to identify unique and shared gene sets among the DLKP-SQ-Mitox resistant cell lines. 1.5 fold lists were generated which showed that 1872 probesets were significantly different in the SQ-Mitox- BCRP line and 1472 probesets were significant in the SQ-Mitox-MDR line. These lists were overlapped using a Venn diagram to identify 823 probesets in common between the two gene lists. 1049 probesets were specific to BCRP and 649 probesets were specific to MDR1.

Table 3.1-4: The gene ontology (GO) identified by functional analyses – exclusively differentially expressed genes in SQ-Mitox

Go ID	Go term	Foreground Freq.	Background Freq	P-value	Benjamini Hochberg	FDR
SQ-Mitox-BCRP: David analysis of 1049 probesets (Figure 3.1-8)						
GO:0006396	RNA processing	52/651	547/20192	4.10E-6	0.0106	0.0073
GO:0046907	Intracellular transport	59/651	657/20349	4.9E-6	0.0006	0.0087
GO:0033554	Cellular response to stress	53/651	566/21223	5.0E-6	0.0043	0.0089
GO:0044265	Cellular macromolecule catabolic process	61/651	725/22950	2.5E-5	0.0158	0.0043
GO:0009057	Macromolecule catabolic process	64/651	781/22950	3.3E-5	0.0168	0.058
GO:0022403	Cell cycle phase	40/651	414/21309	4.5E-5	0.0193	0.08
GO:0016071	mRNA metabolic process	36/651	370/22305	1.0E-4	0.0368	0.1794
GO:0010605	Negative regulation of macromolecule metabolic process	40/651	734/20336	1.2E-4	0.0379	0.2113
SQ-Mitox-MDR: David analysis of 649 probesets (Figure 3.1-8)						
GO:0016568	omatin modification	23/404	274/218517	2.5E-5	0.0527	0.0429
GO:0048598	Embryonic morphogenesis	24/404	307/235521	4.8E-5	0.0515	0.0839
GO:0006325	Chromatin organization	25/404	278/218517	4.2E-4	0.2640	0.7266
GO:0010629	Negative regulation of gene expression	30/404	504/227069	5.5E-4	0.2598	0.9498
GO:0051276	Chromosome organization	28/404	485/218517	1.4E-3	0.4578	2.3982
GO:0010608	Postranscriptional regulation of gene expression	16/404	211/1560817	1.7E-3	0.4554	2.8504
GO:0048568	Embryonic organ development	14/404	172/235521	1.9E-3	0.4541	3.3054
GO:0048706	Embryonic skeletal system development	9/404	77/235521	2.0E-3	0.4256	3.4572

3.1.11 Proteomic analysis of DLKP-SQ and SQ-Mitox-BCRP-4P by 2D-DIGE.

3.1.11.1 Introduction

The work outlined earlier resulted in the generation of SQ-Mitox-BCRP cells, a cell line model of mitoxantrone resistance, which over-expressed the drug resistance pump, BCRP. Little is currently known of the intracellular protein changes associated with BCRP overexpression. Two-dimensional differential in-gel electrophoresis (2D-DIGE) analysis was employed to examine alterations in the levels of proteins in SQ-Mitox-BCRP-4P compared to DLKP-SQ parental cells. Proteins of interest were identified by MALDI-ToF mass spectrometry. Western blotting confirmed these changes.

3.1.11.2 Generation of a list of significantly altered proteins

To investigate proteins potentially involved in mitoxantrone resistance in this model for human lung cancer, we systematically analysed protein expression from DLKP-SQ and DLKP-SQ- Mitox using 2D-DIGE as described in section 2.11. For this, three biological replicate samples from each cell line were prepared separately. Samples from each cell line were differentially labelled with 2D-DIGE dyes (i.e. Cy3 and Cy5). A pooled internal control containing a mixture of all biological replicate samples in the experiment was labelled with Cy2 dye.

Proteins were initially defined as differentially regulated if the observed fold change was greater than 1.2 with p-values less than 0.05 to look for even subtle changes in expression across the drug-resistant variant and the parent. Biological variation analysis of spots was significant, showing greater than 1.2-fold change in expression (*t*-test, $p < 0.05$), and revealed 293 differentially expressed proteins between DLKP-SQ and DLKP-SQ-Mitox-BCRP (identified proteins are tabulated in table 3.1-5).

3.1.11.3 Comparison of proteomic analysis with microarray analysis

The list of alterations in the levels of -proteins in SQ-Mitox-BCRP-4P compared to DLKP-SQ parental cell were compared with the significant differences in transcript levels from the microarray data. There was concordance between the proteomic and microarray data for EEF1A1, β-tubulin, p47, Ku80 and galactin 1 (table 3.1-5).

Table 3.1-5: Up- (↑) and Down-Regulated (↓) Proteomic Analysis and Microarray Analysis: DLKP-SQ *vs* SQ-Mitox-BCRP-4P

Protein Name	Gene Symbol	Accession Number	Molecular Function	SQ *vs* 4P Protein expression		SQ *vs* 4P Microarray analysis	
				Fold Change	*P*-Value	Fold change	*P*-Value
EF1a-like protein		gi|12006049|	translation	2.55	$<< 1 \times 10^{-4}$	1.8	$<< 1 \times 10^{-4}$
β-tubulin	TUBB	gi|338695|	cytoskeleton constituent	2.16	$<< 1 \times 10^{-4}$	1.29	$<< 1 \times 10^{-4}$
α-tubulin	TUBA	gi|340021|	cytoskeleton constituent	1.93	$<< 1 \times 10^{-4}$	na	na
Triosephosphate isomerase 1	TPI1	gi|17389815|	glycolysis	1.84	$\approx 1 \times 10^{-4}$	na	na
Phosphoglycerate Mutase	PGAM1	gi|67464305|	glycolysis	1.76	$< 1 \times 10^{-2}$	na	na
Heat Shock 70kDa protein 8, isoform 2 variant	HSPA8	gi|62896815|	stress	1.70	$<< 1 \times 10^{-4}$	na	na
Chaperonin containing TCP1; subunit 7 isoform b	CCT7	gi|58331185|	protein folding	1.53	$<< 1 \times 10^{-4}$	na	na
erbB3 binding protein	EBP1	gi|4099506|	cell proliferation	1.49	$<< 1 \times 10^{-4}$	na	na
p47	NSFL1C	gi|33150522|	protein binding	1.40	$< 1 \times 10^{-2}$	2.52	$< 1 \times 10^{-2}$
Nuclear Factor IV/Ku80	XRCC5	gi|35038|	DNA repair	1.33	$<< 1 \times 10^{-4}$	1.39	$<< 1 \times 10^{-4}$
Thioredoxin-like protein		gi|3646128|		1.29	$<< 1 \times 10^{-4}$	na	na
Chaperonin containing TCP1; subunit 3, isoform a	CCT3	gi|63162572|	protein folding	1.26	$< 1 \times 10^{-3}$	na	na
Peroxiredoxin 1	PRDX1	gi|55959887|	apoptosis/redox	1.26	$< 1 \times 10^{-3}$	na	na
fatty acid binding protein 5	FABP5	gi|30583737|	lipid metabolism	1.25	$< 1 \times 10^{-1}$	na	na
Thioredoxin Peroxidase B		gi|9955016|		1.25	$<< 1 \times 10^{-4}$	na	na
CCT2	CCT2	gi|48146259|	protein folding	1.24	$<< 1 \times 10^{-4}$	na	na
Cl^- intracellular channel 1	CLIC1	gi|55961618|	Cl^- ion binding	1.24	$< 1 \times 10^{-3}$	na	na
Glycyl tRNA synthetase	GARS	gi|3845409|	nucleotide binding	1.22	$<< 1 \times 10^{-4}$	na	na

Table 3.1-5: Up- (↑) and Down-Regulated (↓) Proteomic Analysis and Microarray Analysis: DLKP-SQ *vs* SQ-Mitox-BCRP-4P

Protein Name	Gene Symbol	Accession Number	Molecular Function	SQ *vs* 4P Protein expression		SQ *vs* 4P Microarray analysis	
				Fold Change	*P*-Value	Fold change	*P*-Value
Tu translation elongation factor, mitochondrial	TUFM	gi|32425705|	translation	1.21	$<< 1 \times 10^{-4}$	na	na
Putative protein product of Nbla10058	Nbla 10058	gi|76879893|	glycolysis	-1.6	$<< 1 \times 10^{-4}$	na	na
actin related protein 2/3 complex, subunit 2,	ARPC2	gi|7959903|	actin binding	-1.58	$<< 1 \times 10^{-4}$	na	na
Galectin-1	LGALS1	gi|56554352|	apoptosis/redox	-1.50	$<< 1 \times 10^{-4}$	-1.35	$<< 1 \times 10^{-4}$
phosphoglycerate kinase1	PGK1	gi|48145549|	glycolysis	-1.41	$< 1 \times 10^{-3}$	na	na
Phosphoglycerate Mutase	PGAM1	gi|67464305|	glycolysis	-1.34	$< 1 \times 10^{-2}$	na	na
Down syndrome cell adhesion molecule like-protein 1b	DSCAML 1	gi|23450945|	cell junction organisation	-1.28	$< 1 \times 10^{-2}$	na	na
heat shock 70kDa protein 5 (glucose-regulated protein, 78kDa)	BiP	gi|1143492|	anti-apoptosis /stress	-1.23	$< 1 \times 10^{-3}$	na	na
ATP synthase; H^+ transporting; mitochondrial F_1 complex	ATP5B	gi|50345982|	ion binding	-1.22	0.01	na	na
proteasome subunit; alpha type 1	PSMA1	gi|30582133|	protein turnover	-1.21	$< 1 \times 10^{-2}$	na	na

ns, not statistically significant; na: not available

3.1.11.4 Western blot confirmation of changes in protein expression

The following proteins were selected for validation by Western blotting as described in section 2.6 – EEF1a1 (instead of EF1a-like protein, for which there was no available antibody at the time of analysis), DSCAM and EBP1 binding protein. The proteomic results for these four proteins are shown in table 3.1-5. In all cases, the results were consistent with proteomic analysis. These proteins will be discussed further in section 6.2.6.

3.1.11.4.1 EEF1A1

Elongation factor 1-alpha 1 (eEF1a1) is a protein that in humans is encoded by the *EEF1A1* gene[302]. This gene encodes an isoform of the alpha subunit of the elongation factor-1 complex, which is responsible for the enzymatic delivery of aminoacyl tRNAs to the ribosome. Western blotting confirmed the increase in protein levels of EEF1A1 in SQ-Mitox-BCRP cells compared to DLKP-SQ-parent cells (figure 3.1-9).

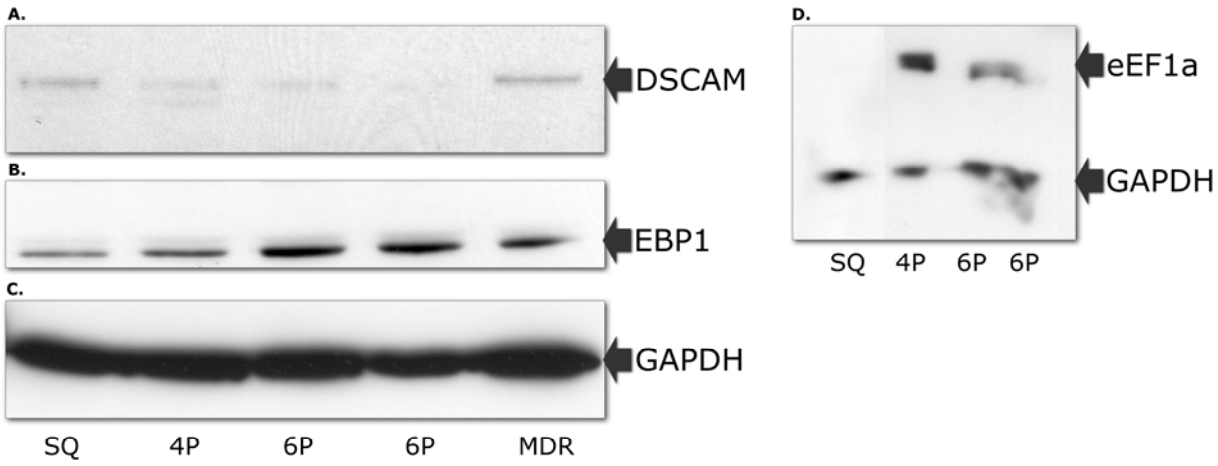

Figure 3.1-9: Western blotting for **(A)** DSCAM and **(B)** EBP1 in the DLKP-SQ (*SQ*), SQ-Mitox-BCRP-4P (*4P*), SQ-Mitox-BCRP-6P (*6P*) and SQ-Mitox-MDR (*MDR*) cell lines. Western blotting for **(D)** EEF1A1 in the DLKP-SQ (*SQ*), SQ-Mitox-BCRP-4P (*4P*) and SQ-Mitox-BCRP-6P (*6P*) cell lines. GAPDH was used as an equal loading control. SQ-Mitox-BCRP-6P (*6P*) is described in section 4.2.2

3.1.11.4.2 EBP1

EBP1 encodes an RNA-binding protein that is involved in growth regulation. Western blotting confirmed the decrease in protein levels in the SQ-Mitox-BCRP cell lines compared to the DLKP-SQ and SQ-Mitox-MDR cell lines (figure 3.1-9). The differential expression of EBP1 in the BCRP over-expressing cells lines warrants further investigation.

3.1.11.4.3 DSCAM

DSCAM encodes a neural cell adhesion molecule belonging to the Ig superfamily that mediates homophilic binding[303]. DSCAM and Dscam are both abbreviations for Down Syndrome Cell Adhesion Molecule [304]. The case difference between the two acronyms is significant as DSCAM refers to the gene that codes for the Dscam protein [305] and the DSCAM-like gene, DSCAMLl located on chromosome band 11q23, a locus associated with Gilles de la Tourette and Jacobsen syndromes[306].

DSCAML1 was identified from the proteomic data but DSCAM was investigated instead as a more likely candidate because of its role as a cell adhesion molecule associated with other diseases. As little is known about the DSCAM protein, it was decided to investigate the expression of DSCAM in the SQ-Mitox cell lines. As shown in figure 3.1-9, DSCAM was present in the DLKP-SQ parent and SQ-Mitox-MDR and decreased in the SQ-Mitox-BCRP cell lines.

IHC analysis of DSCAM expression in human cancer

Western blot analysis of DSCAM showed that it decreased with BCRP overexpression. There have been a few reports on the association of DSCAM with cancer but its role in tumourigenesis and drug resistance remains to be understood[307]. DSCAM expression in human cancer was investigated further (table 3.1-6). A lung cancer tissue microarray (TMA) (Biomax, LC817) was immunohisto-chemically stained using primary antibodies specific for DSCAM. The array contained 17 cases of squamous cell carcinoma, 16 adenocarcinoma, 1 bronchioloalveolar carcinoma and 6 small cell carcinoma. There were single cores per case with matched lymph node metastasis for each, providing 40 cases for analysis of expression (total 80 TMA cores). TMA cores were scored semi-quantitatively, according to the intensity of the DSCAM immunoreactivity observed (weak, moderate, strong). Membrane staining was observed in a

number of squamous carcinomas and adenocarcinomas. In squamous and adenocarcinoma samples where immunoreactivity was observed in the primary tumour, staining was also observed in matched metastatic tumours derived from the same patients (figure 3.1-10). Primary tumours from small cell carcinomas did not show any staining. Interestingly, in metastatic tumours from these small cell carcinomas, weak staining was observed in 3 out of 6 even though the primary tumours were negative. The potential role of DSCAM in cancer will be discussed further in section 6.2.6.

Figure 3.1-10 illustrates that negligible staining for DSCAM is observed in normal lung tissue, while intense immunoreactivity is observed in high-grade adenocarcinoma, known particularly for their poor differentiation but aggressive growth and metastasis. Likewise, a representative squamous cell carcinoma also shows immunoreactivity and intense immunoreactivity is also observed in an invasive ductal breast carcinoma.

Table 3.1-6: DSCAM Immunoreactivity in squamous, adeno and small cell lung primary tumours

Tumour type	DSCAM staining intensity
17 squamous	8/17 - negative 2/17 - weak 5/17- moderate 2/17 - strong
16 adenocarcinoma	5/16 - negative 5/16 – weak 3/16 – moderate 3/16 - strong
6 small cell carcinoma Lymph node metastatic small cell	6/6 negative 3/6 weak

3.1.12 *ABCB1* and *ABCG2* expression in SQ-Mitox-MDR and SQ-Mitox-BCRP

3.1.12.1 Introduction

Several mechanisms have been previously described that facilitate transcriptional up-regulation of *ABCG2* in different MDR cell line models: 1) *ABCG2* gene amplification, 2) chromosomal rearrangements and 3) alternative 3′-untranslated-mediated mRNA stability[308]. Until recently,

the most frequently occurring mechanism of *ABCG2* overexpression in MDR tumour cell lines was *ABCG2* gene amplification[53,309,310]. Drug-induced epigenetic modulation of *ABCB1* and *ABCG2* gene expression has gained increasing focus in a number of recent publications[311]. Epigenetics is the term for regulation of gene expression, other than via changes in the DNA sequence. Well-characterised modifications of DNA or histone scaffolding proteins include methylation, acetylation, phosphorylation, and ubiquitination. The enzymes responsible for these modifications chemically alter genomic DNA and histones, as well as epigenetic chromatin remodeling factors and regulate chromatin accessibility and ultimately gene expression.

The results presented earlier (table 3.1-1) have shown that SQ-Mitox-MDR and SQ-Mitox-BCRP cells were 174-fold and 313-fold resistant to mitoxantrone respectively and that this was attributed to the over-expression of the ABC transporters ABCB1 (P-gp) and ABCG2 (BCRP) (figure 3.1-7). This presented an interesting question as to whether the drug resistant cells were pre-existing in the DLKP-SQ population or arose by DNA damage and mutation. To further illucidate the mechanisms leading to this overexpression, gene copy number profiling and methylation analysis were performed. Additionally, 5-Aza-2' deoxycytidine (5-aza-dC) treatment of the SQ-Mitox cell lines was also carried out to look at the effects of methylation inhibition.

3.1.12.2 Gene Copy Number profiling

Genomic DNA was extracted from DLKP-SQ, SQ-Mitox-BCRP and SQ-Mitox-MDR cell lines. The Taqman real-time quantitative PCR (qPCR) method was used to test the copy number of *BCRP* and *MDR1* in these cell lines according to the protocol of Applied Biosystems (see section 2.9). Relative quantitation analysis was performed by CopyCaller Software (version v1.0), using the known calibrator sample method. In this study, limbal stromal cells were used as the known calibrator and were presumed to be diploid. Limbal stromal cells are a stem cell population which were isolated from the limbus of the corneal epithelia of the eye[283]. The *MDR1* copy number of the DLKP-A cell line was also investigated. The DLKP-A cell line is an adriamycin-selected MDR cell line containing multiple clonal subpopulations which exhibit significantly different drug resistances[277]. The C_T values were at the upper limits of detection and as a result there were errors. The minimum and maximum copy numbers are shown in table 3.1-7.

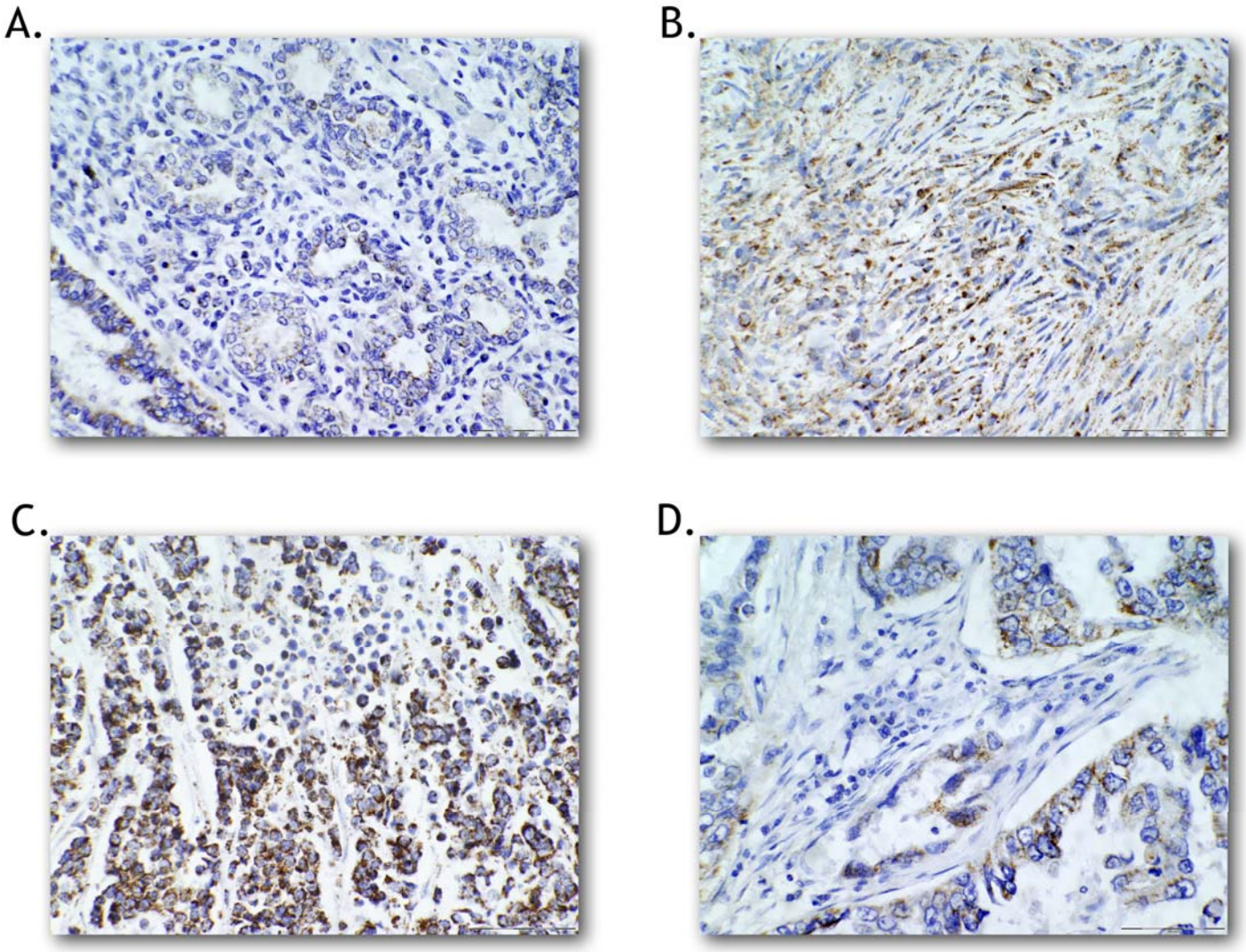

Figure 3.1-10: IHC analysis of DSCAM expression in human cancer. Normal lung, squamous, adeno, small cell carcinoma and invasive ductal breast carcinoma were immunohisto-chemically stained using a primary antibody specific for DSCAM. Representative photomicrographs are shown (A.) Negligible staining is observed in normal lung tissue. (B.) In contrast, intense DSCAM immunoreactivity is observed in invasive ductal breast carcinoma. (C.) High grade lung adenocarcinoma also shows marked staining for DSCAM. (D.) Squamous cell carcinoma of the lung also shows distinct immunoreactivity. (Original magnification of all photomicrographs, 400×, scale bar = 100 μm).

The PCR investigation showed that no copy number changes were detected in either SQ-Mitox-BCRP or SQ-Mitox-MDR cells using the primers to detect the BCRP genomic DNA target. (table 3.1-7). A positive control for BCRP internal copy number was not available. A copy number of 2 was detected in the SQ-Mitox-MDR cells, while a copy number of six was detected in the DLKP-A cells using the primers to detect genomic MDR1. Surprisingly a copy number change of 3 was detected in the DLKP-SQ and the SQ-Mitox-BCRP cell line using the primers to detect genomic *MDR1* DNA.

Table 3.1-7: TaqMan Copy Number Assays.

Cell Line	BCRP	min/max	MDR1	min/max
Limbal stromal	2	1-3	2	1-3
DLKP-SQ	2	1-3	3	3-4
SQ-Mitox-BCRP	2	1-4	3	2-5
SQ-Mitox-MDR	2	1-3	2	1-4
DLKP-A	-	-	6	5-6

3.1.12.3 Methylation

Introduction

Chemotherapeutic drug-induced transcriptional up-regulation of *BCRP* and other methylated genes occurs as early as 12 hours after initial drug exposure, hence resulting in as much as a 55-fold increase in *BCRP* (*ABCG2*) transcript levels within a single cell cycle[312]. The lack of *MDR1* and *BCRP* gene amplification in the SQ-Mitox cell lines suggest the possibility that the dramatic upregulation of both genes observed in these drug-resistant cell lines may be due to a loss of transcriptional silencing. To illucidate this further, a direct experiment examining the effects of inhibiting methylation on gene expression was performed using 5-azacytidine in DLKP-SQ cells (section 2.12.7). 5-azacytidine is one of many different chemical analogs for the nucleoside cytidine. When these analogs are integrated into growing DNA strands, some, including

5-azacytidine, severely inhibit the action of the DNA methyltransferase enzymes that are responsible for DNA methylation. Thus, methylation may be inhibited by flooding cellular DNA with 5-azacytidine, and cell lines can be compared before and after treatment to see what impact the loss of methylation has on BCRP and P-gp protein expression.

Methylation analysis was performed for the *BCRP* promoter as it has only one CpG island and therefore is relatively easy to design primers and probes for a successful analysis. In contrast, the *MDR1* promoter has several CpG islands which make such an analysis more difficult. Toward this end, the methylation status of the *BCRP* promoter in the DLKP-SQ cell line and its *BCRP*-overexpressing counterpart was investigated.

5-Aza-2' deoxycytidine (5-aza-dC) treatment of DLKP-SQ cells

DLKP-SQ and SQ-Mitox cells were incubated with 1μM concentration of the DNA methyltransferase inhibitor 5-aza-dC as described in section 2.12.7. After treatment for 72 hours, whole cell proteins from these cell lines were obtained, and protein isolated for Western blot analysis of BCRP and P-gp. The results confirmed little change between BCRP or P-gp protein in the DLKP-SQ or SQ-Mitox cell lines (figure 3.1-11).

Semiquantitative MethyLight real-time PCR with methylation-specific primers

For semiquantitative MethyLight analysis (as described in section 2.12), a dual-labeled probe is used together with a set of PCR primers that specifically binds to the methylation sites of interest. Bisulfite converted DNA requires a different primer sequence for methylated and unmethylated CpG sites, so the primers need to be specific to methylated, bisulfite converted DNA. If the methylation-specific primer binds to the DNA, it will be elongated, and the 5' → 3' exonuclease activity of Taq DNA Polymerase will lead to the degradation of the primer and the release of the fluorophore.

The Ct values obtained when using control DNA and a primer pair for the unmethylated BCRP gene (bisulfite converted) are shown in table 3.1-8. The probe was located between primers that bound the sites under investigation. Primers in this case are specific for unmethylated sequences,

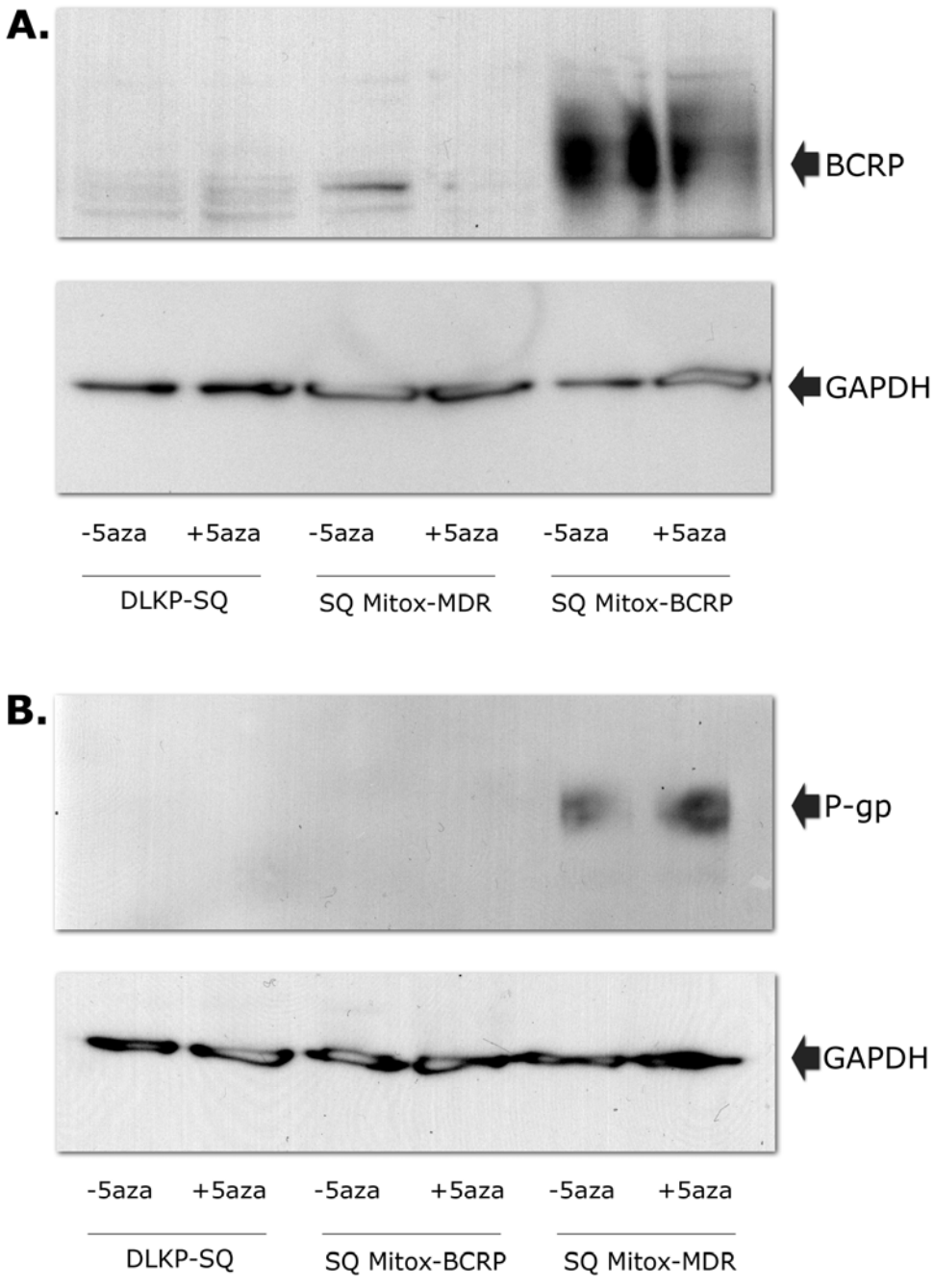

Figure 3.1-11: 5-Aza dC treatment has no effect on DLKP-SQ and SQ-Mitox cells. Western blots show BCRP and P-gp expression in DLKP-SQ, SQ-Mitox-BCRP and SQ-Mitox-MDR cells treated with 1μM 5-aza-dC. (**A.**) BCRP protein migrated at approximately 70 kDa. Lanes 1 and 2: DLKP-SQ with and without treatment. Lanes 3 and 4: SQ Mitox-MDR with and without treatment. Lanes 5 and 6: SQ –Mitox-BCRP with and without treatment. (**B.**) P-gp migrated at approximately 170kDa. Lanes 1 and 2: DLKP-SQ with and without treatment. Lanes 3 and 4: SQ Mitox-BCRP with and without treatment. Lanes 5 and 6: SQ –Mitox-MDR with and without treatment. GAPDH was used as an equal loading control in all blots.

annealing only to unmethylated DNA, and not to methylated DNA. During the PCR extension step released fluorophore was quantitated through its fluorescence. Surprisingly, there was a Ct value of 34.845 observed using the methylated control DNA. This value was quite high and perhaps there was some non-specific binding. Despite this, it was decided to use these primers for the actual methylation analysis.

Similarly, the Ct values obtained when using control DNA and a primer pair for the methylated *BCRP* gene (bisulfite converted) are also shown in table 3.1-8. The results indicated that these primers were suitable for use in detecting methylated stretches of DNA.

Table 3.1-8: Positive control results for methylation analysis using primers to detect methylated and unmethylated BCRP promoters

Primer for unmethylated BCRP gene		Primer for methylated BCRP gene	
Sample	**Ct value (Ct std err)**	**Sample**	**Ct value (Ct std err)**
Unmethylated control DNA	Undetermined	Unmethylated control DNA	Undetermined
Unmethylated control DNA (bisulfite converted)	25.762 (0.216)	Unmethylated control DNA (bisulfite converted)	Undetermined
Methylated control (bisulfite converted)	34.845 (1.103)	Methylated control (bisulfite converted)	26.373 (0.384)
No template control	Undetermined	No template control	Undetermined

The Ct values obtained when using the DLKP-SQ and SQ-Mitox-BCRP cell line DNA and primer pairs are shown in table 3.1-9. The first set of primers were specific for unmethylated *BCRP* sequences, annealing only to unmethylated DNA, and not to methylated DNA. The second set of primers were specific for methylated *BCRP* sequences alone. The results indicate that the *BCRP* promoter was unmethylated in both the DLKP-SQ and SQ-Mitox-BCRP cells. As expected, the results also illustrate that the primer pair for detection of a methylated *BCRP* gene did not produce a signal (thereby also confirming no DNA methylation). Future work examining the methylation state of the *MDR1* promoter is also warranted.

Table 3.1-9: Cell line DNA results for methylation analysis using primers to detect methylated and unmethylated BCRP promoters

Sample	Primer pair	Ct value (Ct std err)
DLKP-SQ	ACTB	27.76 (0.253)
SQ-Mitox-BCRP	ACTB	28.653 (0.448)
DLKP-SQ	Primer for unmethylated BCRP gene (bisulfite converted)	28.976 (0.123)
SQ-Mitox-BCRP	Primer for unmethylated BCRP gene (bisulfite converted)	28.933 (0.177)
DLKP-SQ	Primer for methylated BCRP gene (bisulfite converted)	Undetermined
SQ-Mitox-BCRP	Primer for methylated BCRP gene (bisulfite converted)	Undetermined

3.1.13 miRNA Expression Analysis of DLKP-SQ, SQ-Mitox-BCRP-4P and SQ-Mitox-MDR-4P

In order to further illucidate the mechanism of resistance in the mitoxantrone resistant variants, miRNA lists were generated from the raw Taqman Array data that may potentially reveal whether miRNAs are involved in the development of drug resistance in the SQ-Mitox variants. Changes in miRNA expression between DLKP-SQ parental cells and the derived drug resistant cell lines were generated using the data analysis tool, DataAssist software, with a P-value adjustment of $p \leq 0.05$. 1.5 fold lists of miRNAs with significant changes in expression ($p \leq 0.05$) in each cell line compared to the drug sensitive parental cell line were generated. Even though the TaqMan Human Micro RNA Array A enables quantitation of 377 human miRNAs, only 4 miRNAs with significant changes in expression in each cell line compared to the drug sensitive parental cell line were generated. The differentially expressed miRNAs, with their primary functions, are summarised in tables 3.1-10 and 3.1-11. These miRNAs will be discussed further in section 6.2.7.

Table 3.1-10: Significantly Up/Down regulated miRNAs in SQ-Mitox-BCRP vs DLKP-SQ

Assay	SQ-Mitox-BCRP vs DLKP-SQ Fold Change	P-value	Function
hsa-miR-218-4373081	22.0117	1.00E-04	tumour suppressor
hsa-miR-27a*-4395556	1.8303	0.0112	Activator of Wnt signaling pathway
hsa-miR-639-4380987	-3.071253071	0.0071	Controls cell proliferation
hsa-miR-335*-4395296	-8.196721311	0.0141	unknown

Table 3.1-11: Significantly Up/Down regulated miRNAs in SQ-Mitox-MDR vs DLKP-SQ

Assay	SQ-Mitox-MDR vs DLKP-SQ Fold Change	p-value	Function
hsa-miR-342-3p-4395371	1.6167	0.0119	tumour suppressor
hsa-miR-935-4395289	-4.012841091	0.0032	unknown
hsa-miR-524-3p-4378087	-2.569373073	0.0069	unknown
hsa-miR-550-4395521	-2.112824847	0.0145	unknown

3.1.14 Summary

In summary, two mitoxantrone resistant cell lines with distinct P-glycoprotein and BCRP expression were established. These two cell lines were selected from the same cell population and under identical conditions. Microarray analysis was performed in DLKP-SQ-Mitox-BCRP (4^{th} pulse) and DLKP-SQ-Mitox-P-gp (4th pulse). Functional annotation analysis of probesets exclusively differentially expressed in the BCRP overexpressing cell line revealed that the most significant GO categories were related to RNA processing, the cellular response to stress and cell cycle control. Functional annotation analysis of genes exclusively differentially expressed in the P-gp over-expressing cell line revealed that the most significant GO categories were related to chromatin organization, chromatin modification and embryonic morphogenesis.

Proteomic analysis of the DLKP-SQ and its drug resistant variant SQ-Mitox-BCRP revealed many intracellular protein changes including those involved in various processes such as glycolysis, protein turnover and translational elongation. Interestingly, increased IHC staining of the cell adhesion molecule DSCAM was shown to be associated with aggressive, metastatic lung and breast carcinomas. In contrast, Western blot analysis of SQ-Mitox-BCRP showed an absence of DSCAM. However, the presence of DSCAM in the DLKP-SQ and SQ-Mitox-MDR cells was observed.

miRNA analysis of the DLKP-SQ and its drug resistant variant SQ-Mitox-BCRP revealed differential expression of 4 miRNAs involved as tumour suppressors, in cell proliferation and Wnt signalling. miRNA analysis of the DLKP-SQ and its drug resistant variant SQ-Mitox-MDR revealed differential expression of 4 miRNAs of unknown function.

The gene copy number of *ABCG2* and *ABCB1* was investigated using qPCR. While the DLKP-A cell line exhibited a *ABCB1* gene copy number of 6, the SQ-Mitox-MDR cells exhibited no change in copy number. Surprisingly the DLKP-SQ and the SQ-Mitox-BCRP cells exhibited an *MDR1* gene copy number of 3. The elevated expression of these genes cannot be solely explained by gene copy number.

Treatment with 5-azacytidine of the DLKP-SQ, SQ-Mitox-BCRP and SQ-Mitox-MDR cells had no effect on BCRP or P-gp protein expression. DNA methylation analysis of the BCRP over-expressing cell line revealed that the promoter of *BCRP* was unmethylated in both the DLKP-SQ and SQ-Mitox-BCRP cells.

Based on these results, this chapter provides a preliminary insight into new candidate genes associated with P-gp and BCRP-mediated resistance. These sublines may also prove to be useful models for the study of new modulators of resistance aimed at improving the outcome of acquired drug resistance.

CHAPTER 4

Characterisation of clonal subpopulations of DLKP and drug resistant variants.

Introduction

Resistance to chemotherapy drugs is a major problem in cancer treatment. Consequently, a better understanding of the mechanisms of drug resistance would help to overcome this problem. Intrinsic and acquired drug resistance are believed to cause treatment failure in over 90% of patients with metastatic cancer[36]. Some tumours are initially sensitive to an anticancer agent and, over time, develop a resistance to it – this is referred to as acquired resistance. Whereas, other tumours are resistant before treatment and this is known as intrinsic resistance. Both intrinsic and acquired resistance lead to tumour progression and metastatic changes, making treatment difficult in such patients.

As a result, the overall 5-year survival of patients diagnosed with some cancers, such as lung cancer, remains dismal and is less than 15%. Mechanisms of lung cancer invasion and metastasis and the link with drug resistance has not been fully elucidated and a better understanding of these processes could contribute to better treatment of this disease.

The work described in this chapter was undertaken to increase understanding of the molecular nature of invasion in human lung cancer cell lines using the following approaches:

1. To characterise the morphologically distinct populations of the lung cancer cell line DLKP – extensive characterisation in the form of microarray analysis.
2. To examine the temporal relationship between the emergence of drug resistance and invasiveness in a clone of the DLKP cell line model of mitoxantrone resistance development in order to better understand any links which may exist between multidrug resistance and cancer invasion.

4.1 Characterisation of clonal subpopulations of DLKP

4.1.1 Introduction

Most human tumours are heterogenous at the morphological level and are a mix of different types of cells. Lung cancer is a good example and it's remarkable heterogeneity has become more apparent over the last decade. Heterogeneity is important in terms of predicting the clinical behaviour of the tumour, therapeutic responses and also in trying to understand what sustains heterogeneity[313]. In this section, I have exploited the availability of clonal populations of a human lung cancer cell line DLKP to investigate the development of *in vitro* invasiveness and to investigate some aspects of the mRNA and protein expression changes associated with these changing phenotypes.

4.1.2 Investigation into clonal variation in sub-populations of DLKP

In tumour progression, populations of cancer cells with different patterns of growth and invasion often arise within the same tissue and within individual neoplasms. Previous studies[280] have found that DLKP, a human lung cell line established from a tumour histologically diagnosed as a "poorly differentiated squamous carcinoma", contains at least 3 morphologically distinct populations. Three clones corresponding to these populations were established from the parental DLKP cells — DLKP-SQ (squamous), DLKP-M (mesenchymal like), and DLKP-I (intermediate), that are characterised by their morphologies and growth patterns [281,280]. On prolonged subculture, DLKP-SQ and DLKP-M can each interconvert with DLKP-I, but DLKP-SQ and DLKP-M do not appear to interconvert.

This panel of DLKP cell lines provides an *in vitro* model of invasion. In addition, these cell lines differing in levels of invasiveness (but all derived from the same parent), offer a unique opportunity to study tumour heterogeneity. To characterise the morphologically distinct populations of the human lung cancer cell line DLKP, an extensive characterisation in the form of microarray analysis and mutation profiling was performed.

4.1.3 Morphology of DLKP clones

The three clones are morphologically distinct (figure 4.1-1). All grow as monolayers. The DLKP-SQ clones are squamous in appearance with distinct cell boundaries. The DLKP-I cells grow in colonies with indistinct cell boundaries, while the DLKP-M clone is of intermediate size with an irregular, fibroblastoid-like morpholgy and does not appear to form colonies[280].

4.1.4 Invasion assays of DLKP clones

Degradation of the extracellular matrix (ECM) by cancer cells is an important event in the dissemination of cells and spread of disease[314]. In this study, the invasive activity of the DLKP clones was examined using an *in vitro* invasion assay as described in section 2.3.1. A visual analysis of the levels of invasion of the clones showed that the DLKP-M cells were more invasive than the DLKP-SQ or DLKP-I cell lines. The relative invasiveness of the sub-lines compared to each other after 48 hours (shown in figure 4.1-1) remained constant.

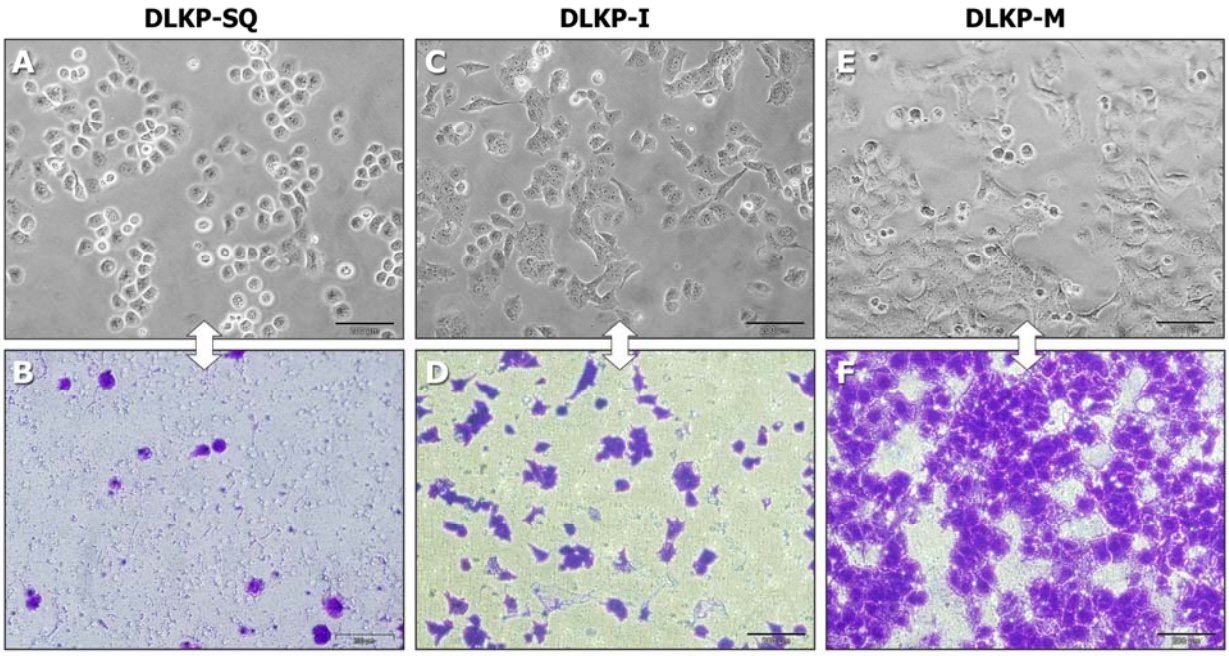

Figure 4.1-1: Growth of DLKP clones on plastic (**A**, **C** and **E**) and visual analysis of the level of invasion of the DLKP clones. Cells suspended in media were seeded in Matrigel invasion inserts. After 48h in culture, cells that invaded the lower surface of the filters were recorded (**B**, **D** and **F**) (original magnification = 100×, scale bar = 200 μm).

4.1.5 Adhesion assays of DLKP clones

Many studies have suggested a correlation between the metastatic potential and the expression of adhesion molecules and/or their receptors on tumour cell surface membranes[315,316]. Thus, the expression of functional fibronectin, vitronectin, laminin and collagen IV and V receptors on the DLKP cells were investigated which included an adherence assay to determine the *in vitro* binding capability of the clones to these molecules (figure 4.1-2) (as described in section 2.3.3). Overall, the highest level of adhesion was observed through fibronectin and vitronectin for the cell lines DLKP-I and DLKP-M. In contrast, no *in vitro* binding to collagens type IV and V was displayed by any of the clones. The increase in adhesion to vitronectin could be explained by the increased expression of integrin αV in the DLKP-I and DLKP-M cell lines.

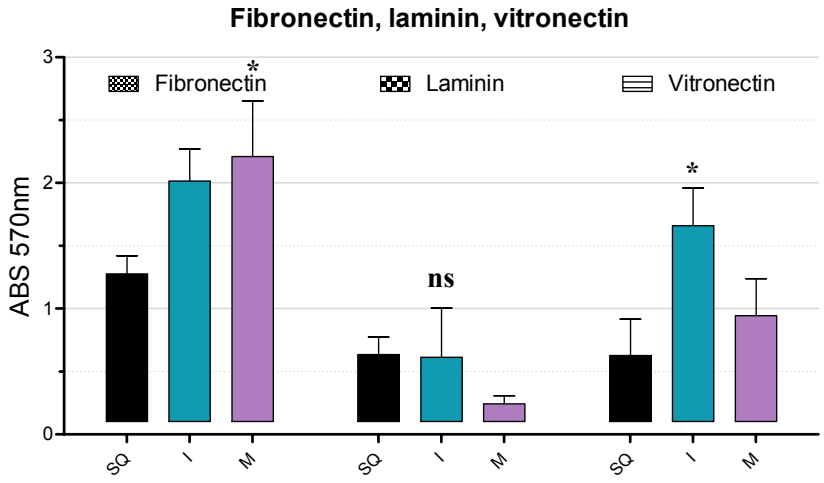

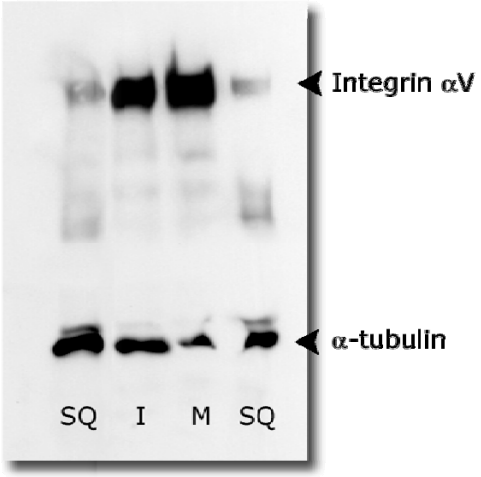

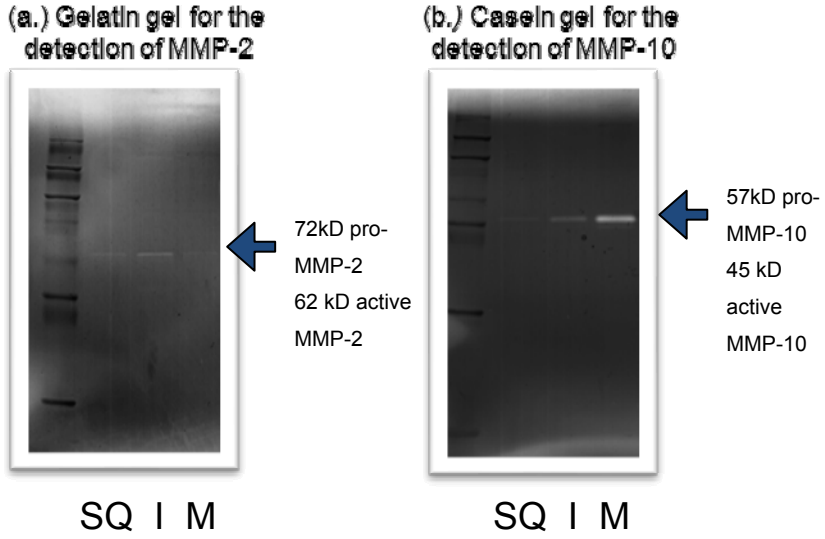

Figure 4.1-2. Adhesion of DLKP-SQ, DLKP-I and DLKP-M clones to extracellular matrix proteins. Results are expressed as absorbance at 570nm. Data shown is mean ± standard deviation (n = 3). Fibronectin: SQ vs M, $p < 0.05$; Laminin: not significant (ns); Vitronectin: SQ vs I, $p < 0.05$, 1-way ANOVA. Zymography confirms that there are higher levels of MMP-2 in DLKP-I and higher levels of MMP-10 in DLKP-M. The Western blot above displays integrin alpha V protein expression in DLKP clones.

4.1.6 Microarray analysis of DLKP clones

The expression profiles of the DLKP clones were analysed and compared to each other using microarray analysis as described in section 2.10. The invasion status of the DLKP clones are shown in the invasion assay results (figure 4.1-1). The purpose of the microarray analysis was to compare invasive and non-invasive cell lines in order to identify genes and compare gene transcription profiles descriptive of invasion.

4.1.6.1 Hierarchical clustering

Before generating the gene lists, it was important to examine the relationship between different cell lines as observed by hierarchical clustering (figure 4.1-3). In hierarchical clustering, genes with similar expression patterns are grouped together and are connected by a series of branches, which is called a clustering tree (or dendrogram) (see section 2.10.9). Two way hierarchical cluster analysis (HCA) was carried out using Euclidean distance and the Ward clustering algorithm in the R statistical environment and applied to all probesets and filtered probesets.

Generally, the data can be divided into two distinct groups, one consisting of all the DLKP-SQ and DLKP-I clones, and one consisting of the DLKP-M clone.

All of the samples used in the experiment were run in triplicate, all three replicates of a particular sample were expected to cluster together, and all such clusters would be expected to be significantly differently from each of the other clusters. This was not the case for one of the sets of samples (figure 4.1-3). DLKP-I did not behave as expected and did not cluster with its replicates. Two of the DLKP-I samples clustered with the DLKP-SQ samples and one clustered with the DLKP-M sample.

4.1.6.2 Generation of gene lists

The aim of the microarray analysis was to generate gene lists that:

1. were specific to an invasive phenotype, in order to identify genetic markers for invasion,
2. were specific to the DLKP-I and DLKP-M clone.

Before generating these gene lists, it was important to examine the relationship between different cell lines as observed by hierarchical clustering (section 4.1.6.1). As already mentioned, the

DLKP-I replicates did not behave as expected, and this was obvious from the way they clustered. Despite this, it was decided to remove the outlier and continue with the remaining samples.

The purpose of initial comparisons (SQ *vs* I and SQ *vs* M) was to determine the number of genes changed between the baseline and experiment samples. Gene filters employed for this analysis included a raw value difference (between baseline and experiment) of at least 100, and a fold

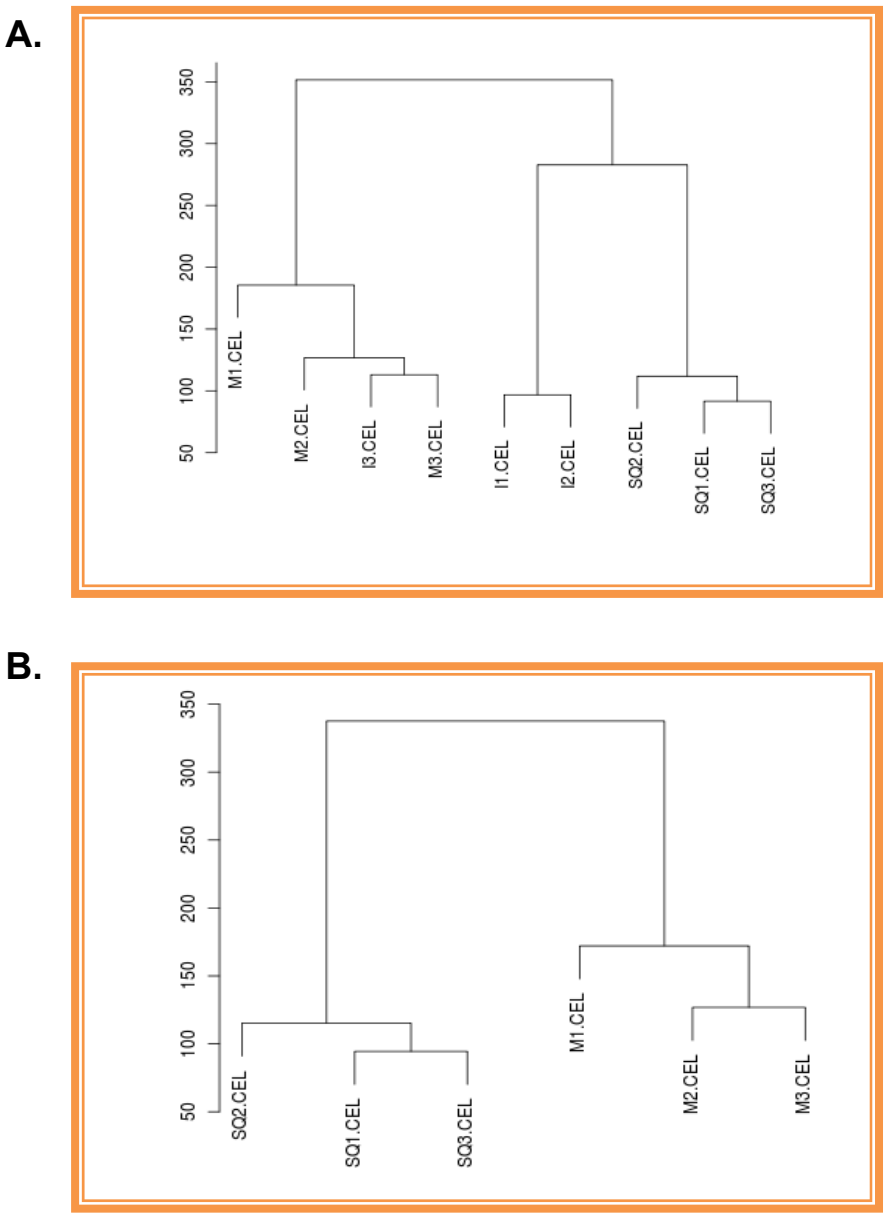

Figure 4.1-3: Hierarchical cluster analysis dendrogram of filtered probesets for DLKP-SQ, DLKP-I and DLKP-M samples used in microarray analysis. The tree represents relationships amongst genes in which branch lengths represent degrees of similarities. (**A.**) All probesets for DLKP-SQ, DLKP-I and DLKP-M samples. (**B.**) Dendrogram of filtered probesets for DLKP-SQ and DLKP-M cell lines.

change of at least 1.5. After these filters were in place and the irrelevant genes were removed, a Welch modified two-sample t-test was carried out to generate p-values for each probe. Only P-values of less than 0.05 were accepted. Gene list comparisons were made using dChip (section 2.17.1) and are summarised in table 4.1-1.

Comparison of DLKP-SQ (baseline) to DLKP-M (experiment) resulted in a list of 2746 genes. That is, the expression of 2746 genes was up- or down-regulated in DLKP-M (1753 genes up-regulated and 993 genes down-regulated). The top 15 over-expressed and under-expressed genes are shown in Table 4.1-1a.

Comparison of DLKP-SQ (baseline) to DLKP-I (experiment) resulted in a list of 1319 genes. That is, the expression of 1319 genes was up- or down-regulated in DLKP-I (490 genes up-regulated and 829 genes down-regulated). The top 15 over-expressed and under-expressed genes are shown in tables 4.1-1b.

4.1.6.3 Confirmation of differences in gene expression among the three DLKP clones

To investigate whether the invasive potentials of the DLKP clones were associated with differential gene expression, seven genes that were previously shown to be differentially expressed in the invasive DLKP-M and DLKP-I and poorly invasive DLKP-SQ cell lines, were picked for analysis by Western blot and immunofluorescence. These included genes that coded for proteins with a known role in invasion such as integrin αV. Piccolo, a presynaptic cytoskeletal matrix protein was also analysed because of high expression change in DLKP-M (but absent from the DLKP-I list). Olfactomedin 3 was previously shown to be highly expressed in the DLKP-SQ clone relative to the DLKP-I and DLKP-M clones[281]. A Western blot investigation was carried out on integrin αV (figure 4.1-2), ROBO2/SLIT2 and ALCAM (figures 4.1-6 and 4.1-7 respectively) as described in section 2.6. Immunofluorescence was performed on Piccolo, N-cadherin, MMP-2 and MMP-10 as described in section 2.5.1. Zymgraphy was carried out on MMP-2 an MMP-10 as described in section 2.4. Integrin αV, N-cadherin, ROBO2/SLIT2, ALCAM and MMP-10 confirmed the trends indicated in the microarray analysis (i.e. increased expression relative to the SQ parent cell line). These genes will be discussed further in section 6.4.3.

Table 4.1-1a: Top fifteen over- and down-expressed genes

	DLKP-SQ vs DLKP-M genelist:					
	Gene symbol	***Main function***	***Fold change***	***Gene symbol***	***Main function***	***Fold change***
	Top 15 over-expressed genes			*Top 15 down-expressed genes*		
01	VGLL3	transcription	321	OLFM3	protein binding	-139
02	PCLO	calcium ion binding	204	HAPLN1	cell adhesion	-127
03	NELL2	Cell adhesion	165	CTCFL	gene regulation	-66
04	DDX3Y	RNA helicase	149	HSP1A	member of heat shock protein 70 famiily	-64
05	LHX9	transcription factor	140	PMAIP1	pro-apoptotic member of Bcl-2 family	-49
06	SCN9A	sodium ion transport	126	HTR2B	serotonin receptor	-37
07	ECRG4	G1 to G0 transition	121	LXN	metalloendopeptidase inhibitor activity	-32
08	CADM2	Cell adhesion	107	PDE4B	3',5'-cyclic phosphodiesterase act.	-31
09	PLCB4	signal transducer activity	102	VCAN	cell adhesion	-21
10	Camk2b	calcium signalling	101	VCAN	cell adhesion	-28
11	SLC6A15	amino acid transporterer	100	PMAIP1	promotes apoptosis	-27
12	MARCKS	actin filament binding	95	NOX4	oxygen sensor	-25
13	SLC6A15	neuronal amino acid transport	94	RGMB	coordinate BMP signaling	-18
14	MIR100HG	unknown	80	PRSS21	serine-type endo. activity I	-18
15	GBRG1	neurotransmission	75	IGF1R	tyrosine kinase activity	-18

Table 4.1-1b: Top fifteen over- and down-expressed genes

	DLKP-SQ vs DLKP-I genelist:					
	Gene symbol	***Main function***	***Fold change***	***Gene symbol***	***Main function***	***Fold change***
	Top 15 over-expressed genes			*Top 15 down-expressed genes*		
01	CDH2	cell adhesion	155	HAPLN1	cell adhesion	-179
02	TTF1	nuclear transcription factor	154	IFITM3	cytokine-mediated signalling pathway	-84
03	DSG2	calcium ion binding	132	BACE2	aspartic type endopeptidase acitivity	-55
04	PTPRC	T cell activation	120	IGFBP2	IGFR signalling pathway	-52
05	DSG3	calcium ion binding	119	IFITM2	cytok-medi signal. path.	-49
06	CADM2	adherins junct organis	103	ARHGAP18	signal transduction	-46
07	FST	BMP signalling pathway	94	STGC3	not known	-40
08	DSC1	homophilic cell adhesion	84	TRIM56	ubiquitin-protein lig act	-39
09	ROBO2	axon guidance	67	APOBEC3B	deoxycytid deamin activi	-36
10	ALCAM	cell adhesion	74	FAM155A	not known	-36
11	hypo prot LOC144977	unknown	70	CLONE=IMAGE :2369365	not known	-37
12	DKK1	wnt signalling pathway	69	PSMB8	DNA damage response	-32
13	SLC6A15	neurotrans trans activity	63	IGF1R	Insulin recep sign pathw	-31
14	gb:N25883	unknown	63	QPRT	NAD metabolic process	-30
15	AW291402	unknown	58	VCAN	cell adhesion	-28

(1) Integrin alpha V

Integrin alpha V was over-expressed in both the DLKP-SQ vs DLKP-M (3-fold) and DLKP-SQ vs DLKP-I (3 fold) genelists. Previous studies have confirmed the pivotal role of alphaV integrins in cell invasion and metastasis[317,318]. Integrin alpha V was expressed at higher levels in the DLKP-I and DLKP-M clones (figure 4.1-2).

(2) N-cadherin (cadherin 2)

N-cadherin was over-expressed in the DLKP-SQ vs DLKP-I (155 fold) genelist only. It is also known as neural cadherin and is a classical cadherin from the cadherin superfamily. Immunofluorescence was performed on N-cadherin to illustrate the localisation of the protein within the cells. Investigation of N-cadherin expression in the DLKP clones revealed that it was overexpressed in the DLKP-I clone only (figure 4.1-4).

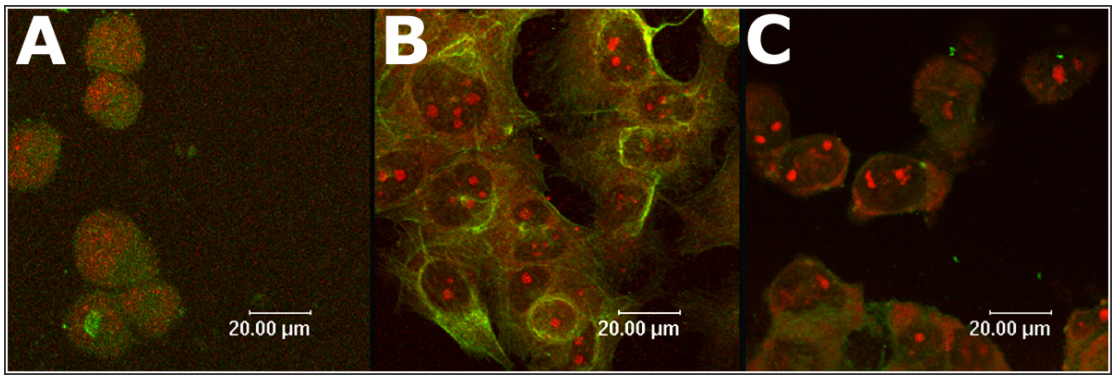

DLKP-SQ **DLKP-I** **DLKP-M**

Figure 4.1-4: Immunofluorescence cell surface staining of N-cadherin. DLKP-SQ (**A**), DLKP-I (**B**) and DLKP-M (**C**) cells stained with an N-cadherin antibody. Immunoreactivity is observed in invasive DLKP-I cells only. DLKP-SQ and DLKP-M cells show very weak immunoreactivity. Counter stained with propidium iodide. Original magnification of all photomicrographs, ×400, scale bar = 20 µm.

(3) Piccolo

Piccolo was over-expressed in the DLKP-SQ vs DLKP-M (83 fold) microarray genelist only. Piccolo encodes a protein that functions as part of the presynaptic cytoskeletal matrix thought to be involved in regulating neurotransmitter release. Immunofluorescence was performed on

piccolo to illustrate the localisation of the protein within the cells. Strongest expression was observed in the DLKP-I clone, with some cells in the DLKP-M population also showing strong expression of the protein.

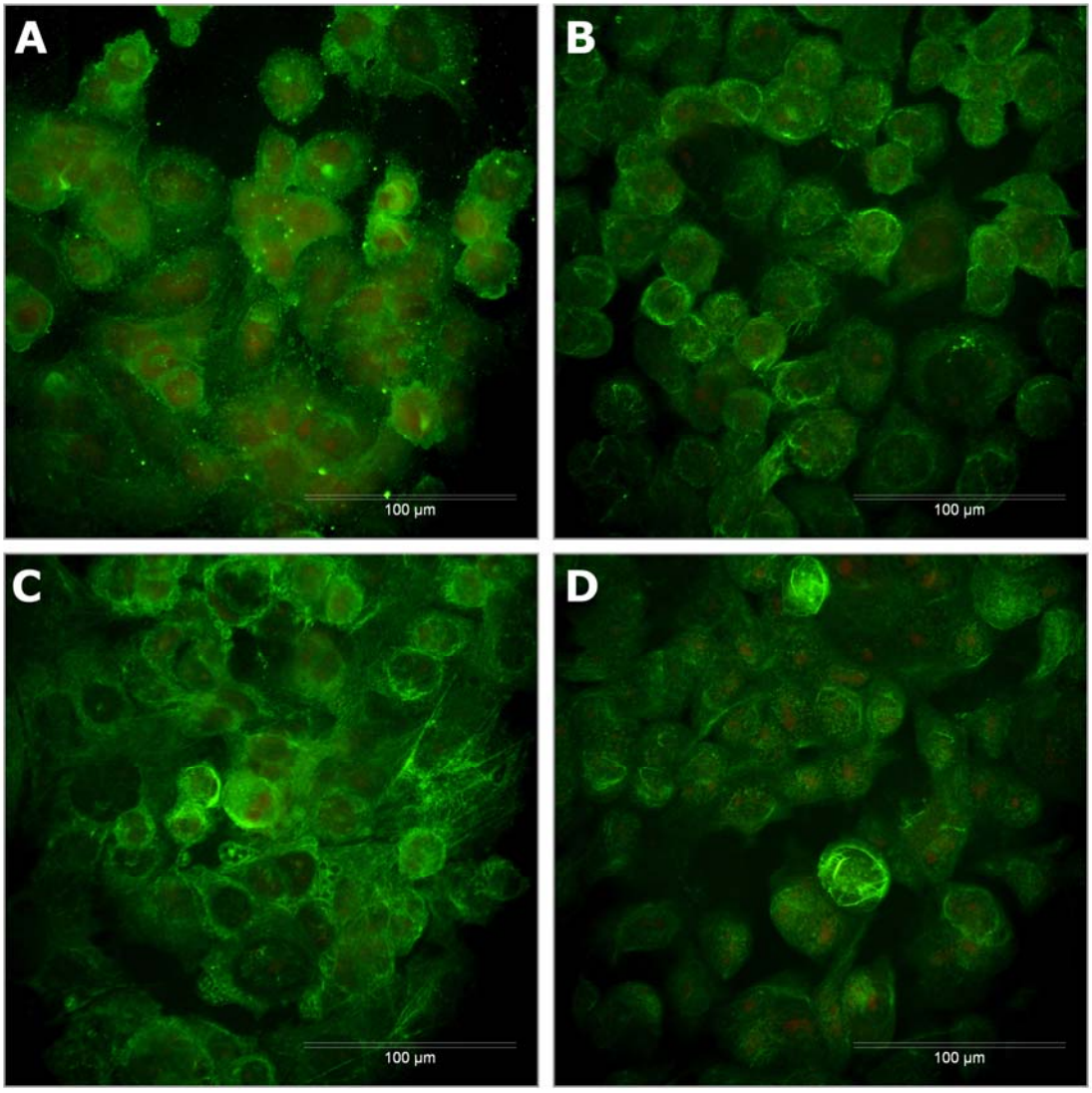

Figure 4.1-5: Immunofluorescence cell surface staining of piccolo. DLKP parent (**A**), DLKP-SQ (**B**), DLKP-I (**C**) and DLKP-M (**D**) cells stained with a piccolo antibody. Strongest immunoreactivity is observed in the invasive DLKP-I cells with some cells in the DLKP-M population showing some immunoreactivity. DLKP and DLKP-SQ cells show weak immunoreactivity. Counter stained with propidium iodide. Original magnification of all photomicrographs, ×,400 scale bar = 100µm.

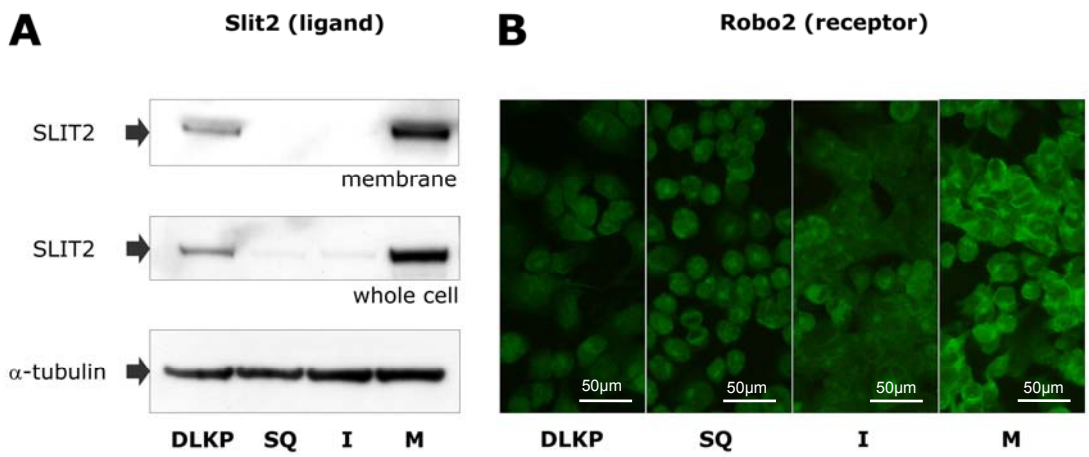

Figure 4.1-6: Expression of SLIT2 and its receptor ROBO2 in the DLKP clones. (**A.**) Immunoblot showing expression of SLIT2 in the DLKP clones. SLIT2 migrated at approximately 165 kDa. α-tubulin was used as an equal loading control. (**B.**) Immunofluorescence cell surface staining of ROBO-2**.** DLKP parental cells, DLKP-SQ, DLKP-SQ, DLKP-I and DLKP-M cells stained with a ROBO-2 antibody. Immunoreactivity was observed in all of the cells with the DLKP-M cells showing the strongest immunoreactivity. Original magnification of all photomicrographs, ×400, scale bar = 50µm. Results facilitated by Andrew McCann. This work is currently unpublished.

(4) SLIT2 / ROBO2

Microarray analysis indicated that ROBO2 is overexpressed in the DLKP-I cells only (table 4.1-1). ROBO2 is a receptor for SLIT2, and probably SLIT1, which is thought to act as molecular guide in cellular migration during neuronal development. Western blot analysis confirmed that the DLKP-M cells express high levels of SLIT2 and ROBO2, whereas the DLKP parental cells, DLKP-SQ and DLKP-I express low levels of SLIT2 (figure 4.1-6). Using immunofluorescence, ROBO2 was detected in all of the clones with the strongest expression observed in the DLKP-M cells.

(5) ALCAM

CD166, also known as activated leukocyte cell adhesion molecule (ALCAM), is a highly conserved 110-kDa multidomain, transmembrane type-1 glycoprotein of the immunoglobulin super family, which was first described as a CD6 ligand on leukocytes[319]. Microarray analysis indicated that ALCAM was overexpressed in the DLKP-I cell line relative to the DLKP-SQ cell

line (table 4.1-1). Western blot analysis confirmed that the DLKP parental, DLKP-SQ and DLKP-M cell lines express low levels of ALCAM whereas the DLKP-I cells expressed high levels of this protein (figure 4.1-7).

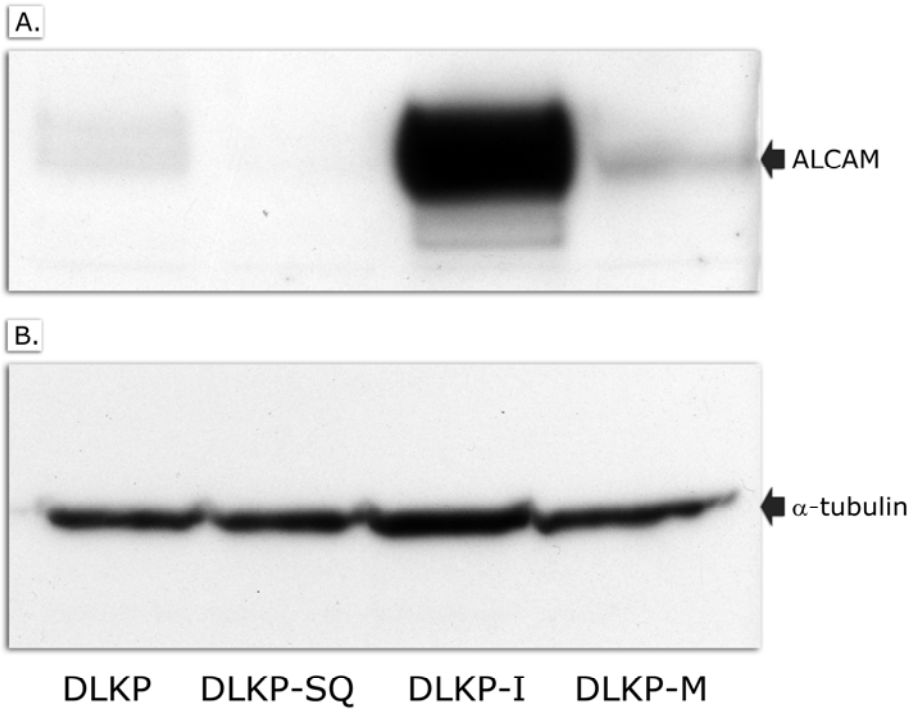

Figure 4.1-7. Western blot analysis showing expression of ALCAM in the DLKP clones. (**A.**) ALCAM migrated at approximately 105 kDa. ALCAM is clearly overexpressed in the DLKP-I cell line. (**B.**) α-tubulin was used as an equal loading control. Blot facilitated by Andrew McCann. This work is currently unpublished.

(5) OLFM3

Microarray analysis indicated that olfactomedin 3 (OLFM3) is down-expressed in the DLKP-M cell line (table 4.1-1a). OLFM3 belongs to a family of glycoproteins containing a conserved C terminal olfactomedin domain. OLFM3 may have a role in anoikis-resistance in the DLKP cell line as shown in a study carried out in collaboration with Dr. Joanne Keenan and others in this laboratory[281] (Appendix II).

4.1.7 Expression of MMP-2 and MMP-10 in the DLKP clones

Since the major enzymes implicated in extracellular matrix remodelling are the matrix metallo proteinases (MMPs), the MMP expression profile of the DLKP clones was examined using

immunofluorescence studies and zymography. Since MMP-2 was previously shown to be increased in drug resistant DLKP-SQ cells in our laboratory[196] and MMP-10 was shown to be increased in the DLKP-SQ *vs* DLKP-M and SQ *vs* SQ-Mitox microarray genelists, the further investigation of the role of these MMPs in DLKP invasion was warranted.

Using immunofluorescence studies as described in section 2.5.1, MMP-2 was detected in all of the cell lines with the the DLKP parent showing similar staining to DLKP-I (figure 4.1-8). The DLKP-SQ clone shows diffuse staining while for the DLKP-I clone, the MMP-2 antigen is asymmetrically distributed upon the cell surface, with major concentrations of the enzyme found along the lamellopodia. The DLKP-M clone shows the strongest staining.

The DLKP parent cells show less MMP-10 staining overall (figure 4.1-9). The DLKP-I clone appears to have the most MMP-10. Like MMP 2, it appears to be located on the surface and on the lamellopodia. The DLKP-M clone shows less staining than the DLKP-I clone even though the zymogram analysis indicates that it has a much higher level of MMP 10 (figure 4.1-2). It is likely that it may be secreted into the conditioned medium by the DLKP-M clone.

Zymography analysis of MMPs from the conditioned media is illustrated in figure 4.1-2. This shows that the DLKP parent and all of the clones secrete MMP-2 protein. The levels of MMP-2 protein detected are similar in both DLKP-SQ and DLKP-M cell lines while the DLKP-I cells may produce more latent MMP-2 than the DLKP-SQ and DLKP-M cells. However, the DLKP-I cell line also expressed low levels of active MMP-2 as seen by the presence of a faint lower molecular weight band in figure in 4.1-2. In contrast, DLKP-M appeared to produce more latent MMP-10 than the DLKP-SQ and DLKP-I cells.

4.1.7.1 Effect of MMP-2 and MMP-10 blocking antibodies on the in vitro invasiveness of the DLKP-I and DLKP-M cell lines

Following observations that the DLKP-I and DLKP-M cell lines were more invasive than the DLKP-SQ cell line and subsequent to the MMP analysis, there were dramatic differences observed between the cell lines in their MMP-2 and MMP-10 expression patterns. These results suggested that MMP-2 and MMP-10 expression in DLKP-I and DLKP-M may play a role in the increased invasiveness of these cells. In order to address this question, MMP-2 and MMP-10 blocking antibodies were employed to investigate their effects, if any, on the invasiveness of the DLKP-I and DLKP-M cell lines.

The addition of 5µg/ml of MMP-2 antibody saw a significant reduction in the invasiveness of the DLKP-I and DLKP-M cell lines (approximately 50-30% respectively). Cells treated with an IgG control antibody for MMP-2 showed no decrease in invasion in comparison to DLKP-I and DLKP-M control cells (figures 4.1-10 and 4.1-11) ($p < 0.001$ for DLKP-I and $p < 0.05$ for DLKP-M).

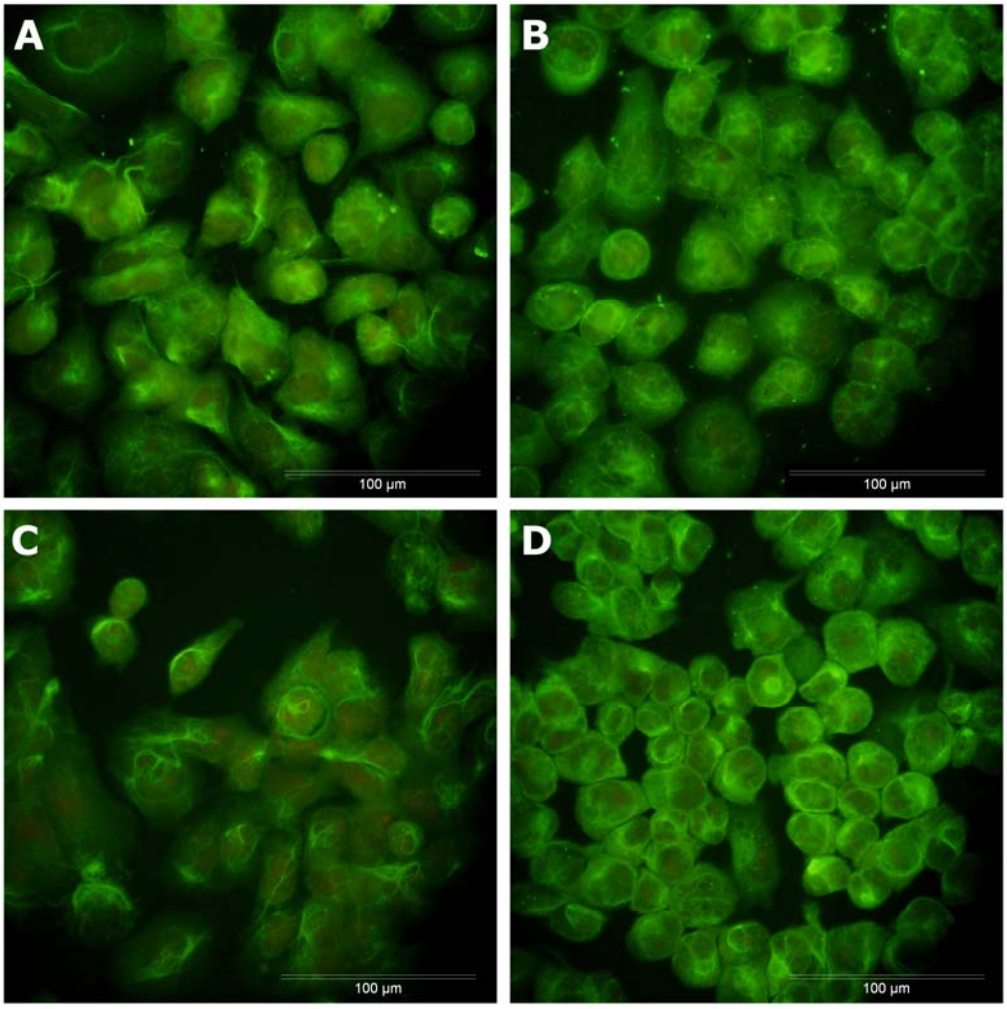

Figure 4.1-8: Immunofluorescence cell surface staining of MMP-2 in DLKP clones. DLKP parent (A), DLKP-SQ (B), DLKP-I (C) and DLKP-M (D) cells stained with an MMP-2 antibody which detects both the pro- and active forms of human MMP-2. Immunoreactivity is observed in all of the cells with the DLKP parental cells showing similar staining to the DLKP-I cells. Strongest immunoreactivity is observed in the DLKP-M cells. Counter stained with propidium iodide. Original magnification of all photomicrographs, ×400, scale bar = 100 µm.

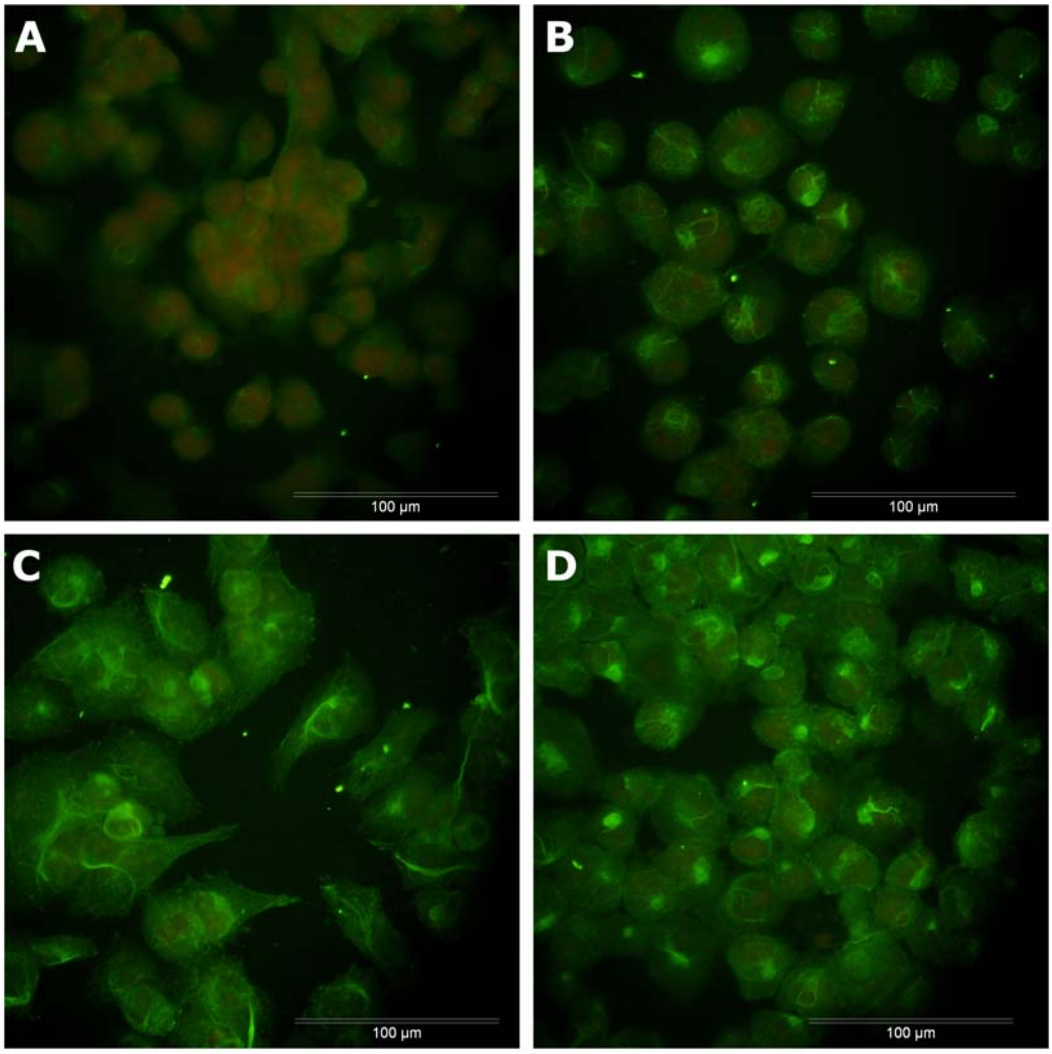

Figure 4.1-9: Immunofluorescence cell surface staining of MMP-10 in DLKP clones. DLKP parent (A), DLKP-SQ (B), DLKP-I (C) and DLKP-M (D) cells stained with an MMP-10 antibody which detects both the pro- and active forms of human MMP-10. Immunoreactivity is observed in all of the cells with the DLKP parental cells showing the weakest staining. Counter stained with propidium iodide. Original magnification of all photomicrographs, ×400, scale bar = 100µm.

In contrast, the addition of 10µg/ml of MMP-10 antibody had no effect on the invasiveness of DLKP-I and DLKP-M cells. There was a small but variable effect in MMP-10 treated DLKP-I cells while there was a highly variable effect in MMP-10 treated DLKP-M cells.

4.1.8 Sequenom analysis of DLKP clones

The DLKP clones and the cell line DLRP were evaluated for the presence of mutations using sequenom technology (section 2.14 and section 1.2.6). DLRP (see section 2.1) is a poorly differentiated squamous cell lung carcinoma which was developed in the National Institute for Cellular Biotechnology (NICB)[282] within Dublin City University (DCU).

Analysis of the clones (table 4.1-2) using Sequenom's mutation panel (section 2.14 and appendix I) showed a sequence alteration within the following genes:

1. the Sema domain of MET (MET_N375S_A1124G),
2. the p85α regulatory subunit of PI3K3R1 (PIK3R1_M3261_G978ATC) (DLKP, DLKP-SQ and DLKP-M clones only),
3. TP53 (TP53_G245VDA_G734TAC) (all DLKP clones and DLRP)
4. EGFR (EGFR_V769LMG2305AT) (DLKP-SQ clone only)
5. IDH1 (IDH1_V1781_G532A) (DLRP only)
6. NRAS (NRAS_G12SRC_G34ACT) (DLRP only)

Table 4.1-2: Sequenom Mutation Analysis of DLKP Clones and DLRP

Mutation	DLKP Parent	DLKP-SQ	DLKP-I	DLKP-M	DLRP
EGFR_V769LM_G2305AT	G	AG	G	G	G
IDH1_V1781_G532A	G	G	G	G	AG
MET_N375S_A1124G	AG	AG	AG	G	A
NRAS_G12SRC_G34ACT	G	G	G	G	GT
PIK3R1_M3261_G978ATC	AG	AG	G	AG	G
TP53_G245VDA_G734TAC	AG	AG	AG	AG	AG

The results indicate that there may be differential activation of EGFR, Met and PIK3R1 within the clones.

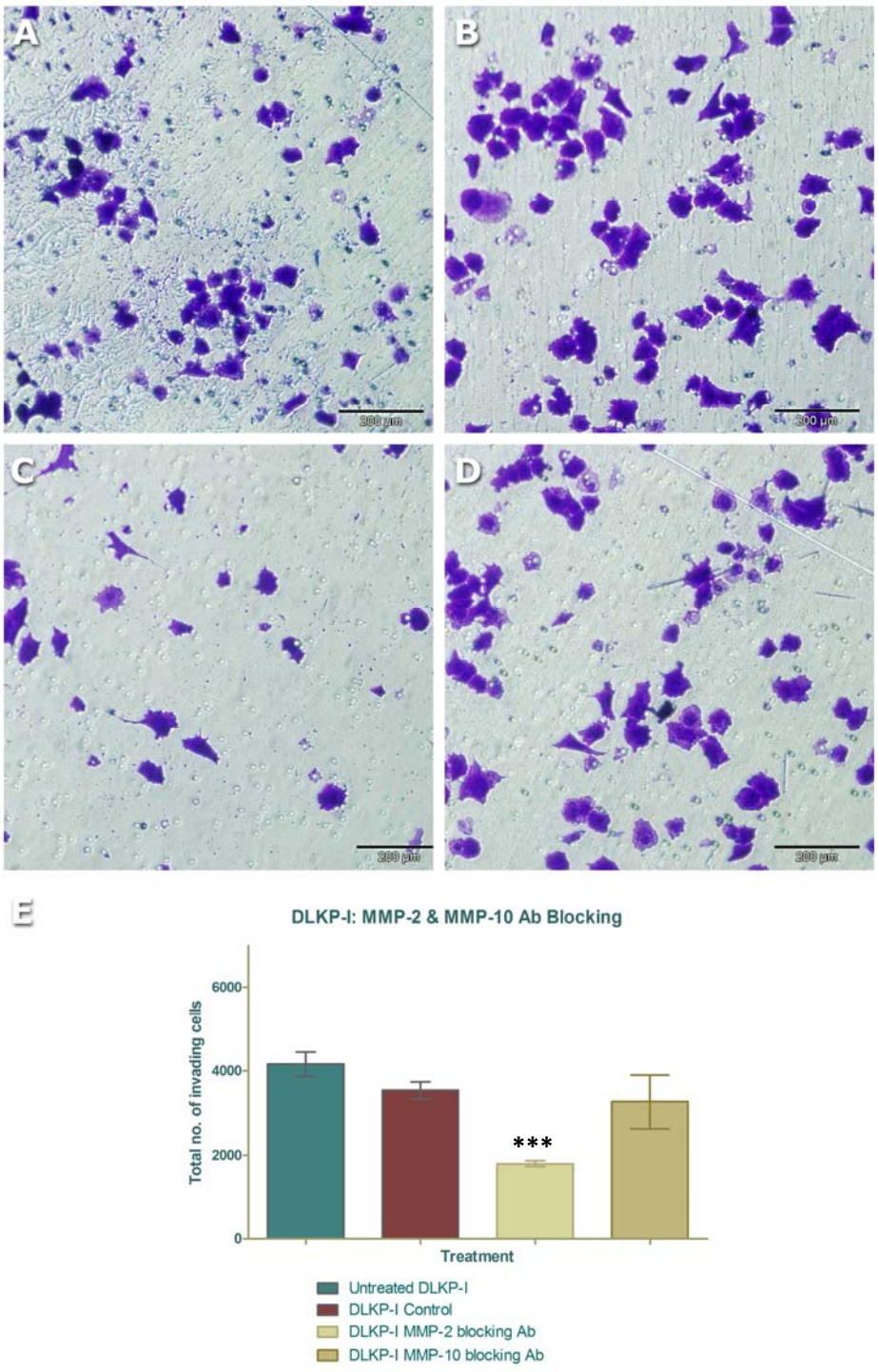

Figure 4.1-10: The effect of MMP-2 and MMP-10 blocking antibodies on the *in vitro* invasion activity of DLKP-I. Within the DLKP-I cell line, invasion is decreased with blocking of MMP 2 relative to non-treated cells while there is a variable and small effect in MMP-10 treated cells. After 48 hours incubation, the invading cells on the underside of the insert were stained with crystal violet and allowed to air dry: (**A.**) untreated; (**B.**) 5.0 µg/ml of control mouse IgG1 monoclonal antibody; (**C**.) 5.0 µg/ml of MMP 2 monoclonal antibody and (**D**.) 10.0 µg/ml of MMP 10 monoclonal antibody. Magnification, ×200. Scale bar, 200µm Results are presented as the mean +/- standard deviation (SD) of three independent experiments. Statistics: *** $p < 0.005$ (unpaired t-test to DLKP-I IgG control).

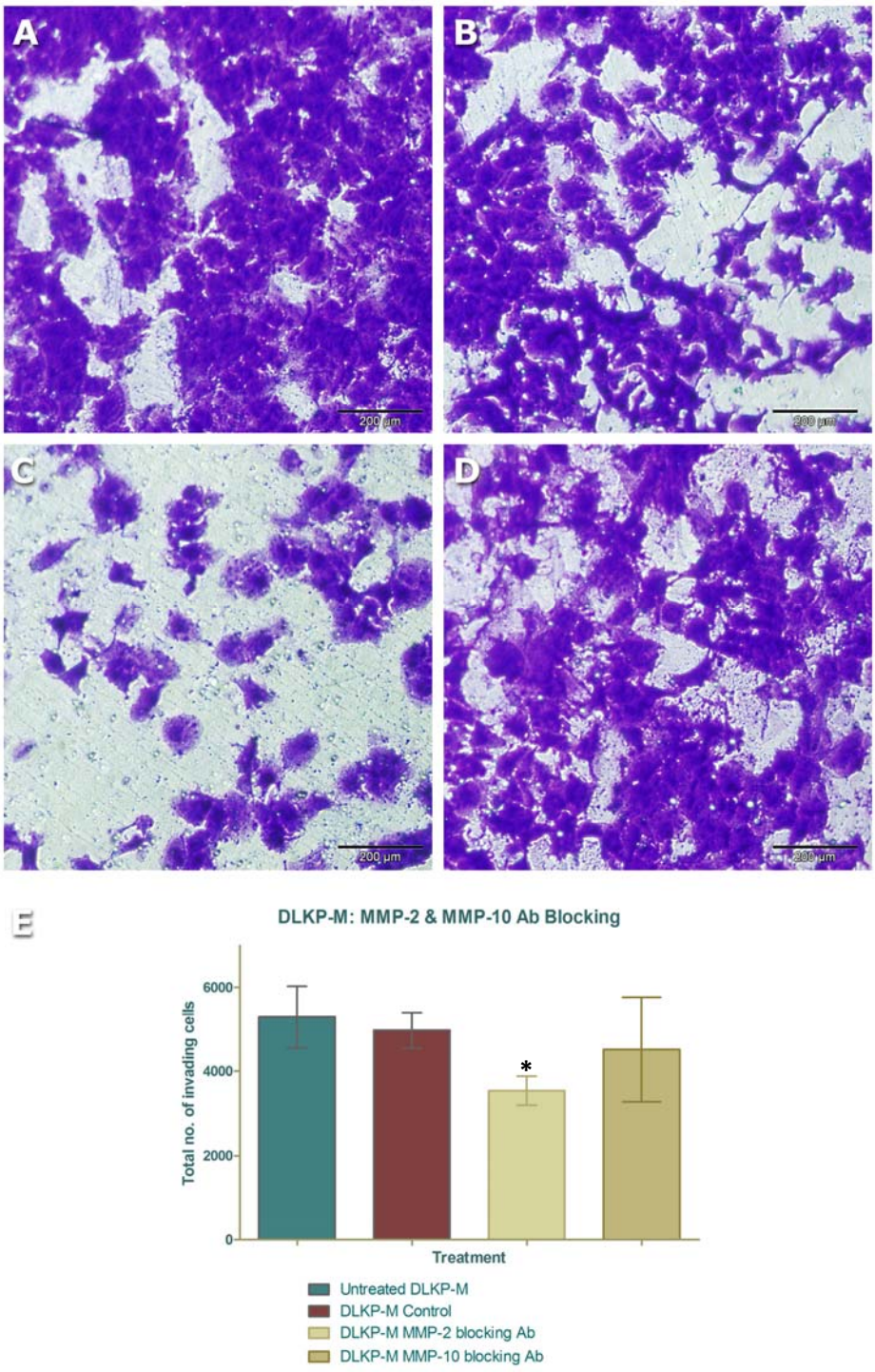

Figure 4.1-11: The effect of MMP-2 and MMP-10 blocking antibodies on the *in vitro* invasion activity of DLKP-M. Within the DLKP-M cell line, invasion is decreased with blocking of MMP 2 relative to non-treated cells while there is a highly variable effect in MMP-10 treated cells. After 48 hours incubation, the invading cells on the underside of the insert were stained with crystal violet and allowed to air dry: (**A.**) untreated; (**B.**) 5.0 µg/ml of control mouse IgG1 monoclonal antibody; (**C**.) 5.0 µg/ml of MMP 2 monoclonal antibody and (**D**.) 10.0 µg/ml of MMP 10 monoclonal antibody. Magnification, ×200. Scale bar, 200µm. Results are presented as the mean +/- standard deviation (SD) of three independent experiments. Stats: * $p < 0.05$ (unpaired t-test to DLKP-M IgG control).

4.1.8.1 c-Met Alterations in the DLKP clones

Analysis of the clones showed an insertion in the Sema domain (MET_N375S_A1124G) in the DLKP parent, DLKP-SQ and DLKP-I cells. A missense change was seen in the DLKP-M clone.

4.1.8.2 TP53 Alterations in the DLKP clones

Also identified were TP53_G245VDA_G734TAC mutations in all of the DLKP clones and the DLRP cell line.

4.1.8.3 PI3K3R1 alterations in the DLKP clones

Analysis of the clones showed an insertion in the p85α regulatory subunit of PI3K3R1 (PIK3R1_M3261_G978ATC). This alteration occurred in the DLKP, DLKP-SQ and DLKP-M clones only.

4.1.8.4 EGFR alterations in the DLKP clones

Analysis of the clones showed an insertion within the EGFR receptor in the DLKP-SQ only.

4.1.9 DLKP clones – investigation of stem cell markers

Cancer stem cells (CSCs) are cancer cells found within tumours that possess characteristics associated with normal stem cells, specifically the ability to give rise to all cell types found in a particular cancer sample. CSCs are therefore tumourigenic (tumour-forming), in contrast to other non-tumourigenic cancer cells [320]. CSCs have been isolated and characterised from more than 20 cancer types[321-323] and emerging evidence supports the notion that CSCs are responsible for tumour development including tumour initiation, invasion, angiogenesis, therapy resistance and recurrence. Since the parental DLKP contains at least three phenotypically different subclonal populations, the possibility of a stem cell model in these cells was investigated with the expression of a small panel of markers for embryonic stem cells (figure 4.1-12). Oct-4 (POU5F1) and NANOG have been suggested as two of the four major factors that allow the reprogramming of adult cells into germ-line competent, induced pluripotent cells. Oct-4 plays a critical role in the development and self-renewal of embryonic stem cells and has been linked to oncogenic processes. NANOG maintains pluripotency of embryonic stem cells and functionally blocks differentiation[324]. The transcription factor, KLF4 has been demonstrated to be a good indicator of stem-like capacity. The DLKP clones were found to be negative for KLF4 and NANOG. Very low levels of Oct-4 were detected in all the clones. The result was not visible when photographed. Therefore, no results are shown for this gene.

Myc (c-Myc) is activated upon various mitogenic signals such as Wnt, Shh and EGF (via the MAPK/ERK pathway). By modifying the expression of its target genes, Myc activation results in numerous biological effects. The first to be discovered was its capability to drive cell proliferation (upregulates cyclins, downregulates p21), but it also plays a very important role in regulating cell growth (upregulates ribosomal RNA and proteins), apoptosis (downregulates Bcl-2), differentiation and stem cell self-renewal. c-Myc was present in all of the clones.

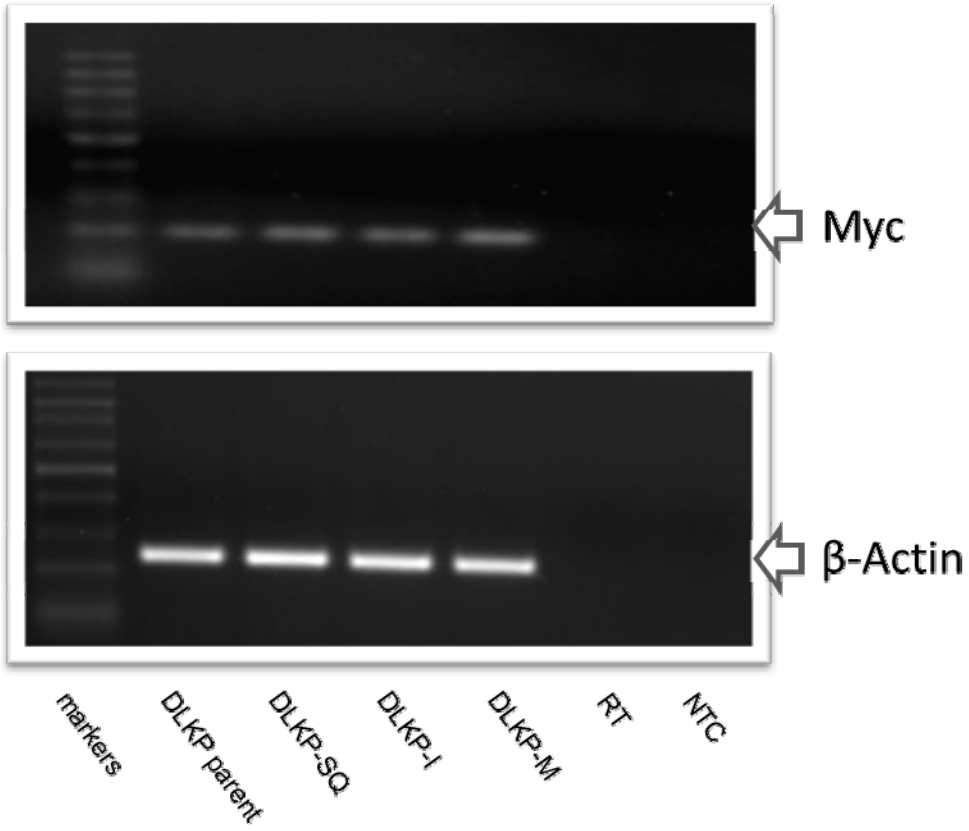

Figure 4.1-12: DLKP parents and clones were negative for Oct-4, KLF4, and pluripotency marker NANOG. Barely detectable levels of Oct-4 were observed, and though not quantifiable, seemed to represent similar levels in parent and clones. RT and NTC are negative controls used to ensure there is no contaminating DNA in the reverse transcription reaction or RNA in the PCR reagents.

4.2 Establishment of drug resistant invasive DLKP-SQ variants

4.2.1 Introduction

The major causes of treatment failure in cancer are the development of multidrug resistance and cancer invasion/metastasis. There is indirect evidence that these two traits may be linked or at least often occur together, but it is unclear whether they share any mechanisms[228]. Drug resistance to chemotherapy in patients is often associated with increased malignancy. One explanation for the link between resistance and malignancy may simply be that resistance facilitates cancer progression and invasion. There is some evidence that the two processes can be linked to each other (reviewed in *Liang et al.,* 2002[325]). Acquisition of P-gp-mediated multidrug-resistance does not however, always correlate with observed malignant behavior of lung cancer[196]. Additionally, many of the model systems used to study the link between drug resistance and invasion bypass the earliest events. Consequently, the critical first step in the transition from a preinvasive to an invasive phenotype during the development of drug resistance has been less well studied than at later stages.

To delineate molecular alterations important for this transition, we pulse selected the clone DLKP-SQ with mitoxantrone and established isogenic sub-populations, overexpressing BCRP and P-gp. The DLKP-SQ-Mitox-BCRP and DLKP-SQ-Mitox-MDR cell lines overexpress BCRP and P-gp respectively and displayed the invasive phenotype after the 6th pulse. Microarray analysis was used to search for changes which may be functionally significant in the transition from a preinvasive to an invasive phenotype.

4.2.2 Generation of invasive mitoxantrone resistant cell lines

DLKP-SQ-Mitox-BCRP and DLKP-SQ-Mitox-MDR were previously established by mitoxantrone pulsing (chapter 3). These cell lines were pulsed two more times to generate the DLKP-SQ-Mitox-BCRP-6P and DLKP-SQ-Mitox-MDR-6P cell lines as shown in the flow diagram in figure 4.2-1. Invasion was induced in the 6th pulse, which was independent of transporter expression (see section 3.1.6). A stable, higher drug resistant cell population isolate, was subsequently isolated from the SQ-Mitox-BCRP-6P cell line. This new cell population was named SQ-Mitox-BCRP-6P-(isolate 2). Figure 4.2-1 outlines the phenotypes observed during mitox treatment.

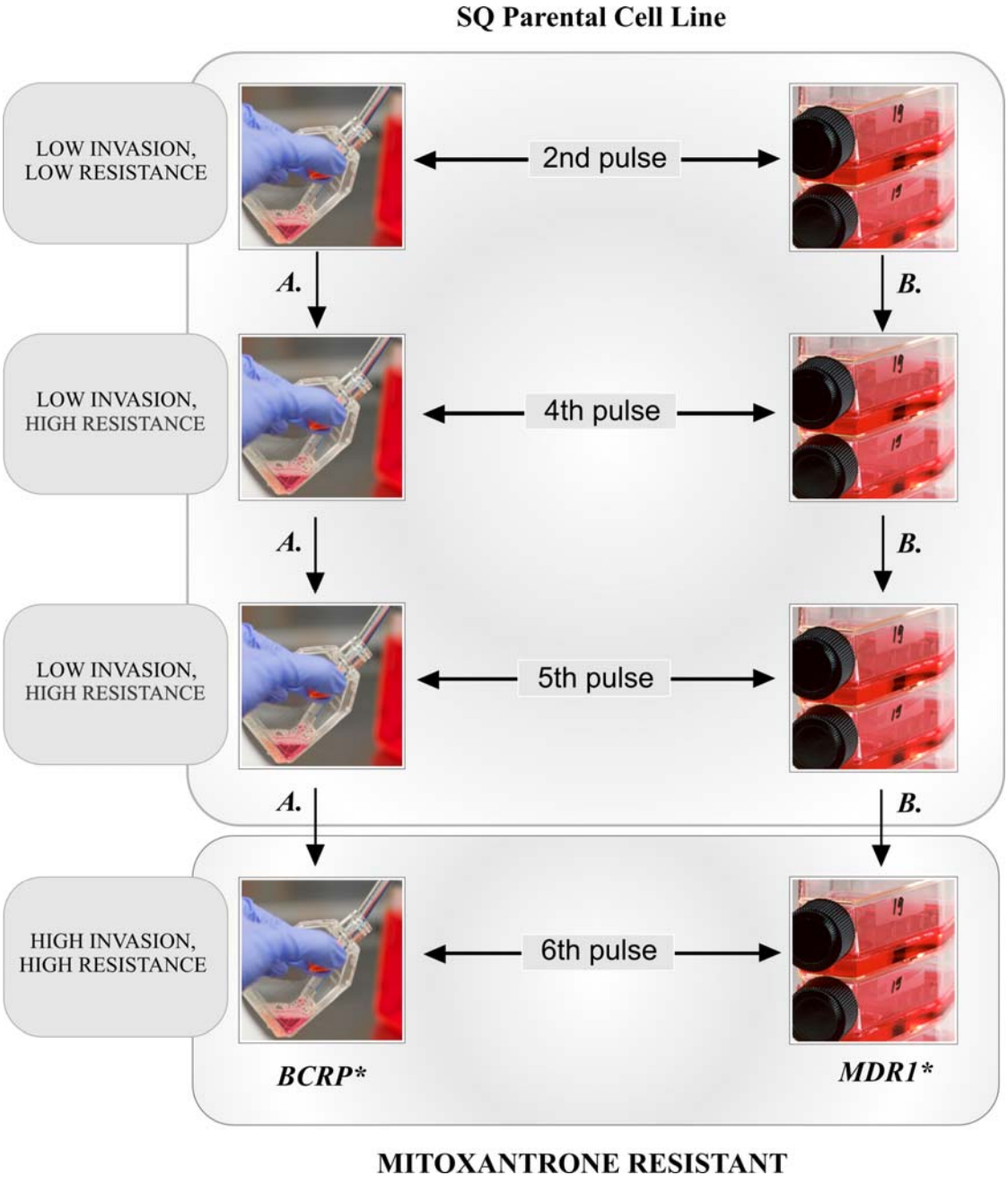

Figure 4.2-1: Flow diagram outlining the generation of the mitoxantrone resistant cell lines. *These eflux pumps were later identified through microarray analysis and revealed to be overexpression of BCRP and P-gp in flasks A and B respectively.

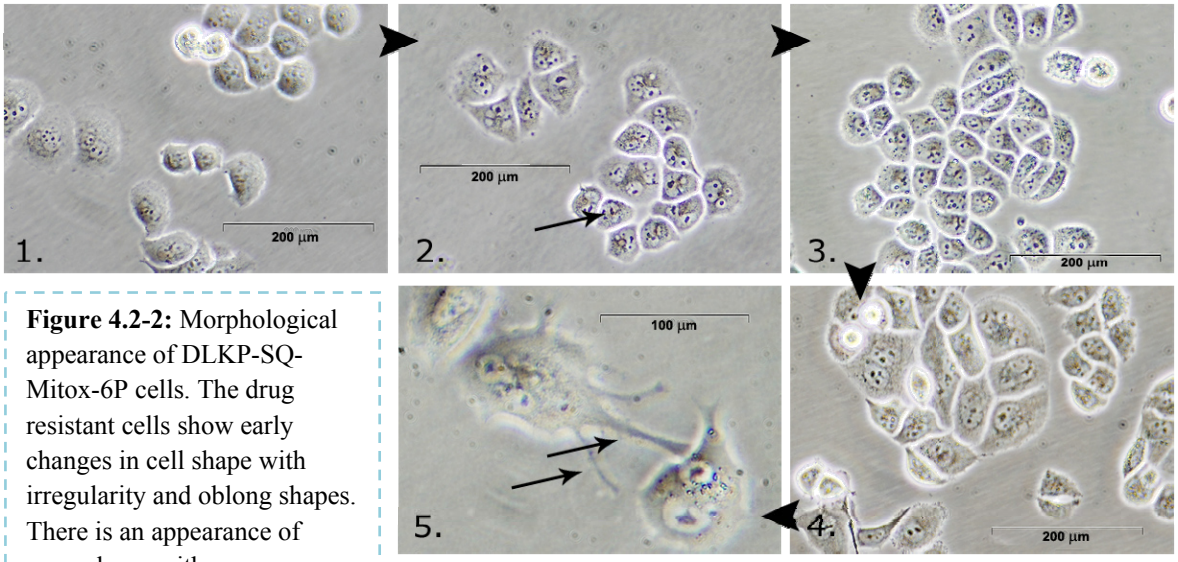

Figure 4.2-2: Morphological appearance of DLKP-SQ-Mitox-6P cells. The drug resistant cells show early changes in cell shape with irregularity and oblong shapes. There is an appearance of appendages with a multinuclate, light nucleoplasm and a granular cytoplasm.

4.2.3 Morphology of SQ-Mitox-BCRP cells

The DLKP-SQ cells are squamous in appearance with distinct cell boundaries. During the development of drug resistance, early changes in cell shape were observed with a spindle-like morphology which is commonly associated with increased tumour invasiveness (figure 4.2-2).

4.2.4 Microarray analysis of mitoxantrone resistant cell lines

Accumulating evidence suggests a tight relationship between chemo-resistance and metastasis. Following the development of MDR variants overexpressing BCRP and P-gp with different levels of invasion (as described earlier in chapter 3), the gene expression profiles of these cell lines were compared using microarray analysis as described in section 2.10. Such analysis has the potential of identifying genes of importance in the metastatic process by identifying differentially expressed genes. These cell lines all share a common genetic background, thus studying their genetic differences is simplified because background genetic variation is minimised and any significant expression changes may likely represent metastasis associated events as opposed to transporter specific changes.

4.2.4.1 Gene expression differences between drug resistant poorly invasive and invasive lung cancer cell lines

To identify genes involved in the acquisition of an invasive potential during the development of drug resistance, the gene expression profiles of poorly invasive DLKP-SQ, SQ-Mitox-BCRP-4P, SQ-Mitox-MDR-4P and invasive SQ-Mitox-BCRP-6P and SQ-Mitox-MDR-6P were compared using microarray analysis. The experimental design enabled the identity of genes changing between the following comparisons:

1. SQ-Mitox-BCRP-4P (poorly invasive) *versus* SQ-Mitox-BCRP-6P (invasive) (Genelist 1);
    - (79 genes (1.2 fold); 62 upregulated, 17 downregulated)
2. SQ-Mitox-MDR-4P (poorly invasive) *versus* SQ-Mitox-MDR-6P (invasive) (Genelist 2);
    - (553 genes (1.2 fold) ; 220 upregulated, 333 downregulated)

Changes in gene expression between DLKP-SQ parental cells and the derived drug resistant cell lines were observed using "D-chip" as described in section 2.17.1. "D-chip" was used to generate a list of genes significantly over- or under-expressed with false discovery rates of 0.05, with a cut-off value of ± 1.2-fold change in gene expression. The top 10 upregulated and downregulated genes for both genelists 1 and 2 with a p-value (p) ≤ 0.05 and fold change ≥ 1.2 are shown in table 4.2-1.

Table 4.2-1: Top ten over- and down-expressed genes on Genelist 1 and Genelist 2 with a p-value (p) ≤ 0.05 and fold change ≥ 1.2 in DLKP-SQ-Mitox cell lines.

SQ-Mitox-BCRP-4P vs SQ-Mitox-BCRP-6P			*SQ-Mitox-MDR-4P vs SQ-Mitox-MDR-6P*		
Gene symbol	**Fold change**	**Main function**	**Gene symbol**	**Fold change**	**Main function**
Over-expressed					
ADAMTS1	54.1	Metallopeptidase activity	*DKK1*	9.61	Wnt receptor signalling pathway
CDH2	13.74	Adherens junction organization	*KIAA0559 protein*	9.61	unknown
IGF1R	4.64	Tyrosine kinase activity	*ABCC9*	7.03	Ion channel binding
Slit2	4.28	Axon guidance	*Slit2*	6.52	Axon guidance
WASH3P	3.36	Arp2/3 complex-mediated actin nucleation	*Neuregulin1*	5.77	ErbB signalling pathway
PRRC2C	3.32	Protein c-terminus binding	*FAM46A*	5.11	Not known
SRRM2	3.02	mRNA splicing	*NAP1L3*	5.03	Nucleosome assembly
PRRC2C	2.99	Protein c-terminus binding	C5orf23	4.67	unknown
HELLS4	2.99	Chromatin binding	*KCNJ8*	4.66	Potassium channel activity
KRAS	2.75	RAS/MAPK pathway	*PDE5A*	4.63	Catalytic activity
Down-expressed					
TTL7	-1.4	Cell differentiation	*TIMP2*	–3.83	Metalloendopeptidase activity
THAP10	–1.36	Unknown	*cDNA clone IMAGE:4811567*	–2.88	Unknown
CYBRD1	-1.35	Cellular iron ion homeostasis	*CDKN2C*	-2.67	Cell cycle
Trim4	-1.34	Zinc ion binding	*CGI-146*	-2.46	Peptidase activity
EIF5	-1.34	Translation activity	*COL6A1*	-2.28	Cell adhesion
HSPCA	-1.31	Molecular chaperone, ATPase activity	*ARL7*	-2.21	Cholesterol transport
ATP1B1	-1.3	Microfilament motor activity	*IPS-1*	-2.19	inositol biosynthetic process
SCOC	-1.28	Autophagy	*ATF5*	-2.14	Heat shock protein binding
CGI-07	-1.25	Protein transport	*MT1E*	-2.07	Zinc ion binding
EID1	-1.24	Histone acetylation	*MT1H*	-2.05	Zinc ion binding

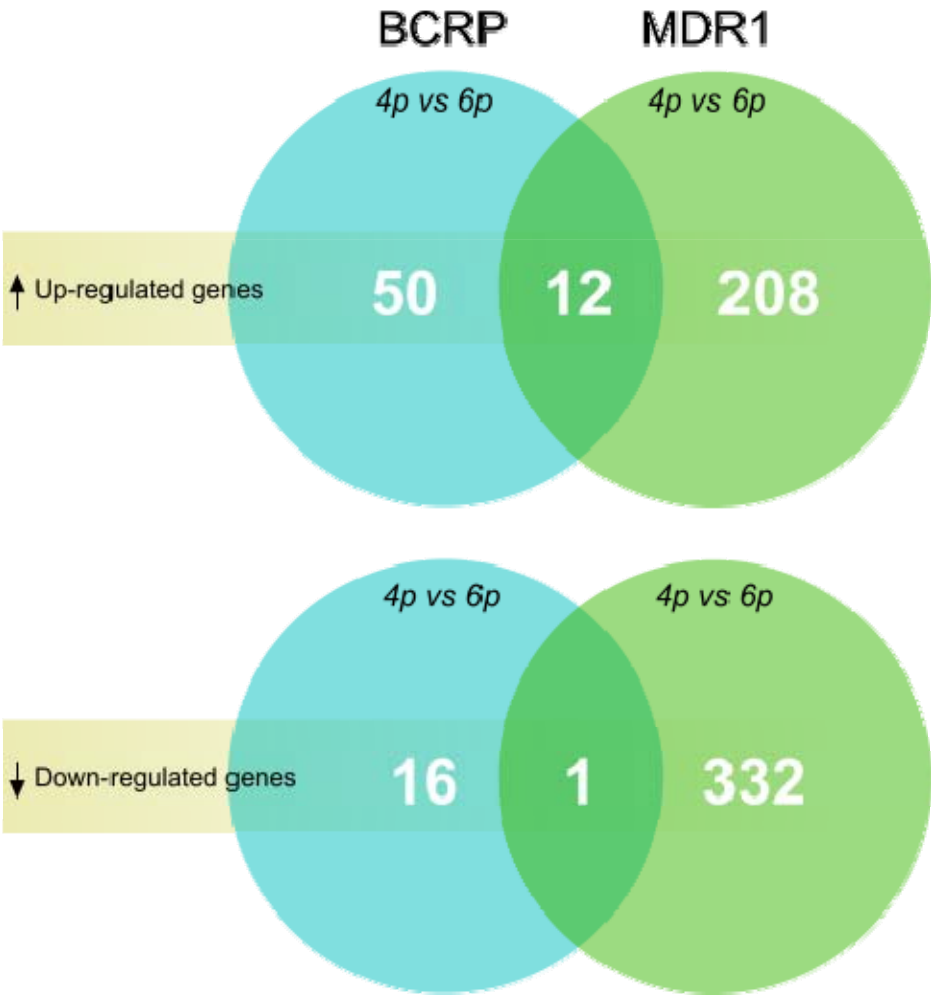

Figure 4.2-3: Two gene lists were generated - DLKP-SQ-Mitox-BCRP-4P *versus* DLKP-SQ-Mitox-BCRP-6P cells (Genelist 1), and DLKP-SQ-Mitox-MDR-4P *versus* DLKP-SQ-Mitox-MDR-6P cells (Genelist 2). These were used in the search for molecular mechanisms involved in the invasive phenotype. These lists were overlapped to identify common/uncommon genes. There were 12 genes identified as common between the upregulated lists; an overlap of almost 20% on the shorter list. By contrast, only one common gene from the downregulated lists was identified and this was most likely an artefact of the analysis.

Table 4.2-2: Up-regulated and Down-regulated genes common to both invasion lists: SQ-Mitox-BCRP-4P *vs.* SQ-Mitox-BCRP-6P and SQ-Mitox-MDR-4P *vs.* SQ-Mitox-MDR-6P.

No.	Affy ID	Description
Up-regulated:		
01	232797_at	CDNA FLJ11397 fis, clone HEMBA1000622/ Integrin alpha V
02	230130_at	SLIT homolog 2 (Drosophila)
03	224576_at	endoplasmic reticulum-golgi intermediate compartment 32 kDa protein
04	213258_at	Tissue factor pathway inhibitor (lipoprotein-associated coagulation inhibitor)
05	210664_s_at	tissue factor pathway inhibitor (lipoprotein-associated coagulation inhibitor)
06	209897_s_at	SLIT homolog 2 (Drosophila)
07	209676_at	tissue factor pathway inhibitor (lipoprotein-associated coagulation inhibitor)
08	206858_s_at	homeo box C6
09	205433_at	butyrylcholinesterase
10	204602_at	dickkopf homolog 1 (Xenopus laevis)
11	203282_at	glucan (1,4-alpha-), branching enzyme 1 (glycogen branching enzyme, Andersen disease, glycogen storage disease type IV)
12	201952_at	activated leukocyte cell adhesion molecule/CD166
Down-regulated:		
13	213428_s_at	collagen, type VI, alpha 1

4.2.4.2 Ontology analysis of Genelist 1 and 2

PANTHER analysis, Pathway Studio and GO analyses were carried out on Genelist 1 and 2. No meaningful results were obtained from the latter two procedures. In contrast, PANTHER analysis reavealed common pathways in the two genelists.

(1) Ontology analysis using PANTHER (Protein ANalysis THrough Evolutionary Relationships)

PANTHER is a unique resource that classifies genes and proteins by their function using published scientific experimental evidence and evolutionary relationships abstracted by curators with the goal of predicting function, even in the absence of direct experimental evidence (section

2.17.4). PANTHER was used to define a list of enriched pathways that are represented by the list of geneslists 1 and 2.

(2) Pathways affected by SQ-Mitox-BCRP-4P versus 6P genelist (identified by PANTHER)

Ontology analysis of Genelist 1 identified several pathways of interest (table 4.2-3 and figure 4.2-4): Ontology analysis of Genelist 2 also identified several interesting pathways (figure 4.2-5 and table 4.2-5) such as p53 and Wnt signaling pathways.

Table 4.2-3: Pathways affected by SQ-Mitox-BCRP-4P versus 6P genelist (identified by PANTHER)

Category name (Accession)	no. genes	% gene hit against total no. genes	% gene hit against total no. pathway hits
Wnt signaling pathway (P00057)	31	10.90%	16.50%
Inflammation mediated by chemokine and cytokine signaling pathway (P00031)	15	5.30%	8.00%
Integrin signalling pathway (P00034)	14	4.90%	7.40%
p53 pathway feedback loops 2 (P04398)	8	2.80%	4.30%
EGF receptor signaling pathway (P00018)	8	2.80%	4.30%
Axon guidance mediated by Slit/Robo (P00008)	6	2.10%	3.20%
Insulin/IGF pathway-protein kinase B signaling cascade (P00033)	6	2.10%	3.20%
Insulin/IGF pathway-mitogen activated protein kinase kinase/MAP kinase cascade (P00032)	6	2.10%	3.20%

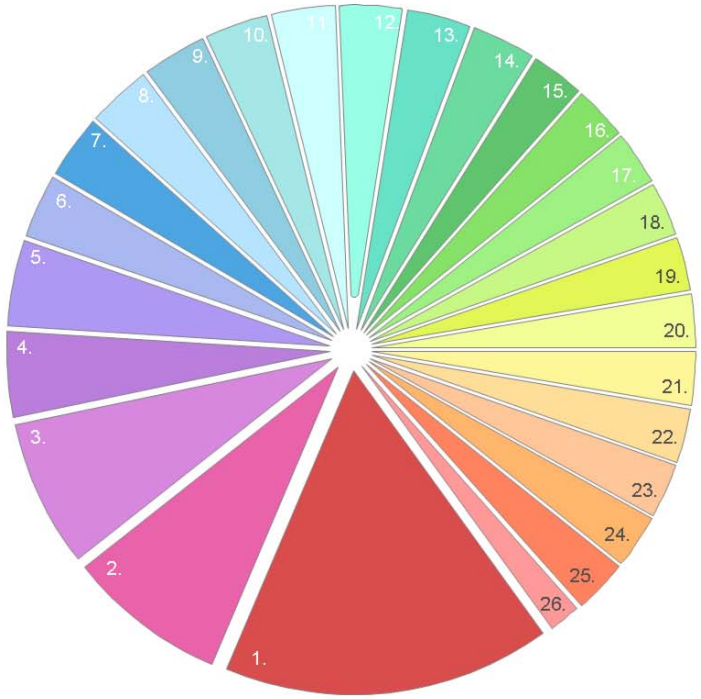

Figure 4.2-4. Genes were functionally classified based on the PANTHER system (http://www.pantherdb.org). SQ-Mitox-BCRP-4P (poorly invasive) versus SQ-Mitox-BCRP-6P (invasive; 79 genes; 62 upregulated, 17 downregulated).

1. Wnt signaling pathway, 16.5 %
2. Inflammation by chemokine and cytokine pathway, 8.0 %
3. Integrin signalling pathway, 7.4%
4. p53 pathway feedback loops 2, 4.3 %
5. EGF receptor signaling pathway, 4.3 %
6. Axon guidance mediated by Slit/Robo, 3.2 %
7. Insulin/IGF pathway-protein kinase B signaling cascade, 3.2 %
8. Insulin/IGF pathway-mitogen activated protein kinase kinase/MAP kinase cascade, 3.2%
9. Angiotensin II-stimulated signaling through G proteins and beta-arrestin, 3.2 %
10. Nicotinic acetylcholine receptor, 3.2 %
11. Muscarinic acetylcholine receptor 2 and 4, 3.2 %
12. Blood coagulation, 3.2 %
13. Muscarinic acetylcholine receptor 1 and 3, 3.2 %
14. Heterotrimeric G-protein signaling pathway-Gi alpha & Gs alpha, 3.2 %
15. Angiogenesis, 2.7%
16. Interleukin signaling pathway, 2.7%
17. PI3 kinase pathway, 2.7%
18. PDGF signaling pathway, 2.7%
19. Cadherin signaling pathway, 2.7%
20. Ras Pathway, 2.7%
21. B cell activation, 2.7%
22. VEGF signaling pathway, 2.7%
23. T cell activation, 2.7%
24. TGF-beta signaling pathway, 2.7%
25. FGF signaling pathway, 2.7 %
26. p53 pathway, 1.6%

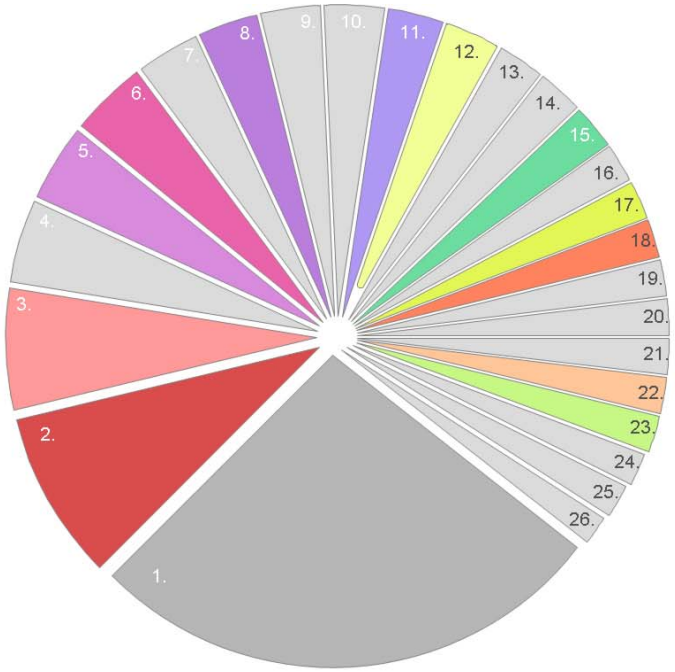

Figure 4.2-5. Genes were functionally classified based on the PANTHER system (http://www.pantherdb.org). SQ-Mitox-MDR-4P (poorly invasive) versus SQ-Mitox-MDR-6P (invasive; genelist 2; 553 genes; 220 upregulated, 333 downregulated). Colour codes indicate pathways shared with figure 4.2-4.

1. All other pathways (36), 27.0 %
2. Wnt signalling pathway, 8.8 %
3. p53 pathway, 6.3%
4. Huntington disease, 4.3 %
5. Integrin signalling pathway, 4.0 %
6. Inflammation mediated by chemokine and cytokine signaling, 4.0 %
7. Parkinson disease, 3.3 %
8. p53 pathway feedback loops 2, 3.1%
9. Hedgehog signaling pathway, 3.1 %
10. Circadian clock system, 3.1 %
11. EGF receptor signaling pathway, 2.9 %
12. Cadherin signaling pathway, 2.9 %
13. Cytoskeletal regulation by Rho GTPase 2.4 %
14. Oxidative stress response, 2.4 %
15. Heterotrimeric G-protein signaling pathway-Gi alpha and Gs alpha mediated pathway, 2.3%
16. Heterotrimeric G-protein signaling pathway-Gq alpha and Go alpha mediated pathway, 2.0%
17. Ras Pathway, 2.0%
18. FGF signaling pathway, 2.0%
19. Alzheimer disease-presenilin pathway, 1.9%
20. Hypoxia response via HIF activation, 1.9%
21. Ubiquitin proteasome pathway, 1.9%
22. T cell activation, 1.9%
23. PDGF signaling pathway, 1.9%
24. Apoptosis signaling pathway, 1.7%
25. Transcription regulation by bZIP transcription factor, 1.7 %
26. Androgen/estrogene/progesterone biosynthesis, 1.5%

Table 4.2-4: Top 8 pathways affected by SQ-Mitox-MDR-4P *vs* 6P genelist (as identified by PANTHER)

Category name (Accession)	no. genes	% gene hit against total no. genes	% gene hit against total no. pathway hits
Wnt signaling pathway (P00057)	69	3.70%	8.80%
p53 pathway (P00059)	49	2.60%	6.30%
Huntington disease (P00029)	34	1.80%	4.30%
Integrin signalling pathway (P00034)	31	1.60%	4.00%
Inflammation mediated by chemokine and cytokine signaling pathway (P00031)	31	1.60%	4.00%
Parkinson disease (P00049)	26	1.40%	3.30%
p53 pathway feedback loops 2 (P04398)	24	1.30%	3.10%
Hedgehog signaling pathway (P00025)	24	1.30%	3.10%

4.2.5 Isolation of a new stable, higher drug resistant clone of SQ-Mitox-BCRP-6P

The DLKP-SQ-Mitox-BCRP and DLKP-SQ-Mitox-MDR cell lines discussed to-date overexpress BCRP and P-gp respectively and display the invasive phenotype after the 6th pulse. However, this invasive phenotype is only stable directly after the sixth drug pulse and is lost on freezing and re-thawing of the cells. Out of the original population of DLKP-SQ-Mitox-BCRP-6P cells a sub population was isolated which appeared to be even more resistant and invasive than their forebears. Toxicity assays appeared to confirm this because the new isolates have higher IC_{50} values when treated with mitoxantrone (table 4.2-5) which may account for up to a 560-fold resistance to this drug relative to the DLKP-SQ parental cell line (or > 4-fold above that of the original resistant isolate 1).

Careful observation of this new, second isolate of BCRP over-expressing cells revealed morphological differences, characterised by large numbers of spiky cells which grow in a more dispersed manner. Further investigation of these cells show that indeed, they have higher levels of BCRP protein (figure 4.2-6). In addition, the invasive phenotype within this population of cells appears to be stable and is from here on in referred to as SQ-Mitox-BCRP-6P (isolate 2).

Furthermore, it would also appear that the activity of both MMP-2 and MMP-10 are also increased within this new population of DLKP-SQ-Mitox-BCRP-6P cells (figure 4.2-6).

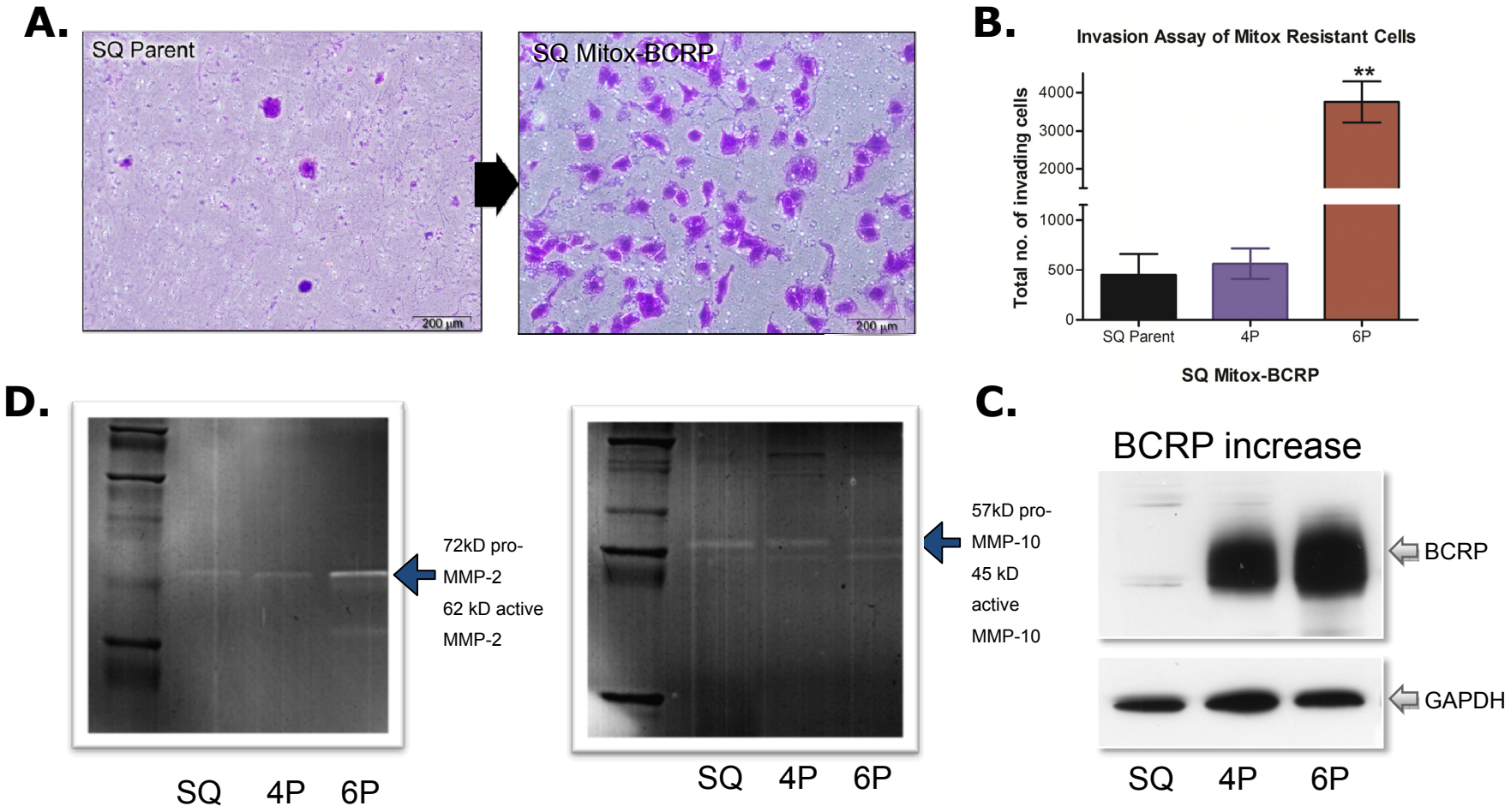

Figure 4.2-6: **A**. Visual analysis of the level of invasion of DLKP-SQ and SQ-Mitox-BCRP variants. **B**. The total number of invading cells was determined by counting the number of cells per field in 10 random fields, at 200× magnification. The average number of cells per field was then multiplied by a factor of 140 (growth area of membrane/field area viewed at 200× magnification (calibrated using a microscope graticule)). Error bars represent the standard deviation of triplicate invasion assay experiments (n=3). **C.** Western blotting analysis (3µg protein) shows upregulation of BCRP protein in the SQ-Mitox-BCRP-6P (Isolate 2) cells. **D**. Zymography analysis showing the presence of increased active MMP2 and MMP10 in the conditioned medium of SQ-Mitox-BCRP-6P (isolate 2).

Table 4.2-5: IC_{50} and fold resistance of all of the DLKP-SQ Mitox resistant variants relative to the parental DLKP-SQ cell line.

CELL LINE	IC_{50}	FOLD RESISTANCE
DLKP-SQ	0.08 ng/ml	1
DLKP-SQ Mitox-BCRP- 4th pulse	16.79 ng/ml	209.8
DLKP-SQ Mitox-BCRP- 6th pulse (isolate 1)	10.89 ng/ml	134.8
DLKP-SQ Mitox-BCRP-6th pulse (isolate 2)	44.82 ng/ml	560
DLKP-SQ Mitox-MDR- 4th pulse	25.59 ng/ml	319.8
DLKP-SQ Mitox-MDR- 6th pulse	19.35 ng/ml	241.8

4.2.5.1 Increased activity and expression levels of MMP-2 and MMP-10 in SQ-Mitox BCRP-6P (isolate 2) cells

Earlier when describing the role of MMP-2 and MMP-10 in DLKP, it was shown that MMP-2 but not MMP-10 may be involved in the process of invasion. To determine if MMP-2 was up-regulated in the invasive and drug-resistant SQ-Mitox-BCRP-6P (isolate 2) cell population, the activity of gelatinases was qualitatively accessed (figure 4.2-6). Zymographic analysis indicated that the proteolytic activity of secreted MMP-2 was remarkably elevated in the isolate 2 cells, relative to that of SQ-Mitox-BCRP-4P and parental DLKP-SQ cells. Thus, the acquisition of drug resistance is accompanied by an increased activity of MMP-2 in DLKP-SQ cells.

MMP-10 was over-expressed in the DLKP-SQ *vs* DLKP-M microarray gene list and on the DLKP-SQ *vs* SQ-Mitox-BCRP-4P microarray gene list. Stromolysin zymography (MMP 10) indicated that the proteolytic activity of secreted MMP-10 was also remarkably elevated in the isolate 2 cells, relative to that of SQ-Mitox-BCRP-4P and parental DLKP-SQ cells (figure 4.2-6).

Effect of MMP 2 blocking antibody on the invasiveness of SQ-Mitox-BCRP-6P cells

To determine the role of MMPs in SQ-Mitox-BCRP-6P invasion, the invasion potential of SQ-Mitox-BCRP-6P (isolate 2) cells in the presence of a specific MMP-2 monoclonal antibodies were investigated. As shown in figure 4.2-7, the number of SQ-Mitox-BCRP-6P cells that migrated through the extracellular matrix gel (ECM) was moderately decreased by specific blocking of MMP-2. However, there was no significant alteration in the invasiveness of the cells treated with the control isotype antibody. These results support the idea of increased expression of MMP2 in SQ-Mitox-BCRP-6P associated with increased invasion.

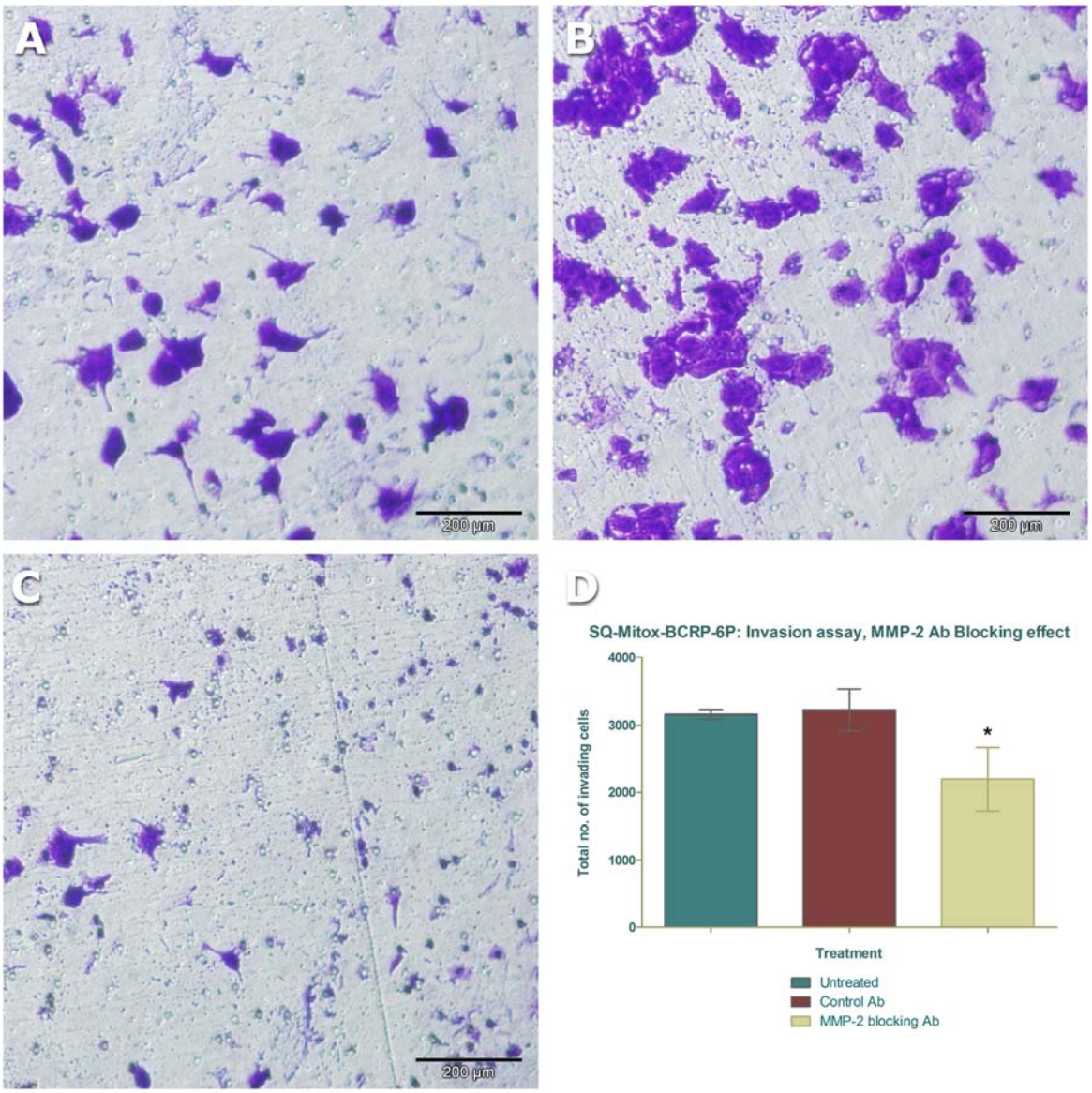

Figure 4.2-7: SQ-Mitox BCRP-6P cell line: invasion is decreased in MMP 2 treated cells compared with non-treated cells. After 24 hours incubation, the invading cells on the underside of the insert were stained with crystal violet and allowed to air dry. (**A.**) Untreated; (**B.**) with the addition of 5.0 µg/ml of control mouse IgG1 monoclonal antibody; (**C.**) with the addition of 5.0 µg/ml of MMP 2 monoclonal antibody. Magnification, ×200. Scale bar, 200µm (**D.**) Invasion assay of MMP-2 blocking antibody and their effect on SQ-Mitox BCRP-6P cells. Statistics: * $p < 0.05$ (unpaired t-test to IgG control antibody).

4.2.6 Post array analysis and confirmation of selected genes

Following the identification of genes that were significantly up- or down-regulated from the microarray analysis (tables 4.2-1 and 4.2-2), literature searches, immunofluorescence and Western blot analysis allowed the confirmation of their expression (as described in section 2.5.2 and 2.6). Western blot verification was carried out on ALCAM, IGF1Rβ, integrin alpha V, SLIT2/ROBO2 and BCHE confirming the microarray trends (i.e. in this case all up-regulated in the SQ-Mitox-BCRP-6P (isolate 2) cell line). Immunofluorescence studies were performed on ALCAM to illustrate the localisation of the protein within the cells. In contrast, the DLKP-SQ and SQ-Mitox-BCRP-4P cell lines expressed low levels of these proteins. These proteins will be discussed further in section 6.3.2.

4.2.6.1 Activated leukocyte cell adhesion molecule (ALCAM)

Previously ALCAM was shown to be up-regulated in the DLKP-SQ *vs* DLKP-I microarray gene list (table 4.1-1b) and subsequently confirmed to be overexpressed in the DLKP-I cells only. Surprisingly, ALCAM was also upregulated in SQ-Mitox Genelists 1 and 2 (table 4.2-2). A progressive up-regulation of ALCAM expression was observed in the cell lysate and on the membrane enriched preparation of SQ-Mitox-BCRP-6P (isolate 2) cells (figure 4.2-8). This up-regulation occurred in parallel with an increasing level of BCRP (figure 4.2-8). Immunofluorescence was performed on ALCAM to illustrate the localisation of the protein within the cells. Immunofluorescence studies confirm the up-regulation of ALCAM on the membrane of the BCRP overexpressing cells (figure 4.2-9)

4.2.6.2 Insulin-like growth factor 1 receptor (IGF1R)

IGF1R was 4.6-fold up-regulated on the SQ-Mitox-BCRP-4P *vs* SQ-Mitox-BCRP-6P gene list (Genelist 1, table 4.2-1). Western blot analysis confirmed that DLKP-SQ and SQ-Mitox-BCRP-4P cell lines expressed low levels of IGF1Rβ, whereas the SQ-Mitox-BCRP-6P cell line expressed high levels of this protein (figure 4.2-10, A).

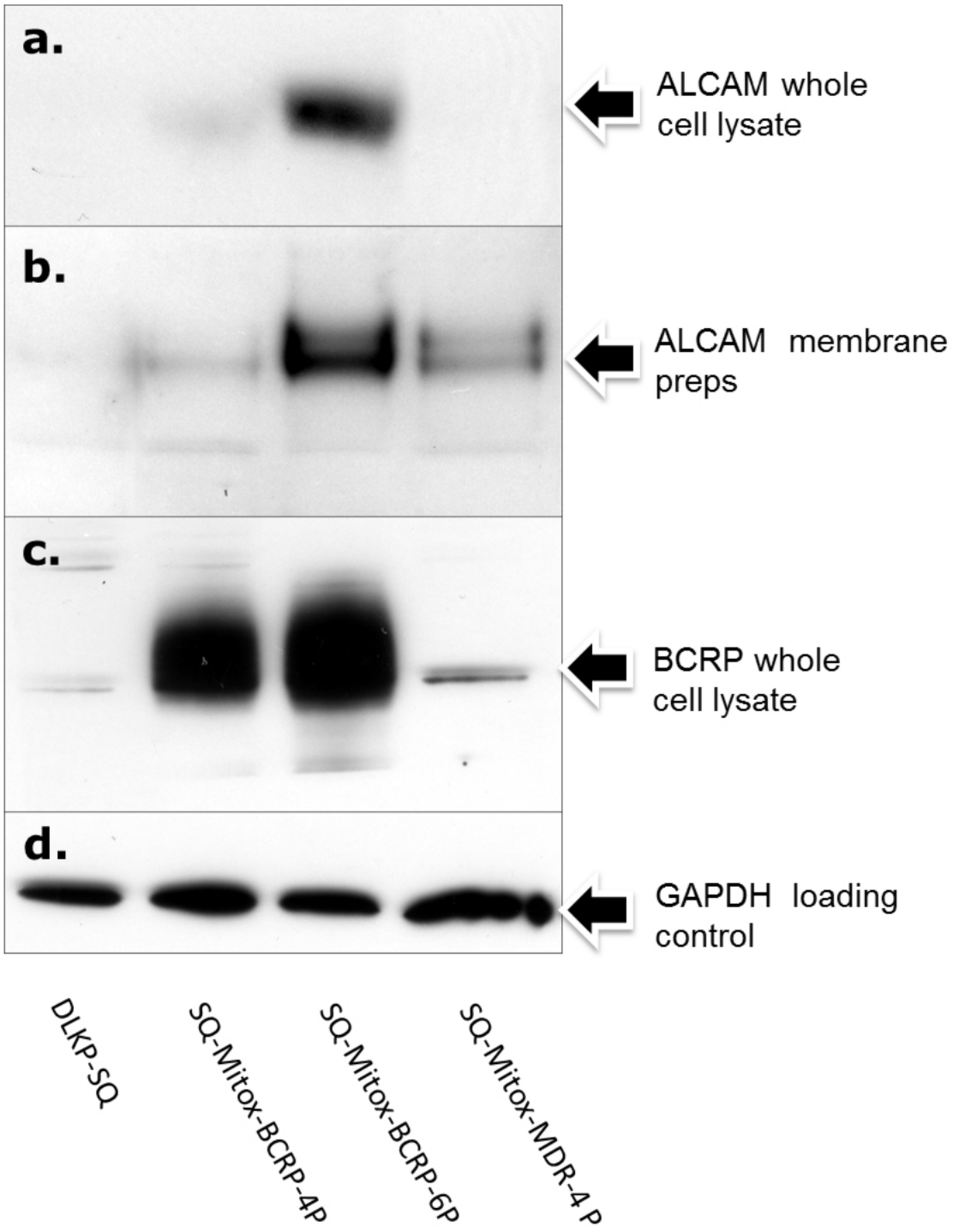

Figure 4.2-8: Western blot showing expression of cell adhesion molecule ALCAM in the SQ-Mitox cells. Different levels of ALCAM were expressed in the DLKP-SQ, SQ-Mitox-BCRP-4P and 6P (isolate 2), and SQ-Mitox-MDR cells. A progressive up-regulation of ALCAM expression in the cell lysate and on the membrane was observed in SQ-Mitox-BCRP-6P (isolate 2).

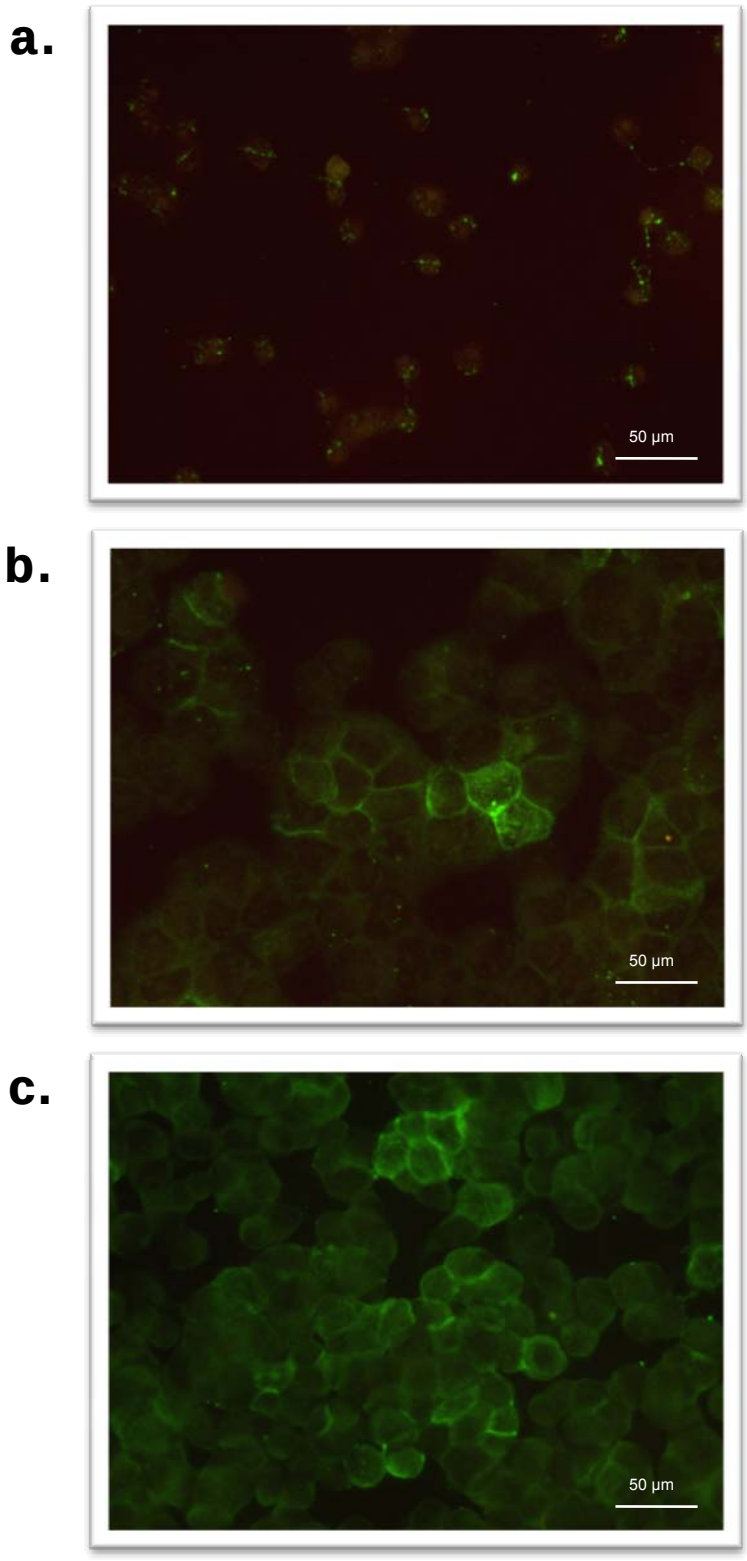

Figure 4.2-9: Expression of cell adhesion molecule ALCAM in drug sensitive and drug resistant lung cancer cell lines. (**A.**) DLKP-SQ; (**B.**) SQ-Mitox-BCRP-4P and (**C.**) SQ-Mitox-BCRP-6P (isolate 2)). There are different levels of expression amongst the cell lines of the drug transporter BCRP. A substantial up-regulation of ALCAM expression is observed in the cell lysate and on the surface membrane of SQ-Mitox-BCRP- 6P (isolate 2) (**C.**) Counter stained with propidium iodide. Original magnification of all photomicrographs, ×400, scale bar = 50 µm.

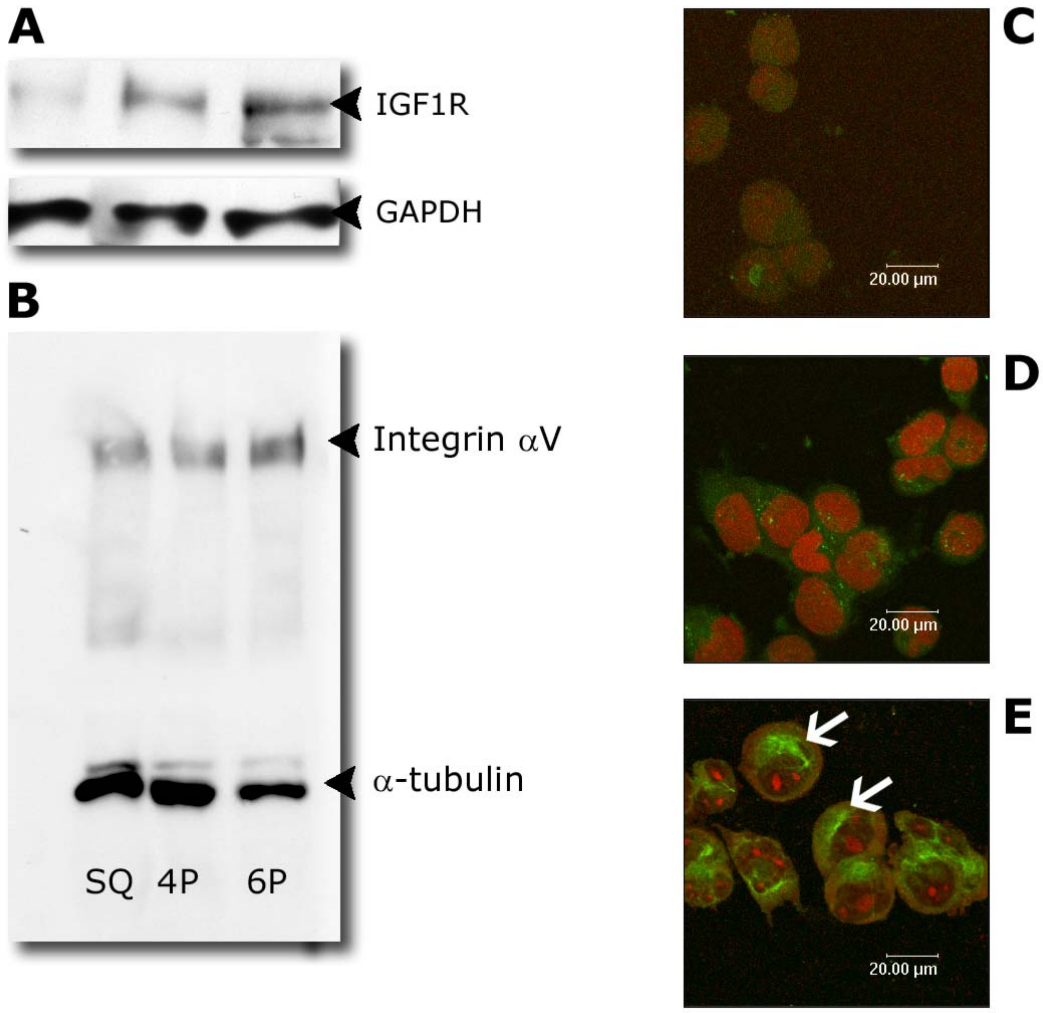

Figure 4.2-10: IGF1Rβ, integrin alpha V and N-cadherin expression in SQ-Mitox cells **A. and B.** Western blot showing a progressive up-regulation of IGF1R and Integrin alpha V expression in drug resistant, invasive SQ-Mitox-BCRP- 6P (isolate 2) relative to drug sensitive DLKP-SQ and drug resistant poorly invasive SQ-Mitox-BCRP-4P cells. Insulin-like growth factor I Receptor (IGF1R) has been shown to cooperate with integrins to promote tumour cell migration *in vitro*. GAPDH and α-tubulin were used as equal loading controls. **C., D., & E**. Immunofluorescence cell surface staining of N-cadherin in drug sensitive (**C.**) DLKP-SQ and drug resistant lung cancer cell lines (**D.**) SQ-Mitox-BCRP-4P and (**E**.) DLKP-SQ-Mitox-BCRP-6P (isolate 2), white arrows. Strong immunoreactivity is observed in invasive SQ-Mitox-BCRP-6P cells. SQ-Mitox-BCRP-4P cells show very weak immunoreactivity. Counter stained with propidium iodide. Original magnification of all photomicrographs, ×400, scale bar = 20 µm.

4.2.6.3 Integrin alpha V

Previously Integrin alpha V was shown to be up-regulated in the DLKP-SQ *vs* DLKP-I and DLKP-SQ *vs* DLKP-M microarray gene list and subsequently confirmed by Western Blot (figure 4.1-2) to be overexpressed in the DLKP-I and DLKP-M cells. Integrin alpha V was also upregulated in SQ-Mitox Genelists 1 and 2 (table 4.2-2). Integrins are cell surface transmembrane glycoproteins involved in the assembly of the actin cytoskeleton as well as in modulating signal transduction pathways that control biological and cellular functions including cell adhesion, migration, proliferation, cell differentiation and apoptosis[326]. *ITAGV* encodes integrin alpha chain V. Alpha V undergoes post-translational cleavage to yield disulfide-linked heavy and light chains, that combine with multiple integrin beta chains to form different integrins.

Western blot analysis confirmed that the DLKP-SQ and SQ-Mitox-BCRP-4P cell lines expressed low levels of integrin alpha V, whereas the SQ-Mitox-BCRP-6P cell line expressed high levels of this protein (figure 4.2-10, B).

4.2.6.4 N-cadherin

The cadherin superfamily comprises a large number of cell surface glycoproteins involved in Ca^{2+}-dependent cell-cell adhesion. Cells containing N-cadherin tend to cluster with other N-cadherin-expressing cells.

Microarray analysis indicated that N-cadherin is overexpressed in the SQ-Mitox-BCRP-6P cell line relative to the SQ-Mitox-BCRP-4P cell line (table 4.2-1). Immunofluorescence was performed on N-cadherin to illustrate the localisation of the protein within the cells. Figure 4.2-10 (C – E) confirms that N-cadherin is expressed in the SQ-Mitox-BCRP-6P cell line. An earlier investigation of N-cadherin expression in the DLKP clones also revealed that it was overexpressed in the DLKP-I but not the DLKP-M clones (figure 4.1-4).

4.2.6.5 SLIT2/ROBO2

The SLIT family of proteins consists of three members (SLIT1-3) that signal by binding to one of four Roundabout (ROBO1-4) receptors. The SLIT family are large, secreted glycoproteins that are subject to proteolytic cleavage resulting in fragments with variable activities. ROBO1,

ROBO2, and ROBO3 are predominantly expressed in the nervous system and SLIT-ROBO interactions have been shown to regulate axon repulsion and neuronal outgrowth.

An up-regulation of SLIT2 expression in the cell lysate was revealed in the BCRP over expressing cell lines but not in the SQ-Mitox-MDR cell line. Interestingly, there was an upregulation of SLIT2 in the membrane fraction of the higher drug resistant SQ-Mitox-BCRP-6P (isolate-2) invasive cell line (figure 4.2-11, A).

ROBO2 is a receptor for SLIT2 and is overexpressed in the DLKP-I and DLKP-M cells (figure 4.1-6). Further investigation of the expression of ROBO2 in SQ-Mitox cells using immunofluorescence revealed that ROBO2 was present in all of the cells to varying extents, with the strongest signal in the SQ-Mitox-BCRP-6P (isolate-2) cells (figure 4.2-11, B).

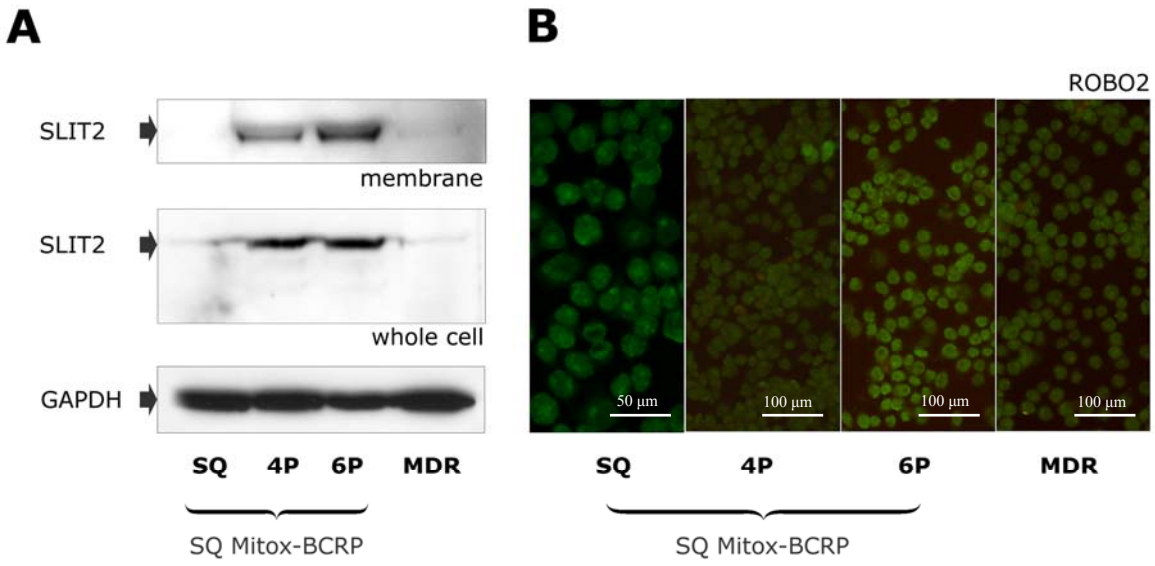

Figure 4.2-11: Expression of SLIT2 and its receptor ROBO2 in the SQ-Mitox cells. (**A.**) Western blot showing expression of SLIT2 in the SQ-Mitox cells. SLIT2 migrated at approximately 165 kDa. GAPDH was used as an equal loading control. (**B.**) Immunofluorescence cell surface staining of ROBO2: DLKP-SQ, SQ-Mitox-BCRP-4P, SQ-Mitox-BCRP-6P and SQ-Mitox-MDR cells stained with ROBO2 antibody. Immunoreactivity is observed in all of the cells but the SQ-Mitox-BCRP-6P cells show the strongest signal. Original objective magnification ×400 for SQ and ×200 for all others.

4.2.7 Effect of ITGAV and BCHE siRNA on proliferation of SQ-Mitox-BCRP-6P cells

The effect of silencing ITGAV and BCHE protein expression on proliferation was investigated as described in section 2.15. Figure 4.2-12 displays the percentage survival of SQ-Mitox-BCRP-6P cells transfected with ITGAV and BCHE siRNAs. Loss of ITGAV and BCHE did not affect proliferation in SQ-Mitox-BCRP-6P cells, indicating they are not essential factors for proliferation in these cells.

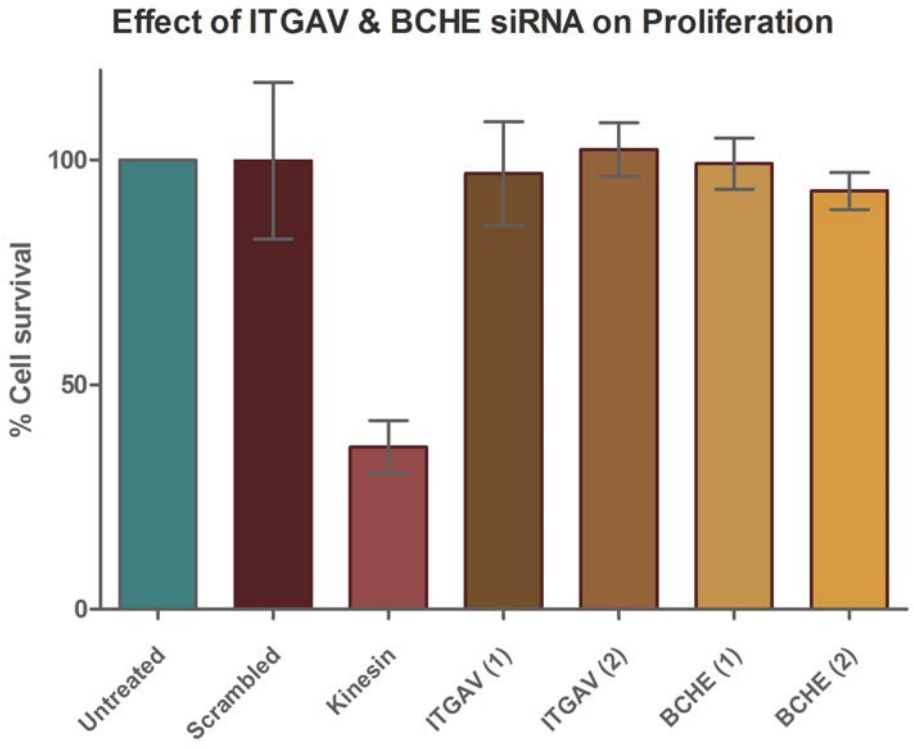

Figure 4.2-12: Proliferation assays on siRNA-transfected 6P cells indicating that monolayer cell growth was not affected by ITGAV or BCRP gene silencing. Proliferation assay of SQ-Mitox-BCRP-6P (isolate 2) untreated control, scrambled and transfected with siRNA ITGAV (1) and (2), BCHE (1) and (2). Results graphed as % survival relative to nontreated control (n=3).

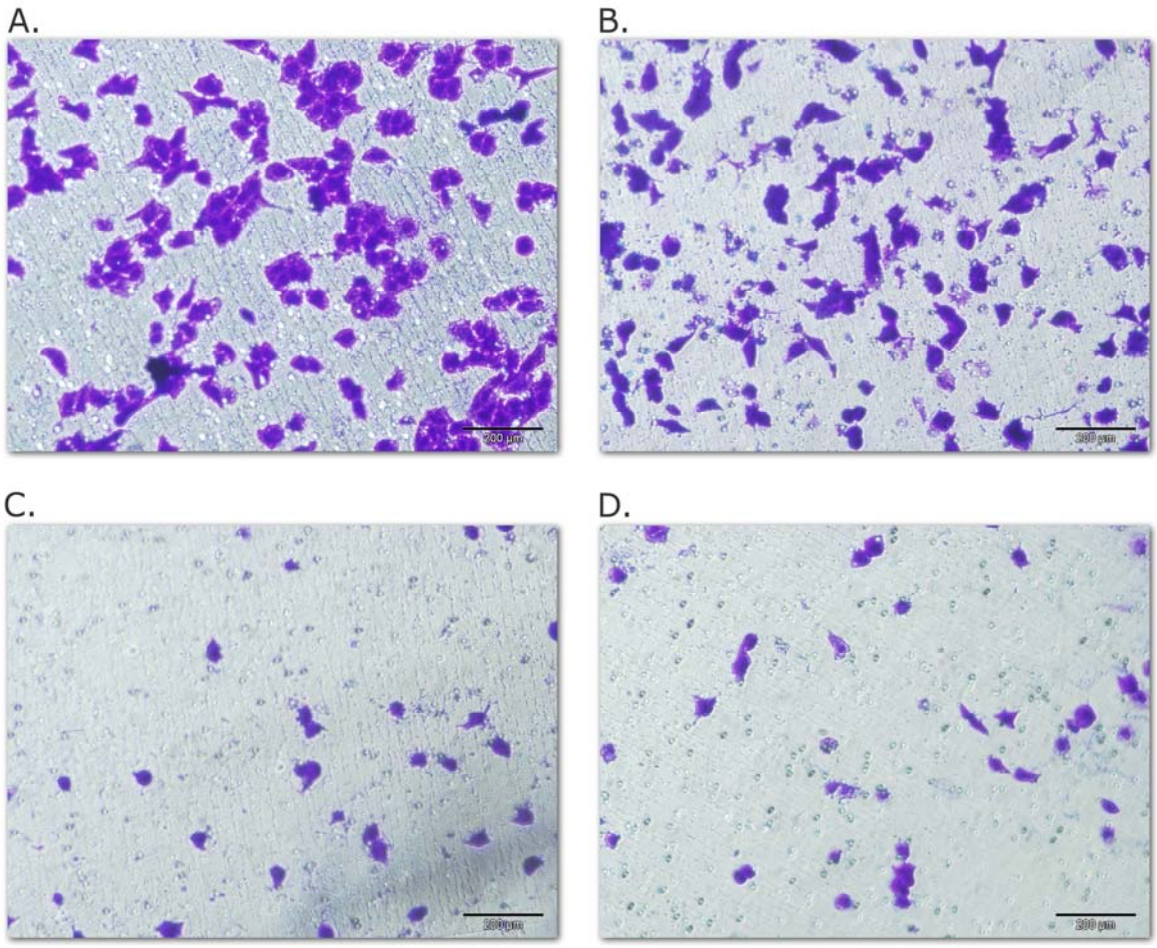

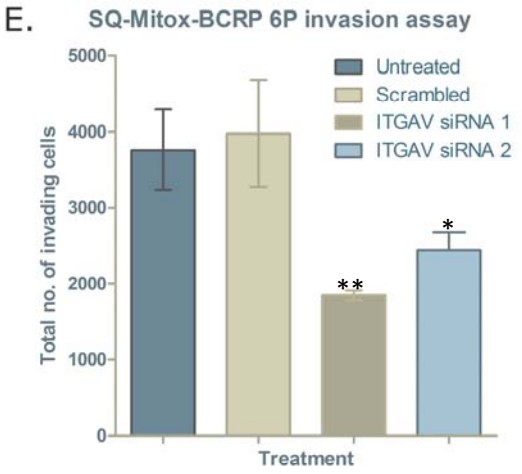

Figure 4.2-13: *ITGAV* gene silencing hampers SQ-Mitox-BCRP-6P invasiveness. Invasion assays of DLKP-SQ-Mitox-BCRP-6P (isolate 2) cells (**A.**) under control conditions; (**B.**) transfected with scrambled siRNA; (**C.**) transfected with integrin alpha V (1); (**D.**) transfected with integrin alpha V (2). Magnification, ×200. Scale bar, 200µm. (**E.**) Invasion assay of DLKP-SQ-Mitox-BCRP-6P (isolate 2) of total number of cells invading post siRNA integrin alpha V transfection. Statistics: $p \leq 0.05$*, 0.01**, 0.005*** (unpaired t-test to scrambled control).

4.2.7.1 siRNA mediated interference knockdown of ITGAV reduces the invasive capacity of SQ-Mitox-BCRP-6P cells

Integrin alpha V was identified as up-regulated in both Genelist 1 and 2. To investigate whether Integrin alpha V plays a role in DLKP lung cancer invasion, *ITGAV*-siRNA was used to knockdown Integrin alpha V expression in the stable, higher drug resistant SQ-Mitox-BCRP overexpressing cell line. *ITGAV* knockdown by small interfering (si)RNA reduces the invasion of DLKP-Mitox cells (figure 4.2-13). This preliminary experiment supports the hypothesis that increased expression of integrin alpha V plays a role in the aggressive invasive phenotype observed *in vitro*. Further investigation confirming the knockdown of Integrin alpha V protein by Western blot is warranted.

4.2.7.2 siRNA mediated interference knockdown of BCHE reduces the invasive capacity of SQ-Mitox-BCRP-6P cells

Microarray profiling revealed differential expression of BCHE, a secretory butyrylcholinesterase, between the SQ-Mitox-BCRP-4P and SQ-Mitox-BCRP-6P cell lines. BCHE was confirmed by Western blot analysis to be abundantly up-regulated in the SQ-Mitox-BCRP-6P (isolate2) compared to the parental cell line, DLKP-SQ and its resistant variant, SQ-Mitox-BCRP-4P (figure 4.2-14). Increasing evidence suggests the involvement of cholinesterases in tumourigenesis[327, 328]. To investigate whether BCHE plays a role in DLKP lung cancer invasion, BCHE siRNA was used to knockdown BCHE in the invasive cell line, SQ-Mitox-BCRP-6P. BCHE siRNA transfected into SQ-Mitox-BCRP-6P resulted in a significant decrease in invasion through matrigel. Figure 4.2-14 shows a Western blot showing knockdown of BCHE in the SQ-Mitox-BCRP-6P cell line after BCHE siRNA transfection.

4.2.7.3 IHC analysis of BCHE Expression in Lung Cancer

Western blot analysis of BCHE showed that it is positively associated with an increase in drug resistance and invasion in the SQ-Mitox-BCRP-6P cell line. BCHE expression in human cancer was investigated further (table 4.2-6). A lung cancer tissue array (TMA) (Biomax, LC817) was immunohisto-chemically stained using primary antibodies specific for BCHE. The array contained 16 cases of squamous cell carcinoma, 16 adenocarcinoma, 1 bronchioloalveolar carcinoma and 6 small cell carcinoma. There were single cores per case with matched lymph node metastasis for each case, providing 40 cases for analytical interpretation.

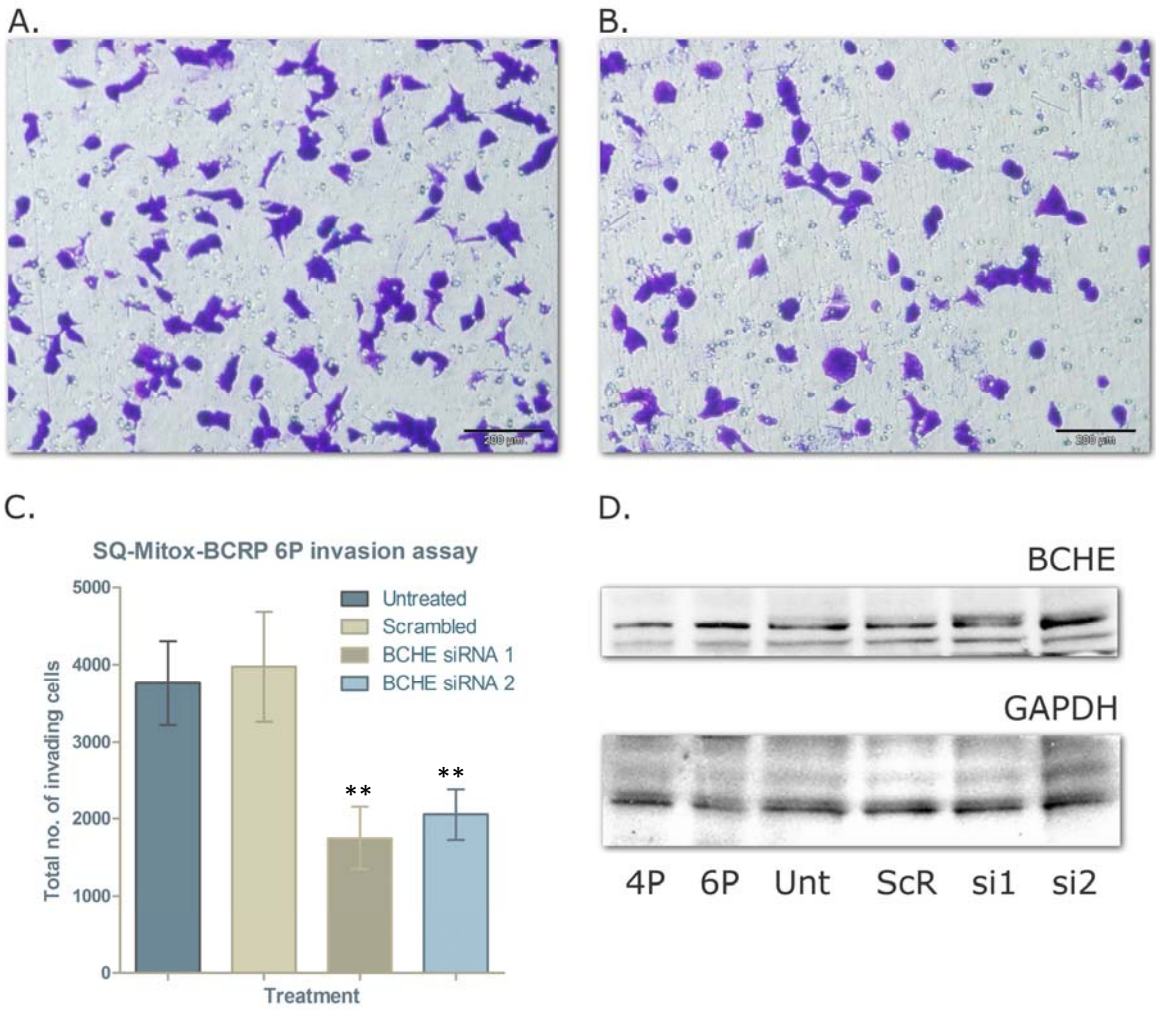

Figure 4.2-14: BCHE gene silencing hampers SQ-Mitox-BCRP-6P invasiveness. Invasion assays of DLKP-SQ-Mitox-BCRP-6P (isolate 2) cells. (**A.**) Transfected with scrambled siRNA. (**B.**) Transfected with BCHE, magnification, 200× scale bar 200µm. (**C.**) Invasion assay of SQ-Mitox-BCRP-6P of total number of cells invading post siRNA BCHE transfection. (**D.**) Western blot showing an increase in BCHE in SQ-Mitox-BCRP-6P relative to SQ-Mitox-BCRP-4P. Also, a Western blot showing knockdown of BCHE at 48 hours post-transfection in SQ-Mitox-BCRP-6P cells transfected with two independent siRNAs targeting BCHE relative to scrambled control siRNA transfected cells. GAPDH served as a loading control. Statistics: $p \leq 0.05$*, 0.01**, 0.005*** (unpaired t-test to scrambled control).

Table 4.2-6: BCHE Immunoreactivity in squamous, adeno and small cell lung tumours from a lung cancer tissue array with matched lymph node metastatic tissue.

US Biomax, Inc. LC817 (serial)

	1	2	3	4	5	6	7	8	9	10
A	3_1	5_2	6_2	5_2	2_2	2_2	2_3	2_3	2_3	3_3
B	$-_3$	$-_3$	3_3	3_-	5_3	3_3	5_3	3_2	4_2	$-_1$
C	5_2	5_2	6_2	5_2	5_3	4_-	4_3	4_2	3_2	3_3
D	$-_3$	4_3	5_3	4_3	5_-	4_-	5_-	3_-	4_-	$-_-$
E	$-_1$	5_2	3_-	6_2	5_2	5_2	4_2	5_3	4_3	2_3
F	$-_3$	6_3	$-_3$	2_3	5_1	5_3	5_-	5_-	3_2	$-_2$
G	2_2	5_2	6_2	6_2	2_2	5_2	2_3	6_3	5_3	4_3
H	$-_3$	3_2	5_3	5_3	5_-	6_-	6_-	$-_-$	5_-	5_-

Main numbers indicate BCHE staining intensity score, superscript indicates tumour grade (where 1-3 is equivalent to well-differentiated, moderately-differentiated or poorly differentiated, respectively).

Colour coding indicates tumour stage; lilac = Stage II; green = Stage IIIa; red = Stage IIIb.

Yellow shading indicates the cognate or matched lymph node metastatic tumour, e.g. A1 is matched with E1, A2 is matched with E2, etc.

Tumour diagnosis: A1 – B7: Squamous cell carcinoma; B8 – D4: Adenocarcinoma, except C6: Bronchioloalveolar carcinoma; D5 – D10: Small cell carcinoma. E1 – H10: the corresponding matched lymph node metastatic tisssues to those in A1 – D10.

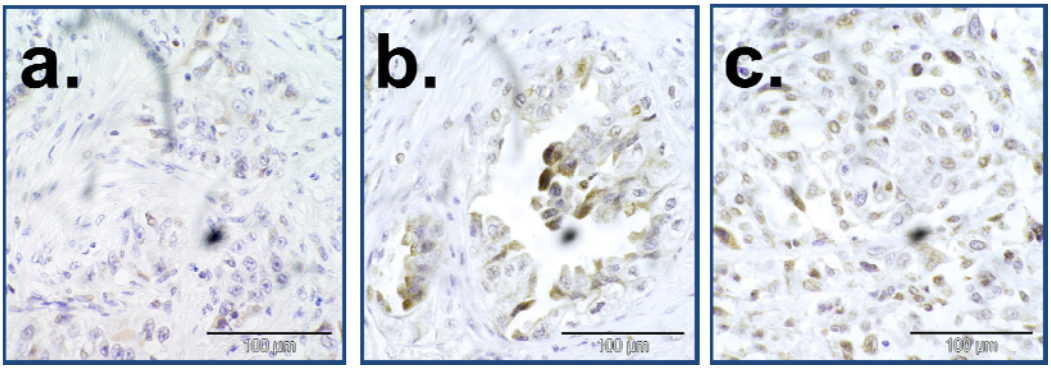

Figure 4.2-15: Immunohistochemical Analysis of BCHE Expression in a Lung Cancer TMA. (**A.**) Weak BCHE positive staining is observed in a grade III (high grade, histologically more aggressive) squamous cell carcinoma. (**B.**) Increased BCHE expression observed in a grade II (histologically less aggressive) adenocarcinoma. (**C.**) Intense BCHE staining was observed in a number of metastatic lung tumours, a representative lymph node metastasis from a squamous tumour is shown. Original magnification of all photomicrographs, ×400. Scale bar = 100 µM.

A total of 80 TMA cores were analysed. TMA cores were scored semi-quantitatively, according to the intensity of the BCHE immunoreactivity observed (weak, moderate, or strong). Each tissue was scored based on the intensity of staining observed and the percentage of cells staining. (figure 4.2-15).

Variable staining was observed in both primary (22/40) and metastatic (26/40) lung tumours. Strong staining was observed in 7/40 metastatic lung carcinomas and 2/40 primary tumours. The pattern of staining was granular and was located in both the cell nucleus and cytoplasm of the cells. Interestingly, a higher percentage of cells stained in the primary tumours of the adenocarcinomas (9/15) and in the metastatic tissues of the small cell carcinomas (5/6).

4.3 Summary

The DLKP clones with various degrees of invasiveness (derived from the same parent) offered a unique opportunity to study mechanisms of invasion. These cell lines provided an ideal *in vitro* model of invasion. One of the aims of this thesis was to identify genes involved in the development of an invasive phenotype in lung cancer cell lines.

The strategy of deriving isogenic drug resistant cell lines from the DLKP-SQ clone eliminates variability due to intrinsic genetic differences between cell lines. An important point to remember when considering the SQ-Mitox analysis is that there are potentially two ways to approach this data; (1) one could look at drug resistance and/or (2) look at invasion. Theoretically however, any differentially expressed genes identified by the microarray analysis of the SQ-Mitox cell lines could relate to drug resistance. Thus, gene-expression profiles of human lung cancer cell lines with differing levels of invasion and drug resistance were analysed using microarray analysis.

The novel cell line model of mitoxantrone resistant lung cancer was developed by pulse selecting a clone of DLKP-SQ with mitoxantrone. In this instance drug resistance developed first, followed by invasion. Induction of invasion was independent of which type of xenobiotic transporter was expressed. Microarray analysis was performed in poorly invasive mitoxantrone resistant DLKP-SQ-Mitox-BCRP (4^{th} pulse) and DLKP-SQ-Mitox-P-gp (4^{th} pulse) and compared with invasive mitoxantrone resistant DLKP-SQ-Mitox-BCRP (6^{th} pulse) and DLKP-SQ-Mitox-P-gp (6^{th} pulse).

Table 4.2-7: summarises the findings in this chapter for genes with increased expression in invasive cell lines.

Gene	Identified from genelist	SQ vs I	SQ vs M×	SQ-Mitox-BCRP-4P vs 6P
Integrin alpha V	SQ vs I SQ vs M 4P vs 6P genelist 1 and 2	↑ DLKP-I	↑ DLKP-M	↑ in 6P vs 4P
ALCAM	Top 15 SQ vs I 4P vs 6P genelist 1 and 2	↑ DLKP-I	↓ DLKP-M	↑ in 6P vs 4P
SLIT2	SQ vs M 4P vs 6P genelist 1 and 2	low in DLKP-I	↑ DLKP-M	↑ in 6P in the membrane vs 4P
ROBO2	Top 15 SQ vs I 4P vs 6P genelist 1 and 2	↑ DLKP-I	↑ DLKP-M	↑ in 6P vs 4P
N-cadherin	Top 15 SQ vs I 4P vs 6P genelist 1 and 2	↑ DLKP-I	absent DLKP-M	↑ in 6P vs 4P
MMP-2	Not present on DE genelists	↑ DLKP-I	↑ DLKP-M	↑ in 6P vs 4P
MMP-10	SQ vs I SQ vs M 4P vs 6P genelist 1 and 2	↑ DLKP-I	↑ DLKP-M	↑ in 6P vs 4P

Two gene lists were generated – (1) DLKP-SQ-Mitox-BCRP-4P *vs* DLKP-SQ-Mitox-BCRP-6P cells (gene list 1) and (2) DLKP-SQ-Mitox-MDR-4P *vs* DLKP-SQ-Mitox-MDR-6P cells (gene list 2), in search of molecular mechanisms involved in the invasive phenotype. The genes were analysed for over-expression of gene ontology terms in categories assigned by PANTHER pathways. The most significant pathways were related to Wnt signalling, inflammation, integrin signalling and p53 pathways – these were common to both gene list 1 and gene list 2.

A stable, higher drug resistant variant was established from the 6th pulse population of BCRP overexpressing cells (SQ-Mitox-BCRP-6P (isolate 2) with a 560-fold resistance to the selecting agent). Western blot and immunofluorescence confirmed the up-regulation of the proteins, integrin alpha V, BCHE, ALCAM and SLIT2 (in the membrane) as identified by the microarray analysis. Of particular interest is the identification of the SLIT2 / ROBO2 signaling pathway in the invasive, drug resistant 6th pulse.

It also appears that the acquisition of drug resistance is accompanied by an increase in activity of MMP-2 in DLKP-SQ cells and treatment with an MMP blocking Ab against MMP-2 may negatively modulate the invasiveness of drug-resistant SQ-Mitox-BCRP-6P cells. siRNA knockdown experiments also suggest that integrin alpha V plays a role in the aggressive invasive phenotype observed *in vitro*.

Of particular interest is that the DLKP-SQ clone acquired characteristics common to both the DLKP-I and DLKP-M clones. For example, the DLKP-SQ clone developed an up-regulation of the cell adhesion molecules ALCAM and N-cadherin in common with DLKP-I, and the axon guidance molecules SLIT2/ROBO2 in common with the DLKP-M clone. In addition, it also acquired the cell surface glycoprotein, integrin alpha V, the metalloproteinases MMP-2 and MMP-10 in common with both DLKP-I and DLKP-M (table 4.2-7). It appears that ALCAM and N-cadherin could be a marker for DLKP-I and SLIT2 could be a marker for DLKP-M.

CHAPTER 5

Investigation of the effects of MEK inhibitors on drug resistance and invasion in DLKP

5.1 MEK inhibitors – effect on drug resistance and invasion

5.1.1 Introduction

The mitogen-activated protein kinase (MAPK) signaling pathways involve a family of protein kinases that play critical roles in the regulation of diverse cellular activities including cell proliferation, survival, differentiation, motility and angiogenesis. The MAPK pathways (figure 5.1-1) transduce signals from various extracellular stimuli (growth factors, hormones, cytokines and environmental stresses), leading to distinct intracellular responses via a series of phosphorylation events and protein-protein interactions[329]. These signalling cascades are often dysregulated in human cancer cells and targeting MEK as a central kinase of the MAPK pathway is currently being tested in clinical trials for its therapeutic potential. A class of molecular targeted compounds called small-molecule protein kinase inhibitors can disrupt such mitogenic signalling pathways. These small molecule inhibitors are moving quickly from bench to bedside[330,331].

Dose-limiting side effects are problematic in the use of small molecule inhibitors, and MEK inhibitors that sufficiently reduce ERK activation in patients show a low clinical response. One possible reason for the low response to MEK targeting drugs is thought to be the up-regulation of counteracting signalling cascades as a direct response to MEK inhibition. Therefore, understanding the biology of cancer cells, cross-talk between intracellular pathways and the effects of MEK inhibition on these cells will help to identify new combinatorial approaches that are ultimately efficacious for the patient[332].

MAPK pathways have been implicated in acquired tumour resistance following chemotherapy[333]. Previous studies of MAPK signalling pathways in cancer models have shown that the p44/p42 MAPK cascade is activated by chemotherapeutic agents such as paclitaxel[334], cisplatin[335] and vinblastine[336] and is involved in acquired resistance to these drugs. Hence, the effects of MEK inhibitors on the anti-cancer drug resistance of the SQ-Mitox cell lines were investigated.

Previous studies in the literature have indicated that MEK inhibitors can suppress the invasiveness of UM-SCC-1, a squamous cell carcinoma derived from the oral cavity[337] and A375 melanoma cells[338]. The differential expression and activation of p44/p42-MAPK among the three distinct DLKP clones and the corresponding effects of targeting p44/p42-MAPK on growth and survival have not previously been examined. Thus, an investigation of the MEK/ERK inhibitor U0126 and its affects on invasion in the DLKP clones was warranted.

5.1.2 Inhibitors used in this study

U0126 is a mitogen activated protein kinase kinase (MAPKK) inhibitor that inhibits MEK1/2 (See table 2-2). It can penetrate cells and selectively inhibit MEK1/2 to inhibit the phosphorylation and activation of MAP kinase (Erk1/2 or p42/44 MAPK)[339]. It can also suppress the activation of AP-1-dependent gene transcription.

PD98059 can also penetrate cells and selectively inhibit MEK1 to inhibit the phosphorylation and activation of MAP kinase (Erk1/2 or p44/42MAPK)[340]. When compared with PD98059, U0126 shows a significantly higher affinity for MEK1. U0126 and PD98059 both bind to this enzyme in a mutually exclusive fashion suggesting that they share a common binding site[339].

The benzimidazole ARRY-142886 (AZD6244) has been reported to be a highly potent MEK inhibitor[341]. AZD6244 is an oral, non-ATP competitive inhibitor and highly specific for MEK1/2, a key enzyme in the Ras-Raf-MEK-ERK pathway. AZD6244 is probably the most widely studied MEK inhibitor for clinical use. For example a Phase II clinical trial is currently underway to compare the efficacy of AZD6244 in combination with docetaxel alone in patients with KRAS mutation positive non small cell lung cancer patients[342].

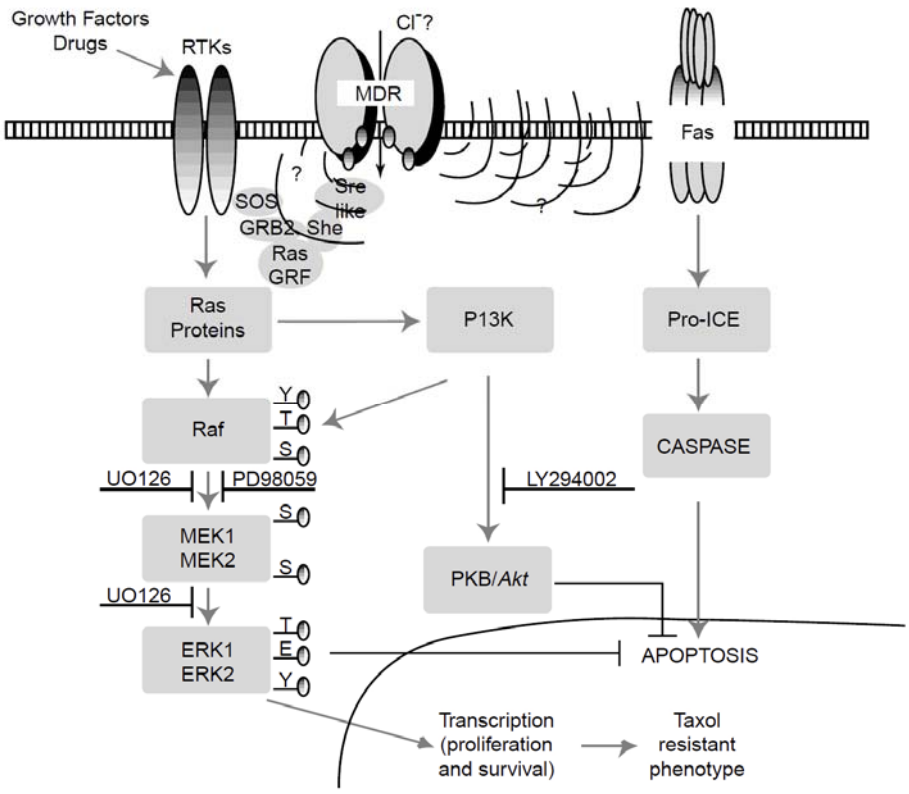

Figure 5.1-1: Diagram taken from *Ding et al.,* (2001)[343] – Cross-talk between signalling pathways and the multidrug resistant protein MDR-1.

5.1.3 Effects of MEK inhibitors on anti-cancer drug resistance of SQ-Mitox cells

The results described in chapter 3 explained the generation of SQ-Mitox-BCRP and SQ-Mitox-MDR cells, a cell line model of mitoxantrone resistance. These cell lines over-expressed the xenobiotic or drug resistance pumps, BCRP and P-gp. The association between the expression of these ABC transporter proteins and cell signalling pathways has recently generated some interest[344,345]. The present study has attempted to further clarify the regulatory mechanisms underlying ABC transporter protein expression, focusing on P-gp and BCRP and to identify inhibitors that specifically target these expression mechanisms. Prior to testing the effects of PD98059 and U0126 on anticancer drug resistance, the appropriate concentration range for each inhibitor was established with the aim of finding a concentration which caused approximately 10% cytotoxicity.

5.1.3.1 Effects of PD98059 and U0126 on cell growth of DLKP-SQ and SQ-Mitox cells

The cell viability of DLKP-SQ and SQ-Mitox cells following treatment with PD98059 was determined by the acid phosphatase assay as described in section 2.2. Different concentrations of inhibitor were used, ranging from 1 μM to 50 μM over a 3-day study period. Results indicated that the growth inhibitory effects of PD98059 on the drug resistant cells are approximately less than 10% (≤ 20 μM, figure 5.1-2, top graph). A concentration of 20 μM PD98059 was thus established for subsequent experiments.

The cell viability of DLKP-SQ and SQ-Mitox cells was also determined by the acid phosphatase assay following treatment with U0126. Different concentrations of inhibitor were used, up to 10 μM over a 3-day study period. The growth suppressive effects of U0126 on the SQ-Mitox-MDR cells was less than 10% but there was an increase in sensitivity of the parental DLKP-SQ and SQ-Mitox-BCRP cells which appeared to plateau at 1 μM (figure 5.1-2, lower graph). A concentration of 10 μM U0126 was thus established for subsequent experiments.

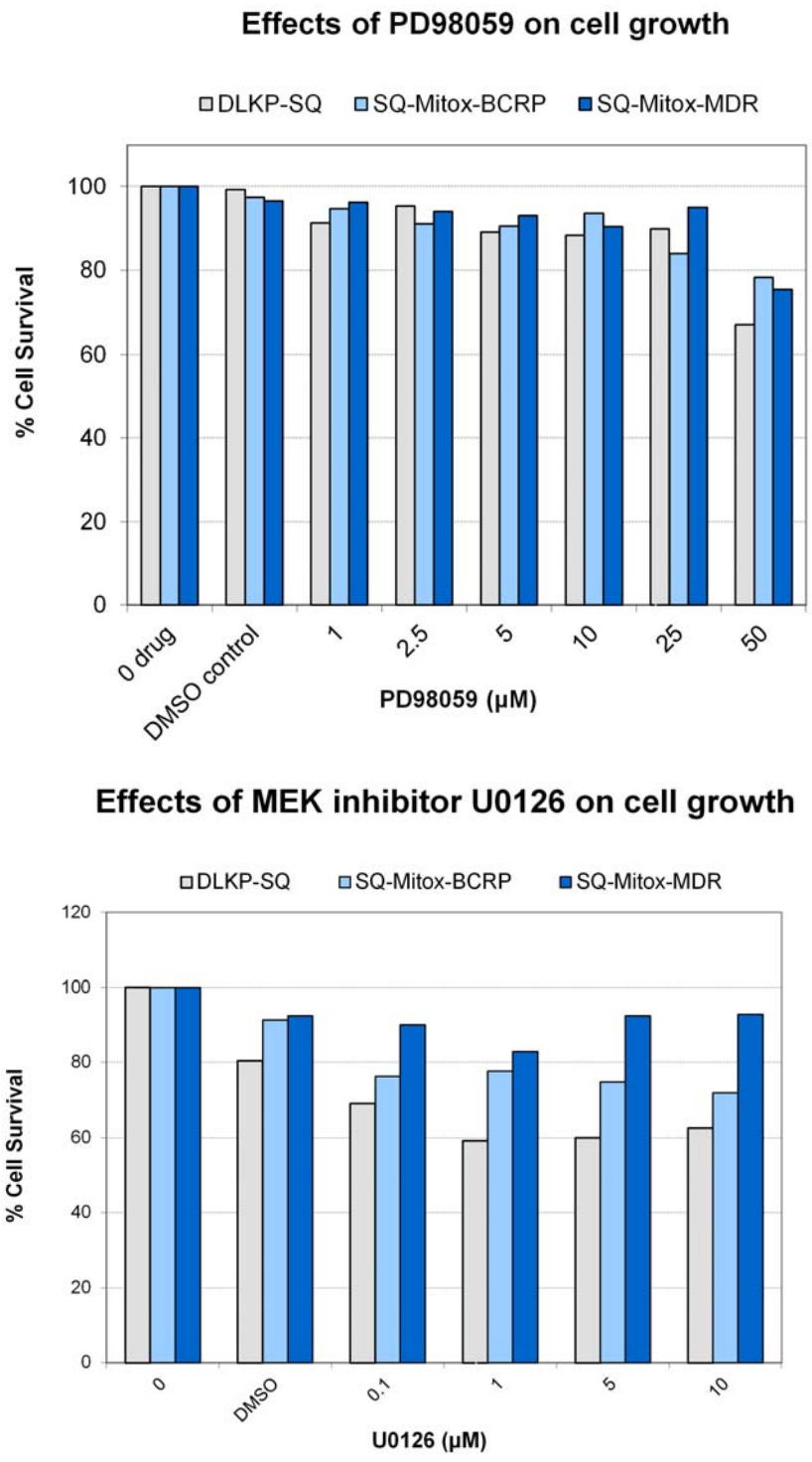

Figure 5.1-2: Effects of PD98059 and U0126 on cell growth. DLKP-SQ, SQ-Mitox-BCRP and SQ-Mitox-MDR cells were seeded into 96 well plates and cultured in the absence or presence of PD98059 and U0126 for 3 days. Cell survival was determined using the alkaline phosphatase assay and presented as percentages relative to those of control cells cultured in the absence of the MEK inhibitor. DMSO was used as a control. The data shown are the means ± SD of at least 4 wells, and are representative of two independent experiments.

5.1.3.2 Effects of PD98059 and U0126 on anticancer drug resistance of SQ-Mitox-BCRP cells

Inhibition of the MAPK kinase pathway can potentially affect the resistant phenotype of cancer cell lines[346-348]. The efficacy of the MAPK signalling inhibitors, U0126 and PD98059 in combination with an anticancer therapeutic such as mitoxantrone was investigated. The cytotoxicity of mitoxantrone was significantly potentiated in the BCRP over-expressing cell line after combination treatment with PD98059 and U0126 for 48 hours (figure 5.1-3). This combination of mitoxantrone with MEK inhibitors produced a substantial and pronounced reduction in cell survival when compared with treatment with mitoxantrone alone. Intriguingly, the effect plateaued at approximately 20% cell survival at all concentrations tested. This is an important result because it questions the potential for a therapeutic regime to effectively eliminate a tumourigenic cell population.

5.1.3.3 Inhibition of MAPK kinase pathway has no effect on BCRP expression levels

In the previous section results show that the inhibitor PD98059 is capable of decreasing anticancer drug resistance in the SQ-Mitox-BCRP cells. Was PD98059 therefore capable of reducing BCRP protein expression? SQ-Mitox-BCRP cells were exposed to PD98059 at a concentration of 20 μM for 24 and 48 hours and BCRP protein expression levels measured by Western blot analysis.

The level of BCRP protein in the SQ- Mitox-BCRP cells was unchanged after treatment with PD98059, suggesting that down-regulation of BCRP is not the molecular change in this cell line responsible for decreasing its mitoxantrone resistance (figure 5.1-4, A).

5.1.3.4 Effects of PD98059 and U0126 on anticancer drug resistance of SQ-Mitox-MDR cells

MEK inhibitors reverse drug resistance significantly in cell lines overexpressing BCRP. Would inhibition of the MAPK kinase pathway also affect the resistant phenotype of the SQ-Mitox-MDR cells? MAPK signalling inhibitors in combination with mitoxantrone were similarly assessed in this cell line. The results demonstrated that combination treatment with PD98059 but not U0126, substantially increased the drug resistance of SQ-Mitox-MDR cells (figure 5.1-5). U0126 had a small but insignificant effect on cell survival.

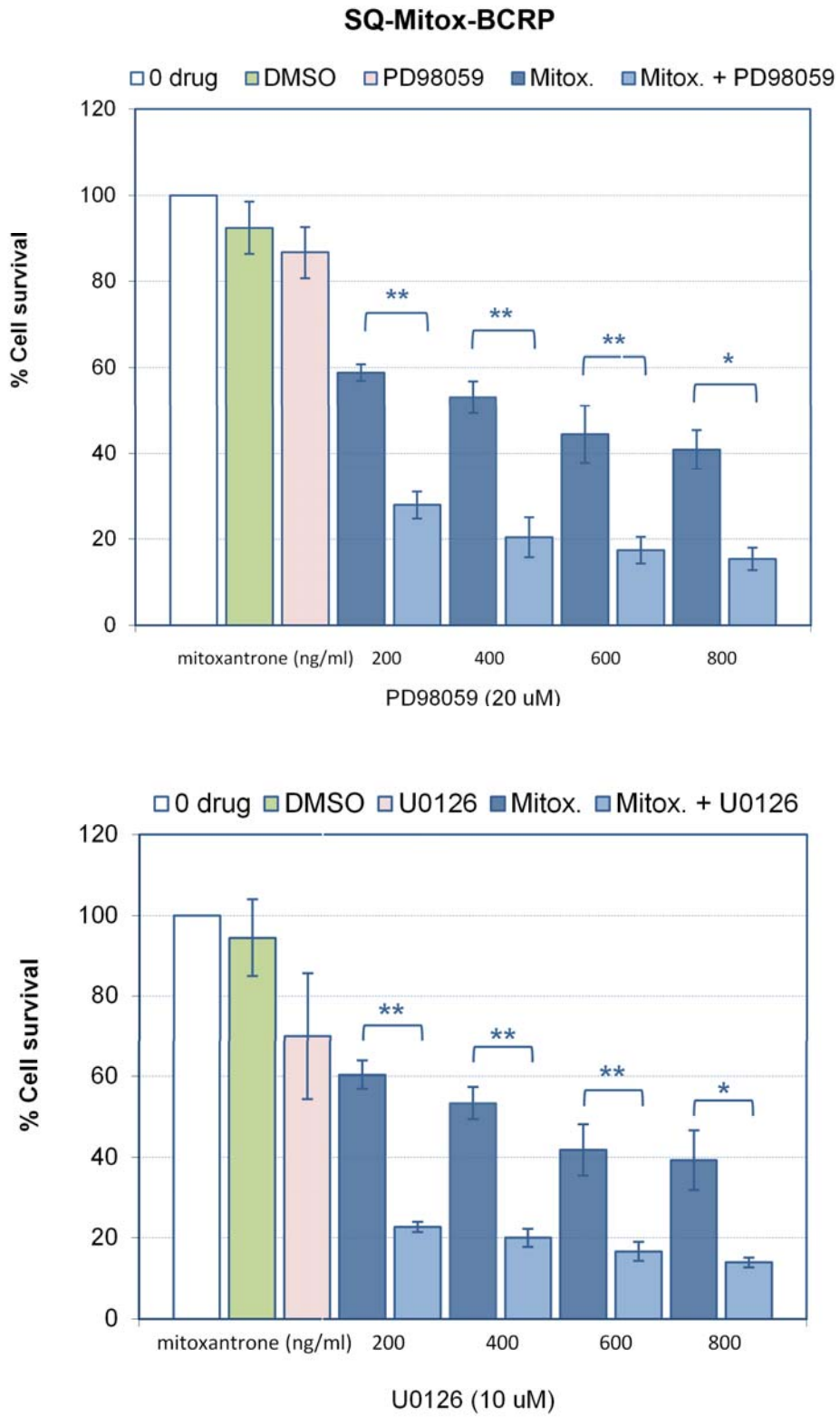

Figure 5.1-3: Effects of PD98059 and U0126 on anticancer drug resistance of SQ-Mitox-BCRP cells. SQ-BCRP cells were seeded into 96 well plates and cultured in the absence or presence of PD98059 and U0126, with and without Mitox for 48 hours. Cell survival was determined using the alkaline phosphatase assay and presented as percentages relative to those of control cells cultured in the absence of the MEK inhibitor. DMSO was used as a control. The data shown are the means ± SD of at least 4 wells, and are representative of three independent experiments. Statistics: $p \leq 0.05$*, 0.01**,

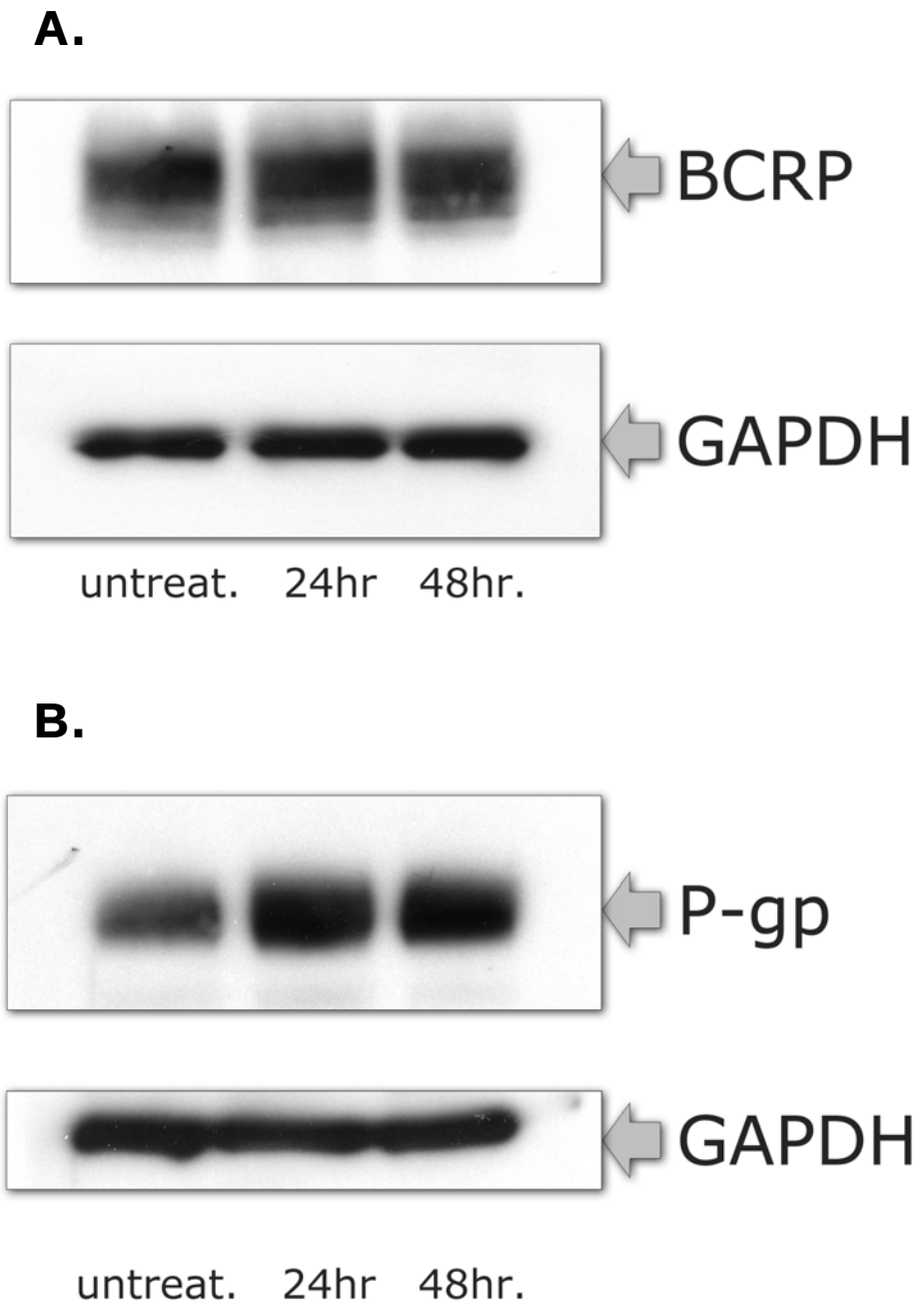

Figure 5.1-4: (**A.**) PD98059 treatment of SQ-Mitox-BCRP**.** SQ-Mitox-BCRP cells were exposed to DMSO (controls) and PD98059 at a concentrations 20 μM for 24 and 48 hours. Lysates were prepared for analysis by Western blot to detect BCRP. (Representative results of two independent treatments). (**B.**) PD98059 treatment of SQ-Mitox-MDR. SQ-Mitox-MDR cells were exposed to DMSO and PD98059 at a concentration of 20 μM for 24 and 48 hours. Lysates were prepared for analysis by Western blot to detect P-gp. (Representative results of two independent treatments).

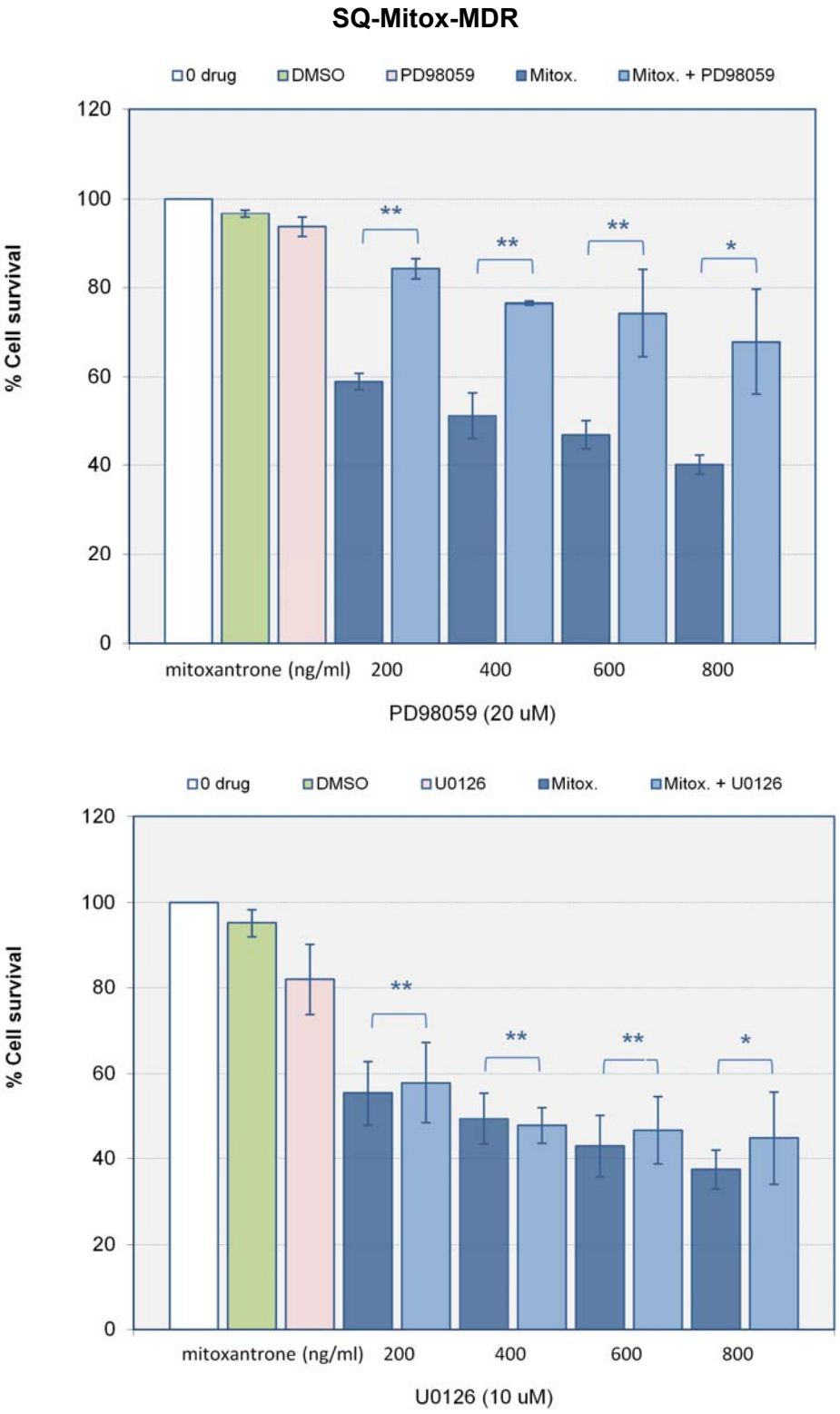

Figure 5.1-5: Effects of PD98059 and U0126 on anticancer drug resistance of SQ-MDR1 cells. SQ-MDR1 cells were seeded into 96 well plates and cultured in the absence or presence of PD98059 and U0126, with and without mitoxantrone for two days. Cell survival was determined using the alkaline phosphatase assay and presented as percentages relative to those of control cells cultured in the absence of the MEK inhibitor. DMSO was used as a control. The data shown are the means ± SD of at least 4 wells, and are representative of three independent experiments. Statistics: $p \leq 0.05$*, 0.01**.

5.1.3.5 Inhibition of MAPK kinase pathway increases P-gp protein expression levels

PD98059 increased anticancer drug resistance in SQ-Mitox-MDR cells. Could PD98059 stimulate P-gp protein expression? SQ-Mitox-MDR cells were exposed to PD98059 at a concentration of 20 μM for 24 and 48 hours. The expression of P-gp protein expression levels was measured by Western blot analysis. The level of P-gp protein was increased after treatment with PD98059, suggesting that PD98059 enhanced the expression of the P-gp protein (figure 5.1-4, B) and that this might help explain the increase in drug resistance.

5.1.3.6 Effects of Elacridar on anticancer drug resistance on SQ-Mitox- MDR

The inhibitor PD98059 stimulated P-gp protein expression in the SQ-Mitox-MDR cell line. Was the resistance mechanism in this cell-line mediated through increased P-gp expression and / or activity? The experiment was repeated with a P-gp inhibitor to investigate if suppression of P-gp expression ameliorated the effect. Elacridar is a P-gp inhibitor which is known to inhibit P-gp at a concentration of 0.25μM[50]. Elacridar was added to the cell culture media in the mitoxantrone and PD98059 combination assay. This had a significant impact on mitoxantrone toxicity, substantially reducing cell survival indicating that P-gp is responsible for the enhanced PD98059 induced drug resistance (figure 5.1-6). Of note is the background basal level of cell survival. Elacridar has the same effect in both the presence and absence of MEK inhibitor. Even with P-gp activity ameliorated there are other mechanisms at work responsible for the albeit low level of cell survival.

5.1.3.7 Effects of AZD6244 on anticancer drug resistance of SQ-Mitox-BCRP and SQ-Mitox-MDR1 cells.

AZD6244 is an oral, non-ATP competitive inhibitor and is highly specific for MEK1/2, a key enzyme in the Ras-Raf-MEK-ERK pathway. AZD6244 is one of the most widely studied MEK inhibitors in the clinical setting and thus a suitable candidate to investigate effects on the anti-cancer drug resistance of the SQ-Mitox cell line. Preliminary results from a single investigation (figure 5.1-7) indicate that there is a small but insignificant increase in anticancer drug resistance of SQ-Mitox-MDR after treatment with AZD6244. In contrast, AZD6244 diminishes the anti-cancer drug resistance of BCRP over-expressing cells – a similar response to that observed with PD98059 and U0126.

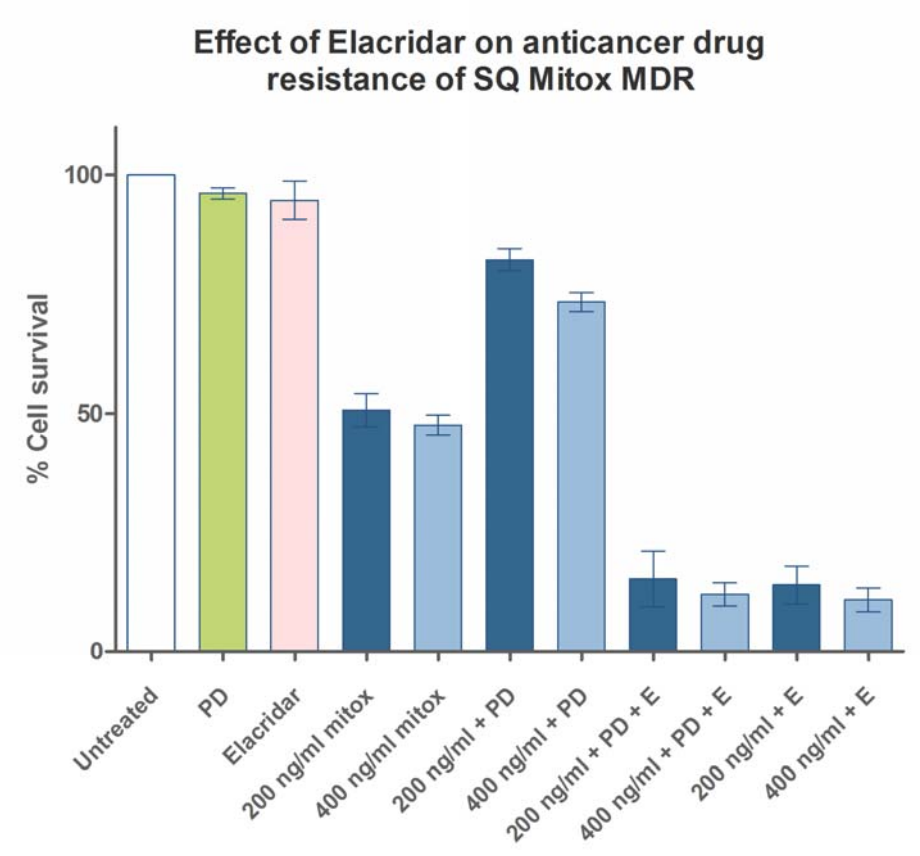

Figure 5.1-6: Effects of Elacridar on anticancer drug resistance on SQ-Mitox- MDR. Previous results showed that PD98059 induced a higher level of P-gp expression in the SQ-Mitox-MDR cell line. The presence of inhibitor and mitoxantrone enhances cell survival by approximately 60% relative to treatment with mitoxantrone alone. This enhanced survival could be reversed by the P-gp inhibitor, Elacridar. Elacridar substantially reduces cell survival with all treatments regardless of the combinatorial treatments employed. The data shown are the means ± SD of at least 4 wells, and are representative of three independent experiments.

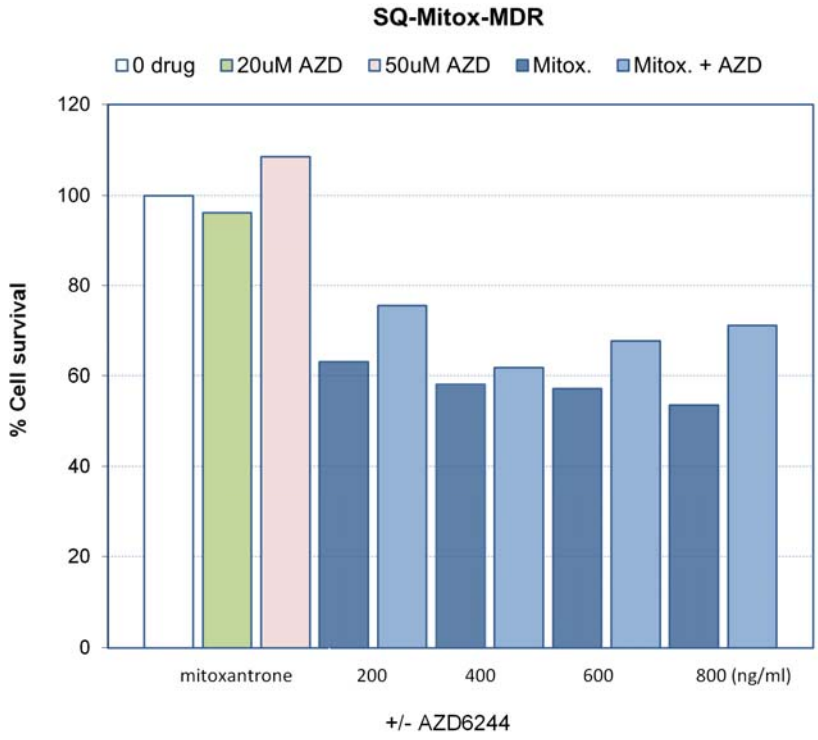

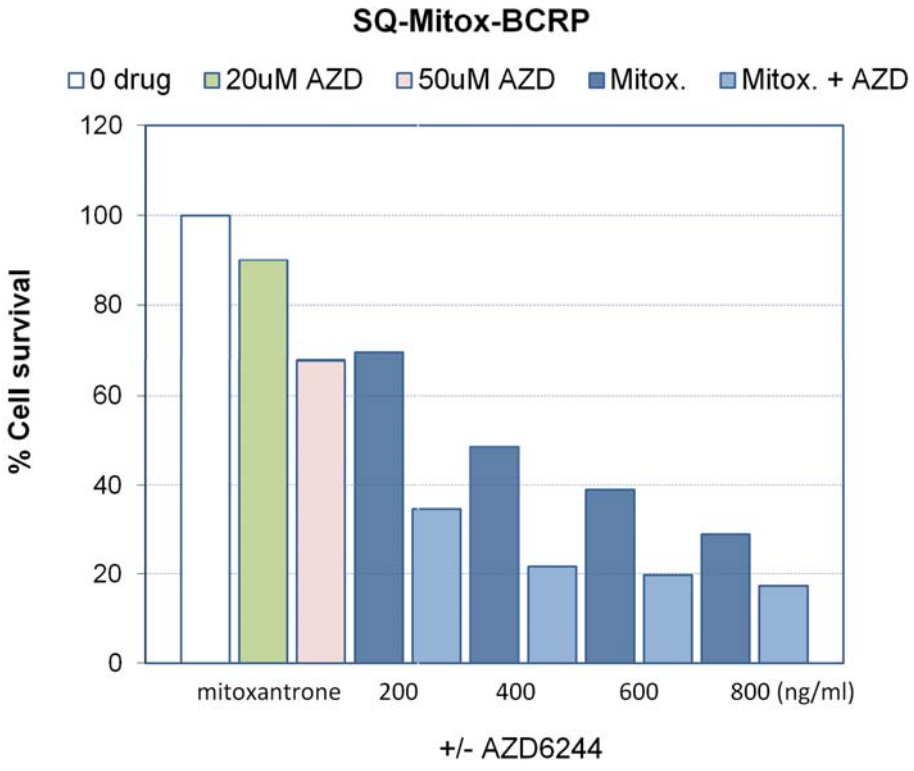

Figure 5.1-7: Effects of AZD6244 on anticancer drug resistance of SQ-Mitox-BCRP and SQ-Mitox-MDR1 cells. There is a small but insignificant increase in anticancer drug resistance of SQ-Mitox-MDR after treatment with AZD6244. This may question the clinical efficaciousness of such inhibitors used in cancer therapy. The decrease in anticancer drug resistance of SQ-Mitox-BCRP is similar to the results observed in treatments with PD98059 and U0126.

5.1.3.8 Effects of PD98059 on anticancer drug resistance of DLKP-SQ

PD98059 decreased anticancer drug resistance in the SQ-Mitox-BCRP cells. Would it have the same effect on the DLKP–SQ parental cell line which contain low levels of BCRP protein (and display little mitoxanrone resistance). Preliminary results from a single investigation indicate that there is a small but insignificant decrease in anticancer drug resistance of DLKP-SQ after treatment with PD98059 (figure 5.1-8).

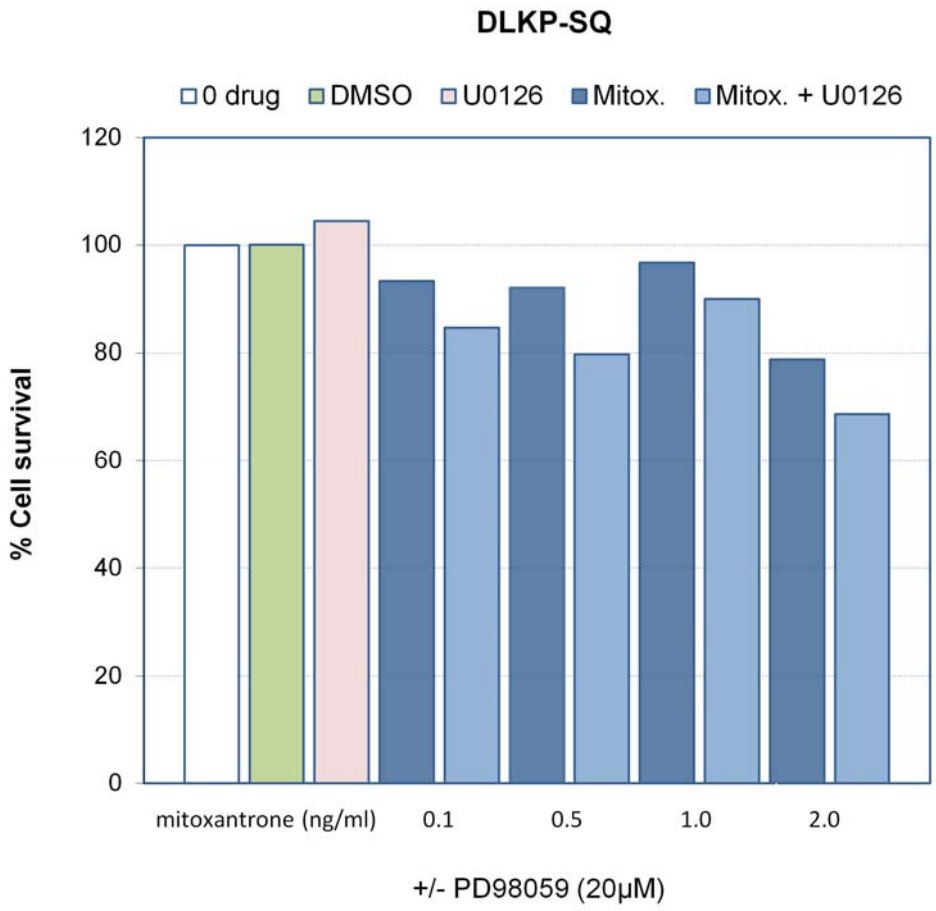

Figure 5.1-8: Effects of PD98059 on anticancer drug resistance of SQ. SQ (2000 cells/well) were seeded into 96 well plates and cultured in the absence or presence of PD98059 and increasing concentrations of mitoxantrone for two days. Cell survival was determined using the alkaline phosphatase assay and presented as percentages relative to those of control cells cultured in the absence of the MEK inhibitor. DMSO was used as a control.

5.1.3.9 Effects of PD98059 on anticancer drug resistance of DLKP-A

PD98059 up-regulates P-gp expression in the SQ-Mitox-MDR cell line. Does it have the same effect on other DLKP derived, drug resistant P-gp overexpressing cell lines? DLKP-A is a drug resistant variant, which was initially selected by exposure to adriamycin and over-expresses P-gp [277]. Inhibition of MEK had a small but not statistically significant effect on the drug resistance profile of DLKP-A (figure 5.1-9). These results suggest that the DLKP-A cells may contain a different mechanism of regulation of P-gp to the SQ-Mitox cells.

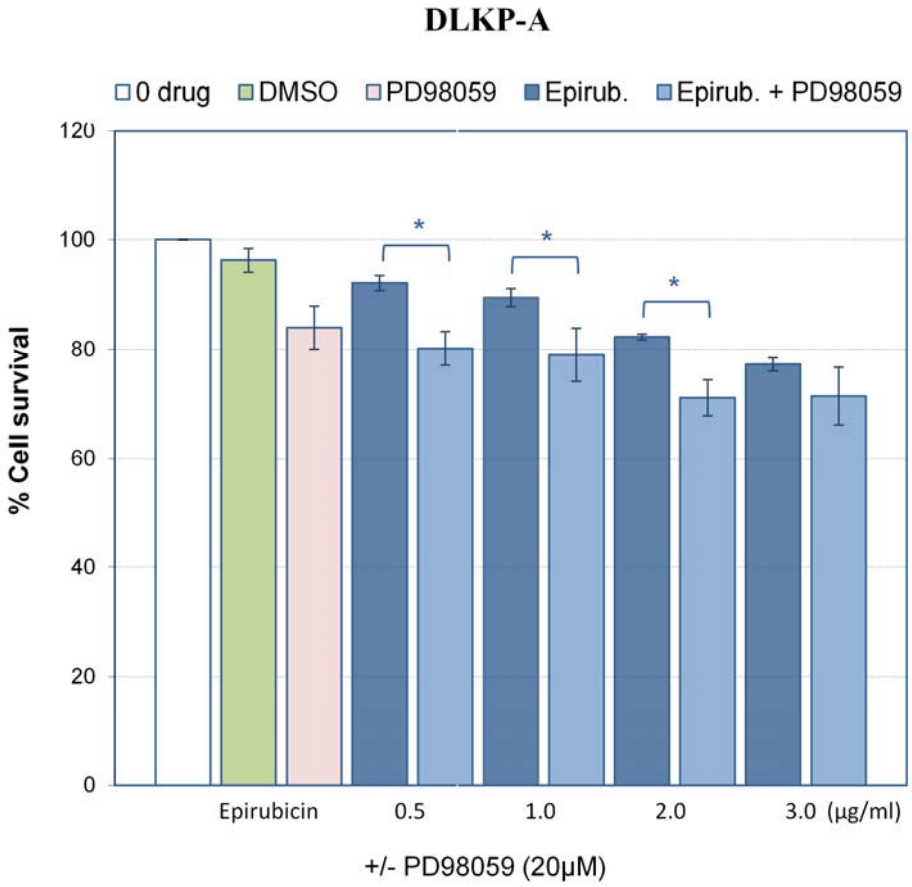

Figure 5.1-9: Effects of PD98059 on anticancer drug resistance of DLKP-A. DLKP-A cells were seeded into 96 well plates and cultured in the absence or presence of PD98059 and increasing concentrations of epirubicin for 48 hours. Cell survival was determined using the alkaline phosphatase assay and presented as percentages relative to those of control cells cultured in the absence of the MEK inhibitor. DMSO was used as a control. The data shown are the means +/- SD of three independent experiments.

5.1.4 Summary of effects of MEK inhibitors on drug resistant DLKP cell lines

In this section, the effects of signal transduction inhibitors upon multidrug resistance of the DLKP cell lines and its drug resistant variants were investigated. Table 5.1-1 summarises the effects of the MEK inhibitors on the drug resistance of the SQ-Mitox and DLKP-A cell lines.

Table 5.1-1: Summary of Effects of MEK inhibitors on drug resistant DLKP cell lines.

MEK Inhibitor	SQ-MitoxBCRP	SQ-Mitox-MDR	DLKP-SQ	DLKP-A
PD98059	++	++	+	+
U0126	++	+	_	_
AZD6244	ns	+	_	_

++ very significant; + significant; ns: not significant

The MEK inhibitor PD98059 diminishes the drug resistance of BCRP over-expressing cells but increases the drug resistance of P-gp over-expressing cells. Western blot analysis reveals that PD98059 up-regulates P-gp expression in the SQ-Mitox-MDR cells, while having little effect on the expression of BCRP protein levels in the SQ-Mitox-BCRP cell line. The role that the MAPK kinase pathway may play in the regulation of ABC transporter protein expression is a complex one and much remains to be elucidated.

5.2 Investigation of the effects of MEK inhibitors on invasion of DLKP- cells

5.2.1 Introduction

Earlier, DLKP-I and DLKP-M cells were observed to over-express MMP-2 and MMP-10. The MEK/ERK pathway has been implicated in the up-regulated expression of MMPs in tumour cells[338,347,349,350]. Common transcription factors stimulated by the MAPK effector molecules include those of the AP-1 and ETS family. Many of the MMP gene promoters contain DNA binding regions for these transcription factors and therefore activation of the MAPK pathway may lead to increased MMP gene transcription. We therefore examined whether this pathway is involved in DLKP cell invasion. In this section, the MEK inhibitor, U0126 was investigated for potential effects on the invasive capacity of DLKP-I and DLKP-M cell lines.

5.2.2 Effects of U0126 on cell growth of DLKP-I and DLKP cells

The cell viability of DLKP-I and DLKP-M cells following treatment with U0126 was determined by the acid phosphatase assay. Different concentrations of inhibitor ranging from 1 μM to 100 μM were utilised over a 3-day study period. Results indicated that the growth inhibitory effects of U0126 on the clones were less than approximately 20% at ≤ 20 μM (figure 5.2-1). A concentration of 10 μM U0126 was established for subsequent experiments.

5.2.3 Investigation of the effect of U0126 on matrigel invasion of DLKP-I and DLKP-M cells

Matrigel invasion assays were performed to evaluate the effects of the MEK inhibitor, U0126 on the invasive capacity of the DLKP clones. Cells were incubated with U0126 (5 μM and 10 μM) for 24 h in transwell inserts with 8 μm pores coated with matrigel. As shown in figure 5.2-2 and 5.2-3, the invasion of DLKP-M cells through the matrigel membrane was inhibited by approximately 50% after the addition of U0126, while the same treatment did not change the matrigel invasion of DLKP-I cells. These results indicate that the MAPK kinase pathway may be a prime candidate involved in DLKP-M invasion but not in DLKP-I invasion.

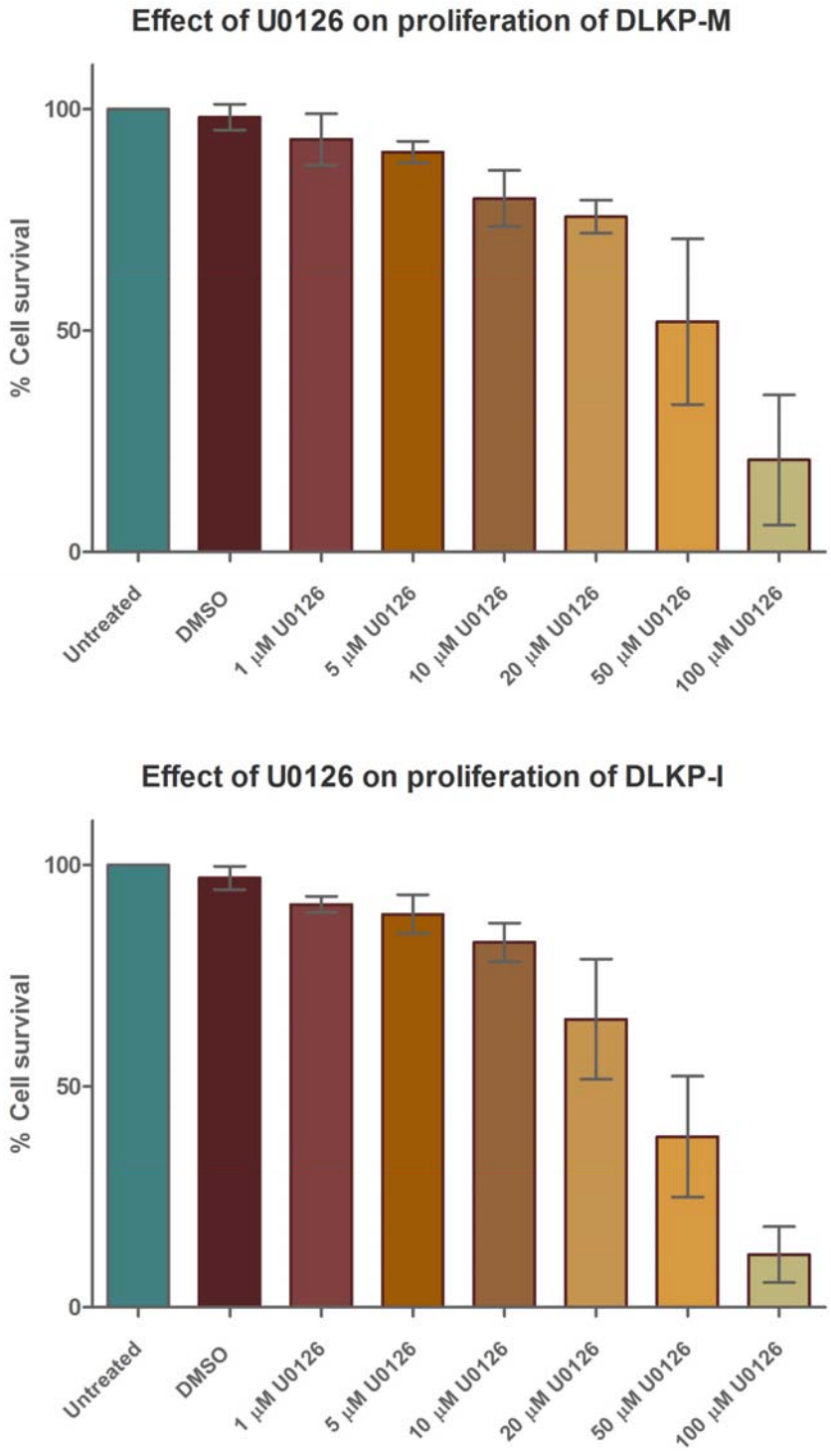

Figure 5.2-1: Effect of U0126 on DLKP-I and DLKP-M on cell growth and survival. DLKP-I and DLKP-M cells were seeded into 96 well plates and cultured in the absence or presence of U0126 for 3 days. Cell survival was determined using the alkaline phosphatase assay and presented as percentages relative to those of control cells cultured in the absence of the MEK inhibitor. DMSO was used as a control. The data shown are the means ± SD of at least 4 wells, and are representative of three independent experiments.

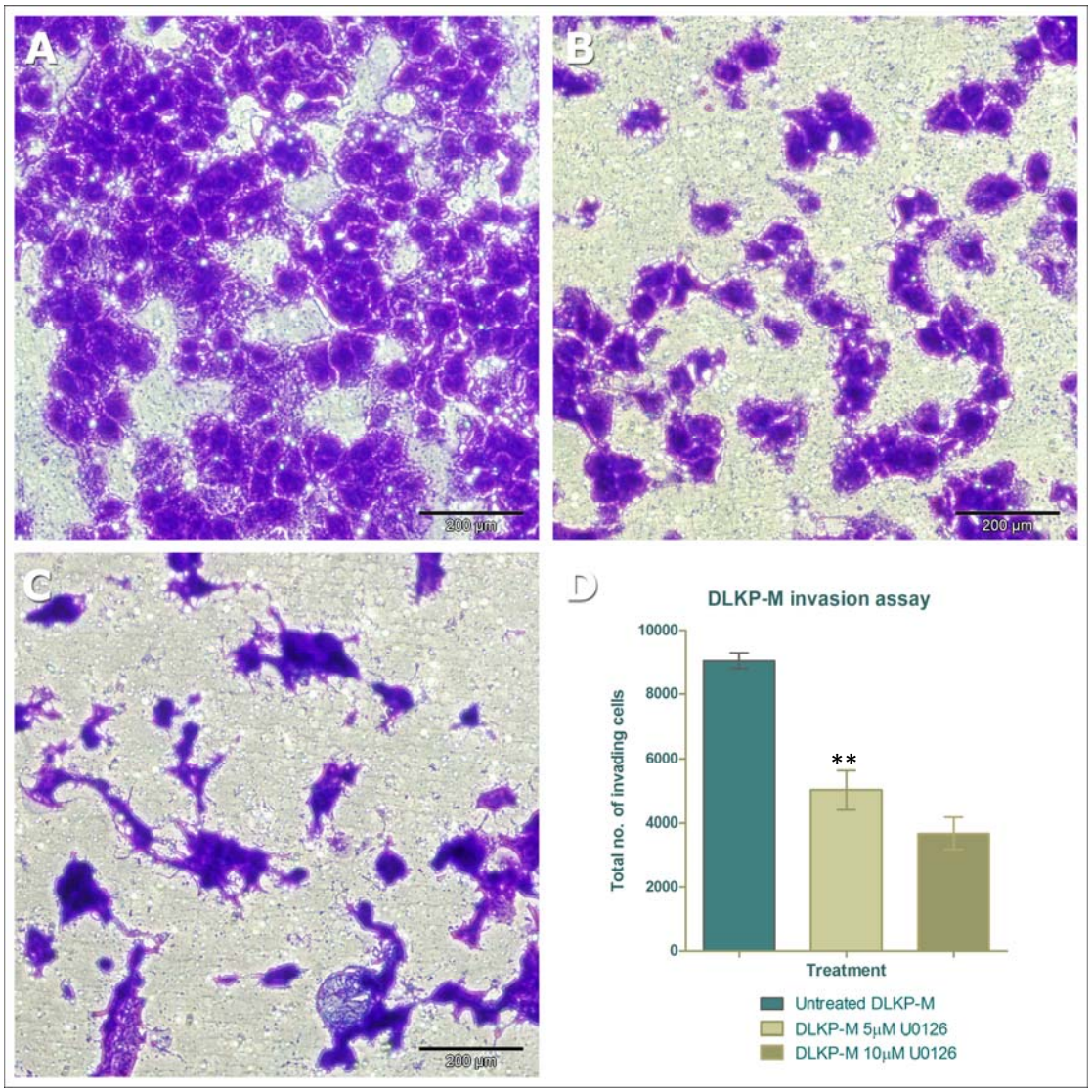

Figure 5.2-2: *The DLKP-M cell line*: invasion is reduced in U0126 treated cells compared with non-treated cells. After 24 hours incubation, the invading cells on the underside of the insert were stained with crystal violet and allowed to air dry. (A) Untreated; (B) with the addition of 5.0 µM U0126; (C) With the addition of 10 µM U0126. Magnification, ×200. Scale bar, 200µm. Results are presented as mean +/- standard deviation (SD) of three independent experiments except for the last treatment (10 µM) where only two mean values were generated. Statistics: $p \leq 0.01$**, (unpaired t-test to untreated control).

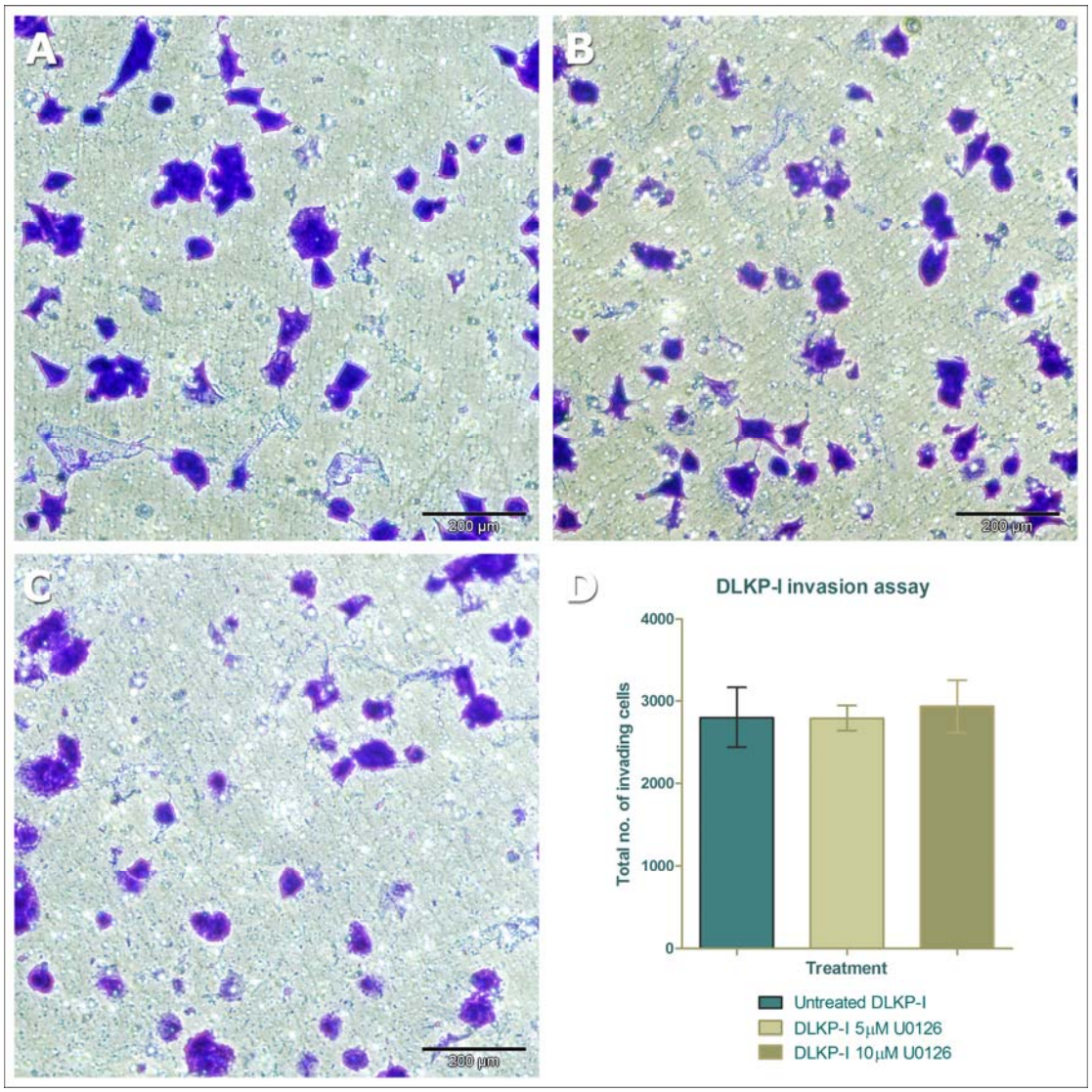

Figure 5.2-3: *The DLKP-I cell line:* invasion in U0126 treated cells compared with non-treated cells. After 24 hours incubation, the invading cells on the underside of the insert were stained with crystal violet and allowed to air dry. (A.) Untreated; (B.) with the addition of 5.0 µM U0126 and (C) with the addition of 10 µM U0126. Magnification, ×200. Scale bar, 200µm Results are presented as mean+/- standard deviation (SD) of three independent experiments except for the last treatment (10 µM) where only two mean values were generated.

5.2.4 U0126 treated DLKP-M cells demonstrate different phosphorylation response compared to U0126 treated DLKP-I cells

In the previous section, results show that the MAPK kinase pathway may be involved in DLKP-M invasion but not in DLKP-I invasion. Would other signalling pathways also be involved in DLKP-I and DLKP-M invasion? The investigation of other MAPKs and intracellular signaling of DLKP-1 and DLKP-M cells under U0126 treatment was investigated using a commercial array kit. A Human Phospho-MAPK array kit was used, which screens for the activation of 28 kinases including 9 MAPKs. The array kit allows the recognition of specific phosphorylation sites (amino acid residues) related to the activations of the MAPKs and the signaling proteins. The human phospho-MAPK array kit provides phosphorylation information of 29 intracellular biochemical signalling proteins. In addition, analyzing multiple pathways simultaneously tests for signalling pathway crosstalk. With this tool, the intracellular signalling patterns in DLKP-I and DLKP-M cells treated with U0126 were investigated. JNK, p38 and p53 were the three phosphorylated proteins with most significant changes in the untreated DLKP-I cells compared to the untreated DLKP-M cells.

The JNK stress pathways participate in many different intracellular signalling pathways that control a spectrum of cellular processes, including cell growth, differentiation, transformation, or apoptosis. JNK binds to and phosphorylates p53. In most cases, p38-MAPKs are simultaneously activated with JNKs.

The MAPK assay data (figure 5.2-4) shows that before U0126 treatment, DLKP-I cells had higher phosphorylated JNK, p38 and p53 than the DLKP-M cells.

After U0126 treatment, DLKP-M cells showed increased phosphorylation in p53 and slightly increased phosphorylation in p38 and JNK, which suggests induced signalling in the p38 and JNK pathways by U0126. Interestingly, U0126 treated DLKP-I cells do not present a significant increase in any of the intracellular signalling proteins.

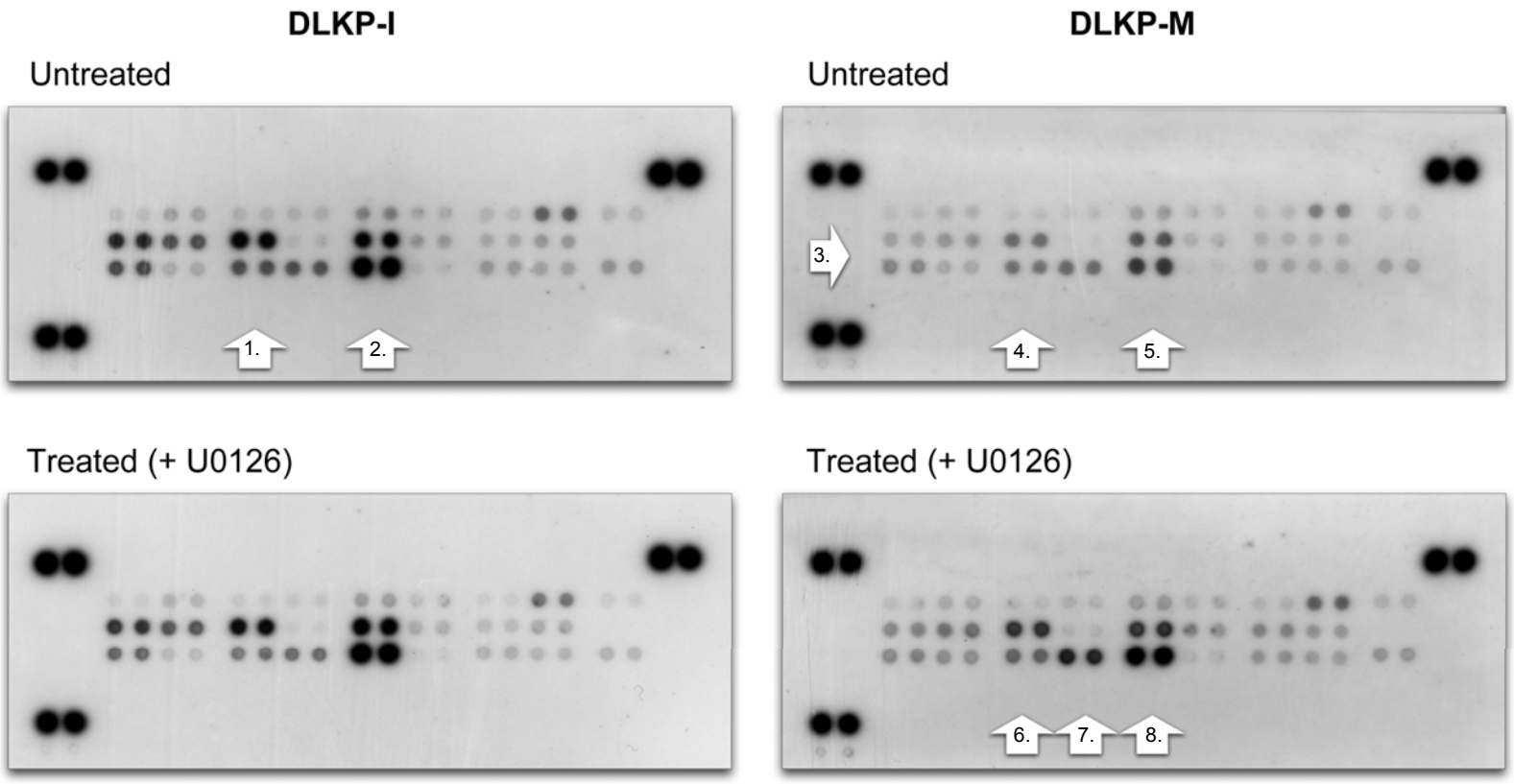

Figure 5.2-4: The Human Phospho-MAPK array shows the effect of inhibitors on specific pathways. All arrays were incubated with 250 µg of lysate. DLKP-I and DLKP-M cells were grown overnight on matrigel coated flasks. After 24 hrs, one flask of each was treated with 10 µM of the MEK inhibitor U0126 for 1 hour. A 1 ½ hour exposure to film is shown. This experiment was carried out once.

1. JNK2, p38δ **2.** JNK pan, p53 **3.** HSP27, p38α **4**. JNK2, p38δ 4. **5.** JNK pan, p53 **6.** JNK2, p38α **7.** p38γ **8.** JNK pan, p53

5.2.5 U0126 inhibits ERK activation in the DLKP-M cell line

To confirm that the pathway inhibitors were hitting their intended targets in DLKP-M and DLKP-I cells in the invasion assay, Western blot analysis was carried out under similar conditions as in the invasion assay to assess activation of pERK in the MAPK kinase pathway. (figure 5.2-5). U0126 inhibited ERK activation in the DLKP-M cell line. This data shows that the reduction of invasion of DLKP-M in the invasion assay is associated with inhibition of the intended targets (MAK kinase pathway).

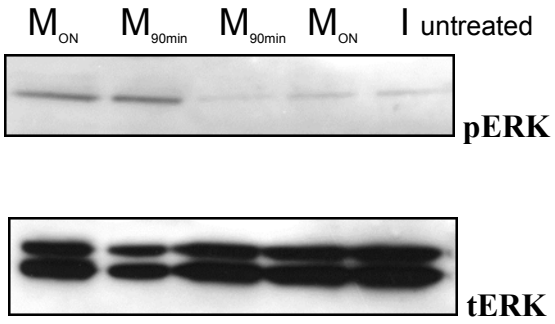

Figure 5.2.5: Western blot analysis of pERK levels in the DLKP-M cell line after treatment with the MEK inhibitor U0126 (grown on matrigel). U0126 treatment significantly represses the levels of pERK in the DLKP-M cell line. The DLKP-I cell line (untreated) contains less levels of phosphorylation of pERK compared to the DLKP-M cell line (untreated).

5.2.6 DLKP clones show differential activation of extracellular signal-regulated kinase

U0126 significantly inhibits invasion in the DLKP-M cell line but has no effect on DLKP invasion. To determine the level of ERK activation in DLKP cells, activation of ERK, as well as total levels of expression was assessed using phospho-specific or native antibodies, respectively. Western blot analysis reveals that the DLKP-M cells show higher levels of endogenous ERK activation compared to the DLKP-I and DLKP parent cells (figure 5.2-6) and this might help explain the significant inhibition of DLKP-M invasiveness with the inhibitor, U0126.

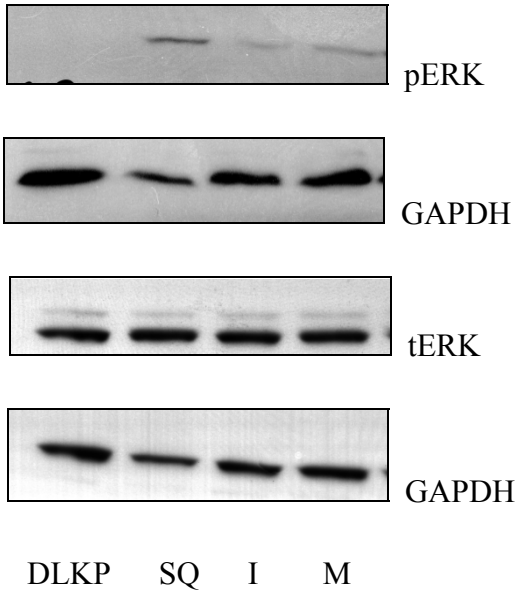

Figure 5.2-6: Expression levels of ERK1/2 and phospho-ERK protein in the DLKP parent and its clones. DLKP-SQ and DLKP-M cells showed high levels of endogenous ERK activation compared to DLKP-I and DLKP parent (In collaboration with Edel McAuley).

5.2.7 Treatment with a MAP kinase inhibitor inhibits the invasiveness of drug-resistant SQ-Mitox-BCRP

Earlier in this chapter the MEK inhibitor, U0126 was observed to inhibit invasion in the DLKP-M cells but not the DLKP-I cells. In addition, in chapter 3 (table 4.2-1)), microarray analysis revealed an upregulation of KRAS and IGF1R in the invasive SQ-Mitox-BCRP-6P cells. As KRAS and IGF1R and known to mediate their effects through the MAPK pathway, the effect of U0126 on the invasion of SQ-Mitox-BCRP-6P cells was investigated. SQ-Mitox-BCRP-6P (isolate 2) cells were incubated with U0126 (10 μM) for 24 h in transwell inserts with 8 μm pores coated with matrigel. As shown in figure 5.2-7, the invasion of SQ-Mitox-BCRP-6P cells through the matrigel membrane was inhibited by approximately 50% after the addition of U0126, indicating that the MAPK pathway may also be involved in the invasive phenotype of drug resistant SQ-Mitox-BCRP.

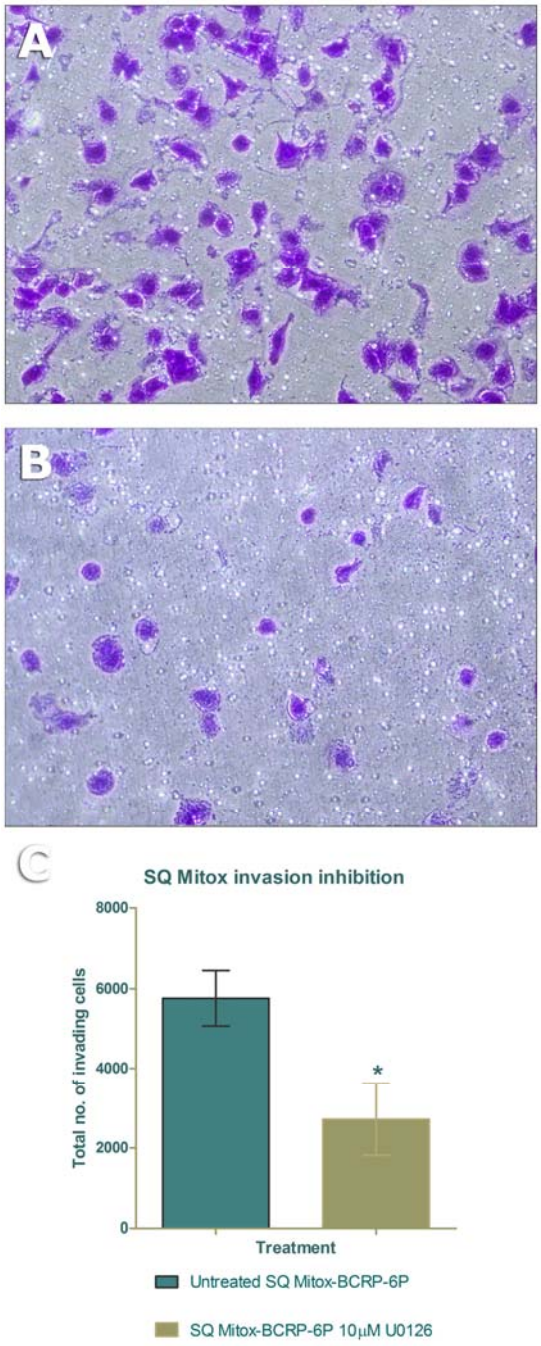

Figure 5.2-7: *The SQ-Mitox-BCRP-6P cell line:* invasion in U0126 treated cells compared with non-treated cells. After 24 hours incubation, the invading cells on the underside of the insert were stained with crystal violet and allowed to air dry. **A**. Untreated **B**. with the addition of 10 μM U0126. Results are presented as mean+/- standard deviation (SD) of three independent experiments. Statistics: * $p < 0.05$ (unpaired t-test to untreated control).

5.3 Summary of Effects of MEK inhibitors on invasive DLKP cell lines

The effects of signal transduction inhibitors upon invasion of the DLKP cell lines and its drug resistant variants were investigated. Table 5.2-1 summarises the effects of the MEK inhibitors on the invasion of the SQ-Mitox and DLKP clones. Interestingly, the SQ-derived mitoxantrone cells show a similar response to the DLKP-M clone.

Table 5.2-1: Summary of effects of MEK inhibitors on invasion of the DLKP cell lines

MEK Inhibitor	SQ-Mitox-BCRP- 6P	DLKP-I	DLKP-M
U0126	+	-	+

5.4 Sequenom analysis of DLKP clones

The DLKP clones show differential activation of extracellular signal-regulated kinase. Genetic alterations that activate the mitogen-activated protein kinase (MAP kinase) pathway occur commonly in cancer. Do the DLKP clones harbour mutations in the signaling pathways which would explain the differential activation of extracellular signal-regulated kinase between the clones? Mutation profiling has the potential to quickly identify which signalling pathway(s) have been co-opted to drive the proliferation of a specific human tumour type. In chapter 4, the DLKP clones were evaluated for the presence of mutations using sequenom technology (table 5.2-2). Of particular interest are the genes showing sequence alterations in the DLKP-SQ and/or DLKP-M clones only as these clones have higher levels of ERK activation compared to the DLKP-I clone. In addition, treatment of the DLKP-M clone and the DLKP-SQ derived mitoxantrone resistant cells with a MAP kinase inhibitor inhibited the invasiveness of these cells but had no effect on the DLKP-I cells. Further investigation of the role of EGFR, Met and PIK3R1 genes in the DLKP clones is warrented. The role that the MAPK kinase pathway may play in the invasive phenotype of the DLKP clones is a complex one and much remains to be elucidated.

Table 5.2-2: Sequenom Mutation Analysis of DLKP Clones

Mutation	DLKP Parent	DLKP-SQ	DLKP-I	DLKP-M	DLRP
EGFR_V769LM_G2305AT	G	AG	G	G	G
IDH1_V1781_G532A	G	G	G	G	AG
MET_N375S_A1124G	AG	AG	AG	G	A
NRAS_G12SRC_G34ACT	G	G	G	G	GT
PIK3R1_M3261_G978ATC	AG	AG	G	AG	G
TP53_G245VDA_G734TAC	AG	AG	AG	AG	AG

5.3 Summary

Drug resistance and invasion were investigated using MEK inhibition. The cell lines used were the DLKP clones (DLKP-SQ, DLKP-I and DLKP-M) and the mitoxantrone resistant variants of DLKP-SQ (SQ-Mitox-BCRP and SQ-Mitox-MDR).

Combination treatment with mitoxantrone and/or PD98059/U0126 significantly reversed drug resistance in the SQ-Mitox-BCRP cell line with no effect on BCRP protein expression levels. In contrast combination treatment with mitoxantrone and PD98059 increased drug resistance in the SQ-Mitox-MDR cell line with an increase in the levels of P-gp protein.

MEK inhibitor treatment of DLKP-M cells had a considerable effect on its invasiveness while having no effect on the DLKP-I cells. Western blot analysis revealed that the DLKP-M cells show higher levels of endogenous ERK activation compared to the DLKP-I and DLKP parent cells and this might help explain the significant inhibition of DLKP-M invasiveness with the inhibitor, U0126.

The poorly invasive DLKP-SQ clone had the highest level of phosphorylation of ERK of all the clones. Interestingly, MEK inhibition of the SQ-Mitox-BCRP-6P cells, which are DLKP-SQ derived also had a significant effect on its invasiveness.

The DLKP clones were evaluated for the presence of mutations using sequenom technology and sequence alterations were revealed in the EGFR, MET, and PIK3R1 genes. Generally the results indicate that there may be differential activation of EGFR, Met and PIK3R1 within the clones.

CHAPTER 6

Discussion

6.1 Drug resistance and cancer invasion

This thesis examined the temporal relationship between the emergence of drug resistance and invasiveness in a human carcinoma cell line model of mitoxantrone resistance in order to better understand the link between the development of multidrug resistance and cancer metastasis or invasion under the confines of the cell culture techniques employed here.

Almost all types of cancer are characterised by their ability to progress toward increased malignancy. Evolutionary processes are clearly very important because the most crucial problem during cancer chemotherapy is the development of resistance by the cancer cells with the subsequent ability to acquire in some cases, an aggressive invasiveness or ability to break through the normal tissue boundaries and spread to disparate sites throughout the body. For example, most small cell lung carcinomas (SCLCs) are drug sensitive at diagnosis, but any recurrence of the disease is usually characterised by an acquired drug resistance. In contrast, other neoplasms such as non small cell lung carcinomas (NSCLCs) are predominantly, intrinsically resistant to chemotherapy to start with. The various cancer phenotypes displayed by different tumours contribute to the slow pace of progress with respect to developing more effective and specific treatments.

One of the primary reasons for the difficulty encountered during chemotherapy is the lack of understanding at a fundamental level of how cells evolve in response to drug treatment and how malignant tissues develop drug resistance. There is indirect evidence that multidrug resistance and invasion/metastasis may be linked or at least, often occur together but it is unclear at this time whether they share any mechanisms. The possibility of a relationship between drug resistance and invasion/ metastasis phenotypes has been raised by at least two types of observations[325] : firstly, some drug resistant tumour cells are more invasive/metastatic relative to non-resistant parental cells; secondly, in some cases, secondary (more metastatic) tumours are more resistant to chemotherapeutic drugs than their primary counterparts. In support of these ideas, many studies have been performed. *Colone et al.,*[199] decribed a doxorubicin-selected, multidrug-resistant human melanoma line expressing high levels of *ABCB1* (P-gp) that showed a more invasive phenotype that the parental cell line and knockdown of *ABCB1* by siRNA substantially reduced the invasiveness of this cell line *in vitro*. Reduction of *ABCB1* levels by siRNA also reduced the migration of MCF-7 breast cancer cells in transwell migration and matrigel invasion assays[351]. However, in some cases, no correlation was seen between drug resistance and cancer invasion/metastasis[196,198].

DLKP-SQ, a clone of DLKP, was chosen for the establishment of a mitoxantrone resistant cell line at the start of this project. The parental cell line, DLKP has a heterogeneous population of cells and was derived from a secondary site of the original tumour. These cells are very sensitive to adriamycin, vincristine, VP-16 and cisplatin[282]. In addition, invasion assays have demonstrated a low level of invasiveness in the DLKP-SQ clone. In this way, isogenic drug resistant cell lines could be generated from the DLKP-SQ clone which would serve to eliminate variability due to intrinsic genetic differences between different cell lines.

The primary aim of this study was to establish if the resistant and invasive phenotypes emerged at the same or at different time points, and to this end the differences in invasion between the mitoxantrone resistant SQ cells and poorly invasive SQ parent were monitored during the development of drug resistance. Table 4.2-5 summarises the association between mitoxantrone drug resistance and invasion in selected cell lines. The SQ parent displayed low invasion and low drug resistance. Following successive drug pulsing with mitoxantrone (in both BCRP and P-gp overexpressing cell lines), cells were isolated from the fourth (4^{th}) pulse population, which displayed high drug resistance but low invasiveness, similar to the SQ parent. In contrast, the cells isolated from the sixth (6^{th}) pulse population displayed high invasiveness with similar drug resistance to the 4^{th} pulse. Results indicate that invasion was increased in the 6^{th} pulse cells relative to the 4^{th} pulse cells and the original SQ parent for both the SQ-Mitox-BCRP and SQ-Mitox-MDR cells. Large standard deviations were observed in these assays which may have been due to the instability of the invasive phenotype in these new drug resistant cells. Subsequently, a sub-population of stable invasive cells were isolated from the 6^{th} pulse BCRP over-expressing cells. Careful observations of these cells revealed morphological features characterised by large numbers of spiky, elongated cells – consistent with the view that this sub-population of cells were more invasive and more resistant than those observed to date. Further investigations of these cells confirmed they had a higher IC_{50} and higher levels of BCRP protein. This drug resistant, stable invasive cell line has provided an excellent base model for further studies. In addition, this work suggests that future studies to clone or isolate a stable invasive sub-population of the P-gp over-expressing cells could also yield further valuable insights into the cancer cell phenotype.

Section 6.2 discusses the characterisation of the resistant phenotype of the mitoxantrone resistant SQ cell lines using microarray analysis and proteomic analysis. Interestingly, induction of invasion was independent of the type of transporter expressed.

Tumour cells can evade death induced by exposure to drugs through various mechanisms. The most simplistic strategy is to move to an environment that contains a lower concentration of a cytotoxic drug. This is achieved through metastasis by tumour cells. In the mitoxantrone selection, the cells developed the membrane-bound drug efflux pumps, BCRP and P-gp to eliminate the drug or its metabolites out of the cell cytoplasm, subsequent drug pulsing initiates the next stage of cell survival, i.e. cell cytoskeletal remodelling and movement of cells away from local high concentrations of drug.

Two observations suggested that the emergence of invasion may be independent of the drug transporter induced. The first observation indicated that the 6th pulse SQ-Mitox BCRP over-expressing variant was significantly more invasive than the 4th pulse SQ-Mitox BCRP over-expressing variant (figure 3.1-1 and figure 3.1-3). The second observation showed that the 6th pulse SQ-Mitox P-gp overexpressing variant was also significantly more invasive than the 4th pulse SQ-Mitox P-gp overexpressing variant (figure 3.1-1 and figure 3.1-3). Do BCRP and P-gp indirectly promote invasion of SQ-Mitox cells? Are common transcription factor or signalling pathways responsible for increased cell invasion (such as switching on MMP genes)? Microarray analysis allowed further examination of the impact of mitoxantrone resistance on the invasive phenotype in both SQ-Mitox-BCRP and SQ-Mitox-MDR cell lines. This analysis identified genes involved in the invasion process for both BCRP and P-gp overexpressing cell lines (see section 4.2). These cell lines share a common genetic background, i.e. BCRP over-expression in the case of the SQ-Mitox-BCRP cell lines and P-gp over-expression in the case of the SQ-Mitox-MDR cell lines. Genetic variation is minimised and expression changes most likely represent invasion as opposed to BCRP or P-gp transporter specific changes. Accumulating evidence suggests that P-gp may promote invasion and metastasis of cancer cells *in vitro* [199,351,352].

The elevated level of BCRP in the SQ-Mitox-BCRP-6P (isolate 2) cells was associated with stable invasion (see section 4.2.4). Concurrently there was also an elevated expression of the cell adhesion molecule ALCAM (figure 4.2-8). The newly developed DLKP-SQ and SQ-Mitox cell lines were thus employed as a model to study the relationship between drug resistance and invasion/metastasis (discussed in section 6.3).

6.2 Development of MDR- and BCRP-mediated resistant lung cancer cell lines

Multidrug resistance (MDR) is still a major obstacle to cancer chemotherapy. The establishment of drug resistant cancer cell lines *in vitro* could provide an important model for studying the mechanism of MDR and the reversal of resistance. The establishment of drug resistant cancer cell lines *in vitro* can therefore enhance the screening of chemotherapeutic drugs, improve the sensitivity of cancer cells to drugs and provide a model for understanding the molecular basis of drug resistance and allow the establishment of reversing strategies to be employed in the fight against cancer. The overcoming of tumour multidrug resistance will allow significant progress to be made in chemotherapeutic efficacy. *In vitro* drug resistant cell lines have a history of more than 20 years as a primary tool for studying the mechanism of tumour multidrug resistance. Generally, high-dose drug intermittent induction or increasing drug concentrations are used on parental cells to establish these cell lines. Intermittent high-dose induction is similar to clinically periodic chemotherapy, and therefore can simulate the drug resistant phenomena in patients following representative treatments.

The DLKP-SQ Mitox resistant cell lines were successfully established by intermittent high-dose Mitox-induced method for four months (see section 3.1). The resistance index was 210- and 320-fold for the DLKP-SQ-Mitox-BCRP and DLKP-SQ-Mitox-MDR cell line respectively (table 3.1-1). In order to investigate changes in the gene expression pattern during mitoxantone selection, microarray analysis was performed in highly resistant DLKP-SQ-Mitox cells (see section 3.1.10). Interestingly, BCRP was the primary over-expressed gene in the DLKP-Mitox-BCRP cell line and P-gp was the primary over-expressed gene in the DLKP-Mitox-MDR cell line (figure 3.1-4). Induction and overexpression of *ABCB1* (*MDR1*) and *ABCG2* (BCRP) were demonstrated by microarray analysis (table 3.1-2) and qPCR and Western blot (figure 3.1-4) in SQ-Mitox-MDR and SQ-Mitox-BCRP respectively. The level of mRNA detected in the drug resistant cell lines positively correlated with the level of protein detected. Low levels of BCRP were detected in the drug sensitive parental cell line while P-gp protein was not detectable. Despite the similar selection strategy, the mechanism of mitoxantrone resistance differs significantly between these two cell lines. *Nieth et al.,*[353], reported that mitoxantrone treatment influences the expression of several ABC-transporters but in the end, merely a single extrusion pump will be dominant. *Yang et al.,*[354] showed that P-glycoprotein-mediated multi-drug resistance and CDDP-resistance phenotypes can coexist in colon cancer cells with primary

resistance to CDDP. *Tegze et al.,* developed multiple drug resistant cell lines in parallel from MCF-7 and MDA-MB-231 breast cancer cells and concluded that heterogeneity caused evolution of multiple resistant clones with different resistance characteristics.[355]. It is also interesting to note that the expression of P-gp did not correlate with resistance in the cell line models, despite the development of models with two P-gp substrates (doxorubicin and paclitaxel)[355].

6.2.1 Cross-resistance in the DLKP-SQ cell line and its mitoxantrone resistant variants

To determine if the SQ-Mitox-BCRP and SQ-Mitox- MDR cell lines displayed cross-resistance, a panel of drugs that differed in their structure and function were tested. As observed (table 3.1-1), the SQ-Mitox-MDR cells demonstrate a "typical" MDR phenotype which has been correlated with P-glycoprotein-mediated drug resistance and its associated cross-resistance to taxol, epirubicin, vinblastine, irinotecan and VP16. SQ-Mitox-MDR cells showed neither significant cross resistance nor sensitivity to cisplatin or 5-fluorouracil, when compared with the parental cell line.

In contrast, the SQ-Mitox-BCRP cell line exhibited resistance to mitoxantrone and irinotecan but not to taxol, epirubicin, vinblastine, VP16 or 5-FU. The efflux protein BCRP has a more selective transport profile than P-gp. BCRP does not transport taxol, vincristine or verapamil. However, irinotecan and its active metabolite SN-38 are substrates of BCRP.

BCRP can have functional variants, for example, a mutation in its primary sequence leads to an amino acid substitution[298]. The wild-type BCRP has an arginine (R) at position 482. Two known variants exist; variant R482T which has threonine (T) at position 482 and variant R482G where position 482 is occupied by the amino acid glycine (G). These variations can lead to functional changes in BCRP. Wild type BCRP does not transport the anthracycline, epirubicin, where as the R482G variant does transport anthracyclines[356]. In this study, the SQ-Mitox-BCRP cell line was not resistant to epirubicin, implying that this cell line contains wild-type BCRP.

6.2.2 MDR and BCRP confer drug resistance to Mitoxantrone-selected DLKP-SQ

siRNA techniques were utilised to confirm that the BCRP and P-gp proteins were contributing to the resistant phenotype observed in the SQ-Mitox-BCRP and SQ-Mitox-MDR cells respectively. The siRNA investigations were coupled with toxicity assays, with the protein of interests' effects on drug sensitivity ultimately being analysed (see section 3.1.9). To evaluate if BCRP and

MDR1 were conferring resistance to mitoxantrone in the BCRP and P-gp overexpressing cell line respectively, cytotoxicity assays were performed in the presence and absence of elacridar, a specific inhibitor of BCRP and MDR1. With the addition of 443nM Elacridar, the BCRP-mediated and MDR1- mediated resistance to mitoxantrone were reversed (figure 3.1-6). Elacridar is a very potent MDR modulator that exerts its MDR reversal effect in nanomolar concentrations. In order to down regulate the genes over-expressed in the resistance cells, highly efficacious and target specific siRNA sequences were selected. An siRNA for kinesin was included in this study as a positive control which resulted in 100% knockdown. Western blot analysis confirmed the knockdown of BCRP protein in the SQ-Mitox-BCRP cells and P-gp protein in the SQ-Mitox-MDR cells (figure 3.2.7). Due to the very high level of overexpression of BCRP and P-gp respectively in the two resistant variants, only partial knockdown could be achieved using siRNAs. There was a corresponding effect on resistance, which supported a role for these pumps in resistance but because complete knockdown was not possible, the results do not allow us to determine whether or not these are the only, or even the main, determinants of resistance, although the Elacridar data would suggest that this is the case. Elacridar, however, is less specific in its effect than an siRNA would be.

6.2.3 *ABCB1* and *ABCG2* expression in SQ-Mitox-MDR and SQ-Mitox-BCRP

There are generally two possibilities for the origin of drug resistance in cells: (1) it is an inherent property of the cells, or (2) it may be acquired following exposure to drugs and other xenobiotics. The chemotherapeutic drugs may therefore act as gene inducers through activation of xenobiotic sensors, or mutagens causing genetic changes which result in MDR cells, or as selective agents, eliminating the sensitive cells from the population. DLKP was established from a primary human squamous lung carcinoma and exhibited high levels of cytogenetic variability[282]. Consequently, the potential existed for drug resistant cells to have been selected from a pre-existing resistant population or to have been acquired following exposure to mitoxantrone.

Western blot analysis showed that BCRP and P-gp overexpression occurred early on in the drug pulsing process (figure 3.1-4). This posed the question as to whether the drug resistant cells were pre-existing in the DLKP-SQ population or arose by gene induction or mutation arising from the drug treatment. During the initial selection process by which eventually the mitoxantrone cell lines were derived, the DLKP-SQ clones were grown at high density to approximately 70% confluency, prior to the initial drug exposure (see section 3.1). The initial four hour

mitoxantrone treatment reduced the cell population to approximately 5% and consisting of single, dispersed cells. These cells then grew into colonies and were maintained until they appeared healthy. The cells were then trypsinised and this whole cyclic treatment was repeated five more times, generating the replicate SQ-Mitox cell lines (figure 3.1-1). Selection with the mitoxantrone drug could therefore have resulted in the isolation of a cell population that already exists in the culture. This has been demonstrated for other drug resistant models. For example, *Barr et al.*, identified cisplatin resistant subpopulations of NSCLC cells with a putative stem-like signature[357].

6.2.3.1 Gene amplification

Gene amplification has long been recognised as a major contributor to the increased expression of *ABCB1* and *ABCG2*[358,359]. Initially it seemed possible that the increased expression of BCRP and P-gp in the SQ-Mitox cells might also be due to gene amplification.

ABCG2 gene amplification was first shown in a study of a few mitoxantrone-selected derivative cell lines of MCF-7[359] and in Adriamycin-selected MCF- 7/AdVp3000 cells[309]. The mitoxantrone-sensitive parental cell line MCF-7, had no amplification or chromosome translocation of the *ABCG2* gene. It has also been shown that the resistance level to SN-38 in colorectal cancer cells positively correlates with *ABCG2* gene amplification[360], suggesting that gene amplification of *ABCG2* is not restricted to MCF-7 breast cancer cells. *Rao et al.*[310] examined the mechanisms of *ABCG2* gene amplification during the stepwise drug selection of the glioblastoma cell line SF395. It was found that double minute chromosomes were responsible for *ABCG2* gene amplification in the drug resistant SF395 derivative cell lines selected with low concentrations of mitoxantrone (50 and 100nM). However, in the derivative cell lines selected with high concentration of mitoxantrone (250 and 500nM), *ABCG2* gene amplification appears to be due to chromosomal reintegration of the amplicon at multiple chromosomes to generate a more stable genotype.

The amplification of the *MDR/ABCB1* chromosomal region has been reported from *in vitro* acquired drug-resistant cell lines from various cancers, including breast[361,362], liver[363], neuroblast[364], esophagus [365] and ovary [366,367]. In the present study, the gene copy number of *ABCG2* and *ABCB1* was investigated using qPCR (see section 3.1.12.2). . The C_T values were at the upper limits of detection and as a result there were errors. The minimum and maximum

copy numbers are shown in table 3.1-7. Future studies should include increasing the concentration of the template (gDNA) and using ten replicates instead of four.

While the DLKP-A cell line[277] exhibited a *ABCB1* gene copy number of 6, the SQ-Mitox-MDR cells exhibited no change in copy number (table 3.1-7). DLKP-A is a cell line composed of a mixture of cells, with respect to their level of resistance to chemotherapeutic drugs and mode of resistance to these drugs[277]. Increased expression of P-gp in some of the clones of DLKP-A may be due to gene amplification. Surprisingly the DLKP-SQ and the SQ-Mitox-BCRP cells exhibited an *MDR1* gene copy number of 3. In summary, the elevated expression of these genes cannot be solely explained by gene copy number.

6.2.3.2 Methylation

The lack of *ABCB1* and *ABCG2* gene amplification in the SQ-Mitox cell lines suggested that the dramatic upregulation of *ABCB1* and *ABCG2* in these drug-resistant cell lines may be due to the loss of transcriptional silencing of these genes. Epigenetic alterations are potential driving forces for acquired chemoresistance[368]. A typical epigenetic modification, which is frequently observed in tumour cells, is aberrant methylation of cytosine bases (C) located 5′ of a guanine base (G), so called CpG dinucleotides [369]. Although CpG dinucleotides are generally underrepresented in mammalian genomes, they frequently cluster around the transcription start site (TSS) of genes, in genomic areas referred to as CpG islands (CGIs)[370].

5-aza-2'-deoxycytidine treatment of DLKP-SQ cells

To further understand the mechanisms leading to this overexpression, two different approaches were employed. Firstly, a direct experiment examining the effects of inhibiting methylation on gene expression using 5-aza-2′-deoxycytidine (5-aza-dC) was performed (see section 3.1.12.3). This agent has been shown to increase gene expression by inhibiting DNA–methyltransferase I, thereby decreasing epigenetic methylation of DNA. DLKP-SQ and SQ-Mitox cells were treated with 1μM 5-aza-dC, and its effects on both BCRP and P-gp protein expression were investigated. Treatment with 5-aza-dC did not result in any change in *ABCG2* or *ABCB1* in the DLKP-SQ or SQ-Mitox cell lines, as assessed by Western blot analysis as shown in figure 3.1-11.

Methylation analysis

The second approach to understanding gene over-expression was the use of methylation analysis. This was performed for the *BCRP* promoter as it has only one CpG island and therefore it is relatively easy to design primers and probes for a successful investigation. In contrast, the *MDR1* promoter has several CpG islands, which make such an analysis more difficult. The methylation status of the *BCRP* promoter in the DLKP-SQ cell line and its *ABCG2* over-expressing MDR counterpart was investigated using MethylLight technology[269]. MethyLight is a sodium bisulfite ($NaHSO_3$) dependent, quantitative, fluorescence-based, real-time PCR method to sensitively detect and quantify DNA methylation in genomic DNA. The results indicated that the *BCRP* promoter was unmethylated in both the DLKP-SQ and SQ-Mitox-BCRP cells (see section 3.1.12.3). As expected, the results also illustrated that the primer pair for detection of a methylated *BCRP* gene did not produce a signal (thereby also confirming no DNA methylation).

Future work examining the methylation state of the *MDR1* promoter is also warranted as it is probably the most prominent gene involved in drug resistance being transcriptionally regulated via CpG island (CGI) promotor methylation. Epigenetic alterations such as promoter demethylation, leading to upregulation of *ABCB1* was described in adriamycin-selected CCRF-CEM cells (CEM-A7R)[371] and vincristine-selected KB3-1 cells[372]. *Baker et al.,*[373] demonstrated the direct epigenetic up-regulation of the *MDR1* gene within a single cell cycle, in antiapoptotic, bcl2-transfected CCRF-CEM-bcl2 cells, occurring in response to chemotherapeutic drug exposure. *To et al.,*[374] have shown an active CpG island within the proximal *ABCG2* promoter region, thereby facilitating its transcriptional silencing in aberrantly methylated renal cell carcinoma lines. While *Turner et al.,*[75] demonstrated that *ABCG2* expression in multiple myeloma patients is regulated in part by promoter methylation, one report documented the impact of single-step anticancer drug selection and concomitant *ABCG2* expression in doxorubicin-selected cancer cells[311]. Histone acetylation and deacylation has also been shown to possibly regulate *ABCG2* promoter activity. Following drug selection in several cancer cell lines and the subsequent overexpression of *ABCG2*, *To et al.,*[374] observed an increase in acetylated histone H3 but a decrease in class I HDACs associated with the *ABCG2* promoter.

6.2.4 Other mechanisms of gene regulation

Regulation of the expression of the major human drug transporter gene *ABCB1* is highly complex[375]. As well as gene amplification and chromosomal tranlocation[376], mRNA

stabilization[377] can also contribute to the elevelated ABCB1 protein levels in highly drug-resistant cell lines. Alternative promoter usage[378,379] and promoter mutation[380,381] also influence the transcription of the *ABCB1* gene. Like many TATA-less promoters, the promoter of the *MDR1* gene contains multiple start sites. The MDR promoter elements include the GC-box, inverted CCAAT element (Y-box), p53 element, AP-1 element, CAAT element, C/EBP element, heat shock element (HSE), TCF elements and steroid xenobiotic (SXR elements)[381]. The inverted CCAAT box can potentially interact with the regulatory protein YB-1 or the transcription factor NF-Y. Previous studies implicated YB-1 as a fundamental regulatory factor for the *MDR1* gene in human cancers[382].

A large number of studies have suggested that ABCB1 is phosphorylated, however, it is still unclear what role phosphorylation plays in regulating ABCB1 function [383,384,385]. In 1987, *Mellado and Horwitz* published the first evidence suggesting that ABCB1 was phosphorylated[386]. Their work showed that phosphorylation of ABCB1 increased when cells were treated with cAMP. Treatment of partially purified ABCB1 with recombinant PKA (i.e., the catalytic subunit) results in increased phosphorylation of ABCB1 *in vitro*[386]. It is now apparent that ABCB1 is likely phosphorylated by a number of kinases, including PKC and PKA.

Other mechanisms of drug-induced up-regulation of gene expression have been proposed for the BCRP transporter (figure 6.2-1). The BCRP (*ABCG2*) promoter also lacks a TATA-box and contains a CAAT-box, lots of AP1, AP2 sites and several putative Sp1 sites, which are downstream of a putative CpG island. Thus potential transcriptional control points have been identified [79]. The upstream region contains functional oestrogen[77] and hypoxia[78] response elements, consistent with its expression in mammary glands and a role in haemopoietic stem cell protection. Furthermore, *ABCG2* expression has been shown to be suppressed by DNA methylation[75], up-regulated by the aryl hydrocarbon receptor[74] and up-regulated by Oct4[76] (with respect to hepatobiliary cancer). Several other transcription factors, such as nuclear factor-κB (NF-κB), hypoxia-inducible factors (HIFs), nuclear factor erythroid 2-related factor 2 (Nrf2), peroxisome proliferator-activated receptors (PPARs) and Krüppel-like factor 5 (KLF5), have also been recently shown to bind to their response elements in the promoter/enhancer to activate the transcription of BCRP[70]. BCRP transcription can be influenced by proinflammatory cytokines, growth factors, and the homeobox protein MSX2. Signaling pathways, such as Sonic hedgehog (Shh), Notch and RAR/RXR pathways, may also be involved in the transcriptional regulation of BCRP. In addition, promoter methylation and histone acetylation are essential for BCRP

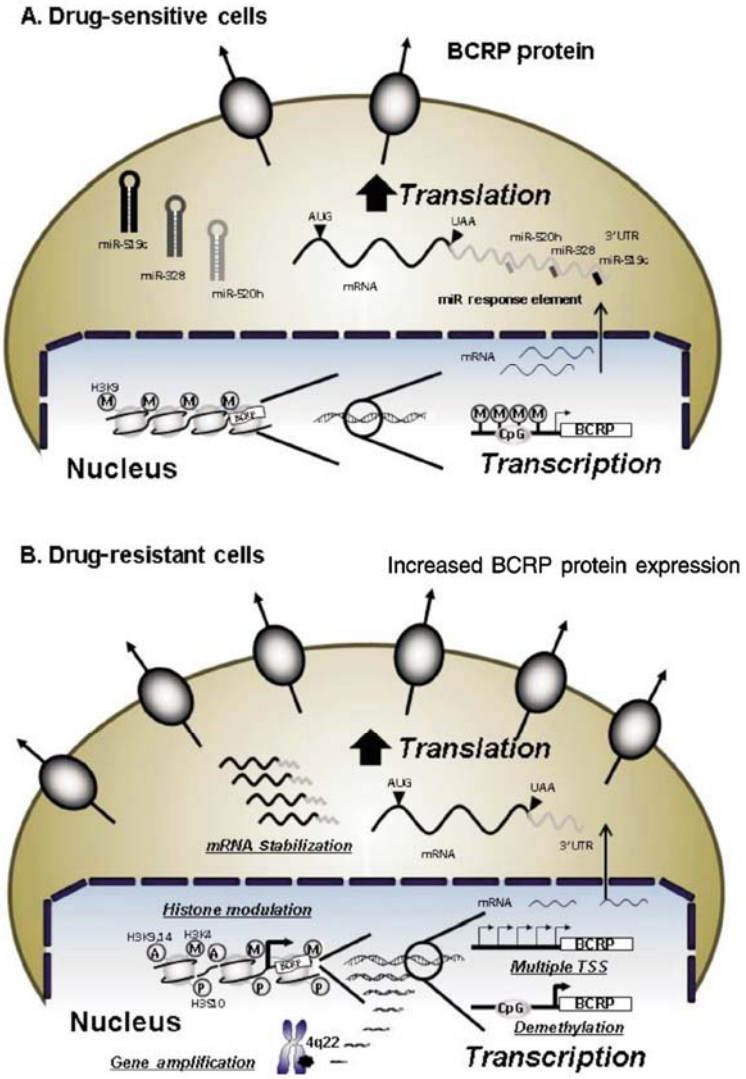

Figure 6.2-1: Putative mechanisms for BCRP overexpression in drug-resistant cells. **A.** In drug-sensitive cells, BCRP transcription is regulated by histone 3 trimethylated at lysine 9 (H3K9me3) and the proximal promoter region is reported to be methylated in cells prior to drug selection or treatment. Synthesized mRNA is negatively regulated by possible candidate miRs, including miR-519c, miR-32 8, and miR-520h, which are purported to bind miR response elements in 3'UTR of BCRP mRNA. Thus, BCRP expression is transcriptionally and post transcriptionally regulated. **B.** BCRP gene amplification is observed in some drug selected cancer cells. Transcription factors become more accessible because of histone 3 modifications, including acetylation at lysine 9 and 14 (H3K9ac, H3K14ac), methylation at lysine 4 (H3K4me), and phosphorylation at serine 10 (H3S10p). Multiple TSSs are likely used for induction of BCRP. Demethylation of CpG islands around promoter regions may contribute to overexpression of BCRP in response to drugs. Once BCRP mRNA is synthesised, its 3'UTR becomes truncated, resulting in deletion of miR response elements, which in turn increases BCRP mRNA stability and levels. M: methylation; A: acetylation; P: phosphorylation. Taken from *Nakanishi et al.* (2012).

transcription, especially for drug-induced BCRP expression. *Wu et al.,* reviews the recent research progresses in this field with an emphasis on the roles of transcription factors and epigenetics in the transcriptional regulation of BCRP[387].

In addition, phosphorylation has been implicated in the regulation of BCRP, with phosphorylation of Thr-362 by Pim-1 kinase affecting the oligomerisation and plasma membrane localisation of BCRP, with unknown effects on the substrate specificity of the transporter [388].

BCRP is also under post-transcriptional regulation by microRNAs. The miRNAs miR-519c and miR-328 decrease the level of *ABCG2* mRNA and thus protein by binding to a putative binding site located within the 3′ untranslated region. However, these binding sites are proposed to be absent from some drug selected, BRCP over-expressing cell lines[389-391]. Similarly, miR-520h has also been reported to target BCRP in hematopoietic stem cells during their differentiation into progenitor cells[392].

The ABC transporters may also undergo post-transcriptional modifications such as glycosylation. A study by *Liang et al.,* showed that glycosylation defects on ABCC1 (also known as MRP1), leads to the mislocalization of multidrug transporters in cisplatin-resistant cancer cell lines[393]. It was also observed that increased levels of glycosylation-defective ABCC1 and ABCC4 are associated with resistance to platinum compounds in ovarian carcinoma cell lines[394]. Glycosylation of P-gp occurs on the first extracellular loop, which contains three putative glycosylation sites[54]. Even though glycosylation of P-gp was not found to be necessary for the drug transport activity of P-gp, glycosylation of P-gp was shown to be important for proper quality control of P-gp in the endoplasmic reticulum[54] and proper transport of P-gp to the plasma membrane[52]. Similarly, glycosylation might also regulate BCRP transporter levels, as altered glycosylation of BCRP results in increased degradation[395]. N-linked glycans are thought to be crucial regulators of the stability of BCRP in the endoplasmic reticulum[395,396]. Studies have shown that N-glycosylated wild-type BCRP is degraded in lysosomes, whereas misfolded mutant proteins have been shown to undergo ubiquitin-mediated degradation in the proteasome[396,397].

In addition *Diop et al*., have shown that within BCRP, there is a single residue (N596) which is glycosylated and this modification is associated with correct assembly and effective trafficking of stable protein to the plasma membrane but is not required for protein function[398].

6.2.5 Microarray analysis of SQ-Mitox sub variants

The mitroxantrone selection activated, exclusively and in parallel, a P-gp and a BCRP-related resistance mechanism. There may also be alternate pathways, activated randomly by drug exposure. The aim of the microarray analysis was to identify the differences at the genetic level between the mechanisms of resistance amongst the two cell lines (see section 3.1.10).

Different genes functionally involved in cellular assembly and organisation (including cell adhesion and cytoskeleton organisation) were induced or suppressed following exposure to mitoxantrone (table 3.1-2). Cell adhesion has been demonstrated to modulate drug response and prevent cell death, implicating the interaction of cell-cell or cell-extracellular matrix as a potentially important determinant in the emergence of drug resistance[399]. Indeed, a number of cell adhesion-related and microtubule related genes, including CD36, KIF1A, MDK and MYH10 were commonly down-regulated in both BCRP and P-gp over-expressing cell lines. CD36, which is a cell surface molecule, is causally involved in suppressing the stromal remodelling that accompanies tumourigenesis[400]. MYH10 encodes a member of the myosin superfamily with diverse functions including regulation of cytokinesis, cell motility, and cell polarity[401].

KIF1A (Kinesin family member 1A) encodes a protein that is a microtubule-dependent molecular motor involved in important intracellular functions such as organelle transport and cell division[402]. Midkine (MDK) is a heparin-binding molecule involved in the regulation of growth and differentiation during embryogenesis, which is overexpressed in most of human malignant tumours and may act as an oncoprotein [403].

The online tool, DAVID was used for the functional annotation analysis using the BP_FAT category of Gene Ontology (GO). Functional annotation analysis of probesets differentially expressed using gene ontology (GO) categories were performed for 'biological process'. This allows for the discovery of over-represented categories of genes. Firstly, gene expression patterns between the DLKP-SQ cells and DLKP-SQ-Mitox-BCRP and DLKP-Mitox-MDR cells were compared in a search for common markers and/or molecular mechanisms involved in drug action. A subset of 823 probesets were found to be similarly deregulated in SQ-Mitox-BCRP and SQ-Mitox-MDR with respect to the parental DLKP-SQ cell line (figure 3.1-8). Gene ontology analysis revealed that the most significant GO categories were related to the broad functional categories of mRNA metabolic processing and RNA splicing.

In surveying the changes in gene expression which were exclusively differentially expressed between DLKP-SQ and DLKP-SQ-Mitox-BCRP, it is clear that the BCRP over-expressing cell

line exhibits an altered expression of genes whose products are involved in RNA processing, intracellular transport, cellular responses to stress and cell cycle regulation (table 3.1-4). ABCG2 may be protecting against the cytotoxic effects of mitoxantrone in this selection, as it does in stem cells [404]. *Pisco et al.,*[405] suggested that dynamic non-genetic heterogeneity of clonal cell populations continuously produces metastable phenotypic variants (persisters), some of which represent stem-like states that confer resistance and that even without genetic mutations, Darwinian selection can expand these resistant variants. This could explain the invariably rapid emergence of stem-like resistant cells. A recent study by *Ming Zhuet al., (2012)* [406] showed that the JNK1/c-jun signaling pathway was also involved in ABCG2-mediated multidrug resistance in colon cancer cells. *Meyer et al., (2006)*[407] reported that EGF increases the expression of ABCG2 by activation of the mitogen-activated protein kinase cascade via phosphorylation of extracellular regulated kinase (ERK)1/2 and c-jun iNH-terminal kinase/stress-activated protein kinase (JNK/SAPK) in cytotrophoblasts. *Imai et al., (2009)*[347] reported that MEK inhibitor could induce transcriptional upregulation of endogenous BCRP through the inhibition of the MEK-ERK-RSK pathway. They also suggested BCRP was post-transcriptionally downregulated through the inhibition of the MEK-ERK-non-RSK pathway in breast cancer MCF-7 cells. The cell cycle genes cyclin A2 and cyclin-dependent kinase inhibitor 1A have been shown to be 2 fold down-regulated while genes involved in DNA repair were upregulated (RAD50 homolog, RAD51 homolog and RecQ protein-like) suggesting that the SQ-Mitox-BCRP cell line can repair DNA more effectively than the parental line, consistent with recent studies that suggest that DNA repair contributes to general drug resistance[408, 409]. Some limited evidence has previously been reported on the cell cycle dependence of ABC transporter expression[410,411]. However, it has never been demonstrated that the functional activity of these transporters correlate with a particular phase of the cell cycle.

Gene ontology analysis revealed that the 649 probesets identified as exclusively, differentially expressed in the P-gp overexpressing cell line belonged to the functional categories of chromatin modification and organisation, embryonic morphogenesis and negative regulation of gene expression (table 3.1-4). As mitoxantrone is a DNA interchelator and topoismerase poison, it is likely that selection for mitoxantrone resistance may result in changes in gene expression within the resistant cell lines that alter the drug's ability to bind to DNA either through slight base sequence changes, DNA scaffolding changes or increased metabolic activity within the resistant cells. Several proteins affecting gene expression were identified in the microarray results (results not shown). These included the SWI/SNF family and chromodomain helicase DNA-binding

proteins (CHDs). In recent years, research has indicated that chromatin accessibility or epigenetic modifications, play a large role in controlling the endogenous *MDR1* expression state[412].

Several candidate proteins are involved in the complex regulation of chromatin accessibility which can have a profound effect on gene transcription. The proteins encoded by SMARCA5, SMARCC1 and SMARCE1 are members of the SWI/SNF family of proteins. Members of this family are chromatin remodeling proteins, which move, destabilise, eject or restructure nucleosomes, thereby changing chromatin structure and adding an extra layer of regulation[413]. Lymphoid-specific helicase is an enzyme that in humans is encoded by the *HELLS* gene and is required for *de novo* or maintenance DNA methylation. The chromodomain helicase DNA-binding proteins (CHDs) are known to affect transcription through their ability to remodel chromatin and modulate histone deacetylation. Chromodomain helicase DNA binding protein 5 plays a tumour suppressor role in human breast cancer[414]. Coactivator-associated arginine methyltransferase 1 (CARM1) is a protein arginine methyltransferase that methylates histones and transcriptional regulators. Interestingly, *Hajihassan et al.,* [415] have shown that mitoxantrone binds to chromatin with higher affinity compared to DNA, implying that the histone proteins may also play an important role in the chromatin-mitoxantrone interaction/accessibility process.

6.2.6 Proteomic analysis of DLKP-SQ and drug resistant variant SQ-Mitox-BCRP-4P by two-dimensional difference in-gel electrophoresis

Analysis using Decyder in Biological Variation analysis revealed a total of 293 proteins to be differentially regulated with $p<0.05$ and fold differences ranging from 2.55-fold up-regulation to -1.9-fold down-regulation (DLKP-SQ versus SQ-Mitox-4th pulse) (see section 3.1.11). Of the 130 proteins identified by MALDI-ToF mass spectrometry, 19 were found to be up-regulated and 9 were down-regulated. EF1a-like protein and beta-tubulin were over 2-fold higher in the mitoxantrone-resistant variant (table: 3.1-5, Up- and Down-Regulated expression) while NBLa10058 protein, ARPC2 and Galectin-1 were more than 1.5-fold down-regulated. Ontology analysis through PubMed searches, identified many cellular processes associated with these proteins with glycolysis, protein turnover and translational elongation constituting the greatest number of protein expression changes (table 3.1-5).

On the whole, the number of differentially expressed proteins may be underestimated because the 2D-PAGE approach poorly recovers some proteins[416]. The BCRP transporter protein was not

detected among the differentially expressed proteins, even though the SQ-Mitox-BCRP cell lines have been demonstrated to overexpress BCRP (chapter 3). However BCRP is a membrane protein and 2D-PAGE is known to underrepresent these proteins.

The primary up-regulated protein was EF1a-like protein. Western blotting confirmed the increase in protein levels of EEF1A1 as a surrogate for EF1a-like protein in SQ-Mitox-BCRP cells and DLKP-SQ-parent cells (figure 3.1-9). No antibodies were available for EF1a-like protein at the time of the investigation. Eukaryotic translation elongation factor 1A (eEF1A) is one of the most abundant proteins in cells[417]. In advanced vertebrates, a gene family encodes for two distinct isoforms, eEF1A1 and eEF1A2[302]. The coding region of the *eEF1A* gene is highly conserved throughout eukaryotes. In humans, the almost identical (92% sequence identity) amino-acid sequences of the eEF1A isoforms differ in length only by one additional C-terminal amino-acid residue present in the second isoform. eEF1A belongs to the family of GTP-binding proteins and promotes the GTP-dependent binding of aminoacyl-tRNA to the A-site of the ribosome during the elongation cycle in protein biosynthesis. eEF1A1 has been shown to be involved in additional non-canonical functions, including actin-binding and bundling, apoptosis, nuclear transport, proteasomal-mediated degradation of damaged proteins, heat shock and transformation[418]. It is known that different signalling pathways, such as the phosphatidylinositol 3-kinases/Protein Kinase B/mammalian target of rapamycin and the Ras-mitogen-activated protein kinase signalling cascades, are involved in the control of the translation apparatus[419]. Not much is clear about the direct regulation of eEF1A even though several groups have been studying phosphorylation and regulation of this elongation factor[420]. High levels of eEF1A1 were associated with pro-survival activity and resistance to chemotherapy [421,422] and down-regulation of eEF1A1 expression resulted in cell death[423]. Overexpression of EF1A mRNA has been correlated with increased metastastic potential in mammary adenocarcinoma probably due to its interaction with the actin cytoskeleton, an effector in metastasis[424] and to have a reduced affinity for F-actin [425].

Western blotting confirmed the decrease in EBP1 protein levels in the SQ-Mitox-BCRP cell lines compared to the DLKP-SQ and SQ-Mitox-MDR cell lines (figure 3.1-9). *EBP1* encodes an RNA-binding protein that is involved in growth regulation. It is also known as proliferation-associated protein 2 G4. This protein is present in pre-ribosomal ribonucleoprotein complexes and may be involved in ribosome assembly and the regulation of intermediate and late steps of rRNA processing. This protein can interact with the cytoplasmic domain of the ErbB3 receptor

and may contribute to transducing growth regulatory signals. This protein is also a transcriptional co-repressor of androgen receptor-regulated genes and other cell cycle regulatory genes through its interactions with histone deacetylases. Overexpression of *EBP1* inhibits the growth of breast cancer cells[426]. Ectopic expression of EBP1 in breast cancer cells reduces the levels of HER2 protein, *HER2* promoter activity and reduces HER2 protein stability[427],[426]. EBP1 also interacts with AKT via the PKC pathway to regulate cell survival and suppress apoptosis[428]. There are two different isoforms of EBP1, the longer form p48, suppresses apoptosis whereas the shorter from p42 promotes cell differentiation [429]. This suggests that EBP1 has different effects on cell growth on survival depending on the expression of its isoforms.

Groups of functionally related proteins display similar dynamics, for example, CCT2, CCT3 and CCT7 showed an increase of 1.2- to 1.5-fold (table 3.1-5). CCT chaperonin was initially identified as a molecular chaperone specifically required for the folding of the cytoskeletal proteins tubulin and actin. In a more recent study searching for CCT substrates, up to 15% of cellular proteins were proposed to require the assistance of CCT for correct folding upon translation.

There was a burst of glycolytic activity in the 4th pulse cell population as indicated by the changes in the enzymes of the glycolytic pathway exemplified by trisephosphate isomerise 1 (1.84 fold) and phosphoglycerate mutase (1.76 fold). Trisephosphate isomerise 1 is a glycolytic enzyme which rapidly interconverts dihydroxyacetone phosphate with glyceraldehyde 3-phosphate, increasing the effectiveness of glycolysis and simplifying its regulation. Proteins involved in the response to stress such as heat shock 70kDa protein also increased (1.7 fold) in the 4th pulse cell population. Heat shock 70kDa (Hsc70, Hsc71, or HspA8) is a member of the Hsp70 family. Hsc70 is constitutively expressed in the cytosol of all eukaryotic cellular organisms and performs functions related to normal cellular processes. Annexin 1 was 1.35 fold up-regulated and was consistent with previous results[430]. Annexin 1 belongs to a family of calcium- and phospholipid-binding proteins which may contribute to drug efflux through exocytosis of drug-filled vesicles[431]. Galectin-1 (down-regulated), Nbla10058 (down-regulated) and Heat Shock 70kDa protein 8 (up-regulated) expression are also consistent with previous results in our laboratory[430]. Galactin-1 has been described as a small protein with major functions [432]. Galectins bind to cell-surface and extracellular matrix glycans and thereby affect a variety of cellular processes[433]. Nbla10058, also known as PSMB2, has been associated with

anthracyclines nuclear transport[434, 435]. Heat Shock 70kDa protein 8 is a major cytosolic molecular chaperone[436].

FABP5 was also 1.2 fold up-regulated in the 4th pulse cell population. It is involved in lipid metabolism. FABPs may also modulate cell growth and proliferation, possibly by virtue of their ability for lipid ligands, (eg prostaglandins, leukotrienes and fatty acids). In a proteomic study on lung cancer cells to elucidate the mechanisms that determine histological phenotype, *Seike et al.,* [437] suggested that FABP5 may play an important role in the differentiation of lung cancer. This protein was also shown to be up-regulated in a mitoxantrone resistant pancreatic cell line by *Sinha et al.,*[438]. They suggested that mitoxantrone could bind to cellular FABPs and lead to its sequestration in cytoplasm, thus inhibiting transfer of mitoxantrone to the nucleus.

ARPC2 protein, also known as PRO2446, was decreased in the SQ-Mitox-BCRP-4P cells. This gene encodes one of seven subunits of the human Arp2/3 protein complex. The Arp2/3 protein complex has been implicated in the control of actin polymerisation in cells and has been conserved through evolution. The exact role of the protein encoded by this gene, the p34 subunit, has yet to be determined although it was found to be down-regulated in human gastric cancers [439].

The DNA repair protein XRCC5 (Ku80) was 1.33 fold up-regulated in the SQ-Mitox-BCRP-4P cells. This correlated with the microarray analysis result of a 1.39 fold up-regulation. Interestingly a functional anti-invasive antibody, 7B7 generated using the Mia PaCa-2 clone 3 cell line as an immunogen in our laboratory and directed against the Ku70/Ku80 heterodimer demonstrated strong membrane reactivity in the SQ-Mitox-BCRP-6P cells[440].

DSCAML1 was identified as 1.2-fold down-regulated in the SQ-Mitox-BCRP-4P cells (table 3.1-5). However, Down Syndrome Cell Adhesion Molecule (DSCAM) was investigated instead as a more likely candidate to provide information because of its role in cell adhesion and cell-cell interactions. Western blotting confirms the decrease in protein levels of DSCAM in SQ-Mitox-BCRP-4P SQ-Mitox-BCRP-6P cells, compared to DLKP-SQ parent cells (figure 3.1-9).

Down Syndrome (DS), caused by trisomy 21, is the most common birth defect associated with cognative impairment. It is expressed in the developing nervous system with the highest level of expression occurring in the fetal brain. DSCAM is a member of the Ig superfamily that maps to a region in chromosome 21 and is one amongst several genes associated with Down Syndrome cognative impairment (figure 6.2-1). It encodes a 230 kDa type I membrane protein with a large

extracellular domain comprising ten C2-type Ig-like domains and six fibronectin type III repeats. Human DSCAM is expressed in axonal and dendritic processes of the central and peripheral nervous system. When this gene is over-expressed in the developing fetal central nervous system, it leads to Down syndrome.

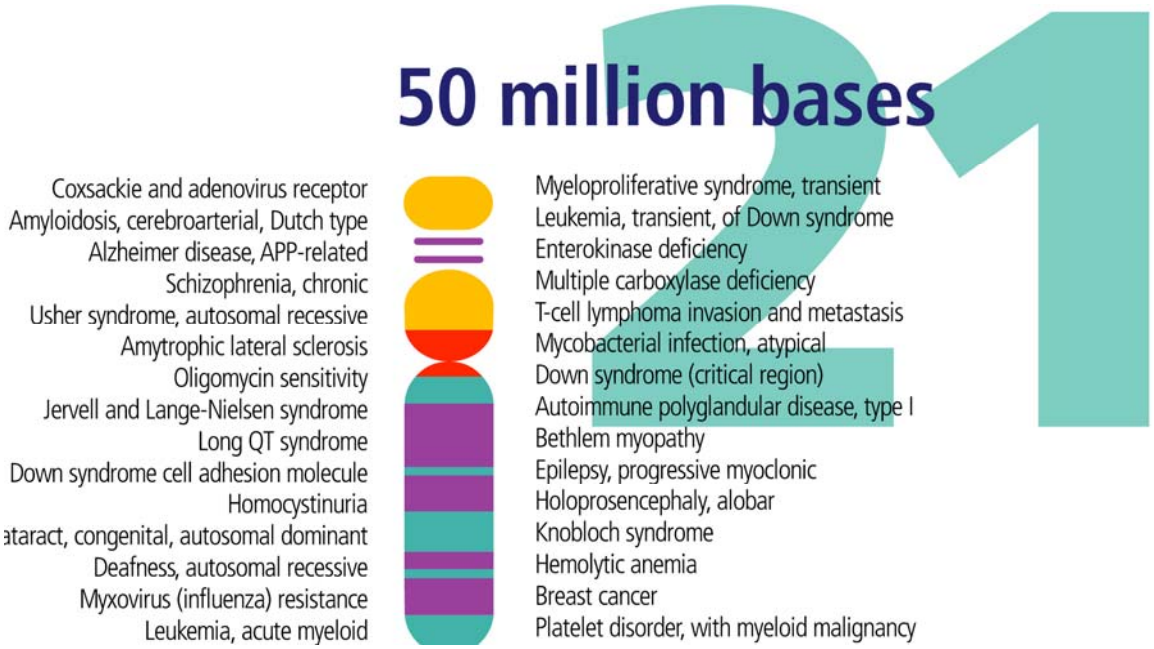

Figure 6.2-2: Chromosome 21 from Human Genome Program. Adapted from the US Human Genome Project Information Archive 1990-2003 website at http://web.ornl.gov/sci/techresources /Human_Genome/posters/chromosome/chromo21.shtml.

Despite its molecular classification as a cell adhesion molecule, DSCAM is recognised for its physiological role in "self-avoidance" in Drosophila and mammals. Self-avoidance involves the repulsion of processes from the same cell during axon branching and the prevention of clumping of cells of the same subtype during the development of structures with well-defined anatomies such as the mammalian retina. In this way, self-avoidance counteracts cell adhesion, which knits cells together[441].

Garrett [441] *et al.,* pointed out, that in neurodevelopmental processes, the phenomenon of not adhering is often viewed as the passive alternative to adhesion, and that in some cases this may be true. However, it is becoming increasingly clear that active signaling pathways are involved in preventing adhesion between cells[441]. The same principal may apply to cancer. A lung cancer

tissue array (Biomax, LC817) was immune-histochemically stained using primary antibodies specific for DSCAM (figure 3.1-10 and table 3.1-6). Variable membrane staining was observed in a number of squamous carcinomas and adenocarcinomas but in contrast, lung small cell carcinomas did not show any staining. Interestingly, in metastatic tumours from small cell carcinomas, weak staining was observed in 3/6 even though the primary tumours were negative. Interestingly, the work of *Sato et al.,* [307], illustrated in a genome-wide association study, a SNP in the DSCAM gene which was associated significantly with shortened overall survival.

The proteomics data supports the concept that MDR development requires several adjustments by cancer cells in order to prevent chemotherapeutic drug-induced damage, and thus provides further insights into the complex mechanisms of mitoxantrone chemoresistance. In particular, this data highlights the role of various proteins involved in a myiad of processes including but not confined to glycolysis, protein turnover and translational elongation, as well as the BCRP protein itself, a key component in the cellular efflux of xenobiotics. This information may be useful as it may lead to the development of new functional tests for the investigation of the mechanisms responsible for MDR.

6.2.7 miRNA Expression Analysis of DLKP-SQ, SQ-Mitox-BCRP-4P and SQ-Mitox-MDR-4P

MicroRNAs (miRs) are small non-coding, endogenous, single stranded RNAs that regulate gene expression (see section 1.2.4). By regulating the gene expression at a posttranscriptional level, miRs have a large impact on a wide variety of pathways, including those pathways related to cancer development. Several research groups have shown that the expression of miRNAs in chemoresistant cancer cells and their parental chemosensitive ones are different[442,443]. The objective of this section was to investigate how the miRNA profile is altered in the SQ-Mitox-BCRP and SQ-Mitox-MDR cell lines (see section 3.1.13).

miRNA lists with significant changes in expression ($p < 0.05$) in each cell line compared to the drug sensitive parental cell line, DLKP-SQ were generated (table 3.1-10 and table 3.1-11). Four miRs were significantly different in the SQ-Mitox-BCRP cell line. There were two upregulated miRs (miR-218 and miR-27*) and two downregulated miRs (miR-639 and miR-335*). Four miRs were also significantly different in the SQ-Mitox-MDR cell line. There was one upregulated miR (miR-342-3p) and three downregulated miRs (miR-935, miR-524 and miR-550).

miR218 was the most highly upregulated miRNA in the SQ-Mitox-BCRP cells (table 3.1-10). A down-regulation of miR-218 has been reported as tumour suppressive miRNA in several kinds of tumours, including gastric cancer[444,445], lung cancer[446], cervical cancer[447], head and neck cancer[284] and prostate cancer[448]. miR-218, along with miR-585, has been found to be silenced by DNA methylation in oral squamous cell carcinoma[449]. It is also downregulated in nasopharyngeal carcinoma, with artificially-induced expression serving to slow tumour growth[450]. miR-218 has also been found to have tumour suppressing qualities in bladder cancer cells[451]. One study reported that miR-218 was a potent activator of Wnt signaling, contributed to osteoblastogenesis, and facilitated the metastasis of breast cancer cells into the bone[452].

There are two genes that code for mature miR-218. miR-218-1 is located on chromosome 4p15.31, and miR-218-2 is located on chromosome 5p34[451]. The gene code for mature miR-218-1 is located within the intron 15 of *slit homologue 2* (SLIT2), a tumour suppressor gene. Interestingly, Western blot analysis also shows an upregulation of the SLIT2 protein in the BCRP over-expressing cell line (figure 4.2-11). miR218-1 expression may be under the control of the SLIT2 promoter[254]. ROBO2 was also present in all of the BCRP over-expressing cells to varying extents (figure 4.2-11). *Tie et al*.,[445] have suggested that there may be a Slit-miR-218-Robo1 regulatory circuit whose disruption may contribute to gastric cancer metastasis. Further investigation of the role of miR218 and SLIT2 in BCRP-mediated drug resistance is warrented.

The second upregulated miRNA was miR27a*. miR27a* is located at chromosome 19 and is known to regulate components involved in numerous types of cancer, including breast[453] and ovarian[454]. miR-27* is an activator of the Wnt signalling pathway, affecting the differentiation of mesenchymal stem cells into osteoblasts[455]. Expression levels of miR-27* are positively correlated with beta-catenin[455] a key protein in Wnt signaling. miR-27* has been found to target and inhibit gene expression of the adenomatous polyposis coli (APC) protein, enabling it to regulate osteoblast differentiation[455]. Inhibition of miR-27* by antisense molecules decreases cell proliferation[456]. Antisense RNA directed against miR-27a* has been shown to decrease the percentage of cells in S phase whilst also increasing those in the G2-M phase[457].

Interestingly an experiment in doxorubicin-resistant ovarian cancer cell lines showed downregulation of P-gp was mediated by antagonizing miR-451 and miR-27a*[458]. Downregulation of miR-27a* resulted in a decrease of P-gp expression in oesophageal squamous carcinoma and in gastric cancer cells[459,460]. After transfection of miR-27a inhibitor, *Li et al*.,[214] reported a downregulation of P-gp and an increased sensitivity to paclitaxel in the paclitaxel-

resistant ovarian cancer cell line (A2780/Taxol) gastric cancer cells. Previous studies in this laboratory showed that miR27a* was increased in the adriamcyin resistant cell line, DLKP-A compared to the DLKP parent[461].

miR335 was 8 fold downregulated in the SQ-Mitox-BCRP cells compared to the DLKP-SQ cells. miR-335, which is transcribed from the genomic region chromosome 7q32.2, has been reported to be differentially expressed in benign and malignant tumours[462] and regulates Rb1 and controls cell proliferation in a p53- dependent manner[463]. It participates in the development of breast cancer[464] and regulates growth and invasion of malignant cells[465]. Other research reports that miR-335 might function as a metastasis suppressor in gastric cancer by targeting Bcl-2 and SP1, and could be further developed as a potential prognostic factor[466]. *Yan et al.*,[467] suggested that hsa-miR-335 is involved in regulating target genes in several oncogenic signal-pathways, such as p53, MAPK, TGF-b, Wnt, ERbB, mTOR, Toll-like receptor and focal adhesion. Finally *Peng et al*.,[468] suggested that miR-335 was downregulated in a majority of primary gallbladder carcinoma patients and may be associated with the aggressive tumour behaviours.

There was one upregulated miR (miR-342-3p) and three downregulated miRs (miR-935, miR-524 and miR-550) in the SQ-Mitox-MDR cell line. *Cittelly et al.,* suggest that miR-342 regulates tamoxifen response in breast tumor cell lines by regulating the expression of genes involved in tamoxifen mediated tumor cell apoptosis and cell cycle progression[469] and has also been found to be aberrantly expressed in prostate cancer[470]. miR-550 has been found to be differentially expressed in the transformation of gastritis into MALT lymphoma[471] . In addition, miR-550 is differentially expressed in childhood acute lymphoblastic leukemia[472] and has been shown to promote the migration and invasion of hepatocellular carcinoma[473]. The function of miR-935 and miR-524-3P is unknown.

This thesis reports the establishment of novel cell lines with resistance to mitoxantrone while over-expressing BCRP and P-gp pumps. These events coincide with early events in the drug pulsing and selection processes. The strategy of deriving isogenic drug resistant cell lines from one cell line eliminates variability due to intrinsic genetic differences between cell lines. The cause of the early upregulation of the BCRP and P-g transporters seen in these investigations remains to be elucidated.

The expression profiling approach outlined here was successful in identifying differentially expressed genes which may contribute to P-gp and BCRP-mediated resistance. The over-expression of a particular ABC transporter during drug selection also appears to depend on a

multitude of factors which include but are not limited to the cell type, the selection regimen, the drug used for selection pressure as well as the concentrations utilised. These factors suggest that a number of ABC transporters in addition to ABCB1 should be evaluated following drug selection.

The establishment of multi-drug resistant cell lines from DLKP-SQ-Mitox has provided a powerful tool for further study of the cancer multi-drug resistant phenotype. This model allows detailed studies on mechanisms of cross-resistance and the direct investigation of drug resistance (e.g. by siRNA knockdown). In addition, these cell lines may prove to be useful models for the study of new modulators of resistance aimed at improving the outcome of acquired drug resistance. The conclusions from these investigations remain to be validated in human tumour biopsies.

6.3 Establishment of drug resistant invasive DLKP-SQ variants

Several publications have suggested an association between advanced malignancy and drug resistance in many cancers[196]. In this thesis, lung cancer invasion potential *in vitro* was investigated using drug-sensitive cell lines and their MDR variants – the results indicate MDR variants possess an enhanced invasive capacity.

Resistance to chemotherapy drugs is a major problem in cancer treatment. Scientific advances made in the last two decades have resulted in the identification of genes and molecular signalling pathways that contribute to drug resistance. However, to further complicate our understanding of drug resistance, patients given chemotherapy gradually develop mutations or metabolic potentiation and adaptation which leads to tumour progression and metastatic changes, making treatment difficult for such patients.

Previous studies[196] show that exposure of the human lung carcinoma cell line, DLKP to mitoxantrone, an anthracenedione, can result in not only an MDR phenotype but also enhanced cell invasion *in vitro*. Array technology can help answer increasingly complex questions and allow for more intricate experiments to be performed. Arrays can infer the probable functions of new genes based on similarities in expression patterns with those of known genes. This can aid the understanding of how genes and their products coordinate and interrelate, and speed the identification of genes involved in the development of various diseases.

Expression array data have led to crucial insights into fundamental cancer biology, including the mechanisms of tumourigenesis, metastasis, and drug resistance[474]. They have also had enormous clinical impact, e.g., several cancers can now be fractionated into therapeutic subsets with unique prognostic outcomes based on their molecular phenotypes[475-481].

The primary aims within this section of the thesis were to establish an *in vitro* model of mitoxantrone resistance and to identify changes in gene expression associated with the transition from pre-invasive to an invasive phenotype. DLKP-SQ, a clone of DLKP was chosen for the establishment of a mitoxantrone resistant cell line in order to eliminate variability due to intrinsic genetic differences between cell lines (chapter 3).

Four sub-populations displaying differences in invasion were further analysed to characterise the *in vitro* invasive phenotype. DLKP-SQ-Mitox-BCRP-4P and DLKP-SQ-Mitox-MDR-4P were characterised as poorly invasive and DLKP-SQ-Mitox-BCRP-6P and DLKP-SQ-Mitox-MDR-6P were characterised as invasive (chapter 4.2).

Matsuo and colleagues[482] reported that increased expression of MDR-1 in tumour tissue obtained at initial cytoreduction surgery is associated with increased risk of developing brain metastases in women with epithelial ovarian, fallopian tube, or peritoneal cancer. Consistent with these observations, our results indicated that BCRP and P-gp were over-expressed in the 4th pulse cell population, followed by the appearance of the invasive phenotype in the 6th pulse cell population. These results suggest a strong relationship between drug resistance and metastasis (figure 4.2-1).

6.3.1 Microarray analysis of SQ-Mitox sub variants

In order to investigate changes in gene expression pattern during the transition from a pre-invasive to an invasive phenotype during the development of drug resistance, microarray analysis was performed in poorly invasive mitoxantrone resistant DLKP-SQ-Mitox-BCRP (4th pulse) and DLKP-SQ-Mitox-P-gp (4th pulse) and invasive mitoxantrone resistant DLKP-SQ-Mitox-BCRP (6th pulse) and DLKP-SQ-Mitox-P-gp (6th pulse) (see section 4.2.4).

Two gene lists were generated - DLKP-SQ-Mitox-BCRP-4P *versus* DLKP-SQ-Mitox-BCRP-6P cells (Genelist 1) and DLKP-SQ-Mitox-MDR-4P *versus* DLKP-SQ-Mitox-MDR-6P cells (Genelist 2), in search of molecular mechanisms involved in the invasive phenotype.

6.3.1.1 Genes related to invasion and specific to SQ-Mitox-BCRP-4P vs 6P

In identifying genes changing between SQ-Mitox-BCRP-4P (poorly invasive) *versus* SQ-Mitox-BCRP-6P (invasive) (Genelist 1), a comparison of the two cell lines resulted in a list of 79 genes being up- or down-regulated (1.2 fold) in SQ-Mitox-BCRP-6P (62 genes up-regulated and 17 genes down-regulated). The top 10 over-expressed and under-expressed genes are shown in table 4.2-1.

The top over-expressed gene was *ADAMTS1*. *ADAMTS1* is a disintegrin and metalloproteinase with thrombospondin motifs. The expression of this gene may be associated with various inflammatory processes as well as development of cancer cachexia[483]. While elevated ADAMTS1 has been shown to promote pro-tumourigenic changes, other studies depict it as a tumour suppressor[484].

N-cadherin was expressed at higher levels in the SQ-Mitox-BCRP-in 6P compared to the DLKP-SQ and SQ-Mitox-BCRP-4P cell lines (figure 4.2-10). Cadherins (named for "calcium-dependent adhesion") are a class of type-1 transmembrane proteins. They play important roles in cell adhesion, forming adherens junctions to bind cells within tissues together. They are dependent on calcium (Ca^{2+}) ions to function. Cells containing specific cadherin subtypes tend to cluster together to the exclusion of other types, both in cell culture and during development[485]. For example, cells containing N-cadherin tend to cluster with other N-cadherin-expressing cells and bind cells within tissues together.

Cadherin switching (i.e. E-cadherin to N-cadherin) associated with epithelial-mesenchymal transition (EMT) is implicated in the transition from benign tumours to invasive, malignant cancer and the subsequent metastatic dissemination of tumour cells[486]. Ectopic expression of N-cadherin increases tumour cell motility, implicating cadherin switching in the regulation of cell behaviour[146,487].

Microarray analysis showed that the kras gene may be up-regulated in the SQ-Mitox-BCRP-6P cells. Interestingly, oncogenic K-ras is sufficient to upregulate N-cadherin expression in pancreatic ductal cells suggesting that K-ras may play an active role in cadherin switching in pancreatic cancer[488].

The under-expressed gene list consisted of low fold changes. In mammals, the HSP90 family consists of four major types, two cytosolic isoforms, the heat-inducible HSP90a encoded by gene *HSP90AA1* and *HSP90AA2* and the constitutively-expressed HSP90b encoded by *HSP90AB1*.

Recent studies suggest that *HSP90AA1* but not *HSP90AA2* is expressed extracellularly and involved in cancer cell invasiveness[489].

6.3.1.2 Genes related to invasion and specific to SQ-Mitox-MDR-4P vs 6P

Comparison of SQ-Mitox-MDR-6P to SQ-Mitox-MDR-4P resulted in a list of 533 genes. That is, the expression of 533 genes was up- or down-regulated (1.2 fold) in SQ-Mitox-MDR-6P (220 genes up-regulated and 333 genes down-regulated). The top 10 over-expressed and under-expressed genes are shown in table 4.2-1.

Different genes involved in signaling were induced or suppressed in the transition to the invasive phenotype (table 4.2-1). The primary over-expressed gene was DKK1 (9.6-fold over-expressed). Although Dickkopf-1 (DKK1) is known to be a negative regulator of the Wnt/β-catenin pathway, it has been recently found to be upregulated in cancers[490]. NRG1 (5.77-fold over-expressed) is one of four proteins in the neuregulin family that act on the EGFR family of receptors. The neuregulins are cell-cell signaling proteins that are ligands for receptor tyrosine kinases of the ErbB family. Through their interaction with ERBB receptors, NRG1 isoforms induce the growth and differentiation of epithelial, neuronal, and glial cells. There is evidence that NRG1 is a tumour suppressor gene[491]. Tissue inhibitor of metalloproteinase-2 (TIMP2), was the primary suppressed gene (reduced 3.8-fold). Matrix metalloproteinases (MMP) have also been implicated in multiple stages of cancer metastasis. TIMP-2 plays an important role in regulating MMP-2 activity[492].

6.3.1.3 Comparison of genelist 1 and 2

Gene expression patterns between the BCRP cell lines (Genelist 1) and MDR cell lines (Genelist 2) were compared with each other to search for molecular mechanisms involved in the invasive phenotype. These lists contained both well and poorly annotated genes. Several of the annotated genes can be related to invasion, cell survival, motility and apoptosis. The possibility that some of the unanotated genes are also relevant to cancer invasion awaits further investigation.

These lists were overlapped to identify common and uncommon genes (figure 4.2-3). Twelve genes were identified as common between the upregulated genes. Different genes involved in cell adhesion, axon guidance and wnt signaling were induced in the transition from the pre-invasive to invasive phenotype.

6.3.1.4 PANTHER analysis of microarray gene lists

The classification of genes was determined by the web program PANTHER[493,494]. PANTHER pathway analysis revealed that the most significant pathways were related to Wnt signalling, inflammation, integrin signalling and p53 in both Genelist 1 and Genelist 2 (see section 4.2.3.2).

Abberations in the Wnt signalling pathway have been linked to many human cancers [495-496]. Wnt signalling is important for cell migration, invasion, adhesion and survival. The Wnt signaling pathway is also strongly implicated as a stem cell regulator[497]. Three Wnt signaling pathways have been characterised: (1) the canonical Wnt pathway, (2) the noncanonical planar cell polarity pathway, and (3) the noncanonical Wnt/calcium pathway. Wnt proteins are secreted glycoproteins that bind to the N-terminal extra-cellular cysteine-rich domain of the plasma membrane located Frizzled (Fz) receptor family of G-protein coupled receptors, which passes the biological signal to the protein Dishevelled inside the cell. The canonical Wnt pathway leads to regulation of gene transcription, the noncanonical planar cell polarity pathway regulates the cytoskeleton and is responsible for the shape of the cell, and the noncanonical Wnt/calcium pathway regulates calcium inside the cell[498 - 499].

PANTHER pathway analysis is generally useful in assisting in the interpretation of microarray analysis. It has allowed the enrichment of pathways that were represented by Genelists 1 and 2. However, many of the pathways as indicated by PANTHER may have been based on only one gene for example, SLIT2. Despite this, it did give an indication of the pathways represented on both gene lists.

The results indicate that chronic treatment with anticancer agents leads to the acquisition of drug-resistance in DLKP cells. Importantly, along with the acquisition of drug resistance, there is also a marked increase in the expression and activity of MMP-2 and integrin alpha V.

In summary, this model provides a unique *in vitro* representation of an invasive, drug resistant lung carcinoma. If the critical alterations of tumour cells after treatment with chemotherapeutic drugs can be understood, it may enable the determination of the key molecules and signaling pathways involved (table 6.3-1).

Table 6.3-1: Key protein expression changes in each cell line

Protein	SQ parent	SQ-Mitox-4P	SQ-Mitox-6P (Isolate 2)
Mitoxantrone IC_{50}	**0.08 ng/ml**	**16.79 ng/ml**	**44.82 ng/ml**
BCRP	low	present	high
ALCAM	absent	trace	high
IGF1Rβ	low	low	high
Integrin alpha V	absent	present	high
MMP2	low	present	high
MMP10	low	present	high
SLIT2	low	high	high
ROBO2	low	low	high
BCHE	low	low	high

6.3.2 Confirmation of array results

6.3.2.1 Role of integrin alpha V expression

The initial step of tumour metastasis is a movement of invasive tumour cells migrating through the basement membrane, which implicates major roles for cell adhesion and migration as well as proteolysis of the extracellular matrix (ECM). This step involves many molecules including matrix metalloproteinases (MMPs) and integrins [500 501 502 503 504 505 506 507 508 509 510]. Cell–cell adhesion is a prerequisite for the maintenance of epithelial integrity and is thus often altered during carcinogenesis and particularly during the metastatic process. As the primary linkage between a cell and the ECM, integrins have an essential role in the invasion process. Indeed, changes in the expression and/or function of integrins have been implicated in all steps of tumour progression, including detachment of tumour cells from the primary site, migration through the basement membrane, invasion of the ECM, intravasation into the blood stream, dissemination through the circulation, extravasation into distant target organs, and formation of the secondary lesions [155 511 512 513 514]. Some integrins, especially αVβ3, seem to promote tumour progression and metastasis[515]. *Blaheta et al.,* [516] reported that chemoresistance induces enhanced adhesion of neuroblastoma cells by down-regulating NCAM surface expression. In recent years, cell adhesion-mediated drug resistance (CAM-DR) has become an active area of investigation in the study of tumour drug resistance [517,518519]. In the present work, siRNAs directed against the

mRNA of the αV chain of integrin alpha V obtained a significant reduction in invasion of the SQ-Mitox-BCRP-6P cell population (figure 4.2.13).

6.3.2.2 Role of BCHE expression

Microarray profiling revealed differential expression of a secretory butyrylcholinesterase, BCHE, between the SQ-Mitox-BCRP-4P and SQ-Mitox-BCRP-6P cell line. There is increasing evidence that suggests the involvement of cholinesterases in tumourigenesis[327, 328].

BCHE protein was differentially expressed in subpopulations of the DLKP lung cancer cell line displaying distinct invasive phenotypes (figure 4.2-14). Mitoxantrone drug pulsing of the least invasive subpopulation induced an upregulation of the BCHE protein. BCHE knockdown by small interfering RNA (siRNA) reduces the invasion of DLKP-SQ-Mitox. Immuno-histochemical analysis indicated that decreased BCHE expression is associated with higher grade lung cancer (table 4.2-6 and figure 4.2-15). The observed intense BCHE staining in metastatic tumours needs to be investigated further to establish its role in lung cancer invasion and drug resistance.

6.3.2.3 Role of ALCAM expression

Immunofluorescence and Western blot analysis has revealed a higher level of expression of ALCAM in the stable, invasive BCRP over-expressing variant, with lower levels in the DLKP-SQ parental cell line and DLKP-SQ-BCRP-4P (figure 4.2-8 and figure 4.2-9). ALCAM mediates cell–cell adhesion through homophilic and heterophilic protein–protein interactions and is thought to be involved in cell migration and guided outgrowth in neurogenesis, in hematopoiesis, and in immune responses[520,521].

ALCAM is a member of a subfamily of immunoglobulin receptors with 5-immunoglobulin-like domains. It is a type 1 transmembrane molecule, with an extracellular domain of 500 amino acids, a transmembrane domain of 22 amino acids and a short cytoplasmic domain of 34 amino acids[522]. It is mainly found in the spleen, placenta, and liver. ALCAM was also identified on thymic epithelial cells and activated leukocytes, fibroblasts, neurones, pancreatic acinar and islet cells, and bone marrow[523].

Its functions have been studied in detail with regard to T-cell biology where the co-stimulatory role of ALCAM in T-cell activation suggests an involvement in the immunological response to

tumour cells[524]. Altered ALCAM expression has also been associated with the differentiation state and progression in melanoma[525], prostate[526,527], colorectal[528], and breast cancers[523]. ALCAM is up-regulated in some of these cancers and down-regulated in others and the major functions of this cell adhesion molecule in cancer remain poorly understood[522].

ALCAM increased with increased BCRP expression in the present studies but it was barely detectable in the Pgp over-expressing cell lines. Presently there are no reports in the published literature of an ALCAM association with BCRP. In pancreatic cancer cells, a reduced ALCAM expression has been shown to be associated with chemoresistance[529].

ALCAM is a membrane protein, confirmed in these studies by the presence of ALCAM in the membrane preparations. Indeed, the stable invasive BCRP over-expressing variant has a higher membranous expression of ALCAM (figure 4.2-8). This would suggest that it is the membranous expression or localisation of ALCAM which is more significant for invasion in the SQ-Mitox cells. *Ishiguro et al.,* [530]*,* found membranous expression in NSCLC and its localisation in the membrane was associated with decreased overall survival.

Although ALCAM has been implicated in different cancers, it is as yet unclear how ALCAM contributes to metastasis. ALCAM expression may be necessary for motility and invasiveness in the SQ-Mitox-BCRP- invasive 6P cell line. One likely way in which ALCAM could promote an invasive phenotype is through regulation of matrix metalloproteinases (MMPs). MMPs are zinc-dependent proteinases whose expression has been implicated in processes such as tissue remodeling and cancer metastasis[531]. MMP-2, a 72 kDa protein also called gelatinase A, is the most abundant of the MMPs. Activation of MMP-2, and the additional gelatinase family protein MMP-9, allows degradation of type IV collagen which is a primary component of basement membranes. MMPs are synthesised as pro-enzymes that must be processed to their active form by proteolytic cleavage. Pro-MMP-2 is recruited from the extracellular milieu and processed by a complex consisting of Type I MMP (MT1-MMP/MMP-14) and tissue inhibitor of metalloproteinase-2 (TIMP-2); this process is known to require full-length ALCAM[532]. MMP-2 levels in the SQ-Mitox-BCRP-6P cell line were assayed using gelatin zymography and western bloting, where pro-MMP-2 appears as a 72 kDa band, and active MMP-2 appears as a ~64 kDa band.

Functional reports indicate a functional link between ALCAM and cadherins, another major family of cell adhesion molecules. The cadherins have been known to link to the actin cytoskeleton via their intracellular binding partners, the catenins[533]. Interestingly, N-cadherin

was expressed at higher levels in the SQ-Mitox-BCRP-in 6P compared to the DLKP-SQ and SQ-Mitox-BCRP-4P cell lines (figure 4.2-10). *Jannie et al.* [534], suggest a mechanism by which ALCAM might differentially enhance or decrease invasiveness in uveal melanoma cells, depending on the type of cadherin adhesion complexes present in tissues surrounding the primary tumour, and on the cadherin status of the tumour cells themselves.

6.3.2.4 Role of MMP-2 expression

The MMP family is comprised of more than 25 members that are divided into 5 groups based on their target substrates: (1) collagenase, (2) stromelysin, (3) gelatinase, (4) matrilysin and (5) membrane type (MT)-MMP8. Although MMPs are secreted by most tumour cells, gelatinases, including MMP-2 (gelatinase A; M_r 72KDa) and MMP-9 (gelatinase B; M_r 92KDa), have been implicated as critical enzymes in the invasion of cells into secondary sites. *Liang et al.,* [196] reported that anticancer drug-selected lung carcinoma cell variants showed enhanced *in vitro* invasive abilities through up-regulation of MMPs. *Song et al.,* [535] reported that advanced malignancy due to acquired drug resistance is responsible for the progressive invasiveness of leukemia cell via MMP-2. The level of MMP-2 in the stable, drug-resistant SQ-Mitox-BCRP-6P cell variant was evaluated. While there was no change in the stable, drug-resistant SQ-Mitox-BCRP-4P cell variants, the 6th pulse cell variant of the SQ-Mitox-BCRP demonstrated a significant increase in the expression and gelatinolytic activity of MMP-2 as well as in its invasiveness.

To confirm the precise role of MMP-2 on SQ-Mitox-BCRP-6P cell invasiveness, invasion assays of these cells were performed in the presence of a specific anti-MMP-2 monoclonal antibody. As shown in figure 4.2-7, the number of SQ-Mitox-BCRP 6th pulse cells that migrated through the ECM gel was significantly decreased by specific blocking of MMP-2. However, there was no significant alteration in the invasiveness of the cells treated with the control isotype antibody. Taken together, these findings clearly indicate that the enhanced invasiveness of drug-resistant SQ-Mitox-BCRP 6th pulse cell variants is associated with an increased level of MMP-2. The incomplete suppression of invasiveness in this assay suggests that other factors, such as regulation by other MMPs and integrins, may also be involved in the invasiveness of drug-resistant cancer cell variants.

6.3.2.5 Role of MAPK kinase pathway in SQ-Mitox-BCRP-6P invasion

IGF-1R was identified as a gene potentially involved in invasion in Genelist 1. I The insulin-like growth factors (IGF) and their receptors play pivotal roles in cellular signaling transduction and regulation of cell growth, differentiation, apoptosis, transformation and other important progresses. IGF1R mainly engages in the Ras/mitogen-activated protein kinase (MAPK) and the phosphoinositide 3-kinase/protein kinase B (PI3K/AKT) pathways, with significant cross-talk with the epidermal growth factor receptor (EGFR) pathway also in evidence[536,537].

Increased IGF-1R expression has been previously linked with tumour invasion[538]. Former investigations in this lab (*Pierce, A.,* PhD thesis, 2006[279]) previously demonstrated that decreasing IGF-1R expression reduces the *in vitro* invasiveness of the DLKP drug resistant variants. Additionally, KRAS was shown to be 2.75-fold up-regulated in the DLKP-SQ-Mitox-BCRP-6P cells relative to the SQ-Mitox-BCRP-4P cells. Activated KRAS engages multiple effector pathways, notably the RAF-mitogen-activated protein kinase, phosphoinositide-3-kinase (PI3K). ERK was shown to be activated in the DLKP clones (section 5.2.7). The poorly invasive DLKP-SQ clone had the highest level of phosphorylation of ERK of all the clones when grown on plastic. Genetic factors may require the cooperation of another genetic event to manifest the invasive phenotype. For example the DLKP-SQ clone contains low levels of integrin αV and MMP-2 and the DLKP-M and DLKP-I clones contain high levels of these proteins (figure 4.1-2 and 4.2-6). Experiments with MEK inhibitors showed that invasion of the SQ-derived SQ-Mitox-BCRP-6P and DLKP-M cell lines was reduced when the MAPK kinase inhibitor, U0126 was added to the invasion assay suggesting that the MEK/ERK pathway contributes to cell invasion in these cells (section 5.2).

6.4 Characterisation of clonal subpopulations of DLKP

The DLKP parental population has been shown to contain at least 3 phenotypically different clonal subpopulations[281, 280]. On prolonged subculture, SQ and M can each interconvert with I, but SQ and M do not interconvert. Of the three, M-type cells are the most invasive, I-type cells are slightly less invasive, wherease SQ-type cells are the least invasive *in vitro*.

Scientific concepts are fashioned by the experimental models used and molecular biologists, working on cancer cell lines or transformed cells often tend to consider their cell lines as a homogeneous population. However, pathologists confronted with real tumours have a different

view and recognise the heterogeneity of cancers[539]. In the clinical setting, the primary obstacle to the success of therapy is the heterogeneous composition of tumours, where highly metastatic cells can escape from the effect of therapeutic agents or are metabolically enhanced and can eliminate or degrade a xenobiotic with ease. Invading tumour cells appear to have lost the control mechanisms which prevent normal cells from invading neighbouring tissues at inappropriate times and places. Thus, the fundamental difference between normal and malignant cells is one of regulation. The differences must lie in the proteins that start, stop or maintain the invasion programme at times and places that are inappropriate for non-malignant cells. A major goal is to understand what signals and signal transduction pathways are perpetually activated or deregulated in malignant invasion[540]. The DLKP cell lines with differing levels of invasiveness (derived from the same parent) offer a unique opportunity to study tumour heterogeneity (figure 4.1-1).

The adherence properties of the DLKP clones to a number of ECM proteins and their invasion potential were assayed to determine what roles individual tumour subpopulations may play in the progression of malignant disease figure 4.1-2). Microarray analysis was used to search for differences between the three distinct clonal subpopulations, DLKP-SQ, DLKP-I and DLKP-M (aee section 4.1.6).

6.4.1 Adhesion and invasion assays of DLKP clones

The adherence properties of DLKP clones to a number of ECM proteins were found to differ from each other (figure 4.1-2). Of the three cell lines investigated, the highest level of adhesion was observed through fibronectin and vitronectin (as observed in *in vitro* binding assays) for the DLKP-M and DLKP-I clones. The increased adhesion to vitronectin could be explained by the increased expression of integrin αV in the DLKP-I and DLKP-M clones (figure 4.1-2). The alpha-V integrins are receptors for a variety of molecules associated with the extracellular matrix including vitronectin, cytotactin, fibronectin, fibrinogen, laminin, matrix metalloproteinase-2, osteopontin, osteomodulin, prothrombin, thrombospondin and vWF. Integrin alpha V is expressed at higher levels in the DLKP-I and DLKP-M clones (figure 4.1-2). Interestingly, the DLKP-I and DLKP-M populations also displayed increased invasion through matrigel compared to the DLKP-SQ clone (figure 4.1-1). There were no significant differences in attachment to laminin among the clones. Nor did any of the clones adhere to collagen IV or collagen V.

6.4.2 Expression of MMP-2 and MMP-10 in the DLKP clones

The acquired ability of tumour cells to migrate and invade through the extracellular matrix between tissues has long been accepted as a hallmark of metastatic potential. Numerous signal transduction pathways and a wide variety of protein classes have been implicated as important players in cell migration and/or invasion. For example, matrix-metalloproteinases (MMPs) have been implicated in the degradation of components of the basal lamina, that is presumably required for the movement of cells through the extracellular matrix. The contribution of the MMPs to cell invasion in the clones was investigated to determine if they played a role in the process. The levels of MMP-2 and MMP-10 were evaluated in the DLKP clones. The DLKP-I and DLKP-M clones demonstrated a significant increase in the expression and gelatinolytic activity of MMP-2 and MMP-10 (figure 4.1-2).

To confirm and illucidate the role of MMP-2 in DLKP-I and DLKP-M invasiveness, an invasion assay of these cells was performed in the presence of a specific anti-MMP-2 monoclonal antibody. As shown in figures 4.1-10 and 4.1-11, the number of DLKP-I and DLKP-M cells that migrated through the ECM gel was significantly decreased by blocking antibodies directed towards MMP-2. There was no significant alteration in the invasiveness of the cells treated with non-specific, control isotype antibody. These findings indicate that the invasiveness of DLKP-I and DLKP-M cell variants is associated with increased levels of MMP-2. The incomplete suppression of invasiveness in this assay suggests that other molecules (other MMPs and integrins) may also be involved in determining the invasive phenotype.

Matrix metalloproteinase 10 (MMP-10, stromelysin-2) is a secreted metalloproteinase which functions in skeletal development, wound healing, and vascular remodelling. Its over-expression is implicated in lung tumourigenesis and general tumour progression. To investigate the role if any of MMP-10 on DLKP-I and DLKP-M invasiveness, the invasion assay of these cells was repeated in the presence of a specific anti-MMP-10 monoclonal antibody (figure 4.1-10 and 4.1-11). Results were negative, there was no effect on invasion. MMP-10 is up-regulated in human non-small cell lung carcinoma (NSCLC), where it is associated with poor clinical outcome[541]. In addition, MMP-10 was identified as a major downstream effector of two NSCLC oncogenes, Kras and PKCι[542,543]. Silencing of MMP-10 expression in lung cancer cells blocks anchorage-independent growth and invasion[542]. Silencing of MMP-10 expression also suppresses the enhanced self-renewal and tumourigenic properties of a subpopulation of lung cancer cells with stemlike characteristics as described by *Justilien et al., 2012*[544] Genetic loss of Mmp10

suppresses tumourigenesis and tumour growth in mouse models of oncogenic Kras-mediated lung adenocarcinoma[543].

6.4.3 Microarray analysis of DLKP clones

In order to investigate changes in gene expression patterns between the clones, hierarchical clustering was performed on the data derived from the microarray analysis of poorly invasive DLKP-SQ and invasive DLKP-I and DLKP-M clones (see section 4.1.6).

In hierarchical clustering, genes with similar expression patterns are grouped together and are connected by a series of branches to form a diagram which is called a clustering tree (or dendrogram). All of the samples used in the experiment were run in triplicate, and all three replicates of a particular sample were expected to cluster together. These clusters were expected to be significantly different from those of each cell line. This was not the case for one of the sets of samples (figure 4.1-13). DLKP-I did not behave as expected and did not cluster with its replicates. Two of the DLKP-I samples clustered with the DLKP-SQ samples and one clustered with the DLKP-M sample (figure 4.1-3).

This was a surprising result as all biological replicates were treated in the same way prior to RNA extraction and microarray processing. Due to the sensitivity of microarray analysis, all cell culture conditions including media, incubation and cell number were kept the same for all samples. Despite this, it is clear that some event occurred that brought about 'drift' in the genetic profile. Previous studies from this laboratory proposed that the DLKP-I clones could possibly undergo interconversions to either DLKP-SQ and/or DLKP-M cells[280]. It is possible that over a number of passages a different sub-population of DLKP-I could have inadvertently been selected.

6.4.3.1 Genes changing between DLKP-SQ (poorly invasive) vs DLKP-M (invasive)

Following the clustering analysis results, studies were continued to identify genes changing between DLKP-SQ (poorly invasive) *vs* DLKP-M (invasive). This comparison resulted in a list of 2746 genes. That is, the expression of 2746 genes was up- or down-regulated in DLKP-M relative to the DLKP-SQ clones (1753 genes up-regulated and 993 genes down-regulated). The primary 15 over-expressed and under-expressed genes are shown in table 4.1-1a.

The primary over-expressed gene was *Vgll3*. Mammalian Vgll3 is related to the transcriptional cofactor *Vestigial* (*Vg*), originally described in *Drosophila melanogaster. Drosophila Vestigial* is

involved in determining cell fate in the developing fly wing and muscle. In mammals, there are four highly conserved "vestigial-like" genes. Previous reports have suggested that members of this protein family are associated with muscle development and function. For example, *Vgll3* has been reported to be expressed in developing muscle tissues of the mouse embryo[545]. Further investigation into the role of *Vgll3* in DLKP lung cancer invasion is warranted.

The second over-expressed gene was *Piccolo*. Piccolo is a neuronal synaptic vesicle protein. The protein encoded by this gene is part of the presynaptic cytoskeletal matrix, which is involved in establishing active synaptic zones and in synaptic vesicle trafficking. A role for *PCLO* gene in calcium sensing has also been suggested[546], but a role in cancer has not been previously reported. Piccolo is a very large protein (520kDa)[547 548]. Genes encoding extremely large proteins are reported to have low expression and are late in DNA replication timing. As a result the mutation rate is higher and it has been suggested that such potentially spurious genes that have been nominated as cancer associated genes in the recently published cancer genome studies are false positives[548]. Immunofluorescence staining showed strongest expression in the DLKP-I clone, with some cells in the DLKP-M population showing less expression of the protein, despite the fact that this gene is not present on the DLKP-SQ vs I genelist (figure 4.1-5).

The primary down-expressed gene was *Olfactomedin 3*. Olfactomedin 3, encodes an olfactomedin domain-containing protein and was previously studied in this laboratory[281]. High expression of *OLFM3* was confirmed at the RNA level by qRT-PCR in DLKP-SQ and at the protein level by Western blotting. Little or no OLFM3 was detected in the other two clones (DLKP-M and DLKP-I). Anoikis is a form of programmed cell death which is induced by anchorage-dependent cells detaching from the surrounding extracellular matrix and OLFM3 was shown to contribute to anoikis-resistance in the clones. This is the first instance of OLFM3 being linked with anoikis resistance in a human cancer cell line[281] (Appendix II).

In surveying genes which were differentially expressed between DLKP-SQ and DLKP-M, it is clear that the DLKP-M cell line exhibits altered expression of genes whose products are involved in cell adhesion and signalling. For example the gene CADM2 is over-expressed in both the DLKP-I and DLKP-M genelists. This gene encodes a member of the synaptic cell adhesion molecule 1 (SynCAM) family which belongs to the immunoglobulin (Ig) superfamily. Recent studies suggest that cell adhesion molecules (CADM), might serve as tumour suppressors[549,550]. For example *He et al.,* [551] suggested that CADM2 might be involved in the maintenance of cell

polarity and adhesion in renal cell carcinoma and that it may serve as a tumour suppressor gene by inducing apoptosis and inhibiting tumour growth both *in vitro* and *in vivo*.

The large extracellular matrix proteoglycan, versican (VCAN) was 28 fold down-expressed in the DLKP-M clone compared to DLKP-SQ. The role of versican in cell adhesion, migration, and proliferation is extensively studied. Versican is often considered an anti-adhesive molecule[552].

6.4.3.2 Genes changing between DLKP-SQ (poorly invasive) vs DLKP-I (invasive)

Despite the clustering analysis results, studies were continued using the remaining two DLKP-I replicates to identify genes changing between DLKP-SQ (poorly invasive) *vs* DLKP-I (invasive). Comparison of DLKP-SQ (baseline) to DLKP-I (experiment) resulted in a list of 1319 genes. That is, the expression of 1319 genes was up- or down-regulated in DLKP-I relative to DLKP-SQ clones (490 genes up-regulated and 829 genes down-regulated). The primary 15 over-expressed and under-expressed genes are shown in table 4.1-1b.

The primary over-expressed gene was N-cadherin. Interestingly, this gene was also over-expressed in the mitoxantrone resistant DLKP-SQ. Cadherins (named for "calcium-dependent adhesion") play important roles in cell adhesion, forming adherens junctions to bind cells together within tissues. It has been observed that cells containing a specific cadherin subtype tend to cluster together to the exclusion of other types, both in cell culture and during development [485]. Immunofluorescence staining showed that N-cadherin is expressed in the DLKP-I clone only (figure 4.1-4). N-cadherin is associated with a more aggressive behavior of cell lines and tumours, such as invasion[146,553].

The second over-expressed gene in the DLKP-I genelist was thyroid transcription factor 1 (TTF1). This gene was also over-expressed in the DLKP-M genelist. Thyroid transcription factor-1 is a protein that regulates transcription of genes specific for the thyroid, lung, and diencephalon. For lung cancers, adenocarcinomas are usually positive, while squamous cell carcinomas and large cell carcinomas are rarely positive. Small cell carcinomas (of any primary site) are usually positive[554,555].

Desmosomes are cell-cell junctions between epithelial, myocardial, and certain other cell types. The desmogleins are a family of cadherins associated with desmosomes consisting of proteins DSG1, DSG2, DSG3, and DSG4. Three of these four desmogleins (DSG 1, 2 and 3) are up-regulated in the DLKP-I genelist but are not present on the DLKP-M genelist. DSG3 (98 fold

over-expressed) is a calcium-binding transmembrane glycoprotein component of desmosomes in vertebrate epithelial cells and has recently been shown to be upregulated in squamous cell carcinoma (SCC)[556]. It has been identified as a good tumour-specific marker for clinical staging of cervical sentinel lymph nodes in head and neck squamous-cell carcinoma[557]. In addition, DSG2 (93 fold over-expressed) has been shown to interact wth desmcollin-1[558] which is 84.3 fold over-expressed. These desmosomal family members, along with the desmogleins, are found primarily in epithelial cells where they constitute the adhesive proteins of the desmosome cell-cell junction and are required for cell adhesion and desmosome formation. The desmoglein gene family members are located in a cluster on chromosome 18[559]. However, little else is known about their biological function in cancer and further investigation of the role of the desmoglein family in DLKP-I invasion is warranted.

ROBO2, an axon guidance receptor, is over-expressed in the DLKP-I cell lines. ROBO2 is a receptor for SLIT2 and these molecules are known to function in axon guidance and cell migration. Both of these proteins were shown to be over-expressed in the SQ-Mitox-BCRP-6P cell line. In addition, ALCAM, which was discussed earlier in this chapter is also over-expressed in the DLKP-I and DLKP-M cells. ALCAM and ROBO2 are both membrane proteins while SLIT2 is both a membrane and secreted protein, suggesting the importance of interactions between tumour cells and their microenvironment in the development of invasion.

The primary down-expressed gene in both the DLKP-I and DLKP-M genelists was hyaluronan and proteoglycan link protein 1 (HAPLN1). The function of HAPLN1 is to link proteoglycans to hyaluronic acid thus participating in the architecture of the extracellular matrix[560]. Interestingly, this gene was previously found to be up-regulated in aggressive melanoma[561] and is often up-regulated in highly metastatic cell lines or aggressive human tumours[562,563]. The expression of HAPLN1 in the DLKP-SQ parental cell line should be confirmed.

The second down-expressed gene in the DLKP-I genelist was interferon-induced transmembrane protein 3. Interferon-induced transmembrane proteins (IFITM) are a family of transmembrane proteins that contain two α helical domains. To date, there are five IFITMs (IFITM1, IFITM2, IFITM3, IFITM5 and IFITM10) that are all clustered on chromosome 11 with less than 2 kb next to each fragment. IFITMs have diverse roles, including the control of cell proliferation, promotion of homotypic cell adhesion, protection against viral infection, promotion of bone matrix maturation and mineralisation, and mediating germ cell development[564,565]. Recent studies identified possible roles of IFITM genes in carcinogenesis. For example, the IFITM1 and

IFITM3 genes were shown to be expressed at higher levels in astrocytoma cells than in normal astrocytes in mice[566]. In addition, IFITM3 expression has been suggested as a preferential marker for ulcerative colitis-associated colon cancer and has been found to be up-regulated in gastric cancer, colorectal tumours, glioma and breast cancer[567-570]. IFITM3 is transcribed in most tissues and highly interferon-inducible.

The third down-expressed gene in the DLKP-I genelist was BACE2. This gene codes for the enzyme beta-secretase-2. BACE2 is a close homolog of BACE1 which is a protease known to be an important enzyme involved in the cellular pathways that some believe lead to Alzheimer's disease. The physiological function and role of BACE2 in Alzheimer's disease is unknown and it has not been reported in cancer. Western blot analysis showed this protein to be down-expressed in the DLKP-I and DLKP-M cells (Edel McAuley, unpublished results).

6.4.4 Microarray lists from DLKP-SQ (Mitoxantrone) and SQ vs. M and SQ vs I clones

An important point to ponder when considering the SQ-Mitox analysis is that there are potentially two ways to approach this data: look at drug resistance and/or invasion. Theoretically however, any differentially expressed genes identified by the microarray analysis of the SQ-Mitox cell lines could relate solely to drug resistance. The DLKP clones with differing levels of invasiveness (derived from the same parent) also offer a unique opportunity to study mechanisms of invasion. These cell lines provide an *in vitro* model of invasion. One of the aims of this thesis was to identify genes involved in the development of an invasive phenotype in lung cancer cell lines.

SQ-Mitox-4P cells may be pre-disposed to an invasive phenotype, already having some of the genes necessary for invasion 'switched on'. They may require only the up regulation of some key genes to push the phenotype into a highly-invasive one. The genes most highly up-regulated in the SQ-Mitox-BCRP-4P *versus* 6P and SQ-Mitox-MDR-4P *versus* 6P genelists may be part of a group of genes essential for invasion. It is significant that three of the primary twelve probesets over-expressed in the SQ-Mitox-BCRP and SQ-Mitox-MDR 4P versus 6P genelist (N-cadherin, ALCAM and SLIT2) were also differentially expressed in the SQ vs I genelists. In addition, integrin alpha V and MMP10 were differentially expressed in the SQ-Mitox 4P vs 6P genelists and confirmed as overexpressed in the DLKP-I and DLKP-M clones. Indeed, N-cadherin expression seems to be associated with the DLKP-I clone only and SLIT2 appears to be associated with the DLKP-M cell lines.

Interestingly the differentially expressed proteins identified in this chapter are all heavily *N*-glycosylated and studies have shown that N-glycosylation is a key regulator of various aspects of tumourigenesis[571]. For example diverse sALCAM forms have been reported in different tissues. A glycosylated 96 kDa form consisting of most of the extracellular domain has been described in epithelial ovarian cancer sera and cells[572] and in epithelial cells[573]. A 60 kDa isoform has been reported in conditioned media of thyroid cancer cells as the result from alternative cleavages and related glycosylation patterns[574,575]. N-glycosylation impacts cell adhesion and cytoskeletal dynamics and studies have shown that the N-glycosylation state of N-cadherin impacts the intrinsic kinetics of cadherin-mediated intercellular binding[576]. In addition although integrin-mediated adhesion to ECM proteins is based on the interaction of specific amino-acid residues, the strength of binding may be modulated by various factors including glycosylation of integrins[577].

6.4.5 Investigation of stem cell markers in DLKP clones

Putative cancer stem cells (CSCs) have been identified in many cancers, often by markers associated with normal stem cells. This is similar with the situation in lung cancer where the accumulated data on side population cells, CD133, CD166, CD44 and ALDH1 are beginning to clarify the true phenotype of the lung cancer stem cell. However, the results presented in this thesis argue against the cancer stem cell model operating in the DLKP cell line. The expression of a small panel of markers for embryonic stem cells was investigated and DLKP clones were found to be negative for KLF4 and NANOG. Very low levels of Oct-4 were seen and c-Myc was present in all of the clones. Myc is a potent oncogene that can promote tumourigenesis in a wide range of tissues[578,579]. c-Myc functions as a master transcriptional regulator of a wide number of target genes that execute various cellular responses, including cell cycle progression, cell differentiation, angiogenesis and apoptosis. It will be critical to determine which cancers follow a stem cell model and which cancers do not, so therapies designed to target rare subpopulations of cells are appropriately tested in patients whose disease is driven by many diverse cancer cells.

6.4.6 Sequenom analysis of DLKP clones

Mutation profiling has the potential to quickly identify which signalling pathway(s) have been co-opted to drive the proliferation of a specific human tumour type. DLKP clones and the cell line DLRP[282] were evaluated for the presence of mutations using sequenome technology (see

table 4.1-2). This mutation panel was designed to look at point mutations. By altering just one amino acid, the entire peptide may change, thereby changing the entire protein. However in this study, in some cases there were two allele insertions and in these cases the mutation is heterozygous. This could lead to the nucleotides'still being read in triplets, but in different frames.

Results showed a two allele insertion within the Sema domain (MET_N375S_A1124G). This heterozygous mutation was notably seen in the DLKP parent, DLKP-SQ and DLKP-I. A missense change was seen in the DLKP-M clone. The MET receptor tyrosine kinase and its cognitive ligand the hepatocyte growth factor (HGF)/scatter factor, play a major role in tumour development. *Krishnaswamy et al.,*[580] showed the majority of the MET mutations to be germline in lung cancer. MET mutation N375S was detected in a high proportion of East Asian samples and was correlated to the incidence of squamous cell carcinoma. The MET-N375S mutation seems to confer resistance to MET inhibition[580]. However, *Shieh et al.,* [581] suggested that the c-Met-N375S sequence variant was not associated with lung cancer susceptibility and prognosis.

There were TP53_G245VDA_G734TAC mutations present in all of the DLKP clones and the DLRP cell line. The tumour suppressor gene *TP53* is frequently mutated in human cancers [582]. Abnormality of the TP53 gene is one of the most significant events in lung cancers and plays an important role in the tumourigenesis of lung epithelial cells. TP53 is mutated in 80% to 100% of small cell lung cancers (SCLC) and 50% to 80% of non-SCLC (NSCLC)[583]. *TP53* gene mutations can occur in association with *EGFR* and *KRAS* mutations[584].

Analysis of the clones showed an AG insertion within the EGFR receptor in the DLKP-SQ only. The DLKP-SQ clone also has the highest levels of phosphorylation of the pERK and so further investigation of this pathway in the clones would be of interest.

6.5 Investigation of the effects of MEK inhibitors on drug resistance and invasion in DLKP

6.5.1 Effects of MEK inhibitors on drug resistance in DLKP

Molecular targeted therapies are of recent interest for the treatment of cancer[585, 586]. These agents can disrupt tumourigenesis by specifically targeting molecular signals regulating cellular proliferation and/or enhancing apoptosis. Molecular targeted therapies may overcome mechanisms by which cancer cells resist traditional cytotoxic chemotherapeutic agents. A class

of molecular targeted compounds called small-molecule protein kinase inhibitors can disrupt mitogenic signaling pathways. Mitogen-activated protein kinase pathways are conserved signaling pathways that enable cells to respond to external stresses and stimuli. The MAPK family includes Jun amino-terminal kinases (JNK1/2/3), p38 proteins, the extracellular signal–related kinases (p44/p42-MAPK or ERK1/2), and ERK5 [587]. The extra-cellular signal-regulated (ERK), mitogen-activated protein kinase (p42/p44 MAPK) pathway is a target that has received significant attention[588].

The p44/p42-MAPK pathway can be activated through G-protein–coupled receptors or receptor tyrosine kinases. Signals travel through the small oncogenic G-protein Ras and ultimately to Raf (or MEK kinase), which then activates the downstream signaling proteins MEK1/2 (MAPK/ERK kinase or MAP kinase kinase) and ERK1/2 (p44/p42-MAP kinase). Activated ERK1/2 control a diverse range of cellular processes through their many substrates (>160) that are located in cellular membranes, the cytoplasm and nucleus. Many of these are transcription factors that are important in cellular proliferation, differentiation, survival, angiogenesis and migration.

The association between the expression of ABC transporter proteins and cell growth signaling has recently generated some interest[589]. Among the complex signaling networks, mitogen-activated protein kinase (MAPK) pathways have been implicated in acquired tumour resistance to chemotherapy[333]. Previous studies of MAPK signaling pathways in cancer models have shown that the p44/p42 MAPK cascade is activated by chemotherapeutic agents such as paclitaxel[334], cisplatin[335], and vinblastine[336] and is involved in acquired resistance to these drugs[590]. In one study, drug-resistant neuroblastoma cells generated from doxorubicin or MDL 28842 demonstrated decreased ERK activation and nuclear translocation[590]. The authors speculated that ERK down-regulation slowed cell cycle progression, affording drug-resistant cells an opportunity to repair drug-induced damage. This implies that inhibiting ERK may grant neuroblastoma cells protection from cytotoxic agents, although this has not been confirmed[590].

Despite demonstrating *in vitro* activity, major *in vivo* limitations were identified for the early first generation MEK inhibitors, PD098059[340] and U0126[339] due to their rapid turnover rate. Although both compounds were deemed unsuitable for clinical consideration due to their pharmaceutical properties, they have proven to be invaluable tools for investigating the Ras/MAPK pathway. In this study, we examined the effects of these signal transduction inhibitors, upon the expression levels of P-gp and BCRP and find that PD98059 up-regulates P-gp expression in the SQ-Mitox–MDR cells and that PD98059 and U0126 diminish the anti-

cancer drug resistance of BCRP, while having no effect on the expression of BCRP protein levels in SQ-Mitox-BCRP cells.

P-gp, BCRP and pMEK expression levels were analysed in DLKP-SQ-Mitox-MDR and DLKP-SQ-Mitox-BCRP cell lines treated with or without the specific inhibitor of MEK, PD09059 and the inhibitor of ERK, U0126. The PNP assay was used to determine the susceptibility of SQ-Mitox-MDR and SQ-Mitox-BCRP to mitoxantrone, treated with or without PD98059 and U0126. The cytotoxicity of mitoxantrone was found to be significantly potentiated by PD98059 and U0126 in DLKP-SQ-Mitox-BCRP. The cytotoxicity of mitoxantrone was found to be significantly decreased by PD98059 but unchanged by U0126 in DLKP-SQ-Mitox-MDR.

Table 6.5-1: Summary of Effects of MEK inhibitors on drug resistant DLKP cell lines.

MEK Inhibitor	SQ-MitoxBCRP	SQ-Mitox-MDR	DLKP-SQ	DLKP-A
PD98059	++	++	+	+
U0126	++	+	_	_
AZD6244	ns	+	_	_

++ very significant; + significant; ns: not significant

Despite the fact that the cytotoxicity of mitoxantrone was found to be significantly potentiated by PD98059 and U0126 in DLKP-SQ-Mitox-BCRP, Western blot analysis revealed that there was no change in BCRP protein expression. This would suggest that up-regulation of BCRP is not the only molecular change in this cell line compared to the parental cell line. There are other lines of evidence to support this argument. Previous studies in this laboratory[591] showed that the IC_{50} of epirubicin alone was 40nM and in combination with elacridar, this reduced to 28nM. This suggests that DLKP-Sq/Mitox-BCRP contains another resistance mechanism. In addition, inhibition of BCRP with elacridar increased the toxicity of dasatinib in DLKP-Sq/Mitox-BCRP to beyond that of the parental cell-line. Src kinase, one of the targets for dasatinib, is upstream of the Raf-MEK pathway and up-regulation of BCRP as a response to mitoxantrone may also up-regulate *p*-src, a target of dasatinib, thus making the resistant BCRP expressing DLKP-Sq/Mitox more sensitive to dasatinib. It has been shown by others that inhibition of the mitogen-activated protein kinase pathway results in the down-regulation of P-gp[346], BCRP[347], MRP1 and MRP3[348]. In the case of BCRP positive cells, there are mixed reports of MEK inhibitors transcriptionally upregulating BCRP but simultaneously enhancing its protein degradation[347]. *Lin et al.,*[348]

showed that MEK inhibitors reduced MRP1 as well as MRP3 expression in hepatocellular carcinoma.

Table 6.5-2 provides a list of well-known and novel signaling pathway inhibitors that alter P-gp function in drug-resistant cells. Many of these pathways (e.g., Ras/MAPK, JNK, p38 MAPK, protein kinase A- and PKC-related proteins, and PI3K) involve cell proliferation status, mediate apoptotic signaling, or generate the stress response. To our knowledge, this is the first report that inhibition of a signaling pathway can increase P-gp expression.

There are only two reports in the literature of a down-regulation of the ERK1/ERK2 proteins resulting in an increase in P-glycoprotein-mediated multidrug resistance. *Wartenberg et al.,*[411] found that UO126 induced upregulation of P-glycoprotein as well as HIF-1 under control conditions that was even more increased under conditions of hyperthermia. These results point towards the notion that inactivation of JNK as well as ERK1,2 are a prerequisite for the induction of a MDR phenotype in multicellular prostate tumour spheroids and that active JNK as well as ERK1,2 may be involved in negative regulation the *mdr-1* and *HIF-1* genes. They previously demonstrated that in small tumour spheroids that are drug sensitive and devoid of P-glycoprotein expression a high level of endogenous JNK and ERK1,2 activity occurs, whereas only minor activation of p38 was observed. Also, *Yan et al.,*[592] reported a down-regulation of ERK 1/2 activity in P-glycoprotein-mediated multidrug resistant hepatocellular carcinoma cells.

There are a variety of mechanisms by which this could occur. In the first case, the ERK1/2 cascade is involved in the phosphorylation of a number of proteins, including transcription factors involved in determining cell survival and death[593]. Studies on the role of signal crosstalk in the transcriptional control of ABCB1 indicate that ABCB1 is a target of the Ras/Raf signalling pathway[594]. PD098059 could therefore reverse changes in drug resistance mediated by this pathway directly. Alternatively, there may be direct cross-talk between the ERK1/2 signalling cascade and MDR-1 function i.e. that activation of the ERK1/2 either directly or indirectly affects the activity of the MDR-1 protein, by changing its phosphorylation state for example. In a minireview by Callaghan *et al.,* 2014[595] they discuss the implications of the phosphorylation of the P-gp protein. The protein has of numerous PKC consensus motifs within in the linker region. Moreover, it has been demonstrated that P-gp is phosphorylated by PKC at several of these motifs within the linker region. A number of studies examined the phosphorylation status of P-gp in cell lines selected for drug resistance and suggested that it played a key role in the resistant phenotype[595,596].

It is feasible that the effects of PD98059 are by an alternative unknown mechanism. However, these would still be linked to *MDR-1* expression. The fact that PD098059 could increase drug resistance and that the alternative MEK inhibitor U0126 had no significant effect indicates that there may be an additional targets for this chemical. This is substantiated by evidence that PD098059 can interact with other cellular targets such as the aryl hydrocarbon receptor and inhibit other signalling cascades such as those mediated by ERK 5 and the COX1/2 pathways for instance[597]. In addition, *Zuber et al.,* [598] report that in a genome-wide survey of Ras transformation targets, PD098059 treatment of cells has effects on 61 Ras targetted genes, blocking down-regulation of 36 genes and up-regulation of 25 targets.

Increased MEK hyperphosphorylation has been reported in p-gp over-expressing cells. Increased P-MEK levels have been reported after treatment with other MEK inhibitors, such as CI-1040 and AZD6244; therefore, MEK phosphorylation appears to be a common response to MEK inhibitors and may be due to interference with the feedback regulation of the Ras-Raf-MEK-ERK pathway[599]. The increase in MEK phosphorylation may overwhelm the ability of the MEK inhibitor to suppress P-ERK, thus allowing reactivation of the targeted pathway, thereby inducing P-gp.

Further investigation of the role of the MAPK kinase pathway in the SQ-Mitox-MDR and SQ-Mitox-BCRP cells is warrented. The regulatory mechanisms underlying the expression of ABC transporters, including P-gp and BCRP, still remain to be clarified.

Table 6.5-2: Selection of novel compounds and inhibitors found to reverse P-gp MDR by altering signal transduction (Adapted from Callaghan *et al.*, 2014[595])

Compound	Probable Pathway or Target	Reference
FTI-277,U0126 & 17AAG	MAPK/ERK, HSP90	Katayama *et al.,* 2007[346]
REM	JNK1/2	Choi *et al.*, 2013[600]
SC-51089	Prostaglandin E2 receptor	Pekcec et al., 2009[601]
PHII-7idarubicin derivative	JNK phosphorylation	Peng et al., 2013[602]
siRNA Bile extract	Wnt/β-catenin	Shen *et al.,* 2013[603]
PEITC (phenethyl isothiocyanate)	PI3K-Akt	Tang *et al.*, 2013[604]
Dioscin	NF-kB	Wang et al., 2013[605]
Parthenolide	NF-kB and Hsp70	Xin et al., 2013[606]
Procyanidin	NF-kB and MAPK/ERK	Zhao et al., 2013[607]

6.5.2 Effects of MEK inhibitors on invasion in DLKP

MEK Inhibitor	DLKP-I	DLKP-M	SQ-Mitox-BCRP-6P
U0126	-	++	++

Previous studies in the literature have indicated that PD98059 and U0126 suppresses the invasiveness of squamous cell carcinoma [337] and melanoma cells[338]. Could these inhibitors affect the invasion of the DLKP clones? The role of MAPK kinase signalling in cell invasion was investigated using the MEK1/2 inhibitor U0126. U0126 showed no effect on invasion of DLKP-I under the conditions tested. The effect on cell invasion of DLKP-M was very evident, with U0126 inhibiting invasion by approximately 50% at 5 and 10 μM. Data shown as the mean ± 3 experiments. The inhibitor, U0126 had no effect on proliferation at the concentrations tested. The p44/p42 MAPK pathway intermediate ERK was subsequently shown to be expressed in all three DLKP clone types. However, the DLKP-SQ and DLKP-M cells showed high levels of endogenous ERK activation compared to DLKP-I and DLKP parent (figure 5.2-5). Interestingly, microarray results for the SQ vs M clones showed a 1.63-fold change in DLKP-M for MAPK1.

Post-translational modifications are important processes in the regulation of protein activity. One of the primary and reversible protein modifications is phosphorylation. It is estimated that nearly 30% of all the proteins in a eukaryotic cell are transiently phosphorylated and by inference under dynamic control. The phosphorylation patterns of proteins within a cell are determined by the sum of all the protein kinases active at that point in time. These protein kinases are themselves also under active dynamic control and are principally involved in signalling pathways which are responsible for diverse processes such as those involved in angiogenesis, apoptosis, cell migration and cell cycle control. It is easy to appreciate that dysregulation at any point in this system could upset the normal homeostatic mechanisms within a cell and lead to a series of molecular events culminating in a malignant phenotype.

Dysregulation of normal protein kinase activity may simply occur by a mutation that renders the kinase constitutively active (or a phosphatase inactive or a combination of reversal activities). Sequenom analysis for example revealed mutations in EGFR, Met and PIK3R1 which may help explain the higher levels of ERK activation and effects of the MEK inhibitors on the invasiveness of the DLKP-M cell line.

However, it is not possible to relate regulation through phosphorylation to levels of mRNA (microarray results). Therefore, the investigation of MAPKs and intracellular signaling of DLKP-1 and DLKP-M cells under U0126 treatment was extended using a commercial array kit (Human Phospho-MAPK array kit), which screens for the activation of 28 kinases including 9 MAPKs. The array kit allows the recognition of specific phosphorylation sites (amino acid residues) related to the activations of MAPKs and signaling proteins. JNK, p38 and p53 were the three phosphorylated proteins with the most significant changes in untreated DLKP-I cells compared to the untreated DLKP-M cells. The JNK stress pathways participate in many different intracellular signalling pathways that control a spectrum of cellular processes, including cell growth, differentiation, transformation, or apoptosis. Particularly relevant to this study is the connection between JNK, p53 and p38. JNK binds to and phosphorylates p53 and in most cases, p38-MAPKs are simultaneously activated with JNKs.

Following U0126 treatment, DLKP-M cells showed increased phosphorylation in p53 and slightly increased phosphorylation in p38 and JNK, which suggests induced signaling in the p38 and JNK pathways. Interestingly, U0126 treated DLKP-I cells do not present a significant increase in any of the intracellular signalling proteins.

Results from this study have demonstrated that MEK inhibitor treatment of DLKP-M had a considerable effect on its invasiveness. The resistance of DLKP-I cells to MEK inhibition in the cell invasion assay indicates the MAPK targeted treatment may be unsuccessful against this subtype within a heterogeneous DLKP tumour. MAPK plays a major role in inducing proteolytic enzymes that degrade the basemant membrane, enhancing cell migration, initiating several pro-survival genes and maintaining growth. Activated MAPK pathways have been detected in many tumours including breast, lung, colon and kidney, implicating it in tumour progression and metastasis[608]. Understanding the differences in DLKP type MAPK expression/activity, MAPK signaling and the functional response to MEK activity may help to further elucidate the phenotype and behavioural traits of DLKP.

These experiments suggest that the DLKP cell line does not adopt a hierarchy consisting of a minor subpopulation of tumourigenic cells and a majority population of non-tumourigenic cells. Markers were successfully identified that robustly distinguish the invasive DLKP-I and DLKP-M clones from the examination of genes which were over-expressed in the microarray results for both the DLKP clones and the mitoxantrone resistant DLKP-SQ cell lines. All of the clones had the capacity to grow *in vivo* (unpublished results). The phenotypically distinct and poorly invasive DLKP-SQ cell line (in vitro) had the capacity to form tumours *in vivo*. This suggests that the poorly invasive DLKP-SQ cell line appeared to undergo reversible changes *in vivo*. Thus, tumourigenic capacity is not restricted to a small subpopulation of the DLKP cell line but is shared among all three of the DLKP-SQ, DLKP-I and DLKP-M clones.

While the morphology of each of the clones is stable, the DLKP-I clone did not cluster well – two clustered with DLKP-SQ and one clustered with the DLKP-M clones. The Sequenom data indicated that there might be important mutational differences while the experiments with MEK inhibitors indicate pathway activation at a post DNA level. The clones, being from the same tumour may interconvert[609]. As *Floor et al.,*[539] pointed out, hallmarks are often interpreted as applying to a canonic cancer cell, or equally to all cells within a cancer. In their article, they discuss the separate concepts of causes, oncogenic events, signal transduction programs, and hallmarks. They argue that there is no unimodal relation between these concepts but a complex network of interrelations that vary in different cells, between cells, and at different times in any given cell.

6.6 Summary and Conclusions

An overview of the current state of research in the field is presented in Chapter 1.

Chapter 2 presents details of materials and methods used to generate the data from the numerous studies described herein.

Chapter 3 characterises the resistant phenotype of mitoxantrone resistant lung cancer cell lines and describes the establishment of two novel cell lines resistant to mitoxantrone, one overexpressing the BCRP and the other the P-gp efflux pumps. Resistance occurred early on in the drug pulsing process. These cell lines were selected in an identical manner in the same study using the same source of DLKP-SQ cells. The strategy of deriving isogenic drug resistant cell lines from one cell line is a method that can reduce variability due to intrinsic genetic differences between cell lines. The establishment of multi-drug resistant DLKP-SQ-Mitox cell lines has provided a powerful tool for further study of multi-drug resistant phenotypes. It is anticipated that these cell lines will continue to be useful models for the study of new modulators and markers of resistance, ultimately aimed at improving the outcome for patient acquired drug resistance that is often observed in the clinical setting.

Chapter 4 describes the molecular characterisation of morphologically and behaviourly distinct populations of the lung cancer cell line DLKP using mRNA expression microarray analysis. DLKP-SQ and its BCRP- and P-gp–overexpressing, mitoxantrone resistant variant were used to investigate lung cancer drug resistance and invasion potential *in vitro*.

Chapter 5 describes the effect of MEK inhibitors on DLKP drug resistance and invasion. The association between the expression of ABC transporter proteins and cell signalling pathways was first explored. Inhibition of MEK with the MEK inhibitor PD98059 led to an up-regulation of P-gp expression in SQ-Mitox suggesting a role for the MAPK kinase pathway in regulation of P-gp. There is a need for caution in the use of such inhibitors as co-therapeutic options designed to reverse multidrug resistance in cancer because cancer cell survival may be increased under certain conditions. The MAPK kinase pathway may also play a role in DLKP invasion.

6.6.1 Development of P-gp- and BCRP-mediated mitoxantrone resistant cell lines.

1. Two mitoxantrone resistant variants of the DLKP-SQ cell line were established one with P-glycoprotein (SQ-Mitox-MDR-4th pulse) and one with BCRP (SQ-Mitox-

BCRP-4th pulse) overexpression. These two cell lines were selected from the same cell population and under identical conditions.

2. Over-expression of P-gp and BCRP was revealed by microarray analysis and was confirmed by RT-PCR and Western blotting.

3. *SQ-Mitox-MDR-4th pulse cells* – cross resistance profiling showed resistance to: mitoxantrone (320×); taxol (303×); epirubicin (179×); vinblastine (128×); irinotecan (5.8×); and VP-16 (1727×), but displayed no significant resistance to cisplatin (0.79×) or 5-FU (1.74×). *SQ-Mitox-BCRP-4th pulse cells* – cross resistance profiling showed resistance to mitoxantrone (210×) and irinotecan (4.03×) but displayed no significant resistance to taxol (0.67×), epirubicin (1.34×), vinblastine (1.07×), cisplatin (0.63×) VP-16 (1.25×) or 5-FU (2.25×).

4. When P-gp was silenced in SQ-Mitox-MDR cells and BCRP was silenced in SQ-Mitox-BCRP cells, an increase in sensitivity to mitoxantrone was observed across all concentrations. Because of the very high level of overexpression of BCRP and P-gp respectively in the two resistant variants, only partial knockdown could be achieved using siRNAs. There was a corresponding effect on resistance, which supported a role for these pumps in resistance, but because complete knockdown was not possible, the results do not allow us to determine whether or not these are the only, or even the main, determinants of resistance, although the Elacridar data would suggest that this is the case. Elacridar, however, is less specific in its effect than an siRNA would be.

5. Western blots confirmed that P-gp siRNAs and BCRP siRNAs reduced the expression of P-gp and BCRP respectively in the cell lines. A reduced amount of the protein was observed with both siRNAs for BCRP and P-gp. In contrast, with the addition of 443 nM Elacridar, both ABCG2-mediated and ABCB1- mediated resistance to mitoxantrone was reversed.

6. Microarray analysis was performed in DLKP-SQ-Mitox-BCRP (4th pulse) and DLKP-SQ-Mitox-P-gp (4th pulse). Functional annotation analysis of probesets exclusively differentially expressed in the BCRP overexpressing cell line revealed that the most significant GO categories were related to RNA processing, cellular response to stress and cell cycle. Functional annotation analysis of genes

exclusively and differentially expressed in the P-gp overexpressing cell line revealed that the most significant GO categories were related to chromatin organisation and modification and embryonic morphogenesis.

7. Gene copy number analysis revealed no alterations in either the BCRP or P-gp copy number.
8. 5-azacytidine treatment of the DLKP-SQ, SQ-Mitox-BCRP and SQ-Mitox-MDR cells had no effect on BCRP or P-gp protein expression. DNA methylation analysis of the BCRP over-expressing cell line revealed that the promoter of BCRP was unmethylated in both the DLKP-SQ and SQ-Mitox-BCRP cells.
9. miRNA analysis identified 4 miRNAs with differential expression relating to mitoxantrone and/or BCRP expression in the SQ-Mitox-BCRP cell line. The miRNAs were involved in tumour suppression, cell proliferation and Wnt signalling. miRNA analysis identified 4 miRNAs (of unknown function) with differential expression relating to mitoxantrone and/or P-gp expression in the SQ-Mitox-MDR cell line.
10. Proteomic analysis identified 28 proteins with differential expression relating to mitoxantrone exposure. The majority are involved in glycolysis, protein turnover and translational elongation. DSCAM protein was investigated. Intense immunoreactivity was observed in squamous and adenocarcinoma and where immunoreactivity was observed in the primary tumour, staining was also observed in matched metastatic tumours in the same patients. Small cell carcinomas did not show any staining. Interestingly, in metastatic tumours from small cell carcinomas, weak staining was observed in 3/6 even though the primary tumours were negative.

In summary, overexpression of P-gp, and BCRP, play an important role in drug resistance in SQ-Mitox cells. The combination of microarray and proteomic techniques and suitable *in vitro* models presents an excellent setting for dissecting the processes and players involved in drug resistance. These sublines may also prove to be useful models for the study of new modulators of resistance aimed at improving the outcome of acquired drug resistance.

6.6.2 Establishment of drug resistant invasive DLKP-SQ variants

Many of the model systems used to study the link between drug resistance and invasion bypass the earliest events. Consequently, the critical first step in the transition from a preinvasive to an invasive phenotype during the development of drug resistance is less well studied than later stages. DLKP-SQ-Mitox-BCRP and DLKP-SQ-Mitox-MDR were previously established by mitoxantrone pulsing. These cell lines were pulsed two more times to generate the DLKP-SQ-Mitox-BCRP-6P and DLKP-SQ-Mitox-MDR-6P cell lines. A stable, higher drug resistant cell population, DLKP-SQ-Mitox-BCRP-6P (isolate 2) was subsequently isolated from the DLKP-SQ-Mitox-BCRP-6P cell line.

1. The SQ parent displayed low invasion and low drug resistance.
2. Successive drug pulsing (in both BCRP and MDR1 overexpressing cell lines) isolated the 4^{th} pulse cell population, which displayed high drug resistance but low invasion, similar to the SQ parent.
3. The 6^{th} pulse cell population displayed high invasion and similar resistance to the 4^{th} pulse cell population. The invasive phenotype was lost upon freezing and thawing.
4. A sub-population (6^{th} pulse) of the BCRP over-expressing cells was subsequently isolated. Careful observation of these cells revealed morphological differences, characterised by large numbers of spiky, elongated cells. This sub-population of cells was believed to be more invasive and more resistant than those observed to date. Further investigation of these cells showed that indeed, they did have a higher IC_{50} and higher levels of BCRP protein.
5. Microarray analysis gave two gene lists – DLKP-SQ-Mitox-BCRP-4P versus DLKP-SQ-Mitox-BCRP-6P cells (Genelist 1) and DLKP-SQ-Mitox-MDR-4P versus DLKP-SQ-Mitox-MDR-6P cells (Genelist 2). PANTHER pathway analysis revealed that the most significant pathways were related to Wnt signalling, inflammation, integrin signalling and p53 pathways in both Genelist 1 and Genelist 2. Twelve genes were identified as common between the up-regulated gene lists. Different genes functionally involved in cell adhesion, axon guidance and wnt signaling were induced during the transition from the pre-invasive to the invasive phenotype.

6. Western blot and immunofluorescence validation confirmed the upregulation (in the SQ-Mitox-BCRP- 4P versus SQ-Mitox-BCRP-6P cell lines) of the proteins, integrin alpha V, BCHE, ALCAM, N-cadherin. Of particular interest is the identification of the SLIT2/ROBO2 signaling pathway in the invasive, drug resistant 6th pulse cell line. The cell adhesion molecule, ALCAM increased with increased BCRP expression and was barely detectable in the Pgp over-expressing cell lines.
7. The acquisition of drug resistance is accompanied by an increased activity of MMP-2 in DLKP-SQ cells and treatment with an MMP blocking antibody against MMP-2 inhibits the invasiveness of drug-resistant SQ-Mitox-BCRP-6P cells.
8. siRNA knockdown experiments suggest that integrin alpha V plays a role in the invasive phenotype observed *in vitro*.
9. Treatment with a MAP kinase inhibitor, U0126, inhibits the invasiveness of drug-resistant SQ-Mitox-BCRP-invasive-6P and the DLKP-M cells, suggesting a role for the MAPK kinase pathway in these cell lines. Western blot analysis revealed that the DLKP-M cells showed higher levels of endogenous ERK activation compared to the DLKP-I and DLKP parent cells and this might help explain the significant inhibition of DLKP-M invasiveness with the inhibitor, U0126.

In summary, mitoxantrone treatment can increase invasiveness of the surviving DLKP cells. An important question concerns exactly what mechanisms link mitoxantrone resistance to cell invasion, *i.e.* what events are triggered by mitoxantrone treatment that lead to increased cell invasion and metastasis? The occurrence of an elevated invasive capability and an acquired multiple drug resistance in the SQ-Mitox-BCRP cells suggest strong links between drug resistance and invasion. Future work should focus on whether a common transcription factor exists to turn on multiple sets of genes. It is plausible that proteins that act as drug sensors such as those of the nuclear receptor family could act to initiate the first events that result in gene transcription and may ultimately be responsible for mitoxantrone resistance. The activation of BCRP genes and those responsible for increased cell invasion, e.g. MMP genes would be amongst a series of events leading to the resistant/invasive phenotype.

6.6.3 Characterisation of clonal subpopulations of DLKP

Heterogeneity within tumours may signify the existence of sub-populations with different and inherent invasive / metastatic and drug resistance potentials[143]. The DLKP cell line contains at least three morphologically distinct subpopulations with different levels of invasiveness. Microarray analysis was used to generate gene lists that were specific to an invasive phenotype, in order to identify genetic markers for invasion.

1. The DLKP-I and DLKP-M cells exhibit higher adhesiveness to fibronectin and vitronectin.
2. Seven genes were shown to be differentially expressed in the invasive DLKP-M and DLKP-I and poorly invasive DLKP-SQ cells. These included integrin αV, SLIT2/ROBO2, ALCAM, piccolo, MMP-2 (from previous studies) and MMP-10.
3. Western blotting showed that:
    a. Expression of ALCAM was undetectable in the DLKP-SQ cells, low in DLKP-M cells and highly expressed in the DLKP-I cells.
    b. Expression of SLIT2 was undetectable in the DLKP-SQ and DLKP-I cells but highly expressed in the DLKP-M cells.
    c. Expression of integrin αV was undetectable in the DLKP-SQ but highly expressed in the DLKP-I and DLKP-M cells.
4. Immunofluorescence demonstrated that:
    a. ROBO2 was detected in all of the clones with strongest expression in the DLKP-M cells.
    b. N-cadherin is overexpressed in the DLKP-I clone only.
    c. MMP-2 and MMP-10 was detected in all of the cell lines.
    d. Piccolo was highly expressed in the DLKP-I cells with some cells in the DLKP-M population also showing strong expression of the protein.
5. The DLKP-I and DLKP-M cells expressed high levels of MMP-2 and MMP-10 whereas the parental cells did not, as detected by zymography.
6. In the DLKP-I and DLKP-M cell line, invasion is decreased with blocking of MMP-2 with no effect in MMP-10 treated cells.

7. Cell adhesion molecules such as ALCAM and N-cadherin may be associated with DLKP-I while axon guidance molecule SLIT2, with DLKP-M. These proteins may be possible markers which are capable of distinguishing between the clones.

6.6.4 MEK inhibitors and anti-cancer drug resistance of SQ-Mitox cells

Cancer often arises when normal cellular growth goes awry due to defects in critical signal transduction pathways. A growing number of inhibitors that target specific components of these pathways are in clinical use, but the success of these agents has been limited by the resistance to inhibitor therapy that ultimately develops.

Combination treatment with (1) mitoxantrone and PD98059 and (2) mitoxantrone and U0126, significantly reversed drug resistance in the SQ-Mitox-BCRP cell line. However, inhibition of the MAPK kinase pathway had no effect on BCRP expression levels, suggesting that down-regulation of BCRP is not the only molecular change in this cell line responsible for increasing its mitoxantrone sensitivity.

In contrast, combination treatement with (1) mitoxantrone and PD98059, but not (2) mitoxantrone and U0126, significantly increased drug resistance in the SQ-Mitox-MDR cell line. That is, the inclusion of the small molecule inhibitors significantly enhanced the survivability of the cell line when co-treated with mitoxantrone. The level of P-gp protein was increased after treatment with PD98059, suggesting that PD98059 enhanced the expression of the P-gp protein. Supression of P-gp with the P-gp inhibitor elacridar, ameliorated the effect, confirming that P-gp was responsible for the enhanced PD98059 induced drug resistance.

Inhibition of MEK had a small but not statistically significant effect on the drug resistance profile of DLKP-A. DLKP-A cells may contain a different mechanism of regulation of P-gp to the SQ-Mitox cells as also suggested by the copy number assay results with a copy number of 6 for *MDR1*, a far higher number than that exhibited by the other cell lines.

The complexity of cell signaling pathways has profound implications on our understanding of tumour cell behavior and on our ability to use this knowledge for better treatmemts in the clinical setting. Cancer cells undergo multiple genetic changes, and continuously evolve in response to selective pressures. Even if an activated pathway can be blocked by an inhibitor (e.g. as in the case of SQ-Mitox-MDR cells treated with PD98059), tumour cells may evade the inhibitor by activating other pathways. Care must therefore be used in the interpretation of experiments with

inhibitors, as is the case with all other pharmacological tools. It will always be more appropriate to conduct experiments with at least two pharmacologically distinct inhibitors where possible and to confirm the results with other cell types.

6.6.5 Investigation of the effects of MEK inhibitors on invasion of DLKP

MEK inhibitor treatment of DLKP-M had a considerable effect on its invasiveness. The resistance of DLKP-I cells to MEK inhibition in the cell invasion assay indicates the MAPK targeted treatment may be unsuccessful against this subtype within a heterogeneous DLKP tumour. During tumour development and progression, aberrations in cellular behaviour are strongly correlated with alterations in kinase expression and/or activity. The identification of novel kinase targets which may play a pivotal role in the progression of DLKP cancer invasion may offer new therapeutic vantage points. Functional evaluation of the DLKP-I and DLKP-M clones, using immunoblotting to validate the Sequenom analysis as well as assessment of response to kinase inhibitor treatment will be carried out explain how cancer cells metastasize.

6.6.6 Conclusions

The work presented in this thesis has a very wide scope and as we have seen, throws up further questions as to the mechanism of action with respect to the molecular events that contribute towards resistance and metastasis. Cancer is caused by genetic changes in genes which results in defects to regulatory circuits which give cancer cells survival and growth advantages. As a result, populations of tumour cells can display variability in their phenotypes with the ability to be able to adapt and become resistant to therapeutics allowing them to invade into tissues and metastase to others. The mitoxantrone resistant cell line model demonstrates that the same parent cell line treated with the same chemotherapy agent can lead to the development of two different mechanisms of resistance. This demonstrates that individual cells within a cancer, even though initially clonally derived from one or a small population to begin with, can exhibit high levels of heterogeneity with respect to drug resistance. Even if tumours are initially not resistant to a specific anticancer treatment, this heterogeneity with selective pressure imposed by potent anticancer drugs can result in overgrowth of drug-resistant variants with the rapid acquisition of drug resistance. Clinically, this heterogeneity has been associated with poor prognosis and treatment resistance in cancer patients. Understanding this heterogeneity is central to the development of targeted, cancer-preventative and-therapeutic interventions. The DLKP cell line

is a good example of this heterogeneity. The genes ALCAM, SLIT2 and N-cadherin have been identified as potential biomarkers capable of distinguishing between the clones. Their protein products may serve as quantitative markers in future studies of the DLKP cells and may be used more effectively to study aspects of the tumourigenic process with a clearer understanding of how information obtained from these cells may be applied *in vivo*.

REFERENCES

1. National Cancer Registry Ireland. Cancer in Ireland 1994-2011: Annual report of the National Cancer Registry 2014. 96 (2014).
2. Ferlay, J. *et al.* Estimates of worldwide burden of cancer in 2008: GLOBOCAN 2008. *Int J Cancer.* **127**, 2893-917. doi: 10.1002/ijc.25516. (2010).
3. Schiller, J.H. *et al.* Comparison of four chemotherapy regimens for advanced non-small-cell lung cancer. *N Engl J Med.* **346**, 92-8. (2002).
4. Jemal, A. *et al.* Global cancer statistics. *CA Cancer J Clin.* **61**, 69-90. doi: 10.3322/caac.20107. Epub 2011 Feb 4. (2011).
5. Rosti, G. *et al.* Small cell lung cancer. *Ann Oncol.* **17**, ii5-10. (2006).
6. Hecht, S.S. Cigarette smoking and lung cancer: chemical mechanisms and approaches to prevention. *Lancet Oncol.* **3**, 461-9. (2002).
7. Thun, M.J. *et al.* Lung cancer occurrence in never-smokers: an analysis of 13 cohorts and 22 cancer registry studies. *PLoS Med.* **5**, e185. doi: 10.1371/journal.pmed.0050185. Epub 2008 Sep 9. (2008).
8. Chua, Y.J., Steer, C. & Yip, D. Recent advances in management of small-cell lung cancer. *Cancer Treat Rev.* **30**, 521-43. (2004).
9. Hoffman, P.C., Mauer, A.M. & Vokes, E.E. Lung cancer. *Lancet.* **355**, 479-85. (2000).
10. Subramanian, J. & Govindan, R. Lung cancer in never smokers: a review. *J Clin Oncol.* **25**, 561-70. (2007).
11. Raz, D.J., He, B., Rosell, R. & Jablons, D.M. Bronchioloalveolar carcinoma: a review. *Clin Lung Cancer.* **7**, 313-22. (2006).
12. Rom, W.N., Hay, J.G., Lee, T.C., Jiang, Y. & Tchou-Wong, K.M. Molecular and genetic aspects of lung cancer. *Am J Respir Crit Care Med.* **161**, 1355-67. (2000).
13. Beadsmoore, C.J. & Screaton, N.J. Classification, staging and prognosis of lung cancer. *Eur J Radiol.* **45**, 8-17. (2003).
14. Dancey, J. & Le Chevalier, T. Non-small cell lung cancer: an overview of current management. *Eur J Cancer.* **33**, S2-7. (1997).
15. Socinski, M.A. Cytotoxic chemotherapy in advanced non-small cell lung cancer: a review of standard treatment paradigms. *Clin Cancer Res.* **10**, 4210s-4214s. (2004).
16. Riedel, R.F. & Crawford, J. Small-cell lung cancer: a review of clinical trials. *Semin Thorac Cardiovasc Surg.* **15**, 448-56. (2003).
17. Lee, W. *et al.* The mutation spectrum revealed by paired genome sequences from a lung cancer patient. *Nature.* **465**, 473-7. doi: 10.1038/nature09004. (2010).
18. Larsen, J.E. & Minna, J.D. Molecular biology of lung cancer: clinical implications. *Clin Chest Med.* **32**, 703-40. doi: 10.1016/j.ccm.2011.08.003. Epub 2011 Oct 7. (2011).
19. Cooper, W.A., Lam, D.C., O'Toole, S.A. & Minna, J.D. Molecular biology of lung cancer. *J Thorac Dis.* **5**, S479-S490. (2013).
20. Li, T., Kung, H.J., Mack, P.C. & Gandara, D.R. Genotyping and genomic profiling of non-small-cell lung cancer: implications for current and future therapies. *J Clin Oncol.* **31**, 1039-49. doi: 10.1200/JCO.2012.45.3753. Epub 2013 Feb 11. (2013).
21. West, L. *et al.* A novel classification of lung cancer into molecular subtypes. *PLoS One.* **7**, e31906. doi: 10.1371/journal.pone.0031906. Epub 2012 Feb 21. (2012).
22. Weinstein, I.B. & Joe, A. Oncogene addiction. *Cancer Res.* **68**, 3077-80; discussion 3080. doi: 10.1158/0008-5472.CAN-07-3293. (2008).
23. Bunn, P.A., Jr. & Franklin, W. Epidermal growth factor receptor expression, signal pathway, and inhibitors in non-small cell lung cancer. *Semin Oncol.* **29**, 38-44. (2002).
24. Downward, J. Targeting RAS signalling pathways in cancer therapy. *Nat Rev Cancer.* **3**, 11-22. (2003).

25. Karnoub, A.E. & Weinberg, R.A. Ras oncogenes: split personalities. *Nat Rev Mol Cell Biol.* **9**, 517-31. doi: 10.1038/nrm2438. (2008).
26. Harris, R.E., Zang, E.A., Anderson, J.I. & Wynder, E.L. Race and sex differences in lung cancer risk associated with cigarette smoking. *Int J Epidemiol.* **22**, 592-9. (1993).
27. Aylon, Y. & Oren, M. New plays in the p53 theater. *Curr Opin Genet Dev.* **21**, 86-92. doi: 10.1016/j.gde.2010.10.002. Epub 2010 Nov 4. (2011).
28. Toyooka, S., Tsuda, T. & Gazdar, A.F. The TP53 gene, tobacco exposure, and lung cancer. *Hum Mutat.* **21**, 229-39. (2003).
29. Greenblatt, M.S., Bennett, W.P., Hollstein, M. & Harris, C.C. Mutations in the p53 tumor suppressor gene: clues to cancer etiology and molecular pathogenesis. *Cancer Res.* **54**, 4855-78. (1994).
30. Hainaut, P. & Pfeifer, G.P. Patterns of p53 G-->T transversions in lung cancers reflect the primary mutagenic signature of DNA-damage by tobacco smoke. *Carcinogenesis.* **22**, 367-74. (2001).
31. Heymach, J.V., Nilsson, M., Blumenschein, G., Papadimitrakopoulou, V. & Herbst, R. Epidermal growth factor receptor inhibitors in development for the treatment of non-small cell lung cancer. *Clin Cancer Res.* **12**, 4441s-4445s. (2006).
32. Pirker, R. Novel drugs against nonsmall-cell lung cancer. *Curr Opin Oncol* **8**, 8 (2014).
33. Shames, D.S. & Wistuba, II. The evolving genomic classification of lung cancer. *J Pathol.* **232**, 121-33. doi: 10.1002/path.4275. (2014).
34. Di Costanzo, F. *et al.* Bevacizumab in non-small cell lung cancer. *Drugs.* **68**, 737-46. (2008).
35. Sasaki, T., Rodig, S.J., Chirieac, L.R. & Janne, P.A. The biology and treatment of EML4-ALK non-small cell lung cancer. *Eur J Cancer.* **46**, 1773-80. doi: 10.1016/j.ejca.2010.04.002. Epub 2010 Apr 24. (2010).
36. Longley, D.B. & Johnston, P.G. Molecular mechanisms of drug resistance. *J Pathol.* **205**, 275-92. (2005).
37. Biedler, J.L. & Riehm, H. Cellular resistance to actinomycin D in Chinese hamster cells in vitro: cross-resistance, radioautographic, and cytogenetic studies. *Cancer Res.* **30**, 1174-84. (1970).
38. Juliano, R.L. & Ling, V. A surface glycoprotein modulating drug permeability in Chinese hamster ovary cell mutants. *Biochim Biophys Acta.* **455**, 152-62. (1976).
39. Riehm, H. & Biedler, J.L. Cellular resistance to daunomycin in Chinese hamster cells in vitro. *Cancer Res.* **31**, 409-12. (1971).
40. Dano, K. Cross resistance between vinca alkaloids and anthracyclines in Ehrlich ascites tumor in vivo. *Cancer Chemother Rep.* **56**, 701-8. (1972).
41. Dano, K. Active outward transport of daunomycin in resistant Ehrlich ascites tumor cells. *Biochim Biophys Acta.* **323**, 466-83. (1973).
42. Gottesman, M.M. & Pastan, I. Biochemistry of multidrug resistance mediated by the multidrug transporter. *Annu Rev Biochem.* **62**, 385-427. (1993).
43. Bellamy, W.T. P-glycoproteins and multidrug resistance. *Annu Rev Pharmacol Toxicol.* **36**, 161-83. (1996).
44. Wang, Z. *et al.* P-glycoprotein substrate models using support vector machines based on a comprehensive data set. *J Chem Inf Model.* **51**, 1447-56. doi: 10.1021/ci2001583. Epub 2011 Jun 3. (2011).
45. Chen, L., Li, Y., Yu, H., Zhang, L. & Hou, T. Computational models for predicting substrates or inhibitors of P-glycoprotein. *Drug Discov Today.* **17**, 343-51. doi: 10.1016/j.drudis.2011.11.003. Epub 2011 Nov 18. (2012).
46. Wang, X.K. & Fu, L.W. Interaction of tyrosine kinase inhibitors with the MDR- related ABC transporter proteins. *Curr Drug Metab.* **11**, 618-28. (2010).
47. Hegedus, T. *et al.* Interaction of tyrosine kinase inhibitors with the human multidrug transporter proteins, MDR1 and MRP1. *Biochim Biophys Acta.* **1587**, 318-25. (2002).
48. Cordon-Cardo, C. *et al.* Expression of the multidrug resistance gene product (P-glycoprotein) in human normal and tumor tissues. *J Histochem Cytochem.* **38**, 1277-87. (1990).

49. Gottesman, M.M., Ludwig, J., Xia, D. & Szakacs, G. Defeating drug resistance in cancer. *Discov Med.* **6**, 18-23. (2006).
50. Szakacs, G., Paterson, J.K., Ludwig, J.A., Booth-Genthe, C. & Gottesman, M.M. Targeting multidrug resistance in cancer. *Nat Rev Drug Discov.* **5**, 219-34. (2006).
51. Greer, D.A. & Ivey, S. Distinct N-glycan glycosylation of P-glycoprotein isolated from the human uterine sarcoma cell line MES-SA/Dx5. *Biochim Biophys Acta.* **1770**, 1275-82. Epub 2007 Jul 19. (2007).
52. Schinkel, A.H., Kemp, S., Dolle, M., Rudenko, G. & Wagenaar, E. N-glycosylation and deletion mutants of the human MDR1 P-glycoprotein. *J Biol Chem.* **268**, 7474-81. (1993).
53. Allen, J.D., Brinkhuis, R.F., Wijnholds, J. & Schinkel, A.H. The mouse Bcrp1/Mxr/Abcp gene: amplification and overexpression in cell lines selected for resistance to topotecan, mitoxantrone, or doxorubicin. *Cancer Res.* **59**, 4237-41. (1999).
54. Loo, T.W. & Clarke, D.M. Quality control by proteases in the endoplasmic reticulum. Removal of a protease-sensitive site enhances expression of human P-glycoprotein. *J Biol Chem.* **273**, 32373-6. (1998).
55. Ambudkar, S.V. *et al.* Biochemical, cellular, and pharmacological aspects of the multidrug transporter. *Annu Rev Pharmacol Toxicol.* **39**, 361-98. (1999).
56. Breier, A., Gibalova, L., Seres, M., Barancik, M. & Sulova, Z. New insight into p-glycoprotein as a drug target. *Anticancer Agents Med Chem.* **13**, 159-70. (2013).
57. Robertson, S.J., Kania, K.D., Hladky, S.B. & Barrand, M.A. P-glycoprotein expression in immortalised rat brain endothelial cells: comparisons following exogenously applied hydrogen peroxide and after hypoxia-reoxygenation. *J Neurochem.* **111**, 132-41. doi: 10.1111/j.1471-4159.2009.06306.x. Epub 2009 Jul 25. (2009).
58. Wang, X., Sykes, D.B. & Miller, D.S. Constitutive androstane receptor-mediated up-regulation of ATP-driven xenobiotic efflux transporters at the blood-brain barrier. *Mol Pharmacol.* **78**, 376-83. doi: 10.1124/mol.110.063685. Epub 2010 Jun 14. (2010).
59. Durk, M.R. *et al.* 1alpha,25-Dihydroxyvitamin D3-liganded vitamin D receptor increases expression and transport activity of P-glycoprotein in isolated rat brain capillaries and human and rat brain microvessel endothelial cells. *J Neurochem.* **123**, 944-53. doi: 10.1111/jnc.12041. Epub 2012 Nov 1. (2012).
60. Nishio, N., Katsura, T., Ashida, K., Okuda, M. & Inui, K. Modulation of P-glycoprotein expression in hyperthyroid rat tissues. *Drug Metab Dispos.* **33**, 1584-7. Epub 2005 Aug 3. (2005).
61. Saeki, M., Kurose, K., Hasegawa, R. & Tohkin, M. Functional analysis of genetic variations in the 5'-flanking region of the human MDR1 gene. *Mol Genet Metab.* **102**, 91-8. doi: 10.1016/j.ymgme.2010.08.019. Epub 2010 Sep 19. (2011).
62. Apostoli, A.J. & Nicol, C.J. PPAR Medicines and Human Disease: The ABCs of It All. *PPAR Res.* **2012:504918.**, 10.1155/2012/504918. Epub 2012 Aug 7. (2012).
63. Germann, U.A., Pastan, I. & Gottesman, M.M. P-glycoproteins: mediators of multidrug resistance. *Semin Cell Biol.* **4**, 63-76. (1993).
64. Doyle, L.A. *et al.* A multidrug resistance transporter from human MCF-7 breast cancer cells. *Proc Natl Acad Sci U S A.* **95**, 15665-70. (1998).
65. Allikmets, R., Schriml, L.M., Hutchinson, A., Romano-Spica, V. & Dean, M. A human placenta-specific ATP-binding cassette gene (ABCP) on chromosome 4q22 that is involved in multidrug resistance. *Cancer Res.* **58**, 5337-9. (1998).
66. Miyake, K. *et al.* Molecular cloning of cDNAs which are highly overexpressed in mitoxantrone-resistant cells: demonstration of homology to ABC transport genes. *Cancer Res.* **59**, 8-13. (1999).
67. Kage, K. *et al.* Dominant-negative inhibition of breast cancer resistance protein as drug efflux pump through the inhibition of S-S dependent homodimerization. *Int J Cancer.* **97**, 626-30. (2002).
68. Ozvegy, C. *et al.* Functional characterization of the human multidrug transporter, ABCG2, expressed in insect cells. *Biochem Biophys Res Commun.* **285**, 111-7. (2001).

69. Mo, W. & Zhang, J.T. Human ABCG2: structure, function, and its role in multidrug resistance. *Int J Biochem Mol Biol.* **3**, 1-27. Epub 2011 Mar 30. (2012).
70. Natarajan, K., Xie, Y., Baer, M.R. & Ross, D.D. Role of breast cancer resistance protein (BCRP/ABCG2) in cancer drug resistance. *Biochem Pharmacol.* **83**, 1084-103. doi: 10.1016/j.bcp.2012.01.002. Epub 2012 Jan 11. (2012).
71. Mo, W. & Zhang, J.T. Human ABCG2: structure, function, and its role in multidrug resistance. *International journal of biochemistry and molecular biology* **3**, 1-27 (2012).
72. Jonker, J.W. *et al.* The breast cancer resistance protein protects against a major chlorophyll-derived dietary phototoxin and protoporphyria. *Proc Natl Acad Sci U S A.* **99**, 15649-54. Epub 2002 Nov 12. (2002).
73. Jonker, J.W. *et al.* Role of breast cancer resistance protein in the bioavailability and fetal penetration of topotecan. *J Natl Cancer Inst.* **92**, 1651-6. (2000).
74. Ebert, B., Seidel, A. & Lampen, A. Identification of BCRP as transporter of benzo[a]pyrene conjugates metabolically formed in Caco-2 cells and its induction by Ah-receptor agonists. *Carcinogenesis.* **26**, 1754-63. Epub 2005 May 25. (2005).
75. Turner, J.G. *et al.* ABCG2 expression, function, and promoter methylation in human multiple myeloma. *Blood.* **108**, 3881-9. Epub 2006 Aug 17. (2006).
76. Wang, X.Q. *et al.* Octamer 4 (Oct4) mediates chemotherapeutic drug resistance in liver cancer cells through a potential Oct4-AKT-ATP-binding cassette G2 pathway. *Hepatology.* **52**, 528-39. doi: 10.1002/hep.23692. (2010).
77. Benderra, Z. *et al.* Breast cancer resistance protein and P-glycoprotein in 149 adult acute myeloid leukemias. *Clin Cancer Res.* **10**, 7896-902. (2004).
78. Krishnamurthy, P. *et al.* The stem cell marker Bcrp/ABCG2 enhances hypoxic cell survival through interactions with heme. *J Biol Chem.* **279**, 24218-25. Epub 2004 Mar 24. (2004).
79. Bailey-Dell, K.J., Hassel, B., Doyle, L.A. & Ross, D.D. Promoter characterization and genomic organization of the human breast cancer resistance protein (ATP-binding cassette transporter G2) gene. *Biochim Biophys Acta.* **1520**, 234-41. (2001).
80. Honjo, Y. *et al.* Single-nucleotide polymorphism (SNP) analysis in the ABC half-transporter ABCG2 (MXR/BCRP/ABCP1). *Cancer Biol Ther.* **1**, 696-702. (2002).
81. Nakanishi, T. *et al.* Quantitative analysis of breast cancer resistance protein and cellular resistance to flavopiridol in acute leukemia patients. *Clin Cancer Res.* **9**, 3320-8. (2003).
82. Suvannasankha, A. *et al.* Breast cancer resistance protein (BCRP/MXR/ABCG2) in adult acute lymphoblastic leukaemia: frequent expression and possible correlation with shorter disease-free survival. *Br J Haematol.* **127**, 392-8. (2004).
83. Suvannasankha, A. *et al.* Breast cancer resistance protein (BCRP/MXR/ABCG2) in acute myeloid leukemia: discordance between expression and function. *Leukemia.* **18**, 1252-7. (2004).
84. Ozvegy, C., Varadi, A. & Sarkadi, B. Characterization of drug transport, ATP hydrolysis, and nucleotide trapping by the human ABCG2 multidrug transporter. Modulation of substrate specificity by a point mutation. *J Biol Chem.* **277**, 47980-90. Epub 2002 Oct 8. (2002).
85. Volk, E.L. *et al.* Methotrexate cross-resistance in a mitoxantrone-selected multidrug-resistant MCF7 breast cancer cell line is attributable to enhanced energy-dependent drug efflux. *Cancer Res.* **60**, 3514-21. (2000).
86. Volk, E.L. *et al.* Overexpression of wild-type breast cancer resistance protein mediates methotrexate resistance. *Cancer Res.* **62**, 5035-40. (2002).
87. Munoz, M., Henderson, M., Haber, M. & Norris, M. Role of the MRP1/ABCC1 multidrug transporter protein in cancer. *IUBMB Life.* **59**, 752-7. (2007).
88. Young, L.C., Campling, B.G., Cole, S.P., Deeley, R.G. & Gerlach, J.H. Multidrug resistance proteins MRP3, MRP1, and MRP2 in lung cancer: correlation of protein levels with drug response and messenger RNA levels. *Clin Cancer Res.* **7**, 1798-804. (2001).

89. Hsia, T.C., Lin, C.C., Wang, J.J., Ho, S.T. & Kao, A. Relationship between chemotherapy response of small cell lung cancer and P-glycoprotein or multidrug resistance-related protein expression. *Lung.* **180**, 173-9. (2002).
90. Kuo, T.H. *et al.* To predict response chemotherapy using technetium-99m tetrofosmin chest images in patients with untreated small cell lung cancer and compare with p-glycoprotein, multidrug resistance related protein-1, and lung resistance-related protein expression. *Nucl Med Biol.* **30**, 627-32. (2003).
91. Rayburn, E.R., Ezell, S.J. & Zhang, R. Anti-Inflammatory Agents for Cancer Therapy. *Mol Cell Pharmacol.* **1**, 29-43. (2009).
92. Tan, B., Piwnica-Worms, D. & Ratner, L. Multidrug resistance transporters and modulation. *Curr Opin Oncol.* **12**, 450-8. (2000).
93. Thomas, H. & Coley, H.M. Overcoming multidrug resistance in cancer: an update on the clinical strategy of inhibiting p-glycoprotein. *Cancer Control.* **10**, 159-65. (2003).
94. Krishna, R. & Mayer, L.D. Multidrug resistance (MDR) in cancer. Mechanisms, reversal using modulators of MDR and the role of MDR modulators in influencing the pharmacokinetics of anticancer drugs. *Eur J Pharm Sci.* **11**, 265-83. (2000).
95. Bates, S. *et al.* A Phase I study of infusional vinblastine in combination with the P-glycoprotein antagonist PSC 833 (valspodar). *Cancer.* **92**, 1577-90. (2001).
96. Wandel, C. *et al.* P-glycoprotein and cytochrome P-450 3A inhibition: dissociation of inhibitory potencies. *Cancer Res.* **59**, 3944-8. (1999).
97. Hyafil, F., Vergely, C., Du Vignaud, P. & Grand-Perret, T. In vitro and in vivo reversal of multidrug resistance by GF120918, an acridonecarboxamide derivative. *Cancer Res.* **53**, 4595-602. (1993).
98. Schinkel, A.H. & Jonker, J.W. Mammalian drug efflux transporters of the ATP binding cassette (ABC) family: an overview. *Adv Drug Deliv Rev.* **55**, 3-29. (2003).
99. Morschhauser, F. *et al.* Phase I/II trial of a P-glycoprotein inhibitor, Zosuquidar.3HCl trihydrochloride (LY335979), given orally in combination with the CHOP regimen in patients with non-Hodgkin's lymphoma. *Leuk Lymphoma.* **48**, 708-15. (2007).
100. Kuppens, I.E. *et al.* A phase I, randomized, open-label, parallel-cohort, dose-finding study of elacridar (GF120918) and oral topotecan in cancer patients. *Clin Cancer Res.* **13**, 3276-85. (2007).
101. Shukla, S., Wu, C.P. & Ambudkar, S.V. Development of inhibitors of ATP-binding cassette drug transporters: present status and challenges. *Expert Opin Drug Metab Toxicol.* **4**, 205-23. doi: 10.1517/17425255.4.2.205. (2008).
102. Nobili, S., Landini, I., Giglioni, B. & Mini, E. Pharmacological strategies for overcoming multidrug resistance. *Curr Drug Targets.* **7**, 861-79. (2006).
103. Minderman, H., O'Loughlin, K.L., Pendyala, L. & Baer, M.R. VX-710 (biricodar) increases drug retention and enhances chemosensitivity in resistant cells overexpressing P-glycoprotein, multidrug resistance protein, and breast cancer resistance protein. *Clin Cancer Res.* **10**, 1826-34. (2004).
104. Palmeira, A., Sousa, E., Vasconcelos, M.H. & Pinto, M.M. Three decades of P-gp inhibitors: skimming through several generations and scaffolds. *Curr Med Chem.* **19**, 1946-2025. (2012).
105. Minotti, G., Menna, P., Salvatorelli, E., Cairo, G. & Gianni, L. Anthracyclines: molecular advances and pharmacologic developments in antitumor activity and cardiotoxicity. *Pharmacol Rev.* **56**, 185-229. (2004).
106. Thomas, X., Le, Q.H. & Fiere, D. Anthracycline-related toxicity requiring cardiac transplantation in long-term disease-free survivors with acute promyelocytic leukemia. *Ann Hematol.* **81**, 504-7. Epub 2002 Sep 21. (2002).
107. Gonsette, R.E. Mitoxantrone in progressive multiple sclerosis: when and how to treat? *J Neurol Sci.* **206**, 203-8. (2003).
108. Paul, F., Dorr, J., Wurfel, J., Vogel, H.P. & Zipp, F. Early mitoxantrone-induced cardiotoxicity in secondary progressive multiple sclerosis. *BMJ Case Rep.* **2009.**, bcr06.2009.2004. doi: 10.1136/bcr.06.2009.2004. Epub 2009 Jul 7. (2009).

109. Cornbleet, M.A. *et al.* Mitoxantrone for the treatment of advanced breast cancer: single-agent therapy in previously untreated patients. *Eur J Cancer Clin Oncol.* **20**, 1141-6. (1984).
110. Smith, P.J., Morgan, S.A., Fox, M.E. & Watson, J.V. Mitoxantrone-DNA binding and the induction of topoisomerase II associated DNA damage in multi-drug resistant small cell lung cancer cells. *Biochem Pharmacol.* **40**, 2069-78. (1990).
111. Bowden, G.T., Roberts, R., Alberts, D.S., Peng, Y.M. & Garcia, D. Comparative molecular pharmacology in leukemic L1210 cells of the anthracene anticancer drugs mitoxantrone and bisantrene. *Cancer Res.* **45**, 4915-20. (1985).
112. Shen, F. *et al.* Dynamic assessment of mitoxantrone resistance and modulation of multidrug resistance by valspodar (PSC833) in multidrug resistance human cancer cells. *J Pharmacol Exp Ther.* **330**, 423-9. doi: 10.1124/jpet.109.153551. Epub 2009 May 7. (2009).
113. Abe, Y. *et al.* P-glycoprotein-mediated acquired multidrug resistance of human lung cancer cells in vivo. *Br J Cancer.* **74**, 1929-34. (1996).
114. Shanker, M., Willcutts, D., Roth, J.A. & Ramesh, R. Drug resistance in lung cancer. *Lung Cancer: Targets and Therapy* **1**, 23-26 (2010).
115. Yabuki, N. *et al.* Gene amplification and expression in lung cancer cells with acquired paclitaxel resistance. *Cancer Genet Cytogenet.* **173**, 1-9. (2007).
116. Bessho, Y. *et al.* ABCC10/MRP7 is associated with vinorelbine resistance in non-small cell lung cancer. *Oncol Rep.* **21**, 263-8. (2009).
117. Zhao, Y. *et al.* ABCC3 as a marker for multidrug resistance in non-small cell lung cancer. *Sci Rep.* **3:3120.**, 10.1038/srep03120. (2013).
118. Stuckler, D. *et al.* RLIP76 transports vinorelbine and mediates drug resistance in non-small cell lung cancer. *Cancer Res.* **65**, 991-8. (2005).
119. Vatsyayan, R. *et al.* Role of RLIP76 in doxorubicin resistance in lung cancer. *Int J Oncol.* **34**, 1505-11. (2009).
120. Kasahara, K. *et al.* Metallothionein content correlates with the sensitivity of human small cell lung cancer cell lines to cisplatin. *Cancer Res.* **51**, 3237-42. (1991).
121. Kelley, S.L. *et al.* Overexpression of metallothionein confers resistance to anticancer drugs. *Science.* **241**, 1813-5. (1988).
122. Hishikawa, Y. *et al.* Overexpression of metallothionein correlates with chemoresistance to cisplatin and prognosis in esophageal cancer. *Oncology.* **54**, 342-7. (1997).
123. Mattern, J. & Volm, M. Increased resistance to Doxorubicin in human non-small-cell lung carcinomas with metallothionein expression. *Int J Oncol.* **1**, 687-9. (1992).
124. Theocharis, S. *et al.* Expression of metallothionein in lung carcinoma: correlation with histological type and grade. *Histopathology.* **40**, 143-51. (2002).
125. Hishikawa, Y. *et al.* Metallothionein expression correlates with metastatic and proliferative potential in squamous cell carcinoma of the oesophagus. *Br J Cancer.* **81**, 712-20. (1999).
126. Barabas, K., Milner, R., Lurie, D. & Adin, C. Cisplatin: a review of toxicities and therapeutic applications. *Vet Comp Oncol.* **6**, 1-18. doi: 10.1111/j.1476-5829.2007.00142.x. (2008).
127. Gossage, L. & Madhusudan, S. Current status of excision repair cross complementing-group 1 (ERCC1) in cancer. *Cancer Treat Rev.* **33**, 565-77. Epub 2007 Aug 17. (2007).
128. Andarawewa, K.L. *et al.* Ionizing radiation predisposes nonmalignant human mammary epithelial cells to undergo transforming growth factor beta induced epithelial to mesenchymal transition. *Cancer Res.* **67**, 8662-70. (2007).
129. Liu, A., Yoshioka, K., Salerno, V. & Hsieh, P. The mismatch repair-mediated cell cycle checkpoint response to fluorodeoxyuridine. *J Cell Biochem.* **105**, 245-54. doi: 10.1002/jcb.21824. (2008).
130. Adhikari, S. *et al.* Targeting base excision repair for chemosensitization. *Anticancer Agents Med Chem.* **8**, 351-7. (2008).
131. Friesen, C. *et al.* DNA-ligase IV and DNA-protein kinase play a critical role in deficient caspases activation in apoptosis-resistant cancer cells by using doxorubicin. *Mol Biol Cell.* **19**, 3283-9. doi: 10.1091/mbc.E08-03-0306. Epub 2008 May 28. (2008).

132. Biswas, R.S., Cha, H.J., Hardwick, J.M. & Srivastava, R.K. Inhibition of drug-induced Fas ligand transcription and apoptosis by Bcl-XL. *Mol Cell Biochem.* **225**, 7-20. (2001).
133. Oh, K.T. *et al.* The reversal of drug-resistance in tumors using a drug-carrying nanoparticular system. *Int J Mol Sci.* **10**, 3776-92. doi: 10.3390/ijms10093776. (2009).
134. Mehlen, P. & Puisieux, A. Metastasis: a question of life or death. *Nat Rev Cancer.* **6**, 449-58. (2006).
135. Bissell, M.J. & Hines, W.C. Why don't we get more cancer? A proposed role of the microenvironment in restraining cancer progression. *Nat Med.* **17**, 320-9. doi: 10.1038/nm.2328. (2011).
136. Leber, M.F. & Efferth, T. Molecular principles of cancer invasion and metastasis (review). *International journal of oncology* **34**, 881-895 (2009).
137. Luzzi, K.J. *et al.* Multistep nature of metastatic inefficiency: dormancy of solitary cells after successful extravasation and limited survival of early micrometastases. *Am J Pathol.* **153**, 865-73. (1998).
138. Chambers, A.F., Groom, A.C. & MacDonald, I.C. Dissemination and growth of cancer cells in metastatic sites. *Nat Rev Cancer.* **2**, 563-72. (2002).
139. Paget, S. The distribution of secondary growths in cancer of the breast. 1889. *Cancer Metastasis Rev.* **8**, 98-101. (1989).
140. Valastyan, S. & Weinberg, R.A. Tumor metastasis: molecular insights and evolving paradigms. *Cell.* **147**, 275-92. doi: 10.1016/j.cell.2011.09.024. (2011).
141. Perlikos, F., Harrington, K.J. & Syrigos, K.N. Key molecular mechanisms in lung cancer invasion and metastasis: a comprehensive review. *Crit Rev Oncol Hematol.* **87**, 1-11. doi: 10.1016/j.critrevonc.2012.12.007. Epub 2013 Jan 16. (2013).
142. De Wever, O. *et al.* Molecular and pathological signatures of epithelial-mesenchymal transitions at the cancer invasion front. *Histochem Cell Biol.* **130**, 481-94. doi: 10.1007/s00418-008-0464-1. Epub 2008 Jul 22. (2008).
143. Fidler, I.J. Tumor heterogeneity and the biology of cancer invasion and metastasis. *Cancer Res* **38**, 2651-60 (1978).
144. Thiery, J.P., Acloque, H., Huang, R.Y. & Nieto, M.A. Epithelial-mesenchymal transitions in development and disease. *Cell.* **139**, 871-90. doi: 10.1016/j.cell.2009.11.007. (2009).
145. Thiery, J.P. Epithelial-mesenchymal transitions in development and pathologies. *Curr Opin Cell Biol.* **15**, 740-6. (2003).
146. Hazan, R.B., Phillips, G.R., Qiao, R.F., Norton, L. & Aaronson, S.A. Exogenous expression of N-cadherin in breast cancer cells induces cell migration, invasion, and metastasis. *J Cell Biol.* **148**, 779-90. (2000).
147. Marsan, M. *et al.* A Core Invasiveness Gene Signature Reflects Epithelial-to-Mesenchymal Transition but Not Metastatic Potential in Breast Cancer Cell Lines and Tissue Samples. *PLoS One.* **9**, e89262. doi: 10.1371/journal.pone.0089262. eCollection 2014. (2014).
148. Talmadge, J.E. & Fidler, I.J. AACR centennial series: the biology of cancer metastasis: historical perspective. *Cancer Res.* **70**, 5649-69. doi: 10.1158/0008-5472.CAN-10-1040. Epub 2010 Jul 7. (2010).
149. Sheen, Y.Y., Kim, M.J., Park, S.A., Park, S.Y. & Nam, J.S. Targeting the Transforming Growth Factor-beta Signaling in Cancer Therapy. *Biomol Ther (Seoul).* **21**, 323-331. (2013).
150. Bartel, D.P. MicroRNAs: genomics, biogenesis, mechanism, and function. *Cell.* **116**, 281-97. (2004).
151. Korpal, M. & Kang, Y. The emerging role of miR-200 family of microRNAs in epithelial-mesenchymal transition and cancer metastasis. *RNA Biol.* **5**, 115-9. (2008).
152. Wan, L., Pantel, K. & Kang, Y. Tumor metastasis: moving new biological insights into the clinic. *Nat Med.* **19**, 1450-64. doi: 10.1038/nm.3391. (2013).
153. Wang, Y. & Shang, Y. Epigenetic control of epithelial-to-mesenchymal transition and cancer metastasis. *Exp Cell Res.* **319**, 160-9. doi: 10.1016/j.yexcr.2012.07.019. Epub 2012 Aug 1. (2013).

154. Farahani, E. *et al.* Cell adhesion molecules and their relation to (cancer) cell stemness. *Carcinogenesis* **15**, 15 (2014).
155. Makrilia, N., Kollias, A., Manolopoulos, L. & Syrigos, K. Cell adhesion molecules: role and clinical significance in cancer. *Cancer Invest.* **27**, 1023-37. doi: 10.3109/07357900902769749. (2009).
156. Guo, W. & Giancotti, F.G. Integrin signalling during tumour progression. *Nat Rev Mol Cell Biol.* **5**, 816-26. (2004).
157. Humphries, M.J. Integrin structure. *Biochem Soc Trans.* **28**, 311-39. (2000).
158. Nawrocki-Raby, B. *et al.* E-Cadherin mediates MMP down-regulation in highly invasive bronchial tumor cells. *Am J Pathol.* **163**, 653-61. (2003).
159. Chetty, C. *et al.* MMP-9 induces CD44 cleavage and CD44 mediated cell migration in glioblastoma xenograft cells. *Cell Signal.* **24**, 549-59. doi: 10.1016/j.cellsig.2011.10.008. Epub 2011 Oct 17. (2012).
160. Cox, T.R. & Erler, J.T. Remodeling and homeostasis of the extracellular matrix: implications for fibrotic diseases and cancer. *Dis Model Mech.* **4**, 165-78. doi: 10.1242/dmm.004077. Epub 2011 Feb 14. (2011).
161. Iizasa, T. *et al.* Elevated levels of circulating plasma matrix metalloproteinase 9 in non-small cell lung cancer patients. *Clin Cancer Res.* **5**, 149-53. (1999).
162. Iniesta, P. *et al.* Biological and clinical significance of MMP-2, MMP-9, TIMP-1 and TIMP-2 in non-small cell lung cancer. *Oncol Rep.* **17**, 217-23. (2007).
163. Bourboulia, D. & Stetler-Stevenson, W.G. Matrix metalloproteinases (MMPs) and tissue inhibitors of metalloproteinases (TIMPs): Positive and negative regulators in tumor cell adhesion. *Semin Cancer Biol.* **20**, 161-8. doi: 10.1016/j.semcancer.2010.05.002. Epub 2010 May 12. (2010).
164. Yadav, L. *et al.* Matrix metalloproteinases and cancer - roles in threat and therapy. *Asian Pac J Cancer Prev.* **15**, 1085-91. (2014).
165. Nikiforov, M.A. *et al.* p53 modulation of anchorage independent growth and experimental metastasis. *Oncogene.* **13**, 1709-19. (1996).
166. Nikiforov, M.A. *et al.* Suppression of apoptosis by bcl-2 does not prevent p53-mediated control of experimental metastasis and anchorage dependence. *Oncogene.* **15**, 3007-12. (1997).
167. Kaul, S.C., Yaguchi, T., Taira, K., Reddel, R.R. & Wadhwa, R. Overexpressed mortalin (mot-2)/mthsp70/GRP75 and hTERT cooperate to extend the in vitro lifespan of human fibroblasts. *Exp Cell Res.* **286**, 96-101. (2003).
168. Wadhwa, R. *et al.* Upregulation of mortalin/mthsp70/Grp75 contributes to human carcinogenesis. *Int J Cancer.* **118**, 2973-80. (2006).
169. Wadhwa, R. *et al.* Inactivation of tumor suppressor p53 by mot-2, a hsp70 family member. *J Biol Chem.* **273**, 29586-91. (1998).
170. Ma, Z. *et al.* Mortalin controls centrosome duplication via modulating centrosomal localization of p53. *Oncogene.* **25**, 5377-90. Epub 2006 Apr 17. (2006).
171. Frisch, S.M. & Ruoslahti, E. Integrins and anoikis. *Curr Opin Cell Biol.* **9**, 701-6. (1997).
172. Frisch, S.M. & Francis, H. Disruption of epithelial cell-matrix interactions induces apoptosis. *J Cell Biol.* **124**, 619-26. (1994).
173. Frisch, S.M., Schaller, M. & Cieply, B. Mechanisms that link the oncogenic epithelial-mesenchymal transition to suppression of anoikis. *J Cell Sci.* **126**, 21-9. doi: 10.1242/jcs.120907. (2013).
174. McLean, G.W. *et al.* The role of focal-adhesion kinase in cancer - a new therapeutic opportunity. *Nat Rev Cancer.* **5**, 505-15. (2005).
175. Onder, T.T. *et al.* Loss of E-cadherin promotes metastasis via multiple downstream transcriptional pathways. *Cancer Res.* **68**, 3645-54. doi: 10.1158/0008-5472.CAN-07-2938. (2008).
176. Folkman, J. Fighting cancer by attacking its blood supply. *Sci Am.* **275**, 150-4. (1996).
177. Liekens, S., De Clercq, E. & Neyts, J. Angiogenesis: regulators and clinical applications. *Biochem Pharmacol.* **61**, 253-70. (2001).

178. Klagsbrun, M. & D'Amore, P.A. Regulators of angiogenesis. *Annu Rev Physiol.* **53**, 217-39. (1991).
179. Herbst, R.S., Onn, A. & Sandler, A. Angiogenesis and lung cancer: prognostic and therapeutic implications. *J Clin Oncol.* **23**, 3243-56. (2005).
180. Al-Hajj, M., Wicha, M.S., Benito-Hernandez, A., Morrison, S.J. & Clarke, M.F. Prospective identification of tumorigenic breast cancer cells. *Proc Natl Acad Sci U S A.* **100**, 3983-8. Epub 2003 Mar 10. (2003).
181. Krystal, G.W., Hines, S.J. & Organ, C.P. Autocrine growth of small cell lung cancer mediated by coexpression of c-kit and stem cell factor. *Cancer Res.* **56**, 370-6. (1996).
182. Kim, C.F. *et al.* Identification of bronchioalveolar stem cells in normal lung and lung cancer. *Cell.* **121**, 823-35. (2005).
183. Eramo, A. *et al.* Identification and expansion of the tumorigenic lung cancer stem cell population. *Cell Death Differ.* **15**, 504-14. Epub 2007 Nov 30. (2008).
184. Sullivan, J.P., Minna, J.D. & Shay, J.W. Evidence for self-renewing lung cancer stem cells and their implications in tumor initiation, progression, and targeted therapy. *Cancer Metastasis Rev.* **29**, 61-72. doi: 10.1007/s10555-010-9216-5. (2010).
185. Goldsmith, K.C. & Hogarty, M.D. Targeting programmed cell death pathways with experimental therapeutics: opportunities in high-risk neuroblastoma. *Cancer Lett.* **228**, 133-41. (2005).
186. Shah, A.N. & Gallick, G.E. Src, chemoresistance and epithelial to mesenchymal transition: are they related? *Anticancer Drugs.* **18**, 371-5. (2007).
187. Liu, F. *et al.* Co-expression of cytokeratin 8 and breast cancer resistant protein indicates a multifactorial drug-resistant phenotype in human breast cancer cell line. *Life Sciences* **83**, 496-501 (2008).
188. Blaheta, R.A. *et al.* Chemoresistance induces enhanced adhesion and transendothelial penetration of neuroblastoma cells by down-regulating NCAM surface expression. *BMC Cancer.* **6**, 294. (2006).
189. Blaheta, R.A. *et al.* Valproic acid inhibits adhesion of vincristine- and cisplatin-resistant neuroblastoma tumour cells to endothelium. *Br J Cancer.* **96**, 1699-706. Epub 2007 May 15. (2007).
190. Fernandez-Luna, J.L. Regulation of pro-apoptotic BH3-only proteins and its contribution to cancer progression and chemoresistance. *Cell Signal.* **20**, 1921-6. doi: 10.1016/j.cellsig.2008.04.015. Epub 2008 May 8. (2008).
191. Robbiani, D.F. *et al.* The leukotriene C(4) transporter MRP1 regulates CCL19 (MIP-3beta, ELC)-dependent mobilization of dendritic cells to lymph nodes. *Cell.* **103**, 757-68. (2000).
192. Randolph, G.J. *et al.* A physiologic function for p-glycoprotein (MDR-1) during the migration of dendritic cells from skin via afferent lymphatic vessels. *Proc Natl Acad Sci U S A.* **95**, 6924-9. (1998).
193. van de Ven, R. *et al.* A role for multidrug resistance protein 4 (MRP4; ABCC4) in human dendritic cell migration. *Blood.* **112**, 2353-9. doi: 10.1182/blood-2008-03-147850. Epub 2008 Jul 14. (2008).
194. Meyers, M.B. & Biedler, J.L. Evidence for reverse transformation in multidrug-resistant human neuroblastoma cells. *Prog Clin Biol Res.* **271**, 449-61. (1988).
195. Greene, G.F. *et al.* Correlation of metastasis-related gene expression with metastatic potential in human prostate carcinoma cells implanted in nude mice using an in situ messenger RNA hybridization technique. *Am J Pathol.* **150**, 1571-82. (1997).
196. Liang, Y. *et al.* Enhanced in vitro invasiveness and drug resistance with altered gene expression patterns in a human lung carcinoma cell line after pulse selection with anticancer drugs. *International journal of cancer.Journal international du cancer* **111**, 484-493 (2004).
197. Furukawa, T. *et al.* Chemosensitivity of breast cancer lymph node metastasis compared to the primary tumor from individual patients tested in the histoculture drug response assay. *Anticancer Res.* **20**, 3657-8. (2000).

198. Liang, Y. *et al.* Selection with melphalan or paclitaxel (Taxol) yields variants with different patterns of multidrug resistance, integrin expression and in vitro invasiveness. *Eur J Cancer.* **37**, 1041-52. (2001).
199. Colone, M. *et al.* The multidrug transporter P-glycoprotein: a mediator of melanoma invasion? *The Journal of investigative dermatology* **128**, 957-971 (2008).
200. Barakat, S. *et al.* Regulation of brain endothelial cells migration and angiogenesis by P-glycoprotein/caveolin-1 interaction. *Biochem Biophys Res Commun.* **372**, 440-6. doi: 10.1016/j.bbrc.2008.05.012. Epub 2008 May 15. (2008).
201. Nokihara, H. *et al.* A new quinoline derivative MS-209 reverses multidrug resistance and inhibits multiorgan metastases by P-glycoprotein-expressing human small cell lung cancer cells. *Jpn J Cancer Res.* **92**, 785-92. (2001).
202. Bjornland, K. *et al.* Human hepatoma cells rich in P-glycoprotein display enhanced in vitro invasive properties compared to P-glycoprotein-poor hepatoma cells. *Oncol Res.* **10**, 255-62. (1998).
203. Yang, H., Zou, W., Li, Y., Chen, B. & Xin, X. Bridge linkage role played by CD98hc of anti-tumor drug resistance and cancer metastasis on cisplatin-resistant ovarian cancer cells. *Cancer Biol Ther.* **6**, 942-7. Epub 2007 Mar 26. (2007).
204. Reimers, N. *et al.* Expression of extracellular matrix metalloproteases inducer on micrometastatic and primary mammary carcinoma cells. *Clin Cancer Res.* **10**, 3422-8. (2004).
205. Marieb, E.A. *et al.* Emmprin promotes anchorage-independent growth in human mammary carcinoma cells by stimulating hyaluronan production. *Cancer Res.* **64**, 1229-32. (2004).
206. Miletti-Gonzalez, K.E. *et al.* The CD44 receptor interacts with P-glycoprotein to promote cell migration and invasion in cancer. *Cancer research* **65**, 6660-6667 (2005).
207. Bajorath, J., Greenfield, B., Munro, S.B., Day, A.J. & Aruffo, A. Identification of CD44 residues important for hyaluronan binding and delineation of the binding site. *J Biol Chem.* **273**, 338-43. (1998).
208. Misra, S., Ghatak, S., Zoltan-Jones, A. & Toole, B.P. Regulation of multidrug resistance in cancer cells by hyaluronan. *J Biol Chem.* **278**, 25285-8. Epub 2003 May 8. (2003).
209. Zhang, F. *et al.* Anxa2 plays a critical role in enhanced invasiveness of the multidrug resistant human breast cancer cells. *Journal of proteome research* **8**, 5041-5047 (2009).
210. Zhang, F. *et al.* P-glycoprotein associates with Anxa2 and promotes invasion in multidrug resistant breast cancer cells. *Biochem Pharmacol.* **87**, 292-302. doi: 10.1016/j.bcp.2013.11.003. Epub 2013 Nov 15. (2014).
211. Slotman, G.J. *et al.* The incidence of metastases after multimodal therapy for cancer of the head and neck. *Cancer.* **54**, 2009-14. (1984).
212. Stefani, S., Eells, R.W. & Abbate, J. Hydroxyurea and radiotherapy in head and neck cancer. Results of a prospective controlled study in 126 patients. *Radiology.* **101**, 391-6. (1971).
213. Tofilon, P.J., Basic, I. & Milas, L. Prediction of in vivo tumor response to chemotherapeutic agents by the in vitro sister chromatid exchange assay. *Cancer Res.* **45**, 2025-30. (1985).
214. Abolhoda, A. *et al.* Rapid activation of MDR1 gene expression in human metastatic sarcoma after in vivo exposure to doxorubicin. *Clin Cancer Res.* **5**, 3352-6. (1999).
215. Zochbauer-Muller, S. *et al.* P-glycoprotein and MRP1 expression in axillary lymph node metastases of breast cancer patients. *Anticancer Res.* **21**, 119-24. (2001).
216. Heimerl, S., Bosserhoff, A.K., Langmann, T., Ecker, J. & Schmitz, G. Mapping ATP-binding cassette transporter gene expression profiles in melanocytes and melanoma cells. *Melanoma Res.* **17**, 265-73. (2007).
217. Nurwidya, F., Takahashi, F., Murakami, A. & Takahashi, K. Epithelial mesenchymal transition in drug resistance and metastasis of lung cancer. *Cancer Res Treat.* **44**, 151-6. doi: 10.4143/crt.2012.44.3.151. Epub 2012 Sep 30. (2012).

218. Hoshino, H. *et al.* Epithelial-mesenchymal transition with expression of SNAI1-induced chemoresistance in colorectal cancer. *Biochem Biophys Res Commun.* **390**, 1061-5. doi: 10.1016/j.bbrc.2009.10.117. Epub 2009 Oct 25. (2009).
219. Zhuo, W. *et al.* Knockdown of Snail, a novel zinc finger transcription factor, via RNA interference increases A549 cell sensitivity to cisplatin via JNK/mitochondrial pathway. *Lung Cancer.* **62**, 8-14. doi: 10.1016/j.lungcan.2008.02.007. Epub 2008 Mar 26. (2008).
220. Kurrey, N.K. *et al.* Snail and slug mediate radioresistance and chemoresistance by antagonizing p53-mediated apoptosis and acquiring a stem-like phenotype in ovarian cancer cells. *Stem Cells.* **27**, 2059-68. doi: 10.1002/stem.154. (2009).
221. Saxena, M., Stephens, M.A., Pathak, H. & Rangarajan, A. Transcription factors that mediate epithelial-mesenchymal transition lead to multidrug resistance by upregulating ABC transporters. *Cell death & disease* **2**, e179 (2011).
222. Huang, S. Genetic and non-genetic instability in tumor progression: link between the fitness landscape and the epigenetic landscape of cancer cells. *Cancer Metastasis Rev* **3**, 3 (2013).
223. Reya, T., Morrison, S.J., Clarke, M.F. & Weissman, I.L. Stem cells, cancer, and cancer stem cells. *Nature.* **414**, 105-11. (2001).
224. Magee, J.A., Piskounova, E. & Morrison, S.J. Cancer stem cells: impact, heterogeneity, and uncertainty. *Cancer Cell.* **21**, 283-96. doi: 10.1016/j.ccr.2012.03.003. (2012).
225. Visvader, J.E. & Lindeman, G.J. Cancer stem cells: current status and evolving complexities. *Cell Stem Cell.* **10**, 717-28. doi: 10.1016/j.stem.2012.05.007. (2012).
226. Lee, G.Y. *et al.* Stochastic acquisition of a stem cell-like state and drug tolerance in leukemia cells stressed by radiation. *Int J Hematol.* **93**, 27-35. doi: 10.1007/s12185-010-0734-2. Epub 2010 Dec 18. (2011).
227. Ghisolfi, L., Keates, A.C., Hu, X., Lee, D.K. & Li, C.J. Ionizing radiation induces stemness in cancer cells. *PLoS One.* **7**, e43628. doi: 10.1371/journal.pone.0043628. Epub 2012 Aug 21. (2012).
228. Alexander, S. & Friedl, P. Cancer invasion and resistance: interconnected processes of disease progression and therapy failure. *Trends Mol Med.* **18**, 13-26. doi: 10.1016/j.molmed.2011.11.003. Epub 2011 Dec 15. (2012).
229. Muller, M. *et al.* One, two, three--p53, p63, p73 and chemosensitivity. *Drug Resist Updat.* **9**, 288-306. Epub 2007 Feb 6. (2006).
230. Derisi, J. Overview of nucleic acid arrays. *Curr Protoc Mol Biol.* **Chapter**, Unit 22.1. doi: 10.1002/0471142727.mb2201s49. (2001).
231. Klose, J. Protein mapping by combined isoelectric focusing and electrophoresis of mouse tissues. A novel approach to testing for induced point mutations in mammals. *Humangenetik.* **26**, 231-43. (1975).
232. Alban, A. *et al.* A novel experimental design for comparative two-dimensional gel analysis: two-dimensional difference gel electrophoresis incorporating a pooled internal standard. *Proteomics.* **3**, 36-44. (2003).
233. Unlu, M., Morgan, M.E. & Minden, J.S. Difference gel electrophoresis: a single gel method for detecting changes in protein extracts. *Electrophoresis.* **18**, 2071-7. (1997).
234. Karas, M. & Hillenkamp, F. Laser desorption ionization of proteins with molecular masses exceeding 10,000 daltons. *Anal Chem.* **60**, 2299-301. (1988).
235. Blackstock, W.P. & Weir, M.P. Proteomics: quantitative and physical mapping of cellular proteins. *Trends Biotechnol.* **17**, 121-7. (1999).
236. Brummelkamp, T.R., Bernards, R. & Agami, R. A system for stable expression of short interfering RNAs in mammalian cells. *Science.* **296**, 550-3. Epub 2002 Mar 21. (2002).
237. Elbashir, S.M. *et al.* Duplexes of 21-nucleotide RNAs mediate RNA interference in cultured mammalian cells. *Nature.* **411**, 494-8. (2001).
238. Pecot, C.V., Calin, G.A., Coleman, R.L., Lopez-Berestein, G. & Sood, A.K. RNA interference in the clinic: challenges and future directions. *Nat Rev Cancer.* **11**, 59-67. doi: 10.1038/nrc2966. Epub 2010 Dec 16. (2011).

239. Matzke, M.A., Primig, M., Trnovsky, J. & Matzke, A.J. Reversible methylation and inactivation of marker genes in sequentially transformed tobacco plants. *Embo J.* **8**, 643-9. (1989).
240. Hamilton, A., Voinnet, O., Chappell, L. & Baulcombe, D. Two classes of short interfering RNA in RNA silencing. *Embo J.* **21**, 4671-9. (2002).
241. Nicholson, A.W. Function, mechanism and regulation of bacterial ribonucleases. *FEMS Microbiol Rev.* **23**, 371-90. (1999).
242. Agrawal, N. *et al.* RNA interference: biology, mechanism, and applications. *Microbiol Mol Biol Rev.* **67**, 657-85. (2003).
243. Blaszczyk, J. *et al.* Crystallographic and modeling studies of RNase III suggest a mechanism for double-stranded RNA cleavage. *Structure.* **9**, 1225-36. (2001).
244. Hammond, S.M., Bernstein, E., Beach, D. & Hannon, G.J. An RNA-directed nuclease mediates post-transcriptional gene silencing in Drosophila cells. *Nature.* **404**, 293-6. (2000).
245. Martinez, J., Patkaniowska, A., Urlaub, H., Luhrmann, R. & Tuschl, T. Single-stranded antisense siRNAs guide target RNA cleavage in RNAi. *Cell.* **110**, 563-74. (2002).
246. Novina, C.D. & Sharp, P.A. The RNAi revolution. *Nature.* **430**, 161-4. (2004).
247. JOYCE, H., BRAY, I. & CLYNES, M. RNA Interference with siRNA. *Cancer Genomics - Proteomics* **3**, 127-135 (2006).
248. Ghildiyal, M. & Zamore, P.D. Small silencing RNAs: an expanding universe. *Nat Rev Genet.* **10**, 94-108. doi: 10.1038/nrg2504. (2009).
249. He, L. & Hannon, G.J. MicroRNAs: small RNAs with a big role in gene regulation. *Nat Rev Genet.* **5**, 522-31. (2004).
250. Reinhart, B.J. *et al.* The 21-nucleotide let-7 RNA regulates developmental timing in Caenorhabditis elegans. *Nature.* **403**, 901-6. (2000).
251. Pasquinelli, A.E. *et al.* Conservation of the sequence and temporal expression of let-7 heterochronic regulatory RNA. *Nature.* **408**, 86-9. (2000).
252. Osada, H. & Takahashi, T. MicroRNAs in biological processes and carcinogenesis. *Carcinogenesis.* **28**, 2-12. Epub 2006 Oct 6. (2007).
253. Singh, S.K., Pal Bhadra, M., Girschick, H.J. & Bhadra, U. MicroRNAs--micro in size but macro in function. *Febs J.* **275**, 4929-44. doi: 10.1111/j.1742-4658.2008.06624.x. Epub 2008 Aug 27. (2008).
254. Inui, M., Martello, G. & Piccolo, S. MicroRNA control of signal transduction. *Nat Rev Mol Cell Biol.* **11**, 252-63. doi: 10.1038/nrm2868. Epub 2010 Mar 10. (2010).
255. Kozomara, A. & Griffiths-Jones, S. miRBase: integrating microRNA annotation and deep-sequencing data. *Nucleic Acids Res.* **39**, D152-7. doi: 10.1093/nar/gkq1027. Epub 2010 Oct 30. (2011).
256. Calin, G.A. *et al.* Human microRNA genes are frequently located at fragile sites and genomic regions involved in cancers. *Proc Natl Acad Sci U S A.* **101**, 2999-3004. Epub 2004 Feb 18. (2004).
257. Friedman, R.C., Farh, K.K., Burge, C.B. & Bartel, D.P. Most mammalian mRNAs are conserved targets of microRNAs. *Genome Res.* **19**, 92-105. doi: 10.1101/gr.082701.108. Epub 2008 Oct 27. (2009).
258. Raza, U., Zhang, J.D. & Sahin, O. MicroRNAs: master regulators of drug resistance, stemness, and metastasis. *J Mol Med (Berl).* **92**, 321-36. doi: 10.1007/s00109-014-1129-2. Epub 2014 Feb 9. (2014).
259. Ambros, V. *et al.* A uniform system for microRNA annotation. *Rna.* **9**, 277-9. (2003).
260. Griffiths-Jones, S., Grocock, R.J., van Dongen, S., Bateman, A. & Enright, A.J. miRBase: microRNA sequences, targets and gene nomenclature. *Nucleic Acids Res.* **34**, D140-4. (2006).
261. Izquierdo, M. Short interfering RNAs as a tool for cancer gene therapy. *Cancer Gene Ther.* **12**, 217-27. (2005).
262. Robertson, K.D. DNA methylation and human disease. *Nat Rev Genet.* **6**, 597-610. (2005).
263. Phillips, T. The Role of Methylation in Gene Expression. *Nature Education* **1**, 116 (2008).

264. Frommer, M. *et al.* A genomic sequencing protocol that yields a positive display of 5-methylcytosine residues in individual DNA strands. *Proc Natl Acad Sci U S A* **89**, 1827-31 (1992).
265. Shapiro, R., DiFate, V. & Welcher, M. Deamination of cytosine derivatives by bisulfite. Mechanism of the reaction. *J Am Chem Soc* **96**, 906-12 (1974).
266. Shapiro, R., Braverman, B., Louis, J.B. & Servis, R.E. Nucleic acid reactivity and conformation. II. Reaction of cytosine and uracil with sodium bisulfite. *J Biol Chem* **248**, 4060-4 (1973).
267. Wang, R.Y., Gehrke, C.W. & Ehrlich, M. Comparison of bisulfite modification of 5-methyldeoxycytidine and deoxycytidine residues. *Nucleic Acids Res* **8**, 4777-90 (1980).
268. Herman, J.G., Graff, J.R., Myohanen, S., Nelkin, B.D. & Baylin, S.B. Methylation-specific PCR: a novel PCR assay for methylation status of CpG islands. *Proc Natl Acad Sci U S A.* **93**, 9821-6. (1996).
269. Eads, C.A. *et al.* MethyLight: a high-throughput assay to measure DNA methylation. *Nucleic Acids Res.* **28**, E32. (2000).
270. Chan, M.W., Chu, E.S., To, K.F. & Leung, W.K. Quantitative detection of methylated SOCS-1 , a tumor suppressor gene, by a modified protocol of quantitative real time methylation-specific PCR using SYBR green and its use in early gastric cancer detection. *Biotechnol Lett.* **26**, 1289-93. (2004).
271. Kristensen, L.S., Mikeska, T., Krypuy, M. & Dobrovic, A. Sensitive Melting Analysis after Real Time- Methylation Specific PCR (SMART-MSP): high-throughput and probe-free quantitative DNA methylation detection. *Nucleic Acids Res.* **36**, e42. doi: 10.1093/nar/gkn113. Epub 2008 Mar 15. (2008).
272. Shen, L. & Waterland, R.A. Methods of DNA methylation analysis. *Curr Opin Clin Nutr Metab Care.* **10**, 576-81. (2007).
273. Trinh, B.N., Long, T.I. & Laird, P.W. DNA methylation analysis by MethyLight technology. *Methods.* **25**, 456-62. (2001).
274. Colella, S., Shen, L., Baggerly, K.A., Issa, J.P. & Krahe, R. Sensitive and quantitative universal Pyrosequencing methylation analysis of CpG sites. *Biotechniques.* **35**, 146-50. (2003).
275. Ehrich, M. *et al.* Quantitative high-throughput analysis of DNA methylation patterns by base-specific cleavage and mass spectrometry. *Proc Natl Acad Sci U S A.* **102**, 15785-90. Epub 2005 Oct 21. (2005).
276. Gabriel, S., Ziaugra, L. & Tabbaa, D. SNP genotyping using the Sequenom MassARRAY iPLEX platform. *Curr Protoc Hum Genet.* **Chapter**, Unit 2.12. doi: 10.1002/0471142905.hg0212s60. (2009).
277. Heenan, M., O'Driscoll, L., Cleary, I., Connolly, L. & Clynes, M. Isolation from a human MDR lung cell line of multiple clonal subpopulations which exhibit significantly different drug resistance. *Int J Cancer.* **71**, 907-15. (1997).
278. Bray, I. Doctoral thesis, Dublin City University, Ireland, Dublin City University (2006).
279. Pierce, A. Doctoral thesis, Dublin City University, Ireland, (2006).
280. McBride, S., Meleady, P., Baird, A., Dinsdale, D. & Clynes, M. Human lung carcinoma cell line DLKP contains 3 distinct subpopulations with different growth and attachment properties. *Tumour Biol.* **19**, 88-103. (1998).
281. Keenan, J. *et al.* Olfactomedin III expression contributes to anoikis-resistance in clonal variants of a human lung squamous carcinoma cell line. *Exp Cell Res.* **318**, 593-602. doi: 10.1016/j.yexcr.2012.01.012. Epub 2012 Jan 13. (2012).
282. Law, E. *et al.* Cytogenetic comparison of two poorly differentiated human lung squamous cell carcinoma lines. *Cancer Genet Cytogenet.* **59**, 111-8. (1992).
283. O'Sullivan, F. & Clynes, M. Limbal stem cells, a review of their identification and culture for clinical use. *Cytotechnology.* **53**, 101-6. doi: 10.1007/s10616-007-9063-6. Epub 2007 Mar 22. (2007).
284. Albini, A. *et al.* A rapid in vitro assay for quantitating the invasive potential of tumor cells. *Cancer Res.* **47**, 3239-45. (1987).

285. Laemmli, U.K. Cleavage of structural proteins during the assembly of the head of bacteriophage T4. *Nature.* **227**, 680-5. (1970).
286. Wong, M.L. & Medrano, J.F. Real-time PCR for mRNA quantitation. *Biotechniques.* **39**, 75-85. (2005).
287. Livak, K.J. & Schmittgen, T.D. Analysis of relative gene expression data using real-time quantitative PCR and the 2(-Delta Delta C(T)) Method. *Methods.* **25**, 402-8. (2001).
288. Pepper, S.D., Saunders, E.K., Edwards, L.E., Wilson, C.L. & Miller, C.J. The utility of MAS5 expression summary and detection call algorithms. *BMC Bioinformatics.* **8**, 273. (2007).
289. Irizarry, R.A. *et al.* Exploration, normalization, and summaries of high density oligonucleotide array probe level data. *Biostatistics.* **4**, 249-64. (2003).
290. Li, C. & Hung Wong, W. Model-based analysis of oligonucleotide arrays: model validation, design issues and standard error application. *Genome Biol.* **2**, RESEARCH0032. Epub 2001 Aug 3. (2001).
291. Schwanhausser, B. *et al.* Global quantification of mammalian gene expression control. *Nature.* **473**, 337-42. doi: 10.1038/nature10098. (2011).
292. Chen, G. *et al.* Discordant protein and mRNA expression in lung adenocarcinomas. *Mol Cell Proteomics.* **1**, 304-13. (2002).
293. Lin, M. *et al.* dChipSNP: significance curve and clustering of SNP-array-based loss-of-heterozygosity data. *Bioinformatics.* **20**, 1233-40. Epub 2004 Feb 10. (2004).
294. Eglen, S.J. A quick guide to teaching R programming to computational biology students. *PLoS Comput Biol.* **5**, e1000482. doi: 10.1371/journal.pcbi.1000482. Epub 2009 Aug 28. (2009).
295. Huang da, W., Sherman, B.T. & Lempicki, R.A. Systematic and integrative analysis of large gene lists using DAVID bioinformatics resources. *Nat Protoc.* **4**, 44-57. doi: 10.1038/nprot.2008.211. (2009).
296. Huang da, W., Sherman, B.T. & Lempicki, R.A. Bioinformatics enrichment tools: paths toward the comprehensive functional analysis of large gene lists. *Nucleic Acids Res.* **37**, 1-13. doi: 10.1093/nar/gkn923. Epub 2008 Nov 25. (2009).
297. Thomas, P.D. *et al.* PANTHER: a library of protein families and subfamilies indexed by function. *Genome Res.* **13**, 2129-41. (2003).
298. Polgar, O., Robey, R.W. & Bates, S.E. ABCG2: structure, function and role in drug response. *Expert Opin Drug Metab Toxicol.* **4**, 1-15. doi: 10.1517/17425255.4.1.1 . (2008).
299. Dunne, G. Master of Science thesis, Dublin City University, Ireland, (2010).
300. Bolstad, B.M., Irizarry, R.A., Astrand, M. & Speed, T.P. A comparison of normalization methods for high density oligonucleotide array data based on variance and bias. *Bioinformatics.* **19**, 185-93. (2003).
301. Irizarry, R.A. *et al.* Summaries of Affymetrix GeneChip probe level data. *Nucleic Acids Res.* **31**, e15. (2003).
302. Lund, A., Knudsen, S.M., Vissing, H., Clark, B. & Tommerup, N. Assignment of human elongation factor 1alpha genes: EEF1A maps to chromosome 6q14 and EEF1A2 to 20q13.3. *Genomics.* **36**, 359-61. (1996).
303. Yamagata, M. & Sanes, J.R. Dscam and Sidekick proteins direct lamina-specific synaptic connections in vertebrate retina. *Nature.* **451**, 465-9. doi: 10.1038/nature06469. (2008).
304. Schmucker, D. *et al.* Drosophila Dscam is an axon guidance receptor exhibiting extraordinary molecular diversity. *Cell.* **101**, 671-84. (2000).
305. Alves-Sampaio, A., Troca-Marin, J.A. & Montesinos, M.L. NMDA-mediated regulation of DSCAM dendritic local translation is lost in a mouse model of Down's syndrome. *J Neurosci.* **30**, 13537-48. doi: 10.1523/JNEUROSCI.3457-10.2010. (2010).
306. Agarwala, K.L. *et al.* Cloning and functional characterization of DSCAML1, a novel DSCAM-like cell adhesion molecule that mediates homophilic intercellular adhesion. *Biochem Biophys Res Commun.* **285**, 760-72. (2001).

307. Sato, Y. *et al.* Genome-wide association study on overall survival of advanced non-small cell lung cancer patients treated with carboplatin and paclitaxel. *J Thorac Oncol.* **6**, 132-8. doi: 10.1097/JTO.0b013e318200f415. (2011).
308. Krek, A. *et al.* Combinatorial microRNA target predictions. *Nat Genet.* **37**, 495-500. Epub 2005 Apr 3. (2005).
309. Knutsen, T. *et al.* Amplification of 4q21-q22 and the MXR gene in independently derived mitoxantrone-resistant cell lines. *Genes Chromosomes Cancer.* **27**, 110-6. (2000).
310. Rao, V.K. *et al.* Characterization of ABCG2 gene amplification manifesting as extrachromosomal DNA in mitoxantrone-selected SF295 human glioblastoma cells. *Cancer Genet Cytogenet.* **160**, 126-33. (2005).
311. Calcagno, A.M. *et al.* Single-step doxorubicin-selected cancer cells overexpress the ABCG2 drug transporter through epigenetic changes. *Br J Cancer.* **98**, 1515-24. doi: 10.1038/sj.bjc.6604334. Epub 2008 Apr 1. (2008).
312. Bram, E.E., Stark, M., Raz, S. & Assaraf, Y.G. Chemotherapeutic drug-induced ABCG2 promoter demethylation as a novel mechanism of acquired multidrug resistance. *Neoplasia.* **11**, 1359-70. (2009).
313. Bhatia, S., Frangioni, J.V., Hoffman, R.M., Iafrate, A.J. & Polyak, K. The challenges posed by cancer heterogeneity. *Nat Biotechnol.* **30**, 604-10. doi: 10.1038/nbt.2294. (2012).
314. Lu, P., Weaver, V.M. & Werb, Z. The extracellular matrix: a dynamic niche in cancer progression. *J Cell Biol.* **196**, 395-406. doi: 10.1083/jcb.201102147. (2012).
315. Cavallaro, U. & Christofori, G. Cell adhesion in tumor invasion and metastasis: loss of the glue is not enough. *Biochim Biophys Acta.* **1552**, 39-45. (2001).
316. Behrens, J. The role of cell adhesion molecules in cancer invasion and metastasis. *Breast Cancer Res Treat.* **24**, 175-84. (1993).
317. Canel, M., Serrels, A., Frame, M.C. & Brunton, V.G. E-cadherin-integrin crosstalk in cancer invasion and metastasis. *J Cell Sci.* **126**, 393-401. doi: 10.1242/jcs.100115. Epub 2013 Mar 22. (2013).
318. Akiyama, S.K., Olden, K. & Yamada, K.M. Fibronectin and integrins in invasion and metastasis. *Cancer Metastasis Rev.* **14**, 173-89. (1995).
319. Bowen, M.A. *et al.* Cloning, mapping, and characterization of activated leukocyte-cell adhesion molecule (ALCAM), a CD6 ligand. *J Exp Med.* **181**, 2213-20. (1995).
320. Hess, D.A. *et al.* Selection based on CD133 and high aldehyde dehydrogenase activity isolates long-term reconstituting human hematopoietic stem cells. *Blood.* **107**, 2162-9. Epub 2005 Nov 3. (2006).
321. Pang, R. *et al.* A subpopulation of CD26+ cancer stem cells with metastatic capacity in human colorectal cancer. *Cell Stem Cell.* **6**, 603-15. doi: 10.1016/j.stem.2010.04.001. (2010).
322. Liu, H. *et al.* Cancer stem cells from human breast tumors are involved in spontaneous metastases in orthotopic mouse models. *Proc Natl Acad Sci U S A.* **107**, 18115-20. doi: 10.1073/pnas.1006732107. Epub 2010 Oct 4. (2010).
323. Hermann, P.C. *et al.* Distinct populations of cancer stem cells determine tumor growth and metastatic activity in human pancreatic cancer. *Cell Stem Cell.* **1**, 313-23. doi: 10.1016/j.stem.2007.06.002. (2007).
324. Major, A.G., Pitty, L.P. & Farah, C.S. Cancer stem cell markers in head and neck squamous cell carcinoma. *Stem Cells Int.* **2013:319489.**, 10.1155/2013/319489. Epub 2013 Mar 3. (2013).
325. Liang, Y., McDonnell, S. & Clynes, M. Examining the relationship between cancer invasion/metastasis and drug resistance. *Curr Cancer Drug Targets.* **2**, 257-77. (2002).
326. Berman, A.E. & Kozlova, N.I. Integrins: structure and functions. *Membr Cell Biol.* **13**, 207-44. (2000).
327. Martinez-Moreno, P. *et al.* Cholinesterase activity of human lung tumours varies according to their histological classification. *Carcinogenesis.* **27**, 429-36. Epub 2005 Nov 5. (2006).

328. Bernardi, C.C., Ribeiro Ede, S., Cavalli, I.J., Chautard-Freire-Maia, E.A. & Souza, R.L. Amplification and deletion of the ACHE and BCHE cholinesterase genes in sporadic breast cancer. *Cancer Genet Cytogenet.* **197**, 158-65. doi: 10.1016/j.cancergencyto.2009.10.011. (2010).
329. Akinleye, A., Furqan, M., Mukhi, N., Ravella, P. & Liu, D. MEK and the inhibitors: from bench to bedside. *J Hematol Oncol.* **6:27.**, 10.1186/1756-8722-6-27. (2013).
330. Thompson, N. & Lyons, J. Recent progress in targeting the Raf/MEK/ERK pathway with inhibitors in cancer drug discovery. *Curr Opin Pharmacol.* **5**, 350-6. (2005).
331. Hsueh, C.T., Liu, D. & Wang, H. Novel biomarkers for diagnosis, prognosis, targeted therapy and clinical trials. *Biomark Res.* **1**, 1. doi: 10.1186/2050-7771-1-1. (2013).
332. Ferguson, J., Arozarena, I., Ehrhardt, M. & Wellbrock, C. Combination of MEK and SRC inhibition suppresses melanoma cell growth and invasion. *Oncogene.* **32**, 86-96. doi: 10.1038/onc.2012.25. Epub 2012 Feb 6. (2013).
333. Pritchard, A.L. & Hayward, N.K. Molecular pathways: mitogen-activated protein kinase pathway mutations and drug resistance. *Clin Cancer Res.* **19**, 2301-9. doi: 10.1158/1078-0432.CCR-12-0383. Epub 2013 Feb 13. (2013).
334. Wang, T.H. *et al.* Microtubule dysfunction induced by paclitaxel initiates apoptosis through both c-Jun N-terminal kinase (JNK)-dependent and -independent pathways in ovarian cancer cells. *J Biol Chem.* **274**, 8208-16. (1999).
335. Persons, D.L., Yazlovitskaya, E.M., Cui, W. & Pelling, J.C. Cisplatin-induced activation of mitogen-activated protein kinases in ovarian carcinoma cells: inhibition of extracellular signal-regulated kinase activity increases sensitivity to cisplatin. *Clin Cancer Res.* **5**, 1007-14. (1999).
336. Stone, A.A. & Chambers, T.C. Microtubule inhibitors elicit differential effects on MAP kinase (JNK, ERK, and p38) signaling pathways in human KB-3 carcinoma cells. *Exp Cell Res.* **254**, 110-9. (2000).
337. Simon, C., Juarez, J., Nicolson, G.L. & Boyd, D. Effect of PD 098059, a specific inhibitor of mitogen-activated protein kinase kinase, on urokinase expression and in vitro invasion. *Cancer Res.* **56**, 5369-74. (1996).
338. Ge, X., Fu, Y.M. & Meadows, G.G. U0126, a mitogen-activated protein kinase kinase inhibitor, inhibits the invasion of human A375 melanoma cells. *Cancer Lett.* **179**, 133-40. (2002).
339. Favata, M.F. *et al.* Identification of a novel inhibitor of mitogen-activated protein kinase kinase. *J Biol Chem.* **273**, 18623-32. (1998).
340. Dudley, D.T., Pang, L., Decker, S.J., Bridges, A.J. & Saltiel, A.R. A synthetic inhibitor of the mitogen-activated protein kinase cascade. *Proc Natl Acad Sci U S A.* **92**, 7686-9. (1995).
341. Yeh, T.C. *et al.* Biological characterization of ARRY-142886 (AZD6244), a potent, highly selective mitogen-activated protein kinase kinase 1/2 inhibitor. *Clin Cancer Res.* **13**, 1576-83. (2007).
342. Janne Passi, D.-F.C.I., Boston, USA. A Phase II, Double-Blind, Randomised, Placebo-Controlled Study to Assess the Efficacy of AZD6244 (Hyd-Sulfate) in Combination With Docetaxel, Compared With Docetaxel Alone, in 2nd Line Patients With KRAS Mutation Positive Locally Advanced Metastatic Non Small Cell Lung Cancer (Stage IIIB- IV). in *ClinicalTrials.gov identifier: NCT00890825* (First received: April 29, 2009 Last updated: March 26, 2014).
343. Ding, S. *et al.* Cross-talk between signalling pathways and the multidrug resistant protein MDR-1. *Br J Cancer.* **85**, 1175-84. (2001).
344. Cossa, G. *et al.* Modulation of sensitivity to antitumor agents by targeting the MAPK survival pathway. *Curr Pharm Des.* **19**, 883-94. (2013).
345. Perego, P., Cossa, G., Zuco, V. & Zunino, F. Modulation of cell sensitivity to antitumor agents by targeting survival pathways. *Biochem Pharmacol.* **80**, 1459-65. doi: 10.1016/j.bcp.2010.07.030. Epub 2010 Aug 3. (2010).
346. Katayama, K., Yoshioka, S., Tsukahara, S., Mitsuhashi, J. & Sugimoto, Y. Inhibition of the mitogen-activated protein kinase pathway results in the down-regulation of P-glycoprotein. *Mol Cancer Ther.* **6**, 2092-102. (2007).

347. Imai, Y. *et al.* Breast cancer resistance protein/ABCG2 is differentially regulated downstream of extracellular signal-regulated kinase. *Cancer Sci.* **100**, 1118-27. (2009).
348. Lin, S. *et al.* MEK inhibition induced downregulation of MRP1 and MRP3 expression in experimental hepatocellular carcinoma. *Cancer Cell Int.* **13**, 3. doi: 10.1186/1475-2867-13-3. (2013).
349. Horiuchi, H. *et al.* A MEK inhibitor (U0126) markedly inhibits direct liver invasion of orthotopically inoculated human gallbladder cancer cells in nude mice. *J Exp Clin Cancer Res.* **23**, 599-606. (2004).
350. Holvoet, S., Vincent, C., Schmitt, D. & Serres, M. The inhibition of MAPK pathway is correlated with down-regulation of MMP-9 secretion induced by TNF-alpha in human keratinocytes. *Exp Cell Res.* **290**, 108-19. (2003).
351. Miletti-Gonzalez, K.E. *et al.* The CD44 receptor interacts with P-glycoprotein to promote cell migration and invasion in cancer. *Cancer Res.* **65**, 6660-7. (2005).
352. Li, Q.Q. *et al.* Involvement of CD147 in regulation of multidrug resistance to P-gp substrate drugs and in vitro invasion in breast cancer cells. *Cancer Sci.* **98**, 1064-9. Epub 2007 Apr 18. (2007).
353. Nieth, C. & Lage, H. Induction of the ABC-transporters Mdr1/P-gp (Abcb1), mrpl (Abcc1), and bcrp (Abcg2) during establishment of multidrug resistance following exposure to mitoxantrone. *Journal of chemotherapy (Florence, Italy)* **17**, 215-223 (2005).
354. Yang, L.Y. *et al.* Distinct P-glycoprotein expression in two subclones simultaneously selected from a human colon carcinoma cell line by cis-diamminedichloroplatinum (II). *International journal of cancer.Journal international du cancer* **53**, 478-485 (1993).
355. Tegze, B. *et al.* Parallel evolution under chemotherapy pressure in 29 breast cancer cell lines results in dissimilar mechanisms of resistance. *PLoS One.* **7**, e30804. doi: 10.1371/journal.pone.0030804. Epub 2012 Feb 2. (2012).
356. Honjo, Y. *et al.* Acquired mutations in the MXR/BCRP/ABCP gene alter substrate specificity in MXR/BCRP/ABCP-overexpressing cells. *Cancer Res.* **61**, 6635-9. (2001).
357. Barr, M.P. *et al.* Generation and characterisation of cisplatin-resistant non-small cell lung cancer cell lines displaying a stem-like signature. *PLoS One.* **8**, e54193. doi: 10.1371/journal.pone.0054193. Epub 2013 Jan 17. (2013).
358. Riordan, J.R. *et al.* Amplification of P-glycoprotein genes in multidrug-resistant mammalian cell lines. *Nature.* **316**, 817-9. (1985).
359. Ross, D.D. *et al.* Atypical multidrug resistance: breast cancer resistance protein messenger RNA expression in mitoxantrone-selected cell lines. *J Natl Cancer Inst.* **91**, 429-33. (1999).
360. Candeil, L. *et al.* ABCG2 overexpression in colon cancer cells resistant to SN38 and in irinotecan-treated metastases. *Int J Cancer.* **109**, 848-54. (2004).
361. Davies, R. *et al.* Regulation of P-glycoprotein 1 and 2 gene expression and protein activity in two MCF-7/Dox cell line subclones. *Br J Cancer.* **73**, 307-15. (1996).
362. Turton, N.J. *et al.* Gene expression and amplification in breast carcinoma cells with intrinsic and acquired doxorubicin resistance. *Oncogene.* **20**, 1300-6. (2001).
363. Pang, E. *et al.* Karyotypic imbalances and differential gene expressions in the acquired doxorubicin resistance of hepatocellular carcinoma cells. *Lab Invest.* **85**, 664-74. (2005).
364. Bedrnicek, J. *et al.* Characterization of drug-resistant neuroblastoma cell lines by comparative genomic hybridization. *Neoplasma.* **52**, 415-9. (2005).
365. Obara, K. *et al.* Comparative genomic hybridization study of genetic changes associated with vindesine resistance in esophageal carcinoma. *Int J Oncol.* **20**, 255-60. (2002).
366. Takano, M. *et al.* Analyses by comparative genomic hybridization of genes relating with cisplatin-resistance in ovarian cancer. *Hum Cell.* **14**, 267-71. (2001).
367. Wang, Y.C. *et al.* Regional activation of chromosomal arm 7q with and without gene amplification in taxane-selected human ovarian cancer cell lines. *Genes Chromosomes Cancer.* **45**, 365-74. (2006).

368. Glasspool, R.M., Teodoridis, J.M. & Brown, R. Epigenetics as a mechanism driving polygenic clinical drug resistance. *Br J Cancer.* **94**, 1087-92. (2006).
369. Bird, A. DNA methylation patterns and epigenetic memory. *Genes Dev.* **16**, 6-21. (2002).
370. Saxonov, S., Berg, P. & Brutlag, D.L. A genome-wide analysis of CpG dinucleotides in the human genome distinguishes two distinct classes of promoters. *Proc Natl Acad Sci U S A.* **103**, 1412-7. Epub 2006 Jan 23. (2006).
371. El-Osta, A., Kantharidis, P., Zalcberg, J.R. & Wolffe, A.P. Precipitous release of methyl-CpG binding protein 2 and histone deacetylase 1 from the methylated human multidrug resistance gene (MDR1) on activation. *Mol Cell Biol.* **22**, 1844-57. (2002).
372. Kusaba, H. *et al.* Association of 5' CpG demethylation and altered chromatin structure in the promoter region with transcriptional activation of the multidrug resistance 1 gene in human cancer cells. *Eur J Biochem.* **262**, 924-32. (1999).
373. Baker, E.K., Johnstone, R.W., Zalcberg, J.R. & El-Osta, A. Epigenetic changes to the MDR1 locus in response to chemotherapeutic drugs. *Oncogene.* **24**, 8061-75. (2005).
374. To, K.K., Zhan, Z. & Bates, S.E. Aberrant promoter methylation of the ABCG2 gene in renal carcinoma. *Mol Cell Biol.* **26**, 8572-85. Epub 2006 Sep 5. (2006).
375. Scotto, K.W. Transcriptional regulation of ABC drug transporters. *Oncogene.* **22**, 7496-511. (2003).
376. Mickley, L.A., Spengler, B.A., Knutsen, T.A., Biedler, J.L. & Fojo, T. Gene rearrangement: a novel mechanism for MDR-1 gene activation. *J Clin Invest.* **99**, 1947-57. (1997).
377. Yague, E. *et al.* P-glycoprotein (MDR1) expression in leukemic cells is regulated at two distinct steps, mRNA stabilization and translational initiation. *J Biol Chem.* **278**, 10344-52. Epub 2003 Jan 13. (2003).
378. Ueda, K., Pastan, I. & Gottesman, M.M. Isolation and sequence of the promoter region of the human multidrug-resistance (P-glycoprotein) gene. *J Biol Chem.* **262**, 17432-6. (1987).
379. Raguz, S. *et al.* Production of P-glycoprotein from the MDR1 upstream promoter is insufficient to affect the response to first-line chemotherapy in advanced breast cancer. *Int J Cancer.* **122**, 1058-67. (2008).
380. Stein, U., Walther, W. & Wunderlich, V. Point mutations in the mdr1 promoter of human osteosarcomas are associated with in vitro responsiveness to multidrug resistance relevant drugs. *Eur J Cancer.* **30A**, 1541-5. (1994).
381. Loeuillet, C. *et al.* Promoter polymorphisms and allelic imbalance in ABCB1 expression. *Pharmacogenet Genomics.* **17**, 951-9. (2007).
382. Kuwano, M. *et al.* The role of nuclear Y-box binding protein 1 as a global marker in drug resistance. *Mol Cancer Ther.* **3**, 1485-92. (2004).
383. Chambers, T.C., McAvoy, E.M., Jacobs, J.W. & Eilon, G. Protein kinase C phosphorylates P-glycoprotein in multidrug resistant human KB carcinoma cells. *J Biol Chem.* **265**, 7679-86. (1990).
384. Chambers, T.C. Identification of phosphorylation sites in human MDR1 P-glycoprotein. *Methods Enzymol.* **292**, 328-42. (1998).
385. Chambers, T.C., Zheng, B. & Kuo, J.F. Regulation by phorbol ester and protein kinase C inhibitors, and by a protein phosphatase inhibitor (okadaic acid), of P-glycoprotein phosphorylation and relationship to drug accumulation in multidrug-resistant human KB cells. *Mol Pharmacol.* **41**, 1008-15. (1992).
386. Mellado, W. & Horwitz, S.B. Phosphorylation of the multidrug resistance associated glycoprotein. *Biochemistry.* **26**, 6900-4. (1987).
387. Wu, X.G., Peng, S.B. & Huang, Q. [Transcriptional regulation of breast cancer resistance protein]. *Yi Chuan.* **34**, 1529-36. (2012).
388. Xie, Y. *et al.* The 44-kDa Pim-1 kinase phosphorylates BCRP/ABCG2 and thereby promotes its multimerization and drug-resistant activity in human prostate cancer cells. *J Biol Chem.* **283**, 3349-56. Epub 2007 Dec 5. (2008).

389. Pan, Y.Z., Morris, M.E. & Yu, A.M. MicroRNA-328 negatively regulates the expression of breast cancer resistance protein (BCRP/ABCG2) in human cancer cells. *Mol Pharmacol.* **75**, 1374-9. doi: 10.1124/mol.108.054163. Epub 2009 Mar 6. (2009).
390. To, K.K. *et al.* Escape from hsa-miR-519c enables drug-resistant cells to maintain high expression of ABCG2. *Mol Cancer Ther.* **8**, 2959-68. doi: 10.1158/1535-7163.MCT-09-0292. (2009).
391. Nakanishi, T. *et al.* Novel 5' untranslated region variants of BCRP mRNA are differentially expressed in drug-selected cancer cells and in normal human tissues: implications for drug resistance, tissue-specific expression, and alternative promoter usage. *Cancer Res.* **66**, 5007-11. (2006).
392. Liao, R. *et al.* MicroRNAs play a role in the development of human hematopoietic stem cells. *J Cell Biochem.* **104**, 805-17. doi: 10.1002/jcb.21668. (2008).
393. Liang, X.J., Shen, D.W., Garfield, S. & Gottesman, M.M. Mislocalization of membrane proteins associated with multidrug resistance in cisplatin-resistant cancer cell lines. *Cancer Res.* **63**, 5909-16. (2003).
394. Beretta, G.L. *et al.* Increased levels and defective glycosylation of MRPs in ovarian carcinoma cells resistant to oxaliplatin. *Biochem Pharmacol.* **79**, 1108-17. doi: 10.1016/j.bcp.2009.12.002. Epub 2009 Dec 31. (2010).
395. Wakabayashi-Nakao, K., Tamura, A., Furukawa, T., Nakagawa, H. & Ishikawa, T. Quality control of human ABCG2 protein in the endoplasmic reticulum: ubiquitination and proteasomal degradation. *Adv Drug Deliv Rev.* **61**, 66-72. doi: 10.1016/j.addr.2008.08.008. Epub 2008 Dec 11. (2009).
396. Nakagawa, H. *et al.* Disruption of N-linked glycosylation enhances ubiquitin-mediated proteasomal degradation of the human ATP-binding cassette transporter ABCG2. *Febs J.* **276**, 7237-52. doi: 10.1111/j.1742-4658.2009.07423.x. Epub . (2009).
397. Furukawa, T. *et al.* Major SNP (Q141K) variant of human ABC transporter ABCG2 undergoes lysosomal and proteasomal degradations. *Pharm Res.* **26**, 469-79. doi: 10.1007/s11095-008-9752-7. Epub 2008 Oct 29. (2009).
398. Diop, N.K. & Hrycyna, C.A. N-Linked glycosylation of the human ABC transporter ABCG2 on asparagine 596 is not essential for expression, transport activity, or trafficking to the plasma membrane. *Biochemistry.* **44**, 5420-9. (2005).
399. Liu, F. *et al.* Overexpression of cell surface cytokeratin 8 in multidrug-resistant MCF-7/MX cells enhances cell adhesion to the extracellular matrix. *Neoplasia.* **10**, 1275-84. (2008).
400. DeFilippis, R.A. *et al.* CD36 repression activates a multicellular stromal program shared by high mammographic density and tumor tissues. *Cancer Discov.* **2**, 826-39. Epub 2012 Jul 9. (2012).
401. Wang, F. *et al.* Kinetic mechanism of non-muscle myosin IIB: functional adaptations for tension generation and maintenance. *J Biol Chem.* **278**, 27439-48. Epub 2003 Apr 17. (2003).
402. Okada, Y., Higuchi, H. & Hirokawa, N. Processivity of the single-headed kinesin KIF1A through biased binding to tubulin. *Nature.* **424**, 574-7. (2003).
403. Xu, Y. *et al.* Midkine positively regulates the proliferation of human gastric cancer cells. *Cancer Lett.* **279**, 137-44. doi: 10.1016/j.canlet.2009.01.024. Epub 2009 Feb 27. (2009).
404. Zhou, S. *et al.* The ABC transporter Bcrp1/ABCG2 is expressed in a wide variety of stem cells and is a molecular determinant of the side-population phenotype. *Nat Med.* **7**, 1028-34. (2001).
405. Pisco, A.O. *et al.* Non-Darwinian dynamics in therapy-induced cancer drug resistance. *Nat Commun.* **4:2467.**, 10.1038/ncomms3467. (2013).
406. Zhu, M.M. *et al.* Increased JNK1 signaling pathway is responsible for ABCG2-mediated multidrug resistance in human colon cancer. *PLoS One.* **7**, e41763. doi: 10.1371/journal.pone.0041763. Epub 2012 Aug 1. (2012).
407. Meyer zu Schwabedissen, H.E. *et al.* Epidermal growth factor-mediated activation of the map kinase cascade results in altered expression and function of ABCG2 (BCRP). *Drug Metab Dispos.* **34**, 524-33. Epub 2006 Jan 13. (2006).
408. Kruh, G.D. Introduction to resistance to anticancer agents. *Oncogene.* **22**, 7262-4. (2003).

409. Baird, R.D. & Kaye, S.B. Drug resistance reversal--are we getting closer? *Eur J Cancer.* **39**, 2450-61. (2003).
410. Koshkin, V. & Krylov, S.N. Correlation between multi-drug resistance-associated membrane transport in clonal cancer cells and the cell cycle phase. *PLoS One.* **7**, e41368. doi: 10.1371/journal.pone.0041368. Epub 2012 Jul 25. (2012).
411. Wartenberg, M., Fischer, K., Hescheler, J. & Sauer, H. Modulation of intrinsic P-glycoprotein expression in multicellular prostate tumor spheroids by cell cycle inhibitors. *Biochim Biophys Acta.* **1589**, 49-62. (2002).
412. Baker, E.K. & El-Osta, A. MDR1, chemotherapy and chromatin remodeling. *Cancer Biol Ther.* **3**, 819-24. Epub 2004 Sep 23. (2004).
413. Wilting, R.H. & Dannenberg, J.H. Epigenetic mechanisms in tumorigenesis, tumor cell heterogeneity and drug resistance. *Drug Resist Updat.* **15**, 21-38. doi: 10.1016/j.drup.2012.01.008. Epub 2012 Feb 20. (2012).
414. Wu, X. *et al.* Chromodomain helicase DNA binding protein 5 plays a tumor suppressor role in human breast cancer. *Breast Cancer Res.* **14**, R73. (2012).
415. Hajihassan, Z. & Rabbani-Chadegani, A. Studies on the binding affinity of anticancer drug mitoxantrone to chromatin, DNA and histone proteins. *J Biomed Sci.* **16:31.**, 10.1186/1423-0127-16-31. (2009).
416. Rahbar, A.M. & Fenselau, C. Unbiased examination of changes in plasma membrane proteins in drug resistant cancer cells. *J Proteome Res.* **4**, 2148-53. (2005).
417. Andersen, G.R., Nissen, P. & Nyborg, J. Elongation factors in protein biosynthesis. *Trends Biochem Sci.* **28**, 434-41. (2003).
418. Ejiri, S. Moonlighting functions of polypeptide elongation factor 1: from actin bundling to zinc finger protein R1-associated nuclear localization. *Biosci Biotechnol Biochem.* **66**, 1-21. (2002).
419. Sanges, C. *et al.* Raf kinases mediate the phosphorylation of eukaryotic translation elongation factor 1A and regulate its stability in eukaryotic cells. *Cell Death Dis.* **3:e276.**, 10.1038/cddis.2012.16. (2012).
420. Browne, G.J. & Proud, C.G. Regulation of peptide-chain elongation in mammalian cells. *Eur J Biochem.* **269**, 5360-8. (2002).
421. Johnsson, A. *et al.* Identification of genes differentially expressed in association with acquired cisplatin resistance. *Br J Cancer.* **83**, 1047-54. (2000).
422. Lamberti, A. *et al.* C-Raf antagonizes apoptosis induced by IFN-alpha in human lung cancer cells by phosphorylation and increase of the intracellular content of elongation factor 1A. *Cell Death Differ.* **14**, 952-62. Epub 2007 Mar 2. (2007).
423. Talapatra, S., Wagner, J.D. & Thompson, C.B. Elongation factor-1 alpha is a selective regulator of growth factor withdrawal and ER stress-induced apoptosis. *Cell Death Differ.* **9**, 856-61. (2002).
424. Edmonds, B.T. *et al.* Elongation factor-1 alpha is an overexpressed actin binding protein in metastatic rat mammary adenocarcinoma. *J Cell Sci.* **109**, 2705-14. (1996).
425. Lamberti, A. *et al.* The translation elongation factor 1A in tumorigenesis, signal transduction and apoptosis: review article. *Amino Acids.* **26**, 443-8. Epub 2004 Apr 26. (2004).
426. Lu, Y., Zhou, H., Chen, W., Zhang, Y. & Hamburger, A.W. The ErbB3 binding protein EBP1 regulates ErbB2 protein levels and tamoxifen sensitivity in breast cancer cells. *Breast Cancer Res Treat.* **126**, 27-36. doi: 10.1007/s10549-010-0873-4. Epub 2010 Apr 9. (2011).
427. Zhang, Y., Akinmade, D. & Hamburger, A.W. Inhibition of heregulin mediated MCF-7 breast cancer cell growth by the ErbB3 binding protein EBP1. *Cancer Lett.* **265**, 298-306. doi: 10.1016/j.canlet.2008.02.024. Epub 2008 Mar 19. (2008).
428. Ahn, J.Y. *et al.* Nuclear Akt associates with PKC-phosphorylated Ebp1, preventing DNA fragmentation by inhibition of caspase-activated DNase. *Embo J.* **25**, 2083-95. Epub 2006 Apr 27. (2006).
429. Liu, Z., Ahn, J.Y., Liu, X. & Ye, K. Ebp1 isoforms distinctively regulate cell survival and differentiation. *Proc Natl Acad Sci U S A.* **103**, 10917-22. Epub 2006 Jul 10. (2006).

430. Murphy, L., Clynes, M. & Keenan, J. Proteomic analysis to dissect mitoxantrone resistance-associated proteins in a squamous lung carcinoma. *Anticancer Res.* **27**, 1277-84. (2007).
431. Wang, Y. *et al.* Annexin-I expression modulates drug resistance in tumor cells. *Biochem Biophys Res Commun.* **314**, 565-70. (2004).
432. Camby, I., Le Mercier, M., Lefranc, F. & Kiss, R. Galectin-1: a small protein with major functions. *Glycobiology.* **16**, 137R-157R. Epub 2006 Jul 13. (2006).
433. Yang, R.Y., Rabinovich, G.A. & Liu, F.T. Galectins: structure, function and therapeutic potential. *Expert Rev Mol Med.* **10:e17.**, 10.1017/S1462399408000719. (2008).
434. Kiyomiya, K., Matsuo, S. & Kurebe, M. Proteasome is a carrier to translocate doxorubicin from cytoplasm into nucleus. *Life Sci.* **62**, 1853-60. (1998).
435. Kiyomiya, K., Matsuo, S. & Kurebe, M. Mechanism of specific nuclear transport of adriamycin: the mode of nuclear translocation of adriamycin-proteasome complex. *Cancer Res.* **61**, 2467-71. (2001).
436. Place, S.P. & Hofmann, G.E. Comparison of Hsc70 orthologs from polar and temperate notothenioid fishes: differences in prevention of aggregation and refolding of denatured proteins. *Am J Physiol Regul Integr Comp Physiol.* **288**, R1195-202. Epub 2005 Jan 6. (2005).
437. Seike, M. *et al.* Proteomic signatures for histological types of lung cancer. *Proteomics.* **5**, 2939-48. (2005).
438. Sinha, P. *et al.* Increased expression of epidermal fatty acid binding protein, cofilin, and 14-3-3-sigma (stratifin) detected by two-dimensional gel electrophoresis, mass spectrometry and microsequencing of drug-resistant human adenocarcinoma of the pancreas. *Electrophoresis.* **20**, 2952-60. (1999).
439. Kaneda, A., Kaminishi, M., Sugimura, T. & Ushijima, T. Decreased expression of the seven ARP2/3 complex genes in human gastric cancers. *Cancer Lett.* **212**, 203-10. (2004).
440. O'Sullivan, D. *et al.* 7B7: a novel antibody directed against the Ku70/Ku80 heterodimer blocks invasion in pancreatic and lung cancer cells. *Tumour Biol* **18**, 18 (2014).
441. Garrett, A.M., Tadenev, A.L. & Burgess, R.W. DSCAMs: restoring balance to developmental forces. *Front Mol Neurosci.* **5:86.**, 10.3389/fnmol.2012.00086. (2012).
442. Zheng, T., Wang, J., Chen, X. & Liu, L. Role of microRNA in anticancer drug resistance. *Int J Cancer.* **126**, 2-10. doi: 10.1002/ijc.24782. (2010).
443. Haenisch, S., Werk, A.N. & Cascorbi, I. MicroRNAs and their relevance to ABC transporters. *Br J Clin Pharmacol.* **77**, 587-96. doi: 10.1111/bcp.12251. (2014).
444. Gao, C. *et al.* Reduced microRNA-218 expression is associated with high nuclear factor kappa B activation in gastric cancer. *Cancer.* **116**, 41-9. doi: 10.1002/cncr.24743. (2010).
445. Tie, J. *et al.* MiR-218 inhibits invasion and metastasis of gastric cancer by targeting the Robo1 receptor. *PLoS Genet.* **6**, e1000879. doi: 10.1371/journal.pgen.1000879. (2010).
446. Davidson, M.R. *et al.* MicroRNA-218 is deleted and downregulated in lung squamous cell carcinoma. *PLoS One.* **5**, e12560. doi: 10.1371/journal.pone.0012560. (2010).
447. Martinez, I. *et al.* Human papillomavirus type 16 reduces the expression of microRNA-218 in cervical carcinoma cells. *Oncogene.* **27**, 2575-82. Epub 2007 Nov 12. (2008).
448. Leite, K.R. *et al.* Change in expression of miR-let7c, miR-100, and miR-218 from high grade localized prostate cancer to metastasis. *Urol Oncol.* **29**, 265-9. doi: 10.1016/j.urolonc.2009.02.002. Epub 2009 Apr 16. (2011).
449. Uesugi, A. *et al.* The tumor suppressive microRNA miR-218 targets the mTOR component Rictor and inhibits AKT phosphorylation in oral cancer. *Cancer Res.* **71**, 5765-78. doi: 10.1158/0008-5472.CAN-11-0368. Epub 2011 Jul 27. (2011).
450. Alajez, N.M. *et al.* MiR-218 suppresses nasopharyngeal cancer progression through downregulation of survivin and the SLIT2-ROBO1 pathway. *Cancer Res.* **71**, 2381-91. doi: 10.1158/0008-5472.CAN-10-2754. Epub 2011 Mar 8. (2011).

451. Tatarano, S. *et al.* miR-218 on the genomic loss region of chromosome 4p15.31 functions as a tumor suppressor in bladder cancer. *Int J Oncol.* **39**, 13-21. doi: 10.3892/ijo.2011.1012. Epub 2011 Apr 20. (2011).
452. Hassan, M.Q. *et al.* miR-218 directs a Wnt signaling circuit to promote differentiation of osteoblasts and osteomimicry of metastatic cancer cells. *J Biol Chem.* **287**, 42084-92. doi: 10.1074/jbc.M112.377515. Epub 2012 Oct 11. (2012).
453. Li, X. *et al.* MicroRNA-27a Indirectly Regulates Estrogen Receptor {alpha} Expression and Hormone Responsiveness in MCF-7 Breast Cancer Cells. *Endocrinology.* **151**, 2462-73. doi: 10.1210/en.2009-1150. Epub 2010 Apr 9. (2010).
454. Kontorovich, T., Levy, A., Korostishevsky, M., Nir, U. & Friedman, E. Single nucleotide polymorphisms in miRNA binding sites and miRNA genes as breast/ovarian cancer risk modifiers in Jewish high-risk women. *Int J Cancer.* **127**, 589-97. doi: 10.1002/ijc.25065. (2010).
455. Wang, T. & Xu, Z. miR-27 promotes osteoblast differentiation by modulating Wnt signaling. *Biochem Biophys Res Commun.* **402**, 186-9. doi: 10.1016/j.bbrc.2010.08.031. Epub 2010 Aug 12. (2010).
456. Mertens-Talcott, S.U., Chintharlapalli, S., Li, X. & Safe, S. The oncogenic microRNA-27a targets genes that regulate specificity protein transcription factors and the G2-M checkpoint in MDA-MB-231 breast cancer cells. *Cancer Res.* **67**, 11001-11. (2007).
457. Guttilla, I.K. & White, B.A. Coordinate regulation of FOXO1 by miR-27a, miR-96, and miR-182 in breast cancer cells. *J Biol Chem.* **284**, 23204-16. doi: 10.1074/jbc.M109.031427. Epub 2009 Jul 1. (2009).
458. Zhu, H. *et al.* Role of MicroRNA miR-27a and miR-451 in the regulation of MDR1/P-glycoprotein expression in human cancer cells. *Biochem Pharmacol.* **76**, 582-8. doi: 10.1016/j.bcp.2008.06.007. Epub 2008 Jun 24. (2008).
459. Zhang, H. *et al.* Down-regulation of miR-27a might reverse multidrug resistance of esophageal squamous cell carcinoma. *Dig Dis Sci.* **55**, 2545-51. doi: 10.1007/s10620-009-1051-6. Epub 2009 Dec 4. (2010).
460. Zhao, X., Yang, L. & Hu, J. Down-regulation of miR-27a might inhibit proliferation and drug resistance of gastric cancer cells. *J Exp Clin Cancer Res.* **30:55.**, 10.1186/1756-9966-30-55. (2011).
461. Muniyappa, M.K. Doctoral thesis, Dublin City University, Ireland, DCU (2009).
462. Schmitz, K.J. *et al.* Differential expression of microRNA-675, microRNA-139-3p and microRNA-335 in benign and malignant adrenocortical tumours. *J Clin Pathol.* **64**, 529-35. doi: 10.1136/jcp.2010.085621. Epub 2011 Apr 6. (2011).
463. Scarola, M., Schoeftner, S., Schneider, C. & Benetti, R. miR-335 directly targets Rb1 (pRb/p105) in a proximal connection to p53-dependent stress response. *Cancer Res.* **70**, 6925-33. doi: 10.1158/0008-5472.CAN-10-0141. Epub 2010 Aug 16. (2010).
464. Heyn, H. *et al.* MicroRNA miR-335 is crucial for the BRCA1 regulatory cascade in breast cancer development. *Int J Cancer.* **129**, 2797-806. doi: 10.1002/ijc.25962. Epub 2011 May 25. (2011).
465. Shu, M. *et al.* Targeting oncogenic miR-335 inhibits growth and invasion of malignant astrocytoma cells. *Mol Cancer.* **10:59.**, 10.1186/1476-4598-10-59. (2011).
466. Xu, Y. *et al.* MicroRNA-335 acts as a metastasis suppressor in gastric cancer by targeting Bcl-w and specificity protein 1. *Oncogene.* **31**, 1398-407. doi: 10.1038/onc.2011.340. Epub 2011 Aug 8. (2012).
467. Yan, Z. *et al.* Identification of hsa-miR-335 as a prognostic signature in gastric cancer. *PLoS One.* **7**, e40037. doi: 10.1371/journal.pone.0040037. Epub 2012 Jul 3. (2012).
468. Peng, H.H., Zhang, Y.D., Gong, L.S., Liu, W.D. & Zhang, Y. Increased expression of microRNA-335 predicts a favorable prognosis in primary gallbladder carcinoma. *Onco Targets Ther.* **6:1625-30.**, 10.2147/OTT.S53030. (2013).
469. Cittelly, D.M. *et al.* Downregulation of miR-342 is associated with tamoxifen resistant breast tumors. *Mol Cancer.* **9:317.**, 10.1186/1476-4598-9-317. (2010).

470. Li, X. *et al.* MicroRNA-185 and 342 inhibit tumorigenicity and induce apoptosis through blockade of the SREBP metabolic pathway in prostate cancer cells. *PLoS One.* **8**, e70987. doi: 10.1371/journal.pone.0070987. eCollection 2013. (2013).
471. Thorns, C. *et al.* Deregulation of a distinct set of microRNAs is associated with transformation of gastritis into MALT lymphoma. *Virchows Arch.* **460**, 371-7. doi: 10.1007/s00428-012-1215-1. Epub 2012 Mar 7. (2012).
472. Xu, L., Liang, Y.N., Luo, X.Q., Liu, X.D. & Guo, H.X. [Association of miRNAs expression profiles with prognosis and relapse in childhood acute lymphoblastic leukemia]. *Zhonghua Xue Ye Xue Za Zhi.* **32**, 178-81. (2011).
473. Tian, Q. *et al.* MicroRNA-550a acts as a pro-metastatic gene and directly targets cytoplasmic polyadenylation element-binding protein 4 in hepatocellular carcinoma. *PLoS One.* **7**, e48958. doi: 10.1371/journal.pone.0048958. Epub 2012 Nov 7. (2012).
474. Rhodes, D.R. *et al.* Probabilistic model of the human protein-protein interaction network. *Nat Biotechnol.* **23**, 951-9. (2005).
475. Buyse, M. *et al.* Validation and clinical utility of a 70-gene prognostic signature for women with node-negative breast cancer. *J Natl Cancer Inst.* **98**, 1183-92. (2006).
476. Dhanasekaran, S.M. *et al.* Delineation of prognostic biomarkers in prostate cancer. *Nature.* **412**, 822-6. (2001).
477. Lowe, J.A., Jones, P. & Wilson, D.M. Network biology as a new approach to drug discovery. *Curr Opin Drug Discov Devel.* **13**, 524-6. (2010).
478. Pegram, M.D. *et al.* Phase II study of receptor-enhanced chemosensitivity using recombinant humanized anti-p185HER2/neu monoclonal antibody plus cisplatin in patients with HER2/neu-overexpressing metastatic breast cancer refractory to chemotherapy treatment. *J Clin Oncol.* **16**, 2659-71. (1998).
479. Slamon, D.J. & Press, M.F. Alterations in the TOP2A and HER2 genes: association with adjuvant anthracycline sensitivity in human breast cancers. *J Natl Cancer Inst.* **101**, 615-8. doi: 10.1093/jnci/djp092. Epub 2009 Apr 28. (2009).
480. Spentzos, D. *et al.* Gene expression signature with independent prognostic significance in epithelial ovarian cancer. *J Clin Oncol.* **22**, 4700-10. Epub 2004 Oct 25. (2004).
481. Zhu, C.Q. *et al.* Prognostic gene expression signature for squamous cell carcinoma of lung. *Clin Cancer Res.* **16**, 5038-47. doi: 10.1158/1078-0432.CCR-10-0612. Epub 2010 Aug 25. (2010).
482. Matsuo, K. *et al.* Multidrug resistance gene (MDR-1) and risk of brain metastasis in epithelial ovarian, fallopian tube, and peritoneal cancer. *Am J Clin Oncol.* **34**, 488-93. doi: 10.1097/COC.0b013e3181ec5f4b. (2011).
483. Krampert, M. *et al.* ADAMTS1 proteinase is up-regulated in wounded skin and regulates migration of fibroblasts and endothelial cells. *J Biol Chem.* **280**, 23844-52. Epub 2005 Apr 20. (2005).
484. Tan Ide, A., Ricciardelli, C. & Russell, D.L. The metalloproteinase ADAMTS1: a comprehensive review of its role in tumorigenic and metastatic pathways. *Int J Cancer.* **133**, 2263-76. doi: 10.1002/ijc.28127. Epub 2013 Mar 16. (2013).
485. Bello, S.M., Millo, H., Rajebhosale, M. & Price, S.R. Catenin-dependent cadherin function drives divisional segregation of spinal motor neurons. *J Neurosci.* **32**, 490-505. doi: 10.1523/JNEUROSCI.4382-11.2012. (2012).
486. Wheelock, M.J., Shintani, Y., Maeda, M., Fukumoto, Y. & Johnson, K.R. Cadherin switching. *J Cell Sci.* **121**, 727-35. doi: 10.1242/jcs.000455. (2008).
487. Nieman, M.T., Prudoff, R.S., Johnson, K.R. & Wheelock, M.J. N-cadherin promotes motility in human breast cancer cells regardless of their E-cadherin expression. *J Cell Biol.* **147**, 631-44. (1999).
488. Agbunag, C. & Bar-Sagi, D. Oncogenic K-ras drives cell cycle progression and phenotypic conversion of primary pancreatic duct epithelial cells. *Cancer Res.* **64**, 5659-63. (2004).

489. Eustace, B.K. *et al.* Functional proteomic screens reveal an essential extracellular role for hsp90 alpha in cancer cell invasiveness. *Nat Cell Biol.* **6**, 507-14. Epub 2004 May 16. (2004).
490. Chen, L., Li, M., Li, Q., Wang, C.J. & Xie, S.Q. DKK1 promotes hepatocellular carcinoma cell migration and invasion through beta-catenin/MMP7 signaling pathway. *Mol Cancer.* **12:157.**, 10.1186/1476-4598-12-157. (2013).
491. Chua, Y.L. *et al.* The NRG1 gene is frequently silenced by methylation in breast cancers and is a strong candidate for the 8p tumour suppressor gene. *Oncogene.* **28**, 4041-52. doi: 10.1038/onc.2009.259. Epub 2009 Oct 5. (2009).
492. DeClerck, Y.A. *et al.* Inhibition of invasion and metastasis in cells transfected with an inhibitor of metalloproteinases. *Cancer Res.* **52**, 701-8. (1992).
493. Mi, H., Muruganujan, A., Casagrande, J.T. & Thomas, P.D. Large-scale gene function analysis with the PANTHER classification system. *Nat Protoc.* **8**, 1551-66. doi: 10.1038/nprot.2013.092. Epub 2013 Jul 18. (2013).
494. Mi, H., Muruganujan, A. & Thomas, P.D. PANTHER in 2013: modeling the evolution of gene function, and other gene attributes, in the context of phylogenetic trees. *Nucleic Acids Res.* **41**, D377-86. doi: 10.1093/nar/gks1118. Epub 2012 Nov 27. (2013).
495. Clevers, H. & Nusse, R. Wnt/beta-catenin signaling and disease. *Cell.* **149**, 1192-205. doi: 10.1016/j.cell.2012.05.012. (2012).
496. Khramtsov, A.I. *et al.* Wnt/beta-catenin pathway activation is enriched in basal-like breast cancers and predicts poor outcome. *Am J Pathol.* **176**, 2911-20. doi: 10.2353/ajpath.2010.091125. Epub 2010 Apr 15. (2010).
497. Beachy, P.A., Karhadkar, S.S. & Berman, D.M. Tissue repair and stem cell renewal in carcinogenesis. *Nature.* **432**, 324-31. (2004).
498. Katoh, M. Comparative genomics on Wnt5a and Wnt5b genes. *Int J Mol Med.* **15**, 749-53. (2005).
499. Moon, R.T., Kohn, A.D., De Ferrari, G.V. & Kaykas, A. WNT and beta-catenin signalling: diseases and therapies. *Nat Rev Genet.* **5**, 691-701. (2004).
500. Artym, V.V., Zhang, Y., Seillier-Moiseiwitsch, F., Yamada, K.M. & Mueller, S.C. Dynamic interactions of cortactin and membrane type 1 matrix metalloproteinase at invadopodia: defining the stages of invadopodia formation and function. *Cancer Res.* **66**, 3034-43. (2006).
501. Danen, E.H. Integrins: regulators of tissue function and cancer progression. *Curr Pharm Des.* **11**, 881-91. (2005).
502. Deryugina, E.I. & Quigley, J.P. Matrix metalloproteinases and tumor metastasis. *Cancer Metastasis Rev.* **25**, 9-34. (2006).
503. Fu, X., Parks, W.C. & Heinecke, J.W. Activation and silencing of matrix metalloproteinases. *Semin Cell Dev Biol.* **19**, 2-13. Epub 2007 Jul 6. (2008).
504. Haass, N.K., Smalley, K.S., Li, L. & Herlyn, M. Adhesion, migration and communication in melanocytes and melanoma. *Pigment Cell Res.* **18**, 150-9. (2005).
505. Hofmann, U.B., Westphal, J.R., Van Muijen, G.N. & Ruiter, D.J. Matrix metalloproteinases in human melanoma. *J Invest Dermatol.* **115**, 337-44. (2000).
506. Kajita, M. *et al.* Membrane-type 1 matrix metalloproteinase cleaves CD44 and promotes cell migration. *J Cell Biol.* **153**, 893-904. (2001).
507. Makela, M. *et al.* Matrix metalloproteinase 2 (gelatinase A) is related to migration of keratinocytes. *Exp Cell Res.* **251**, 67-78. (1999).
508. McCawley, L.J. & Matrisian, L.M. Matrix metalloproteinases: multifunctional contributors to tumor progression. *Mol Med Today.* **6**, 149-56. (2000).
509. Murphy, G. & Nagase, H. Progress in matrix metalloproteinase research. *Mol Aspects Med.* **29**, 290-308. doi: 10.1016/j.mam.2008.05.002. Epub 2008 May 24. (2008).
510. Page-McCaw, A., Ewald, A.J. & Werb, Z. Matrix metalloproteinases and the regulation of tissue remodelling. *Nat Rev Mol Cell Biol.* **8**, 221-33. (2007).
511. Felding-Habermann, B. *et al.* Integrin activation controls metastasis in human breast cancer. *Proc Natl Acad Sci U S A.* **98**, 1853-8. (2001).

512. Bates, R.C. *et al.* Transcriptional activation of integrin beta6 during the epithelial-mesenchymal transition defines a novel prognostic indicator of aggressive colon carcinoma. *J Clin Invest.* **115**, 339-47. (2005).
513. Mercurio, A.M., Rabinovitz, I. & Shaw, L.M. The alpha 6 beta 4 integrin and epithelial cell migration. *Curr Opin Cell Biol.* **13**, 541-5. (2001).
514. Brooks, P.C. *et al.* Localization of matrix metalloproteinase MMP-2 to the surface of invasive cells by interaction with integrin alpha v beta 3. *Cell.* **85**, 683-93. (1996).
515. Koistinen, P., Ahonen, M., Kahari, V.M. & Heino, J. alphaV integrin promotes in vitro and in vivo survival of cells in metastatic melanoma. *Int J Cancer.* **112**, 61-70. (2004).
516. Blaheta, R.A. *et al.* Chemoresistance induces enhanced adhesion and transendothelial penetration of neuroblastoma cells by down-regulating NCAM surface expression. *BMC cancer* **6**, 294 (2006).
517. Hazlehurst, L.A. *et al.* Cell adhesion to fibronectin (CAM-DR) influences acquired mitoxantrone resistance in U937 cells. *Cancer Res.* **66**, 2338-45. (2006).
518. Hazlehurst, L.A., Landowski, T.H. & Dalton, W.S. Role of the tumor microenvironment in mediating de novo resistance to drugs and physiological mediators of cell death. *Oncogene.* **22**, 7396-402. (2003).
519. Damiano, J.S., Cress, A.E., Hazlehurst, L.A., Shtil, A.A. & Dalton, W.S. Cell adhesion mediated drug resistance (CAM-DR): role of integrins and resistance to apoptosis in human myeloma cell lines. *Blood.* **93**, 1658-67. (1999).
520. Swart, G.W. Activated leukocyte cell adhesion molecule (CD166/ALCAM): developmental and mechanistic aspects of cell clustering and cell migration. *Eur J Cell Biol.* **81**, 313-21. (2002).
521. Weiner, J.A. *et al.* Axon fasciculation defects and retinal dysplasias in mice lacking the immunoglobulin superfamily adhesion molecule BEN/ALCAM/SC1. *Mol Cell Neurosci.* **27**, 59-69. (2004).
522. Weidle, U.H., Eggle, D., Klostermann, S. & Swart, G.W. ALCAM/CD166: cancer-related issues. *Cancer Genomics Proteomics.* **7**, 231-43. (2010).
523. Burkhardt, M. *et al.* Cytoplasmic overexpression of ALCAM is prognostic of disease progression in breast cancer. *J Clin Pathol.* **59**, 403-9. Epub 2006 Feb 16. (2006).
524. Ofori-Acquah, S.F. & King, J.A. Activated leukocyte cell adhesion molecule: a new paradox in cancer. *Transl Res.* **151**, 122-8. doi: 10.1016/j.trsl.2007.09.006. Epub 2007 Oct 23. (2008).
525. Degen, W.G. *et al.* MEMD, a new cell adhesion molecule in metastasizing human melanoma cell lines, is identical to ALCAM (activated leukocyte cell adhesion molecule). *Am J Pathol.* **152**, 805-13. (1998).
526. Kristiansen, G. *et al.* ALCAM/CD166 is up-regulated in low-grade prostate cancer and progressively lost in high-grade lesions. *Prostate.* **54**, 34-43. (2003).
527. Kristiansen, G. *et al.* Expression profiling of microdissected matched prostate cancer samples reveals CD166/MEMD and CD24 as new prognostic markers for patient survival. *J Pathol.* **205**, 359-76. (2005).
528. Weichert, W., Knosel, T., Bellach, J., Dietel, M. & Kristiansen, G. ALCAM/CD166 is overexpressed in colorectal carcinoma and correlates with shortened patient survival. *J Clin Pathol.* **57**, 1160-4. (2004).
529. Hong, X. *et al.* ALCAM is associated with chemoresistance and tumor cell adhesion in pancreatic cancer. *J Surg Oncol.* **101**, 564-9. doi: 10.1002/jso.21538. (2010).
530. Ishiguro, F. *et al.* Membranous expression of activated leukocyte cell adhesion molecule contributes to poor prognosis and malignant phenotypes of non-small-cell lung cancer. *J Surg Res.* **179**, 24-32. doi: 10.1016/j.jss.2012.08.044. Epub 2012 Sep 7. (2013).
531. Noel, A. *et al.* New and paradoxical roles of matrix metalloproteinases in the tumor microenvironment. *Front Pharmacol.* **3:140.**, 10.3389/fphar.2012.00140. eCollection 2012. (2012).

532. Lunter, P.C. *et al.* Activated leukocyte cell adhesion molecule (ALCAM/CD166/MEMD), a novel actor in invasive growth, controls matrix metalloproteinase activity. *Cancer Res.* **65**, 8801-8. (2005).
533. Tomita, K., van Bokhoven, A., Jansen, C.F., Bussemakers, M.J. & Schalken, J.A. Coordinate recruitment of E-cadherin and ALCAM to cell-cell contacts by alpha-catenin. *Biochem Biophys Res Commun.* **267**, 870-4. (2000).
534. Jannie, K.M., Stipp, C.S. & Weiner, J.A. ALCAM regulates motility, invasiveness, and adherens junction formation in uveal melanoma cells. *PLoS One.* **7**, e39330. doi: 10.1371/journal.pone.0039330. Epub 2012 Jun 26. (2012).
535. Song, J.H. *et al.* Enhanced invasiveness of drug-resistant acute myeloid leukemia cells through increased expression of matrix metalloproteinase-2. *International journal of cancer.Journal international du cancer* **125**, 1074-1081 (2009).
536. van der Veeken, J. *et al.* Crosstalk between epidermal growth factor receptor- and insulin-like growth factor-1 receptor signaling: implications for cancer therapy. *Curr Cancer Drug Targets.* **9**, 748-60. (2009).
537. Guha, M. Anticancer IGF1R classes take more knocks. *Nat Rev Drug Discov.* **12**, 250. doi: 10.1038/nrd3992. (2013).
538. Chitnis, M.M., Yuen, J.S., Protheroe, A.S., Pollak, M. & Macaulay, V.M. The type 1 insulin-like growth factor receptor pathway. *Clin Cancer Res.* **14**, 6364-70. doi: 10.1158/1078-0432.CCR-07-4879. (2008).
539. Floor, S.L., Dumont, J.E., Maenhaut, C. & Raspe, E. Hallmarks of cancer: of all cancer cells, all the time? *Trends Mol Med.* **18**, 509-15. doi: 10.1016/j.molmed.2012.06.005. Epub 2012 Jul 13. (2012).
540. Liotta, L.A. & Kohn, E.C. The microenvironment of the tumour-host interface. *Nature.* **411**, 375-9. (2001).
541. Gill, J.H. *et al.* MMP-10 is overexpressed, proteolytically active, and a potential target for therapeutic intervention in human lung carcinomas. *Neoplasia.* **6**, 777-85. (2004).
542. Frederick, L.A. *et al.* Matrix metalloproteinase-10 is a critical effector of protein kinase Ciota-Par6alpha-mediated lung cancer. *Oncogene.* **27**, 4841-53. doi: 10.1038/onc.2008.119. Epub 2008 Apr 21. (2008).
543. Regala, R.P. *et al.* Matrix metalloproteinase-10 promotes Kras-mediated bronchio-alveolar stem cell expansion and lung cancer formation. *PLoS One.* **6**, e26439. doi: 10.1371/journal.pone.0026439. Epub 2011 Oct 17. (2011).
544. Justilien, V. *et al.* Matrix metalloproteinase-10 is required for lung cancer stem cell maintenance, tumor initiation and metastatic potential. *PLoS One.* **7**, e35040. doi: 10.1371/journal.pone.0035040. Epub 2012 Apr 24. (2012).
545. Halperin, D.S., Pan, C., Lusis, A.J. & Tontonoz, P. Vestigial-like 3 is an inhibitor of adipocyte differentiation. *J Lipid Res.* **54**, 473-81. doi: 10.1194/jlr.M032755. Epub 2012 Nov 13. (2013).
546. Fujimoto, K. *et al.* Piccolo, a Ca2+ sensor in pancreatic beta-cells. Involvement of cAMP-GEFII.Rim2. Piccolo complex in cAMP-dependent exocytosis. *J Biol Chem.* **277**, 50497-502. Epub 2002 Oct 24. (2002).
547. Cases-Langhoff, C. *et al.* Piccolo, a novel 420 kDa protein associated with the presynaptic cytomatrix. *Eur J Cell Biol.* **69**, 214-23. (1996).
548. Lawrence, M.S. *et al.* Mutational heterogeneity in cancer and the search for new cancer-associated genes. *Nature.* **499**, 214-8. doi: 10.1038/nature12213. Epub 2013 Jun 16. (2013).
549. Takai, Y., Irie, K., Shimizu, K., Sakisaka, T. & Ikeda, W. Nectins and nectin-like molecules: roles in cell adhesion, migration, and polarization. *Cancer Sci.* **94**, 655-67. (2003).
550. Chang, G. *et al.* Hypoexpression and epigenetic regulation of candidate tumor suppressor gene CADM-2 in human prostate cancer. *Clin Cancer Res.* **16**, 5390-401. doi: 10.1158/1078-0432.CCR-10-1461. Epub 2010 Nov 9. (2010).

551. He, W. *et al.* Aberrant methylation and loss of CADM2 tumor suppressor expression is associated with human renal cell carcinoma tumor progression. *Biochem Biophys Res Commun.* **435**, 526-32. doi: 10.1016/j.bbrc.2013.04.074. Epub 2013 May 3. (2013).
552. Ricciardelli, C., Sakko, A.J., Ween, M.P., Russell, D.L. & Horsfall, D.J. The biological role and regulation of versican levels in cancer. *Cancer Metastasis Rev.* **28**, 233-45. doi: 10.1007/s10555-009-9182-y. (2009).
553. Hulit, J. *et al.* N-cadherin signaling potentiates mammary tumor metastasis via enhanced extracellular signal-regulated kinase activation. *Cancer Res.* **67**, 3106-16. (2007).
554. Kwei, K.A. *et al.* Genomic profiling identifies TITF1 as a lineage-specific oncogene amplified in lung cancer. *Oncogene.* **27**, 3635-40. doi: 10.1038/sj.onc.1211012. Epub 2008 Jan 21. (2008).
555. Kendall, J. *et al.* Oncogenic cooperation and coamplification of developmental transcription factor genes in lung cancer. *Proc Natl Acad Sci U S A.* **104**, 16663-8. Epub 2007 Oct 9. (2007).
556. Savci-Heijink, C.D. *et al.* The role of desmoglein-3 in the diagnosis of squamous cell carcinoma of the lung. *Am J Pathol.* **174**, 1629-37. doi: 10.2353/ajpath.2009.080778. Epub 2009 Mar 26. (2009).
557. Chen, Y.J. *et al.* DSG3 is overexpressed in head neck cancer and is a potential molecular target for inhibition of oncogenesis. *Oncogene.* **26**, 467-76. Epub 2006 Jul 31. (2007).
558. Chitaev, N.A. & Troyanovsky, S.M. Direct Ca2+-dependent heterophilic interaction between desmosomal cadherins, desmoglein and desmocollin, contributes to cell-cell adhesion. *J Cell Biol.* **138**, 193-201. (1997).
559. Arnemann, J., Spurr, N.K., Wheeler, G.N., Parker, A.E. & Buxton, R.S. Chromosomal assignment of the human genes coding for the major proteins of the desmosome junction, desmoglein DGI (DSG), desmocollins DGII/III (DSC), desmoplakins DPI/II (DSP), and plakoglobin DPIII (JUP). *Genomics.* **10**, 640-5. (1991).
560. Spicer, A.P., Joo, A. & Bowling, R.A., Jr. A hyaluronan binding link protein gene family whose members are physically linked adjacent to chondroitin sulfate proteoglycan core protein genes: the missing links. *J Biol Chem.* **278**, 21083-91. Epub 2003 Mar 27. (2003).
561. Xu, L. *et al.* Gene expression changes in an animal melanoma model correlate with aggressiveness of human melanoma metastases. *Mol Cancer Res.* **6**, 760-9. doi: 10.1158/1541-7786.MCR-07-0344. (2008).
562. Yau, C. *et al.* A multigene predictor of metastatic outcome in early stage hormone receptor-negative and triple-negative breast cancer. *Breast Cancer Res.* **12**, R85. doi: 10.1186/bcr2753. Epub 2010 Oct 14. (2010).
563. Zhuang, Z., Jian, P., Longjiang, L., Bo, H. & Wenlin, X. Oral cancer cells with different potential of lymphatic metastasis displayed distinct biologic behaviors and gene expression profiles. *J Oral Pathol Med.* **39**, 168-75. doi: 10.1111/j.1600-0714.2009.00817.x. Epub 2009 Aug 12. (2010).
564. Hickford, D., Frankenberg, S., Shaw, G. & Renfree, M.B. Evolution of vertebrate interferon inducible transmembrane proteins. *BMC Genomics.* **13:155.**, 10.1186/1471-2164-13-155. (2012).
565. Friedman, R.L., Manly, S.P., McMahon, M., Kerr, I.M. & Stark, G.R. Transcriptional and posttranscriptional regulation of interferon-induced gene expression in human cells. *Cell.* **38**, 745-55. (1984).
566. Seyfried, N.T. *et al.* Up-regulation of NG2 proteoglycan and interferon-induced transmembrane proteins 1 and 3 in mouse astrocytoma: a membrane proteomics approach. *Cancer Lett.* **263**, 243-52. doi: 10.1016/j.canlet.2008.01.007. Epub 2008 Feb 20. (2008).
567. Andreu, P. *et al.* Identification of the IFITM family as a new molecular marker in human colorectal tumors. *Cancer Res.* **66**, 1949-55. (2006).
568. Seo, G.S. *et al.* Identification of the polymorphisms in IFITM3 gene and their association in a Korean population with ulcerative colitis. *Exp Mol Med.* **42**, 99-104. doi: 10.3858/emm.2010.42.2.011. (2010).
569. Zhao, B., Wang, H., Zong, G. & Li, P. The role of IFITM3 in the growth and migration of human glioma cells. *BMC Neurol.* **13:210.**, 10.1186/1471-2377-13-210. (2013).

570. Yang, M., Gao, H., Chen, P., Jia, J. & Wu, S. Knockdown of interferon-induced transmembrane protein 3 expression suppresses breast cancer cell growth and colony formation and affects the cell cycle. *Oncol Rep.* **30**, 171-8. doi: 10.3892/or.2013.2428. Epub 2013 Apr 26. (2013).
571. Varki, A., Kannagi, R. & Toole, B.P. Glycosylation Changes in Cancer.
572. Rosso, O. *et al.* The ALCAM shedding by the metalloprotease ADAM17/TACE is involved in motility of ovarian carcinoma cells. *Mol Cancer Res.* **5**, 1246-53. doi: 10.1158/1541-7786.MCR-07-0060. (2007).
573. Bech-Serra, J.J. *et al.* Proteomic identification of desmoglein 2 and activated leukocyte cell adhesion molecule as substrates of ADAM17 and ADAM10 by difference gel electrophoresis. *Mol Cell Biol.* **26**, 5086-95. (2006).
574. Micciche, F. *et al.* Activated leukocyte cell adhesion molecule expression and shedding in thyroid tumors. *PLoS One.* **6**, e17141. doi: 10.1371/journal.pone.0017141. (2011).
575. Carbotti, G. *et al.* Activated leukocyte cell adhesion molecule soluble form: a potential biomarker of epithelial ovarian cancer is increased in type II tumors. *Int J Cancer.* **132**, 2597-605. doi: 10.1002/ijc.27948. Epub 2012 Dec 13. (2013).
576. Langer, M.D., Guo, H., Shashikanth, N., Pierce, J.M. & Leckband, D.E. N-glycosylation alters cadherin-mediated intercellular binding kinetics. *J Cell Sci.* **125**, 2478-85. doi: 10.1242/jcs.101147. Epub 2012 Feb 17. (2012).
577. Janik, M.E., Przybylo, M., Pochec, E., Pokrywka, M. & Litynska, A. Effect of alpha3beta1 and alphavbeta3 integrin glycosylation on interaction of melanoma cells with vitronectin. *Acta Biochim Pol.* **57**, 55-61. Epub 2010 Jan 11. (2010).
578. Meyer, N. & Penn, L.Z. Reflecting on 25 years with MYC. *Nat Rev Cancer.* **8**, 976-90. doi: 10.1038/nrc2231. (2008).
579. Wasylishen, A.R. & Penn, L.Z. Myc: the beauty and the beast. *Genes Cancer.* **1**, 532-41. doi: 10.1177/1947601910378024. (2010).
580. Krishnaswamy, S. *et al.* Ethnic differences and functional analysis of MET mutations in lung cancer. *Clin Cancer Res.* **15**, 5714-23. doi: 10.1158/1078-0432.CCR-09-0070. Epub 2009 Sep 1. (2009).
581. Shieh, J.M. *et al.* Lack of association of C-Met-N375S sequence variant with lung cancer susceptibility and prognosis. *Int J Med Sci.* **10**, 988-94. doi: 10.7150/ijms.5944. Print 2013. (2013).
582. Hainaut, P. & Wiman, K.G. 30 years and a long way into p53 research. *Lancet Oncol.* **10**, 913-9. doi: 10.1016/S1470-2045(09)70198-6. (2009).
583. Wistuba, II *et al.* Molecular changes in the bronchial epithelium of patients with small cell lung cancer. *Clin Cancer Res.* **6**, 2604-10. (2000).
584. Kosaka, T. *et al.* Mutations of the epidermal growth factor receptor gene in lung cancer: biological and clinical implications. *Cancer Res.* **64**, 8919-23. (2004).
585. Santarpia, L., Lippman, S.M. & El-Naggar, A.K. Targeting the MAPK-RAS-RAF signaling pathway in cancer therapy. *Expert Opin Ther Targets.* **16**, 103-19. doi: 10.1517/14728222.2011.645805. Epub 2012 Jan 12. (2012).
586. Rusconi, P., Caiola, E. & Broggini, M. RAS/RAF/MEK inhibitors in oncology. *Curr Med Chem.* **19**, 1164-76. (2012).
587. Johnson, G.L. & Lapadat, R. Mitogen-activated protein kinase pathways mediated by ERK, JNK, and p38 protein kinases. *Science.* **298**, 1911-2. (2002).
588. Roberts, P.J. & Der, C.J. Targeting the Raf-MEK-ERK mitogen-activated protein kinase cascade for the treatment of cancer. *Oncogene.* **26**, 3291-310. (2007).
589. McCubrey, J.A. *et al.* Mutations and deregulation of Ras/Raf/MEK/ERK and PI3K/PTEN/Akt/mTOR cascades which alter therapy response. *Oncotarget.* **3**, 954-87. (2012).
590. Eppstein, A.C. *et al.* Differential sensitivity of chemoresistant neuroblastoma subtypes to MAPK-targeted treatment correlates with ERK, p53 expression, and signaling response to U0126. *J Pediatr Surg* **41**, 252-9 (2006).

591. Roche, S. Doctoral thesis, Dublin City University, Ireland, (2011).
592. Yan, F., Wang, X.M., Pan, C. & Ma, Q.M. Down-regulation of extracellular signal-regulated kinase 1/2 activity in P-glycoprotein-mediated multidrug resistant hepatocellular carcinoma cells. *World J Gastroenterol.* **15**, 1443-51. (2009).
593. Janknecht, R. & Hunter, T. Activation of the Sap-1a transcription factor by the c-Jun N-terminal kinase (JNK) mitogen-activated protein kinase. *J Biol Chem.* **272**, 4219-24. (1997).
594. Sui, H., Fan, Z.Z. & Li, Q. Signal transduction pathways and transcriptional mechanisms of ABCB1/Pgp-mediated multiple drug resistance in human cancer cells. *J Int Med Res.* **40**, 426-35. (2012).
595. Callaghan, R., Luk, F. & Bebawy, M. Inhibition of the multidrug resistance p-glycoprotein: time for a change of strategy? *Drug Metab Dispos.* **42**, 623-31. doi: 10.1124/dmd.113.056176. Epub 2014 Feb 3. (2014).
596. Stolarczyk, E.I., Reiling, C.J. & Paumi, C.M. Regulation of ABC transporter function via phosphorylation by protein kinases. *Curr Pharm Biotechnol.* **12**, 621-35. (2011).
597. Borsch-Haubold, A.G., Pasquet, S. & Watson, S.P. Direct inhibition of cyclooxygenase-1 and -2 by the kinase inhibitors SB 203580 and PD 98059. SB 203580 also inhibits thromboxane synthase. *J Biol Chem.* **273**, 28766-72. (1998).
598. Zuber, J. *et al.* A genome-wide survey of RAS transformation targets. *Nat Genet.* **24**, 144-52. (2000).
599. Huynh, H., Soo, K.C., Chow, P.K. & Tran, E. Targeted inhibition of the extracellular signal-regulated kinase kinase pathway with AZD6244 (ARRY-142886) in the treatment of hepatocellular carcinoma. *Mol Cancer Ther.* **6**, 138-46. (2007).
600. Choi, Y.K. *et al.* JNK1/2 Activation by an Extract from the Roots of Morus alba L. Reduces the Viability of Multidrug-Resistant MCF-7/Dox Cells by Inhibiting YB-1-Dependent MDR1 Expression. *Evid Based Complement Alternat Med.* **2013:741985.**, 10.1155/2013/741985. Epub 2013 Jul 24. (2013).
601. Pekcec, A. *et al.* Targeting prostaglandin E2 EP1 receptors prevents seizure-associated P-glycoprotein up-regulation. *J Pharmacol Exp Ther.* **330**, 939-47. doi: 10.1124/jpet.109.152520. Epub 2009 Jun 3. (2009).
602. Peng, H. *et al.* PHII-7 inhibits cell growth and induces apoptosis in leukemia cell line K562 as well as its MDR- counterpart K562/A02 through producing reactive oxygen species. *Eur J Pharmacol.* **718**, 459-68. doi: 10.1016/j.ejphar.2013.07.038. Epub 2013 Jul 30. (2013).
603. Shen, D.Y., Zhang, W., Zeng, X. & Liu, C.Q. Inhibition of Wnt/beta-catenin signaling downregulates P-glycoprotein and reverses multi-drug resistance of cholangiocarcinoma. *Cancer Sci.* **104**, 1303-8. doi: 10.1111/cas.12223. Epub 2013 Aug 6. (2013).
604. Tang, T., Song, X., Liu, Y.F. & Wang, W.Y. PEITC reverse multi-drug resistance of human gastric cancer SGC7901/DDP cell line. *Cell Biol Int.* **38**, 502-10. doi: 10.1002/cbin.10169. Epub 2014 Feb 5. (2014).
605. Wang, L. *et al.* Dioscin restores the activity of the anticancer agent adriamycin in multidrug-resistant human leukemia K562/adriamycin cells by down-regulating MDR1 via a mechanism involving NF-kappaB signaling inhibition. *J Nat Prod.* **76**, 909-14. doi: 10.1021/np400071c. Epub 2013 Apr 26. (2013).
606. Xin, Y. *et al.* Parthenolide reverses doxorubicin resistance in human lung carcinoma A549 cells by attenuating NF-kappaB activation and HSP70 up-regulation. *Toxicol Lett.* **221**, 73-82. doi: 10.1016/j.toxlet.2013.06.215. (2013).
607. Zhao, B.X. *et al.* Grape seed procyanidin reversal of p-glycoprotein associated multi-drug resistance via down-regulation of NF-kappaB and MAPK/ERK mediated YB-1 activity in A2780/T cells. *PLoS One.* **8**, e71071. doi: 10.1371/journal.pone.0071071. eCollection 2013. (2013).
608. Reddy, K.B., Nabha, S.M. & Atanaskova, N. Role of MAP kinase in tumor progression and invasion. *Cancer Metastasis Rev* **22**, 395-403 (2003).
609. McBride, S. Doctoral thesis, Dublin City University, Ireland, (1995).

Appendix I: Sequenom Mutation Panel

	Gene	AA Change		Gene	AA Change		Gene	AA Change
1.	AKT1	E17K	58.	CTNNB1	I35N/S/T	115.	HRAS	G12S/R/C/D/A/V
2.	AKT1	E49K	59.	CTNNB1	H36P/R/Y	116.	HRAS	G13S/R/C
3.	AKT1	G173R	60.	CTNNB1	S37A/P/T/C/F/Y	117.	HRAS	Q61H/H/Q/K/L/P/R
4.	AKT1	K179M	61.	CTNNB1	T41A/P/S/I/N/S	118.	HRAS	E62G
5.	AKT2	E17K	62.	CTNNB1	S45A/P/T/C/F/Y	119.	IDH1	G70D
6.	AKT2	G175R	63.	DDR2	R105S	120.	IDH1	R132C/G/S/H/L
7.	AKT3	E17K	64.	DDR2	N456S	121.	IDH1	V178I
8.	AKT3	G171R	65.	DDR2	T533K	122.	IDH2	R172G/W/M/K/S
9.	ALK	L560F	66.	EGFR	V689M	123.	KIT	M552L
10.	ALK	A877S	67.	EGFR	N700D	124.	KIT	Y553N
11.	ALK	D1091N	68.	EGFR	E709A/V/G/K/Q	125.	KIT	W557G/R/R
12.	ALK	M1166R	69.	EGFR	G719A/D/C/S/R	126.	KIT	K558N/R
13.	ALK	I1171N	70.	EGFR	S720T/P	127.	KIT	V559A/D/G/I
14.	ALK	F1174C/S/L/L/I/V	71.	EGFR	D761N/Y	128.	KIT	V560D/A
15.	ALK	F1245C/L/V/I	72.	EGFR	V769L/M	129.	KIT	G565R
16.	ALK	R1275Q/L	73.	EGFR	T783A	130.	KIT	N566D
17.	APC	R1114X	74.	EGFR	A839T	131.	KIT	Y568D
18.	APC	E1306X	75.	EGFR	K846R	132.	KIT	V569G
19.	APC	E1338X	76.	EGFR	L858M/R	133.	KIT	P573L
20.	APC	Q1367X	77.	EGFR	L861Q/R	134.	KIT	F584S
21.	APC	E1379X	78.	EGFR	G863D	135.	KIT	L576P
22.	APC	Q1429X	79.	EGFR	H870R	136.	KIT	E561K
23.	APC	R1450X	80.	EGFR	E884K	137.	KIT	K642E
24.	BRAF	R444Q	81.	ERBB2	S310F/Y	138.	KIT	V654A
25.	BRAF	R462I	82.	ERBB2	L755S	139.	KIT	T670I
26.	BRAF	I463S	83.	ERBB2	G776S/V	140.	KIT	D716N
27.	BRAF	G464E/V/A/R	84.	ERBB2	D769H	141.	KIT	D816E/H/N/Y/G/V/A
28.	BRAF	G466R/E/V/A	85.	ERBB2	V777A/L/M	142.	KIT	D820E/E/H/Y/A/G/
29.	BRAF	G469A/E/R/V	86.	ERBB2	V842I	143.	KIT	N822K/N/K/Y/H
30.	BRAF	V471F	87.	ERBB2	H878Y	144.	KIT	Y823D/N
31.	BRAF	Y472S	88.	FBXO4	S8R	145.	KRAS	G12D/A/V/S/R/C
32.	BRAF	E586K	89.	FBXO4	S12L	146.	KRAS	G13D/A/V/S/R/C/
33.	BRAF	D587A/E	90.	FBXO4	L23Q	147.	KRAS	L19F/F
34.	BRAF	I592M/V	91.	FBXO4	P76T	148.	KRAS	Q22K
35.	BRAF	D594E/V/G	92.	FBXW7	R465C/H/L	149.	KRAS	T58I
36.	BRAF	F595L/L/L/S	93.	FBXW7	R479G/Q/L	150.	KRAS	A59T/G/E
37.	BRAF	G596R	94.	FBXW7	R505C/S/H/L/P	151.	KRAS	G60D
38.	BRAF	L597R/R/Q/V	95.	FBXW7	S582L	152.	KRAS	Q61E/K/X/H/H/Q/L/P/R
39.	BRAF	T599I	96.	FGFR1	S125L	153.	KRAS	A146P/T
40.	BRAF	V600E/A/G/L/M	97.	FGFR1	P252T	154.	MAP2K1	F53C/S
41.	BRAF	K601E/N/N	98.	FGFR2	S252W	155.	MAP2K1	Q56P
42.	BRAF	S605N	99.	FGFR2	Y375C	156.	MAP2K1	K57N
43.	BRAF	G615R	100.	FGFR2	N549K/K	157.	MAP2K1	P124L/T/S
44.	CDK4	R24C/H	101.	FGFR3	R248C	158.	MAP2K1	E203K/Q
45.	CDKN1B	P117S	102.	FGFR3	S249C	159.	MAP2K2	E207K/Q
46.	CDKN2A	R58X	103.	FGFR3	G370C	160.	MAP2K2	R388Q
47.	CDKN2A	E61X	104.	FGFR3	S371C	161.	MAP3K13	P373S
48.	CDKN2A	E69X	105.	FGFR3	Y373C	162.	MAP3K13	S694L
49.	CDKN2A	R80X	106.	FGFR3	G380R	163.	MAP3K13	R880C
50.	CDKN2A	H83Y	107.	FGFR3	A391E	164.	MAP3K13	A882S
51.	CDKN2A	E88X	108.	FGFR3	K650E/Q/M/T	165.	MET	E168D

	Gene	AA Change		Gene	AA Change		Gene	AA Change
52.	CTNNB1	A13T	109.	FGFR3	G697C	166.	MET	N375S
53.	CTNNB1	A21T	110.	GNA11	Q209L/P	167.	MET	R970C
54.	CTNNB1	V22A	111.	GNA11	R183C	168.	MET	T1010I
55.	CTNNB1	D32A/G/V/H/N/Y	112.	GNAS	R201H/S/C	169.	MET	H1112R/L/Y
56.	CTNNB1	S33A/P/T	113.	GNAS	Q227H/L/R	170.	MET	H1124D
57.	CTNNB1	G34E/V/A/R/R	114.	GNAQ	Q209L/P/R	171.	MET	M1131T
172.	MET	Y1248C/H/D	210.	PIK3CA	M1004I	248.	SMARCD	D391H
173.	MET	Y1253D	211.	PIK3CA	G1007R	249.	SMARCD	Q504X
174.	MET	M1268T	212.	PIK3CA	Y1021C/H/N	250.	SOS1	R248H
175.	MLH1	V384D	213.	PIK3CA	R1023Q	251.	SOS1	R688Q
176.	MYC	P57S	214.	PIK3CA	T1025A/S/I/T	252.	SOS1	H888Q
177.	MYC	T58A	215.	PIK3CA	A1035T/V	253.	SRC	Q531X
178.	NCOR1	R108X	216.	PIK3CA	M1043I/I/I/V	254.	STK11	Q37X
179.	NCOR1	Q313X	217.	PIK3CA	A1046V	255.	STK11	Q170X
180.	NCOR1	E379X	218.	PIK3CA	H1047R/L/Y	256.	STK11	D194N/Y/V
181.	NCOR1	I1422S	219.	PIK3CA	G1049R	257.	STK11	G196V
182.	NCOR1	Q1792X	220.	PIK3CA	I1058F	258.	STK11	E199X/K
183.	NRAS	G12D/A/V/S/R/C	221.	PIK3CA	H1065L	259.	STK11	P281L
184.	NRAS	G13D/A/V/S/R/C	222.	PIK3R1	M326I	260.	STK11	W332X
185.	NRAS	A18T	223.	PIK3R1	G376R	261.	STK11	F354L
186.	NRAS	Q61E/K/X/H/H/Q/R/P/L	224.	PIK3R1	D560Y	262.	TBX3	Y163X
187.	PDGFRA	V561D	225.	PIK3R1	N564D	263.	TBX3	W197X
188.	PDGFRA	N659K/Y	226.	PTEN	R130L/P/Q/X	264.	TP53	V143A
189.	PDGFRA	D842Y/N/V	227.	PTEN	R173C/H	265.	TP53	R175H/P/L
190.	PDGFRA	D846Y	228.	PTEN	R233X	266.	TP53	C176F
191.	PDGFRA	Y849C	229.	PTEN	R335X	267.	TP53	I195S
192.	PDGFRA	D1071N	230.	PTPN11	A72D/V/T	268.	TP53	R196X
193.	PHLPP2	L1016S	231.	PTPN11	E69K	269.	TP53	R213X/L
194.	PIK3CA	R38H	232.	PTPN11	E76A/G/V/Q/K	270.	TP53	Y220C/S/H/N
195.	PIK3CA	Q60K	233.	RB1	E137X	271.	TP53	Y234H/N/D/C
196.	PIK3CA	R88Q	234.	RB1	L199X	272.	TP53	M237I
197.	PIK3CA	K111N	235.	RB1	R320X	273.	TP53	G245D/A/S/C/R
198.	PIK3CA	G118D	236.	RB1	R358X	274.	TP53	R248Q/P/L/W/G
199.	PIK3CA	N345K	237.	RB1	R455X	275.	TP53	R273C/H/P/L/S
200.	PIK3CA	S405F	238.	RB1	R552X	276.	TP53	D281G/H/Y
201.	PIK3CA	E418K	239.	RB1	R556X	277.	TP53	R282W
202.	PIK3CA	C420R	240.	RB1	R579X	278.	TP53	R306X
203.	PIK3CA	E453K	241.	RB1	C706F	279.	VHL	P81S
204.	PIK3CA	P539R	242.	RB1	E748X	280.	VHL	L85P
205.	PIK3CA	E542K/Q/V/G	243.	RET	C634R/W/Y	281.	VHL	L89H
206.	PIK3CA	E545D/K/Q/A/V/G	244.	RET	A664D	282.	VHL	L158Q/V
207.	PIK3CA	Q546H/E/K/L/P/R	245.	RET	E768D	283.	VHL	R161X
208.	PIK3CA	C901F	246.	RET	M918T	284.	VHL	R167W
209.	PIK3CA	F909L/L	247.	SMARCD	Q539X			

Appendix II: Research Article

Olfactomedin III expression contributes to anoikis-resistance in clonal variants of a human lung squamous carcinoma cell line.

EXPERIMENTAL CELL RESEARCH 318 (2012) 593–602

Available online at www.sciencedirect.com

SciVerse ScienceDirect

www.elsevier.com/locate/yexcr

Research Article

Olfactomedin III expression contributes to anoikis-resistance in clonal variants of a human lung squamous carcinoma cell line

Joanne Keenan[a,*], *Helena Joyce*[a,c], *Sinead Aherne*[a,c], *Shirley O'Dea*[b], *Padraig Doolan*[a], *Vincent Lynch*[a], *Martin Clynes*[a]

[a]*National Institute for Cellular Biotechnology (NICB), Dublin City University, Glasnevin, Dublin 9, Ireland*
[b]*Institute of Immunology, Biology Department, National University of Ireland, Maynooth, Co. Kildare, Ireland*
[c]*Molecular Therapeutics for Cancer Ireland, c/o NICB, Ireland*

ARTICLE INFORMATION

Article Chronology:
Received 12 August 2011
Revised version received
9 December 2011
Accepted 7 January 2012
Available online 13 January 2012

Keywords:
Olfactomedin 3
Anoikis
Lung cancer

ABSTRACT

Three clonal subpopulations of DLKP, a poorly differentiated squamous lung carcinoma cell line, display striking differences in ability to survive in suspension (anoikis resistance). DLKP-SQ is anoikis resistant (7.5% anoikis at 24 h). In contrast, DLKP-M and DLKP-I are sensitive to anoikis (49.2% and 42.6% respectively). DLKP-I shows increased apoptosis consistently over all time points tested while DLKP-M appear to slow down metabolically and perhaps delays onset of anoikis by undergoing autophagy. Expression microarray analysis identified pronounced differential expression of Olfactomedin 3 (OLFM3) between the clones. High expression of OLFM3 was confirmed at the RNA level by qRT-PCR in DLKP-SQ and at the protein level by Western blotting (within the cell and secreted). Little or no OLFM3 was detected in the other two clones (DLKP-M and DLKP-I). Following siRNA knockdown of OLFM3 in DLKP-SQ, anoikis was increased 2.8-fold to 21% which was intermediate between the anoikis levels in DLKP-SQ and DLKP-M or DLKP-I. This knockdown correlated with increased apoptosis in suspension but not in attached culture conditions. Addition of recombinant OLFM3 reduced anoikis in DLKP-I. This is the first instance of OLFM3 being linked with anoikis resistance in a human cancer cell line.

Introduction

Cellular heterogeneity within tumours could provide protection against a changing environment, such as exposure to hypoxia or chemotherapeutic drugs or the opportunity for invasion to a more suitable site. Subpopulations can arise by mutation or by alterations in the differentiation state, such as epithelial to mesenchymal and mesenchymal to epithelial transitions (EMT–MET) or by differentiating cancer stem cells [1]. Lung cancer, although the most preventable cancer, kills more people than the next top three cancers (breast, prostate and colon) [2]. Lung cancer is heterogeneous, consisting of two main groups: small cell lung cancer and non-small cell lung cancer (adenocarcinoma, large cell lung cancer and squamous cell carcinoma) and even within these groups there is morphological, functional, genetic as well as proteomic heterogeneity [3–5]. Subpopulations have been found to have differences in their drug resistance profiles and /or in their invasive potential [6,7] and this can impact critically on

* *Corresponding author at:* National Institute for Cellular Biotechnology, Dublin City University, Dublin, Ireland. Fax: +353 1 7005484.
E-mail address: Joanne.keenan@dcu.ie (J. Keenan).

Abbreviations: OLFM, Olfactomedin; 2D, two dimensional; siRNA, small interfering RNA; poly-Hema, poly-2-hydroxyethyl methacrylate; CM, conditioned Media.

0014-4827/$ – see front matter © 2012 Elsevier Inc. All rights reserved.
doi:10.1016/j.yexcr.2012.01.012

treatment [8]. Understanding the biology of these subpopulations and how they interact may provide opportunities to improve treatment or produce new diagnostic markers.

In previous work in our laboratory, three subpopulations (DLKP-SQ, DLKP-M and DLKP-I) of a poorly differentiated squamous lung carcinoma line, DLKP, were isolated and characterised with respect to epithelial, mesenchymal and other lung differentiation markers [4]. In this paper, we explore differences in anoikis-resistance between these clonal subpopulations, and investigate the role of Olfactomedin-3 in regulation of anoikis-resistance.

Materials and methods

Chemicals

All chemicals (unless otherwise stated), FBS, glutamine and cell culture media were obtained from Sigma (Poole, UK). Recombinant OLFM3 (cat. H00118427-P01) was obtained from Abnova (Taiwan).

Cell lines

DLKP is a poorly differentiated human squamous carcinoma cell line established in this laboratory [9] from which the three subclones DLKP-SQ, DLKP-M and DLKP-I were isolated [4]. DLKP-SQ is squamous-like, DLKP-M is mesenchymal cell-like and DLKP-I exhibits an intermediate morphology. DLKP variants were maintained in DMEM/Hams F12 (1:1) supplemented with 5% FBS and 1% L-glutamine. MCF-7, SKBR3 and RPMI-2650 were obtained from the ATCC. RPMI-2650tx was previously obtained by continuous exposure to taxol [10]. MCF-7 and SKBR3 were maintained in RPMI-1640 supplemented with 10% FBS and 1% L-glutamine. RPMI-2650 and RPMI-2650txl were maintained in MEM supplemented with 5% FBS and 1% L-glutamine, 1% sodium pyruvate and 1% NEAA. All cell lines were mycoplasma negative. A frozen cell pellet of 2×10^6 cells of DLKP and variants was submitted to LGC Limited (Middlesex, UK) for DNA fingerprinting. A database search of over 3000 cell lines showed no match with DLKP indicating that it was unique and the sub-clones were confirmed to be derived from DLKP.

qRT-PCR for OLFM3

Total RNA extracted from cell lysates (MirVana miRNA Isolation Kit, cat AM1560, Applied Biosystems) were quantified using the Nanodrop (ND-1000 spectrophotometer), reverse-transcribed using (High capacity RNA-to-cDNA kit, cat 4387406, Ambion) and requantified using the Nanodrop. TaqMan gene expression experiments were performed in 20 µl reactions containing 10 µl of TaqMan® Fast Universal Master Mix (2X), No AmpErase® UNG, 9 µl of cDNA template (80 ng) and 1 µl of TaqMan gene expression assay (20x). The following thermal cycling specifications were performed on the ABI 7500 Fast Real-Time PCR system (Applied Biosystems) 20 s at 95 °C and 40 cycles each for 3 s at 95 °C and 30 s at 60 °C. Expression values were calculated using the comparative threshold cycle (C_t) method. Briefly, this technique uses the formula $2^{-\text{delta deltaC}}t$ to calculate the expression of target genes normalised to a calibrator sample [11]. Glyceraldehyde-3-phosphate dehydrogenase (GAPDH) was selected as the endogenous control.

SiRNA transfection

Transfection assays were carried out with NeoFX transfection reagent (siPORT NeoFX, AM4511, Ambion Inc) and olfactomedin 3 validated siRNAs S26707, Ambion Inc (OLFM3(1)) and S26708, Ambion Inc (OLFM3(2)) with scrambled control 2 (AM4613, Applied Biosystems) in OptiMEM medium (Gibco™) [12]. Cells in log phase of growth were fed prior to setting up transfection at the following conditions: 2×10^5 cells per well (in 1 ml for transfection) and 2 ul NeoFX. Cells were fed after overnight exposure to transfection with 2 ml fresh medium. The cells were allowed to grow for three days at 37 °C and 5%CO_2, over which time, microscopic observations were used to look for changes in morphology and to assess the efficiency of transfection (by looking at the growth in kinesin control (KIF-II, Ambion, Inc). At 72 h the cells were trypsinized, counted and anoikis assays were set up. A duplicate plate was washed in PBS A and lysed with 2D lysis buffer for protein analysis.

Western blotting

Western blotting was performed on cell lysates. Samples with 20–30 µg of protein per well, were separated on a 12% SDS gel [13]. After Western blotting [14], blots with primary antibodies (OLFM3 (Santa Cruz, Germany), Caspase-3 and FAK (BD, Europe, cat 610322 and 610087), phospho-FAK and phospho-PAX (Cell Signalling Cat 8556, 2541) or alpha-tubulin, LC3 (Sigma, cat T6199) were incubated overnight at 4 °C. Secondary antibodies conjugated to horse-radish peroxidase (Sigma, Poole, UK) were detected by enhanced chemiluminesence (Luminol, Santa Cruz, CA, USA).

Anoikis assays

The base of wells in a 24-well tissue culture plate (Costar, Cat 3524) were coated with 200 µl of poly-2-hydroxyethyl methacrylate (poly-HEMA, 12 mg/ml dissolved in 95% ethanol, Sigma P3932) and allowed to dry overnight. Coating was repeated. Immediately before use, the coated wells were washed twice with sterile PBS A. A 1 ml volume of cell suspension at 1x10E5 cells/ml was added to control (no poly-HEMA) and coated wells (3 per assay). The cells were incubated for specified times at 37 °C and 5% CO_2. Three hour prior to the end of the assay, 100 µl Almar Blue (Serotec BUF012B), an indicator dye was added. Metabolically active cells convert Almar Blue (resazurin) to a fluorescent and colormetric indicator (resorufin). Colour development was measured on a Bio-Tek plate reader at 570 nm with reference wavelength of 600 nm. Alternatively at the end of the incubation, cell viability was assessed by trypan blue exclusion dye of cells growing in poly-HEMA coated plates. Apoptosis (Guava Nexin cat 4500–0450) and Cell cycle analysis (Guava Cell cycle reagent 4500-0220) were assessed on a bench top flow cytometer (Guava EasyCyte Instrument).

Collection of conditioned media

Cells were grown in 175 cm2 flasks until about 40–50% confluent. Following extensive washing with fresh medium (no serum), cells were grown for 72 h to generate conditioned medium (CM). The CM was removed and centrifuged at 1000 rpm for 5 min, filter-

sterilised through a 0.22 μm low-protein binding filter and concentrated (to 10x of the starting volume of the CM) in a Vivaspin concentrator (Vivaspin-20, cat Vs2012) with a 5 kDa cut-off and the retentate was filter-sterilised.

Statistics

Statistics were carried out using the Student *t*-test assuming a two-tailed distribution and two samples of unequal variance. Values of $p < 0.05$ were considered as statistically significant.

Results

Anoikis resistance in DLKP clones

The presence of 'floaters' (viable cells that are suspended in the medium without the need for attachment to a surface) in sub-confluent flasks of DLKP-SQ, suggest that either DLKP-SQ or a sub-population of the clone could be resistant to anoikis. These floating cells if placed in a fresh flask attach and grow in the same fashion as DLKP-SQ. In contrast, DLKP-M and DLKP-I have very few floaters, and most of the cells floating were dead. As a result of these observations, the three clones were tested individually for anoikis resistance (Fig. 1). Microscopically, DLKP-SQ in suspension consists mostly of single cells, not forming clumps. DLKP-M and DLKP-I had very few loose single cells and formed aggregates which became more tightly clumped with time (Fig. 1F). When cells were grown for prolonged periods in polyhema-coated flasks (up to 10 passages), DLKP-SQ continued to grow with no lag-phase, the percentage viability remained high and when seeded in normal flasks, the cells attached and grew with the same morphology as the original DLKP-SQ. DLKP-M and DLKP-I, on the other hand, struggled and after three days showed only 42% and 56% viability respectively (data not shown).

Anoikis was measured by monitoring cell counts of attached and suspended cells, cell growth and viability in suspension and the Almar Blue assay (a measure of the metabolic activity of cells). After 24 h in suspension, DLKP-SQ undergo only 7.5% cell death as measured by viable cell counts and Almar Blue measurements (Figs. 1A and B) and with no significant changes in cell viability (Fig. 1E). At 48 h, although there is a slight reduction in growth for suspension cells compared to attached cells and Almar Blue measurement, there is no change in viability. While Annexin V staining suggest some apoptosis is occurring (Fig. 2A), DLKP-SQ is the only clone that continues to grow in suspension (Fig. 1D). These results suggest that no significant adaptation is required to survive anoikis conditions and that the bulk DLKP-SQ population rather than a sub-population is anoikis resistant.

The clones, DLKP-I and DLKP-M, showed 42–50% anoikis by Almar Blue measurement and show similar morphology under anoikis conditions but variations in viable cell counts suggest different mechanisms.

DLKP-I maintained in suspension show a continuous loss of viable cell numbers and viability (Figs. 1A, D–E) over time which is reflected in the metabolic state of the cells (Figs. 1B–C) and correlates with increased apoptosis. Annexin V staining revealed DLKP-I cells to be more susceptible to apoptosis under normal attached conditions (at 13%, higher than DLKP-SQ or DLKP-M at 6% and 8% respectively). In suspension, there was a significant (2.8-fold) increase in apoptosis in DLKP-I, with 33% of the cells being apoptotic at 24 and 48 h (Fig. 2B). Procaspase-3 levels were reduced in DLKP-I in suspension due to cleavage, indicating apoptosis (Fig. 2C). In addition there is a loss of phosphorylated FAK and phosphorylated Paxillin when DLKP-I are maintained in suspension (Fig. 2C).

For DLKP-M, there was a lag phase between the loss of metabolic activity and the reduction in viable cell number (Figs. 1A–C). While there was a slight increase in annexin V staining (Fig. 2B) this was not significant.

We analysed cell cycle progression to see if this could explain the lag phase. For the clones, cell cycle analysis revealed some changes between the clones under attached conditions, notably for DLKP-I, there was a higher proportion of cells in the G2/M phase than the other clones. However at 24 h, comparison of suspension cells to attached cells for each of the clones showed no significant differences, suggesting for this time point, cell cycle analysis was not a determining factor in the lag phase for DLKP-M (Fig. 2A). At 48 h, there was a more distinct increase in the proportion of DLKP-M cells in G0/G1 arrest (Fig. 2A).

At 24 h, an increase in the ratio the LC3-II to LC3-I peptides of the autophagy marker LC3 was observed (Fig. 2C). This in conjunction with the Almar Blue measurements and viable cell counts suggests that DLKP-M may be undergoing autophagy under anoikis conditions during the first 24 h.

Olfactomedin 3 in DLKP clones

Microarray analysis of the three clones of DLKP (Helena Joyce and Padraig Doolan, unpublished results) shows that one of the most highly differentially expressed mRNA among the clones was olfactomedin 3. The levels of OLFM3 in DLKP-I were 6% of those in DLKP-SQ (p-value <0.002) and in DLKP-M were less than 1% of those in DLKP-SQ (p-value <0.003)(Fig. 3A). Other members of the olfactomedin family (OLFM1, 2 and 4) were not differentially or highly expressed in the three clones at the mRNA level from microarray studies. Quantitative RT-PCR was carried out on the clones (Fig. 3B) using GAPDH as the internal control (shown not to be differentially expressed on the mRNA level in microarray results). OLFM3 was shown to be highly expressed in the DLKP-SQ compared to the two clones DLKP-M and DLKP-I. The levels of OLFM3 in DLKP-I were 3.6% of those in DLKP-SQ (p-value 2x10E-13) and in DLKP-M, were less than 1% of those in DLKP-SQ (p-value $<$ 2x10E-12).

Western blotting demonstrated high levels of OLFM3 protein in the DLKP-SQ cells, with little or no expression in the other two clones (Fig. 3C). Densitometry of Western blots for OLFM3 using alpha-tubulin as the loading control (shown not to be differentially regulated at least at transcript level in the microarray data) revealed DLKP-M and DLKP-I to express 1.3% and 1.2% of the OLFM3 expressed in DLKP-SQ (p-values <0.005) (Fig. 3D). OLFM3 is a secreted protein and may be present in the conditioned media (CM). Western blotting showed expression of OLFM3 in DLKP-SQ CM and none in DLKP-M or DLKP-I (Fig. 3E). There was little or no alpha- tubulin in the CM, indicating a lack of intracellular contaminants.

RNAi downregulation of Olfactomedin 3 in DLKP-SQ

Two validated siRNAs targeting OLFM3 were selected (OLFM3(1) and OLFM3(2)) and DLKP-SQ in log phase of growth were

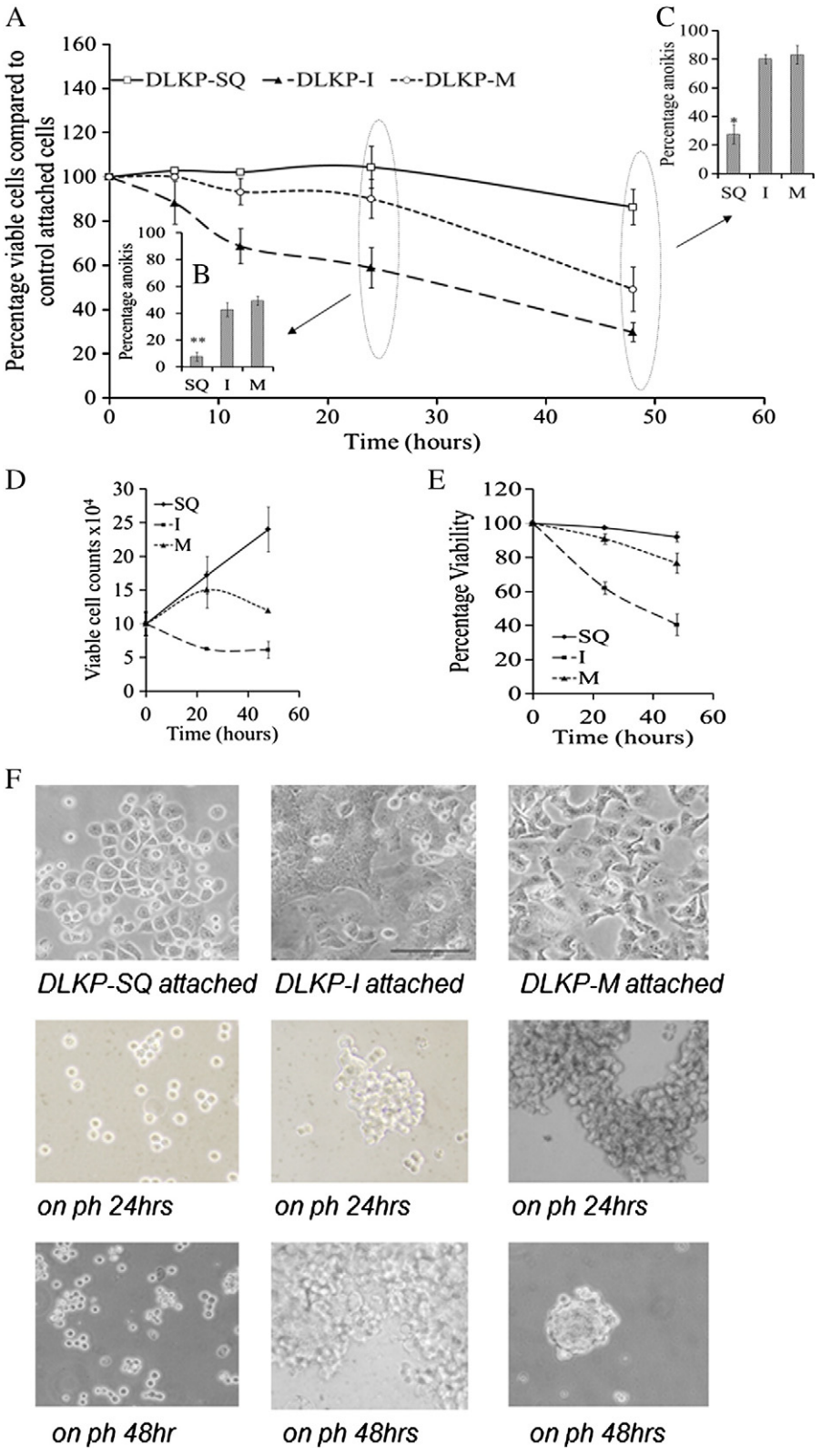

Fig. 1 – Effect of anoikis conditions on cell growth, Almar blue measurements, viability and morphological differences in DLKP clones (DLKP-SQ, DLKP-I and DLKP-M). (A) Anoikis measured as the percentage of cell death when grown in polyhema-coated wells over a 24 hour period (n = 4) compared to control cells in untreated wells. B and C show the results of Almar Blue measurements at 24-hour and 48-hour in polyhema-coated versus control plates respectively. * or ** indicates a p-value of <0.05 or <0.01 comparing DLKP-SQ to either of the other two clones; ph indicates in polyhema-coated wells. D shows the Viable cell number of the cells in the polyhema-coated plates while E shows the viability of those cells. (F) Morphological differences between DLKP clones viewed under 200× magnification at 24 h and 48 h.

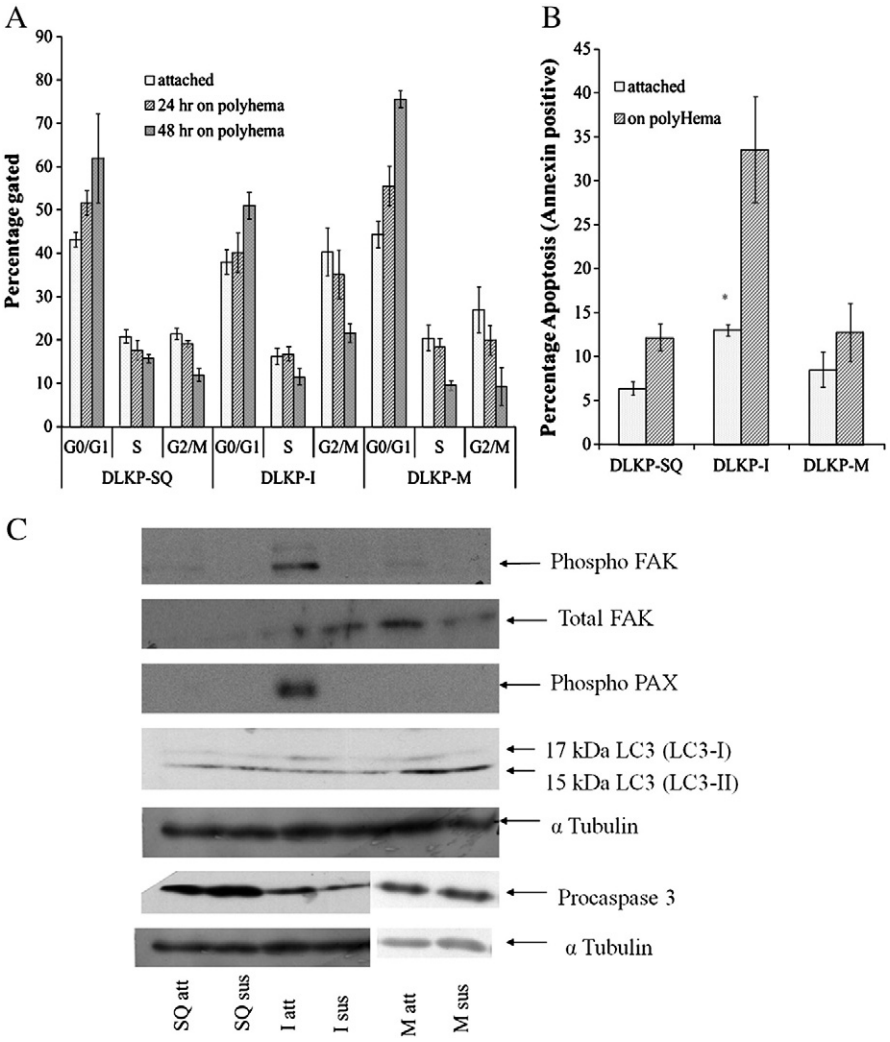

Fig. 2 – Effect of growth under anoikis conditions on cell cycle and apoptosis. (A) Cell cycle analysis on DLKP clones comparing attached versus suspension cells at 24 h and 48 h. (B) Apoptosis in DLKP clones as measured by Annexin-V staining in attached versus suspension cells at 24 h. * indicates a p-value of <0.05 DLKP-I in suspension to DLKP-I attached. For all experiments, results are the average of at least 3 separate repeats. (C) Western blotting of selected proteins in DLKP clones either attached (att) or in suspension (sus).

transfected with OLFM3 siRNA (kinesin siRNA (positive) or scrambled siRNA (negative) were used as controls). Microscopically, transfection of kinesin siRNA was seen to reduce growth as would be expected (by 90%, data not shown) indicating good siRNA transfection conditions. There was no morphological change in the DLKP-SQ as visualised microscopically following OLFM3 siRNA transfection, suggesting that OLFM3 was not a decisive factor in determining the morphological differences between DLKP-SQ and the other clones. At 72 h, cells counts (using trypan blue dye exclusion to look at viable cell numbers) showed no significant change in the total viable cell counts of siRNA-treated DLKP-SQ cells.

Knockdown of OLFM3 in DLKP-SQ had a significant impact on anoikis resistance (Fig. 4A), resulting in a 2.8-fold increase in anoikis compared to the scrambled control which was significant for both siRNAs ($p<0.01$ and $p<0.05$ for OLFM3(1) and OLFM3(2) respectively). Analysis of the protein levels of OLFM3 lysates in transfected samples showed that levels of OLFM3 were reduced by about 80% in the siRNA transfected cells (Figs. 4B and D). The level of anoikis in DLKP-SQ transfected cells was not as high as that seen with DLKP-M or DLKP-I suggesting that other factors may be having an impact on anoikis resistance, or that the remaining levels of OLFM3 are sufficient to maintain some level of anoikis resistance.

Loss of OLFM3 correlates with increased annexin V staining (Fig. 4D) suggesting anoikis may be occurring by apoptosis. There was no significant change in cell cycle profiles on loss of OLFM3 following siRNA transfection (data not shown).

Effect of recombinant OLFM3 on Anoikis sensitive clones

As OLFM3 appears to have a protective role against anoikis in DLKP-SQ, recombinant OLFM3 was tested on DLKP-I and DLKP-M anoikis sensitive cell lines. Recombinant OLFM3 at 1 ng/ml reduced anoikis in DLKP-I significantly ($p<0.001$) by 1.9-fold but not in DLKP-M, supporting a protective role for OLFM3 in apoptosis (Fig. 5). It is interesting to note that DLKP-I is the intermediate clonal type in the interconversion of the DLKP clones. It appears to

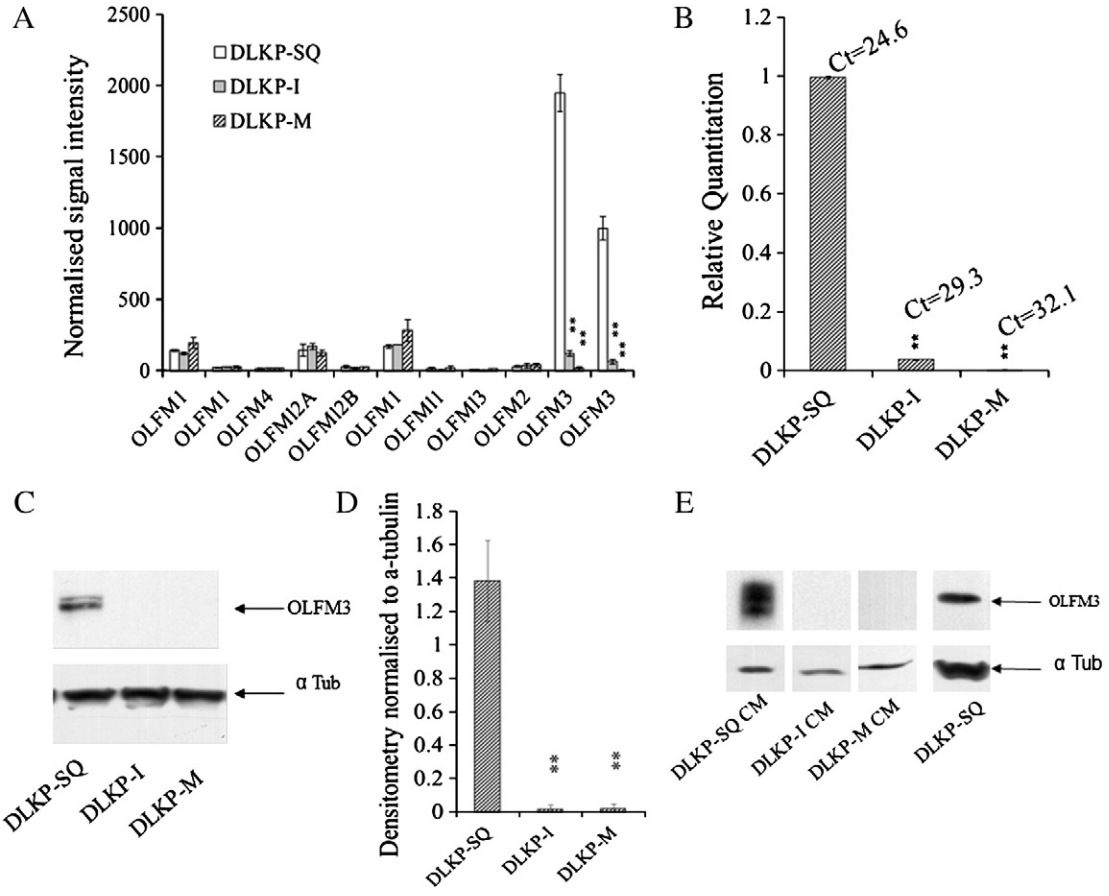

Fig. 3 – Expression of OLFM3. (A) Normalised signal intensity for OLFM species from microarrays. Standard *t*-test with p-value <0.003 compared to DLKP-SQ for DLKP-I or DLKP-M. OLFMl1 refers to OLFM-like 1. (B) Relative quantitation of OLFM3 compared to DLKP-SQ and normalised to GAPDH by qRT-PCR. Results are the average and standard deviation for three biological repeats. Standard *t*-test with p-value <2x10E-12 compared to DLKP-SQ for DLKP-I or DLKP-M. (C) Protein expression of OLFM3 and alpha tubulin as loading control in DLKP clones with (D) densitometry normalised to alpha tubulin. Results are the average and standard deviation for four biological repeats. ** represents Student *t*-test with p-value <0.002 for DLKP-SQ compared to DLKP-M and DLKP-I. (E) Western blot of OLFM3 in conditioned medium from DLKP clones. Image shows average blots from three biological repeats. A typical Western blot for OLFM3 in DLKP-SQ (labelled DLKP-SQ con) and control alpha tubulin is shown.

retain OLFM3 sensitivity without producing it, while DLKP-M not only does not produce OLFM3 but has lost sensitivity to it.

Expression of OLFM3 in other anoikis resistant cell lines

We looked at expression of OLFM3 in number of cancer cell lines with different anoikis resistance levels (Fig. 6). In the nasal carcinoma, the anoikis-sensitive parent RPMI-2650 expressed little or no OLFM3 but the taxol-resistant variant which was anoikis-resistant expressed OLFM3. In breast cell lines, anoikis-resistant SKBR-3 express OLFM3 while anoikis-sensitive MCF-7 does not. These results together with the results for SQ-CM and recombinant OLFM3 suggest that OLFM3 expression may have a role in anoikis resistance.

Discussion

In this work, the presence and possible role in anoikis of Olfactomedin 3 was investigated in clones of a poorly differentiated squamous lung carcinoma cell line. Affymetrix expression microarray studies in our laboratory showing OLFM3 to be one of the most highly differentially expressed mRNAs between the DLKP clones DLKP-SQ (high) and DLKP-M and DLKP-I (both low) were confirmed by qRT-PCR. Western blotting confirmed the presence of OLFM3 at the protein level in DLKP-SQ while the two other clones had little or no expression of OLFM3.

SiRNA knockdown of OLFM3 showed no effect on total viable cell growth or in morphology in the siRNA-transfected DLKP-SQ compared to the parental DLKP-SQ. Knockdown of OLFM3 resulted in increased anoikis (which is a form of cell death resulting from a disruption in the ECM signals). Knockdown of OLFM3 did not alter cell cycle but showed increased apoptosis as measured by annexin V expression (Fig. 4D). While the knockdown of OLFM3 was significant as detected by Western blotting (Fig. 4), the level of anoikis in the siRNA-transfected cells was still less than that observed in the DLKP-M or DLKP-I cells, suggesting that reduction in OLFM3 levels was not sufficiently complete for the time period or that other factors are involved in anoikis resistance in DLKP-SQ compared to DLKP-M and DLKP-I.

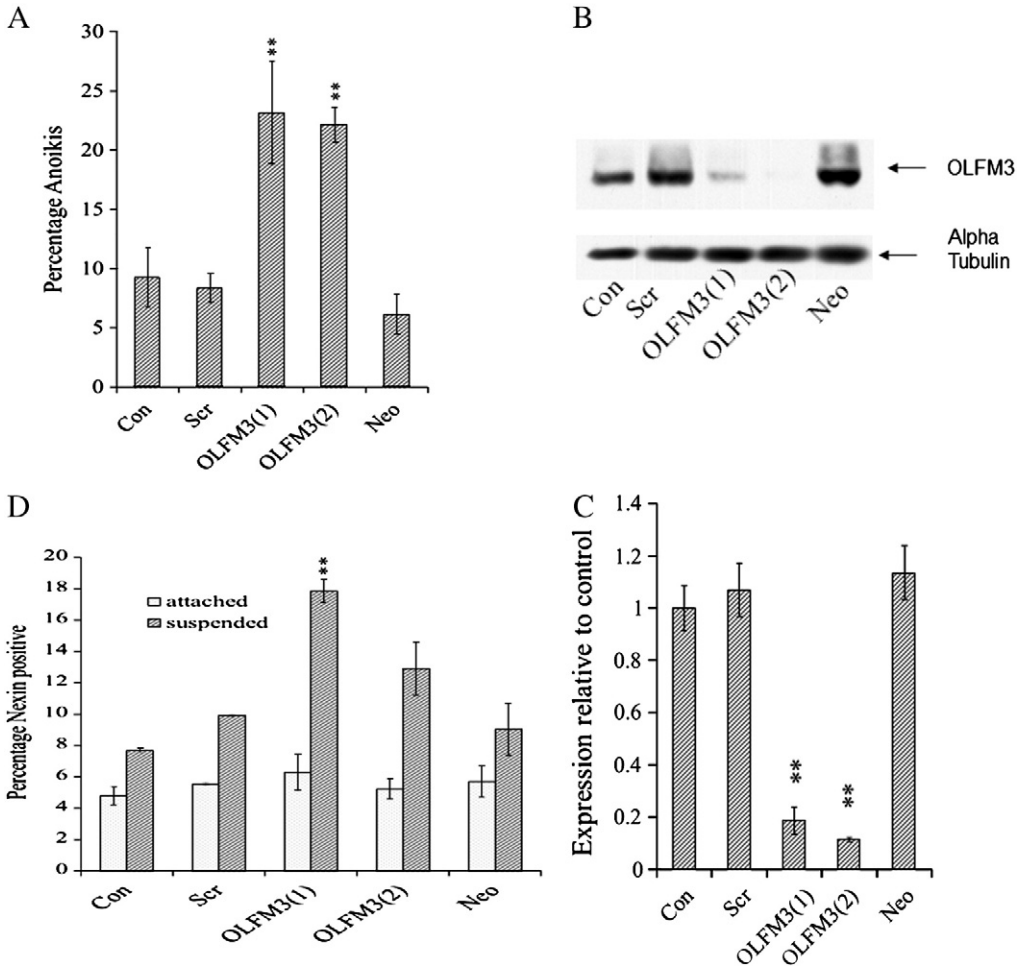

Fig. 4 – Effect of siRNA knockdown on anoikis in DLKP-SQ cells. After siRNA transfection and growth for 72 h, cells were trypsinised and set up under anoikis conditions, allowed to grow for a further 24 h and then counted. Samples were taken for Western blotting at 72 h. (A) Effect of siRNA knock-down on anoikis in DLKP-SQ as measured using Almar blue assay. (B) Western blotting for OLFM3 expression of siRNA-transfected DLKP-SQ and (C) Densitometry of Western blot. (D) Apoptosis assay as measured by Annexin V staining. Results are the average of at least 3 separate experiments. ** denotes Student *t*-test with a p-value of <0.005 compared to the scrambled control.

When recombinant OLFM3 was added to DLKP-I cells in suspension, anoikis was significantly reduced (Fig. 5). This is the first time, to our knowledge, that OLFM3 has been linked with anoikis resistance.

Olfactomedin 3 belongs to a family of glycoproteins containing a conserved C terminal olfactomedin domain, with four main groups OLFM1 to OLFM4 and at least 13 isoforms in mammals [15,16]. Identified first in the olfactory neuroepithelium of the bull frog in the 1990s [17], olfactomedins have been found in diverse species ranging from *C. elegans* to humans. The fact that the olfactomedins have been identified only in multicellular organisms suggests that they play a role in cell–cell interaction and signalling. Olfactomedins are involved in normal development and are associated with several diseases including open-angle glaucoma and cancer [18–22]. OLFM1 and 3 are expressed mainly in the brain, OLFM2 in the pancreas and prostate, and OLFM4 in the bone marrow, small intestine, colon and prostate [15]. Although originally identified in neural tissue, OLFM3 expression has been reported in the lung and spinal cord [23–25] and commercially available OLFM3 antibodies have been shown to stain lung cancer tissue. Lung cancers have also been observed to express OLFM1 and OLFM4 [19,22]. In this study, we also observed OLFM3 expression in lung as well as breast and nasal cancer cell lines that were anoikis resistant. None of the other olfactomedin proteins were differentially regulated at the mRNA level and subsequently were not investigated.

OLFM3, first identified in rat eye tissue and named optimedin [24] is a very conserved protein. OLFM3 forms homodimers (N-terminal important) and heterodimers (C-terminal important) with other olfactomedin domain containing proteins. OLFM3 is often localised to the Golgi and is a secreted protein. In mouse lens, the Pax6 transcription factor directly targets OLFM3 expression [25]. However, while Pax6 was detected in our microarray studies, the mRNA levels were slightly lower in DLKP-SQ than in DLKP-I or DLKP-M.

Olfactomedin 3 is known to interact with myocilin, a protein with cytoskeletal function and is associated with hereditary juvenile-onset open-angle glaucoma [26]. Microarray analysis showed very low levels of myocilin mRNA to be expressed in the clones and no difference was seen in the expression levels.

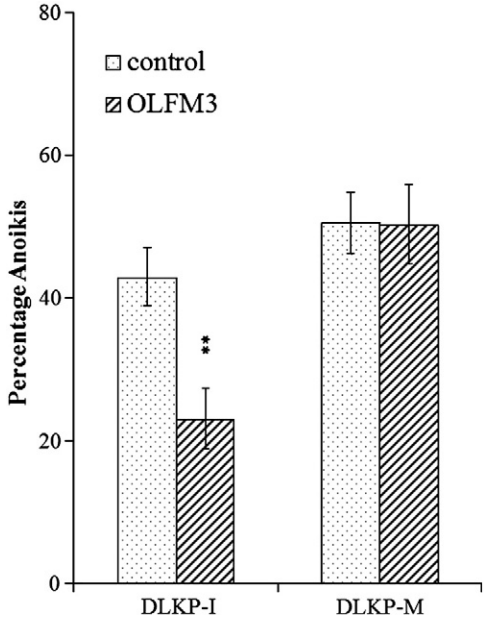

Fig. 5 – Effect of recombinant OLFM3 on DLKP-I and DLKP-M. Results are the average of at least 3 separate experiments. ** denotes Student *t*-test with a p-value of <0.001 compared to DLKP-I.

From the literature, it has been previously found that OLFM3 increased growth rate [27], and modulated cytoskeletal organisation, cell adhesion and migration [15]. Expression of OLFM3 in PC cells increased expression of N-cadherin, alpha-catenin and beta-catenin [27]. When Lee and Tomerav [27] knocked down expression of N-cadherin in OptH cells, the decreased levels of N-cadherin led to beta-catenin destabilisation, reduced formation of aggregates and increased the number of single cells in culture.

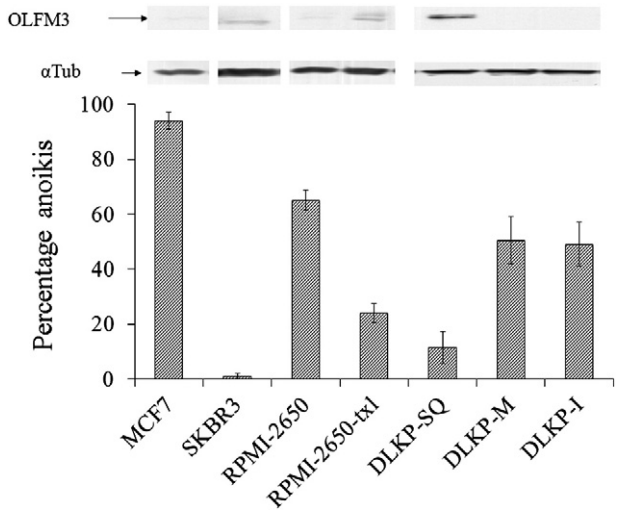

Fig. 6 – Correlation of expression of OLFM3 in anoikis resistant and anoikis sensitive pairs. Results for anoikis are the average of at least 3 separate experiments. Western blots shown are representative of three separate repeats with alpha tubulin being used as the loading control.

Interestingly, for DLKP-SQ which express OLFM3 but not N-cadherin (unpublished), the cells readily grow as single cells in suspension.

While the functions of OLFM3 are mostly unknown, several of the other olfactomedin proteins show similarities to the effects seen with DLKP-SQ. Both OLFM1 and OLFM4 have been implicated in apoptosis. Mutations in OLFM1 [28] and silencing of OLFM1 resulted in increased apoptosis [29]. OLFM4 may have differing roles depending on the tissue, being antiapoptotic in gastric cancers [30] and growth promoting in pancreas and lung cancer cells [31,21]. Recently, OLFM4 in prostate cancer, suppressed growth and metastasis and exerted a negative impact on autophagy through interactions with Cathepsin D and stromal-derived factor 1 [31].

The mechanism by which OLFM3 may regulate anoikis in DLKP-SQ is currently being investigated. Anoikis, meaning 'homelessness' in Greek, describes the induction of programmed cell death due to inappropriate expression of or loss of cell surface attachment to the extracellular matrix, and as such, provides a mechanism for preventing dissemination of cancer cells. There are two major cell death pathways involved in anoikis, apoptosis and autophagy [32]. Apoptosis from the literature appears as the main mechanism of anoikis with autophagy becoming important where apoptosis is blocked as a means of cell death. In autophagy, macromolecules and organelles especially mitochondria are targeted for degradation by lysozymal proteins to recycle nutrients within the cell. As such, autophagy may be a self-conservation response in times of stress. If the stress is excessive, autophagy can lead to cell death and there is extensive cross-talk between the two processes [32].

Mechanisms of anoikis resistance include augmentation of anti-apoptotic signals (such as Bcl-2 or Bcl-Xl [33]) or dampening of extracellular signals. Reducing extracellular signals occur at several levels, through cell surface receptors (such as integrins, cadherins and IGF-IR [34–37]), through the signalling cascades emanating from those receptors (such as the PI3K/Akt and ERK signalling pathways) and through the signalling molecules connecting receptors to pathways (such as Src family kinases and FAK [38]). EMT has been linked to suppression of anoikis via depletion of E-cadherin and expression N-cadherin to protect cells against anoikis [39,40].

It is possible that the activity of OLFM3 in reducing anoikis in DLKP-SQ is related to intracellular interaction with apoptotic machinery within the cell. For example, OLFM4 was found to interact with and inhibit the apoptosis promoting factor GRIM-19 [41]. Alternatively, secreted OLFM3 may interact with cell surface receptors or secreted proteins to prevent anoikis signalling. Secreted OLFM1 interacts with the Wnt signalling system through WIF-1 to regulate apoptosis through a variety of mechanisms [42].

In the clones, phosphorylated FAK is low in DLKP-SQ and DLKP-M suggesting reduced sensitivity to extracellular anoikis signals (Fig. 2C). In DLKP-I, the high levels of phosphorylated FAK in attached cells, are lost when the cells are maintained in suspension together with a loss of phosphorylated Paxillin (Fig. 2C), suggesting that integrin signalling through FAK is active and a source of anoikis signalling in DLKP-I.

There are several interacting proteins that have been previously identified to bind to OLFM3 including N-cadherin, Pax and Myoc [27,23,24]. Interestingly, N-cadherin is the only one of the above connectors that is significantly differentially regulated at the

mRNA level in the DLKP-clones, being up in DLKP-I and low or absent in DLKP-M and DLKP-SQ respectively (also in protein levels as determined by Western blotting (data not shown)).

Given that recombinant OLFM3 was able to reduce anoikis in DLKP-I but not back to the levels of DLKP-SQ and that loss of OLFM3 did not increase anoikis in DLKP-SQ to levels seen in the anoikis sensitive clones, suggests that other factors are involved in anoikis resistance in addition to OLFM3. Further, that FAK is not significantly affected by DLKP-SQ between attached and suspended cells supports more than one mechanism of anoikis resistance. This is not surprising as changes in apoptosis and/or autophagy may result in anoikis resistance. For apoptosis, many sets of molecules interact at the cell surface, inducing different downstream signalling cascades that lead to intracellular machinery controlling apoptosis [43]. In addition, the signalling molecules connecting the cytoskeleton and cytoplasm to the extracellular matrix can exhibit extensive cross-talk between the different signalling pathways [44].

Whether the expression of OLFM3 is a common mechanism is uncertain. Limited analysis has shown some correlation in breast cell lines with expression detected in the anoikis resistant SKBR3 but not in the anoikis sensitive MCF-7. Similarly OLFM3 was shown to be expressed in the anoikis resistant nasal cell line RPMI-2650-Txl variant while not in the anoikis sensitive parent, RPMI-2650.

Recently, both OLFM1 and OLFM4 expression have been linked to early stage lung cancer, while OLFM4 expression has also been implicated in early stages of gastric, colon and breast cancer [19–21]. It may be that expression of OLFM3 in DLKP-SQ reflects an early stage cancer.

In conclusion, this paper shows that expression of OLFM3 contributes to the increased anoikis resistance of DLKP-SQ and reduces anoikis in DLKP-I by reducing apoptosis. These results suggest that OLFM3 expression may have a role in anoikis resistance.

Conflict of interest

The authors declare no conflict of interest.

Acknowledgments

This work was supported by the Irish Higher Education Authority PRTLI Cycle 3 and 4 and Science Foundation Ireland Strategic Research Cluster, ‘Molecular therapeutics for cancer Ireland’.

REFERENCES

[1] A. Eramo, T.L. Haas, R. de Maria, Tools and targets to fight lung cancer, Oncogene 29 (2010) 4625–4635.
[2] R. Danesi, F. De Braud, S. Fogli, T.M. De Pas, A. Di Paolo, G. Curigliano, M. Del Tacca, Pharmacogenetics of anticancer drug sensitivity in non-small cell lung cancer, Pharmacol. Rev. 55 (2003) 57–103.
[3] F. Bianchi, F. Nicassio, P.P. Di Fiore, Unbiased vs biased approaches to the identification of cancer signatures: the case of lung cancer, Cell Cycle 7 (2008) 729–734.
[4] S. McBride, P. Meleady, A. Baird, D. Dinsdale, M. Clynes, Human lung carcinoma cell line DLKP contains 3 distinct subpopulations with different growth and attachment properties, Tumour Biol. 19 (1998) 88–103.
[5] J. Keenan, L. Murphy, M. Henry, P. Meleady, M. Clynes, Proteomic analysis of multidrug-resistance mechanisms in adriamycin resistant variants of DLKP, a squamous lung cancer cell line, Proteomics 9 (2009) 1556–1566.
[6] M. Heenan, L. O'Driscoll, I. Cleary, L. Connolly, M. Clynes, Isolation from a human MDR lung cell line of multiple clonal subpopulations which exhibit significantly different drug resistance, Int. J. Cancer 71 (1997) 907–915.
[7] Y.W. Chu, P.C. Yang, S.C. Yang, Y.C. Shvu, M.J.C. Hendrix, R. Wu, C.W. Wu, Selection of invasive and metastatic subpopulations from a human lung adenocarcinoma cell line, Am. J. Respir. Cell Mol. Biol. 17 (1997) 353–360.
[8] A.C. Borczuk, R.L. Toonkel, C.A. Powell, Genomics of lung cancer, Proc. Am. Thorac. Soc. 6 (2009) 152–158.
[9] E. Law, U. Gilvarry, V. Lynch, B. Gregory, G. Grant, M. Clynes, Cytogenetic comparison of two poorly differentiated human lung squamous cell carcinoma lines, Cancer Genet. Cytogenet. 59 (1992) 111–118.
[10] Y. Liang, P. Meleady, I. Cleary, S. McDonnell, L. Connolly, M. Clynes, Selection with melphalan or paclitaxel (Taxol) yields variants with different patterns of multidrug resistance, integrin expression and in vitro invasiveness, Eur. J. Cancer 37 (2001) 1041–1052.
[11] K.J. Livak, T.D. Schmittgen, Analysis of relative gene expression data using real-time quantitative PCR and the 2(−Delta Delta C(T)) Method, Methods 25 (2001) 402–408.
[12] M.K. Muniyappa, P. Dowling, M. Henry, P. Meleady, P. Doolan, P. Gammell, M. Clynes, N. Barron, MiRNA-29a regulates the expression of numerous proteins and reduces the invasiveness and proliferation of human carcinoma cell lines, Eur. J. Cancer 45 (2009) 3104–3118.
[13] E. Laemmli, M. Favre, Mutation of the head of bacteriophage T4, J. Mol. Biol. 80 (1973) 575–579.
[14] H. Towbin, T. Staehelin, J. Gordon, Electrophoretic transfer of proteins from polyacrylamide gels to nitrocellulose sheets: procedures and some applications, Proc. Natl. Acad. Sci. U. S. A. 76 (1979) 4350–4354.
[15] S. Tomarev, N. Nakaya, Olfactomedin domain-containing proteins:possible mechanisms of action and functions in normal development and pathology, Mol. Neurobiol. 40 (2009) 122–138.
[16] L.C. Zeng, Z.G. Han, W.J. Ma, Elucidation of subfamily segregation and intramolecular coevolution of the olfactomedin-like proteins by comprehensive phylogenetic analysis and gene expression pattern assessment, FEBS Lett. 679 (2005) 5443–5453.
[17] D.A. Snyder, A.M. Rivers, H. Yokoe, B.P. Menco, R.R. Anholt, Olfactomedin: purification, characterisation, and localization of a novel olfactory glycoprotein, Biochemistry 30 (1991) 9143–9153.
[18] E.M. Stone, J.H. Fingert, W.M. Alward, T.D. Nguyen, J.R. Polansky, S.F. Sunden, D. Nishimura, A.F. Clark, A. Nystuen, B.E. Nichols, D.A. Mackey, R. Ritch, et al., Identification of a gene that causes primary open angle glaucoma, Science 275 (1997) 668–670.
[19] L. Wu, W. Chang, J. Zhao, Y. Yu, X. Tan, T. Su, L. Zhao, S. Huang, S. Liu, G. Cao, Development of autoantibody signatures as novel diagnostic biomarkers of non-small cell lung cancer, Clin. Cancer Res. 16 (2010) 3760–3768.
[20] N. Oue, K. Sentani, T. Noguchi, S. Ohara, N. Sakamoto, T. Hayashi, K. Anami, J. Motoshita, M. Ito, S. Tanaka, K. Yoshida, W. Yasui, Serum olfactomedin 4 (GW112, hGC-1) in combination with Reg IV is a highly sensitive biomarker for gastric cancer patients, Int. J. Cancer 125 (2009) 2383–2392.
[21] S. Koshida, D. Kobayashi, R. Moriai, N. Tsuji, N. Watanabe, Specific overexpression of OLFM4GW112/hGC-1 mRNA in colon, breast and lung cancer tissues detected using quantitative analysis, Cancer Sci. 98 (2007) 315–320.
[22] W. Liu, Y. Liu, J. Zhu, E. Wright, I. Ding, G.P. Rodgers, Reduced hGC-1 protein expression is associated with malignant progression of colon carcinoma, Clin. Cancer Res. 14 (2008) 1041–1049.

[23] O. Grinchuk, Z. Kozmik, X. Wu, S. Tomarev, The Optimedin gene is a downstream target of Pax6, J. Biol. Chem. 280 (2005) 35228–35237.
[24] M. Torrado, R. Trivedi, R. Zinovieva, I. Karavanova, S.I. Tomarev, Optimedin: a novel olfactomedin-related protein that interacts with myocilin, Hum. Mol. Genet. 11 (2002) 1291–1301.
[25] L.V. Wolf, Y. Yang, J. Wang, Q. Xie, B. Braunger, E.R. Tamm, J. Zavadil, A. Cvekl, Identification of pax6-dependent gene regulatory networks in the mouse lens, PLoS One 4 (2009) e4159.
[26] M.K. Joe, S. Sohn, W. Hur, Y. Moon, Y.R. Choi, C. Kee, Accumulation of mutant myocilins in ER leads to ER stress and potential cytotoxicity in human trabecular meshwork cells, Biochem. Biophys. Res. Commun. 312 (2003) 592–600.
[27] H.S. Lee, S.I. Tomarev, Optimedin induces expression of N-cadherin and stimulates aggregation of NGF-stimulated PC12 cells, Exp. Cell Res. 313 (2007) 98–108.
[28] N. Nakaya, H.S. Lee, Y. Takada, I. Tzchori, S.I. Tomarev, Zebrafish olfactomedin 1 regulates retinal axon elongation in vivo and is a modulator of Wnt signaling pathway, J. Neurosci. 31 (2008) 7900–7910.
[29] K.K. Kim, K.S. Park, S.B. Song, K.E. Kim, Up regulation of GW112 Gene by NF kappaB promotes an antiapoptotic property in gastric cancer cells, Mol. Carcinog. 49 (2010) 259–270.
[30] D. Kobayashi, S. Koshida, R. Moriai, N. Tsuji, N. Watanabe, Olfactomedin 4 promotes S-phase transition in proliferation of pancreatic cancer cells, Cancer Sci. 98 (2007) 334–340.
[31] L. Chen, L. Hongzhen, L. Wenli, Z. Jianqiong, Z. Xiongce, E. Wright, L. Cao, I. Ding, G.P. Rodgers, Olfactomedin 4 suppresses prostate cancer cell growth and metastasis via negative interaction with Cathespin D and SDF-1, Carcinogenesis 32 (2011) 986–994.
[32] C. Horbinski, C. Mojesky, N. Kyprianou, Live free or die: tales of homeless (cells) in cancer, Am. J. Pathol. 177 (2010) 1044–1052.
[33] R.J. Bold, J. Chandra, D.J. McConkey, Gemcitabine-induced programmed cell death (apoptosis) of human pancreatic carcinoma is determined by Ccl-2 content, Ann. Surg. Oncol. 6 (1999) 279.
[34] J. Grossmann, Molecular mechanisms of 'detachment-induced apoptosis-Anoikis', Apoptosis 7 (2002) 247–260.
[35] D. Lane, N. Goncharenko-Khadier, C. Rancourt, A. Piché, Ovarian cancer ascites protects from TRAIL-induced cell death through αvβ5 integrin-mediated focal adhesion kinase and Akt activation, Oncogene 29 (2010) 3519–3531.
[36] M.J. Martin, N. Melnyk, M. Pollard, M. Bowden, H. Leong, T.J. Podor, M. Gleave, P.H. Sorensen, The insulin-like growth factor 1 receptor is required for Akt activation and suppression of anoikis in cells transformed by the ETV6-NTRK3 chimeric tyrosine kinase, Mol. Cell. Biol. 26 (2006) 1754–1769.
[37] J. Schwock, N. Dhani, M.P. Cao, J. Zheng, R. Clarkson, N. Radulovich, R. Navab, L.C. Horn, D.W. Hedley, Targeting focal adhesion kinase with dominant-negative FRNK or Hsp90 inhibitor 17-DMAG suppresses tumor growth and metastasis of SiHa cervical xenografts, Cancer Res. 69 (2009) 4750–4759.
[38] G. Liu, X. Meng, Y. Jin, J. Bai, Y. Zhao, X. Cui, F. Chen, S. Fu, Inhibitory role of focal adhesion kinase on anoikis in the lung cancer cell A549, Cell Biol. Int. 32 (2008) 663–670.
[39] P.W. Derksen, X. Liu, F. Saridin, H. van der Gulden, J. Zevenhoven, B. Evers, J.R. van Beijnum, A.W. Griffioen, J. Vink, P. Krimpenfort, J.L. Peterse, R.D. Cardiff, et al., Somatic inactivation of E-cadherin and p53 in mice leads to metastatic lobular mammary carcinoma through induction of anoikis resistance and angiogenesis, Cancer Cell 10 (2006) 437–449.
[40] G. Li, K. Satyamoorthy, M. Herlyn, N-cadherin-mediated intercellular interactions promote survival and migration of melanoma cells, Cancer Res. 61 (2001) 3819–3825.
[41] X. Zhang, Q. Huang, Z. Yang, Y. Li, C.Y. Li, GW112, a novel antiapoptotic protein that promotes tumor growth, Cancer Res. 64 (2004) 2474–2481.
[42] N. Pecina-Slaus, Wnt signal transduction pathway and apoptotis: a review, Cancer Cell Int. 1 (2010) 22.
[43] L.D. Nagaprashantha, R. Vatsyayan, P.C.R. Lelsani, S. Awasthi, S.S. Singhal, The sensors and regulators of cell-matrix surveillance in anoikis resistance of tumours, Int. J. Cancer 128 (2011) 743–752.
[44] M.C. Guadamillas, A. Cerezo, M.A. del Pozo, Overcoming anoikis — pathways to anchorage independent growth in cancer, J. Cell Sci. 124 (2011) 3189–3197.